BOILING IN NARROW CHANNELS

Peter Arthur Kew

Submitted for the Degree
of
Doctor of Philosophy

Heriot-Watt University

Department of Mechanical and Chemical Engineering

November 1995

Abstract of Thesis

Heriot-Watt University: POSTGRADUATE EXAMINATIONS

1. NAME

(a) Surname KEW

(b) Other Names PETER ARTHUR

Registration No: 899249782

2. QUALIFICATION SOUGHT

(PhD/MSc/MPhil) PhD

3. TITLE OF THESIS BOILING IN NARROW CHANNELS

Date 16/11/95 Signature R. A Kew

Abstract

An experimental and theoretical study of the phenomena involved during boiling in narrow channels is presented. The channels are of a small size typical of those in the new micro-compact heat exchangers. Correlations and design methods used in the design of conventionally sized evaporators are summarised and the literature covering boiling in confined spaces is reviewed. It is shown that the published data are insufficient to allow the design of novel compact evaporators incorporating narrow channels to be undertaken with confidence.

A dimensionless criterion for determining the channel size at which the effects of confinement are likely to be significant for different fluids has been derived. It has been demonstrated that the flow in narrow channels can be divided into three flow regimes; Isolated Bubble, Confined Bubble and Annular-Slug Flow. A new model has been proposed which allows the prediction of evaporative heat transfer coefficients in each regime and this model has been tested against the Author's and other measured data. A fair degree of corroboration was achieved and it is argued that the model yields a thermal design methodology for narrow channel evaporators.

See reverse side for Notes

TABLE OF CONTENTS

TABLE OF CONTENTS

TABLE OF CONTENTS

TABLE OF CONTENTS

LIST OF TABLES

LIST OF TABLES

LIST OF FIGURES

LIST OF FIGURES

LIST OF FIGURES

LIST OF FIGURES

LIST OF FIGURES

LIST OF FIGURES

LIST OF FIGURES

LIST OF FIGURES

ACKNOWLEDGEMENTS

This work was carried out under the supervision of Professor Keith Cornwell, Dean of the Faculty of Engineering , Heriot-Watt University, whose help and guidance has been greatly appreciated.

Much of the research described in this Thesis was conducted as part of projects supported by the Commission of the European Communities under the JOULE I and JOULE II programmes. The support of the Commission is gratefully acknowledged.

The Author also acknowledges the help of the technical staff of the Department of Mechanical Engineering and thanks them for their assistance with the construction of the test rigs. The collaboration of Dr Ian Grant and his assistance in the development of the single-tube test section as a co-worker on the JOULE II project was particularly appreciated.

Finally, the Author wishes to thank his Wife for her patience and support, especially during the latter stages of preparation of this Thesis

BOILING IN NARROW CHANNELS

ABSTRACT

An experimental and theoretical study of the phenomena involved during boiling in narrow channels is presented. The channels are of a small size typical of those in the new micro-compact heat exchangers. Correlations and design methods used in the design of conventionally sized evaporators are summarised and the literature covering boiling in confined spaces is reviewed. It is shown that the published data are insufficient to allow the design of novel compact evaporators incorporating narrow channels to be undertaken with confidence.

A dimensionless criterion for determining the channel size at which the effects of confinement are likely to be significant for different fluids has been derived. It has been demonstrated that the flow in narrow channels can be divided into three flow regimes; Isolated Bubble, Confined Bubble and Annular-Slug Flow. A new model has been proposed which allows the prediction of evaporative heat transfer coefficients in each regime and this model has been tested against the Author's and other measured data. A fair degree of corroboration was achieved and it is argued that the model yields a thermal design methodology for narrow channel evaporators.

INTRODUCTION

Evaporation is a fundamental part of many processes in the chemical and petro-chemical industries and in refrigeration plant. Additionally, the production of steam is vital in many processes and in power plant. Traditionally, evaporation or boiling occurs in tubular heat exchangers, either within the tubes or on the outside of the tubes. Recently there has been a growing awareness of the benefits of process intensification - the reduction in plant size, for a given capacity, by an order of magnitude or more - and this has led to a requirement for smaller evaporators. Several types of compact heat exchanger previously confined to use in specialist applications are now gaining widespread acceptance in the process and refrigeration industries, while other heat exchanger types have been developed within the last ten years. The common feature of compact heat exchangers is their high (compared to shell-and-tube designs) ratio of heat transfer area to heat exchanger volume. Compact heat exchangers have heat transfer area to volume ratios in excess of $700m^2/m^3$, compared to, typically, $200m^2/m^3$ for a tubular unit. Various types of compact heat exchanger are described in *Chapter 1* .

Utilisation of a physically small heat exchanger for a given duty is advantageous for several reasons: often (although not always) small physical size is associated with relatively low capital cost; installation costs are reduced if the size of a component is reduced;- a lower fluid inventory can be beneficial on both cost and safety grounds; and the nature of many compact heat exchanger designs is such that close approach temperatures can be achieved.

As manufacturing techniques have been developed to facilitate the construction of compact heat exchangers suitable for a range of duties and applications it has become apparent that there is insufficient understanding of the mechanisms involved in boiling in confined channels to permit confident thermal and hydraulic design of compact heat exchangers.

Recognising the importance of this area of research and development the Commission of the European Communities (CEC) has financed collaborative projects in the area of enhanced evaporation and compact heat exchangers under the *JOULE I* and *JOULE II* programmes relating to the rational use of energy. Details of the two projects under which much of the work reported here was carried out are included in *Appendix (1).* Support has also been provided by British Gas in the form of a Fellowship for the author covering the period of this work.

A consequence of the high area density in compact heat exchangers is that the flow passages must be small, having hydraulic diameters of 3mm or less. Established boiling and two-phase pressure drop correlations (discussed further in *Chapter 1)* are based largely on data which have been obtained from experiments with tubes of the order of 10mm diameter and above. Most data relating to smaller dimensions have been obtained with cryogenic fluids. As will be shown in *Chapter 4,* the diameter below which the effects of confinement become significant is a function of the Confinement Number, Co, defined:

$$Co = \frac{\left[\sigma / \left(g(\rho_f - \rho_g)\right)\right]^{1/2}}{d_e}$$

It will be shown in *Section 4.2* that the effects of confinement are expected to be significant for values of Confinement Number greater than 0.5.

The properties of cryogenic fluids are such that the term $\left[\sigma / \left(g(\rho_f - \rho_g)\right)\right]^{1/2}$ is lower than that for most process fluids, water and refrigerants, hence the effects of confinement only become important at lower diameters with cryogenic fluids than with other fluids, as indicated in *Table (0.1).*

The aim of this work is to investigate the mechanisms of evaporation in narrow channels and to provide information of use to designers in the prediction of heat transfer and pressure drop in compact geometries.

The structure of this Thesis is as laid out in the *Contents*. A summary of established methods of predicting heat transfer and pressure drops in boiling two-phase flows in conventionally sized tubes *(Chapter 1)* is followed by a review of the published literature which is relevant to the development of an understanding of the phenomena occurring in boiling flow in narrow channels *(Chapter 2). Chapter 3* describes the experimental programme which was carried out in order to provide data to assist in the formulation of a model applicable to boiling in narrow channels. The published and experimental data is combined with a theoretical analysis of various mechanisms of heat transfer (*Chapter 4))* resulting in the formulation of a semi-empirical model which incorporates the phenomena observed in narrow channel boiling *(Chapter 5)*. It is concluded *(Chapter 6)* that the model described is suitable for use as a tool in the design of compact heat exchangers.

NOMENCLATURE

A	Area	m^2
a,b,c,e,m,n,p,r	Constants used in Equation 1.8	
C	Constant	
D	Appropriate dimension	m
d	Diameter	m
d_e	Mean hydraulic diameter	m
E	Enhancement Factor (Chen type correlation)	
E1,E2	Percentage Errors	
F	Enhancement Factor (Shah type correlation)	
f	Friction factor	
G	Mass flux	kg/m^2
g	Acceleration due to gravity	m/s^2
h_{fg}	Latent heat of vapourisation kJ/kgK	
j	Superficial volume flux	m/s
K	Constant, Drift Coefficient	
L	Length	m
m	Mass flow rate	kg/s
p_{cr}	Critical pressure	bar
p_r	Reduced pressure	
q	Heat flux	W/m^2 (or kW/m^2)
r	Radius	m
S	Suppression factor	
s	Channel gap spacing	m
SR	Slip ratio	
T	Temperature	K
t	Time	s
V	Volumetric flow rate	m^3/s
v	Void fraction	
$v_{\$}$	Specific volume of phase $\$$	m^3/kg
w	Channel width	m
X	Martinelli parameter	
x	Vapour quality	
z	Length	m
ΔP	Pressure difference	Pa (or bar)
ΔT	Temperature difference	K

NOMENCLATURE

Dimensionless Numbers

Bo	Boiling Number
Ca	Capillary Number
Co	Confinement Number
Co_n	Convection Number (Shah Correlation)
Fo	Fourier Number
Fr	Froude Number
N_{EO}	Eotvos Number
NTU	Number of Transfer Units
Nu	Nusselt Number
Pr	Prandtl Number
Re	Reynolds Number
Re_l	Reynolds Number based on liquid flowing alone
We	Weber Number

NOMENCLATURE

Subscripts

0	at time=zero
ASF	Annular Slug Flow
b	bubble
CB	Confined Bubble
conv	convective
exp	experimental
f	film
g	gas or vapour
IB	Isolated Bubble
in	inlet
l	liquid
max	maximum
min	minimum
nb	nucleate boiling
npb	nucleate pool boiling
out	outlet
pred	predicted
sat	saturation conditions
SB	Sliding Bubble
tp	two-phase
w	wall

NOMENCLATURE

Greek

α	Heat transfer coefficient	W/m^2K (or kW/m^2K)
δ	Thickness	m
μ	Dynamic viscosity	Pas
ρ	Density	kg/m^3
σ	Surface tension	N/m
θ	Angle, dimensionless temperature difference	

CHAPTER 1

BACKGROUND

1.1 INTRODUCTION.

This Chapter commences with a general description of the compact heat exchangers which are currently available. It then proceeds to outline the methods which are used by designers in the analysis of heat transfer and pressure drop during evaporation in conventionally-sized equipment. The range of sizes, materials and construction methods incorporated in compact heat exchangers is continually being extended as manufacturing techniques are refined and developed. It is shown that there are correlations available to predict the heat transfer and pressure drop under most conditions of evaporation in round tubes of 6mm and above and although these correlations may be used in the design of compact heat exchangers they must be applied with caution.

1.2 COMPACT HEAT EXCHANGERS

Heat exchangers having very high area densities, typically of greater than $700m^2/m^2$, are classified as compact. Such heat exchangers occupy very much less space and are generally lighter than, for example, a shell-and-tube unit for an equivalent duty. This size reduction is due partly to the large heat transfer area which, by definition, is associated with a given volume of compact heat exchanger and partly to the fact that the small equivalent diameter associated with high area density leads to high heat transfer coefficients.

Utilisation of a physically small heat exchanger for a given duty is advantageous for several reasons: often (but not necessarily always) small physical size is associated with relatively low capital cost; installation costs are decreased if the size of a component is reduced; a lower fluid inventory can be beneficial on cost and safety grounds. Additionally, the nature of compact heat exchangers is such that very close approach temperatures can be achieved since it is possible to have almost pure counter-flow arrangements, this advantage is of less importance with single component phase-change applications than with single-phase applications. The benefits are likely to be greatest if

compact heat exchangers are incorporated in a process at the design stage, however, they can also be very attractive if modification to the process requires further units to be installed in an existing plant. Some designs of compact heat exchanger, particularly the plate-fin and printed circuit heat exchangers can accommodate several fluid streams.

There are several reasons why compact heat exchangers have not been more widely adopted to date. The conventional shell-and-tube heat exchanger is an established and reliable piece of equipment. The savings accruing due to use of a compact unit are likely to be dwarfed by the additional costs if the unit proves unreliable. Design codes applicable to compact heat exchangers are very limited, although the situation is improving. The number of manufacturers of compact heat exchangers of various types is very limited. For example there is only one manufacturer of PCHEs and some five manufacturers of plate-fin heat exchangers world-wide, therefore much thermal design data is proprietary. This contrasts with the situation for tubular heat exchangers for which published thermal design codes are available in the open literature.

It is widely perceived that fouling will be a problem associated with the small passage sizes in compact heat exchangers. Manufacturers claim that the high shear stresses also associated with small passages reduce the tendency to foul. Further work is necessary in this area. It must be remembered that the phenomena involved in fouling are far from fully understood in conventional heat exchangers.

Shell-and-Tube Heat Exchangers

Shell-and-Tube heat exchangers are traditionally the most widely used general purpose heat exchangers in all industries. The general arrangement of a typical shell-and-tube unit is shown in *Fig.1.1*. They comprise a tube bundle mounted in the shell. One fluid stream flows through the tubes while the other flows through the shell. The headers are usually arranged to divide the tube-side into two or more passes and a horizontal baffle may be used to divide the shell. The shell-side is usually well baffled for single-phase fluids to ensure that locally the flow is in cross-flow relative to the tubes. Many header and pass arrangements are possible depending upon the mechanical and heat transfer requirements

of the heat exchanger. The TEMA classification (TEMA, 1978) is generally used to describe shell-and-tube heat exchangers. This, and other standards (e.g. BS5500,1984) specify minimum tube diameters and spacings, however there is no intrinsic reason why very small diameter tubes should not be used. Although shell-and-tube units can be manufactured with small tubes and high surface density they are generally excluded from being described as compact heat exchangers in the literature. If used as evaporators shell-and-tube heat exchangers may be arranged for shell- or tube- side evaporation. When boiling occurs on the shell side the evaporator is said to be flooded and generally incorporates a liquid separation.

Plate Heat Exchangers

The area densities of plate heat exchangers are not necessarily compact but high heat transfer coefficients result in units which are significantly smaller than standard shell-and-tube units for similar duties. Gasketed plate heat exchangers, as shown schematically in *Fig.1.2* comprise a series of pressed, corrugated plates. The plates are assembled, separated by gaskets, in a frame and compressed. Portholes in the corners of the plates and the gaskets are arranged such that the two fluid streams flow through alternative spaces between the plates.

Gasketed plate heat exchangers were originally adapted for use as evaporators and condensers in the mid-1970's for mini-OTEC (*O*cean *T*hermal *E*nergy *C*onversion). Use of gasketed plate heat exchangers then spread to deep mine cooling, dairies, food and drink plants, ships, offshore and the process industries. The fact that gasketed plate heat exchangers can be dismantled for cleaning is a significant advantage. On the other hand, with aggressive media, the gaskets can prove troublesome.

Two relatively recent developments have made the plate heat exchanger more attractive for refrigeration applications, acting as either condenser or evaporator.

As its name suggests, the brazed plate heat exchanger comprises a series of plates vacuum brazed together at all contact points. The gasket is thus eliminated. Brazed plate heat exchangers are available as condensers, evaporators and intermediate heat exchangers for

refrigeration duties up to approximately 250kW. A brazed plate heat exchanger cannot be dismantled for mechanical cleaning.

Welded Plate heat exchangers comprise pairs of plates laser welded around the gasket groove. A series of such pairs of plates is then assembled, with gaskets between each pair and 'O' rings between the ports carrying the fluid (for example refrigerant) carried between the welded plates. The process fluid passes through passages between the pairs of plates. Welded plate heat exchangers are available for refrigeration duties up to about 8000kW.

Plate-Fin heat Exchangers

Plate-fin heat exchangers were developed almost 50 years ago for use in the cryogenics industry. They are now used widely in aircraft and defence applications and, latterly, offshore, and to a lesser extent in process applications.

A plate-fin heat exchanger comprises a series of metal sheets pressed (and sometimes cut) to form fins. Each sheet of fins is then sandwiched between parting plates with bars down each side and the assembly vacuum or salt bath brazed together. The Fins act both as secondary heat transfer surfaces and as structural members. Headers are brazed onto the cores. A significant proportion of the core volume, especially in smaller units, may be used for flow distribution rather than heat transfer.

There is a wide range of fin types available, the most common being plain, serrated, louvered and perforated. *Fig.1.3 (a)* shows a core arrangement and *Fig.1.3(b)-(d)* show typical fin structures. Other surfaces and fabrication methods are under development, for example the highly compact, diffusion bonded surface developed at NEL (Hesselgreaves, 1995) and the superplastically formed, diffusion bonded unit from Rolls-Royce (Adderly and Fowler, 1991). Different types and sizes of fin may be used for each fluid stream in the heat exchanger.

The limitations of the plate-fin heat exchanger lie principally with the widely used brazed aluminium construction. Aluminium is a poor structural material under cyclic loads and at even moderate temperatures. Stainless steel and titanium are possible replacement

materials but they are expensive, difficult to work with and have poor thermal conductivities. The latter point may be of considerable importance when a large proportion of the heat transfer area is secondary surface.

Printed Circuit Heat Exchangers

Printed Circuit Heat Exchangers (PCHEs) are constructed by diffusion bonding a stack of metal plates into which flow passages have been chemically milled. The chemical milling process is similar to that used in the fabrication of electronic printed circuit boards. Fluid headers are welded onto the blocks. Alternatively, the assembly may be encapsulated within a cylindrical pressure vessel to form, for example, a flooded evaporator.

The channels produced by chemical milling are between 0.3-1.5mm deep and approximately semi-circular in section. The area density achieved can be up to $5000m^2/m^3$.

Diffusion bonding involves compressing the stack of plates and heating them to almost their melting point. The resulting bond approaches the strength of the metal and, because no intermediate material or braze is involved, the problems associated with such materials are eliminated. It is claimed that cores may be designed to withstand 1000bar, however the headers are likely to impose a somewhat lower limit. Incidentally, the PCHE is so compact that in some configurations the headers are larger than the core. *Fig.1.4(a)* shows a typical PCHE plate and *Fig.1.4(b)* and *(c)* show a section through the core and an assembled heat exchanger, respectively.

The fluid paths may be milled to give any required flow configuration. In particular they may be shaped so that the flow is tripped from laminar to turbulent at low Reynolds number. Consequently there is a substantial gain in terms of heat transfer coefficient in single-phase applications.

The PCHE was originally developed in the early 1980s at Sydney University as part of a project to design a compact solar absorption refrigerator. In 1985 PCHEs came on to the market manufactured by Heatric, a company founded in Australia and now located in the

UK. Heatric list a considerable number of successful applications, originally in Australia including many as evaporators, condensers and intercoolers in refrigeration plant. Latterly the PCHE is gaining acceptance in many applications in the UK and elsewhere which would traditionally be the preserve of the shell-and-tube unit, both for single and two-phase duties.

1.3 BOILING AND EVAPORATION

The mechanisms involved in boiling are complex and, even in simple geometries, are not yet fully understood. However, prior to investigating the effects of confinement it is worthwhile reprising the processes involved in boiling on surfaces in an otherwise stationary fluid and boiling in relatively large tubes or channels. The situations in which boiling may occur are summarised in *Fig.1.5.* While the terms "boiling" and "evaporation" are used loosely to describe the action of converting a liquid to a vapour by the transfer of energy to the liquid at its saturation temperature it is necessary to be more precise when describing the mechanisms involved.

The distinction between pool boiling and flow boiling is analogous to that between free and forced convection in single-phase terminology. Pool boiling occurs when there is no externally imposed movement of the fluid and motion is due to natural circulation at the heated surface induced by rising vapour and, to a lesser extent, warm liquid. Flow boiling occurs when the boiling fluid flows past the heated surface under the influence of an external circulatory force, either driven by a pump or by circulation induced in a loop. Although the situation encountered when boiling in tubes or channels is clearly flow boiling it is convenient for discussion to review the phenomenon observed during pool boiling.

If a fluid is heated by a flat plate or tubular heater in a reservoir of otherwise stationary fluid at a temperature close to its saturation temperature the relationship between the heat flux at the heater surface, q, and the difference, ΔT_{sat}, between the surface and fluid

saturation temperatures is typically as shown in *Fig.1.6*. For the case of controlled heat flux the various regimes may be described:

For increasing heat flux, in the region 'A'-'B' heat transfer from the heater surface is purely by single-phase natural convection. Superheated liquid rises to the surface of the reservoir and evaporation takes place at this surface. As the heat flux is increased beyond the value at 'B' bubbles begin to form on the surface of the heater, depart from the heater surface and rise through the liquid this process is referred to as nucleate boiling. The point 'B' denotes the incipience of nucleate boiling. At this stage a reduction of heater surface temperature to 'C' may be observed. Reducing the heat flux would now result in the heat flux - temperature difference relationship following the curve 'C'-'B^*'. The difference in the heat flux - temperature difference relationship between 'B^*' and 'C' is known as boiling curve hysterisis. After the commencement of nucleate boiling further increase in heat flux leads to increased heater surface temperature to point 'D'. Further increase beyond the value at 'D' leads to vapour generation at such a rate that it impedes the flow of liquid back to the surface and transition boiling occurs between 'D' and 'E'. At 'E' a vapour film begins to form over the surface of the heater and this has the effect of an insulating layer on the heater. Initially, the film is unstable and quenching of the surface by liquid occurs, but as the surface temperature increases the film becomes stable. The result of attempting to maintain a heat flux at or above the level at 'E' would be an increase in temperature from 'E' to 'F'. The magnitude of the heat flux at 'E' is the critical heat flux. The large temperature increase which occurs if an attempt is made to maintain the heat flux above the level of the critical heat flux is frequently referred to as burn-out. However, if physical burn out does not occur it is possible to maintain boiling at point 'F' and then adjust the heat flux, the heat flux - temperature difference relationship will then follow the line 'G'-'H'. This region on the boiling curve corresponds to the stable film boiling regime. Reduction of the heat flux below the value at 'G' causes a return to the nucleate boiling regime at 'G^*'.

Clearly several relationships, defining both the extent of each region and the appropriate shape of the curve for that region, would be required to describe the entire curve. However, it is the nucleate boiling region, 'C'-'D' which is of greatest importance in this study. Many correlations describing this region of the boiling curve have been published. Additionally, the temperature difference at which nucleation first occurs, i.e. the temperature at 'C' influences the boiling regime during flow boiling and the hysterisis witnessed in the region 'B'-'B*'-'C' may also be significant during boiling in small channels.

The correlations, valid in the nucleate boiling region, which are used in this study are listed in *Table 1.1*. Rohsenow (1952), Forster and Zuber (1955), Mostinski (1963), Armstrong (1966), Stephan and Abdelsalam (1980), Cooper (1982), Cooper (1984). Typically nucleate boiling correlations are presented in one of the following forms:

$$q = a\,\Delta T_{sat}^{m} \tag{1.8(a)}$$

$$\alpha = b\,q^{n} \tag{1.8(b)}$$

$$\Delta T_{sat} = c\,q^{p} \tag{1.8(c)}$$

$$\alpha = e\Delta T_{sat}^{r} \tag{1.8(d)}$$

The exponents m,n,p,r are constant or vary only with the class of fluid, and the constants a,b,c,e are functions of fluid properties, pressure and, in the cases of Rohsenow (1955) and Cooper (1984),(1982), the nature of the boiling surface.

Equations 1.8(a)-(d) are equivalent in that each may be rearranged into any of the other forms. *Figs.1.7* and 1.8 *(a)-(c)* illustrate the correlations tabulated in *Table1.1* applied to water, R113 and R141b at atmospheric pressure and at elevated pressure.

The Yilmaz and Westwater (1980) correlation is included in *Table 1.1* because, although it is of very limited application with regard to fluid and pressure, it was derived as part of a study which included measurement of heat transfer from a cylinder in both stationary and flowing liquid. The results from the study were then used by Chen and Westwater (1984) in deriving a method appropriate for use in the design of plate-fin evaporators.

Values of a and m appropriate to *Equation 1.8(a)* from Yilmaz and Westwater (1980) and derived values of b and n which may be substituted in *Equation 1.8 (b)* are given in *Table 1.2* and their data are reproduced in *Fig 1.9.* It is clear from these results that, in the velocity range 0-6.8m/s, the heat transfer coefficient becomes a weaker function of heat flux as the velocity increases. At low heat flux the heat transfer coefficient increased with velocity, at high heat flux, above approximately 200kW/m^2 it appears that the heat transfer coefficient becomes a weak function of velocity. This form of dependence on velocity and heat flux is a common feature of flow boiling, as will be shown below.

The flow regimes encountered during flow boiling will be discussed fully in *Section 4.3.* It is, however, appropriate to describe the principal regimes observed during boiling in a vertical, relatively large tube before reviewing the calculation methods which are appropriate to heat transfer and pressure drop during in-tube boiling. *Fig 1.10* (Adapted from Collier (1981)) shows the progression from slightly subcooled liquid to superheated vapour which would be observed under evaporating conditions.

In large tubes annular flow predominates at most mass flows and correlations such as the well known Chen (1963) correlation are only strictly applicable in the annular flow regime. Chen suggests that this encompasses the quality range 1%-70%. It is therefore common to apply flow boiling correlations over a wide range of qualities and the influence of the bubbly and slug flow regimes is largely neglected. It will, however, be shown that the confined bubble regime encountered in small channels should not be neglected.

Conventionally, it is assumed that during flow boiling heat may be transferred by convection to the liquid and evaporation then occurs at the liquid vapour interfaces; this mechanism is referred to as convective evaporation or convective boiling. Additionally, nucleate boiling may occur if the wall temperature is sufficiently high to initiate nucleation. Correlations account for these two components of heat transfer in somewhat different ways. In a review of published boiling correlations Webb and Gupte (1992)

suggest that correlations may be classified into three groups: superposition, asymptotic or enhancement, depending upon the methods used to evaluate the nucleate boiling and convective evaporation components of the heat transfer. Examples of correlations used in this work are given in *Table 1.3*. Typically, the smallest diameter of tube from which data were used in the correlation is of the order of 3mm, thus use of the correlations in smaller tubes involves extrapolation. The models are described below, together with an example of a correlation based upon each of the models.

The superposition model, known also as the Chen type model after the first published and widely used application of the model, is based on addition of the nucleate (or microscopic) and the convective (or macroscopic) component of the boiling.

$$q = q_{nb} + q_{conv} \tag{1.9}$$

and, for boiling of a saturated liquid, this implies:

$$\alpha = \alpha_{nb} + \alpha_{conv} \tag{1.10}$$

The nucleate boiling component of the heat transfer is calculated using a pool boiling correlation corrected by a suppression factor, S.

$$\alpha_{nb} = S\alpha_{nbp} \tag{1.11}$$

The convective component is evaluated using the Dittus Boelter equation:

$$\alpha_l = 0.023\frac{k_l}{d_e} Re_l^{0.8} Pr^{0.4} \tag{1.12}$$

Where the Reynolds Number is the liquid only Reynolds Number based upon the liquid superficial velocity:

$$Re_l = \frac{G(1-x)d_e}{\mu_l} \tag{1.13}$$

Corrected by a factor, F.

$$\alpha_{conv} = F\alpha_l \tag{1.14}$$

The total heat transfer coefficient is then given by:

$$\alpha = S\alpha_{nbp} + F\alpha_l \tag{1.15}$$

Chen used the Forster and Zuber correlation to determine the nucleate pool boiling heat transfer coefficient. The enhancement factor was related to the reciprocal of the Martinelli

Parameter, X_{tt}, and S was correlated as a function of the effective two-phase Reynolds Number defined:

$$F = \left(\frac{Re_{tp}}{Re_l} \right)^{0.8}$$
$$\therefore Re_{tp} = F^{1.25} Re_l \tag{1.16}$$

The Martinelli Parameter is defined as the square root of the ratio of the frictional pressure gradients which would be observed if the liquid and gas flowed alone in the channel. Using the Blasius equation to determine friction factor it may be shown that:

$$X_{tt} = \left(\frac{(dp/dz)_l}{(dp/dz)_g} \right)^{0.5} = \left(\frac{1-x}{x} \right)^{0.9} \left(\frac{\rho_g}{\rho_l} \right)^{0.5} \left(\frac{\mu_l}{\mu_g} \right)^{0.1} \tag{1.17}$$

The subscript 'tt' denotes the fact that both gas and liquid flow are assumed to be turbulent.

Chen presented the $F - 1/X_{tt}$ and $S - Re_{tp}$ relationships in graphical form. Collier has suggested that suitable curve fits for Chen's data are given by (Collier 1983):

$$F = 1 \text{ for } 1/X_{tt} \leq 0.1$$
$$F = 2.35\left(\frac{1}{X_{tt}} + 0.213 \right)^{0.736} \text{ for } 1/X_{tt} > 0.1 \tag{1.18}$$
$$S = \frac{1}{1 + 2.53 \text{ x } 10^{-6} Re_{tp}^{1.17}}$$

The Chen correlation has now been superseded by, for example, Liu and Winterton (1988), but is still widely used for comparison purposes.

Asymptotic models, as defined by Webb and Gupte (1992), are similar in concept to superposition models except that the arrangement:

$$q^{n_1} = q_{nb}^{n_1} + q_{conv}^{n_1} \tag{1.19}$$

or

$$\alpha^{n_1} = \alpha_{nb}^{n_1} + \alpha_{conv}^{n_1} \tag{1.20}$$

implies that the heat transfer coefficient approaches the larger of the nucleate or convective boiling components asymptotically. The Liu and Winterton (1988) correlation is generally accepted to be one of the most reliable flow boiling correlations currently available and is of this form. Liu and Winterton calculated the nucleate boiling component using the Cooper (1984) correlation with a suppression factor and the convective component was based upon an enhancement factor and the Dittus Boelter Equation with the Reynolds Number based upon all of the flow being liquid. The use of the Cooper correlation with the implied dependence of the nucleate boiling contribution on the total heat flux is logically inconsistent since the model implies that some of the heat flux is transferred by a convective mechanism.

The enhancement and suppression factors were calculated:

$$F = \left[1 + x\,Pr_l\left(\frac{\rho_l}{\rho_g} - 1\right)\right]^{0.35} \tag{1.21}$$

$$S = \frac{1}{1 + .055 F^{0.1} Re_L^{0.16}} \tag{1.22}$$

and the correlation becomes:

$$q^2 = \left(F\alpha_L \Delta T_{sat}\right)^2 + \left(S\alpha_{nbp}\Delta T_{sat}\right)^2 \tag{1.23}$$

$$\alpha^2 = \left(F\alpha_L\right)^2 + \left(S\alpha_{nbp}\right)^2 \tag{1.24}$$

Shah (1976) proposed an Enhancement model which has been widely used. It was based upon the equation:

$$\alpha = E\alpha_l \tag{1.25}$$

where the liquid only heat transfer coefficient was determined from the Dittus Boelter equation with the liquid only Reynolds Number as defined in *Equation 1.6*. Shah proposed that the Enhancement Factor, E, should be a function of the Boiling Number, Bo, the Convection Number, Co_n, and the Froude Number, Fr. For vertical tubes and

horizontal tubes at all but the lowest flows the Enhancement Factor was found to be independent of Froude Number.

The Boiling and Convection Numbers are defined:

$$Bo = \frac{q}{G h_{fg}} \tag{1.26}$$

$$Co_n = \left(\frac{1-x}{x}\right)^{0.8} \left(\frac{\rho_g}{\rho_l}\right)^{0.5} \tag{1.27}$$

Originally Shah presented the relationship between E and Bo and Co_n graphically as the CHART correlation but later, Shah (1982), presented the equations which best fitted the CHART correlation. Four regions were identified on the Chart: nucleate boiling, bubble suppression, convective boiling (with the surface fully wet) and, for horizontal tubes at low flow rate, convective boiling with a partially dry surface. The equation to be used in determining the enhancement factor was selected to the region.

For Froude number greater than 0.04 in horizontal tubes and for all vertical tubes the equations presented were:

$$E_{cb} = 1.8 Co_n^{-0.8}$$

For $Co_n > 1$:

$$E_{nb} = 230 Bo^{0.5} \qquad (Bo > 0.3 \text{ x } 10^{-4})$$

$$E_{nb} = 1 + 46 Bo^{0.5} \qquad (Bo > 0.3 \text{ x } 10^{-4})$$

For $0.1 < Co_n \leq 1$ (1.28)

$$E_{bs} = 14.7 Bo^{0.5} \exp\left(2.74 Co_n^{-0.1}\right) \qquad (Bo \geq 11 \text{ x } 10^{-4})$$

$$E_{bs} = 15.43 Bo^{0.5} \exp\left(2.74 Co_n^{-0.1}\right) \qquad (Bo < 11 \text{ x } 10^{-4})$$

For $Co_n \leq 0.1$

$$E_{bs} = 14.7 Bo^{0.5} \exp\left(2.47 Co_n^{-0.15}\right) \qquad (Bo \geq 11 \text{ x } 10^{-4})$$

$$E_{bs} = 15.43 Bo^{0.5} \exp\left(2.47 Co_n^{-0.15}\right) \qquad (Bo < 11 \text{ x } 10^{-4})$$

The value of E to be used in *Equation 1.25* was the larger of E_{cb} and the appropriate value of either E_{nb} or E_{bs}..

The philosophy embodied in the Shah correlation implying that either nucleate or convective boiling dominates the heat transfer process and that the larger of the two values should be used has been supported by other Authors, e.g. Cooper (1989) who have proposed that the convective and nucleate boiling regimes may be distinguished by examination of data plotted on a heat transfer - quality plane. An example of one of the data sets analysed by Cooper is reproduced as *Fig. 1.11.* This shows that at low quality the heat transfer coefficient was heat flux controlled and insensitive to quality, while at higher quality (greater than 0.1 in the example shown) the heat transfer was a function of quality and independent of heat flux. Cooper proposed that the heat flux controlled region was dominated by nucleate boiling and the value of the heat transfer coefficient could be calculated from a pool boiling type correlation. The quality controlled region was assumed to be convective boiling and the heat transfer coefficient could be calculated accordingly.

The general shape of the flow boiling map thus derived is shown in *Fig. 1.12 (a).* *Fig.1.12(b)* illustrates the way in which superposition and asymptotic models represent the phenomena. *Fig.1.13(a)-(d)* illustrate the range of predicted heat transfer values for R141b in a 12mm diameter tube flowing under typical conditions for the correlations of Chen, Shah, Liu and Winterton and Kandlikar as listed in *Table1.3.* The conditions illustrated show the dependence of the predicted heat transfer coefficient on heat flux at low quality and on mass flux at higher quality. The behaviour of the four correlations is similar in the range of quality 0.2-0.8 but at low quality the predicted values differ markedly as shown in *Fig 1.13(d).* While each model can provide a satisfactory fit to the data it is regarded by some as conceptually more realistic to propose that one or other mechanism dominates rather than to attempt to combine the contribution of the two mechanisms in a transition region. Alternatively, if the flow is of an intermittent nature, it may be preferable to take what may be regarded as a time average of the heat transfer as predicted the two mechanisms.

It should be noted that the decrease in heat transfer coefficient at high quality (>0.9) predicted by the Chen, Shah and Kandlikar correlations occurs because of the presence of a term including (1-x) in the prediction of the liquid only heat transfer coefficient. This falls to zero as x approaches 1. The correlations are not, however, valid in the region where dryout occurs (i.e. at high quality); the apparent indication of reduced heat transfer coefficient under the conditions at which dryout might occur is essentially coincidental. The correlations do not predict the onset of dryout.

Examination of data in the apparently nucleate regime extracted from five sources allowed Cooper to propose the equation:

$$\alpha = 35\, p_r^{0.12} (-\log_{10} p_r)^{-0.55} M^{-0.5} q^{0.67} \qquad (1.29)$$

Equation 1.29 is of the same form as the pool boiling correlation of Cooper (1984) for unknown surface conditions (*Equation 1.7*). *Equations 1.7* and *1.29* incorporate constants of 55 and 35 respectively hence *Equation 1.29* predicts values of heat transfer coefficient some 65% of those obtained using *Equation 1.7.* The shortage of available data led Cooper to emphasise the tentative nature of his conclusion. In particular he noted that the Forster and Zuber (1955) correlation as used by Chen (1963) would produce equally good agreement with the data.

A method for calculating the heat transfer coefficient in the slug flow regime in vertical tubes has been proposed by Wadekar and Kenning (1990) and modified by Wadekar (1991). The method is based upon the weighted average of the heat transfer coefficients in the liquid slug and through the film surrounding the vapour plugs. Using the nomenclature of *Fig 1.14:*

$$\alpha = \alpha_p \left[\frac{L_p}{L_p + L_s} \right] + \alpha_s \left[\frac{L_s}{L_p + L_s} \right] \qquad (1.30)$$

Convective heat transfer to the liquid slug was calculated using the Dittus Boelter equation, with a modified Reynolds Number obtained using a notional two-phase velocity which was the sum of the liquid and vapour superficial velocities:

$$\alpha_c = 0.023 \frac{k_l}{d} Re_m^{0.8} Pr_l^{0.4} \tag{1.31}$$

$$Re_m = \frac{dG\rho_l}{\mu_l}\left[\frac{x}{\rho_g} + \frac{1-x}{\rho_l}\right] \tag{1.32}$$

This Reynolds Number allowed for enhancement due to the increased velocity of the slug resulting from the increased volume of the gas-liquid mixture but did not take into account any enhancement due to recirculation within the slug.

The vapour plug was assumed to be cylindrical and to be surrounded by a film, the thickness of which was calculated using the method of McQuillan and Whalley(1985). This involved solving the following set of equations:

$$\dot{V}_p = \left[1 - \frac{4\delta}{D}\right] u_p A_c \tag{1.33}$$

where $\dot{V}_p$ is the vapour volumetric flow rate in the plug and u_p is the absolute rise velocity of the slug calculated using the equation of Nicklin, Wilkes and Davison (1962):

$$u_p = 1.2j + 0.35\left[\frac{gd(\rho_l - \rho_g)}{\rho_l}\right]^{0.5} \tag{1.34}$$

and, from continuity:

$$\dot{V}_p = \dot{V}_f + \left(\dot{V}_g + \dot{V}_l\right) \tag{1.35}$$

Where $\dot{V}_p$, $\dot{V}_g$ and $\dot{V}_l$ represent the volumetric vapour flow rate in the plug and the total volumetric vapour and liquid flow rates, respectively, all being positive in the upwards direction. $\dot{V}_f$ represents the film flow rate, positive in the downward direction.

A relationship between liquid film thickness and film flow rate was derived:

$$\delta = \left[\frac{0.00169\, Re_f^{1.8} \mu_l^2}{g(\rho_l - \rho_g)\rho_l} \right]^{1/3} \tag{1.36}$$

with Re_f defined:

$$Re_f = \frac{4 V_l \rho_l}{\pi d \mu_l} \tag{1.37}$$

Iterative solution of *Equations 1.33* to *1.37* then gave the liquid film flow rate and film thickness. The heat transfer coefficient through the film to the plug was then calculated using the Chun and Seban (1971) correlation for heat transfer through a turbulent falling film.

$$\alpha_f = 0.0038 Re_f^{0.4} \left[\frac{g k_l \rho_l}{\mu_l^2} \right] Pr_l^{0.65} \tag{1.38}$$

Having calculated the convective slug heat transfer coefficient, α_s, and the plug film coefficient, α_f, each of these was individually compared with the nucleate boiling coefficient, α_{nb}, proposed by Cooper (1989) and presented here as *Equation 1.29.*

The slug coefficient, α_s, was then chosen as the larger of α_s and α_{nb}, similarly the plug coefficient ,α_p, was chosen as the larger of α_f and α_{nb}.

Finally the length fraction was calculated from continuity of volume:

$$\frac{L_p}{L_p + L_s} = \left[\frac{\pi d^2 v_s u_p - 4\dot{V}_g}{\pi u_p \left(d^2 v_s - (d - 2\delta)^2 \right)} \right] \tag{1.39}$$

Where u_p is the velocity of the liquid plug and v_s is the void fraction in the liquid slug.

This void fraction was taken to be 0.25.

The effective heat transfer coefficient can then be calculated from *Equation 1.30.*

The above is a summary of the methods used in the prediction of boiling heat transfer coefficients in conventionally sized tubes. It should, however, be emphasised that there is, at the current time, debate regarding relative importance of the mechanisms involved in flow boiling. Therefore any attempt to apply the available correlations to conditions other than those for which they were derived should be undertaken with caution.

1.3 PRESSURE DROP IN TWO-PHASE FLOW

It is conventional to consider the pressure drop along a passage in which a vapour-liquid mixture flows to be made up of three components, each of which can be evaluated individually using an appropriate correlation.

$$\frac{dp}{dz} = \frac{dp_f}{dz} + \frac{dp_a}{dz} + \frac{dp_h}{dz} \tag{1.40}$$

where:

$\frac{dp}{dz}$ = Pressure gradient at position z in the channel

$\frac{dp_f}{dz}$ = frictional pressure gradient at position z in the channel

$\frac{dp_a}{dz}$ = Pressure gradient due to the momentum change at position z in the channel

$\frac{dp_h}{dz}$ = Hydrostatic pressure gradient at position z in the channel

and z is the coordinate in the flow direction along the channel

In a flow involving phase change it is necessary to consider the variation in quality. To calculate the pressure drop along a channel it is necessary to integrate the expressions for the three components of pressure change over the length of the channel. In practice this may be carried out analytically or numerically by evaluating the three gradients for a number of sections along the channel, assuming a mean value of quality and physical properties in that section. Each component may be evaluated individually using one of a number of techniques. The basic processes are outlined below.

The hydrostatic pressure gradient is given by:

$$\frac{dp_h}{dz} = g \sin\theta\left[\nu\rho_g + (1-\nu)\rho_l\right] \tag{1.41}$$

Where θ is the angle of inclination of the channel, measured from the horizontal. Clearly the hydrostatic pressure gradient is zero for a horizontal channel. The void fraction, ν, may be evaluated using one of many available correlations. Five correlations which have wide applicability and have been used in the analysis in this study are presented in *Table 1.4*, together with the equation linking void fraction and quality in homogeneous flow..

The change in the static pressure due to acceleration of the fluid is calculated from:

$$\frac{dp_a}{dz} = -G^2 \frac{d}{dz}\left(\frac{x^2}{\nu\rho_g} + \frac{(1-x)^2}{(1-\nu)\rho_l}\right) \tag{1.46}$$

Which, when integrated, gives an expression for the pressure drop between 1 and 2 along the channel:

$$\Delta\rho_{a,1-2} = K_a G^2\left[\frac{x_2^2}{\nu_2\rho_{g,2}} + \frac{(1-x_2)^2}{(1-\nu_2)\rho_{1,2}} - \frac{(1-x_1)^2}{(1-\nu_1)\rho_{l,1}}\right] \tag{1.47}$$

The empirically determined constant, K_a, approximately equal to 2, is introduced to take into account the velocity profiles within the flow. As with the gravitational component, the void fraction, ν, may be evaluated using one of many available correlations.

Estimation of the friction component is somewhat more complex and various approaches have been taken. The Martinelli Parameter, defined by:

$$X^2 = \frac{(dp_F/dz)_f}{(dp_F/dz)_g} \tag{1.48}$$

is frequently used in the correlation of pressure drop data.

The Martinelli Parameter may be related to the single phase liquid pressure drop by:

$$\frac{\Delta P_{tp}}{\Delta P_c} = 1 + \frac{C}{X} + \frac{1}{X^2} \tag{1.49}$$

when the single phase pressure gradient is given by:

$$\left(\frac{dp_F}{dz}\right)_l = f\frac{2G^2}{D\rho_l}(1-x)^2 \tag{1.50}$$

For turbulent flow of both liquid and gas the Martinelli parameter is commonly calculated from:

$$X_{tt} = \left[\frac{1-x}{x}\right]^{0.9}\left[\frac{\rho_g}{\rho_l}\right]^{0.5}\left[\frac{\mu_l}{\mu_g}\right]^{0.1} \tag{1.51}$$

and the Blasius Equation friction factor is used.

$$f = 0.079\left[\frac{G(1-x)d}{\mu_l}\right]^{-0.25} \tag{1.52}$$

The value of the constant, C in *Equation 1.49* is selected from *Table 1.5*. as suggested by Chisholm (1967)

There are several other correlations available for the prediction of the frictional component of two-phase pressure drop, e.g. Chisholm (1973,2), Baroczy (1965), Friedel (1979)

An alternative approach is to use pseudo-single-phase properties and assume homogeneous flow in the evaluation of the frictional pressure gradient. The homogeneous density is given by:

$$\rho_{tp} = \frac{\rho_g\rho_l}{x\rho_l + (1-x)\rho_g} \tag{1.53}$$

The determination of an appropriate viscosity is less well established and various methods have been proposed:

$$\frac{1}{\mu_{tp}} = \frac{x}{\mu_g} + \frac{1-x}{\mu_l} \quad \text{McAdams (1942)} \tag{1.54(a)}$$

$$\mu_{tp} = x\mu_g + (1-x)\mu_l \quad \text{Chichitti (1960)} \tag{1.54(b))}$$

$$\mu_{tp} = \frac{j_l}{j}\mu_l + \frac{j_g}{j}\mu_g \quad \text{Dukler (1964)} \tag{1.54(c))}$$

The friction factor may then be calculated from a single-phase correlation, typically the Blasius Equation, *Equation 1.52*.

Beattie and Whalley (1982) give equations for effective viscosity:

$$\mu_{tp} = \mu_l(1-\beta_B)(1+2.5\beta_B) + \mu_g\beta_B \tag{1.55}$$

$$\beta_B = \frac{x\rho_{tp}}{\rho_g} \tag{1.56}$$

and suggest that these should be used with the Colebrook-White correlation for friction factor:

$$\frac{1}{\sqrt{f}} = 3.48 + 4\log_{10}\left(\frac{9.35}{Re_{tp}\sqrt{f}}\right) \tag{1.57}$$

This latter approach has been tested, amongst others including the Lockhart-Martinelli approach in small tubes by Bao et al (1994). The conclusions of this study are summarised in *Section 2.7*.

1.5 Summary

Several new manufacturing methods for the production of compact heat exchangers are being developed and the use of existing designs such as the plate and plate-fin heat exchanger is becoming more widespread in applications involving evaporation. Thermal and hydraulic design methods are sufficiently well developed for use with confidence in most conventional heat transfer equipment but cannot necessarily be applied to different geometries to narrow passages.

CHAPTER 2

LITERATURE REVIEW

2.1 INTRODUCTION

This review is limited to a discussion of published work which is of use in either providing data for evaluation of correlations or in adding to the understanding of the mechanisms involved in boiling in confined spaces.

The work discussed has been broadly categorised:

2.2. Forced flow boiling in confined spaces

2.3. Natural circulation boiling in confined spaces

2.4. Evaporation in compact heat exchangers

2.5. Microlayer formation.

2.6. Boiling in liquid metals and heat-pipe thermosyphons

Work relating to flow patterns and regimes might be classified in this way, but, since the determination of flow regime is of fundamental importance in the analysis of boiling in narrow channels, the literature covering flow regimes is discussed separately and is covered in *Section 4.3*.

Forced flow boiling involves evaporation of a liquid in a channel with the flow induced by an external driving system. Importantly, it is usual for reports of flow boiling studies to include measurements of mass flow and vapour quality. Natural circulation boiling occurs when the external driving force is provided by a hydrostatic head of liquid and flow through the channel is caused by the difference between this hydrostatic head and the lower hydrostatic head in the channel which contains a mixture of liquid and vapour. The mechanisms involved in forced flow and natural convection boiling are similar, they are differentiated by the control and measurement of the fluid flow rate. In natural circulation boiling the fluid flow rate is uncontrolled and not measured directly, although it is possible to estimate the flow from the known driving pressure and the heat flux.

Fig.2.1 shows a typical natural convection boiling configuration. Some workers have, using this arrangement investigated the effects of channel inclination and the edge conditions. The condition of sides closed and top and base open most closely reflects the flow boiling situation and is therefore of most interest here. The arrangement of sides and base closed is analogous to the situation found in a closed thermosyphon and some studies of such devices are included in this review.

Data are available in the literature covering boiling in compact heat exchangers. Much of this data relates to channels having Confinement Numbers less than 0.5 and to serrated channels, however, it is appropriate that this work be summarised here. It will be shown in *Section 4.2* that the influence of confinement will become significant at Confinement Numbers in excess of 0.5. *Table 0.1* lists the dimension at which the Confinement Number is equal to 0.5 for a range of fluids. It can be seen that the boiling of cryogenic fluids in compact heat exchangers is likely to fall outside the confined range whereas the effect of confinement is likely to be significant for liquid metals in relatively large tubes.

It must be emphasised that the classifications described above are introduced for convenience and there is considerable overlap between classifications in many papers.

Boiling in narrow channels has been investigated by workers wishing to obtain correlations for use in compact heat transfer systems and by those with an interest in specific situations. Bankoff and Rehm (1980), for example, worked with narrow annular channels simulating the annulus formed by a tube passing through a heat exchanger tube support plate. Much of the work on natural circulation boiling in confined spaces has been motivated by a requirement for data for use in the design of ebulliently cooled electronic systems.

2.2 FLOW BOILING

Relatively few workers have studied forced flow boiling in confined spaces or small tubes. As discussed in *Chapter 1* commonly used boiling correlations are based largely upon data obtained from experiments with tubes of 10mm diameter and larger with a few data sources covering tubes of 3-10mm diameter included.

The results of work covering small tubes and channels are summarised in *Table 2.1*. The work of Lazarek and Black (1980), Wambsganns et al (1993) and Tran et al (1993) are all applicable to Confinement Numbers of approximately 0.35, hence, according to the analysis of *Section 4.2* , they fall somewhat outside the definition of a narrow channel. Bankoff and Rehm (1980) and Moriyama and Inoue (1992) worked with very much smaller gaps having Confinement Numbers of the order of 10 and above. There is therefore a considerable range of confinement, including much of the range of interest to the compact heat exchanger designer, which is not covered.

Flow boiling of R113 in up flow and down flow in a vertical 3.15mm diameter tube was studied by Lazarek and Black (1982) and a correlation proposed:

$$Nu = 30\,Re^{0.857}\,Bo^{0.714} \tag{2.1}$$

This may be rearranged:

$$Nu = C\left(\frac{qd_e}{h_{fg}\mu_l}\right)^{0.714}\left(\frac{Gd_e}{\mu_l}\right)^{0.143} \tag{2.2}$$

The first group is a two-phase Reynolds number where the mass flow rate is essentially the vapour flow away from the surface, q/h_{fg} . This group to the power 0.67 has been used successfully for correlating pool boiling on tubes by Cornwell Schuller and Einarsson (1982) and the exponent of 0.714 associated with q is within the range typical of nucleate pool boiling correlations. The second group indicates a slight but positive effect of G on the heat transfer. The low value of the exponent associated with G

suggests that data sets which do not include G, such as those associated with natural circulation boiling, can still be applied to boiling in narrow channels.

Since the Lazarek and Black correlation was derived for a single fluid and tube diameter, it must be viewed with some caution. Wambsganns et al (1993) also worked with R113 in a horizontal tube of a similar size (2.9mm diameter) and compared their measured heat transfer coefficients with those of ten published correlations. The results of their comparison with correlations used in this study are summarised in *Table 2.2.*

Both Lazarek and Black and Wambsganss et al observed that the heat transfer was dominated by nucleate boiling throughout the experimental range. This was deduced from the fact that the heat transfer coefficient was found to be independent of quality and a weak function of mass flow rate. Rearrangement of *Equation (2.1)* gives:

$$\alpha = [\text{Fluid property dependent constant }] \text{ x } \left(\frac{G}{d}\right)^{0.143} q^{0.714} \qquad (2.3)$$

Wambsganss et al noted that those correlations which included a substantial convective component under the conditions of interest performed poorly when compared to their experimental data. The Stephan and Abdelsalam (1980) correlation is a pool boiling correlation, while Liu and Winterton, Shah and Chen were all derived for flow boiling conditions.

A subsequent study by Tran Wambsganss and France (1993) was concerned with R12 flowing in a rectangular channel 1.7mm x 4.06mm. In this case they found that the majority of correlations tested significantly under predicted the heat transfer coefficient, the exceptions, which over predicted the results, were Chen (1963) and Steiner and Taborek (1992). The results of this work confirmed that nucleate boiling dominated the heat transfer for all of the conditions examined. Neither mass flow rate nor quality had a large effect on measured heat transfer coefficient over most of the range. It was, however, observed that the heat transfer coefficient was substantially higher at low

qualities, showing a sharp decrease between x=0 and x=0.1, thereafter remaining constant. This is a trend which is exhibited by the Kandlikar (1990) correlation.

Tran, Wambsganss and France (1993) concluded that the heat transfer in a rectangular channel was higher than that predicted by nucleate boiling correlations because of surface tension effects drawing the liquid into the corners and thus thinning the remaining liquid film on the walls. The enhancement of nucleate boiling in thin layers has been observed by several authors, for example Turmeau (1971) and Mesler (1977). The dominance of nucleate boiling suggested that the results could best be correlated by an equation of the form:

$$\alpha = C_1 q^{c_2} \tag{2.4}$$

with both C_1 and C_2 being functions of geometry, fluid properties, mass flow rate and quality. This equation is otherwise identical to *Equation 1.8(b)*

Recent work by Tran and Wambsganss and France (1995) includes the previously reported conclusions together with experimental results obtained with R-134a in a tube 2.46mm diameter. From all the data it was confirmed that nucleation dominated the boiling process for wall superheats above ≈2.75K. It was also noted that the transition from convection to nucleation dominated boiling was abrupt. The insensitivity of the measured heat transfer coefficient to mass flux was confirmed and *Equation 2.1* derived by Lazarek and Black(1982) for R113 only was modified by replacement of the Reynolds Number by a Weber Number and inclusion of the liquid to vapour density ratio to account for fluid property variations. These substitutions eliminated all dependence upon mass flux and viscosity and bring in the effects of surface tension.

The correlation thus derived is:

$$\alpha = 840\left(Bo^2 We_l\right)^{0.3}\left(\frac{\rho_l}{\rho_g}\right)^{-0.4} \text{ kW / m}^2\text{K} \tag{2.5}$$

$$We_l = \frac{G^2 d}{\rho_l \sigma} \tag{2.6}$$

It is of interest to note that the inclusion of the Weber Number to the power 0.3 leads to a dependence of the constant C_1 in *Equation 2.4* above on $d^{0.3}$, i.e.

$$\alpha \propto d^{0.3}$$

This implies that the heat transfer coefficient would decrease with increasing confinement. The nucleate boiling exponent of 0.6 is within the range which is typical of nucleate pool boiling correlations.

Tran Wambsganss and France (1995) observed that flow boiling correlations derived from large tube data tended to under-predict the heat transfer coefficient when applied to the small tubes tested in their study.

In contrast to the above conclusions regarding the predominance of nucleate boiling, Bankoff and Rehm (1980) found that convection through a thin film dominated the heat transfer to water boiling in a narrow annulus. As a result of this work they suggested that the Chen correlation should be modified for use in such channels. The nucleate boiling component was calculated using the Forster and Zuber correlation and the Chen value of suppression factor was employed. The convective component was calculated using the Dittus-Boelter equation and a modified Chen F factor accounted for enhancement. F_{Chen} was calculated according to *Equation (1.18)* and $F_{Bankoff}$ was then obtained from:

$$F_{Bankoff} = C_1 C_2 F_{Chen} \tag{2.8}$$

C_1 was referred to as a non-dimensional length and expressed as a function of the confinement Number, Reynolds Number and Martinelli Parameter. However, for a gap of greater than 0.203mm C_1 was set equal to unity. C_2 was calculated from the Confinement Number:

$$C_2 = \left(1 + \operatorname{csch}\left(Co^{-1}\right)\right) \tag{2.8}$$

C_2 asymptotically approaches unity as the Confinement Number decreases, and reduces to 1.01 for a gap of 6.35mm.

The model proposed by Moriyama and Inoue (1992,1) was based upon the flow in a small channel being divided into three regimes: single-phase, slug flow and film flow. Slug and film flow correspond to the confined bubble and annular regimes defined in *Chapter 4*. Their flow regime model was developed from observation of adiabatic flow of R113 and nitrogen in a horizontal channel 30mm wide x 265mm long and 0.007-0.01mm thick.). Heat transfer measurements were carried out (Moriyama and Inoue (1992,2)) using R113 in a similar test channel with a thickness of 0.035-0.110mm.

Heat transfer results were presented as the ratio of the measured, two-phase heat transfer coefficient and the single-phase liquid heat transfer coefficient. The single-phase liquid heat transfer coefficient was calculated from:

$$\alpha_{LO} = 2.43\frac{k}{s} \tag{2.9}$$

based upon the assumption that the flow of liquid alone would be laminar.

In the two-phase region heat transfer to the vapour was assumed to be by conduction through and evaporation of the liquid film between the vapour and the wall. The film thickness was determined by one of two methods.

In the Confined Bubble region (defined in *Section 4.3*) the thickness of the liquid layer between wall and confined bubble was determined according to the method of Taylor (1961) and developed by Park and Homsy (1984).

$$\frac{\delta}{s} = \xi\, Ca^{\zeta} \tag{2.10}$$

where Ca is the Capillary Number, defined by:

$$Ca = \frac{j_t \mu_l}{\sigma} \tag{2.11}$$

and the constants were evaluated from:

$$0 < Ca \le 0.09 \qquad \xi = 0.25 \qquad \zeta = 0.50$$
$$0.09 < Ca \le 0.49 \qquad \xi = 0.14 \qquad \zeta = 0.27$$
$$0.49 < Ca \le 2 \qquad \xi = 0.13 \qquad \zeta = 0.12$$

The area fraction of the bubbles was obtained from the adiabatic study and correlated by:

$$\nu' = 5.7 \frac{j_g}{j_t}\left[\frac{\rho_L \sigma s}{\mu_l^2}\right]^{0.17} \tag{2.12}$$

and the heat transfer coefficient was then calculated from:

$$\alpha = \nu' \frac{k_l}{\delta} + (1-\nu')2.43\frac{k_l}{s} \tag{2.13}$$

A combined force and mass balance was used to estimate the liquid film thickness in the annular flow regime yielding:

$$C\mu_g^n \rho_g^{1-n}\left(\frac{s}{\delta}\right)^n \left\{\frac{\delta}{s}\left(3-\frac{2\delta}{s}\right)j_g - 3\left(1-\frac{2\delta}{s}\right)\left(1-\frac{\delta}{s}\right)j_l\right\}^{2-n} - 6 \text{ x } 2^n \mu_l j_l \left(1-\frac{2\delta}{s}\right)^n \left(3-\frac{2\delta}{s}\right)^{1-n} = 0$$

(2.14)

The constants C and n were assigned values depending on whether the vapour flow was laminar or turbulent:

$$Re_g < 2042 \qquad C = 24 \qquad n = 1$$
$$Re_g \geq 2042 \qquad C = 0.079 \quad n = 0.25$$

In the annular flow regime the heat transfer coefficient was then calculated from:

$$\alpha = \frac{k_l}{\delta} \tag{2.15}$$

Transition from confined bubble to annular flow was assumed to occur at the point where the film thickness calculated from *Equation 2.14* was equal to that determined using *Equation 2.10.*

The philosophy underpinning the model of Moriyama and Inoue appears to have general applicability however care must be taken in applying it to intermediate sized channels. The implicit assumption that the liquid film is thin and laminar may not hold for channels of 1mm-3mm (i.e. larger by a factor of up to 30 than the largest gap tested by Moriyama and Inoue). Hewitt and Hall-Taylor (1970) have described the heat transfer across the liquid film for laminar and turbulent film flow and present a graphical relationship between the film Nusselt Number defined:

$$Nu_F = \frac{\alpha \delta}{k_f} \tag{2.16}$$

and the Dimensionless Mass Flow Rate in the film, W^+, defined by *Equation 2.17* below, and the liquid Prandtl Number. Their graph is reproduced here as *Fig. 2.2.*

For the case of Film Nusselt Number being equal to unity the heat transfer coefficient would be given by *Equation 2.16*. Values of Film Nusselt Number in excess of one suggest that heat transfer due to turbulence in the film is significant. The Dimensionless Mass Flow Rate was defined:

$$W^{+} = \frac{\dot{m}_F}{\pi d \mu_f} \equiv 4 Re_F \qquad (2.17)$$

Film models have not been widely used in the prediction of heat transfer coefficients for large tubes. Since it is necessary to determine the film thickness, usually using an empirical approach, prior to evaluating the heat transfer coefficient it is preferable to use an empirical heat transfer correlation directly. However, Robertson (1982) demonstrated that the film flow model could be applied in compact heat exchangers. Robertson tested a representative plate-fin section. The test section was 3.4m long and 76mm wide with serrated fins 6.35mm high and 0.2mm thick and with 590 fins per metre, the serrations were 6.35mm long. Tests were carried out with nitrogen and R11 to represent cryogenic and hydrocarbon fluids respectively. A range of low heat fluxes, up to 4kW/m^2 , and mass fluxes from 15-150 kg/m^{2}s were covered by the tests. Film thickness was calculated by applying a force balance over the film using the measured local two-phase pressure gradient. After application of a correction to allow for the entrainment of droplets in the vapour flow it was shown that the film Nusselt Number was a function of the Dimensionless Mass Flow Rate and the relationship was close to that given by Hewitt and Hall-Taylor (1970).

Robertson suggests that the film flow model is appropriate for use in the small passages typical of plate-fin heat exchangers "particularly those which do not contain interrupted finning".

2.3 NATURAL CIRCULATION BOILING IN CONFINED SPACES

Several workers have reported data covering natural convection boiling in confined spaces. The use of such data for development of flow boiling correlations is limited because the mass flow rate through the space is unknown. The mass flow may, however, be estimated by balancing the calculated two-phase pressure drop through the test section and the available hydrostatic pressure due to the surrounding fluid. This method was originally proposed by Sydoriak and Roberts (1957) for natural convective boiling in small channels and is commonly used to estimate the recirculating flow rate in boilers. It has been developed by Bar-Cohen and Schweitzer (1985) and Fujita and Uchida (1990). The estimation of the natural convection mass flow rate through the channel involves equating the hydrostatic pressure difference in the liquid outside the boiling space with the sum of the gravitational, accelerational, and frictional pressure drops in the fluid flowing through the gap.

Integrating *Equation 1.40* gives:

$$\Delta p_H = \Delta p_g + \Delta p_a + \Delta p_f \tag{2.18}$$

where Δp_H is the pressure difference between the bottom and top of the test section due to the hydrostatic head of the liquid surrounding the test section and Δp_g is the gravitational pressure drop in the test section containing a two-phase vapour liquid mixture.

The method of computing each of the pressure drop components is reviewed in outline in *Section 1.3*. The correlations resulting from work on natural circulation boiling are summarised in *Table 2.3*

Sydoriak and Roberts (1957) were concerned with burn-out in electromagnets cooled with liquid nitrogen or hydrogen, and, neglecting frictional effects, determined that the heat input and exit dryness fraction were related but no relationship between heat flux and temperature difference was examined.

The methods of estimating pressure drop used by Schweitzer (1983) as summarised by Bar-Cohen and Schweitzer (1985) and Fujita and Uchida (1990) differ in the assumptions made. Schweitzer assumed that the slip ratio was invariant along the channel length and the wall shear stress was dependent only upon the liquid properties. It was also assumed that there was an additional loss at inlet to the test section given by:

$$\Delta p_{inlet} = 0.65\frac{\rho_l u^2}{2g} \tag{2.19}$$

Equation 2.18 then becomes:

$$\begin{aligned}\Delta p_H - \Delta p_{inlet} = {} & \frac{2C_{fr}}{d_e\rho_l}\frac{\left(1+\left(A_s-1\right)x_e\right)}{3\left(A_s-1\right)\frac{x_e}{L}}+\frac{G^2x_e}{\rho_l}\left[\left(S_r-1\right)\left(A_s-1\right)x_e+\left(A_s-1\right)+\left(S_r-1\right)\right] \\ & +\frac{g\left(\rho_l-\rho_g\right)A_s\frac{L}{x_e}}{\left(1-A_s\right)^2}\ln\left[\left(\left(A_s-1\right)x_e+1\right)\right]+\rho_l gL-\frac{\rho_l-\rho_g}{\left(1-A_s\right)}gL\end{aligned} \tag{2.20}$$

Where $\bar{A_s} = \rho_l/S_r\rho_g$.

Heat transfer data from the study were correlated using a superposition model. The nucleate boiling component, α_{nb}, was evaluated using the Rohsenow correlation (*Equation 1.1*) with a suppression factor of unity. The Dittus Boelter correlation with a two-phase flow Reynolds Number as defined by *Equation 2.21* was used in evaluating the convective component.

$$\dot{R}e_{tp} = G\left(x\frac{v_{fg}}{v_l}+1\right)\left(\frac{d_e}{\mu_{fl}}\right) \tag{2.21}$$

The mass flux G being calculated from the pressure balance across the test section given here as *Equation 2.20*.

Integrating the Dittus Boelter Equation along the length of the channel with this Reynolds Number and noting that, for the conditions of interest:

$$\frac{2qz}{Gsh_{fg}}\left(\frac{v_{fg}}{v_f}\right) >> 1$$

gave the height averaged convective heat transfer coefficient:

$$\overline{\alpha}_c = 0.0064\frac{k_l}{s}Pr_l^{0.4}\left(\frac{K_h\, qLv_{fg}}{\mu_l\, h_{fg}\, v_l}\right)^{0.8} \qquad (2.22)$$

The value of the constant K_h was either 4 or 2 for symmetric heating and heating on one side of the space only respectively. The convective heat transfer coefficient was then multiplied by a factor, correlated with a group which may be arranged to give the Confinement Number:

$$F_{B-CS} = .022\,Co\,x_e^{-0.533} \qquad (2.23)$$

Finally the heat transfer coefficient was obtained by combining *Equations 2.22* and *2.23* and adding the nucleate boiling contribution :

$$\overline{\alpha} = 0.022\,Co\,\overline{\alpha}_c x_e^{-0.533} + \alpha_{nb} \qquad (2.24)$$

Equations 2.21-2.24 must be solved iteratively since the convective heat transfer coefficient, given by *Equation 2.22* is dependent upon the heat flux. Although the authors asserted that the convective heat transfer coefficient was independent of mass flux it should be noted that *Equation 2.23* shows that the enhancement factor is proportional to $x_e^{-0.533}$ and, for a given heat flux and geometry x_e is inversely proportional to mass flux.

Fuchita and Uchida did not correlate their heat transfer data but presented it graphically as heat flux against ΔT for a range of peripheral conditions and surface inclinations for gap sizes of 0.15-5mm. Data for the vertical heater with closed sides are replotted here as *Fig 2.3*. Fuchita and Uchida equated the pressure drop through the channel with the gravitational head outside the channel and used this to predict critical heat flux by determining the condition at which the quality of the fluid at outlet was unity. The pressure drop in the channels was determined from:

$$-\frac{dp}{dz} = \frac{g\sin\theta}{v_l + x\left(v_g - v_l\right)} + 4\frac{\tau_w}{d_e} + G^2\left(v_g - v_l\right)\frac{dx}{dz} \tag{2.25}$$

The terms on the right of *Equation 2.25* represent frictional, hydrostatic and acceleration pressure gradients respectively. Implicit in the equation is the assumption of homogeneous flow.

The wall shear stress, τ_w, was determined using a friction factor calculated from the Blasius Equation, *Equation 2.27*.

$$\tau_w = \frac{1}{2}C_{fr}G^2 v_l \tag{2.26}$$

$$C_{fr} = \frac{0.079}{\left(Re_l\right)^{0.25}} \tag{2.27}$$

The mean viscosity used in the calculation of the Reynolds Number was defined by:

$$\frac{1}{\mu_m} = \frac{x}{\mu_g} + \frac{(1-x)}{\mu_l} \tag{2.28}$$

Combining *Equations 2.25 -2.28* and integrating over the length of the test section, noting that, for uniform heat flux:

$$x = x_e \frac{z}{L} \tag{2.29}$$

gave the Equation relating the heat flux to the flow rate through the test section and the exit quality:

$$\rho_l g L \sin\theta = \frac{g L \sin\theta}{x_e\left(\nu_g - \nu_l\right)} \ln\left(1 + x_e \frac{\left(\nu_g - \nu_l\right)}{\nu_l}\right) + \frac{0.6324 G^{\frac{7}{4}} (\mu_l \mu_g)^{\frac{1}{4}} L}{3 D^{\frac{5}{4}} (\mu_l - \mu_g)}$$
$$x\left\{\frac{1}{x_e}\left(\left((1-x_e)\mu_g + x_e\mu_l\right)^{\frac{3}{4}}\left((1-x_e)\nu_l + x_e\nu_g\right) - \mu_g{}^{\frac{3}{4}}\nu_l\right) - \frac{4\left(\nu_g - \nu_l\right)}{x_e(\mu_l - \mu_g)}\left(\left((1-x_e)\mu_g + x_e\mu_l\right)^{\frac{7}{4}}\right)\right\}$$
$$+ G^2\left(\nu_g - \nu_l\right)x_e \tag{2.30}$$

Based on the assumptions that were made by Bar-Cohen and Schweitzer (1985) and Fujita and Uchida (1990) , the flow rate and exit quality predicted using *Equations 2.19-2.20* and *2.30* respectively have been calculated for the geometry used by Bar-Cohen and Schweitzer. The results of these calculations are presented in *Figs.2.4-2.7. Fig.2.5* shows that solution of *Equation 2.30* results in an extremely rapid rise of the predicted value of exit quality as the maximum heat flux is approached. This is indicated by the vertical arrows. It can be seen that both equations would lead to predictions of maximum heat flux (occurring when the quality reaches unity) which are of the same order of magnitude. The method of Fujita and Uchida yields a prediction some 2-3 times that of Bar-Cohen and Schweizer. However, the predicted flow rates and qualities at lower heat fluxes diverge markedly. The mass flow rate predicted from *Equation 2.20* reaches a peak at a relatively low heat flux and then decreases, as illustrated in *Fig. 2.4,* decreasing very rapidly as the critical heat flux is approached. The variation of exit quality with heat flux is shown as *Fig 2.5* increases slowly with heat flux and then rises rapidly at the maximum heat flux. Solution of *Equation 2.30,* illustrated in *Figs 2.6* and *2.7* shows that the mass flux would be expected to increase slowly with heat flux and that the quality would vary almost linearly with heat flux. The difference in the behaviour predicted by

the two approaches outlined is indicative of the uncertainties involved in predicting the pressure drop through the channels.

Monde, Kusada and Uehara (1982) report decreasing critical heat flux with increasing values of the ratio (channel length/spacing), confirming the principle that CHF occurs due to insufficient liquid flow through the test section. CHF was observed to occur when a dry patch appeared on the upper portion of the heated plate and then spread downward to the entrance of the channel. As discussed above, both Fujita Bar-Cohen and Schweitzer (1985) and Fujita and Uchida (1990) suggest that CHF occurs when the quality of the fluid leaving the channel is very close to unity. However, Katsuta and Nagata (1992) have shown that, for a partially submerged, narrow vertical channel the heat transfer coefficient increases with void fraction to a maximum at a void fraction of between 0.8 and 0.9 and then decreases rapidly with further increase in void fraction. This indicates that the maximum heat transfer coefficient occurred at a dryness fraction of the order of 0.1, considerably below that at which it would normally be expected that dry out would occur. This observation is consistent with the prediction of Bar-Cohen and Schweitzer since this suggests that the increase in quality with heat flux is extremely rapid once the quality approaches 0.1 implying that a small increase in heat flux would lead to dry-out.

The observation made by the Author in *Section 4.5*, using an analysis of a growing, confined bubble that the slope of the boiling curve would be expected to decrease with decreasing gap size contradicts other studies of confined boiling (e.g., Ishibashi and Nishikawa, 1969) in which it is asserted that the slope of the boiling curve was constant. It is however supported by the correlation of Xia et al (1992), both of these works are reviewed below.

The experiments of Ishibashi and Nishikawa (1969) working with water and other fluids at various pressures boiling in the annulus formed between an electrically heated cylinder and a glass tube permitted flow visualisation and measurement of the effect of

confinement on heat transfer coefficient. Their visualisation studies demonstrated the presence of three flow regimes which they referred to as the Isolated Bubble region, the Coalesced Bubble region and the Liquid Deficient region. From the description given the Coalesced Bubble regime is apparently equivalent to the Confined Bubble regime as defined in *Section 4.3.* A sample of their results for heat transfer to water at atmospheric pressure is presented as *Fig.4.1.* The results were in agreement with those of Chernobyls'kii and Tananaiko (1956) It was concluded that, in the Isolated Bubble region, the heat transfer coefficient, annular gap and heat flux could be related:

$$\alpha \propto q^{\frac{2}{3}} \Delta R^{-0.13} \tag{2.31}$$

while the relationship became:

$$\alpha \propto q^{\frac{3}{4}} \Delta R^{-\frac{3}{4}} \tag{2.32}$$

in the coalesced bubble region. The transition between the two regions occurred at 3mm at atmospheric pressure. This transition corresponds to a Confinement Number of 0.4, based on the equivalent diameter of the annular gap. With increased pressure the transition occurred at a smaller gap size, although the change in Confinement Number with pressure is minimal, the presence of Isolated Bubbles at high values of Confinement Number suggests that the transition is also a function of the volume of vapour generated.

A correlation was proposed for the coalesced bubble region, based on the results with water at atmospheric pressure:

$$Nu = 13.6\left(Re^{*\frac{1}{2}}\right)^{\frac{2}{3}} \tag{2.33}$$

where

$$Re^{*\frac{1}{2}} = \left[\frac{q}{h_{fg}\rho_g}\frac{\Delta R}{\upsilon}\right]^{\frac{1}{2}}\left[\frac{q}{M^2 P}\right]^{\frac{1}{2}} \tag{2.34}$$

M and P being constants having the dimensions m^{-1} and W respectively.

It was noted that this correlation applied only in the coalesced bubble regime and was not applicable in the liquid deficient region or approaching burn-out. A more widely applicable correlation was preferred. This was based upon the frequency of emission of coalesced bubbles and assuming that the main mechanism of heat transfer was transient conduction to liquid which entered the space instantaneously after the rapid nucleation, growth and expulsion of a coalesced bubble.

$$Nu = 4.00\,Fo_{(1)}^{-\frac{2}{3}}\,Pr^{-0.267} \quad \text{(for water at 1.013 bar)}$$

$$Nu = 200\,Fo_{(1)}^{-\frac{2}{3}}\,Pr^{-\frac{2}{3}}\left(\frac{\rho_f}{\rho_g}\right)^{1.085} \quad \text{(for all fluids)} \tag{2.35}$$

$$Fo_{(1)} = \frac{a}{N_{(1)}\Delta R^2} \tag{2.36}$$

and $N_{(1)}$ was the bubble emission frequency measured at the lower end of the heated section. If this was not measured it could be determined for the coalesced bubble region away from partial dry-out by use of the relationship:

$$N_{(1)} = 1.365 \text{ x } 10^{-9}\, q\Delta R^{-\frac{2}{3}}\, Pr^{1.627}\left(\frac{\rho_f}{\rho_g}\right)^{1.085} \tag{2.37}$$

An analytical approach based on the transient conduction model with a 30% contribution due to latent heat transport and convection fitted the above correlations.

Monde, Kusada and Uehara (1982) presented data for boiling in channels immersed in various fluids, including water. The channel considered had a width of 10mm and spacings between heater and cover plate of between 0.45mm and 7.0mm, the vertical length of channel was considered as a variable. Lengths of 20, 35 and 50mm were tested. There was only a weak tendency for the heat transfer coefficient to increase as the spacing decreases. It should be noted that the data of Fujita and Uchida only shows weak enhancement at the relatively high heat fluxes reported by Monde et al.

Yao and Chang (1983) studied boiling heat transfer in the confined, annular space around a vertical, heated tube surrounded by a quartz cylinder. The annulus was closed at the bottom and open at the top. The assembly was immersed in a pool of fluid. Tests were carried out with water, acetone and R113. Results were compared with the data of Yilmaz and Westwater (1980). The authors noted that the boiling curve for an open vertical tube was parallel to that obtained by Yilmaz and Westwater with a horizontal tube. It was observed that heat transfer was enhanced at low heat flux when the annular gap width was such that the Bond Number was less than unity. The significance of this is discussed in *Section 4.2*. At higher heat fluxes "near dry-out" was observed. The level of the heat flux at which near dry-out occurred was, for a given gap, higher in the shorter tube than the longer tubes.

The correlation of Xia et al (1992) was derived from experiments using a heated plate and adiabatic cover immersed in with R113 and with various boundary conditions. It was observed that the heat flux required for incipient boiling was reduced as gap size reduced, presumably due to natural single phase convection being inhibited. All experimental data were fitted into a quasi-dimensionless equation which was quoted as:

$$\frac{q/h_{fg}\rho_g}{\left(\sigma g(\rho_l-\rho_g)/\rho_g^2\right)^{0.25}} = 76.56\left(\frac{\rho_l c_{pf}\Delta T_{sat}}{h_{fg}\rho_g}\right)^{2.07+666(Ls)} Co^{0.21}Pr_l^{0.3} \qquad (2.38)$$

Since *Equation 2.38* was derived for a single fluid the dependence on fluid properties must be questionable, however it is of interest to note that reducing the equation to the form:

$$q = \text{Constant x } s^{-0.4}\Delta T^{2.07+666Ls} \qquad (2.39)$$

This suggests that the variation in the heat transfer coefficient with q or ΔT will decrease with increasing confinement.

2.4 EVAPORATION IN COMPACT HEAT EXCHANGERS

The use of compact and plate heat exchangers is becoming more widespread, but, until comparatively recently, their use has been confined to specialised applications. Plate heat exchangers are now used routinely as evaporators in refrigeration applications and in food the processing industry. However the design philosophy used is largely proprietary and is only available to the heat exchanger manufacturer. Similarly the utilisation of plate-fin heat exchangers is expanding but established, generally applicable design procedures are not available in the open literature. Novel heat exchanger types, such as the Printed Circuit Heat Exchanger and the Super-Plastic Formed Heat Exchanger are also making headway in the market.

The published literature covering evaporation in compact heat exchangers comprises mainly reports of experiments with a limited range of fluids and test geometries, hence, the results are not necessarily applicable to other fluids or situations. Reviews of this published work are available (e.g. Westwater 1983, Carey and Shah 1988, and Thome 1990). These conclude that no generally applicable correlations or design procedures are available for use with compact heat exchangers.

Table 2.4 summarises the correlations and design methods which are available in the literature. The early studies are of extremely limited use, giving order of magnitude values for heat transfer coefficient for specific applications. The recommended coefficients of Lenfestey (1961) and Clark and Thorgood(1971) were regarded as the best available design tools at the time. A similar approach is probably used by many manufacturers today in the selection of plate heat exchangers for refrigeration and food processing.

The work of Sydoriak and Roberts (1957), mentioned in *Section 2.3*, produced a correlation derived from work on channels typical of those used in the cooling of electro-magnets with boiling nitrogen coolant. This semi-theoretical analysis related the pressure drop and flow rate in the channels and hence determined the rate of heat removal

corresponding to dry-out at exit of the channels for a given pressure drop. This correlation is thus equivalent to the burn-out correlations of Bar-Cohen and Schweitzer (1985) and Fujita and Uchida (1990) and gives no indication of the heat transfer coefficients expected.

Galezha et al (1976) presented a correlation based on experiments over a range of pressures with R12 and R22 as working fluids. Five plate-fin geometries were tested in a natural circulation loop. The mass flow rate and mass flux were not measured but were always low (the mass flux was less than 16kg/m^{2}s); it was observed that the mass flux had no effect on the heat transfer coefficient. The measured heat transfer coefficient was the mean over the length of the test section and was correlated by an equation of the form.

$$\overline{\alpha} = C\, f(p_{cr}, p, T_{cr})\, q^{\frac{1}{3}} \tag{2.40}$$

The factor C being a function of geometry. The correlation cannot be used in design since no theoretical or empirical method of determining C is available without recourse to experiment with a particular geometry. *Equation 2.40* does, however serve to indicate that the heat transfer coefficient at low mass flux in compact heat exchanger geometries is likely to be proportional to the heat flux to a low power (approximately 1/3) rather than the power of 0.5-0.7 typical of pool boiling correlations.

Robertson and co-workers have been largely concerned with cryogenic applications but have also published results of experiments using boiling hydrocarbons and refrigerants. Robertson (1982) has suggested that a film flow model based on conduction and convection through a film laid down on the fins is appropriate for use with serrated fin plate fin heat exchangers. Robertson calculated a liquid film thickness using a force balance on a fluid element and a measured pressure gradient.

At low film Reynolds Numbers the film Nusselt Number, defined by:

$$Nu_f = \frac{\alpha \delta_f}{k} \tag{2.41}$$

was found to be equal to unity, indicating that the heat transfer was purely by conduction through the liquid film. At film Reynolds Numbers in excess of 300 the film Nusselt Number was found to be proportional to the Reynolds Number to a power of approximately 0.8, suggesting turbulent flow in the film.

Young, Lorenz and Panchal (1980) have developed a similar model with data obtained with boiling ammonia. Carey (1985) further developed the film flow model to account for the apparently high values of heat transfer coefficient predicted at low vapour qualities. This was explained by the influence of bubbles held by surface tension in the smallest channel sections. High heat transfer coefficients at low quality in a perforated fin test section were partially accounted for by Wadekar (1992) using the slug flow model of Wadekar and Kenning (1990) and Wadekar (1991). Wadekar (1992) suggested that for correlations of the form:

$$\alpha = F\alpha_l \tag{2.42}$$

the liquid heat transfer coefficient, α_l, should be estimated using a correlation appropriate for turbulent flow, even if the Reynolds Number indicated Laminar Flow. This approach eliminated the discontinuity which was otherwise apparent in measured F values at the Reynolds Number corresponding to transition from laminar to turbulent flow for a single-phase liquid.

A method for designing plate fin heat exchangers has been suggested by and reviewed by Westwater (1983) and tested by co-workers based on the "Local Assumption". This model implies that at any point on the heat exchanger surface the heat transfer coefficient is known function of the fluid velocity and the difference between the local surface temperature and the fluid saturation temperature.

$$\alpha = f(u, \Delta T) \tag{2.43}$$

The local surface temperature was calculated from a numerical analysis of the heat flow through the fin with the heat transfer coefficient varying along its length.

The requirement for boiling curves for a range of velocities limits the application of this design method. However, Yilmaz and Westwater (1980) have published curves for R113 at velocities up to 6.8m/s. These curves are discussed in *Chapter 1*. Panitsidis, Graham and Westwater (1975) showed that the Local Assumption gave results which were in agreement with experiment. The conditions which were tested by Panitsidis, Graham and Westwater included a range of heat flux which would be expected to lead to both nucleate and film boiling in different areas of the heat exchanger.

Neither the film flow nor the nucleate boiling based models can be expected to span the complete range of heat and mass fluxes, qualities and geometries which might be encountered. In general the film flow models are appropriate at low heat flux (i.e. low wall superheat) and relatively high quality and velocity. The Local Assumption, which is a nucleate boiling based model, is applicable at high heat fluxes or wall superheat but is limited in application by the availability of boiling curves for non-stationary fluids. The model was verified at relatively low mass flux but, if appropriate boiling curves were available, it could be used at higher values.

2.5 EVAPORATION OF THIN LAYERS

It will be suggested (*Section 4.5*) that conduction through and evaporation of a thin layer of liquid is an important mechanism of heat transfer during boiling in confined spaces. The film flow model in essentially annular flow has been described by Robertson (1982) and Hewitt and Hall-Taylor (1970). Determination of film thickness in both confined bubble and annular flow (Moriyama and Inoue (1992,1)) has been discussed in *Section 2.2*. In this section the evidence for deposition of liquid on the surface beneath a bubble is reviewed and the estimation of its thickness discussed.

Taylor (1961) presented data demonstrating that the velocity of a bubble in a capillary tube and the mean velocity of the liquid immediately in front of the bubble are functions of the Capillary Number. The ratio $(u_b - j)/u$ where u_b is the bubble velocity and j is the velocity of the fluid ahead of the bubble, tends to a value of 0.56 at high velocities. For adiabatic flow it is therefore possible, since volume must be conserved, to calculate the thickness of the liquid film remaining on the wall. Taylor (1961) presented the results graphically, however they are reported in Wallis (1969) in the form:

$$\frac{j - u_b}{u_b} = 0.56\left(1 - e^{-2.64\left(\frac{\mu_l u_b}{\sigma}\right)}\right) \tag{2.44}$$

This form must be used iteratively since the value of u_b is not known. The value of j can, however, be determined as it is equivalent to the total volumetric flux through the tube. Wallis states that the relationship:

$$\frac{A}{A_b} = \frac{u}{u_m} \approx 1 + 1.27\left(1 - e^{-3.8\left(\frac{\mu_l j}{\sigma}\right)^{0.8}}\right) \tag{2.45}$$

is accurate to within 2% and allows the ratio of the cross sectional area of the bubble to that of the tube to be determined from a knowledge of the total volumetric flow rate.

Cornwell and Schuller (1982) noted the important contribution to heat transfer made by bubbles sliding around tubes in a tube bundle under boiling conditions. Analysis of high speed films showing the growth of bubbles in a tube bundle indicated that evaporation of the liquid microlayer between the bubble and the heated surface was the predominant mode of heat transfer. The microlayer thickness was estimated to be of the order of 3μm for R113 boiling in the tube bundle. Hydrodynamic theory (Addlesee, Cornwell and Peace, 1989) suggests that the liquid layer between an isolated bubble and the surface would be somewhat thicker than this. The work of Monde (1988)(1989), discussed below, also indicates that a thicker layer would be expected. Cornwell, Houston and Addlesee (1992) measured the heat transfer to a tube within a bundle under both heating and cooling conditions. A test section representative of a vertical slice through a tube

bundle was constructed such that heat was supplied to all the tubes in the bundle with the exception of the test tube. A representative bubbly flow field was thus established around the test tube. The instrumented test tube itself was then either heated or cooled and the heat transfer coefficient determined for both cases. When the test tube was cooled condensation of the vapour in the bubbles around the tube occurred. This led to a thickening of the microlayer. During heating evaporation of the microlayer caused it to thin. The thermal resistance of the microlayer during the life of a bubble would thus be expected to be less for the heating case than for the cooling case. A theoretical analysis showed that for typical conditions of bubble size and lifetime a microlayer of 5μm thickness would yield a ratio of between 1 and 2.4 between the evaporative and condensing heat transfer coefficients for a given absolute value of temperature difference. The experimental results yielded a ratio of approximately 2.

The work of Cooper and Lloyd (1968) demonstrated the importance of the microlayer formed beneath vapour bubbles during pool boiling above a horizontal surface. The hydrodynamics of the configuration investigated were not the same as would be encountered in situations where the bubble is constrained. It was however noted that the thickness of the layer deposited at the periphery of a bubble increased with time as the bubble grew. Thicknesses of 6 - 75μm were observed with bubbles of 0.4 - 10mm diameter with toluene and isopropyl alcohol as the working fluids. It was proposed that the layer thickness before evaporation could be determined from:

$$\delta \approx 0.8\left(\frac{\mu_l t_g}{\rho_l}\right)^{\frac{1}{2}} \tag{2.44}$$

Where t_g represents the time of bubble growth. This would lead to a film thickness of approximately 80μm with R141b after 20ms, considerably thicker than that observed in *Section 4.5* of this study.

The model of Kusuda (1981) as reported and developed by Monde (1988) assumed that the heat transfer enhancement observed when a bubble passed over a heated surface

forming part of a narrow channel was due principally to transient conduction. The passing bubble was assumed to sweep superheated liquid away from the surface leaving only a thin layer of superheated liquid adhering to the surface. After the passage of the bubble it was assumed that the channel would be refilled with liquid at the bulk temperature. The heat transfer from the wall and the layer of superheated liquid was then calculated using an analysis based upon the liquid behaving as a semi-infinite solid. The model is similar to that outlined in *Section 4.6* for round tubes and applied to boiling in an annular gap by Ishibashi and Nishikawa (1969). Monde (1989) developed the model further by allowing for evaporation of the film during passage of the bubble.

Monde (1988),(1989) and Addlesee, Cornwell and Peace (1989) predict significantly greater film thicknesses, of the order of 100μm, than Cornwell Houston and Addlesee (1992). The differences may be explained by the nature of the flow field around the surface and the bubble. In particular Cornwell Houston and Addlesee (1992) suggest that the frothy conditions within a tube bundle are conducive to the formation of a thin layer. The analysis of microlayer thickness in narrow channels is reported in *Section 4.5* of this thesis.

2. 6 BOILING IN LIQUID METALS AND HEAT-PIPE THERMOSYPHONS.

The development of liquid metal (principally sodium and potassium) cooled nuclear reactors has prompted the study of boiling in liquid metals and it is noted here that the phenomena observed are similar to those seen during boiling in narrow channels. In particular the instability which has been observed during the boiling of liquid metals and has been referred to as "chugging" is similar to that seen in narrow channel boiling with ordinary fluids. It is associated with the rapid growth of a few bubbles in a channel and the associated expulsion of liquid slugs. A similar, intermittent boiling has been observed in thermosyphon heat-pipes. The evaporator wall temperature and liquid temperature rise without any appreciable evaporation occurring then explosive boiling takes place with a rapid drop in temperature. The boiling ceases when the liquid cools to saturation pressure and the cycle is repeated.

Morozov et al (1988) described the important features of liquid metal boiling and stated that high superheats to initiate boiling and low vapour-phase densities result in the formation of bubbles of size commensurate with that of the tube. These bubbles then grow forcing liquid slugs ahead of them. Experimental observations indicated the presence of "pulsative" and non-pulsative regimes. The pulsations affected mass flux, local wall temperature and inlet pressure.

A model based on the formation of a few (less than 10) discrete bubbles which then grow due to evaporation of the thin film deposited on the heated wall is featured in the HOMSEP-2 computer programme (Rudge 1989) used for the analysis of the transient behaviour of the sodium cooling system of a fast-breeder reactor when boiling occurs.

A link between the features of liquid metal boiling and narrow channel boiling is represented by the similarity shown between the boiling of sodium and the boiling which occurs during rapid depressurisation of uniformly heated fluid in a tube. The work of Kosky (1968) observing rapidly depressurised, uniformly superheated water in a tube showed that when the pressure at the free end of the tube was reduced there was a rapid fall in pressure throughout the tube during which time a few bubbles formed. These grew to be the size of the tube diameter at which stage the pressure at the base of the tube rose as the longitudinally expanding bubbles expelled fluid slugs. An analysis of the rate of evaporation from the spherical end caps showed that the rate of bubble growth could not be explained by vapour generation at the end caps alone. Inclusion of evaporation from a thin film deposited on the wall gave good agreement between observed and predicted bubble growth rates.

Liu, Wang, Dong and Ang (1990) have studied pulse boiling in vertical, closed thermosyphons. It was observed that, under certain conditions, boiling in the evaporator of a thermosyphon was intermittent in nature. The mechanism suggested by Liu et al is as described above. Energy is stored in superheated liquid, then nucleation is

followed by rapid bubble growth resulting in the liquid above the bubble being forced up the thermosyphon tube. The study reported involved tubes of 15-30mm diameter and predicted pulse strength and frequency to an accuracy of 50% using a transient conduction model. Some aspects of the analysis are likely to be more accurate when applied to small tubes. In particular the assumption that heat transfer within the liquid is by conduction rather than convection is more appropriate as tube diameter decreases.

Casarosa and Latrofa (1983) have investigated pulse boiling in thermosyphons. Qualitatively their observations are similar to the phenomena observed at low flow rates in the present study. The correlation which they proposed was:

$$Nu_* = 0.0786 Re_*^{0.6} Pr^{1/3} \qquad (2.45)$$

Where:

$$\mathrm{Re}_* = \frac{q\, l^* \rho_l}{\mu_l \rho_g h_{fg}}$$

$$Nu_* = \frac{\alpha'\, l^*}{k_l}$$

$$l^* = \frac{cp_l \rho_l \sigma T_{sat}}{\left(h_{fg} \rho_v\right)^2}$$

It should be noted that the temperature difference used in the definition of the heat transfer coefficient, α', in *Equation 2.27* is defined as the "drop between the wall temperature and the liquid temperature at the end of the quiet phase, as soon as explosive evaporation begins".

Since both fluid and wall temperature varied cyclically during the course of a test it is likely that the above correlation would not be applicable to a situation with differing mechanisms controlling the wall temperature. However, despite the foregoing reservation, the correlation implies:

$$\alpha = Cq^{0.6}$$

where C is a function of fluid properties and geometry.

2.7 VOID FRACTION AND PRESSURE DROP IN NARROW CHANNELS

There are few reported studies of pressure drop and void fraction in narrow channels at the relatively low mass fluxes encountered in compact evaporators. This has been illustrated by Holt, Azzopardi and Biddulph (1993) who showed the number of data points in published works relating to channels of 6mm diameter or smaller and mass flux below 1000kg/m^{2}s was very small. Holt and co-workers have undertaken a systematic study, as part of the Joule II Programme, to produce data relating to small circular, rectangular and trapezoidal channels. Their study covered adiabatic flow of air-water, helium-water and air-glycerol solutions. It was concluded (Azzopardi and Holt, 1995) that no single correlation was consistently good at predicting the data over the range of conditions. However, the best results overall were achieved using the Lockhart-Martinelli (1949) correlation for frictional pressure drop. The Friedel (1979) correlation which is now widely used for conventionally sized tubes was found to overpredict the frictional pressure drop. The Lockhart-Martinelli and CISE predictions (presented here as *Equations 1.61* and *1.64)* were both found to be acceptable for predicting void fraction.

The work described above is broadly in agreement with that of Bao et al. (1993). Working with water-air, aqueous glycerine solution - air and kerosene-water mixtures in tubes of 0.75-3.1 mm Bao et al discriminated between laminar and turbulent flow conditions. The Lockhart-Martinelli and CISE predictions performed equally well in the prediction of void fraction for both flow regimes. The pressure drop results were best

predicted using the Lockhart-Martinelli correlation for the gas liquid flows. This correlation did not, however, give good predicions for kerosene-water mixtures. It was recommended that the correlations of Beattie (1973), Chisholm (1973) and Friedel (1979) should not be used for flow having Reynolds Number of less than 1000.

2.8 SUMMARY OF THE LITERATURE REVIEW.

Literature relating to flow and boiling in confined spaces has been reviewed. It is clear from the review that there are several approaches which have been taken in the determination of heat transfer in confined passages. Data obtained from work involving forced flow boiling in confined spaces is limited and correlations derived from this data must be viewed with caution. It is, however, apparent that the distinction between nucleate boiling and convective boiling which is apparent in conventionally sized tubes can also be made in small tubes. As with conventionally sized tubes, nucleate boiling will dominate at high wall superheats corresponding to low heat fluxes while convective boiling is likely to be the dominant mechanism at low wall superheats and heat flux (Tran , Wambsganss and France , 1995).

If nucleate boiling is the principal mode of heat transfer then it would be expected that the heat transfer coefficient would be essentially independent of mass flux. Therefore, the results of reported studies of natural circulation boiling in confined spaces may be applied to the case of flow boiling for the nucleate dominated region, although the mass flux through the test section is generally unknown.

Workers studying compact heat exchangers have concluded either that the heat transfer is entirely nucleate (e.g. Panchal, 1989, Galezha et al, 1976) or convective boiling (e.g. Robertson, 1979,1982,1983, Carey and Mandrusiak, 1986) and developed correlations accordingly. As with forced flow boiling in tubes the appropriate mechanism depends upon the wall superheat and heat flux; low heat fluxes typical of cryogenic applications would favour convective boiling and high heat fluxes would lead to nucleate boiling dominating the heat transfer.

A general approach to predicting heat transfer in confined spaces requires an understanding of the flow regimes and heat transfer mechanisms which occur. In particular it is necessary to determine whether the flow is in the Confined Bubble or Annular Slug flow regime in order to calculate an appropriate liquid film thickness. It has been shown that when bubbles grow adjacent to a heated surface heat transfer through a liquid layer and evaporation of that layer play a significant part in the heat transfer (Cooper and Lloyd, 1969, Cornwell, Houston and Addlesee, 1992). Estimated values of the thickness of the film deposited under a bubble vary considerably.

Boiling in confined spaces exhibits some of the characteristics observed during boiling in liquid metals and heat-pipe thermosyphons, the pulsations observed during small channel boiling have been analysed in thermosyphon evaporators. The rapid growth of bubbles filling much of the tube has been observed in liquid metal boiling (Morozov et al, 1988) and incorporated in computer codes (Rudge 1989).

It is apparent that the heat transfer coefficient to a boiling fluid depends upon geometry, fluid properties, mass flux and heat flux. Under some conditions flow instabilities due to rapid bubble growth can occur and this further complicates the analysis of the boiling heat transfer. In view of the complexity of the mechanisms involved it is unsurprising that no published work is applicable to all situations involving evaporation in confined space.

CHAPTER 3

EXPERIMENTAL ANALYSIS OF BOILING IN CONFINED SPACES

3.1 PURPOSE AND DESIGN OF RIGS

Two test rigs, referred to as the Mark I and Mark II rigs, respectively, have been constructed to provide data for use in this project. The Mark I rig was adapted from an existing rig and used to establish the existence of the various flow regimes. A test section was incorporated to permit flow visualisation together with the measurement of heat transfer and pressure drop data. This rig was operated at atmospheric pressure and the condenser was vented to atmosphere to ensure that elevated pressures could not occur. After preliminary results were obtained a second rig was constructed which had a relatively small fluid inventory and operated in a closed mode thus reducing the loss of working fluid to the atmosphere and permitting operation at elevated pressure. Low inventory and low venting requirements were regarded as important features in view of both environmental and financial concerns.

The Mark II rig incorporated two flow loops, one for flow visualisation together with the measurement of heat transfer and pressure drop data in geometries with large aspect ratios (76mm wide by up to 4.5mm deep) and a loop for the measurement of local heat transfer and pressure drop in single, narrow channels. The Mark II rig was operated with Water, R141b and Flutec PP1. For preliminary tests using the Mark I rig R113 was used as a test fluid. relevant properties of these fluids are given in *Table 1.1.*

3.2 TEST RIG MARK I

3.2.1 General Description

The flow visualisation rig is shown schematically in *Fig.3.1* and photographically in *Fig.3.2*. Liquid was pumped from the reservoir to the test section via manual flow control valves and two variable orifice flow meters in parallel. A liquid preheater was incorporated in the pipe between the flow meters and the test section. A manifold was machined into the test section outlet and this manifold acted as a liquid separator. Liquid from the test section was be returned to the reservoir via a measuring cylinder. Vapour from the test section passed to the condenser and the condensate returned to the reservoir via a measuring cylinder. Pneumatically operated shut-off valves were situated in the pipes between each of the measuring cylinders and the reservoirs. The air supply to these valves was supplied from a single solenoid valve to ensure simultaneous operation. Use of these valves permitted the outlets of both of these cylinders to be closed simultaneously. All pipe work carrying liquid was copper or glass, while that transporting vapour was glass with some clear PVC connections.

The test section, shown schematically in *Fig.3.3* and Photographically in *Fig. 3.4*, comprised an aluminium block with a liquid inlet manifold machined in the lower end, a test area and a vapour separator/outlet manifold which was machined in the upper end of the block. The active test area, 150mm wide and 300mm long, was situated between the two manifolds. A clear, 6mm thick, glass sheet was clamped over the front of the test section. Five electric cartridge heaters were inserted into the block behind the active area of the test section.

The heated surface for the single channel experiments was as machined. Gap size was adjusted by altering the spacer between the surface and the glass plate so that the heated surface was identical for each test.

A finite difference analysis of the temperature distribution within the block was carried out. It was assumed that the heaters were located 36mm from the base of the channels. The analysis showed that the temperature would, assuming constant heat transfer coefficient between the surface and the fluid and constant fluid temperature, be uniform along the length of the test section at a depth of 24mm below the channels to within +/-0.5K and, at the surface constant to within ±0.005K. *Fig. 3.5* shows the results of the analysis for a total heat input to the test section of 2kW and a heat transfer coefficient, with reference to the plan or superficial area of the test section of 4500 W/m^2K. On the basis of this analysis and the assumption that the heat transfer coefficient would vary relatively little along the test section, hence axial conduction would be negligible, surface temperature of the block was estimated assuming one dimensional conduction from the thermocouples to the base of the flow channels.

The heat input to the cartridge heaters was controlled by a variable auto transformer (Variac) and measured using a digital wattmeter. In order to account for heat losses from the block a relationship between block temperature and heat loss was determined: With the rig drained of fluid and the control valves closed to prevent circulation of air through the test section the heaters were switched on at low power. The power input to the heaters, the temperature of the block in equilibrium with the surroundings and the ambient temperature were measured. *Fig.3.6* is a plot of power input against temperature difference between the block and the environment. The heat loss was related to the block temperature by *Equation 3.1.*

$$Q_{loss} = 1.16\left(T_b - T_{amb}\right)^{1.167} \tag{3.1}$$

For commissioning tests heaters with a maximum rating of 250W each were used. These were replaced with heaters rated at 1000W, capable of providing an average heat flux over the test area of approximately 110kW/m (based on the frontal area of the test section). In practice the maximum heat flux was limited by flooding of the condenser.

3.2.2 Instrumentation and Data Acquisition - Mark I Rig

The instrumentation used with the Mark I rig is shown schematically as *Fig 3.7.*

Calibrated Type K thermocouples were used for temperature measurement. The fluid inlet and outlet temperatures were monitored. Additionally four thermocouples were mounted in the block, nominally 24mm behind the surface of the block in order to permit estimation of the temperature variation up the surface of the test block.

Since the accurate measurement of temperature differences rather than absolute temperature level was regarded as important, the thermocouples used to measure the fluid inlet and outlet temperature and block temperature were calibrated by placing them in an insulated aluminium block and recording the thermocouple outputs using the data logger. The block was electrically heated to various temperature levels and the output of each thermocouple recorded. The calibration constants in the data logging program were then adjusted so that the data logger outputs were in agreement to within ±0.1K over the temperature range of interest. All thermocouples were connected directly to the data logger and the data logger internal reference temperature was used in the conversion of measured voltages to temperatures.

Pressure at inlet and outlet of the test section was measured using calibrated WIKA Type 881.39.600 pressure transducers giving 0-100mV output over a range 0-2.5 bar.

Two data acquisition systems were used. A Hewlett Packard 3421A was used for monitoring and recording steady state and time-averaged values and a Keithley DAS8/EXP16 was used for recording transient values. The Hewlett Packard was a stable instrument with a low susceptibility to noise but a relatively low logging speed.

The Keithley was more susceptible to electrical noise when measuring the low voltages associated with thermocouples but was capable of much higher data acquisition rates. The Keithley Instruments data acquisition system was connected to a PC running EASYLX, data acquisition and analysis software. This arrangement permitted the recording and analysis of rapidly varying signals.

The Hewlett Packard 3421A was controlled using a hand held HP71B microcomputer. This machine was capable of only limited processing of the raw data and the calculated temperatures and pressures were provided as a print-out for manual re-entry into a PC for further processing.

The Heat input to the test section was measured using a Norma D1150 Auto-ranging digital wattmeter.

Liquid flow rate into the test section was measured using variable orifice flow meters having ranges 0.3 - 2.4 l/min and 2.0 - 8.0 l/min when operating with R113. Additionally, the flow rates of the liquid exiting the test section and of the condensed vapour could be determined by measuring the time taken to accumulate a given volume in the respective measuring cylinder after closure of the air operated valves.

3.2.3 Range of Geometries and Parameters Tested - Mark I Rig

Tests were performed with a range of Flat-plate, single channel configurations (confined in one dimension) and two multi-channel geometries (confined in two dimensions):

Flat Plate, Single Channel:

Width 150mm Gap 6mm

Width 150mm Gap 4mm

Width 150mm Gap 3mm

Width 150mm Gap 2mm

Width 150mm Gap 1mm

Where the gap is defined as the distance from the heated surface to the adiabatic glass plate.

Multi-Channel:

Geometry 1 - 75 channels, 1.2mm wide by 0.9mm deep

Geometry 2 - 36 Channels, 3.25mm wide by 1.1mm deep

The Confinement Numbers associated with these geometries are listed in *Table 3.2.*

3.3 TEST RIG MARK II

3.3.1 General Description

A second test rig was constructed to provide data for use in this project. The Test Rig Mark II is shown schematically in *Fig 3.8* and photographically on *Figs. 3.9* and *3.10.* The rig comprised two discrete loops. The data logging equipment, fluid reservoir, circulating pump and condenser were common, however, flow meters and instrumentation were specific to one of two loops of the rig. These loops are referred to as the Single Tube test loop and Flow Visualisation test loop. The relevant test sections are referred to as the Single Tube test section and Flow Visualisation test section respectively. Liquid was pumped from the reservoir through the appropriate test loop via manual flow control

valves and variable orifice flow meters connected in parallel. In each loop an electric liquid preheater was incorporated in the pipe between the flow meters and the test section.

Prior to entering the single tube test section the working fluid was preheated by passage through an electric heater followed by a coil immersed in a water bath. When operating with water the water bath was heated so that it boiled, for other fluids the temperature of the water bath was maintained at or very slightly above the saturation temperature of the working fluid. This method of preheating was found to avoid problems associated with subcooled boiling in an electrically heated preheater at low flow rates.

The Single Tube test section is illustrated schematically in *Fig 3.11*. and photographically in *Fig 3.12*. All test sections were thin-walled stainless steel and were heated by passage of a DC electric current along the tube. The test section was enclosed in a 22mm diameter copper tube which was heated with three independently controlled guard heaters. The environment immediately surrounding the test section was maintained at within 2K of the average temperature measured by the surface thermocouples. The outer wall temperature along the single tube test section was measured using ten equally spaced thermocouples electrically isolated from the wall using PVC tape and held in position beneath a small wad of glass fibre insulation using a second layer of PVC tape. This arrangement was chosen in preference to the more conventional practice of mounting thermocouples on the tube and surrounding the test section with thermal insulation to ensure rapid response of the system and eliminate the thermal inertia inherent in thermal insulation which would be significant with the low absolute values of heat input associated with small tubes. The thermocouples were fabricated from bare 0.2mm diameter wires spot welded to form the junction. The internal wall temperature was calculated from the measured heat flux and outer surface temperature assuming one-dimensional conduction through the tube wall with the electric heating providing a uniform heat source throughout the material.

In addition to the measurement of time averaged values the section could be used to provide qualitative information on variations in local heat transfer with time.

Fig. 3.13 is a schematic representation of the Flow Visualisation test section, which is shown assembled and removed from the test facility in *Fig. 3.14*. The heating was provided by three Watlow firebar heaters mounted behind the heated area and controlled using a variable auto-transformer (Variac). Heat loss from the test section was estimated from an analysis of the heat flow paths by conduction, convection and radiation from the test section. The results of this analysis were compared with a quasi-static test in which the test section inlet and outlet ports were disconnected and plugged and the equilibrium temperature measured at various heat inputs. The measured and calculated rates of heat loss agreed to within 8%. The analysis of heat loss from the test section is discussed further in *Appendix 2*.

Pressure and temperature measuring points were incorporated in the inlet and outlet manifolds of the section. Six thermocouples were mounted in the aluminium test block behind the test area. In the surface temperature was calculated assuming one dimensional conduction between the thermocouple and wall fluid interface. Measurements from the top and bottom thermocouples were not used in subsequent analysis because of the influence of end effects. Although the ends of the test block and the internal surfaces of the manifold were insulated using a coating of silicon rubber it was inevitable that some heat transfer to the fluid occurred in this region. *Fig 3.15* shows the flow configurations which were tested.

3.3.2 Instrumentation and Data Acquisition - Mark II Rig

The instrumentation used with the Mark II rig is shown schematically as *Fig 3.16.*

Calibrated, Type K thermocouples with an ice reference junction were used for temperature measurement. The thermocouples for use on the single tube test section were made from 0.2mm diameter wires with spot welded junctions. All other thermocouples were 1.5mm diameter, stainless steel sheathed type.

Pressure was measured using calibrated WIKA type 891.14.525 pressure transducers giving an output signal of 4-20mA over a 0-2.5bar range.

Flow rates were measured using variable orifice type flow meters. As supplied these were calibrated for water at 20^{o}C. These were individually calibrated for the working fluids R141b and Flutec PP1. Flow meters having ranges permitting measurement of flows from 10-350ml/min of water were used on the single tube circuit and 50-2000ml/min on the flow visualisation circuit.

The data acquisition systems used were similar to those used in conjunction with the Mark 1 rig. The major modification being the replacement of the HP71B micro-computer with a HP Vectra 286 PC-AT compatible microcomputer to permit recording of data to magnetic disc for subsequent processing.

Heat transfer and pressure drop measurements were obtained for a range of heat and mass fluxes in a range of flow configurations based on the 76mm wide x 300mm long heated test area incorporated in the rig. Tests were carried out with R141b and Flutec PP1.

3.3.3 Range of Geometries and Parameters Tested - Mark II Rig

Heat transfer and pressure drop measurements were obtained in the single tube test section for a range of mass and heat fluxes in round tubes of 1.39, 2.05, 2.87 and 3.69mm diameter and for a square section tube having internal sides of length 2.1mm. Most measurements were obtained using R141b as a working fluid. A limited amount of data was collected with water.

Table 3.3 gives the approximate range of variables covered by the tests using the Single Tube Test Section.

The range of parameters investigated using the Flow Visualisation Test Section is summarised in *Table 3.3.*

The Confinement Numbers for the Geometries Tested for each fluid are listed in *Table 3.5.*

3.4 FLOW VISUALISATION AND ANALYSIS TECHNIQUES

3.4.1 General

In order to develop a model of and identify the processes involved during boiling in confined spaces various methods of observing and recording the flow in the channels were attempted. These are summarised below. A problem with all recording methods examined was the inherent difficulty in obtaining a sequential record with high resolution locally while also maintaining an overview of the flow field. Thus representation of the entire flow did not contain sufficient resolution to enable examination of local effects; recordings over short lengths permitted examination of these local effects but these could not be viewed in synchronisation with processes occurring elsewhere, for example, up- and down-stream of the area under examination.

3.4.2 Direct Visual Observation

Direct observation of the flow was possible in the visualisation test section and was useful in that it permitted the observer to view the entire flow field and thus note phenomena occurring concurrently along the length of the test section. It was also possible to identify flow regimes under some conditions. The limitations of direct observation are principally the lack of record and the restricted ability of the viewer to observe short duration or high frequency events.

3.4.3 Flash Photography

Flash photography provided clear pictures with good resolution of either the entire flow field or of localised areas of the flow. Still photographs were useful in identifying flow regimes but were of little use in the analysis of the flow. The clearest record of instantaneous flow patterns within the Flow Visualisation Test Sections of the Mark I and Mark II rigs was obtained with flash photography using a 35mm SLUR camera with a 50mm macro lens and 25mm extension tube. Use of a ring flash mounted on the end of the lens permitted mounting of the camera approximately 50mm from the glass viewing window and gave an acceptable depth of focus

3.4.4 Video Recording

The most flexible and useful method of recording the flow was found to be use of a high speed video camera. The resolution of the Video recording was not as high as that obtained with flash photography but the technique gave the ability to study the instantaneous flow regime and the sequence of regimes in a particular area. This proved useful in studying the growth of bubbles.

A NAC 400 video recorder giving a capability of recording at 200 frames/second in full frame mode or 400 frames/second in half frame mode was used. For the purposes of this project it was operated at 200 frames/second throughout. The recordings were examined on screen at user selected speed or frame by frame and hard copies of selected frames were produced using a frame-grabber and thermal printer.

3.4.5 Laser Doppler Anemometry

The use of Laser Doppler techniques was reviewed for use in measuring wall film thicknesses and for the measurement of instantaneous velocities in fluctuating flow.

The equipment available is summarised in *Table 3.6.*

After discussions with the consultant employed on the relevant JOULE II project (University of Wales) to advise on laser utilisation, it became clear that the equipment available was unsuitable for use in film thickness measurements. Upgrading of the equipment to provide the necessary resolution was beyond the resources of the project and would not necessarily yield reliable results.

The system was used to investigate the presence of liquid slugs or vapour bubble and the variation of liquid velocity with time at a single point in a channel. The measuring volume obtained with the available system was approximately 6mm long, hence even with the larger channels investigated here it extended across the full channel and into the viewing window. It was found that the results obtained could not be interpreted due to the influence of measurements taken in the boundary layer and at the liquid - window interface. The measuring volume is shown schematically in *Fig. 3.17.*

It was initially assumed that no signal would be present when a bubble passed the measuring station, however, since a signal was received from the liquid layer, it was not possible to identify bubbles in this way. Determination of the liquid velocity- time profile required measurement of a representative velocity over a period of time Since the velocity in a channel must vary from zero at the wall to a maximum in the centre of the channel, measurements taken from close to the walls had a very low or zero values. It was not possible to distinguish between measurements which were truly representative of the liquid velocity and those obtained from the boundary layers.

3.4.6 Infra Red Thermometry and Thermochromic Paints

In order to qualitatively assess the variation of wall temperature with time two additional techniques were employed with the single tube test section. An Infra red video camera was used to view the tube while water was boiling. This showed that the tube wall temperature at a particular point on the tube varied with time by up to 10K. This phenomenon was particularly noticeable when it could be seen that slugs of liquid were expelled from the end of the tube and pressure pulsations were recorded. The existence of temperature fluctuations was confirmed using thermochromic paint.

Although the results obtained were limited and qualitative, since all guard heaters and insulation were removed to expose the test section they did serve to indicate that average surface temperatures as indicated by a thermocouple on small tubes must be viewed with caution. This is particularly true when small temperature differences are measured as discussed in *Section 3.5.*

3.5 HEAT TRANSFER RESULTS.

3.5.1 Results from Mark I Rig

Sample results obtained from the gap confined in one dimension and from the multi-channel geometries are presented in *Figs.3.18-3.25* and *Figs.3.26-3.33* respectively. Results for the range of geometries and conditions tested are plotted together as *Fig.3.34.*

The heat transfer results for the single channel configuration are compared with the Mostinski correlation (*Equation 1.3*). It can be seen from an examination of the results that there was an enhancement under all conditions of confinement and mass flux until partial dryout occurred. The enhancement, defined as the ratio between measured heat transfer coefficient and that predicted by Mostinski *(Equation 1.3)* reduced as heat flux increased. Enhancement was greatest at low mass flux and small gap between heated wall and plate; it is assumed that this was due to the tendency towards confined bubble formation under these conditions. At higher heat fluxes partial dryout occurred in the higher levels of the channel. The occurrence of dry patches was more prevalent at high

heat fluxes and lower flow rates, corresponding to higher dryness fraction. For similar flow and heat flux the tendency to dry out increased with decreasing gap, suggesting that the small gap led to poor fluid distribution.

The heat transfer results for the multi-channel geometries are compared with the correlation proposed by Galheza *(Equation 2.)* represented by the straight lines on *Figs 3.26-3.33.* The constant, C, chosen was 11500 and 13000 for geometries 1 and 2, respectively (These are within the range 8000 to 16000 for the configurations tested by Galheza). It should be noted that, since the tests reported here cover a single fluid, *Equation 2.* , with suitable choice of constant, reduces to:

$$\alpha = b\,q^{n} \qquad (1.8(b))$$

The lower mass flux cases for geometry 1 were characterised by unstable flow, with the regime and flow rate varying with time and from channel to channel. It is suggested in *Section 4.7* that this type of flow results from the rapid elongation of confined bubbles which either cause fluctuations in the pressure drop across a channel or a variation in the flow, including the possibility of reverse flow, in individual channels. Under these conditions the heat transfer coefficient was relatively high and, until dryout occurred, insensitive to heat flux. At the highest mass flow the flow was stable and the heat transfer coefficient increased with heat flux.

The instability commented on above was less marked in geometry 2, however the heat transfer coefficient tended to fall with increasing mass flux. It should be noted that for a given heat flux, geometry and flow rate the dryness fraction at any position would decrease with increasing flow rate. Conventional correlations, for example Chen, Shah or Liu and Winterton, would suggest that increasing either x or G would be expected to lead to an increased heat transfer coefficient. In this instance it appears that the effect of increasing G is outweighed by the corresponding decrease in x at a given heat flux or that the mechanisms implicit in the correlations do not apply.

3.5.2 Heat Transfer Results for Mark II Rig - Single Channel Test Section

Heat transfer data were obtained for round tubes in the range 1.39-3.69mm diameter and for a 2.1mm square section tube with water and R141b as working fluids.

Sample results for water are shown in *Figs.3.35-3.37*. As it can be seen the temperature differences encountered in boiling water at low heat flux (*Fig.3.35*) are extremely small, and the measured values are apparently negative in some regions. Clearly this must be accounted for by measurement error. *Fig.3.36* shows the temperature profiles along a tube at higher heat flux and illustrates the variation in saturation pressure which has been estimated along the length of the tube. In estimating the local saturation temperature it was assumed that the pressure varied linearly from the onset of boiling (i.e. quality = 0) between the measured inlet and outlet pressures. The saturation temperature was then determined for the local pressure. From *Fig.3.37* it can be seen that the heat transfer coefficients towards the exit of the tube are of the order of 25kW/m^{2}K. If this value is taken to be representative of the value along the tube, rather than the higher estimated values in the early stages of boiling, then it is apparent that at the low heat flux, 10kW/m^2, shown on *Fig.3.35.* the expected temperature difference would be approximately 0.4K. This corresponds to an error of 1.35kPa in the determination of local pressure. Given the pulsating nature of the flow under some conditions and the reliance on linear interpolation, an error of this order in the estimation of local pressure is not unreasonable. This source of potential error is in addition to errors in temperature measurement which may be ±0.2^{o}C. As noted in *Section 3.4.6* , thermochromic and infra-red measurements showed that wall temperature variations of up to 10K may occur under conditions of high heat flux with water, the calculation of heat transfer coefficients based upon average values of heat flux and wall temperature is likely to be misleading.

For R141b data, as represented on *Figs.3.38-3.41* the heat transfer coefficients at low heat flux were found to be an order of magnitude less than those for water. Hence the error introduced by the measurement and interpolation of local pressures was

proportionally less. The maximum error induced in the temperature difference an heat transfer coefficient from this source is likely to be 10%.

For the reasons outlined above R141b data have been used for comparison with correlations. Sample results for the 3.69mm and 2.87mm tubes presented in *Figs.3.38* and *3.39* respectively exhibit the features which are typical of boiling in larger tubes. At low quality the heat transfer coefficient was independent of quality and a function of heat flux while at higher qualities the heat transfer coefficient increased with quality and was apparently independent of heat flux. In the smaller tubes, 2.05mm and 1.39mm diameter, as shown in *Figs.3.40* and *3.41* respectively, the influence of quality was less clear. Results for the 2.1mm square section tube and 2.05mm diameter tube were found to follow similar trends.

Heat transfer results from the round and square tubes have been compared with a number of correlations. The comparisons for three correlations are shown in *Table 3.10*. The three which are considered here are representative of a large tube flow boiling correlation, a nucleate boiling correlation and two correlations proposed for use in relatively small tubes. Further comparisons are carried out in *Section 5.3*.

3.5.3 Heat Transfer Results for Mark II Rig - Flow Visualisation Test Section

Heat transfer results for R141b are presented in *Figs.3.42-3.50* and for Flutec PP1 in *Figs.3.51 -3.53*. All of the figures, *Figs.3.42-3.53,* are plotted in the form (a) Heat flux against temperature difference and (b) Heat transfer coefficient against heat flux. In each case the results are compared with the Cooper (1984) correlation:

It can be seen from the results that the heat transfer coefficients are generally higher than predicted by *Equation 1.7*. The influence of quality and mass flux is relatively small. The exceptions to this observation being that at high qualities periodic dry out occurred, leading to a reduced measured (i.e. time-averaged) heat transfer coefficient.

Examination of the results suggests that attempts to fit equations of the form:

$$\alpha = b\,q^{n} \qquad (1.8(b))$$

to the data for spaces confined in one dimension are unsatisfactory because there is a clear change in gradient on the q vs ΔT plot (and hence α vs q plot) with increasing heat flux. At relatively high heat flux the gradients tend towards those predicted by *Equation 1.7*, however, for the smaller gaps the measured heat transfer coefficients were higher than predicted.

The heat transfer coefficients at low heat fluxes are very much higher than predicted by *Equation 1.7* and the rate of increase of heat transfer coefficient with heat flux is lower than expected from the exponent n= 0.67. It is suggested that this enhancement is due to evaporation of the liquid film between the heated surface and confined bubbles. It is noticeable that the presence of adiabatic splitters, (i.e. strips of thermally insulating material (PTFE) placed along the length of the plate parallel to the flow direction thus acting as flow dividers) reduces the enhancement due to these bubbles at high mass flux. This is because the presence of the splitters tends to reduce the recirculation of liquid and bubbles which is otherwise apparent.

The results from the multi-channel test specimens do not exhibit the change of gradient in the α vs q plots described above. However mass flux appears to influence the heat transfer coefficient; increasing mass flux leading to a decrease in heat transfer coefficient for a given heat flux. This is illustrated in *Fig. 3.54*. The effect is more marked at low heat flux than high. A complete model of the heat transfer in the multi-channel arrangements must therefore take into account the mass flux, but since the dependence on heat flux is more marked, a correlation of the form given in *Equation 1.8* may be formulated. The constants a,b,m and n are tabulated in *Table 3.7*

3.6 PRESSURE DROP RESULTS

Pressure drops, calculated using *Equations 1.40-1.52* and numerically integrating over the length of the tube have been compared to measured pressure drops for water and R141b flowing in the Single Channel Test Section of the Mark II rig. The CISE correlation (Premilo et al 1970) was used in the estimation of void fraction as this has been shown by Bao et al (1994), and latterly confirmed by Azzopardi and Holt (1995), to be the most appropriate for use in narrow tubes.

A comparison of the predicted and experimental results obtained with R141b flowing in horizontal tubes is presented in *Table 3.8.*

Examination of *Table 3.8* shows that the effect of confinement on the accuracy of the prediction was not significant. *Table 3.9* gives the accuracy of the prediction for all R141b data (90 points in horizontal orientation and 12 in vertical orientation) and water data for all round tubes in the horizontal orientation.

The water data show better agreement with the predicted values then do the data for R141b. This is to be expected since the Lockhart-Martinelli procedure for evaluating frictional pressure drop was developed using water-steam mixtures.

Lazarek and Black (1982), working with R113 in a 3.15mm diameter tube found that use of C=30 and K_a= 2.5 gave agreement to within 20%. Adjustment of the values of C and $K_a$was not found to significantly improve the agreement of the correlation with the data obtained in this project.

It was noted that better agreement was obtained for vertical flow than for horizontal flow. It is unlikely that this is due to the phenomena influencing pressure drop (eg flow regime) being different for each tube orientation. The relatively small number of data points means that the improved agreement may not be statistically significant. Alternatively, the

inclusion of the gravitational component in the vertical orientation may result in two errors cancelling: for example, an over prediction of void fraction would lead to an under prediction of gravitational drop (*Equation 1.41*) and an over prediction of acceleration pressure drop (*Equation 1.46*).

3.7 COMPARISON WITH DATA FROM OTHER SOURCES

3.7.1 General

Ideally, direct comparison with other data sources requires that the data be obtained from experiments with identical fluid, geometry and test conditions. Available data meeting these criteria are very limited, however, comparison has been made with data obtained by IKE (Institut fuer Kernenergetic und Energiesysteme, Universitat Stuttgart), a participant in the JOULE II programme. Alternatively data from different experimental conditions may be compared indirectly through the use of, preferably non-dimensional, correlations. This approach is covered in greater detail in *Chapter 5,* the comparisons made here are therefore limited in scope. The comparison of results from the multi-channel test configurations with the correlation of Galheza et al. has been discussed above.

3.7.2 Comparison with the Work of IKE

There was some overlap between the work carried out by IKE (Universitat Stuttgart) and the present Author under the JOULE II contract "Compact Two-Phase Heat Exchangers". *Figs. 3.55* and *3.56* show comparisons of the results of IKE and the Author at similar conditions. The ranges in which results from the present study for conditions similar to those reported by IKE have been superimposed on figures prepared by IKE and extracted from the JOULE contract report (Cornwell et al 1995). *Fig.3.55* shows the IKE results for a single rectangular channel having cross section 2 x 4mm (mean hydraulic diameter 2.67mm) compared with results for the round tube of 2.87mm with water and R141b at overlapping mass flow rates. The Cooper (1984) nucleate boiling correlation for both fluids has also been added to the figure. Results from the IKE and the Author's multi-channel test sections working with R141b are presented on *Fig.3.56* together with the Cooper (1984) correlation for comparison purposes.

It can be seen from the comparison of the IKE and Author's results that the results from the present study tend to yield higher heat transfer coefficients at a given condition than the IKE results. The difference is greatest at the highest heat fluxes; the Author's results suggest some enhancement over the Cooper (1984) correlation under all conditions shown while IKE results suggest a weak dependence on heat flux with measured heat transfer coefficients below those predicted by Cooper at high heat flux. Both sets of results indicate that higher values of heat transfer coefficient are obtained with multi-channel arrangements than are observed in single channels.

The difference between the IKE results and the Author's results are greatest for water, however, it should be noted that the shaded HWU area is for qualities of 0.1-0.2 while the IKE quality is unknown. Reference to *Fig 2.3* indicates that Fujita and Uchida (1990), again at unknown quality, measured heat transfer coefficients, for water at a heat flux of 100kW/m^2, of approximately 12kW/m^{2}K for natural circulation in a 2mm x 60mm gap (hydraulic diameter 3.87mm) and 40kW/m^{2}K for a gap of 0.6mm x 60mm (hydraulic diameter 1.19mm). These values tend to support the estimate of 25kW/m^{2}K for water in a 2.87mm diameter tube estimated by the present Author despite the reservations expressed in *Section 3.5.2* regarding the accuracy of these results.

It is suggested that the differences in the results obtained by IKE and the present Author arise due to the sensitivity of the results to detail design of the test sections and the resulting instabilities resulting from the pressure fluctuations which are noted in *Section 4.7.* It is to be expected that the design of manifolds and the fluid circulation system will influence the onset of these instabilities which can enhance heat transfer coefficients at low heat flux and, due to temporal or spatial maldistribution, lead to premature dryout and, hence, poor heat transfer high heat flux.

3.7.3 Comparison with the Work of Lazarek and Black (1982) Cooper (1984),(1989) and Liu and Winterton (1988)

In this section the results obtained from the single tube test section of the Mark II rig are compared with four correlations. This work is discussed further in *Chapter 5.*

The work of Lazarek and Black (1982) supported by the study of Wambsganns et al (1993) resulted in a correlation applicable to R113 flowing in a tube approximately 3mm diameter. Although the correlation was obtained with only one fluid it was presented in non-dimensional form, *Equation 2.1* , and therefore could be expected to apply to other fluids.

$$Nu = 30\,Re^{0.857}\,Bo^{0.714} \tag{2.1}$$

As discussed in *Section 2.2* Wambsganns et al (1993), working with a tube 2.92mm diameter noted that the boiling in small tubes (Confinement Number approximately 0.33) was predominantly nucleate in nature and that the Lazarek and Black correlation provided the best agreement . The Lazarek and Black correlation does however show a weak dependence on mass flux and diameter unlike the nucleate boiling correlations of, for example Cooper. Lazarek and Black noted that there was no influence of quality on the heat transfer coefficient.

The Reynolds number used in the Lazarek and Black correlation was based upon the entire mass flowing as liquid. Since the data obtained in this project showed some dependence on quality it was decided to compare it with a modified correlation formed by multiplying the heat transfer coefficient predicted by *Equation 2.1* by a factor $(1-x)^{-0.147}$. Clearly this simple modification can be valid, if at all, only at moderate values of quality since, as a multiplying factor $(1-x)^{-0.147}$ approaches infinity as x approaches unity.

The Cooper (1984) correlation applies to nucleate pool boiling, Cooper (1989) has suggested that the correlation with a reduced constant may be appropriate for the "apparently nucleate" region occurring in flow boiling inside tubes. The nucleate boiling component, α_{nb}, used in the Liu-Winterton correlation is determined from the Cooper (1984) correlation, hence use of Cooper rather other available nucleate boiling correlations is appropriate for reasons of consistency. The correlations are presented in the footnotes to *Table 3.10* and in *Chapter 1*. Both values of heat transfer coefficient predicted by the Cooper correlations have been compared with the experimental data.

Table *3.10* shows the results of the comparison of the data from this study with the above correlations, and, for completeness with the conventional large tube correlation due to Liu and Winterton (1988). The Liu-Winterton correlation is used here in preference to the Chen correlation here because it has been found to compare satisfactorily with databases including organic fluids of the type used here and the original data bank used by Liu and Winterton included tubes down to 2.92mm diameter. This correlation is therefore likely to be one of the best available flow boiling correlations. This has been confirmed by more limited comparisons of this data with Chen (1963) and Shah (1982).

For the 3.69mm tube Liu and Winterton (1988) gives an average deviation of 21% which is comparable with the accuracy of the correlation when used with larger tubes. However the accuracy of this correlation declines significantly with increasing confinement.

Cooper (1984) gives significantly better agreement than Cooper (1989), the percentage deviation is greatest with the smallest tube at 36%. The Percentage deviation for the Lazarek and Black and modified Lazarek and Black equations are similar, the modification slightly increases the average deviation, however the agreement at high quality is significantly improved, particularly in the largest tube.

Comparison of the measured and predicted values of heat transfer coefficient are presented for all tubes for Cooper (1984) and modified Lazarek and Black (1982) in *Figs.3.57-3.61* and *3.62-3.66* respectively. The variation of the average percentage deviation for these correlations and for the Liu and Winterton (1988) correlation is presented in *Fig. 3.67.* This clearly shows the deviation increasing for increasing confinement.

3.7.4 Comparison with the Work of Tran, Wambsganns and France(1995)

Tran, Wambsganns and France (1995) reported on study of boiling in circular tubes of 2.46 and 2.92mm diameter and a rectangular channel of cross section 1.7mm x 4.06mm (d_e=2.4mm). The results of the study are discussed in *Section 2.2.* The correlation recommended is given as *Equation 2.5*:

$$\alpha = 840\left(Bo^2 We_l\right)^{0.3}\left(\frac{\rho_l}{\rho_g}\right)^{-0.4} \text{ kW / m}^2\text{K} \qquad (2.5)$$

It is noted by Tran, Wambsganns and France that nucleate boiling dominates the heat transfer and as with the Lazarek and Black correlation there is no dependency on quality. The results observed in this study have shown some dependency on quality and therefore Equation 2.5 cannot be expected to predict the data where convective boiling occurred. The percentage errors between the measured data and the *Equation 2.5* are presented in *Table 3.10.* It can be seen that the error associated with the smaller tubes is very much less for the Tran, Wambsganns and France (1995) correlation than for the Lazarek and Black (1982) or Liu and Winterton (1988) flow boiling correlation.

Examination of *Figs.3.68-3.71* showing the comparison between measured heat transfer coefficients and those predicted by *Equation 2.5* shows that the correlation generally under-predicts the measured data, especially in the smallest tubes. However, since there is apparently a significant convective component under some of the conditions tested in this

study, it is to be expected that a correlation based upon entirely nucleate boiling will under-predict the data at high quality in the absence of dryout.

It is also notable that the dependence of the heat transfer coefficient on the Weber number to the power 0.3 implies

$$\alpha \propto d^{0.3}$$

which suggests that the heat transfer coefficient decreases with confinement.

3.8 SUMMARY

A database of heat transfer results from narrow channels has been established and the results from single channel test specimens have been compared with correlations. Existing correlations perform well for R141b at 3.69mm (Co=0.33) but less well as confinement increases.

A very recent correlation proposed by Tran, Wambsganns and France (1995) appears to give the give best agreement especially for small tubes but does not account for the increase in heat transfer coefficient with quality observed in this study.

CHAPTER 4

THEORETICAL CONSIDERATIONS

4.1 INTRODUCTION

In this chapter various aspects of the mechanisms of heat transfer and fluid flow during evaporation in confined spaces are examined. Since the mechanisms and interactions between the mechanisms active in pool boiling and evaporation in large channels are not fully understood it is clear that a full theoretical treatment of boiling in narrow channels is not feasible at the present time. Much of the work is of a pioneering nature and should thus be considered as seeding ideas and approaches which may be developed over the next few years. It is, however, possible to evaluate the contribution of various phenomena under limited conditions and hence estimate their importance in the more general case. The calculations presented in this Chapter indicate which aspects of flow in narrow channels contribute most significantly to boiling heat transfer.

The heat transfer coefficient, α, defined as $q/\Delta T$ is widely used in works on single and multi-phase heat transfer. The justification for using the ratio of heat flux to temperature difference as a measure of heat transfer performance when dealing with a boiling fluid lends itself more to tradition than logic: since the relationship between heat flux and temperature difference is not linear the heat transfer coefficient itself is not constant but a function of q (or ΔT).

Additional difficulty occurs when considering the heat transfer to a boiling fluid from a surface having finite heat capacity, neither the local wall temperature nor the local heat flux are constant with time. Furthermore, in small channels at low pressure the local saturation temperature may also vary significantly with time.

The concepts of temperature difference, heat flux and heat transfer coefficient applied to a situation where all vary with position and time is discussed further in *Appendix 3.*

A description of the mechanism of confined bubble and annular slug flows permits the derivation of a relationship between the quantity of fluid carried through the system in liquid slugs and the magnitude of the measured pressure pulses.

4.2 DEFINITION OF A NARROW CHANNEL

It is clear that, before discussing the mechanisms involved in boiling in narrow channels, the term "narrow" must be given a rational definition. This is necessary in order to determine the size of channel below which established correlations may become unreliable and to distinguish data covering channels which, although physically small, behave in the same way as large channels and those where size effects are significant.

The dimensionless group governing small-size effects adopted in this work is defined as the Confinement Number, Co, such that:

$$Co = \frac{\left[\sigma / \left(g(\rho_l - \rho_g)\right)\right]^{1/2}}{d_e} \tag{4.1}$$

The importance of the Confinement Number in determining the nature of two-phase flow in tubes can be deduced from several reported studies in which parameters, which may be rearranged to give the Confinement Number, have been shown to indicate flow regime boundaries. The Confinement Number, first introduced by Cornwell and Kew (1993), is the reciprocal of the Bond Number. Use of a new group is justified because the Confinement Number has an advantage over the Bond Number in that it increases with increasing physical restriction, and hence increasing influence of confinement. The Confinement Number relates the buoyancy force, which is proportional to $\left(g(\rho_l - \rho_g)\right)d_e^3$, and the surface tension force which is proportional to $\sigma d_e.$, for a bubble of the representative dimension. Increasing Confinement Number thus indicates an increase in the influence of surface tension.

Wallis (1969) provides three equations for the rise velocity of a bubble in a vertical round tube. The choice of governing equation depends upon whether inertia, viscosity, or surface tension produces the dominant force. The condition for surface tension to dominate is given by:

$$N_{EO} = \frac{g d^2 (\rho_l - \rho_g)}{\sigma} < 3.37 \qquad (4.2)$$

Which may be rearranged to give:

$$d < 1.84 \left[\frac{\sigma}{g(\rho_l - \rho_g)} \right]^{1/2} \qquad (4.3)$$

or:

$$Co > \frac{1}{1.84}$$

For Confinement greater than this it is observed that bubbles approaching the diameter of the tube will remain motionless in a vertical tube if the liquid is stationary, i.e. the rise velocity is Zero.

In a separate study Wallis and Makkenchery (1974) showed that counter-current flow of gas and liquid does not occur if the dimensionless tube diameter, d^*, defined by *Equation 4.4*, is less than or equal to 2.

$$d^* = d \Big/ \left[g(\rho_l - \rho_g) / \sigma \right]^{1/2} \qquad (4.4)$$

Examination of *Equation 4.4* shows that d^* so defined is the reciprocal of the Confinement Number. Since slug flow in a vertical tubes involves a film of liquid falling around a rising bubble this suggests that slug flow, as commonly defined (e.g. Collier (1982) and *Section 4.3)* cannot exist in channels for which:

$$Co \geq 0.5 \qquad (4.5)$$

This conclusion is consistent with the earlier observation, in a stationary fluid if a bubble is to rise it implies that liquid must flow down past the bubble - if this cannot occur then the bubble cannot rise.

In their study of boiling in a narrow annulus Yao and Chang (1983) demonstrated that the shape of the boiling curves for water, acetone and R113 varied consistently with the Bond Number, Bo, defined with reference to the width of the annular gap, s,:

$$Bo = \frac{s}{\left[\sigma / \left(g\left(\rho_l - \rho_g\right)\right)\right]^{1/2}} \tag{4.6}$$

They observed that the effects of confinement were significant when the Bond Number was of the order of unity or less. Noting that the hydraulic diameter, d_e, for an annular gap is twice the gap width, s, it can be seen that the Bond Number so defined is equal to half of the reciprocal of the Confinement Number. The condition for confinement effects to be significant is thus, $Co \geq 0.5$, as stated in *Equation 4.5*.

Following an examination of boiling heat transfer from closely spaced fins Bondurant and Westwater (1971) reported that the fins acted independently providing that the fin spacing was greater than the bubble departure diameter. At smaller spacings interaction between the fins was observed. Using the expression, quoted by Kutadeladze (1981), for bubble departure diameter:

$$d_b = 0.02\theta\left[\frac{\sigma}{g\left(\rho_l - \rho_g\right)}\right]^{1/2} \tag{4.7}$$

It can be deduced that the effects of confinement would be expected to be significant if:

$$\frac{\left[\sigma / \left(g\left(\rho_l - \rho_g\right)\right)\right]^{1/2}}{s_f} > \frac{1}{0.02\theta} \tag{4.8}$$

where θ is the contact angle expressed in degrees and s_f is the fin spacing. Contact angles for common fluid surface combinations are typically between 25^o and 90^o (Thome, 1990). The hydraulic diameter corresponding to the gap between two fins would depend upon fin height and spacing but would be between s_f and $2s_f$ hence the condition for confinement effects to be significant would be expected to be in the range:

$$Co > 0.5 - 2$$

The results of Chernobyl'skii and Tananaiko (1956) indicated that the heat transfer coefficient for boiling in an annular gap was approximately constant as the gap width was decreased until the width was close to the bursting diameter of a steam bubble, i.e. $\delta \leq 3\text{mm}$, for smaller gaps significant heat transfer enhancement was achieved. Similar results were reported by Ishibashi and Nishikawa (1969), again with water boiling in an annular space. Results from these two studies are reproduced in *Fig.4.1* to illustrate the change in the influence of the gap thickness occurring at 3mm for water boiling in an annulus.

In addition to the above observations which demonstrate that there is a distinction between the flow and heat transfer mechanisms involved in boiling in narrow channels and those which govern boiling in larger channels it should also be noted that laminar flow conditions are more likely to prevail in small channels than in larger channels and, as shown in *Chapter 1,* conventional boiling correlations are based upon turbulent conditions. It will also be shown, in *Section 4.7,* that, for a given heat flux, the acceleration associated with the growth of confined bubbles in a channel is inversely proportional to the square of the equivalent diameter. The pressure pulsations associated with fluid accelerating in front of confined bubbles therefore can be expected to become more significant in small channels.

4.3 FLOW REGIMES IN NARROW CHANNELS

4.3.1 General

In order to determine the appropriate approach to the analysis of a two-phase, vapour-liquid flow it is necessary to have a knowledge of the interactions between the phases. This, in turn, requires identification of the flow regime or pattern pertaining to the particular conditions.

Many terms describing observed flow patterns have been used in the literature and, since the transitions between the regimes are not clearly defined, the existence of various intermediate regimes has been suggested. The patterns described below are those identified by Collier (1982) as the principal regimes observed in adiabatic, co-current, gas-liquid up flow.

- *Bubble flow* The gas phase is present as discrete bubbles dispersed throughout the liquid phase.

- *Slug flow* Gas bubbles approaching the diameter of the pipe move up the pipe, separated from the wall by a descending liquid film. The gas bubbles have approximately spherical caps (in round tubes). The bubbles are separated by slugs of liquid, which may contain entrained gas bubbles.

- *Churn Flow* Long bubbles formed as slug flow develops become unstable and the gas bubbles and liquid slugs become intermingled. The liquid tends to be displaced towards the tube wall but intermittent, irregularly shaped liquid bridges pass up the tube.

- *Wispy Annular* At high mass velocities the majority of the liquid flow is attached to the duct walls but "fingers" of liquid flow in the gas core.

- *Annular Flow* The liquid phase flows principally as a film on the pipe wall while the gas flows up the central core. Waves forming on the film may break up causing liquid to be entrained in the gas core as discrete droplets.

A further flow regime may be present in heated, evaporating flows at high quality:

- *Drop Flow* Since the presence of the heated wall causes the liquid film to evaporate the wall will dry out prior to the thermodynamic quality of the fluid reaching unity. Drops, entrained in the vapour during annular flow remain in the vapour stream, only evaporating when the bulk vapour temperature is increased to a value slightly above the local saturation temperature.

Fig. 4.2 shows the progression from bubbly flow to drop flow along a vertical boiler tube together with an indication of the fluid and wall temperature variation along the tube.

Experimental observations suggest that in boiling flow in small channels the flow regimes differ slightly from those listed above and that three flow regimes are sufficient to describe the patterns observed. These have been defined:

- *Isolated Bubble Flow* Similar to bubble flow in large channels, bubbles detach from the nucleation sites and flow as discrete units in the liquid, as the flow proceeds further heat addition results in an increase in the number and size of the bubbles.

- *Confined Bubble Flow* Bubbles span the gap (in spaces confined in one dimension) or fill the channel (in spaces confined in two dimensions) and they are separated from the wall by a layer of liquid which evaporates and causes the bubble to grow exponentially. The bubbles may be formed by isolated bubbles growing or coalescing, alternatively single bubbles may reach

a sufficient size to be regarded as confined before becoming detached from their nucleation sites. This latter phenomenon has been observed in relatively large tubes having polished surfaces and has been referred to as *cavitation slug flow* (Hsu and Graham 1963). A similar phenomenon also occurs in the boiling of liquid metals (Morozov et al 1989). The rapid growth of confined bubbles can lead to significant fluctuations in the pressure at entry to the channel and apparent instability in multi-channel arrangements.

- *Annular-Slug Flow*: As the Confined bubbles expand liquid in the slugs between them is either displaced (in spaces confined in one dimension) or deposited on the wall (in spaces confined in two dimensions) and the flow becomes basically annular with random, irregular slugs of liquid interspersed with the vapour.

Fig. 4.3(a) and *(b)* show these regimes schematically for flow confined in one dimension (e.g. between plates) and two dimensions (e.g. in a tube) respectively. Photographic examples of each of these regimes are presented in *Fig. 4.4 (a)-(f)*.

Damianades and Westwater (1988) found three regimes, referred to as bubble, intermittent and annular, sufficient to describe the flow in compact heat exchanger sections. Lowry and Kawaji (1988) described bubble and annular flow and sub-divided the intermittent region into slug and churn flow when examining flow in narrow rectangular passages. Mishima, Hibiki and Nisihara (1993) also working with narrow rectangular ducts divided the flow into four regimes, using the terms bubble, slug, churn and annular. Wilmarth and Ishi (1994) used similar designations for their observations, again in rectangular channels. The designations and descriptions used by Wambsganss et al (1991) include bubble flow, plug and slug flows, and annular flow; additionally, two further regimes, stratified and wave were observed in horizontal flow in a 19mm x 3.18mm rectangular duct with the longer side in the vertical plane.

4.3.2 Flow Regime Boundaries

There have been several attempts to produce maps showing the boundaries between the various flow regimes in adiabatic two-phase flow. Such maps tend to be of limited applicability because of the complexity of the processes involved and the number of parameters which may influence the transition between regimes. Furthermore, the properties which determine one transition may differ from the properties which fix the boundary between another pair of regimes. In adiabatic flow the mode of gas and liquid introduction into the test section can influence the flow regime while for evaporating flows the heat flux, heating length and surface condition are also of influence (Hsu and Graham 1963).

Typically, flow pattern maps are drawn by identification of the flow patterns as areas on a graph with co-ordinates representing superficial liquid and phase velocity (e.g. McQuillan and Whalley, 1985) or superficial phase momentum (e.g. Hewitt and Roberts, 1969).

Identification of boundaries between the flow regimes is further complicated by the influence of the liquid supply characteristics on the flow. The supply may be characterised "hard" if the flow remains constant and is independent of the pressure drop along the channel or "soft" if the supply pressure remains constant and the flow rate varies if the pressure drop characteristics of the channel change. In practice supplies have intermediate characteristics and both test section and inlet pressure vary with time if the flow is unsteady. An example of a soft system which has been observed is a multi-channel test section: the overall flow rate and pressure drop can both remain constant while the flow in individual channels varies significantly and may become negative for short periods. Under such conditions the flow regime at a particular point in a test section must be a function of both upstream and downstream conditions. The tendency to reverse flow in some channels at low quality was noted by Clarke and Blundell (1989) in a study of adiabatic two-phase flow of nitrogen and R113 in a multi-channel plain fin test section comprising channels 1.44mm x 6.2mm. The fluid flowed through seven pads of finning,

each separated by a 3mm gap. The reversing or recirculating flow was in individual pads rather than the entire test section and was associated with the collapse of the liquid film around an elongated bubble. Phenomena related to the local instantaneous quality varying with time are likely to be more marked in situations involving heat transfer. The unsteady nature of the flow observed in the current study was extremely marked and reversing or recirculating flow frequently caused the expulsion of gas into the inlet manifold of the test section followed by passage of this gas into adjacent channels.

In general position of the flow regime boundaries may depend upon:

System geometry

Diameter

Shape 1....n

Flow parameters

Liquid Superficial Mass Flux (or Liquid Superficial Velocity)

Vapour Superficial Mass Flux (or Vapour Superficial Velocity)

Equilibrium Quality

Heat Flux

Fluid Properties

Liquid Viscosity

Vapour Viscosity

Liquid Density

Vapour Density

Surface Tension

Latent Heat of Vapourisation

The inclusion of the heat flux and latent heat is necessary as these two parameters determine the rate of change of equilibrium dryness fraction and hence the rate of bubble growth.

The above parameters may be combined in dimensionless form to yield groups which may be important in determining the flow regime.

Examples of appropriate dimensionless groupings include:

Boiling Number : $$Bo = \frac{q}{Gh_{fg}}$$

Confinement Number : $$Co = \left(\frac{\sigma}{g(\rho_l - \rho_g)} \right) \Big/ d_e$$

Momentum Flux Ratio: $$MF_{ratio} = \frac{G_f^2 \rho_g}{G_g^2 \rho_l}$$

Viscosity Ratio: $$\mu_{ratio} = \frac{\mu_g}{\mu_l}$$

Capillary Number $$Ca = \frac{\mu_f J}{\sigma}$$

Providing that the flow is close to its equilibrium quality the influence of quality would be expected to be accounted for in the Momentum Flux Ratio.

Even for conventionally sized round tubes the rationale for determining the flow boundaries has not been established. It is therefore beyond the scope of this study to produce a comprehensive flow map for narrow channels. The transition to annular or Annular Slug Flow is of the most importance in determining heat transfer coefficients and a model is proposed below. Several mechanisms have been reported to explain this transition and criteria for the conditions at this transition have been derived.

Wallis (1969) noted that in annular, upward flow in vertical tubes the liquid and gas flows are concurrent and, based upon experiments with liquid injected through a porous wall into a gas flow, observed that the liquid film so formed flowed downwards at low gas

velocity and upwards at high gas velocity. The transition occurred at a value of dimensionless gas superficial volume flux, j_g *, defined by *Equation 4.9*, of 0.9. It is now a frequently used "rule of thumb" that the onset of annular flow corresponds to j_g * being equal to unity (McQuillan and Whalley 1985).

$$j_g * = j_g \rho_g^{0.5} \left(gD(\rho_l - \rho_g) \right)^{-0.5} \tag{4.9}$$

A similar approach was taken by Mishima and Ishi (1984) leading to a prediction of the onset of annular flow when:

$$j_g * = v - 0.11 \tag{4.10}$$

with the void fraction calculated from:

$$v = \frac{j_g}{C_0 j_T + 0.35 \left(Dg(\rho_l - \rho_g)/\rho_l \right)^{0.5}} \tag{4.11}$$

and

$$C_0 = 1.35 - 0.35 \left(\frac{\rho_g}{\rho_l} \right)^{0.5} \tag{4.12}$$

Based upon an investigation of the variation of slug passing frequency with flow parameters Jones and Zuber (1979) suggested that the transition to annular flow would occur when the predicted passing frequency of liquid slugs becomes zero and showed that this occurred when:

$$j_g * = 4 \left(\frac{\rho_g}{\rho_l} \right) (j_l * + K) \tag{4.13}$$

and:

$$j_l * = j_{;} \rho_g^{0.5} \left(gD(\rho_l - \rho_g) \right)^{-0.5} \tag{4.14}$$

The value of K, the drift coefficient, recommended was 0.35 for tubes and (0.23+0.13*s/w*) for rectangular sections. The value of D recommended for use in the rectangular section was equal to w.

Taitel et al (1980) examined each transition. For the transition to annular flow they suggested that annular flow would occur when the gas velocity was sufficient to entrain and carry the largest stable droplet. Using their analysis the transition occurs at a value of superficial gas velocity determined from:

$$j_g = \frac{3.1\left(\sigma g\left(\rho_l - \rho_g\right)\right)^{0.25}}{\rho_g^{0.5}} \tag{4.15}$$

For air water flows at atmospheric pressure and 20°C this yields a value of approximately 15m/s for the gas superficial gas velocity at transition, irrespective of liquid flow rate or channel dimension. However, implicit in the analysis is a prediction of stable drop size which, for air-water flows at transition, is of the order of 20mm. Clearly such droplets cannot exist in confined passages. However, Caetano et al (1992) showed that the prediction due to Taitel et al proved to give excellent agreement for the transition to annular flow for air and water at water superficial velocities up to 0.5m/s in a concentric annulus with internal diameter 42.2mm and external diameter 76.2mm (i.e. gap spacing 17mm) and agreement up to a water superficial velocity of 1m/s in an eccentric annulus made from the same tubes.

A model specifically derived for flow in confined spaces is that of Lowry and Kawaji (1988). They reported on a study of air and water flow through a narrow passage between two flat plates with a gap width of 0.5-2mm noting that large tube predictions did not give adequate results for the flow transition to annular flow. They derived the following model to predict this transition.

It was observed that in narrow channels neither spherical nor axi-symmetric Taylor bubbles could form therefore predictions based upon the existence of such bubbles (e.g. Jones and Zuber, 1979) would not be valid. In formulating their model it was assumed that as the flow approached the annular transition the majority of the liquid was deposited on the wall and the quantity of liquid contained in liquid bridges was negligible. Annular flow was assumed to occur when the axial pressure gradient was sufficient to overcome the surface tension forces which tend to maintain the bridge. The work was carried out

with vertical channels but, since it was assumed that the gravity forces were negligible it is reasonable to assume that the analysis should apply to horizontal flow. A schematic representation of the bridge is shown in *Fig.4.5*.

With the assumption of negligible liquid flow in the bridges compared with the flow in the film, the gas velocity (assumed uniform in the core) was given by *Equation 4.16*.

$$u_g = \frac{J_g}{v} \tag{4.16}$$

A linear velocity distribution was then assumed for the film with zero velocity at the wall and u_{Li} at the gas-liquid interface.

$$u_{Li} = 2j_l(1-v) \tag{4.17}$$

A further assumption was then made that :

$$u_{Li} = u_g \tag{4.19}$$

This implies that there is continuity of velocity at the gas-liquid interface and hence no shear stress at the interface, an assumption which cannot be justified.

Combining *Equations 4.16-4.18* gave an expression for the void fraction:

$$v = \frac{j_g}{j_g + 2j_l} \tag{4.19}$$

The frictional pressure drop was derived from the velocity gradient in the liquid film and given by:

$$\frac{dp}{dz} = \frac{8\mu_l j_l}{(1-v)^3 s^2} \tag{4.20}$$

For stability of the bridge it was asserted that the pressure force on the bridge must be less than the surface tension forces acting at the intersection of the lower surface of the bridge and the liquid film, i.e.

$$F = 2\sigma w \tag{4.21}$$

The pressure force was calculated from the average bridge thickness, z', and the pressure gradient. When the minimum bridge thickness approaches zero the average thickness is given by:

$$z' = \left(1 - \frac{\pi}{4}\right)\frac{vs}{2} \tag{4.22}$$

Thus, equating the pressure force from *Equation 4.20*, integrated over a length equal to z', and the surface tension force from *Equation 4.21* and rearranging:

$$\frac{(1-v)^3}{v^2} = \frac{(2-\pi/2)\mu_l j_l}{\sigma} \tag{4.23}$$

which can be combined with *Equation 4.19* to yield a value of j_g corresponding to the transition to annular flow for a given value of j_l.

The analysis described above is flawed in that assumptions which were made in its derivation cannot be supported. Firstly the assumptions regarding the velocity profiles, that is, continuity of velocity across the liquid-gas interface and constant velocity in the gas, cannot be sustained, since the liquid film flow must be maintained by the shear stress at the interface. Secondly, the pressure gradient derived was that in the region remote from the bridge. There does not appear to be any justification in assuming that the pressure gradient in the region of the bridge is equal to this gradient.

The predictions of Lowry and Kawaji (1988) give good agreement with their own data for a 2mm gap but under predicted the gas superficial velocity for transition to annular flow for a 1mm gap.

The data of Wilmarth and Ishi (1994) with air and water in narrow rectangular gaps of 1 and 2mm suggests that transition to annular flow occurs at a gas superficial velocity of approximately 5m/s in both sections for liquid superficial velocities of 0.05- 0.5 m/s. This compares with a value of gas superficial velocity of 0.28-1 m/s predicted by Lowry and Kawaji over the same range. Wilmarth and Ishi claim good agreement with the prediction of Lowry and Kawaji for the 2mm section but examination of the figures presented

suggests that they have compared their data for slug-churn flow transition with the Lowry and Kawaji prediction for the onset of annular flow.

It should be noted that Wilmarth and Ishi observed different flow patterns and transitions for horizontal and vertical flow in their 2mm test section. The assumption that vertical and horizontal flows in spaces confined in one dimension must therefore be treated with care. Wambsganss et al (1991) did not observe stratified flow in a horizontal passage 19mm x 3.18mm when the longer side was horizontal.

In addition Wilmarth and Ishi compared their data showing the transition to annular flow with the experimental data of Mishima et al (1991) and Ali and Kawaji (1991) for vertical flow and with the map of Wambsganss et al (1991) for horizontal flow. There was good agreement with the experimental data of Ali and Kawaji and reasonable agreement with that of Mishima et al.

The flow visualisation techniques used in this study were not suitable for use in the determination of the position of flow boundaries because the existence of recirculation or reversing flows coupled with the relatively short length over which the intermediate regimes existed made it impossible to relate local quality, and hence vapour and mass fluxes, with the flow regime at any given time. Not only was it found that, as in other studies, the precise position of the various transitions was unclear it appeared that, under most conditions the position of the transition moved with time.

4.3.3 A Model for the Transition from Confined Bubble to Annular Slug Flow

A model is proposed for the transition from Confined Bubble Flow to Annular Slug Flow based upon the premise that the thickness of the liquid layer on the wall in the Confined Bubble Regime is governed by viscous deposition and the layer is essentially stationary. In the Annular Slug Flow regime the liquid layer flow characteristics are governed by the shear force between the liquid and gas or vapour core. The regime which is predicted by the proposed model is that which would result in the thinner liquid layer on the wall.

In the Confined Bubble Region the mechanism of deposition is described by Taylor (1963) for flow of gas bubbles in a capillary tube. Taylor presented results graphically and demonstrated that the ratio of bubble velocity to the velocity of the liquid in front of the bubble and hence the film thickness could be expressed in the form:

$$\delta = f(Ca) = f\left(\frac{\mu_l j}{\sigma}\right) \tag{4.24}$$

This relationship has been presented by Wallis (1969)

$$C_T = 1 + 1.27(1 - \exp(-3.8Ca^{0.8}) \tag{4.25}$$

$$\delta_{CB} = \frac{(C_T - 1)}{C_T}\frac{D}{4} \tag{4.26}$$

The film thickness which would pertain in Annular Flow may be determined from a force balance across the film and this approach has been used in very narrow channels by Moriyami and Inoue (1992). A simpler approach is to assume that all the liquid flows in the wall film and to estimate the void fraction and thence the film thickness. Several void fraction correlations are available (see *Chapter 1, Table 1.4*) however the CISE correlation for slip ratio (Premoli et al, 1970) presented here as *Equation* 1.*45* is regarded as having wide applicability and has recently been shown by Bao et al (1994) and Azzopardi and Holt (1995) to be appropriate for use in narrow channels.

Having calculated the film thickness using the two approaches above for a given flow it is assumed that the flow regime which exists is that yielding the lower film thickness.

Figures 4.6(a) and *(b)* illustrate the variation in predicted film thickness with dryness fraction (defined by *Equation 4.27*) for air-water mixtures in channels of 1 and 5mm diameter respectively.

The model has been tested against the results of Damianades and Westwater for tubes in the range 1-5 mm diameter. The air and water velocities at transition were calculated from the predicted quality, x, using Equation 4.27 to relate the respective mass flows.

$$x = \frac{\dot{m}_{air}}{\dot{m}_{water} + \dot{m}_{air}} \tag{4.27}$$

The results of this comparison are shown on *Fig. 4.7.*The prediction of the model is also tested against the map of Hewitt and Roberts (1969) and the results are plotted on *Fig 4.8.*

Limited experimental observations from this study are also plotted on *Fig 4.8* for comparison purposes.

The transition values predicted by the proposed model follow the same trend as the experimental values of Damianades and Westwater (1988) as shown on *Fig. 4.7.* The model and the reported experimental results both show that the transition to Annular Slug Flow occurs at a superficial air velocity which is largely independent of the water velocity. The air velocity at transition increased by a factor of 2 over a range of water superficial velocities varying by a factor of almost 100. The predicted value of transition occurs at a value of air velocity approximately one quarter of that observed by Damianades and Westwater. Hewitt and Roberts (1969) suggest that the transition is independent of liquid flow over most of the range of interest. The model under-predicts the vapour momentum flux for transition at low liquid flows and over-predicts the transition value of the transition vapour momentum flux at high flows.

The experimental results which have been plotted suggest that the transition value of vapour momentum flux increases significantly with increasing liquid momentum flux, at least in boiling flow. The value of transition vapour momentum flux is below that observed experimentally.

4.4 HEAT TRANSFER MECHANISMS

4.4.1 General

As outlined in *Chapter 1* it is conventional (e.g. Chen (1963), Shah (1982), Liu and Winterton (1988)), to consider two mechanisms, nucleate boiling and forced convection, to contribute to heat transfer in flow boiling and to combine the contributions of these methods either additively or to take the larger of the two as the total heat transfer. The rationale for assessing the relative combination of the two mechanisms is currently subject of some debate (Hewitt 1995). While the several correlations give satisfactory results over their range of application this can be explained by the incorporation of empirical constants rather than seen as confirmation that they have a sound physical basis.

It has been shown by Cornwell and Schuller (1982) and Cornwell, Houston and Addlesee (1992), that heat transfer through the microlayer deposited under sliding bubbles makes a significant contribution to boiling on tubes in the higher rows of tube bundles. While sliding bubbles contribute little to the heat transfer in boiling in large diameter tubes their contribution is considerable in confined spaces, especially at low flow rates and heat fluxes and low quality. It is argued in *Section 4.2* that in a confined space vapour liquid counter-flow cannot occur, therefore the conventional slug flow regime cannot exist. The slug flow regime is replaced by the confined bubble regime and the heat transfer analysis of these bubbles is similar to that applied to sliding bubbles, at least at low vapour and liquid velocities.. At high quality annular slug flow is likely to occur and the heat transfer mechanism is then by conduction and convection through the annular layer of liquid flowing along the heat transfer surface.

4.4.2 Summary of Mechanisms

Nucleate Boiling

The nucleate boiling contribution to the heat transfer relate to the formation and growth of bubbles on the heated surface. Appropriate correlations, of the form given in *Equation 1.8* are summarised in *Table 1.1* and the most convenient forms of *Equation 1.8* are reproduced below:

$$q_{nbp} = a\,\Delta T_{sat}^{m} \qquad (1.8(a))$$

$$\alpha_{npb} = b\,q^{n} \qquad (1.8(b))$$

In flow boiling correlations it is usually assumed that the nucleate boiling heat transfer coefficient is reduced by a factor S, where S is a suppression factor dependent upon the mass flux and quality. Hence *Equation 1.8(b)* becomes:

$$\alpha_{nb} = Sbq_{nb}^{n} \qquad (4.28)$$

Where the subscript *nb* indicates the nucleate boiling component of the heat transfer.

Table 1.1 shows that the value of the constant, n, is between 0.5 and 0.7 and b is a constant which depends upon fluid properties, and may be determined from the critical and reduced pressures of the fluid or from known fluid properties. The existence of the suppression factor is disputed by some workers.

Forced Convection

Heat is transferred to the liquid flowing over the surface by forced convection, the heat transfer coefficient depends upon the local liquid superficial velocity and the dryness fraction and is conventionally evaluated:

$$\alpha_{conv} = F\alpha_{l} \qquad (4.29)$$

$$\alpha_{l} = 0.023\frac{k_{l}}{d_{e}} Re_{l}^{0.8} Pr_{l}^{0.4} \qquad (4.30)$$

F is an enhancement factor which takes into account the additional turbulence and velocity induced by the presence of vapour in the flow. Various correlations are available for use in the calculation of F. The subscript *l'* in *Equation 4.30* may refer to all fluid flowing as liquid or for the liquid component flowing alone.

An alternative method for evaluating the convective heat transfer coefficient in the annular flow regime is to use a film flow model:

$$\alpha_{conv} = \frac{k_l}{\delta_f} Nu_f \tag{4.31}$$

This model is outlined *Chapter 2* and has been applied to compact heat exchangers by Robertson 1982 and is further developed in *Chapter 5*.

Heat Transfer to Sliding Bubbles

This mechanism has been investigated by Cornwell and co-workers (e.g. Cornwell, Houston and Addlesee (1992)) and has been shown to be a significant factor when boiling occurs in tube bundles. Heat is transferred by conduction through the liquid layer deposited beneath confined bubbles due to viscous forces. Evaporation from this layer to the bubble causes the bubble to grow. In spaces confined in only one dimension the bubbles may move or remain essentially stationary while growing, and the velocity of the bubble perimeter remain relatively low. An allowance must be made for the thinning of the layer due to evaporation, indeed, the layer may eventually dry out. Assuming that a representative film thickness can be determined and dry out does not occur:

$$\alpha_{sb}' = \frac{k_l}{\delta'} \tag{4.32}$$

where α_{sb}' is the heat transfer coefficient pertaining to the area covered by the bubble and δ' is the appropriate film thickness. This is essentially the same as the film model but applies only to the area covered by a bubble and contains the implicit assumption that the film Nusselt Number, Nu_f, is equal to unity.

Heat Transfer to Growing Bubbles

The mechanism of heat transfer to growing bubbles is similar to that described as heat transfer to sliding bubbles, however it is more appropriate to situations where a space is confined in two dimensions, the vapour generated in the bubble must cause the front of the bubble to accelerate and the relatively high velocity of the liquid vapour interface leads to a thickening of the layer deposited. The heat transfer coefficient can be calculated from *Equation 4.32* .

Transient Conduction.

A model which incorporates transient conduction to explain enhanced heat transfer in confined spaces been used by workers investigating natural circulation boiling in narrow channels (Nishikawa and Fujita, 1990) and the enhancement of heat transfer by passing bubbles (Kusuda, 1981 and Monde, 1988). The transient conduction model is described in *Chapter 2* and a modified version is presented in *Section 4.6*. The results of this analysis show that the contribution of transient conduction is small for the conditions investigated.

4.4.3 Combination of Heat Transfer Mechanisms.

The contributions of the various heat transfer mechanisms may be combined.

$$q = f(q_{nb}, q_{conv}, q_{sb}) \tag{4.33(a)}$$

Similarly, for the three mechanisms to the heat transfer coefficient:

$$\alpha = f(\alpha_{nb}, \alpha_{conv}, \alpha_{sb}) \tag{4.33(b)}$$

The way in which the coefficients should be combined is discussed below. The conventional approaches assume that the mechanisms of nucleate boiling and convective heat transfer occur simultaneously and continuously at any particular point on the heat transfer surface. The degree to which the two mechanisms interact is open to debate as discussed in *Chapter 1*. In Annular Slug Flow in confined spaces the situation is essentially the same. However in the Confined Bubble region the situation differs somewhat.

In narrow spaces confined in one dimension it is clear from *Fig. 4.9* that at low quality (and if this is to occur over a significant area this implies relatively low heat flux) heat transfer to confined bubbles may occur over a portion of the surface while nucleate boiling and convection to essentially single phase liquid accounts for the heat transfer over the remainder of the surface.

When the space is confined in two dimensions then the space is occupied at a given instant either by a confined bubble or by a liquid slug, and the heat transfer mechanism thus varies with time.

The case of a channel confined in one dimension is now considered in more detail. In the confined bubble region heat transfer by conduction through the layer under a bubble can only occur in the area covered by a bubble, while nucleate boiling and forced convection occur when the surface is covered by flowing liquid. If it is assumed that the volume of vapour in confined bubbles greatly exceeds the volume which exists in isolated bubbles, and the flow between the confined bubbles behaves as if it is entirely liquid then one of three situations may occur::

$$\alpha = (1 - v')\alpha'_{conv} . + v' \alpha'_{sb} \qquad (4.34(a))$$

or

$$\alpha = (1 - v')\alpha'_{nb} . + v' \alpha'_{sb} \qquad (4.34(b))$$

or

$$\alpha = \alpha_{nb} \qquad (4.34(c))$$

where the " ' " symbol denotes the value of the coefficient in the region where the particular mechanism is active and v' is a modified void fraction defined with reference to *Fig.4.3*. The total heat transfer coefficient, α, is the average coefficient at a given value of the Z co-ordinate for the case of a space which is confined in one dimension. *Equation 4.34(a)* represents the case where both the convective and sliding bubble coefficients are larger than that predicted for nucleate boiling at the relevant temperature difference. *Equation 4.34(b)* would be used if the nucleate boiling coefficient was greater

than the convective, but less than the sliding bubble coefficient and Equation *4.34(c)* represents the case when nucleate boiling dominates.

Table 4.1 gives indicative values for the local convective, nucleate boiling and sliding bubble coefficients for R141b at 1 bar in a channel with a 2mm gap, the nucleate boiling coefficient is evaluated at 3°C, the level above which Tran, Wambsganss and France (1995) suggest nucleate boiling would dominate evaporation in confined spaces.

Since both α_{nb} and α_{conv} are relatively low under these conditions the heat transfer coefficient is approximately equal to $v'\alpha'_{sb}$ for the space confined in one dimension. This has been confirmed by examination of the rate of growth of confined bubbles at low quality and heat flux. The analysis is given in *Section 4.5.*

It can be shown that for tubes and channels of the size considered in this study the sliding bubble heat transfer coefficient must be higher than the laminar convective heat transfer coefficient. For laminar flow the Nusselt Number is a constant of the order of 3, depending upon the duct shape and the boundary conditions.

$$Nu_{conv} = \frac{\alpha_{conv} d_e}{k_l} = \text{Constant} \tag{4.35}$$

The heat transfer coefficient from the surface under a sliding bubble is given by *Equation 4.33.* Combining *Equations 4.33* and *4.35* gives:

$$\frac{\alpha_{sb}}{\alpha_{conv}} = \frac{d_e}{Nu_{conv}\delta_f} \approx \frac{d_e}{3\delta_f} \tag{4.36}$$

and since $\delta_f \approx 10-20\mu m$ this Equation suggests that the sliding bubble heat transfer coefficient would be greater, by a factor of approximately thirty, than the convective heat transfer coefficient to the liquid. The contribution of convection to the liquid can thus be neglected unless significant enhancement occurs due to the presence of confined bubbles.

An analysis of the enhancement of single phase convection due to the presence of the confined bubbles shows that the enhancement is not significant, even in turbulent flow,

and any enhancement will be outweighed by the reduction in area over which the mechanism is effective as the void friction increases. If it is assumed that the flow is homogeneous, that is the vapour and liquid velocities are equal, then the flow may be divided:

$$\dot{m}_{flow} = \dot{m} - \dot{m}_{cb} \tag{4.37}$$

$$A_{flow} = A - A_{cb} \tag{4.38}$$

Where m represents the entire mass flow rate and $\dot{m}_{flow}$ and $\dot{m}_{cb}$ pertain to the mass flowing in the between the confined bubbles and in the confined bubbles. Similarly A, A $_{flow}$ and A_{cb} represent the relevant flow areas.

The areas for the flow are related:

$$A_{cb} / A = L_c / L = v' = (1 - A_{flow}) / A \tag{4.39}$$

Where L is the total width of the channel and L_c is the width covered by vapour in confined bubbles.

Parameters for the flow other than that in the confined bubbles are related to the total flow and flow within the confined bubbles by:

$$G_{flow} = \frac{\dot{m}\left(1 - L_c / L\left(x + (1-x)\rho_g / \rho_f\right)\right)}{(L - L_c)s} \tag{4.40}$$

$$x_{flow} = \frac{\left(x - L_c / L\left(x + (1-x)\rho_g / \rho_f\right)\right)}{\left(1 - L_c / L\left(x + (1-x)\rho_g / \rho_f\right)\right)} \tag{4.41}$$

From *Equations 4.41 and 4.42*

$$G_{flow}\left(1 - x_{flow}\right) = \frac{\dot{m}(1-x)}{(L - L_c)s} \tag{4.42}$$

Alternatively, *Equation 4.42* may be derived intuitively; the liquid flow rate is $\dot{m}(1-x)$ and this flows entirely through the gaps between confined bubbles.

The Reynolds number is then given by:

$$\mathrm{Re}_{l,flow} = \frac{G_{flow}\left(1-x_{flow}\right)d'_e}{\mu} = \frac{\dot{m}(1-x)d'_e}{\left(L-L_c\right)s\mu} \tag{4.43}$$

Considering the flow in the channels between adjacent confined bubbles in may be observed that the wetted perimeter is equal to twice the distance between adjacent bubbles, the remaining channel boundaries being the liquid-vapour interface, and the channel area is equal to the product of the distance between bubbles and the gap spacing. The hydraulic diameter, d'_e for flow channels between the confined bubbles is therefore independent of the distance between bubbles or the void fraction and is equal to twice the gap spacing.

The convective heat transfer coefficient calculated using the Dittus-Boelter Equation is proportional to the Reynolds Number to the power 0.8, the ratio of convective heat transfer coefficient to that which would pertain if all the fluid flowed as liquid using the entire channel may be evaluated:

$$\frac{\alpha_{flow}}{\alpha_L} = \left(\frac{\dot{m}(1-x)d'_e}{\left(L-L_c\right)s\mu} \Big/ \frac{\dot{m}d_e}{Ls\mu}\right)^{0.8} \tag{4.44}$$

which reduces to:

$$\frac{\alpha_{flow}}{\alpha_L} = \left(\frac{L(1-x)}{\left(L-L_c\right)}\right)^{0.8} \tag{4.45}$$

The area through which the heat transfer to the liquid occurs is reduced by the presence of confined bubbles so the net effect on the liquid heat transfer may be determined:

$$\frac{\alpha_{flow} A_{flow}}{\alpha_l A} = \left(\frac{L(1-x)}{(L-L_c)} \right)^{0.8} \left(\frac{(L-L_c)}{L} \right) \approx \left(\frac{(L-L_c)}{L} \right)^{0.2} . \qquad (4.46)$$

at low values of x.

This suggests that the contribution of the heat transfer to the liquid by convection would be reduced by the presence of confined bubbles but by less than the effective area reduction. However, *Equation 4.36* is based upon the assumption that the flow is turbulent under all conditions. If the flow is laminar throughout the range then the liquid convective heat transfer coefficient would be unaffected by the change in Reynolds Number and the contribution of this mode of heat transfer would be proportional to $(L-L_c)/L$. On the other hand, an increase in the Reynolds Number causing transition from laminar to turbulent flow in the gaps between confined bubbles would lead to a greater enhancement in the convective heat transfer coefficient.

Fig. 4.10 indicates the predicted heat transfer coefficients for water and R141b based upon a constant Nusselt Number in the laminar region and the Dittus Boelter Equation in the turbulent region. The shaded regions indicate the range of Reynolds Numbers in which tripping from laminar to turbulent flow would create enhancement.

4.5. THE LAYER EVAPORATION MODEL OF CONFINED BUBBLE HEAT TRANSFER

4.5.1 The Model

The model described in this section is applicable to heat transfer in the Confined Bubble Regime and has been verified by the experimental analysis of bubble growth at low mass flow rate and heat flux. It is based upon the heat transfer being primarily through a thin layer liquid deposited on the surface under the moving and expanding bubble. Bubble growth is then due to the evaporation of this layer. (Note that, since the bubble is assumed to be stationary or moving slowly the subscript 'CB' referring to confined bubble rather than 'SB' referring to sliding bubble). A confined bubble is shown schematically in *Fig 4.11*.

If it is assumed that evaporation from the perimeters of the bubbles is negligible compared to that at the metal surface, then the volume rate of growth of the bubbles is related to the heat flux q_{CB} through the layer of area A_b on the surface by

$$\frac{dV}{dt} = \frac{q_{CB} A_b}{\rho_g h_{fg}} \tag{4.47}$$

It is further assumed that the layer has a characteristic mean thickness of d on both sides of the gap of thickness, s.

$$\frac{dV}{dt} = (s - 2\delta)\frac{dA_b}{dt} \tag{4.48}$$

Equating these equations and integrating from an initial condition (suffix o) yields

$$A_b = A_{bo} \exp\left[B(t - t_o)\right] \tag{4.49}$$

where

$$B = \frac{q_{CB}}{(s - 2\delta)\rho_g h_{fg}} \tag{4.50}$$

This allows an estimate of q_{CB} to be made (independently of δ as it is found that $\delta << s$) which may be related to the measured mean value of heat flux q by

$$q_{CB} = q / \nu \tag{4.51}$$

The voidage, ν, used in *Equation 4.51* is the time averaged void fraction for the area. The value of q_{CB} calculated from *Equations 4.50* and *4.51* are in reasonable agreement under most conditions.

Finally an estimate may be made of the mean layer thickness by assuming pseudo-steady-state conduction through the layer; not unreasonable for the very thin layer involved under sliding bubbles. The surface temperature is taken as the mean measured value for the purposes of the estimate although it will be rather lower under the bubble. Thus

$$q_{CB} = \frac{k_f \Delta T_{sat}}{\delta} \tag{4.52}$$

Substituting this value into *Equation 4.50* and rearranging:

$$\frac{S \rho_g h_{fg}}{\Delta T k_f} \ln \frac{A_b}{A_{bo}} = \frac{1}{\delta}(t - t_o) \tag{4.53}$$

A plot of $\left[\left(S \rho_g h_{fg}\right) / \Delta T k_f\right] \times \ln \frac{A_b}{A_{bo}}$ against $(t - t_o)$ should thus have a gradient equal to δ^{-1}. *Fig.4.12 (a)* and *(b)* shows plots for the conditions detailed in *Table 4.2. Fig 4.13* shows the growth of a bubble typical of those analysed.

The experimental estimate of layer thickness must be taken as very approximate owing to its variation with time and position under the bubble and doubts about the true surface temperature. However, it should be noted that the layer thickness is of the same order of magnitude as that found from heat transfer measurements to and from sliding bubbles in previous work Cornwell, Houston and Addlesee (1992).

Under the conditions analysed there was no local drying-out of the layer under as there was no visual impression of bubbles sticking to the wall within the flow and calculations of the evaporation rate over the time of observation indicate that, even at very low rates of bubble movement the layer would not evaporate entirely. The mean film thickness over the entire area of the bubble is shown in *Section 4.5.2* to be of the order of 75% of the thickness laid down by the moving boundary of the bubble.

The estimated value is also bounded by values which have been obtained under conditions where dryout occurred.

Under some conditions momentary dryout has been observed during the passage of confined bubbles over a flat plate with cover. Most of the surface was observed to be covered with a liquid film which was periodically refreshed by passing liquid bridges or slugs. Examination of high speed (200 frames/second) video recordings permitted an estimate of the time between passage of a slug and appearance of a dry patch to be made.

Conditions observed were:

Fluid R141b

Heat Flux, q, = 30.7kW/m^2

Heat Transfer Coefficient, α,3.6kW/m^{2}K

Time to Dryout (approximate), t_d,=0.1 seconds

Enthalpy of Vapourisation, h_{fg}, = 222kJ/kgK

Liquid Thermal Conductivity, k_l, =88 x 10^{-6}kW/mK

Liquid Density, k_l, =1220kg/m^3

The rate of change of the layer thickness due to evaporation is given by:

$$\frac{d\delta}{dt} = -\frac{q}{\rho_l h_{fg}} \tag{4.54}$$

Integrating:

$$(\delta_0 - \delta) = \frac{q}{\rho_l h_{fg}} t \tag{4.55}$$

At t_d dryout occurs therefore $\delta=0$ and Equation A3.2 yields:

$$\delta_0 = \frac{q}{\rho_l h_{fg}} t_d \tag{4.56}$$

Substitution of the appropriate values leads to an estimate of initial film thickness of 11μm.

The heat transfer coefficient would be expected to be given by:

$$\alpha = \frac{k_l}{\delta_r}$$

since the surface was almost entirely covered by the film. This yields a value of δ_r, the representative film thickness, of 24μm. As expected this is higher than the value estimated from the time to dryout because dry out occurs first at the thinnest portion of the film.

Both of the above estimates must be regarded as approximate but they provide support to the estimate of 10-20μm thickness for the film laid down by slowly moving bubbles.

4.5.2 Representative Film Thickness

The analysis presented above involves the implicit assumption that the film thickness remains constant throughout the period of bubble growth. In reality the film thickness will decrease as the layer evaporates and the average film thickness will therefore be less than the thickness of the film laid down on the surface by the retreating liquid as the bubble expands. If the thickness of film laid down at the perimeter of the bubble remains constant as the bubble expands and it is assumed that the heat flux through the film is constant then the mean thickness of the film as the bubble grows may be related to the original film thickness. For simplicity, it is again assumed in the following analysis that the bubble is cylindrical in shape, having radius r_{max} and height equal to the gap spacing, s.

Equating the mass of liquid evaporating from the film to the mass of vapour generated:

$$\frac{dA}{d\delta} = -\frac{A\rho_l}{s\rho_g} \tag{4.57}$$

and since $A = \pi r^2$ leading to $dA = 2\pi r\, dr$:

$$\frac{dr}{d\delta} = \frac{-r\rho_l}{2s\rho_g} \tag{4.57(a)}$$

The rate of evaporation of the liquid layer is given by:

$$\frac{d\delta}{dt} = \frac{-q_{CB}}{\rho_l h_{fg}} \tag{4.56}$$

Combining *Equations 4.56* and *4.57* gives:

$$\frac{dr}{dt} = \frac{q_{CB}\, r}{2s\rho_g h_{fg}}$$

which may be integrated:

$$\ln\frac{r}{r_0} = \frac{q_{CB}(t - t_0)}{2s\rho_g h_{fg}} \tag{4.58}$$

Therefore the time t is related to the radius of the bubble r_{max} at that time by:

$$(t - t_0) = \frac{2s\rho_g h_{fg}}{q_{CB}} \ln\frac{r_{max}}{r_0} \tag{4.59}$$

and r_0 is the bubble radius at time t_0 and is approximately equal to the gap width, s, when the bubble is first confined.

At the perimeter of the bubble the film thickness is δ_0, prior to evaporation from the film. Integrating *Equation* 4.55 gives:

$$\delta_{r,t} = \delta_0 - \frac{q_{CB}t'}{\rho_l h_{fg}} \tag{4.60}$$

where $t' = (t - t_r)$, $\delta_{r,t}$ is the film thickness at radius r, and t_r is the time at which bubble perimeter reached radius r. i.e.

$$t' = (t - t_0) - (t_r - t_0) \tag{4.61}$$

Combining *Equations 4.59* and *4.60* leads to:

$$\delta_r = \delta_0 - \frac{q_{CB}}{\rho_l h_{fg}}\left((t-t_0) - \frac{2s\rho_g h_{fg}}{q}\ln\frac{r}{r_0}\right) \tag{4.62}$$

and further substitution from *Equation 4.59* and simplification leads to an expression for the film thickness, δ_r, at radius r when the bubble has a radius r_{max}.

$$\delta_r = \delta_0 - 2s\frac{\rho_g}{\rho_l}\ln\frac{r_{\max}}{r} \tag{4.63}$$

The mean film thickness may be determined from:

$$\begin{aligned}\delta_{mean} &= \frac{1}{A}\int_A \delta_r\, dA \\ &= \frac{1}{\pi\left(r_{max}^2 - r_0^2\right)}\int_{r_0}^{r_{\max}} 2\pi r\delta_r\, dr\end{aligned} \tag{4.64}$$

Substituting for δ_r from *Equation 4.63* and simplifying gives:

$$\delta_{mean} = \frac{2}{\left(r_{max}^2 - r_0^2\right)}\int_{r_0}^{r_{\max}} r\left(\delta_0 - 2s\frac{\rho_g}{\rho_l}\ln\frac{r_{\max}}{r}\right)\delta_r\, dr \tag{4.65}$$

Integrating *Equation 4.65* and rearranging yields:

$$\frac{\delta_{mean}}{\delta_0} = 1 - \frac{s\rho_g}{\delta_0\rho_l}\left[1 - \frac{2r_0^2}{\left(r_{max}^2 - r_0^2\right)}\ln\frac{r_{max}}{r_0}\right] \tag{4.66}$$

Equation 4.63 giving the profile of the film thickness and *Equation 4.66* giving the mean value of film thickness over the area of a growing bubble are valid only if the film does not dry out at any point. For the idealised bubble considered here dry out would be expected to first occur in the region $r \le r_0$. The maximum radius to which a bubble can grow prior to dry out occurring may then be determined from *Equation 4.56*. Fig 4.14 illustrates the profile of the film during growth of an idealised bubble.

4.5.3 Influence of Gap Spacing.

The effect of gap spacing on confined bubble boiling can be examined by considering a simple model comprising a single, growing, confined bubble. Using this model it may be shown that the average heat transfer in the confined bubble regime is a function of gap spacing.

The simple model described in *Section 4.5.1* above shows a single cylindrical bubble having radius r at time t and confined in the space, width s, between a heated block and an adiabatic plate. It is assumed that a thin layer of liquid (the micro-layer) having a representative thickness δ remains on the heated surface between the surface and the vapour in the bubble.

To obtain an approximate result several simplifying assumptions have been made:

It is assumed that δ is very small compared with s and that for the period of bubble growth δ may be regarded as constant. Both of these assumptions have been shown to be reasonable in the analysis above.

Furthermore, it is assumed that the temperature of the heated block remains constant throughout. Although this is incompatible with the nominally constant heat flux conditions used in the experimental facilities it is an adequate assumption in the investigation of trends which may occur.

For areas of surface covered by liquid:

$$q_{CB} = 0 \tag{4.67}$$

and for areas under the bubble:

$$q_{CB} = \frac{k\Delta T_s}{\delta} \tag{4.68}$$

The rate of vapour generation is given by :

$$\frac{dV_b}{dt} = \frac{q_{CB}\pi r^2}{h_{fg}\rho_g} \tag{4.69}$$

and this must be equal to the rate of growth of the bubble:

$$\frac{dV_b}{dt} = 2\pi r s \frac{dr}{dt} \tag{4.70}$$

Equating these expressions and simplifying leads to:

$$2\frac{dr}{dt} = \frac{q_{CB} r}{h_{fg}\rho_g}$$

or

$$\frac{dr}{r} = \frac{q_{CB} dt}{2h_{fg}\rho_g s} \tag{4.71}$$

and setting $r = r_0$ at $t = 0$ and integrating leads to:

$$r = r_0 \exp\left(\frac{q_{CB} t}{2h_{fg}\rho_g s}\right) \tag{4.72}$$

The total heat flow to the bubble is then given by:

$$Q_{CB} = q_{CB}\pi r^2$$

or

$$Q_{CB} = q_{CB}\pi r_0^2 \exp\left(\frac{qt}{h_{fg} r_g s}\right) \tag{4.73}$$

During one cycle of bubble formation, i.e. from nucleation to maximum radius:

$$\int_0^{t_{max}} Q_{CB} dt = \text{Total heat transferred} = \int_0^{t_{max}} q_{CB}\pi r_0^2 \exp\left(\frac{qt}{h_{fg} r_g s}\right) dt \tag{4.74}$$

$$\int_0^{t_{max}} Q_{CB} dt = h_{fg}\rho_g s\pi r_0^2 \left(\exp\left(\frac{q_{CB} t}{h_{fg} r_g s}\right) - 1\right) \tag{4.75}$$

The mean heat transfer coefficient is defined by:

$$\alpha_{CB,mean} = \left(\frac{\int_0^{t_{max}} Q_{CB} dt}{t_f \pi r_{max}^2} \right) \Big/ \Delta T_{sat} \tag{4.76}$$

and relating the maximum radius to the time to achieve this radius:

$$r_{max} = r_0 \exp\left(\frac{q_{CB} t_{max}}{h_{fg} r_g s} \right) \tag{4.77}$$

Substitution and rearrangement then yields:

$$\alpha_{CB,mean} = \ln\left(\frac{r_{max}}{r_0} \right)\left(\frac{k}{2\delta} \right)\left(1 - \exp\left(-2 \Big/ \ln\left(\frac{r_{max}}{r_0} \right) \right) \right) \tag{4.78}$$

Which may be expressed in the form:

$$\alpha_{CB} = f\left(\frac{r_{max}}{r_0} \right)\frac{k_l}{\delta} \tag{4.79(a)}$$

Where

$$f\left(\frac{r_{max}}{r_o} \right) = \frac{1}{2}\ln\left(\frac{r_{max}}{r_0} \right)\left(1 - \exp\left(-2 \Big/ \ln\left(\frac{r_{max}}{r_0} \right) \right) \right) \tag{4.79(b)}$$

This term is less than unity for all values of r_{max}/r_0 (providing that $r_{max} > r_0$) and increases with increasing r_{max}/r_0. Furthermore, r_{max} can be assumed to be largely independent upon the gap spacing, s, but a function of the density of nucleation sites and the breadth of the test section. The radius at which the bubble becomes confined is approximately equal to the gap spacing, i.e. $r_0 = s$. Therefore, taking a representative value of r_{max} the variation in heat transfer coefficient due to evaporation of a thin film may be determined from

Equation 4.79 as a function of gap size. *Fig 4.15* shows $f\left(\frac{r_{max}}{r_o}\right)$ plotted against s for r_{max} =25mm.

Also plotted on *Fig.4.15* is the proportional variation in heat transfer coefficient if:

$$\alpha = C' s^{-p} \tag{4.80}$$

for various values of p if C' is chosen to give an identical value of heat transfer coefficient to that predicted by *Equation 4.79* at s=3mm.

Values of α_{CB} for water, R113 and R141b calculated using *Equation 4.79* are presented in *Table 4.3* .

The value of δ_f used in *Table 4.3* is somewhat higher than that estimated from *Fig.4.12* for R113 and R141b. However the combination of r_{max} =25mm and δ_f =20μm gives values of heat transfer coefficient representative of those measured for R113 and R141b at moderate heat flux.

It can be seen from examination of *Fig. 4.15* that, for agreement at s=3mm the slope of the line predicted by *Equation 4.79* is similar to that for *Equation 4.80* with a value of p of approximately 0.15 over the range of gap spacings 1-4mm. Clearly the film evaporation model must break down for low Confinement Numbers corresponding to large gap spacings so as the gap spacing approaches the notional maximum bubble diameter the model is no longer applicable. A very small gap spacings the heat transfer coefficient predicted using an inverse power relationship increases rapidly with decreasing gap size. This increase is not mirrored in the predictions made using the model. Reported experimental results (Fuchita and Uchida, 1990 and Nishikawa, 1969) from tests involving natural circulation suggest greater enhancement at small gap size than predicted by the model. However, it should be noted that the heat transfer coefficient α_{CB} relates only to the heat transfer to the confined bubble. The measured heat transfer coefficients

include contributions from other mechanisms and the influence of transient conduction to the liquid, as examined in *Section 4.6,* becomes more significant with decreasing size.

4.6 HEAT TRANSFER TO LIQUID FLOWING IN NARROW CHANNELS

The liquid only Reynolds Numbers during flow in the narrow channels examined in this project were generally such that the flow would be expected to be laminar or transition. However it has been observed that the flow in the confined bubble regime in channels confined in two dimensions exhibits unsteady characteristics as bubbles rapidly grow and then liquid flows in to fill the space.

A simple model has been developed by the Author while studying the enhancement due to pulsations in laminar single-phase flows. The model is similar in principle to that described by Nishikawa (1969) and outlined in *Chapter 2.* The model is based on "ideal" pulses of very short duration followed by periods of zero movement of the liquid slugs. The analysis is carried out for a round tube.

Several simplifying assumptions were made in deriving the model:

- The total mass flow/unit time is either uniform (the steady flow case) or, in the case of pulsed flow, is zero for most of the time, the entire flow occurring during a very short duration. This is shown schematically in *Fig.4.16*
- The pulses are of very short duration relative to the period, τ, between pulses.
- The volume in a pulse displaces all fluid from a length of tube, l.
- During the equivalent steady flow the flow is fully developed and laminar
- The temperature immediately after a pulse is uniform throughout the fluid in the section
- For the purpose of this analysis it is assumed that the wall temperature is constant with both position and time.

This set of assumptions provides the optimum enhancement. The assumption that the steady flow is fully developed and laminar implies that the baseline heat transfer coefficient is the lowest which can be achieved for that flow, higher heat transfer

coefficients would occur in the entry length or in turbulent flow. If the fluid is not fully mixed during the pulse then the temperature profile would be such that the temperature adjacent to the wall was higher than the mean bulk temperature and hence the initial temperature gradient at the wall would be less than that occurring after perfect mixing. This would reduce the heat transfer and hence the enhancement.

When pulsing occurs heat transfer to the fluid is by conduction to a cylinder of fluid, initially at temperature T_{in} when t=0, For t>0 then $T = T_w$ at $r = r_o$

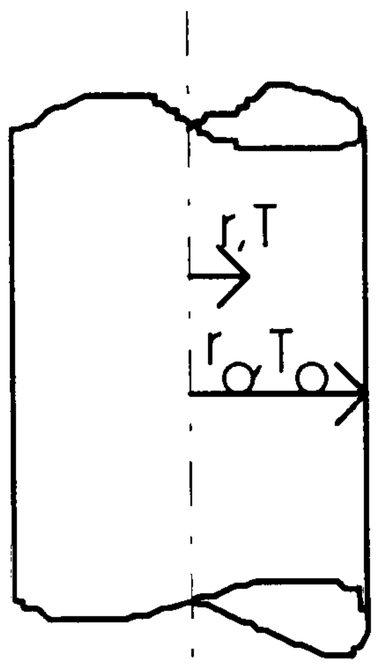

The temperature field for this case is given by:

$$\frac{\theta(r,t)}{\theta_w} = \frac{T(r,t) - T_{in}}{T_w - T_i} = 1 - 2\sum_{k=1}^{\infty} \frac{J_0\left(\lambda_k \frac{r}{r_o}\right)}{\lambda_k J_1(\lambda_k)} \exp\left\{-\frac{A\lambda_k^2}{r_o^2} t\right\} \tag{4.81}$$

To obtain the rate of heat transfer from the wall this may be differentiated.

$$q(t) = k\frac{\partial T(r_o,t))}{\partial r} = k\theta_w \frac{\partial \theta(r,t)}{\partial r} \tag{4.82}$$

From *Equation 4.81*, the only parameter varying with r is $J_o\left(\lambda_k \frac{r}{r_o}\right)$.

and

$$\frac{d}{dr} J_o\left(\lambda_k, \frac{r}{r_o}\right) = -\frac{\lambda_k}{r_o} J_1\left(\lambda_k, \frac{r}{r_o}\right) \tag{4.83}$$

Therefore:

$$\frac{d\theta(x,t)}{dr} = 2\theta\sum_{k=1}^{\infty}\frac{\frac{\lambda_k}{r_o}J_1\left(\lambda_k,\frac{r}{r_o}\right)}{\lambda_k J_1(\lambda_k)}\exp\left(\frac{-A\lambda_k^2}{r_o^2}t\right) \tag{4.84}$$

and, at $r = r_0$:

$$= 2\theta_w\sum_{k=1}^{\infty}\frac{1}{r_o}\exp\left(\frac{-A\lambda_k^2}{r_o^2}t\right) \tag{4.85}$$

hence, applying the Fourier equation for heat transfer by conduction:

$$q(t) = 2k\theta_w\sum_{k=1}^{\infty}\frac{1}{r_o}\exp\left(\frac{-A\lambda_k^2}{r_o^2}t\right) \tag{4.86}$$

and for the period when the fluid is stationary (i.e. the period of the pulse), τ:

$$\int_0^{\tau} q(t)dt = 2k\theta_w\sum_{k=1}^{\infty}-\frac{1}{r_o}\left(\frac{A\lambda_k^2}{r_o^2}\right)^{-1}\left(\exp\left(\frac{-A\lambda_k^2}{r_o^2}t\right)-1\right) \tag{4.87}$$

so the mean rate of heat transfer to a length, ℓ, is given by:

$$\dot{Q}_p = \frac{2\pi r_o l}{\tau}\int_0^{\tau} q(t)dt = \frac{4\pi r_o^2 lk\theta_w}{At'}\sum_{k=1}^{\infty}\left(\frac{1}{\lambda_k^2}\right)\left(1-\exp\left(\frac{-A\lambda_k^2}{r_o^2}t\right)\right) \tag{4.88}$$

the length, l, may be defined as the length of the fluid cylinder in the tube which is displaced by each pulse.

Therefore the mass moved per pulse is equal to the mass of fluid in length l.

$$\text{mass/pulse} = \rho\pi r^2 l$$

and the mean mass flowrate is given by:

$$\text{mass flowrate} = \frac{\rho\pi r^2 l}{\tau} = \dot{m}_p \tag{4.89}$$

The rate of heat transfer determined for the pulsed flow, $\dot{Q}_p$, may then be compared with that for a steady flow having mass flow rare $\dot{m}_p$, with uniform and constant heat transfer coefficient from a wall at constant, uniform temperature.

The temperature, T_f, of the fluid at exit from the section of tube, wall temperature T_W, is given by the expression:

$$\varepsilon = \frac{T_f - T_{in}}{T_w - T_{in}} = 1 - \exp(-NTU) \qquad (4.90(a))$$

$$T_f - T_{in} = (T_w - T_{in})(1 - \exp(-NTU)) \qquad (4.90(b)$$

and

$$NTU = \frac{UA}{\dot{m}c_p} \qquad (4.90(c))$$

thus

$$\dot{Q}_s = \dot{m}_s c_p \theta_w \left(1 - \exp\left(-\frac{UA}{\dot{m}_s c_p}\right)\right) \qquad (4.91)$$

$\dot{Q}_s$ represents the rate of heat transfer with steady flow through the tube length *l*.

For laminar flow it is assumed that the Nusselt Number is constant (it should, however, be noted that the entry length is frequently significant in laminar flow situations).

$$U = \frac{Nuk}{2r_o}, \qquad A = 2\pi r_o l.$$

$$\frac{UA}{\dot{m}_s c_p} = \frac{Nukl}{\dot{m}_s c_p} = \frac{Nu\rho\alpha l}{\dot{m}_s} \qquad (4.92)$$

If the steady mass flow rate is set to the mean mass flow rate for the pulsed system the rate of heat transfer over a length l of the tube becomes:

$$\dot{Q}_s = \frac{\pi r^2 lk\theta_w}{At'}\left(1 - \exp\left(-\frac{ANu\tau}{r^2}\right)\right) \qquad (4.93)$$

Comparing expressions for the heat transferred, *Equations 4.88* and *4.93:*

$$\frac{\dot{Q}_p}{\dot{Q}_s} = \frac{4\sum_{k=1}^{k=\infty}\frac{1}{\lambda_k^2}\left(1 - \exp\left(-\frac{A\lambda_k^2\tau}{r_o^2}\right)\right)}{1 - \exp\left(-\frac{ANu\tau}{r_o^2}\right)} \qquad (4.94)$$

The ratio given in *Equation 4.94* above is the enhancement due to pulsing.

An example of the enhancement predicted for water flowing in a tube radius 0.0143m is shown in *Fig 4.17.*

It can be seen that as the period of the pulse increases the enhancement tends towards unity. Examination of the model suggests that this would be the case: Since, from *Equation 4.89*, the pulse length, l, is proportional to the equivalent mass flow rate and the period of the pulse the value of l must increase with τ, the period. Clearly if l is greater than the physical length of the tube through which the pulses are passing then the model breaks down. Since UA is proportional to l, *Equation 4.80* implies that the heat transfer effectiveness of the tube will tend towards unity as l increases towards infinity. This means that the fluid outlet temperature approaches the tube wall temperature and $\dot{Q}_s \Rightarrow \dot{m}c_p(T_w - T_{in}) = \dot{m}c_p\theta$.

Study of *Equation 4.88*, substituting the value of mass flow from *Equation 4.79* shows that, as τ tends to infinity $\dot{Q}_p \Rightarrow 4\dot{m}c_p\theta\sum_{k=1}^{\infty}\frac{1}{\lambda^2}$ and, since, $4\sum_{k=1}^{\infty}\frac{1}{\lambda^2} = 1$ this implies that $\dot{Q}_p \Rightarrow \dot{m}c_p\theta$. i.e. the enhancement is unity for pulses of long duration.

A similar argument holds if it is assumed that the pulse or tube length remains constant while the mass flow decreases with increasing period; in both cases the rate of heat transfer would approximate to $\dot{m}c_p\theta$.

Examination of *Fig. 4.17* indicates that for the range of conditions observed in this study the enhancement factor predicted is of the order of 3. Thus the heat transfer due to transient conduction is not likely to be high under the conditions examined here. However, it should be noted that the predicted enhancement rises rapidly with decreasing period of pulse at periods below 0.5 seconds, therefore in different geometries transient conduction may be of more importance.

4.7 PRESSURE FLUCTUATIONS DURING BOILING IN NARROW CHANNELS

Experimental results suggest that conventional methods of estimating overall pressure drops can be used with reasonable accuracy in confined spaces. However, it has been observed that during boiling in narrow tubes or channels that when confined bubble boiling occurs, for a nominally constant flow rate and outlet pressure, the inlet pressure varies cyclically. This is illustrated in *Figs.4.18(a)* and *(b)*. A model which would explain the presence of pressure fluctuations during confined bubble boiling is proposed below and the magnitude of the pressure variations expected is calculated.

The relevant processes involved in confined bubble boiling in a single narrow tube may be summarised:

- Saturated or subcooled liquid enters the tube and since the heat transfer coefficient between the tube and the water is relatively low the temperature of the tube wall rises until nucleation occurs at some point upstream of the front of the liquid slug.

- Having nucleated the bubble expands until it fills the cross section of the tube, at which time it begins to expand longitudinally, causing the slug in front of the bubble to accelerate.

- As the slug moves down the tube it deposits a film of liquid on the wall behind it. This film evaporates thus causing the bubble to grow. The slug will accumulate liquid from any film remaining from the previous cycle, however the rate of accumulation of liquid must be less than the deposition rate so the slug becomes shorter as it travels down the tube.

- The slug is expelled from the end of the tube.

This model is illustrated in *Fig 4.19*.

In order to calculate the magnitude of the pressure and temperature variations which will occur during confined bubble boiling it would be necessary to take into account the thermal capacity of the wall, the film thickness and the conditions for bubble nucleation. However a simple estimate of the likely magnitude of the pressure pulses may be made if it is assumed that the wall has zero heat capacity, implying that the wall heat flux is uniform. Furthermore it is assumed that the film thickness, δ, is small compared to the tube diameter, d.

Using the nomenclature of *Fig.4.20*:

$$u = \frac{\text{Rate of vapour generation}}{\text{Cross sectional area}} + \text{Liquid velocity at entry}$$

$$= \frac{\dfrac{q\,p\,dz_b\,v_g}{h_{fg}}}{pd^2/4} + u_e \qquad (4.95)$$

The acceleration of the liquid slug is given by du/dt. Since the liquid velocity at entry is constant, $du/dt = d^2z_b/dt^2$.

$$\frac{dz_b}{dt} = \frac{4q\,v_g\,z_b}{d\,h_{fg}} \qquad (4.96)$$

Integrating *Equation 4.96* gives:

$$\frac{z_b}{z_0} = \exp\left(\frac{4q\,v_g}{d\,h_{fg}}t\right) \qquad (4.97)$$

$$t = \frac{d\,h_{fg}}{4q\,v_g}\ln\left(\frac{z_b}{z_0}\right) \qquad (4.98)$$

where t is the time for expansion from a bubble length of z_o to a length z_b. A reasonable assumption for the value of z_o, assuming that the bubble becomes confined when it fills the tube is z_o= d.

Differentiating *Equation 4.96* to obtain the acceleration of the front of the bubble gives:

$$\frac{\mathrm{d}^2 z}{\mathrm{d}t^2} = \left(\frac{4q v_g}{d h_{fg}}\right)\frac{\mathrm{d}z_b}{\mathrm{d}t} = \left(\frac{4q v_g}{d h_{fg}}\right)^2 z_b \tag{4.99}$$

$$\frac{\mathrm{d}^2 z}{\mathrm{d}t^2} = \left(\frac{4q v_g}{d h_{fg}}\right)^2 z_{bo} \exp\left(\frac{4q v_g}{d h_{fg}} t\right) \tag{4.100}$$

It can be seen that the acceleration of the fluid slug for a given heat flux is inversely proportional to the square of the diameter so the effect will be very much greater in small tubes than in large.

The force required to accelerate the slug of liquid is given by :

Force = mass of slug x acceleration

and the acceleration is given by *Equation 4.100* above.

The mass of the slug is proportional to its length.

Substitution of values for water at atmospheric pressure in a tube 3mm diameter and for a bubble length of 500mm shows that the magnitude of the pulses would be expected to be of the order of one bar, hence the assumption implicit in the above analysis that the specific volume of the steam is constant is not valid. A more accurate estimate of the magnitude of the pressure pulse can be achieved by assuming that the vapour behaves as a perfect gas such that:

$$p(t)v_g(t) = RT \tag{4.101}$$

Where p(t) and v(t) are the instantaneous pressure and specific volume.

$$\frac{\mathrm{d}z}{\mathrm{d}t} = \frac{4q v_g(t)}{d h_{fg}} z_b \tag{4.102}$$

$$\frac{\mathrm{d}^2 z}{\mathrm{d}t^2} = \frac{4q v_g(t)}{d h_{fg}}\frac{\mathrm{d}z}{\mathrm{d}t} \tag{4.103}$$

assuming that $\mathrm{d}v_g/\mathrm{d}t$ is small compared with $\mathrm{d}z/\mathrm{d}t$.

The acceleration at time t when the bubble has a length $z_b(t)$ is given by:

$$\frac{\mathrm{d}^2 z}{\mathrm{d}t^2} = \left(\frac{4q\, v_g(t)}{d\, h_{fg}} \right)^2 z_b(t) = a$$

$$v_g(t) = \frac{RT}{p(t)} \qquad (4.104)$$

$$p(t) = p_a + \frac{m_s}{A} a$$

Rearranging:

$$a = \left(\frac{4q\, RT}{d\, h_{fg}} \right)^2 \left(p_o + a \frac{m_s}{A} \right)^{-2} z_b(t)$$

$$\frac{m_s^2}{A^2} a^3 + 2 p_o \frac{m_s}{A} a^2 + p_o^2 a - \left(\frac{4q\, RT}{d\, h_{fg}} \right)^2 z_b(t) = 0 \qquad (4.105)$$

Equation 4.105 may be solved giving to give a relationship between the magnitude of the pressure pulse and the length of the liquid slug for a given heat flux, fluid and geometry. A sample solutions for water in 2.87mm and 3.69mm diameter tubes are shown as *Fig. 4.21(a)* and *(b)*. Comparison with *Fig 4.18(b)* shows that at the higher heat flux (110kW/m^2) pressure fluctuations of the order of 0.200-0.25bar were observed, this corresponds to slugs of approximately 5mm length. At low heat flux (10kW/m^2) there is little evidence of pulsing and none would be expected with slugs of reasonable length. While a more detailed experimental investigation would be required to confirm the analysis of this section, it appears from the results observed to yield results which are at least qualitatively acceptable.

4.8 CHAPTER SUMMARY

Two-phase gas-liquid flow in confined channels has been divided into three flow regimes and a model has been presented which permits the prediction of the boundary between Confined Bubble and Annular-Slug Flow. The contribution of the various mechanisms of heat transfer, particularly in the Confined Bubble regime have been examined.

The various analyses presented demonstrate that nucleate boiling and conduction through and evaporation through the liquid layer on the wall are likely to be the dominant mode of heat transfer during evaporation in channels at moderate Confinement Number. The Isolated Bubble Regime has not been examined, however at low quality, which must characterise the Isolated Bubble Regime, conventional boiling correlations and the work of Cooper (1988) suggest that nucleate boiling dominates the heat transfer at this condition.

It has also been demonstrated, both by analysis and experimental observation, that when liquid bridging occurs evaporation upstream of the liquid slug so produced causes acceleration of the slug and results in significant pressure fluctuations, or pulses. These pulses are important in two respects: Firstly, they lead to perturbations in the flow, particularly in multiple channels or where the supply is 'soft'. The varying or reversing flows produced leads to difficulty in determining the instantaneous local condition at any specific point and time. Secondly, the pressure variation must lead to a corresponding temporal variation of the local saturation pressure. The combination of these effects inevitably leads to variation in the local heat flux, heat transfer coefficient and wall temperature with time. Predictions and measurements made in this study yield time-averaged results. It has been observed that relatively high heat transfer coefficients have been observed in pulsating flow.

CHAPTER 5

INTERPRETATION OF RESULTS AND DERIVATION OF CORRELATIONS

5.1. INTRODUCTION

In this chapter experimental data from the present study together with published correlations and data are used in the derivation of a semi-empirical model for boiling heat transfer covering all the regimes of boiling observed in confined spaces.

Four approaches may be taken in determining heat transfer coefficients and pressure drops applicable to flow boiling in narrow channels or compact heat exchangers:

- The use of conventional correlations, with some correction for the effects of confinement.
- The application of established nucleate boiling correlations, with constants adjusted to take into account the effect of confinement.
- The fitting of data to correlations of a new form.
- Mechanistic approaches.

The use of conventional, established correlations has the advantage of consistency with existing design techniques. Any correction factor would be expected to approach unity as the channel size increased, hence there would not be a requirement to select the appropriate correlation.

Application of a nucleate boiling-type correlations of the form:

$$\alpha = bq^n \qquad (1.8(b))$$

is attractive because of the apparent simplicity of this form. However, this simplicity can be deceptive in that the constants, b, and to a lesser extent, n, are functions of the geometry and fluid properties. In flow boiling situations they may also be dependent upon the mass flux and vapour quality.

Formulation of a new correlation fitted to measured data is likely to lead to a relationship applicable only to a limited range of conditions. This problem can be overcome if a comprehensive data-base is available (as is the case for large channels, but not for narrow channels) or if the correlation is based upon a sound understanding of the mechanisms underpinning the correlation. Hence the importance of the mechanistic approach.

A mechanistic approach, involving an understanding of the phenomena involved in the evaporative process, has the advantage that relationships based upon the physical reality of the situation can be expected to be reliable. They are also applicable to all conditions where the mechanism proposed is valid. A correlation having a sound physical basis may be validated with relatively few data. Currently, understanding of boiling phenomena is such that it is not possible to produce a correlation based entirely on an analytical model of the processes involved. Empirically determined constants are necessary to complete the correlations and care must be taken to ensure that the presence of such constants does not mask incorrect assumptions regarding the mechanism occurring.

There are examples in the literature of each of the above approach applied to boiling in confined spaces.

5.2. DEVELOPMENT FROM EXISTING CORRELATIONS

As outlined in *Chapter 1* correlations used in conventionally sized tubes recognise the existence of two mechanisms of heat transfer, namely nucleate boiling and convective evaporation, which might be active during boiling. Correlations either add together the contributions from the two mechanisms, take the larger contribution to act alone or effectively offer a compromise in which the terms are raised to some power greater than one prior to addition. Having studied the literature and from initial experimental work carried out in this project it was initially considered appropriate to divide the flow into three regimes, i.e. Isolated Bubble, Confined Bubble and Annular Slug Flow and to develop correlations from each region based upon published large channel correlations and incorporating widely used dimensionless groupings.

Cornwell and Kew (1993) proposed correlations of the form:

Isolated Bubble Region $$Nu = C_1 Bo^{\approx 0.7} Nu_{lo} \quad (5.1)$$

Confined Bubble Region $$Nu = C_2 Bo^{m} Co^{n} Nu_{lo} \quad (5.2)$$

Annular Slug Flow $$Nu = C_3 F Nu_{lo} \quad (5.3)$$

The ≈ signifying the approximate value of the exponent.

Although the liquid only Reynolds Number in narrow channels is usually such that laminar flow would be expected in boiling flow it is reasonable to determine the liquid only Nusselt Number using a correlation based on turbulent flow. This approach has been shown by Wadekar (1992) to be satisfactory in compact heat exchangers from an analysis of data which were correlated over a range of Reynolds Numbers straddling the accepted transition value. Hence, for low values of x, and using the Dittus-Boelter Equation to determine the liquid only heat transfer coefficient, *Equation 5.1.* becomes, for the Isolated Bubble region :

$$\alpha = C_1' q^{\approx 0.7} G^{\approx 0.1} d^{\approx -0.2} \quad (5.4)$$

with C_1' being a function of fluid properties. *Equation 5.4* is then closely equivalent to *Equation 1.8(b)* , the typical form of nucleate pool boiling correlations. The dependence on mass flux is very weak and there is an increasing enhancement with increasing confinement.

In the Confined Bubble region the appropriate value of the constants *m* and *n* depends upon the flow regime assumed in the hypothetical liquid only flow, and hence the method of determining the liquid only Nusselt Number, Nu_{lo} . For the case of turbulent flow:

$$Nu_{lo} \propto Re_{lo}^{0.8} \propto G^{0.8} d^{0.8}$$

Therefore from *Equation* 5.2 ,

$$\alpha \propto G^{(0.8-m)} \quad (5.5(a))$$

$$\alpha \propto d^{-(n+0.2)} \quad (5.5(b))$$

Ishibashi and Nishikawa suggest that in the regime which they refer to as Coalesced Bubble which is equivalent to the Confined Bubble region:

$$\alpha \propto d^{-\frac{2}{3}} \tag{5.6}$$

Comparing *Equations 5.5(b)* and *5.2* suggests a value of n of approximately 0.5 is appropriate.

If a lower dependence of heat transfer coefficient is assumed, for example:

$$\alpha \propto d^{-0.15} \tag{5.7}$$

as indicated by the analysis of *Chapter 4.5.* then it is found that n should be -0.05 implying that the effect of confinement reduces the heat transfer coefficient *with respect to the heat transfer coefficient which would otherwise be found in a channel of that dimension.*

Examination of the results reported here and those of other workers, for example Fujita and Uchida (1990), presented as *Fig 2.3*, suggests that exponent m varies with mass flux, heat flux and confinement. At high heat flux m tends to the nucleate boiling value of 0.6-0.7 while at low heat flux values as low as 0.3 are observed, in agreement with Galezha et al (1975).

In the Annular Slug Flow Regime Bankoff and Rehm (1990) reported here in *Chapter 2* suggested using the Chen *F*-Factor *(Equation 1.18)* with some enhancement *(Equation 2.9).* Other workers have suggested that Chen is appropriate in compact heat exchangers, however work reported in *Chapter 3* and the studies of Lazarek and Black (1982) and Tran, Wambsganss and France (1995) indicate that the dependence on mass flux and quality is weak, at least for quality up to 60%, thus demonstrating that either conventional *F* factors are inappropriate or that the transition to Annular type flow occurs at relatively high quality in small channels. There is also evidence from video observations made during the current work and some published work (Katsuta and Nagata 1992) that dryout occurs at lower qualities in confined spaces than in conventionally sized tubes.

The recent correlation proposed by Tran, Wambsganss and France (1995) presented here as *Equation 2.5* introduces the Weber Number as a correlating Factor.

$$\alpha = 840\left(Bo^2 We_l\right)^{0.3}\left(\frac{\rho_l}{\rho_g}\right)^{-0.4} \text{ kW/m}^2\text{K} \qquad (2.5)$$

The derivation of this correlation was based upon experimental observation that the heat transfer was predominantly through nucleate boiling, and the heat transfer coefficient was independent of mass flux. For a given diameter *Equation 2.5* reduces to *Equation 1.8(b)*, however the constant, *b*, becomes a function not only of fluid properties but also of diameter such that:

$$b \propto d^{0.3}$$

This implies that the heat transfer coefficient is independent of mass flux and quality but *increases* with *increasing* diameter, or *decreases in absolute terms with increasing confinement.*

The above suggests that the use of correlations based upon power laws is unlikely to be entirely satisfactory. In particular it is apparent that the nature of the dependency of heat transfer upon confinement is uncertain and may depend upon the nature of the confinement. The magnitude of the constants and exponents are not only a function of the regime but also vary within regimes. The range of constants and exponents which were obtained in this study are presented in *Table 3.7* and it is clear from this that, from the data available, no guidance can be given to the choice of values in other applications.

5.3. COMPARISON OF EXPERIMENTAL RESULTS WITH PREDICTIONS FROM ESTABLISHED CORRELATIONS

The results obtained from the Mark II single section test section have been discussed in *Chapter 3.5* and compared with the Liu Winterton, Cooper and Lazarek and Black Correlations. In this section the trends observed from these results are considered further and compared with the predictions which can be made using published correlations.

Figs. 5.1(a)-(d) and *5.2(a)-(c)* show selected results from the 1.39mm diameter and 3.69mm diameter tubes, respectively, compared with six correlations. The correlations due to Chen (1963), Liu and Winterton (1988), Schrock and Grossman (1962) and Shah (1982) are summarised in *Table 1.3, Chapter 1* and are appropriate for relatively large tubes. The Lazarek and Black correlation was proposed for use in channels of the order of 3mm with refrigerant fluids and is discussed in *Chapter 2* and summarised in *Table 2.1.*

It can be seen from inspection of *Figs. 5.1* and *5.2* that for qualities of 0.1 and above the conventional correlations, with the exception of Schrock and Grossman, follow similar trends. The Lazarek and Black correlation predicts an essentially constant heat transfer coefficient along the length of the tubes (the slight reduction in predicted coefficient with increasing quality is due to the decrease in local pressure along the length of the tube).

Figs. 5.3(a) and *(b)* show comparisons of sample data from narrow gaps with the same correlations.

It can be seen from *Table 3.10* and *Fig.3.67* that the applicability of the Liu and Winterton correlation to tubes decreases with diameter with the mean error defined:

$$E2 = \frac{100}{N}\sum \frac{\left|\alpha_{pred} - \alpha_{exp}\right|}{\alpha_{exp}}$$

ranging from 21% in the 3.69mm diameter tube to 250% in the 1.39mm diameter tube.

Examination of *Fig.5.1*, presenting data for the smallest tube, shows that the conventional correlations over-predict the heat transfer coefficient in most circumstances. The Schrock and Grossman correlation, derived for water-steam systems from data obtained from tubes in the range 3mm to 11mm diameter, is not now widely used but is included here for comparison purposes since it exhibits somewhat different trends to the more generally used correlations. The trends exhibited by the correlations are best followed at low mass and heat flux (*Fig5.1(a)*) but as the heat flux is increased (*Figs.5.1(b)* and *(c)*) the measured heat transfer coefficient increases less markedly with quality and hence the correlations over-predict the heat transfer coefficient more significantly. At higher mass flux (*Fig5.1(d)*) the correlations incorporating a significant convective component of heat transfer predict that the heat transfer coefficient should rise rapidly with quality. This trend is not observed in the measured data. Since the measured results at low quality show little dependence upon heat flux the Lazarek and Black correlation does not generally give good agreement with the measured values.

As expected, at low heat and mass flux (*Fig5.2(a)*), the Lazarek and Black correlation predicts the measured data well in the 3.69mm diameter tube. The increase in heat transfer coefficient with quality predicted by the conventional correlations is less marked for this tube but all over-predict the heat transfer coefficient. The situation is similar at intermediate heat and mass fluxes (*Fig 5.2(b)*). At higher mass and heat fluxes the measured trend more closely follows that predicted by the conventional correlations (with the exception of Schrock and Grossman) with closest agreement being with Liu and Winterton.

Comparison of the data with the predictions of Tran, Wambsganss and France (1995), *Equation 2.5* has been included in *Chapter 3.7* and it has been shown that the agreement with the single tube data is at least comparable with that of Lazarek and Black (1982). However the Tran, Wambsganss and France correlation generally under predicts the measured data and hence can be regarded as giving a conservative prediction of heat transfer coefficient in the smaller tubes. The predicted reduction in heat transfer

coefficient with decreasing diameter for a given fluid and heat flux may be appropriate for the single tube results but is in conflict with the trend in flat-plate geometries. The Tran, Wambsganss and France correlation shows no quality dependence which is not in agreement with the observations in the current study.

The data obtained from the multi-channel and flat-plate geometries, examples of which are given in *Fig 5.3(a)* and *(b)*, are generally under-predicted by the established flow boiling correlations and by pool boiling correlations. The results obtained for flat-plate and multi-channel geometries show little dependence on quality, an increase in heat transfer coefficient with heat flux and a slightly negative influence of mass flux, as illustrated in *Fig 5.4* for the 2mm square multi-channel test section. It is suggested that if a simple correlation is required the nucleate boiling type correlation is the most appropriate for this class of configuration. This approach has been examined in *Chapter 3*.

5.4 A MODEL FOR THE DETERMINATION OF HEAT TRANSFER COEFFICIENTS IN CONFINED SPACES

5.4.1 Introduction to the Model

This Section outlines a procedure for the prediction of heat transfer coefficients in confined spaces based upon the experimental observations and consideration of the flow mechanisms in confined spaces. It is applicable, with appropriate modifications, to spaces which are confined in one dimension (e.g., between plates) or two dimensions (e.g., small diameter tubes).

Initially, the model is presented in outline and as such is a framework into which appropriate correlations may be inserted. A series of correlations which have been used as a basis for comparison are then listed and, finally, predictions using the model are presented and compared with experimental results.

The model is based upon the observation that heat transfer to a fluid evaporating in a narrow channel may be through one of four mechanisms:

(I) Nucleate Boiling

(II) Confined bubble boiling

(III) Convective boiling

(IV) Partial Dryout

Note that these *mechanisms* do not correspond exactly with the flow *regimes* described in *Chapter 4.3.* The Isolated bubble regime is neglected in the analysis but it is reasonable to assume that heat transfer in this regime occurs entirely through nucleate boiling; this is similar to the situation suggested by Cooper (1989) for larger tubes. It is assumed that at any point in the channel occupied by either the Confined Bubble or Annular Slug Flow regimes then either nucleate boiling may coexist with confined bubble evaporation or convective boiling or that one mechanism dominates. Both of these hypotheses have been tested. . The contribution of single-phase convection is assumed to be small throughout.

It is further assumed that there is a minimum film thickness which can exist on the wall. This minimum thickness may differ depending on the flow regime. It is taken to be that laid down by slowly moving or expanding bubbles in the Confined Bubble regime. In the Annular Slug Flow regime as the film thickness reduces there is a tendency for the film to break up and dry areas form, this leads to the regime referred to as Partial Dryout. Partial Dryout may also occur if the film evaporates fully before being replenished.

The heat transfer coefficient attributable to Mechanism (I) is obtained from an appropriate nucleate boiling correlation. Mechanism (II) is active in the Confined Bubble regime and involves heat transfer by conduction through the layer deposited on the wall by the passing bubble and evaporation of the film. Mechanism (III) occurs when the flow is in the Annular Slug Flow regime with the liquid phase deposited on the wall of the channel or passing through as liquid slugs; heat transfer is by conduction and convection

through and evaporation of the liquid film. Heat transfer by Mechanism (IV) is similar to that for Mechanism (III) except that at any given time a portion of the wall is dry and therefore heat transfer from that portion is negligible.

5.4.2 Determination of Film Thickness and Flow Regime

The mechanisms of heat transfer and the flow regime encountered depend upon the flow conditions as outlined in *Chapter 4.3.* In both the Confined Bubble and Annular Slug Flow regimes it has been noted that heat transfer is from the wall through a layer of liquid to the vapour-liquid interface which is at the fluid saturation temperature. Evaporation occurs at this interface. The determination of the film thickness and its resistance to heat transfer is therefore fundamental to the prediction of heat transfer coefficients.

Confined Bubble Regime

In the Confined Bubble Regime the deposition of liquid on the wall is governed principally by viscous and surface tension forces and, according to Park and Homsy (1984) and Taylor (1961) working with rectangular channels and round tubes respectively, the film thickness on the wall surrounding a bubble passing through a narrow gap may be estimated from an equation of the form:

$$\delta_{f,CB} = f(Ca) \tag{5.8}$$

Where:

$$Ca = \frac{\mu_l J_T}{\sigma}$$

However, observation has shown that even at very low velocity a film is laid down on the wall. It is therefore assumed that there is a minimum thickness of film, $\delta_{f,CB,\min}$

Annular Slug Flow Regime

The void fraction, v, is determined using an appropriate correlation, typically of the form:

$$v = f(\text{fluid properties, mass flux, x, channel dimension}) \qquad (5.9)$$

and the film thickness, $\delta_{f,ASF}$, is then be calculated assuming either that all of the liquid flows along the wall, as in *Equation 5.10*, or an allowance may be made for the liquid flowing in the slugs.

$$\delta_{f,ASF} = \frac{d}{4}(1-v) \quad \text{(for tubes or square section side } d) \qquad (5.10(a))$$

$$\delta_{f,ASF} = \frac{s}{2}(1-v) \quad \text{(for flat plate geometries, gap } s) \qquad (5.10(b))$$

Transition from Confined Bubble to Annular Slug Flow

The transition from Confined Bubble to Annular Slug Flow is taken to be at the value of dryness fraction at which the film thickness predicted by *Equations 5.8* and *5.9* are equal. i.e.:

$$\delta_{f,CB} = \delta_{f,ASF} \qquad (5.11)$$

This transition has been discussed more fully in *Chapter 4.3*.

Partial Dryout

The approach used in the Annular Slug Flow regime would lead to a film thickness approaching zero at as the dryness fraction approached unity. This in turn would result in the heat transfer coefficient approaching infinity. In practice, during evaporation at high dryness fractions, the heat transfer coefficient reaches a peak and then sharply declines due to partial dry-out of the walls.

In order to account for this effect a minimum film thickness, $\delta_{f,ASF,\min}$, must be specified. If the value of $\delta_{f,ASF}$ is less than that of $\delta_{f,ASF,\min}$ then the actual film thickness is taken to be $\delta_{f,ASF,\min}$, and the proportion, P_W, of the wall wetted by the film is given by:

$$P_w = \delta_{f,ASF} / \delta_{f,ASF,\min} . \qquad (5.12)$$

Experimental observation shows that in the smaller diameter tubes which have been tested the measured heat transfer coefficient may fall below that predicted for nucleate boiling alone. It may be argued that this is because, although the mechanism of boiling is related to nucleate pool boiling, correlations derived from pool boiling data are inappropriate in highly confined spaces. Alternatively, the model and correlations applied may be essentially correct except that intermittent dryout occurs under a wider range of conditions than expected.

Appropriate value of film thickness

The appropriate value of film thickness at any value of dryness fraction is shown schematically by the thick line in *Fig 5.5*

The film thickness in the Confined Bubble Regime is taken to be the larger of the minimum value, $\delta_{f,CB,min}$, and the value, δ_{CB}, predicted from a correlation of the form suggested in *Equation. 5.8.* In the Annular Slug flow Regime the thickness, $\delta_{f,ASF}$, is given by *Equation 5.10* .

The liquid film laid down in the Confined Bubble Regime by capillary deposition as defined by Taylor (1961) is essentially stationary and the shear stresses between the vapour and liquid are small compared with the surface tension and viscous forces associated with the liquid. Within the Annular Slug Flow Region the shear stress between the liquid and vapour, the viscous forces within the liquid and, in the case of a vertical channel, gravitational forces determine the film thickness.

5.4.3. Determination of Heat Transfer Coefficient

The component of heat transfer due to each mechanism which is active must be calculated and then these components added to determine the overall heat transfer coefficient.

Nucleate Boiling

A nucleate boiling correlation is used. Typical correlations are of the form:

$$q_{nbp} = a\,\Delta T_{sat}^{m} \qquad (1.8(a))$$

$$\alpha_{npb} = b\,q^{n} \qquad (1.8(b))$$

However care must be taken in determining the appropriate heat flux to use if the form given in *Equation 1.8(b)* is to be used. If the heat flux is only partly transferred by nucleate boiling then, it may be argued that, only that proportion of the heat flux, q_{nb}, should be used in the prediction of the nucleate boiling heat transfer coefficient. The heat transferred by nucleate boiling should be calculated from *Equation 1.8(a)*. This requires an iterative solution if predicting the temperature difference and hence heat transfer coefficient for a given total heat flux and convective heat transfer coefficient.

Confined Bubble Boiling

In the Confined Bubble region the heat transfer coefficient depends on both the film thickness and the proportion of the time which the surface is covered by a bubble. A reasonable approximation of the proportion of the time which a given area of tube will be covered by a bubble is given by the void fraction. Therefore, neglecting the contribution of single-phase convection:

$$\alpha_{CB} = \nu' \frac{k_f}{\delta_{CB}} \qquad (5.13)$$

The modified void fraction, ν', is the proportion of the area covered by bubbles (or the proportion of the time for which a given position is covered by a bubble) and a reasonable approximation may be calculated using an appropriate correlation of the form described in *Table 1.4*.

It is implicit in *Equation 5.13* that the heat transfer through the thin layer is by quasi-steady state conduction.

Annular Slug Flow

For the case of Annular Slug Flow it is assumed that the time taken for a slug to pass is small and therefore the heat transfer surface may be regarded as being covered by a film for the entire time. The heat transfer coefficient is then given by:

$$\alpha_{asf} = Nu_f \frac{k_f}{\delta_{f,ASF}} \tag{5.14}$$

Where Nu_f is the Film Nusselt Number, defined as the ratio of the convective heat transfer coefficient through the film to heat transfer coefficient if all heat was transferred by conduction through the film. The value of Film Nusselt Number may be taken as unity implying quasi-steady state conduction or taken from the data of Hewitt (Hewitt and Hall-Taylor, 1970) which relates Nu_f to the Film Reynolds Number. These data were presented in graphical form and are reproduced here as *Fig.2.2*.

Partial Dryout

In the Partial Dryout region the magnitude of the time-averaged heat transfer coefficient is given by the product of the proportion of the local surface which is wetted and the heat transfer coefficient through the film of thickness $\delta_{f,ASF,min}$.

$$\alpha_{pd} = P_w \frac{k_f}{\delta_{f,ASF,min}} = \left(\frac{\delta_{f,ASF}}{\delta_{f,ASF,\min}} \right) \frac{k_f}{\delta_{f,ASF,min}} \tag{5.15}$$

The rationale for application of this correction for dryout is illustrated in *Fig 5.6.* The total volume in the film is calculated from the void fraction, however, it is assumed that this no longer forms a uniform layer around the circumference, but the entire volume is contained on a portion of the perimeter such that the wetted portion is covered by a layer of thickness $\delta_{f,ASF,\min}$ and the remainder is dry. The heat transfer coefficient from dry wall to the vapour is assumed to be negligible.

The selection of an appropriate value of film thickness at the onset of partial dry out, $\delta_{f,ASF,min}$, is particularly important in that its magnitude determines the onset of partial dry out and the predicted heat transfer coefficient in this regime is inversely proportional to the square of the thickness.

Total Heat Transfer Coefficient

Providing that partial dry out has not been encountered it will be shown that the heat transfer coefficient is best predicted for tubes by taking the larger of the nucleate boiling heat transfer coefficient and the coefficient calculated from *Equation 5.13* in the Confined Bubble Regime or *Equation 5.14* in the Annular Slug Flow Regime. It will, however, be shown that this approach leads to an underestimate of the heat transfer coefficient in spaces confined in one dimension or in multi-channel arrangements, suggesting that an additive combination of the two mechanisms may be appropriate. If partial dry out occurs then the heat transfer coefficient must be calculated using *Equation 5.15* and this value is taken as the total heat transfer coefficient. .

5.4.3 Practical Implementation of the Model

- Select appropriate values for minimum film thickness in the Confined Bubble and Partial Dryout regions $\delta_{f,CB,\min}$ and $\delta_{f,ASF,\min}$ respectively.
- Calculate the film thickness for Confined Bubble flow, $\delta_{f,CB}$.
- Calculate the film thickness for annular flow, $\delta_{f,ASF}$.
- The appropriate flow regime is that which has the lower value of δ_f.
- If $\delta_{f,CB} \leq \delta_{f,ASF}$ then flow is taken to be Confined Bubble and the film thickness is the larger of $\delta_{f,CB}$ and $\delta_{f,CB,\min}$ .The heat transfer coefficient is calculated from *Equation 5.13* with Nu_f=1. and the modified void fraction, v', calculated using an appropriate correlation.

- If the $\delta_{f,CB} > \delta_{f,ASF}$ then the flow is taken to be Annular Slug Flow or Partial Dryout and film thickness is the larger of $\delta_{f,ASF}$ and $\delta_{f,ASF,\min}$. The heat transfer coefficient is calculated from *Equation 5.14* with Nu_f determined from the data of Hewitt and Hall-Taylor (1970) or taken as unity.
- If $\delta_{f,ASF} \leq \delta_{f,ASF,\min}$ then the film thickness is taken to be $\delta_{f,ASF,\min}$ and the film heat transfer coefficient is multiplied by a factor: $\delta_{f,ASF,\min} / \delta_{f,ASF}$.
- Calculate the nucleate boiling coefficient using an appropriate correlation.
- The total heat transfer coefficient for the Confined Bubble or Annular Slug Flow regimes is calculated by a combination of the nucleate boiling coefficient and the film coefficient. Selection of the larger value is conceptually the most satisfying but an additive model may give better results in some situations.

Fig.5.7 illustrates the procedure which has been incorporated into a computer program and used to evaluate different correlations and assumptions within the framework of the model described. The various correlations which have been considered for use within the model are summarised in *Table 5.1*.

In the Confined Bubble region the Taylor or Moriyami and Inoue correlations were used to determine the film thickness in tubes and flat plate geometries respectively. The Chisholm void fraction correlation (*Equation 1.63*) was used to estimate the modified void fraction. Moriyamia and Inoue give a correlation for the modified void fraction (*Equation 1.65*) however this was derived from observations of highly confined flow in flat plate geometries, with a Confinement Number of approximately 10. At low pressure the measured void fraction approaches unity with quality asymptotically and is close to unity at very low quality, hence the predicted results are not sensitive to the choice of correlation used to determine the modified void fraction.

The choice of void fraction correlation (or correlation for determining velocity ratio as a precursor to calculation of void fraction) for use in the Annular Slug Flow regime has been made with reference to the literature. Film thicknesses calculated for R141b with

mass flux 300kg/m^{2}s at a quality of 0.5 in tubes between 0.5 and 10mm diameter are compared in *Fig 5.8*. Under the conditions considered homogeneous flow is not possible. The CISE and Chisholm correlations differ by 25%-50% in the range of interest and Zivi predicts considerably lower values of film thickness. The CISE or Chisholm correlations are recommended (e.g. Whalley (1987) in preference to Zivi. Zivi is used in some applications since it has the advantage of simplicity and since the velocity ratio calculated using the correlation is independent of quality it is useful in simplifying analytical integration. Recent literature regarding pressure gradients in small tubes (Bao et al (1994) and Azzopardi and Holt (1995)) confirms that the CISE correlation (*Equation 1.64*) performs satisfactorily when applied to small channels. The CISE correlation has therefore been applied to the calculation of void fraction.

The minimum film thickness for both the Confined Bubble and Annular Slug Flow regions has been taken to be 20μm for the purposes of initial calculations. This assumption is justified in the case of the Confined Bubble region by the estimate of film thickness observed in slowly moving bubbles (*Section 4.5*) which suggested a value between 10 and 24 μm would be appropriate.

5.4.4 Discussion of Results from the Proposed Model

The model proposed in the previous section has been tested against the single round tube data. The errors associated with five differing sets of assumptions within the proposed framework are given in *Table 5.2*. The errors associated with the Cooper (1984), Lazarek and Black (1982) and Liu and Winterton (1988) correlations are included in the table for comparison.

It can be seen that the lowest mean error for the 3.69mm tube was obtained with the lower value of constant in the Cooper correlation of 35 (as recommended by Cooper (1989) for use in flow boiling rather than the value of 55 as originally proposed), the film Nusselt Number estimated from the data of Hewitt presented here as *Fig.2.2*, and the heat transfer

coefficient being taken to be the larger of the nucleate boiling and film coefficients (the substitution model). The error for all sizes of tube was comparable with that obtained from the Liu and Winterton Correlation. It is of interest to note that, for the smallest (1.39mm diameter) tube the best agreement with the data was obtained if the film Nusselt Number was taken to be unity. This may indicate that the data of *Fig.2.2* are not applicable to very thin films due to wall effects, however, it should also be noted that the Cooper nucleate boiling correlation yielded a somewhat lower mean error when applied alone.

A selected sample of the results from the 2.05mm diameter tube is given as *Fig 5.9* together with the predictions from various implementations of the proposed model. The combination of conditions giving the closest prediction, both in terms of trend and magnitude is clearly that described above as giving the minimum average error for the 3.69mm diameter tube.

Figs.5.10 (a)-(c) show comparisons of the measured and predicted heat transfer coefficients for the 3.69mm diameter tube for three sets of assumptions. Fig.5.10(c) shows the conditions described above to give the minimum average error. *Figs.5.11-5.13* illustrate this set of assumptions applied to the 2.87mm, 2.05mm and 1.39mm diameter tubes, respectively. Increasing scatter with decreasing tube size is evident from these plots. It is also evident from *Figs 5.10(c)* and *5.11 -5.13* and from value of E1 given in *Table 5.2* that the model over predicts the measured values to a greater extent as the diameter decreases.

The model (with the heat transfer coefficient chosen to be the higher of the film and nucleate components, the Film Nusselt Number from *Fig 2.2* and the constant of 35 in the Cooper nucleate boiling correlation) applied to two samples of data from the 1.39mm tube, together with the prediction for corresponding conditions from the Liu and Winterton correlation is shown in *Figs.5.14(a)* and *(b)*. As expected from the value of error E1 reported in *Table 5.2* both the model and Liu and Winterton over-predict the

data. The proposed model and the Liu and Winterton correlation display similar trends until the prediction of partial dryout which occurs at a value of quality of 0.6-0.7 in *Fig.5.14(b)*.

Application of the proposed model to multi-channel and flat-plate geometries has been limited. Data and predicted results for different assumptions are shown in *Table 5.3* and *Figs. 5.15 - 5.17.* The model under-predicts the measured data under all conditions. Application of the substitution model to the multi-channel geometries yields essentially a nucleate boiling correlation. The additive model gives somewhat better results, particularly for the flat plate geometry.

It should be noted that the predicted flow regime in the multi-channel and flat-plate geometries is predominantly Confined Bubble while the single tubes are predominantly Annular Slug Flow. This suggests that the model should be refined for application to the Confined Bubble regime.

A particular shortcoming of the model which must be acknowledged is the implicit assumption that fluid flow and local heat flux are constant with time or may be time averaged without loss of accuracy. Observation the pulsed nature of the flow in small channels indicates that this assumption may not be a valid assumption. In particular the tendency for local dryout to occur in narrow single channels due to a relatively lengthy period between passage of a liquid slug and replenishment of the liquid layer by either flow of liquid in the layer or by passage the next slug may be considerable. In the multi-channel and flat-plate configurations it would be expected that if local vapour generation ceases there would be a tendency for rapid liquid flow into the dry area, with a corresponding reduction in flow and possibly reverse flow in channels or areas of rapid vapour generation. The prolonged local dryout is therefore more likely to occur in single channels rather than multi-channels.

5.5 CONCLUDING REMARKS

Study of the behaviour of evaporating flows in narrow channels has demonstrated that existing commonly used flow boiling correlations, for example Liu and Winterton (1988) are unreliable in confined spaces. Pool boiling correlations, for example Cooper (1984) give predictions which are scattered above and below the measured data, correlations derived for use in small channels by Lazarek and Black (1982) and Tran, Wambsganss and France (1985) are good predictors at 3mm diameter but are less reliable at lower diameters and do not account for the variation with quality which has been observed. It is therefore concluded that simple dimensionless correlations are unlikely to provide more than approximate predictions.

The proposed model based upon the observed phenomena during evaporation in multi-channel and flat plate geometries provides results which are of comparable accuracy with the correlation of Liu and Winterton when applied to single channels. The model requires refinement to include a better criterion for the onset of partial dryout and for the film thickness in the Confined Bubble Regime.

CHAPTER 6

CONCLUSIONS

Most of the commonly-used correlations for the prediction of heat transfer coefficients during boiling in tubes are derived from data obtained from measurements in round tubes of 6mm diameter or larger. Such correlations cannot be applied with confidence to the design of equipment incorporating narrow channels. It has been demonstrated that the effects of confinement can be expected to be significant if the Confinement Number, Co, defined in terms of the surface tension, σ, acceleration due to gravity, g, density, ρ, and equivalent diameter, d_e, as:

$$Co = \frac{\sqrt{\sigma / g(\rho_l - \rho_g)}}{d_e}$$

is greater than 0.5.

The prediction of pressure gradients in two-phase flow using the method of Lockhart and Martinelli produces acceptable results and appears to be suitable for use in confined spaces. Other pressure drop correlations should be used with care under these conditions.

Three flow regimes which can be used as a basis for deriving physical models of the processes involved in evaporative heat transfer in confined spaces have been identified. These regimes have been referred to as **Isolated Bubble**, **Confined Bubble** and **Annular-Slug Flow.**

In the Isolated Bubble regime nucleate boiling occurs. In the Confined Bubble regime, where the bubbles are constrained by more than one surface, a liquid layer forms under

the bubble. Heat transfer is by conduction through this layer and evaporation at its surface. There is enhanced convection from the heated surface to the liquid in the spaces between the confined bubbles. In the Annular-Slug Flow regime there is a similar layer to that under the confined bubbles but spread evenly over the surface. Heat transfer through this layer is by conduction and convection. Thinning of the layer due to evaporation leads to partial dry out of the surface at high quality. The model developed here involves treating each of these various mechanisms separately using regime-specific correlations.

The situation is, however complicated by the unsteady nature of the processes involved in boiling in narrow channels and the resulting temporal variations in local conditions. The occurrence of intermittent local dryout at relatively low values of quality can result in low values of average heat transfer coefficient. The nature of the fluid delivery system is important in determining the influence of unsteady conditions. In general it has been found that the tendency to dry out is greatest in very small single channels and less marked in multiple channels. In multiple channels large local variations in flow are possible with reverse flow occurring in some sections. Rapid liquid replenishment occurs if the heat transfer and hence vapour generation in a channel is reduced. In single channels, after subsequent expulsion of a plug of liquid and dry out of the remaining film, the time taken to replace the liquid is governed by the inlet flow rate.

A model developed to permit the estimation of heat transfer coefficients in narrow tubes has been proposed and this has been shown to yield promising results although it requires further development before it is capable of being used as a comprehensive design tool. The model involves a criterion based on predicted void fraction and film thickness to determine the transition from Confined Bubble to Annular-Slug Flow. It also permits a tentative prediction of the likelihood of local dryout occurring during boiling.

At the present time it is recommended that a pool boiling correlation such as Cooper (1984) may be used to give a conservative value of heat transfer coefficient for spaces confined in only one dimension or for multi-channel arrangements. Other workers have

noted that nucleate boiling tends to dominate the heat transfer in small single tubes even at relatively high dryness fraction and often until dryout occurs. They have recommended the use of pool boiling type correlations such as Cooper (1984) or those based upon confined channel boiling such as Lazarek and Black (1982) which give reasonable results under conditions of moderate confinement providing that there is no local dryout. In this work it has been observed that under some conditions, at moderate to high confinement, there is an appreciable increase in heat transfer coefficient with quality.

Further work should be aimed at developing the model proposed in this study by applying it to a wider database and by incorporating appropriate corrections to the correlations employed. It is also important that the range of applicability of the model be determined and that the criterion for local partial dryout is tested by further experimentation.

In summary, this work has resulted in identification of the flow regimes and the establishment of a model of the mechanisms on which analysis and prediction can be based. It allows the designer of compact heat exchangers to estimate heat transfer coefficients in narrow channels with some confidence.

REFERENCES

Adderley C. and Fowler J.O.,(1991), The use of a novel manufacuring process for high performance titanium plate heat exchangers, Chapter 17, Heat Exchange Engineering, Vol.2, Compact Heat Exchangers Techniques of Size Reduction, Ellis Horwood.

Addlesee A.J., Cornwell K. and Peace D.G., Fluid dynamics of sliding bubbles and the heat transfer implications, Eurotherm Seminar 8, Paderborn.

Ali M. and Kawaji M., The effect of flow channel orientation of two-phase flow in a narrow passage between flat plates, ASME/JSME Thermal Eng. Proc, Vol.2, pp183-190.

Armstrong R.J.,(1966) The temperature difference in nucleate boiling, Int. J. Heat Mass Transfer, Vol.10, pp1148-1151

Azzopardi B.J. and Holt A.J., Two-phase pressure drop and void fraction relevant to compact two-phase heat exchangers, Proc. 4th UK National Conference on Heat Transfer, Manchester UK., I.Mech.E, pp437-442.

Bankoff S.G. and Rehm T.E.,(1980), Convective boiling in narrow concentric annuli, Transactions of ASME - Journal of Engineering for Gas Turbines and Power, Vol.112, pp607-613.

Bao Z-Y, Bosnich M.G. and Haynes B.S.,(1994) Estimation of void fraction and pressure drop for two-phase flow in fine passages, Trans. IChemE, Vol.72, Part A.

Bar-Cohen A.and Schweitzer H.,(1985), Thermosyphon boiling in vertical channels, Trans. ASME Journal of Heat Transfer, Vol.107, pp772-778.

Baroczy C.J., (1966), A systematic correlation for two-phase pressure drop, Chem. Eng. Prog. Symp. Ser., Vol.62, No.64,pp232-249

Beattie D.R.H.,(1973), A note on the calculation of two-phase pressure losses, Nucl. Eng. and Design, Vol.25, pp297-308

Beattie D.R.H. and Whalley P.B., (1982, A simple two-phase frictional pressure drop calculation method, Int. J. Multiphase Flow, Vol.8, pp83-87.

Bondurant D.L. and Westwater J.W.,(1971), Performance of transverse fins for boiling heat transfer,Chem. Eng Prog Symp Series, Vol.67 , No.113, pp30-37

BS5500, (1984), Specification for unfired fusion welded pressure vessels, British Standards Institution

Caeteno E.F., Shoham O.and Brill J.P.,(1992),Upward vertical two-phase flow through an annulus Part 1 and Part 2, Transactions of ASME Journal of Energy Resources Technology, Vol.114, No.1, pp1-30.

Carey V.P.,(1985), Surface tension effects on convective boiling heat transfer in compact heat exchangers with offset strip fins, Transactions of ASME Journal of Heat Transfer, Vol.107, pp 970-975.

Carey V.P. and Mandrusiak G.D.,(1986), Annular film-flow boiling of liquids in a partially heated, vertical channel with offset-strip fins, Int. J. Heat mass Transfer, Vol.29 pp927-939.

REFERENCES

Carey V.P. and Shah R.K., (1988), Design of compact and enhanced heat exchangers for liquid-vapour phase-change applications, Two-phase flow heat exchanges, NATO ASI Series E, Vol143, pp909-968.

Casarosa C., Latrofa E. and Shelginski A., (1983), The geyser effect in a two-phase thermosyphon, Int J Heat mass Transfer, Vol.26, No.6, pp933-941.

Chen C.C. and Westwater J.W., (1984), Application of the local assumption to the design of compact heat exchangers for boiling heat transfer, Trans. ASME Journal of Heat Transfer, Vol. 106, pp204-209.

Chen J.C.,(1963.), A correlation for boiling heat transfer to saturated fluids in convective flow,ASME Paper 63-HT-34, 6th International Heat Transfer Conference, Boston.

Chernobyl'skii I.I. and Tananaiko I.M.,(1956), Heat exchange during boiling of liquids in narrow annular tubes, SovietPhysics Tech Phys, Vol.1, pp2244-2249.

Chichitti A., (1960) Two-phase cooling experiments - pressure drop, heat transfer and burnout measurements, Energi Nucl, Vol.7, No.6, 407-425pp

Chisholm D, (1973,1),Void fraction in two-phase flow, Journal Mech. Eng Sci., Vol.15, pp235-236

Chisholm D, (1973,2), Pressure gradients due to the flow of evaporating two-phase mixtures in smooth tubes and channels, Int. J. Heat Mass Transfer, Vol.16,pp347-358.

Chisholm D, (1967), A theoretical basis for the Lockhart-Martinelli correlation for two-phase flow, Int. J. Heat Mass Transfer, Vol.10,pp1767-1768.

Chun K.R.and Seban R.A.,(1971), Heat transfer to evaporating liquid films, Journal of Heat Transfer,Vol.93, pp391-396.

Clark J.A. and Thorogood R.M,(1971), Selection and design of heat exchangers , Cryogenic Fundamentals, Ed G.G. Haselden, Academic Press

Clarke R.H. and Blundell N.,(1989),The two-phase flow patterns occuring inside a plain-fin passage of a plate-fin heat exchanger, AICHE Symposium Series Vol.269, No.85, pp287-292

Collier, J G. (1981), Convective Boiling and Condensation, McGraw-Hill, 2nd Ed.

Collier J.G., Kennedy T.D.A. and Ward J.A., (1974), Thermal design of plate-fin reboilers, Cryotech 73, IPC technology Press, pp95-100.

Collier J.G.,(1983), Boiling within vertical tubes, Chapter 2.7.3, Heat Exchanger Design Handbook, Schlunder E.U. (Ed), Hemisphere Publishing Co.

Cooper M.G,(1982.),Correlations for nucleate boiling formulation using reduced properties, Physiochem Hydrodyn, Vol.3,No.2,pp89-111

Cooper M.G., (1989), Flow Boiling - the apparently nucleate regime, Int J Heat Mass Transfer, Vol.32,pp3449-464,

REFERENCES

Cooper M.G., (1984), Saturated nucleate pool boiling - a simple correlation, 1st UK National Heat Transfer Conference, IChemE Symposium Series No.86, Vol.2, pp 785-93.

Cooper M.G. and LLoyd A.J.P., (1969), The microlayer in nucleate boiling , Int J Heat mass Transfer, Vol.12, pp895-913.

Cornwell, K and Kew P A., (1993), Boiling in small parallel channels, Proc CEC Conf. on Energy Efficiency in Process Technology, Athens, October 1992, Paper 22, Elseier Applied Scinces, pp624-638

Cornwell K., Schuller R.S. and Einarsson J.G., (1982) The influence of diameter on nucleate boiling outside tubes, Int. J. Heat Mass Transfer, Vol.25, pp683-690.

Cornwell K., Houston S.D. and Addlesee A.J., (1992) Sliding bubble heat transfer on a tube under heating and cooling conditions, Eng. Foundation Conf., Santa Barbara, ASME, pp 49-53.

Cornwell K. et al. (1995), Compact two-phase heat exchangers, Draft Final Report, CEC Contract No JOU2-CT92-0045.

Cornwell K.J and Shuller R.B.,(1982),A study of boiling outside a tube using high speed photography, Int J Heat Mass Transfer, Vol.25, No.5, pp683-690.

Damianides C.A. and Westwater J.W. (1988), Two-phase flow patterns in a compact heat exchanger and in small tubes, 2nd National UK Heat Transfer Conference, Vol.2, IMechE, pp1257-1268

Dukler A.E., (1964), Pressure drop and hold-up in two-phase flow, AIChE Journal, Vol.10, No.1, pp 38-51.

ESDU (1977), The gravitational component of pressure gradient for two-phase gas or vapour liquid flows through straight pipes, Engineering Sciences Data Unit, Item 77016, Appendix J, pp50-51

Ford W.D, Fauske H.K. and Bankoff S.G., (1971), The slug expulsion of freon 113 by rapid depressurisation of a vertical tube, Int J Heat Mass Trans, Vol.14, No.1, pp133-140.

Forster H.K. and Zuber N., (1955), Dynamics of bubble growth and boiling heat transfer, AIChE Journal, Vol.1 pp531-535.

Friedel L., (1979), Improved friction drop correlations for horizontal and vertical flow, European Two-phase Flow Group Meeting, Ispra, Italy.

Fujita Y and Uchida S, (1990), Boiling heat transfer and critical heat flux in a confined narrow space. Effects of gap size, inclination angle and peripheral conditions at the space edge, 9th Int Heat Trans Conf, Vol.2, pp153-158.

Galezha V.B., Usyukin I.P. and Kan K.D.,(1976), Boiling heat transfer with Freons in finned plate heat exchangers, Heat Transfer - Soviet Research, Vol.8, No.3, pp103-110.

Groll M. et al, (1993), Enhanced evaporation heat transfer surfaces, Final Report, CEC Contract No JOUE-0041C.

REFERENCES

Hesselgreaves J.,(1995),Concept proving of a novel compact heat exchanger surface, Proc. 4th UK National Conference on Heat Transfer, Manchester UK., I.Mech.E, pp479-486.

Hewitt G.F., (1995), Forced convective boiling, Proc. 4th UK National Conference on Heat Transfer, Manchester UK., I.Mech.E, Invited Lecture.

Hewitt G.F. and Hall Taylor N.S.,(1970.), Annular two phase flow, Pergamon Press, Oxford, p194.

Hewitt G.F.and Roberts D.N.,(1969), Studies of two phase flow patterns by simultaneous X-ray and flash photography, Harwell Report M2159.

Holt A.J., Azzopardi B.J. and Biddulph M.W., (1993), Pressure drop and void fraction in narrow channels, Eurotherm 26, Edinburgh.

Hsu, Y Y and Graham R W (1976) Transport Processes in Boiling and Two-Phase Flow Systems, Hemisphere Pub Corp/McGraw-Hill.

Hsu Y.Y and Graham R.W,(1963), A visual study of two-phase flow in a vertical tube with heat addition, NASA-TN-D 1564

Ishibashi E. and Nishikawa K., (1969), Saturated boiling heat transfer in narrow spaces.,Int J. Heat Mass Transfer, Vol.12, pp863-894.

Johannes C.and Mollard J.,(1972), Nucleate boiling of helium I in channels, Adv Cryog. Eng, Vol.17, pp332-341.

Jones A.C. and Zuber N, (1979), Slug-annular transition with particular reference to narrow rectangular ducts, in Two-Phase Momentum and Mass Transfer in Chemical, Process and Energy Engineering Systems, Vol. 1 (Edited by Durst, F., Tsiklauri, G.V. and Afgan, N.H.),Hemisphere, Washington, D.C, pp 345-355.

Kandlikar S.G.,(1990),A general correlation for saturated two-phase flow boiling heat transfer inside horizontal and vertical tubes,Trans ASME Journal of Heat Transfer, Vol.112,-pp219-228.

Katsuta. M and Nagata K.,(1992), Boiling induced heat transfer enhancement using a narrow space, Pool and External Boiling Conf. Santa Barbara.

Kew P A and Cornwell, K (1994) Confined Bubble Flow in Narrow Channels, 10th Int. Heat Transfer Conference, Vol.7, pp 473-478, Taylor & Francis.

Kosky P.G.,(1968), Bubble growth measurements in uniformly superheated liquids, Chemical Engineering Science, Vol.23, pp695706.

Kutateladze S.S., (1981) Principle equations of thermohydrodynamics of nucleate boiling, Heat Transfer - Soviet Research, Vol 13, No 3, pp1-14.

Lazarek G.M and Black S.H, (1982.), Evaporative heat transfer, pressure drop and critical heat flux in a small vetical tube with R113, Int J. Heat Mass Transfer., Vol.25, No.7, pp945-960

REFERENCES

Lenfestey A.G.,(1961), Low temperature heat exchangers, Progress in Cryogenics, Vol.3, pp25-47.

Liu, Z and Winterton, R H S (1988), A Wet Wall Flow Boiling Correlation with Explicitly Nucleate Term, 5th Miami Int. Symp. on Multiphase Transport and Particulate Phenomenon.

Liu J.F., Wang J.C.Y., Dong J.C. and Ang X.Y.,(1989), Studies on the pulse boiling phenomenon in thermosyphons, Heat Transfer Digest, Vol.108, pp5763.

Liu Z,. and Winterton R.H.S.,(1988),A wet wall flow boiling correlation with explicit nucleate term, Paper presented at %th International Symposium o Multiphase Transport and Particulate Phenomena.

Lockhart R.W. & Martinelli R.C,(1949), Proposed correlation of data for isothermal two-phase, two-component flow in pipes, Chemical Engineering Progress, Vol45, No1, pp39-48.

Lowry B and Kawaji M.,(1988), Adiabatic vertical two phase flow in narrow flow channels, AIChE Symposium Series, Vol.84,No.263, pp133-139.

Mandrusiak G.D., Carey V.P. and Xu X.,(1986), An experimental study of convective boiling in a partially heated horizontal channel with offset strip fins, Heat Transfer Digest, Vol.10, pp17-27.

McAdams W.H.,(1942) Vaporisation inside horizontal tubes II benzene-oil mixtures, Trans. ASME, Vol.64,p193

McQuillan K.W.and Whalley P.B.,(1985), Flow Patterns in vertical two-phase flow, Int J. Multiphase Flow, Vol.2, No.11, pp161-175.

Mesler R., (1977), An alternative to the Dengler and Addoms convection concept of forced convection boiling heat transfer, AIChE Journal, Vol.23, pp448-453.

Mishima K., Hibiki T. and Nisihara H.,(1993), Some characteristics of gas-liquid flow in narrow rectangular ducts, Int. J. Multiphase Flow, Vol. 19, No.1, pp115-124.

Mishima K. and Ishi M., (1984), Flow regime transition criteria for upward two-phase flow in vertical tubes, Int J Heat mass Transfer, Vol.27, pp723-737.

Monde M, (1988), Characteristic of heat transfer enhancement due to bubbles passing through a narrow vertical channel, Transaction of ASME - Journal of Heat Transfer, Vol.110.

Monde M., Kusuda H. and Uehara H., (1982), Critical heat flux during natural convective boiling in vertical rectangular channels submerged in saturated liquid, Trans ASME - Journal of Heat Transfer, Vol.104, pp300-303.

Monde M.,(1990), Measurement of liquid film thickness during passage of bubbles in a vertical rectangular channel, Transaction of ASME -Journal of Heat Transfer, Vol.112, pp255-258.

REFERENCES

Moriyama K. and Inoue A.,(1992),The thermohydraulic characteristics of two-phase flow in extremely narrow channels (Parts 1 and 2),Heat transfer - Japanese Research, Vol.21, No.8,pp823-856

Morozov Y.D. et al,(1988), Mechanism of the transition to two-phase flow and flow regimes in the boiling of liquid metals in a once through steam boiler, Translated from Teplofizik Vysokikh Temperature, Vol 26, No.6 pp1163-1170

Mostinski I.L.,(1963), Application of the rule of corresponding states for the calculation of heat transfer and critical heat flux, Teploenergetika, Vol.4,P66 (English Abstract in British Chemical Eng., Vol.8,P580,1963

Nicklin D.J.,Wilkes J.O. and Davison J.F,(1962), Two-phase flow in vertical tubes,Trans. IChem.E.,Vol.40, pp61-68.

Panchal C.B.,(1989), Analysis of flow boiling of ammonia and R114 in a matrix heat exchanger,AICHE Symposium Series Vol.269, No.85, pp293-300.

Panitsidis R.D., Gresham R.D. and Westwater J.W.,(1975), Boiling of liquids in a compact plate-fin heat exchanger, Int. J. Heat Mass Transfer, Vol.18, pp37-42.

Park C.-W. and Homsy G.M.,(1984),Two-phase displacement in Hele Shaw cells, J. Fluid Mechanics, Vol.139, pp291-308.

Premoli A., Francesco D. and Prina A., (1970), An empirical corrlation for evaluating two-phase mixture density under adiabatic conditions, European Two-phase Flow Group Meeting, Milan.

Robertson J.M, (1982), The correlation of boiling coefficients in plate-fin heat exchanger passages with a film-flow model,7th Int Heat Trans Conf, Munich, Vol.6, pp341-345.

Robertson J.M.,(1979), Boiling heat transfer with liquid nitrogen in brazed aluminium plate heat exchangers,, AICHE Symposium Series Vol.189, No75, pp151-164.

Robertson J.M., (1983), The boiling characteristics of perforated plat-fin channels with liquid nitrogen in upflow, Heat Transfer Digest, Vol.27, pp35-40.

Robertson J.M. and Lovegrove P.C.,(1983), Boiling heat transfer with Freon 11(R11) in brazed aluminium plate-fin heat exchangers, Transactions of ASME Journal of Heat Transfer, Vol.105, pp605-610.

Robertson J.M. and Lovegrove P.C.,(1980), Boiling heat transfer with Freon 11 in brazed aluminium plate-fin heat exchangers, ASME Paper 80-HT-58.

Robertson J.M. and Wadekar V.V.,(1988), Boiling characteristics of cyclohexane in vertical upflow in perforated plate-fin passages, AICHE Symposium Series Vol.263, No84, pp120-125.

Rohsenow W.M., (1952), A method of correlating heat transfer data for surface boiling of liquids, Trans ASME, Vol 74, pp969ff

Rudge T.,(1989), Homsep-2: a one-dimensional sodium boiling model for the fast reactor, Nuclear Energy, Vol.28, No.3, pp171181

REFERENCES

Shah M.M, (1982),Chart correlation for saturated boiling heat transfer: Equations and further study,Trans ASHRAE, Vol.88,pp185196.

Shah M.M.,(1976),A New Correlation for heat transfer during boiling flow through pipes,Trans ASHRAE, Vol.82,pp66-86.

Shorin C.N. et al., (1974), Experimental investigation of heat transfer with the boiling of oxygen in vertical channels, Int. Chem. Eng. Vol.14, No.3, pp517-521.

Stephan K. and Abdelsalam M.,(1980),Heat-transfer correlations for natural convection boiling, Int J. Heat Mass Transfer, Vol.23,pp73-87.

Sydoriak S.G. and Roberts T.R.,(1957), Study of boiling in short narrow channels and its application to design of magnets cooled by liquid H2 and N2, Journal of Applied Physics, Vol.28, No.2, pp143-149.

Taitel Y., Bornea D, and Dukler A.E.,(1980), Modelling flow transitions for steady upward gas-liquid flow in vertical tubes, AIChE Journal, Vol.26, No.3, pp345-354.

Taylor G.I., (1961), Deposition of a viscous fluid on the wall of a tube, Fluid Mechanics, Vol.10, No.2, pp161-165.

TEMA, (1978), Standards of the Tubular Exchanger Manufacturers Association, 6th Ed, Tubular Exchanger Manufacturers Association, New York.

Thome J.R., (1990), Enhanced boiling heat transfer, Hemisphere.

Tran T.N., Wambsganss M.W., France D.M. and Jendrzejczyk J.A., (1993),Boiling heat transfer in a small horizontal rectangular channel, AIChE Symposium Series - Atlanta, pp253-261

Tran T.N., Wambsganss M.W. and France D.M., (1995), Boiling heat transfer with three fluids in small circular and rectangular channels, Argonne National Laboratory, Report ANL-95-9, NTIS, Springfield VA.

Turmeau W.G.,(1971), Studies of nucleate boiling in thin liquid layers, PhD Thesis, Heriot-Watt University.

Wadekar V.V and Kenning D.B.R, (1990), Flow boiling heat transfer in vertical slug and churn flow regions, 9th Int. Heat Trans Conf., Vol.3, pp449-454.

Wadekar V.V.,(1991), Vertical slug flow heat transfer with nucleate boiling, ASME HTD-Vol.159,pp157-161

Wadekar V.V., (1992), Flow boiling of heptane in a plat-fin heat exchanger passage, Heat Transfer Digest, Vol.201, pp1-6.

Wallis G.B and Makkenchery S.,(1974), The hanging film phenomenon in vertical annular two-phase flow,Transactions of the ASME- Journal of Fluids Engineering, Vol.

Wallis G.B.,(1969), One-dimensional two-phase flow, McGraw-Hill.

REFERENCES

Wambsganss M.W., Jendrzejczyk and J.A, France D.M., (1991), Two-phase flow patterns and transitions in a small horizontal rectangular channel, Int. J. Multiphase Flow, Vol. 17, No.3, pp327-342.

Wambsganss M.W. et al,(1992), Frictional Pressure Gradients in Two-Phase flow in a small horizontal rectangular channel, Experimental Thermal and Fluid Science, Vol.5, pp40-56.

Wambsganss M.W. France D.M. and Jendrzejczyk J.A, (1993), Boiling heat transfer in a horizontal small diameter tube,Trans ASME Journal of Heat Transfer, Vol.115, pp963-972.

Webb R. and Gupte N., (1992), A critical review of correlations for convective vaporization in tubes and tube banks, Heat Transfer Engineering, Vol.13, No.3, pp58-75.

Westwater J.W, (1983), Boiling and heat transfer in compact and finned heat exchangers, Advances in Two Phase Flow and Heat Transfer, NATO ASI Series E, Vol.64, pp827-857.

Whalley P.B. (1987), Boiling, condensation and gas-liquid flow, OUP, Oxford.

Wieting A.R., (1975) Empirical Correlation for Heat Transfer and Flow Friction Characteristics of Offset-Fin Plate-Fin Heat Exchangers, J. Heat Transfer, 97, pp488-490.

Wilmarth T. and Ishi M. (1994), Two-phase flow regimes in narrow rectangular verical and horizontal channels, Int. J. Heat Mass Transfer, Vol.37, No.12 pp1749-1758.

Xia C., Hu W. and Guo Z., (1992) Mechanism of boiling heat transfer in narrow channels, 1st European an 3rd UK National Heat Transfer Conference, Birmingham.

Yao S-C. and Chang Y.,(1983), Pool boiling heat transfer in a confined space, Int J Heat Mass Trans, Vol.26, No.6, pp841-848.

Yilmaz S. and Westwater J W.,(1980), Effect of velocity on heat transfer to boiling Freon113, Journal of Heat Transfer, Vol.102, pp26-31

Yung D., Lorenz J.J. and Panchal C., (1980), Convective vaporization and condensation in serrated fin channels, Heat Transfer Digest - Heat Transfer in OTEC systems, Vol.12, pp29-37.

Zivi S.M.,(1964), Estimation of steady-state steam void fraction by means of the principle of minimum entropy production, Trans. ASME Journal of Heat Transfer, Vol.86, pp247-252.

APPENDICES

APPENDIX 1

EXTRACTS SUMMARISING THE JOULE PROJECTS

Research financed by

The Commission of the European Communities
in the framework of the
JOULE and JOULE II
programmes

2 OBJECTIVES

2.1 Structured Surfaces

- To investigate different planar and tubular specimen in the pool boiling mode under different operating conditions with water and R113 as working fluids in order to discover parametric interdependencies,

- To employ visualisation techniques to study the two-phase flow from the structured surfaces.

2.2 Covered Surfaces

Planar surfaces

- To investigate boiling heat transfer of water and R113 in the confined space between two vertical plates for several gap sizes, orientations, and peripheral boundary conditions.

- To identify, with the use of a high-speed camera (1000 frames/second), the flow patterns occurring in the confined space mentioned above.

- To correlate the effects of the different parameters for the data sets at hand.

- To investigate the boiling performance of mixtures of R113 and lubricant oil in the same geometry.

Tubular surfaces

- To examine the literature pertaining to the physics of boiling in the confined space formed by surrounding a tubular boiling surface by a sleeve, whether perforated or unperforated.

- To test idealised sleeves likely to provide suitable enhancement.

- To test sleeves suitable for practical industrial production and application.

2.3 Narrow Vertical Channels

- To use flow visualisation techniques to improve the understanding of the mechanisms involved in the various regimes observed during evaporation in vertical, narrow channels.

- To formulate a model for the theoretical analysis of evaporative heat transfer in vertical narrow channels.

- To evaluate the performance of a heat exchanger incorporating vertical, narrow channels when operating as an evaporator.

- To evaluate the available literature covering evaporative heat transfer in narrow vertical channels and identify relevant work reported in the literature.

2.4 Rotating Surfaces

Investigations at **CRES**

- To study the heat transfer characteristics of a smooth rotating disc during boiling.
- To study the effect of surface enhancement of the disc on the heat transfer coefficient.

Investigations at **UN**

- To carry out a literature review.
- To design, manufacture and test tailored surfaces.
- To compare the experimental results with published data on smooth surfaces.

2.5 Mathematical Modelling

- To employ CFD techniques to assist the experimental design of the rotating disc heat exchanger.
- To develop computational models to simulate the flow and evaporative heat transfer over rotating surfaces.
- To develop computational models to simulate the flow and conjugate heat transfer inside and over structured surfaces.

3. DATA BASE REPORT

Data Base Report

Contract number: JOUE-CT92-0045

Title: Compact Two-Phase Heat Exchangers

Co-ordinator: Professor K Cornwell

Project Leaders:

WP1	Mr P A Kew, Dr D B R Kenning
WP2	Professor M Groll; Dr A Karayannis
WP3	Dr L Haseler; Professor B Azzopardi
WP4	Dr C Marvillet

Objective: The programme of work is aimed at producing the technical and design information required to produce advanced compact heat exchangers for evaporation duty which have improved performance and reduced size, weight and price.

Description: Process intensification of industrial process plant involves the development of effective and reliable compact heat exchangers. These heat exchangers, which will achieve large energy savings owing to their increased effectiveness, are at an early stage of development where two-phase flow equipment is involved. The Programme, consisting of four work packages (**WP**) with contributions from five EC Countries, represents a major collaborative effort to overcome the technical problems associated with compact heat exchangers:

WP1	Evaporation in Narrow Channel Heat Exchangers	(GB, IE)
WP2	Heat Transfer and Flow Phenomena in Narrow Spaces	(DE, GR)
WP3	Design Implications for Compact Heat Exchangers	(GB)
WP4	Enhanced Plate Evaporators	(FR)

The major work was conducted in R & D Laboratories (in GB, DE, GR and FR) with industry participating as suppliers of equipment and services and as advisers on the manufacture and commercial viability of new heat exchanger designs.

Key Words: Compact Heat Exchangers, Evaporators, Two-Phase Flow, Flow Boiling, Boiling-Confined Spaces, Plate-Fin Heat Exchangers, Printed Circuit Heat Exchangers, Enhanced Flow Boiling

APPENDIX 2

Calculation of Heat Loss from Mark II Test Rig Flow Visualisation Test Section

The rate heat loss from the flow visualisation test section of the Mark II test rig was estimated by adding the contribution to the heat loss from each surface of the test section. This loss was then calculated from the measured temperatures during each test run.

The individual components were calculated:

Heat loss from rear of heater through Vermiculux Insulation

$$\dot{Q}_1 = \frac{k_v}{t_v} A_v \left(T_h - T_R\right)$$

where k_v = Thermal Conductivity of Vermiculux = 0.13 W/AK
t_v = Thickness of Vermiculux = 0.01 m
A_v = Area of Vermiculux = 0.0302 m²
T_h = Temperature at rear of heaters K
T_r = Temperature of back face of insulation K

Heat loss from Glass Front (Radiative)

$$\dot{Q}_2 = \sigma \varepsilon_g A_g \left(T_s^4 - T_a^4\right)$$

where σ = Stefan Boltzmann Constant = 56.7×10^{-9} W/mK^4
ε_g = Emissivity of Glass = 0.94
A_g = Area of Glass = 0.0259 m²
T_s = Temperature of Glass (assumed to equal fluid saturation temperature) K
T_a = Ambient Temperature K

Heat loss from Steel Front Plate (Radiative)

$$\dot{Q}_3 = \sigma \varepsilon_s A_s' \left(T_s^4 - T_a^4\right)$$

where σ = Stefan Boltzmann Constant = 56.7×10^{-9} W/mK^4
ε_s = Emissivity of Steel = 0.9
A_s = Area of Steel (front face only) = 0.0212 m²
T_s = Temperature of Steel (assumed to equal fluid saturation temperature) K
T_a = Ambient Temperature K

Heat loss from Glass and Steel (Convective)

$$\dot{Q}_4 = (A_g + A_s)\,\alpha\,(T_s - T_A)$$

where A_g = Area of Glass = 0.0212 m²
A_s = Area of Steel = 0.0307 m²
T_s = Saturation Temperature of fluid K
T_A = Ambient Temperature K

$$\alpha = 1.42\left(\frac{T_s - T_a}{0.4}\right)^{0.25} \text{ W / m}^2\text{K}$$

Heat loss through Side Wall

$$\dot{Q}_5 = \frac{k_i}{t_i} A_i\,(T_s - T_a)$$

where k_i = Thermal Conductivity of Insulation = 0.05 W/mK
k_i = Thickness of Insulation = 0.01 m
A_i = Area of Insulation = 0.04 m
T_s = Saturation Temperature of Fluid K
T_a = Ambient Temperature K

$$\dot{Q}_{loss} = \dot{Q}_1 + \dot{Q}_2 + \dot{Q}_3 + \dot{Q}_4 + \dot{Q}_5$$

A test was carried out with the inlet and outlet pipes disconnected and the manifolds plugged to ensure no heat transfer to fluid flowing through the test section or conduction through the pipes. A low heat input (41 W) was applied to the heaters and temperature readings were taken until the temperature reached an almost constant value (a period of 1 hour). The following readings were obtained.

Core Temperature (equivalent to T_s) = 56.7°C
Temperature of back face of Vermiculux = 42.5°C
Ambient Temperature = 19.7°C

It was also noted that the rate of change of core temperature was 0.83×10^{-3} K/s which was equivalent to a net heat input to the section, having heat capacity of 5400 J/K, of 4.5 W.

The values of heat loss calculated were

$$\dot{Q}_1 = 5.6 \text{ W}$$
$$\dot{Q}_2 = 6.2 \text{ W}$$
$$\dot{Q}_3 = 4.8 \text{ W}$$
$$\dot{Q}_4 = 9.2 \text{ W}$$
$$\dot{Q}_5 = 7.4 \text{ W}$$
$$\dot{Q}_{loss} = \overline{33.2 \text{ W}}$$

which can be compared with the measured value of

$$(41 - 4.5) = 36.5\ \text{W}$$

Showing that the difference between calculated and measured heat loss was approximately 8%.

This demonstrated that the approximation inherent in deriving the expressions for the components of heat loss the resulting prediction is acceptable.

APPENDIX 3
The Effect of Temperature Fluctuations on Heat Exchanger Operation

If the hypothesis that heat transfer to fluid boiling in a narrow channel involves the nucleation of single bubbles followed by rapid growth of a confined bubble is correct then this has significant implications in the development of design correlations, in particular for heat exchangers operating with low temperature differences.

While some aspects of the analysis presented below apply to all boiling situations where the fluid approaches the boiling surface as a single-phase liquid the effect is likely to be more marked in narrow channels. This is because, in large channels, the nucleate boiling component of heat transfer during low quality boiling is due to the formation of numerous bubbles and the time averaged and instantaneous values of this component are similar.

In narrow tubes it is suggested that the nucleation frequency will be low: formation of a single bubble which fills the channel cross section (i.e. becomes confined) before departing from the wall leads to a change in heat transfer regime to one of transfer through and evaporation of a thin liquid layer on the wall. This regime gives high heat transfer coefficients and hence will lead to a reduction in wall temperature. The time averaged wall temperature will thus be significantly below that necessary to initiate nucleation. The local heat transfer coefficient will decrease again when either the advancing liquid front has passed by or when the liquid layer dries out, whichever occurs first.

Firstly consider the case of flow in a thin walled channel heated electrically. This is generally referred to as a constant heat flux case, however, while the time averaged heat

flux is constant along the channel the instantaneous heat flux at any point may vary with time as the wall temperature changes. Representative temperature profiles, immediately prior to nucleation and post-nucleation are shown in *Figs. A3.1(a)* and *(b)* below. As can be seen the temperature in the region marked "A" would be expected to vary markedly due to the change in heat transfer rates depending whether liquid, a nucleating bubble or a confined bubble was adjacent to the wall.

The wall temperature in the confined bubble and ASF regions is likely to fluctuate as the liquid film thickness varies with time, however the effect of this variation is not fundamental to the boiling process.

It should be emphasised that this phenomena differs from the hysteresis which may be experienced at the initiation of large channel boiling or pool boiling. In a narrow channel the temperature excursions to the temperature necessary to initiate nucleation are repetitive, since after each bubble confined bubble has passed, it is assumed that liquid sweeps the surface.

Considering the case of constant wall temperature (e.g. maintained by a condensing vapour outside the channel) if the wall temperature is below the temperature necessary for nucleation, then the heat transfer throughout the channel will be to single-phase liquid the temperature of which will approach that of the wall asymptotically. The wall temperature may be measured to be above the time-averaged value for the constant heat flux case, but clearly the rate of heat transfer will be extremely low. In effect the heat exchanger will fail to function. This situation is show in *Fig. A3.2*.

	Liquid Density kg/m^3	Vapour Density kg/m^3	Surface Tension mN/m	D^* (Co=1) mm	D* (Co=0.5) mm	Notes
HELIUM	128	10	0.09	0.27	0.54	-269 Deg.C
NITROGEN	815	3.81	0.985	0.35	0.7	-200 Deg.C
FLUTEC PP1	1582	13.5	8.3	0.73	1.46	
FLUTEC PP3	1626	13.8	9.9	0.79	1.58	
CFC114	1499	7.89	13.4	0.95	1.9	
CFC113	1508	7.435	14.7	0.99	1.98	
CFC11	1479	5.85	17.94	1.11	2.22	
HCFC22	1409	4.7	18.18	1.14	2.28	
HCFC141b	1215	4.85	17.28	1.2	2.4	
MERCURY	12763	4.45	382	1.74	3.48	350 Deg.C
NH3	681.6	0.89	34.2	2.26	4.52	
WATER	959	0.498	58.9	2.5	5	
POTASSIUM	675.4	0.486	67.2	3.18	6.36	750 Deg.C
SODIUM	745.4	0.306	113	3.93	7.86	900 Deg.C
LITHIUM	420	0.42	260	7.94	15.88	1330 Deg.C

Table 0.1 Critical Diameter Based on Confinement Number for Various Fluids (at Normal Boiling Point unless Stated Otherwise)

Author	Correlation	Eqn. No.	Comments
Rohsenow (1952)	$\frac{c_{pl}\Delta T_{sat}}{h_{fg}} = C_{sf}\left(\frac{1}{h_{fg}\mu_l}\left\{\frac{\sigma}{g(\rho_l-\rho_g)}\right\}^{1/2}\right)^{0.33}\left(\frac{c_{pl}\mu_l}{k_l}\right)^{s} q^{0.33}$	1.1	C_{sf} surface finish and fluid dependent All fluids except water s = 1.7 Water s = 0.7
Forster and Zuber (1955)	$\alpha = 0.0122\left(\frac{k_l^{0.79}c_{pl}^{0.45}\rho_l^{0.49}}{\sigma^{0.5}\mu_l^{0.29}h_{fg}^{0.24}\rho_g^{0.24}}\right)\Delta T_{sat}^{0.25}\Delta p_{sat}^{0.75}$	1.2	Clapeyron's Equation may be used to determine Δp_{sat} $\Delta p_{sat} = \frac{h_{fg}\Delta T_{sat}}{T_{sat}\left(1/\rho_g - 1/\rho_l\right)}$
Mostinski (1963)	$\alpha = 0.106 p_{cr}^{0.69}\left(1.8 p_r^{0.17} + 4 p_r^{1.2} + 10 p_r^{10}\right) q^{0.7}$	1.3	Pressures in bar Heat flux in W/m^2 Heat transfer coefficient in W/m^{2}K
Armstrong (1966)	$\Delta T_{sat} = 0.602 q^{0.293}$	1.4	Claimed to be applicable to most organic fluids
Stephan and Abelsan (1980)	$\alpha = C_a q^{C_b}$	1.5	C_a is a fuction of the fluid and fluid pressure C_b depends upon class of fluid
Yilmaz and Westwater (1980)	$q = 0.532\Delta T_{sat}^{0.731}$	1.6	Applicable to R113 at atmospheric pressure
Cooper (1984)	$\alpha = 55 p_r^{0.12}(-\log_{10} p_r)^{-0.55} M^{-0.5} q^{0.67}$	1.7	Pressures in bar Heat flux in W/m^2 Heat transfer coefficient in W/m^{2}K

Table 1.1 Nucleate Pool Boiling Correlations Used in this Work

Velocity	a	m	b	n
m/s	(Eqn. 1.8(a))	(Eqn. 1.8(a))	(Eqn. 1.8(b))	(Eqn. 1.8(b))
0.0	0.000532	3.72	0.132	0.731
2.4	0.237	1.96	0.48	0.490
4.0	1.06	1.57	1.038	0.363
6.8	1.48	1.49	1.301	0.329

Table 1.2 Constants from Yilmaz and Westwater (1980)

Correlation	Form	Eqn. No.	Comments
Chen (1963)	$\alpha = S\alpha_{npb} + F\alpha_l$	1.12-1.18	α_{npb} from *Equation (1.2)*
Shah (1982)	$\alpha = E\alpha_l$ $E = f(Bo, Co_n)$	1.25-1.28	Details in main text For horizontal flow at low Froude number $E = f(Bo, Co_n, Fr)$ Minimum tube diameter 2.95mm
Liu and Winterton (1988)	$\alpha^2 = \left((F\alpha_L)^2 + (S\alpha_{npb})\right)$	1.21-1.24	Details in main text α_{npb} from Equation (1.7) Minimum tube diameter 2.95mm
Kandlikar (1990)	$\alpha = E\alpha_l$ $E = D_1(Co_n)^{D_2} + D_3(Bo)^{D_4} F_{fl}$	1.58-1.59	F_{fl} is fluid dependent constant For horizontal flow at low Froude number $E = f(Bo, Co_n, Fr)$ Values of D_n given below. Minimum tube diameter: 4mm (neon) 6.6mm (Freons) 5mm (water)

$$Bo = \frac{q}{G h_{fg}} \qquad Co_n = \left(\frac{1-x}{x}\right)^{0.8}\left(\frac{\rho_g}{\rho_l}\right)^{0.5}$$

$$\alpha_l = 0.023\frac{k_l}{d_e} Re_l^{0.8} Pr^{0.4} \qquad Re_l = \frac{G(1-x)d_e}{\mu_l}$$

$$\alpha_l = 0.023\frac{k_l}{d_e} Re_L^{0.8} Pr^{0.4} \qquad Re_L = \frac{Gd_e}{\mu_l}$$

Constant	Co<0.65	Co>0.65
D_1	1.136	0.6683
D_2	-0.9	-0.2
D_3	667.2	1058
D_4	0.7	0.7

Constants in Kandlikar (1990) Correlation

Table 1.3 Summary of Flow Boiling Correlations Used in this Work

Correlation	Form	Eqn. No.	Comments
Homogeneous	$S_r = 1$		Simplest form, limited applicability
Lockhart and Martinelli (1949) (Adapted by Chisholm 1973)	$v = 1 - \frac{1}{\Phi_{tt}}$ $\Phi_{tt} = 1 + \frac{20}{X} + \frac{1}{X^2}$	1.61	
Zivi (1964)	$S_r = \left(\frac{\rho_l}{\rho_g}\right)^{\frac{1}{3}}$	1.62	Derived from assumption that total kinetic energy in flow is a minimum.
Chisholm (1973,1)	$S_r = \left(1 - x\left(1 - \frac{\rho_l}{\rho_g}\right)\right)^{\frac{1}{2}}$	1.63	Provides "very simple, reasonably accurate result" Whalley(1987)
CISE Premilo et al (1970)	$S_r = 1 + E_1 \frac{\rho_l x}{\rho_l x + \rho_g (1-x)}$ $E_1 = 1.578 Re^{-0.19}\left(\frac{\rho_l}{\rho_g}\right)^{0.22}$ $E_2 = 0.0273 We\, Re^{-0.51}\left(\frac{\rho_l}{\rho_g}\right)^{-0.08}$ $Re = \frac{Gd}{\mu_l}$ $We = \frac{G^2 d}{\sigma \rho_l}$	1.64	Accurate and generally applicable correlation. Conditions for which the correlation may be expected to hold are given in ESDU (1977)
Moriyama and Inoue (1992)	$\nu' = \frac{\beta}{C_o}$ $\beta = \frac{j_g}{j_t}$ $C_0 = 5.7\left(\frac{\rho_l \sigma s}{\mu_l^2}\right)^{-0.17}$	1.65	ν' = the fraction of the surface area covered by bubbles. Derived from experimental observations with Co≈10

In all cases:

$$v = \frac{1}{1 + \left(S_r \frac{1-x}{x} \frac{\rho_l}{\rho_g}\right)} \tag{1.66}$$

Table 1.4 Correlations used in Determining Void Fraction

Re_L	Re_G	C
≥2000	≥2000	20.0
<2000	≥2000	12.0
≥2000	<2000	10.0
<2000	<2000	5.0

Table 1.5 Constant C for use in Equation 1.49

Reference	Fluid	Geometry	Mass Flux	Heat Flux kW/m^{2}K	Quality	Press. bar	Correlation	Eqn. No.
Lazarek and Black (1982)	R113	Tube 3.15mm ϕ	125-750	1.4-380		1.3-4.1	$Nu = 30\,Re^{0.857}\,Bo^{0.714}$	2.1
Tran et al (1993)	R12	Channel 1.7 x 4.06mm	54-396	4.1-33.7		7.6-9.5	$\alpha = C_1 q^{C_2}$	2.4
Wambsnganns et al (1993)	R113	Tube 2.92mmϕ	50-500	8.8-90.75	0-0.9		Lazarek and Black produced good agreement	
Moriyamia and Inoue (1992)	R113	Channel 30mm wide 265mm long .035-.11mm deep	200-1000	4-30		1-2	$\alpha_{tp} = v\alpha_{lf} + (1-v)\alpha_{lf}$ Void fraction ,v, and film and liquid heat transfer coefficients calculated from model.	2.9-2.15
Bankoff and Rehm (1980)	Water	Annular gap 0.0508mm-0.406mm wide <Co<	300-2450	50-350		1-2	$\alpha = \alpha_{mic} + \alpha_{mac}$ α_{mic} and α_{mic} calculated using Chen correlation with modified Enhancement Factor.	2.7-2.8
Tran, Wambsganns and France (1995)	R113 R12 R134a	Tube 2.92mmϕ Channel 1.7 x 4.06mm Tube 2.46mmϕ	500-832	8.8-129	0-0.9	p_r=0.1-0.2	$\alpha = 840\left(Bo^2 We_l\right)^{0.3}\left(\frac{\rho_l}{\rho_g}\right)^{-0.4}$ kW / m^{2}K	2.5

Table 2.1 Summary of Reported Work on Forced Flow Boiling in Confined Spaces

Correlation	**Mean Deviation** $\frac{1}{N}\frac{\sum\lvert\text{Predicted}-\text{Measured}\rvert}{\text{Measured}}$	**Percentage of Data within ±20% of predicted value**
Lazarek and Black (1982)	12.7	84.8
Stephan and Abdelsalam (1980)	12.9	83.8
Liu and Winterton (1988)	15.5	74.3
Shah (1982)	17.6	68.6
Chen (1963)	36.0	41.9

Table 2.2 Comparison of Data from Wambsganns et al (1993) with Selected Correlations

Reference	Fluid	Geometry	Heat Flux kW/m^2	Pressure bar	Correlation	Eqn. No.
Sydoriak and Roberts (1957)					See Table 2.5	
Ishibashi and Nishikawa (1969)	Water	Vertical annulus internal cylinder heated. d_i=80mm, L=304mm	1-67	Atmospheric	$Nu = 13.6\left(Re^{*\frac{1}{2}}\right)^{\frac{2}{3}}$ $Re^{*\frac{1}{2}} = \left(\frac{q}{h_{fg}\rho_g}\frac{\Delta R}{\upsilon}\right)^{\frac{1}{2}}\left(\frac{q}{M^2 P}\right)$ $M = 900\,\mathrm{m}^{-1}, P = 1.976\,\mathrm{W}$ (for coalesced bubble region except liquid deficient region)	2.33 2.34
ibid	Water Aqeous solutions Ethanol	As above	As above	1-10.1	$Nu = 200\,Fo_{(1)}^{-\frac{2}{3}} Pr^{-\frac{2}{3}}\left(\frac{\rho_f}{\rho_g}\right)^{1.085}$ (for coalesced bubble region including liquid deficient region) $N_{(1)} = 1.365 \times 10^{-9} q\Delta R^{-\frac{2}{3}} Pr^{1.627}\left(\frac{\rho_f}{\rho_g}\right)^{1.085}$ (for coalesced bubble region except liquid deficient region)	2.35 2.37
Bar-Cohen and Schweizer(1985)	Water	Heated Vertical plate with adiabatic or heated wall L=240mm,W=66mm,s=2-∞ mm	4-250		Chen type correlation	2.18-2.24
Xia et al (1993)	R113	Vertical flat plate and quartz window. L=56-197mm,W=45mm,s = 0.78-5mm	<1000	Atmospheric	$\frac{q/h_{fg}\rho_g}{\left(\sigma g(\rho_l-\rho_g)/\rho_g^2\right)^{0.25}} = 76.56\left(\frac{\rho_l c_{pf}\Delta T_{sat}}{h_{fg}\rho_g}\right)^{2.07+666(Ls)} Co^{0.21} Pr_l^{0.3}$	2.38

Table 2.3 Reported Correlations from Studies of Natural Circulation Boiling in Confined Spaces

Source	Conditions Investigated				Correlation /Design Method	Eqn. No.*	Notes
	Geometry	**Fluid/ Pressure**	**Superheat/ Heat Flux**	**Mass Flux** kg/m^{2}s			
Sydoriak and Roberts (1957)	Annulus Axis vertical L=75-150mm Gap=0.17-1mm				$Q = A_c h_{fg} \left(\rho_l \rho_g g \Delta p\right)^{\frac{1}{2}}$		At best gives order of magnitude and requires knowledge of Δp
Lenfestey (1961)					$\alpha = 8400 - 10,000 \text{W} / \text{m}^2\text{K}$		Typical heat transfer coefficient in air separation processes
Clark and Thorgood (1971)					$\alpha = 3000 - 4000 \text{W} / \text{m}^2\text{K}$		Typical boiling heat transfer coefficient in cryogenic applications
Johannes and Mollard (1972)	L=100-200mm H=0.35-1.65mm Plain Fins	Helium I 1 bar	0.02-1K	10-30	$Nu = 5.5 Re^{0.8} x^{0.8} \left(\frac{L}{d}\right)^{-0.8} \quad \left(\text{For} \left(\frac{L}{d}\right) < 50\right)$ $Nu = 0.24 Re^{0.8} x^{0.8} \quad \left(\text{For} \left(\frac{L}{d}\right) \geq 50\right)$		
Collier et al (1974)	L=1115mm H=6.35mm t_f=0.2mm 590 fin/metre Plain	Nitrogen 2.5-4.1 bar	0.6-1K	14-130			Chen gives satisfactory results
Shorin et al (1974)	L=1625mm H=6mm t_f=0.22mm 222 fin/metre Serrated & Plain	Oxygen 1.2-1.6 bar	600-4500 W/m^{2}K	34-400	At high mass flux results were similar to those for larger (10.7mm diameter) tube At low mass flux results differed from those in larger tubes because of the predominance of laminar flow. At low mass flux α was essentially constant for qualities from 5-50%.		

Table 2.4 Summary of Reported Correlations and Design Method Appropriate to Boiling Heat Transfer in Compact heat Exchangers

Pantsidis et al (1975)	L=4.67mm H=3.88mm t_f=0.1mm 641 fin/metre Serrated	R113 Isopropanol 1.01bar	0-80K	0-72	Use of local Assumption (see text)		
Galezha et al (1976)	Various Serrated & Plain	R12 & R22 -20- +20^{o}C	0.6-5K	0-16	$\overline{\alpha} = C\left(\frac{p_{cr}^{\frac{1}{3}}}{T_{cr}^{\frac{5}{6}} M^{\frac{1}{6}}}\right)\left(0.65 + 3.3\frac{p}{p_{cr}}\right) q^{\frac{1}{3}}$	2.41	Mean value of heat transfer coefficient for heat exchanger in natural circulation loop.
Robertson (1979)	L=3.18mm H=6.35mm t_f=0.2mm 591 fin/metre Serrated	Nitrogen 2-7 bar	0.3-2K	11-110			
Yung Lorenz and Panchal (1980)	L=3.18mm H=4.mm t_f=0.2mm 591 fin/metre Serrated	Ammonia	0-3	12-28			
Robertson and Lovegrove (1980),(!983)	L=3.18mm H=6.35mm t_f=0.2mm 591 fin/metre Serrated	R11 3-7.2bar	0.3-2K	34-159			
Robertson (1982)	Analysis of data of Robertson (1979) and Robertson and Lovegrove (1980)				Film flow model: Triangular relationship between pressure gradient, liquid film flow rate and film thickness to calculate film thickness. $Nu_f = \frac{\alpha\delta}{k_l} = f\left(Re_f\right)$	2.41	Requires measured value of pressure gradient. Assumptions regarding the extent of entrainment required to determine film thickness.

Table 2.4 Summary of Reported Correlations and Design Method Appropriate to Boiling Heat Transfer in Compact heat Exchangers (Continued)

Robertson (1983)	H=6.35mm t_f=0.2mm 591 fin/metre Perforated	Nitrogen 2-7bar	0.3-2K	11-110	$\frac{\alpha}{\alpha_l} = 7.0X^{-0.36}$		
Panchal (1984)	L=4710mm H=7.1mm t_f=0.4mm 720 fin/metre Perforated	Ammonia 9.4 bar		20-43	Film flow model: Triangular relationship between pressure gradient, liquid film flow rate and film thickness to calculate film thickness. $Nu_f = \frac{\alpha\delta}{k_l} = 1$		Requires measured value of pressure gradient. Assumes film is laminar. Neglects entrainment
Carey (1985)	Used Data of Robertson (1979) and Robertson and Lovegrove (1980),(!983) to derive correlation				$\alpha_{min} = \alpha_l \, Pr_l^{0.295}\left(1+0.34\Omega^{0.68}\right)$ $\alpha = \alpha_l \, Pr_l^{0.295} F(1/X_{tt})$ $\alpha_l = 0.242\left(\frac{L}{d_e}\right)^{-0.322}\left(\frac{t}{d_e}\right)^{0.089}\left(\frac{k_l}{d_e}\right)Pr_l^{\frac{1}{3}}\,\mathrm{Re}^{0.632}$ $\Omega = \left[\frac{2Re^{0.198}}{\gamma_l We}\left(\frac{d_e}{d_{es}}\right)(1-O.25Bo)\right]^{\frac{1}{2}}$ $\gamma_l = 1.136\left(\frac{L}{d_e}\right)^{-0.781}\left(\frac{t}{d_e}\right)^{0.534}$ $We = \frac{G^2 d_{es}}{\sigma\rho_l}$ $Bo = \left(\frac{\rho_l - \rho_v}{\sigma}\right)g d_{es}^2 \sin\theta$		Two correlations, one for bubbly and slug flow and one for film flow.

Table 2.4 Summary of Reported Correlations and Design Method Appropriate to Boiling Heat Transfer in Compact heat Exchangers (Continued)

Carey and Mandrusiak (1986)	L=12.7mm H=3.8mm t_f=1.6mm 105 fin/metre Perforated (vertical)	Water Methanol n-Butanol 1.01bar	0-15K	6-35	$\frac{\alpha}{\alpha_l} = \frac{Re_l Pr_l (d_{eh}/d_e)^{0.5n}}{4.74A^{0.5}\tan^{-1}\left(0.149 Re_l^{0.5} Pr_l^{0.5}(d_{eh}/d_e)^{0.5}\right)}$ x $\left(1+\frac{20}{X_{tt}}+\frac{1}{X_{tt}^2}\right)^{0.5}$ $\frac{1}{X_{tt}} = \left(\frac{\rho_l}{\rho_g}\right)^{0.5}\left(\frac{\mu_g}{\mu_l}\right)^{\frac{n}{2}}\left(\frac{x}{1-x}\right)^{1-\frac{n}{2}}$ $St_l Pr_l = ARe_l^n$		A=0.215 n=0.36
Mandrusiak, Carey and Xu(1986)	L=12.7mm H=3.8mm t_f=1.6mm 105 fin/metre Perforated (horizontal)	Water Methanol 1.01bar	0-15K	6-35	As above		
Robertson and Wadekar (1988)	L=3.4mm H=6.35mm t_f=0.2mm 590 fin/metre Perforated	Cyclohexane 1.5 bar	< 3K <10kW/m^2	50-290			
Panchal (1989)	L=4710mm H=7.1mm t_f=0.4mm 720 fin/metre Perforated	R114 3.5 bar Ammonia 9.4 bar		85-250 20-43			No nucleate boiling existed at any point

Table 2.4 Summary of Reported Correlations and Design Method Appropriate to Boiling Heat Transfer in Compact heat Exchangers (Continued)

Wadekar (1992)	L=3.4mm H=6.35mm t_f=0.2mm 590 fin/metre Perforated	Cyclohexane Heptane 1.5 bar	< 3K <10kW/m^2	50-290	Intermittent or Slug Flow $\left(j_G^* < 1\right)$: Model of Wadekar and Kenning (1990) and Wadekar (1991). Non-Intermittent: $\left(j_G^* \geq 1\right)$: $\alpha = F\alpha_l$ $Y = \left[\left(\frac{x}{1-x}\right)^{0.75}\left(\frac{p}{p_c}\right)^{-0.375} M^{0.125}\right]$ $F = 3.2Y + 1$		Cyclohexane data from Robertson and Wadekar (1988) Slug flow model underpredicts data in the intermittent flow region Wadekar (1990) Correlation underpredicts data but less so than Chen (1963) Liquid heat transfer coefficient, α_l, obtained by extrapolating turbulent data into laminar region if appropriate.

* Equation Numbers are assigned only if the Equation is used elsewhere.

Table 2.4 Summary of Reported Correlations and Design Method Appropriate to Boiling Heat Transfer in Compact heat Exchangers (Continued)

FLUID	Normal Boiling Point °C	Viscosity		Density		Surface Tension	Specific Heat	Thermal Conductivity	Latent Heat	Critical Temperature	Critical Pressure	Mol Weight
		Liquid m Pa s	Vapour m Pa s	Liquid kg/m³	Vapour kg/m³	m Nm	J kg K	W/m K	kJ/kg	°C	bar	
Water	100	0.279	.012	959	0.498	58.9	4219	0.681	2256	374	221	18
Flutec PP1	57	0.425		1582	13.5	8.3	1200	0.632	85.5	178	18	338
R113	48	0.516	.011	1508	7.435	14.7	984	0.0705	144	214	34.1	187
R141B	32	0.393	.010	1215	4.85	17.28	790	.0886	223	204	42.5	117

Table 3.1 Heat Transfer Properties of Fluids Used in This Study

Single Channel Gap /mm	Confinement No. (Based on d_e)	Confinement No. (Based on min. d)
1	0.97	1.93
2	0.49	0.97
3	0.33	0.64
4	0.25	0.48
6	0.17	0.32
Geometry 1	1.88	2.14
Geometry 2	1.17	1.74

Table 3.2 Confinement Number (Co) for Test Geometries, Mark I Rig.

(Fluid R113)

Parameter	**Range**	
Mass Flux	100-1500	kg/m^2s
Heat Flux	10-100	kW/m^2
Quality	0.0-0.9	

Table 3.3 Test Parameters for Single Tube Test Section.

Single Channel	1.125-4.5 mm x 76mm
Single Channel with adiabatic splitter(s)	1.5mm x 76mm 1 & 2 splitters
Multiple Channel	2mm x 2mm x 12 channels
Multiple Channel	3mm x 3mm x 10 channels
Multiple Channel	4mm x 4mm x 6 channels
Heat Flux	5-95 kW/m^2
Mass Flux	10-565 kg/m^2s
Pressure	1.0-1.5 bar
Fluids	R141b Flutec PP1

Table 3.4 Test Parameters for Flow Visualisation Test Section.

Geometry	Confinement No. (Based on d_e)			Confinement No. (Based on min. d)		
	Water	PP1	R141b	Water	PP1	R141b
1.125mm Gap	1.11	0.32	0.53	2.22	0.64	1.07
1.5mm Gap	0.83	0.24	0.40	1.67	0.48	0.4
4.5mm Gap	0.28	0.08	0.13	0.56	0.16	0.27
1.39mm ϕ	1.80	0.52	0.86			
2.05mm ϕ	1.22	0.35	0.59			
2.87mm ϕ	0.87	0.25	0.42			
3.69mm ϕ	0.68	0.20	0.33			
2.10mm□	1.19	0.34	0.57			
2.00mm□	1.25	0.36	0.60			
3.00mm□	0.83	0.24	0.40			
4.00mm□	0.63	0.18	0.30			

Table 3.5 Confinement Numbers For Geometries Investigated with Mark II Rig

Type	5mW Helium-Neon
Manufacturer	Dantec
Configuration	One component backscatter system with frequency shift.
Mounting	3-D Traverse 600x600x600mm
Lens	Focal length 310mm
Beam separation	60mm
Measuring Volume	$0.28mm^3$

Table 3.6 Specification of LDA system

Geometry	Fluid	Co	m	n	a	b
2mm □	R141b 1bar	0.6	1.4	0.3	2.3	1.8
2mm □	R141b 1.5bar	0.6	1.4	0.3	2.6	1.9
3mm □	R141b 1bar	0.4	1.7	0.4	1.4	1.2
4mm □	R141b 1bar	0.3	2.7	0.6	0.25	0.6
Equation 6.1.3	R141b 1bar		3.0	0.67	0.015	0.254
Equation 6.1.3	R141b 1.5bar		3.0	0.67	0.022	0.283
3mm □	PP1 1bar	0.24	2.6	0.6	0.27	0.6
4mm □	PP1 1bar	0.18	2.5	0.6	0.49	0.75
Equation 6.1.3	PP1 1bar		3.0	0.67	0.007	0.192

(Units α-kW/m^{2}K, q-kW/m^2,ΔT -K)

Table 3.7 Constants for Equation 1.8 Applied to Results from Flow Visualisation Test Section

Tube Description	Co	No. of Points	Percentage Deviation	
			E1	E2
3.69mm ϕ	0.33	16	-16.3	49.7
2.87mm ϕ	0.42	14	-27.1	52.7
2.05mm ϕ	0.59	21	+26.3	58.8
1.39mm ϕ	0.87	23	- 5.3	53.0
2.10mm □	0.57	16	- 1.3	49.0
Average			- 2.5	53.7

$$\text{Percentage Deviation } E1 = \frac{100}{N}\sum\frac{\left(\Delta p_{\exp} - \Delta p_{pred}\right)}{\Delta p_{\exp}}$$

$$\text{Percentage Deviation } E2 = \frac{100}{N}\sum\frac{\left|\Delta p_{\exp} - \Delta p_{pred}\right|}{\Delta p_{\exp}}$$

Table 3.8 Comparison of R141b Pressure Drop Data with Prediction

Fluid	No. of Points	Percentage Deviation	
		E1	E2
R141b	102	+9.9	49.8
Water	12	+0.1	21.7

(Percentage deviation defined as for Table 3.8)

Table 3.9 Comparison of R141b and Water Pressure Drop Data with Prediction

Tube Description	Co	No. of Points	Percentage Deviation				
			L&W	Cooper (a)	Cooper (b)	L&B	L&B (Mod)
3.69mm ϕ	0.33	146	21	25	36	22	23
2.87mm ϕ	0.42	141	42	21	46	19	19
2.05mm ϕ	0.59	182	118	30	43	47	48
1.39mm ϕ	0.87	79	250	36	69	69	71
2.10mm □	0.57	149	72	33	54	39	39
2.92mm ϕ (c)	0.34		15				

$$\text{Percentage Deviation} = \frac{100}{N}\sum\frac{\left|\alpha_{exp}-\alpha_{pred}\right|}{\alpha_{exp}}$$

L & W : Liu and Winterton (1988)

$$\alpha^2 = \left(S\alpha_{npb}\right)^2 + \left(F\alpha_L\right)^2$$

Cooper (a) : Cooper (1984)

$$\alpha = 55\,p_r^{0.12}\left(-\log_{10} p_r\right)^{-0.55} M^{-0.5} q^{0.67}$$

Cooper (b) : Cooper (1989)

$$\alpha = 35\,p_r^{0.12}\left(-\log_{10} p_r\right)^{-0.55} M^{-0.5} q^{0.67}$$

L & B: Lazarek and Black (1982)

$$Nu = 30\,Re^{0.857}\,Bo^{0.714}$$

L & B(Mod): Modified Lazarek and Black (1982)

$$Nu = 30\,Re^{0.857}\,Bo^{0.714}\left(1-x\right)^{-0.143}$$

Table 3.10 Comparison of Measured Single-Tube Heat Transfer Data with Selected Correlations

Geometry	Percentage Deviation	
	E1	E2
3.69mmϕ	-8	24.9
2.87mmϕ	-31.6	32.7
2.05mmϕ	-32.5	37.3
1.39mmϕ	-31.5	39.3

$$\alpha = 840\left(Bo^2 We_l\right)^{0.3}\left(\frac{\rho_l}{\rho_g}\right)^{-0.4} \text{ kW / m}^2\text{K}$$

Table 3.11 Comparison of Measured Single-Tube Data with Correlation of Tran, Wambsganns and France (1995)

Coefficient	Water	R141b	
α'_{nb} $(\Delta T = 3\text{K})$	685	134	W/m^{2}K
α'_{sb} $(\delta = 20\mu\text{m})$	29.4 x 10^3	4435	W/m^{2}K
α'_{conv} (Laminar, Nu = 3)	510	66.5	W/m^{2}K
α'_{conv} (Turbulent, *Re* = 2000)	2132	428	W/m^{2}K

α'_{nb} predicted by *Equation 1.7*

Table 4.1 Representative Heat Transfer Coefficients in 2mm Channel

Bubble Ref	Symbol (Fig. 4.12(a))	s mm	ΔT K
1	○	0.5	1.5
2	○		
3	○		
4	○		
5	□	0.5	3.3
6	□		
7	●	1	4.3
8	■	1	5.2
9	■		
10	■		

(a) Conditions for bubbles analysed - R113 Data
(Kew and Cornwell 1994)

Bubble Ref	Symbol (Fig. 4.12(b))	s mm	ΔT K
1	○	1.125	2.72
2	●	1.125	2.62

(b) Conditions for bubbles analysed R141b Data

Table 4.2 Data Used in Determination of Film Thickness of Growing Bubbles

Gap mm	$f\left(\frac{r_{max}}{r_0}\right)$	Heat Transfer Coefficient Predicted by Equation kW/m^{2}K		
		Water	R141b	R113
0.5	0.783	13.252	1.722	1.37
0.75	0.762	12.896	1.676	1.333
1	0.745	12.609	1.639	1.303
1.5	0.716	12.118	1.575	1.253
2	0.691	11.695	1.52	1.209
3	0.647	10.95	1.423	1.132
4	0.609	10.307	1.339	1.065
5	0.572	9.681	1.258	1.001
6	0.538	9.105	1.183	0.941
8	0.471	7.971	1.036	0.824
10	0.406	6.871	0.893	0.71
12	0.343	5.805	0.754	0.6
14	0.281	4.755	0.618	0.491
16	0.221	3.74	0.486	0.386
18	0.164	2.775	0.36	0.287
20	0.112	1.895	0.246	0.196
22	0.064	1.083	0.14	0.112
24	0.02	0.338	0.044	0.035

Table 4.3 Prediction of α_{CB} Using Thin Film Evaporation Model
(Micro-Layer = 20μm, r_{max} =25mm)

Isolated Bubble/ Nucleate Boiling	Confined Bubble		Annular Slug Flow	
	Void Fraction	**Film Thickness**	**Void Fraction and Film Thickness**	**Film Nusselt Number**
Mostinski (1)	Homogeneous Flow	Taylor (5)	Homogeneous Flow	Hewitt (9)
Cooper (2)	Moriyama and Inoue (3)	Moriyama and Inoue (6)	CISE (7)	
	Chisholm (4)		Zivi (8)	

(1)Mostinski (1963) *Equation 1.3*

(2)Cooper (1984), (1989), *Equations 1.7,1.7(a)*

(3)Moriyama and Inoue (1992), *Equation 2.12*

(4) Chisholm (1972) *Equation 1.64*

(5) Wallis (1969) *Equation 2.45*

(6)Moriyama and Inoue (1992), *Equation 2.14*

(7) Premoli (1970) , *Equation 1.64*

(8) Zivi (1964), *Equation 1.62*

(9) Hewit and Hall Taylor (1970), *Figure 2.2.*

Table 5 1. Correlations Tested in Model for Evaporation in Narrow Channels

	3.69mm Diameter		2.87mm Diameter		2.05mm Diameter		1.39mm Diameter	
	E1	**E2**	**E1**	**E2**	**E1**	**E2**	**E1**	**E2**
Assumption 1	105	105	119	119	202	204	344	345
Assumption 2	61	63					298	299
Assumption 3	19	28					229	231
Assumption 4	15	28					20	41
Assumption 5	-2	23	25	32	98	109	227	231
L&B (1982)		22		19		47		69
Cooper(1984)		25		21		30		36
L&W (1988)		21		42		118		250

$$E1 = \frac{100}{N}\sum\frac{(a_{pred} - a_{exp})}{a_{exp}}, \qquad E2 = \frac{100}{N}\sum\frac{|a_{pred} - a_{exp}|}{a_{exp}}$$

	Nucleate Boiling Constant (Eq 1.7)	**Film Nusselt No.**	**Method of Combination**
Assumption 1	55	From Fig 2.2	$\alpha = \alpha_{nb} + \alpha_f$ -Substitution
Assumption 2	35	From Fig 2.2	$\alpha = \alpha_{nb} + \alpha_f$ -Substitution
Assumption 3	55	From Fig 2.2	α = Larger of α_{nb} or α_f - Additive
Assumption 4	55	1	α = Larger of α_{nb} or α_f - Additive
Assumption 5	35	From Fig 2.2	α = Larger of α_{nb} or α_f - Additive

L & W : Liu and Winterton (1988)

$$\alpha^2 = \left(S\alpha_{npb}\right)^2 + \left(F\alpha_L\right)^2 \quad \textit{(Equations 1.21-1.24)}$$

Cooper (1984)

$$\alpha = 55\,p_r^{0.12}\left(-\log_{10} p_r\right)^{-0.55} M^{-0.5} q^{0.67} \quad \textit{(Equation 1.7)}$$

Cooper (1989)

$$\alpha = 35\,p_r^{0.12}\left(-\log_{10} p_r\right)^{-0.55} M^{-0.5} q^{0.67} \quad \textit{(Equation 1.7(a))}$$

L & B: Lazarek and Black (1982)

$$Nu = 30\,Re^{0.857} Bo^{0.714} \quad \textit{(Equation 2.1)}$$

Table 5.2 Errors Associated with Model Applied with Various Conditions

	No Splitter		1 Splitter		2 Splitter	
	E1	**E2**	**E1**	**E2**	**E1**	**E2**
Assumption 1	-5.5	29	-3.5	37	2.6	27
Assumption 3	-31	43	-7.4	48	-31	38
Assumption 4	-7.40	43	-35	48	-31	38

(a) Flat Plates

	2mm Square		3mm Square	
	E1	**E2**	**E1**	**E2**
Assumption 1	-6	29	-28	31
Assumption 3	-46	46	-55	56
Assumption 4	-51	51	-56	56

(b) Multi-Channels

$$E1 = \frac{100}{N}\sum\frac{(a_{pred} - a_{exp})}{a_{exp}} \qquad E2 = \frac{100}{N}\sum\frac{|a_{pred} - a_{exp}|}{a_{exp}}$$

	Nucleate Boiling Constant (Eq 1.7)	Film Nusselt No.	Method of Combination
Assumption 1	55	From Fig 2.2	$\alpha = \alpha_{nb} + \alpha_f$
Assumption 3	55	From Fig 2.2	α = Larger of α_{nb} or α_f
Assumption 4	55	1	α = Larger of α_{nb} or α_f

Table 5.3 Errors Associated with Model Applied with Various Assumptions (Flat Plate and Multi-Channel Geometries, R141b)

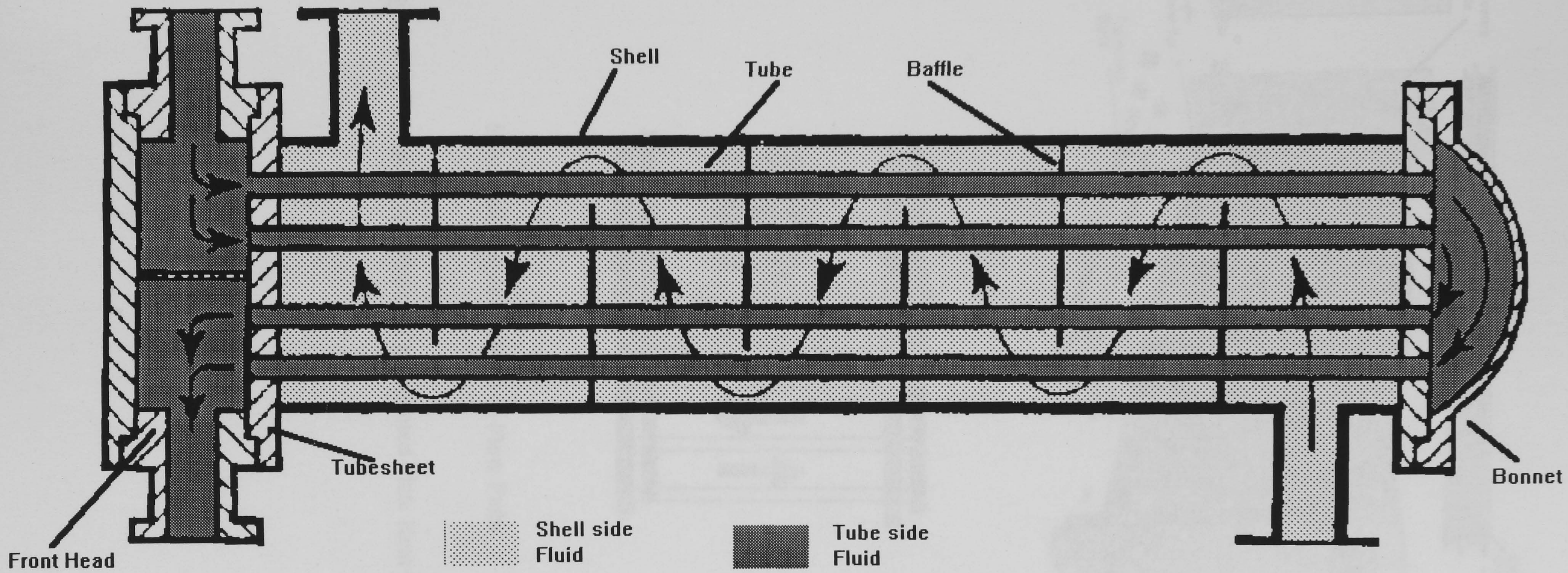

Figure 1.1 Typical Layout of Shell-and-Tube Heat Exchnger
(TEMA Type AEM)

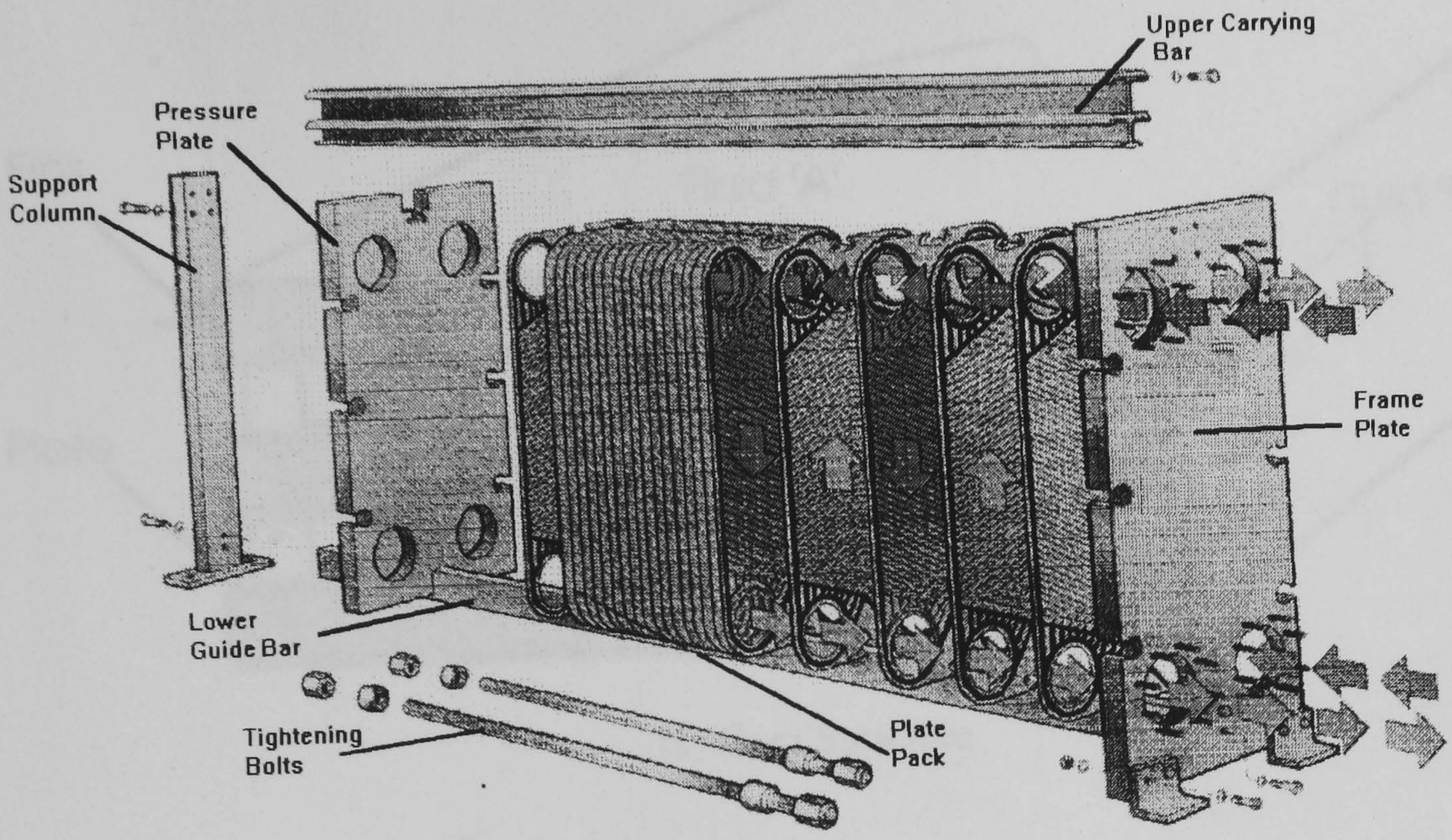

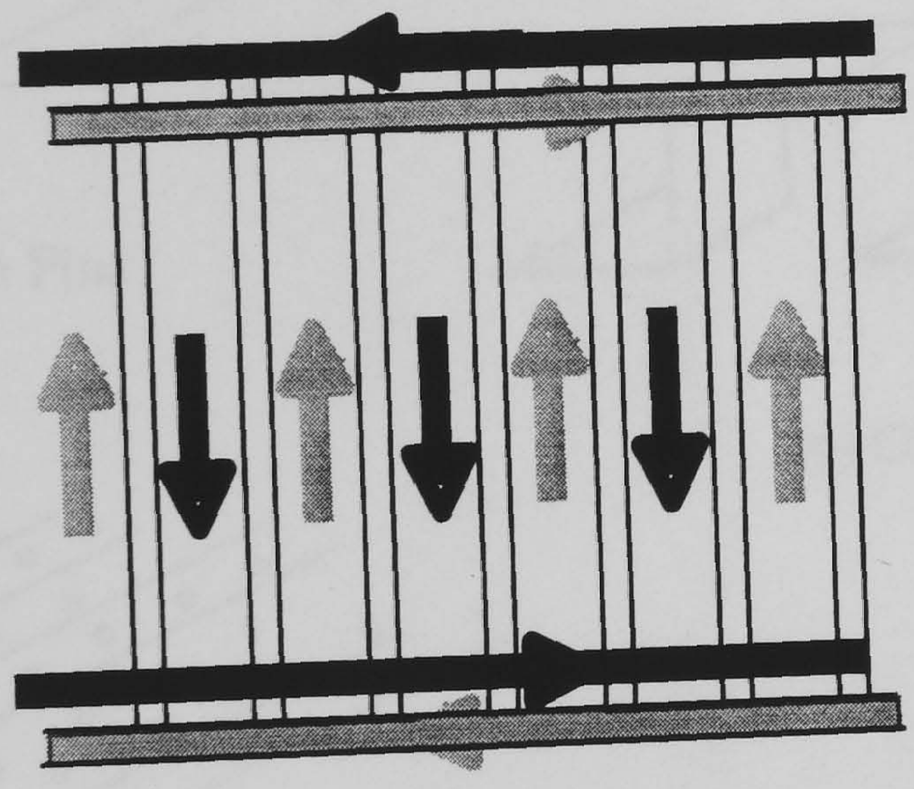

Schematic Representation of Flow Paths

Figure 1.2 General Arrangement of a Gasketed Plate Heat Exchanger

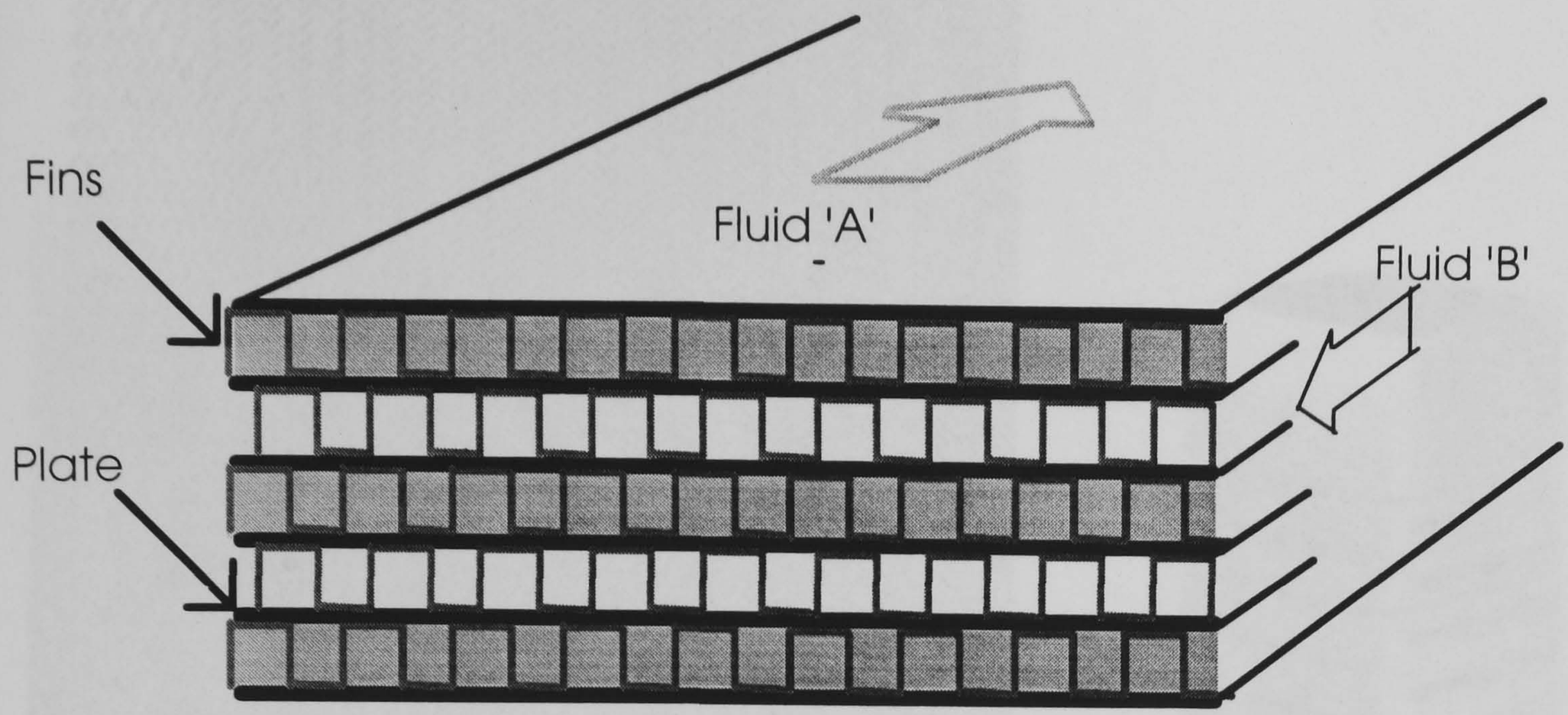

(a) Core Structure

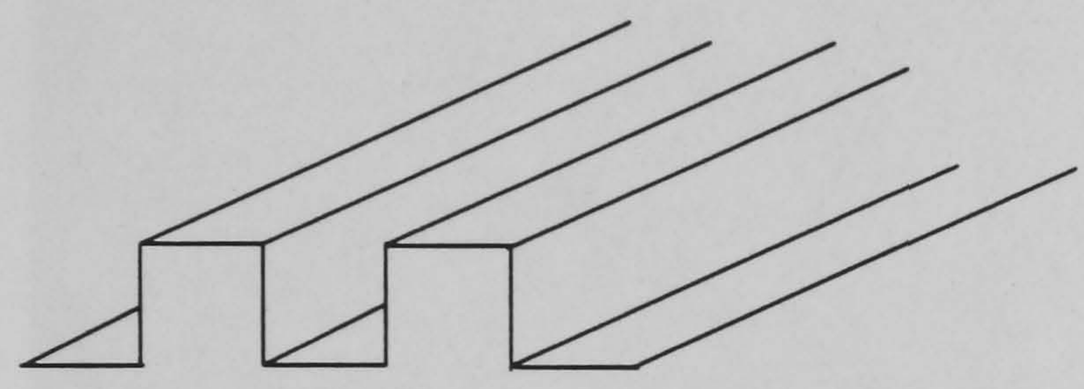

(a) Plain Fins

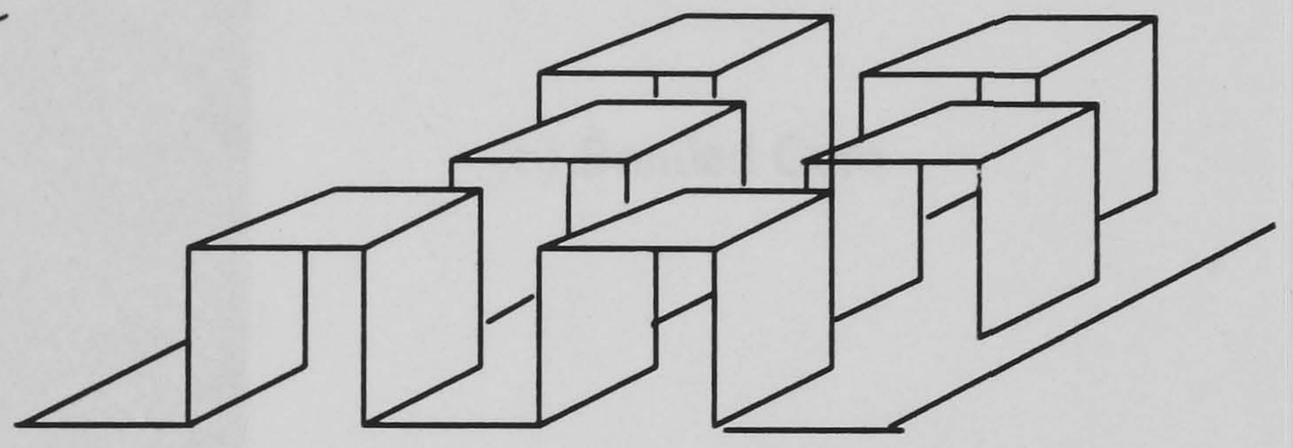

(c) Offset-Strip Fins

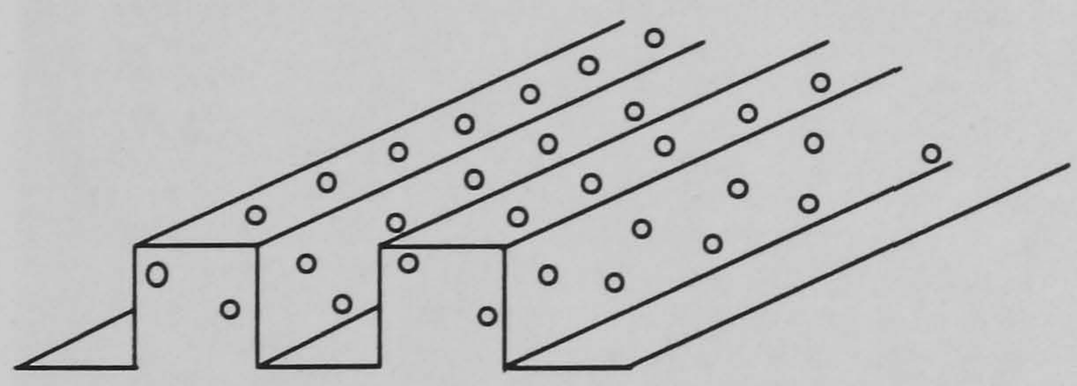

(b) Perforated Fins

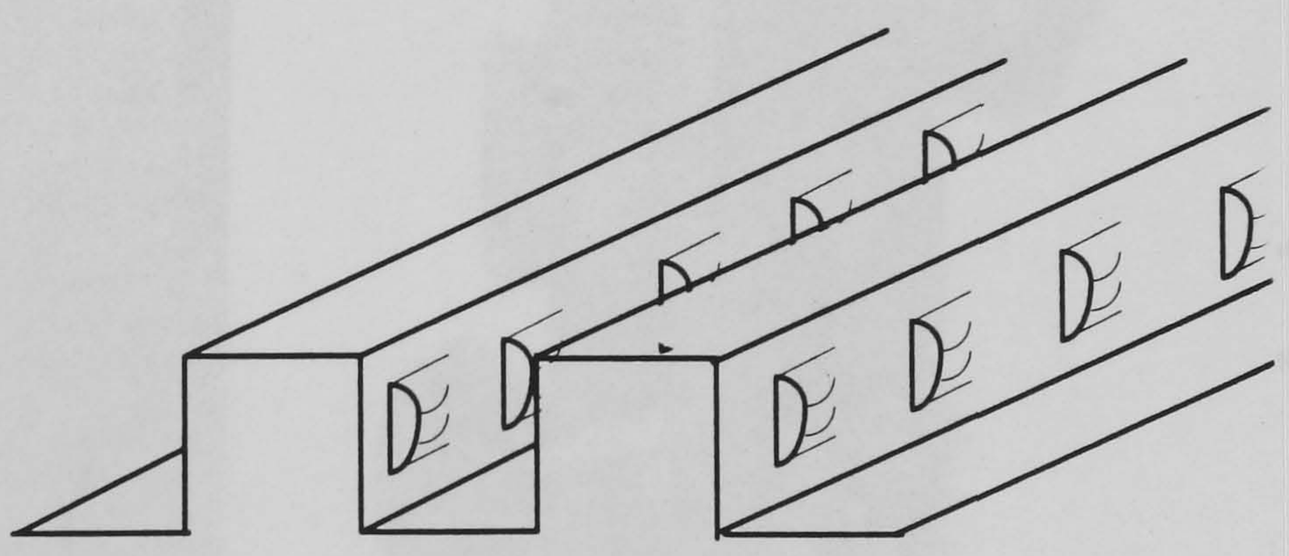

(d) Perforated Fins

Figure 1.3 Core Structure and Typical Fins for Plate-Fin Heat Exchangers

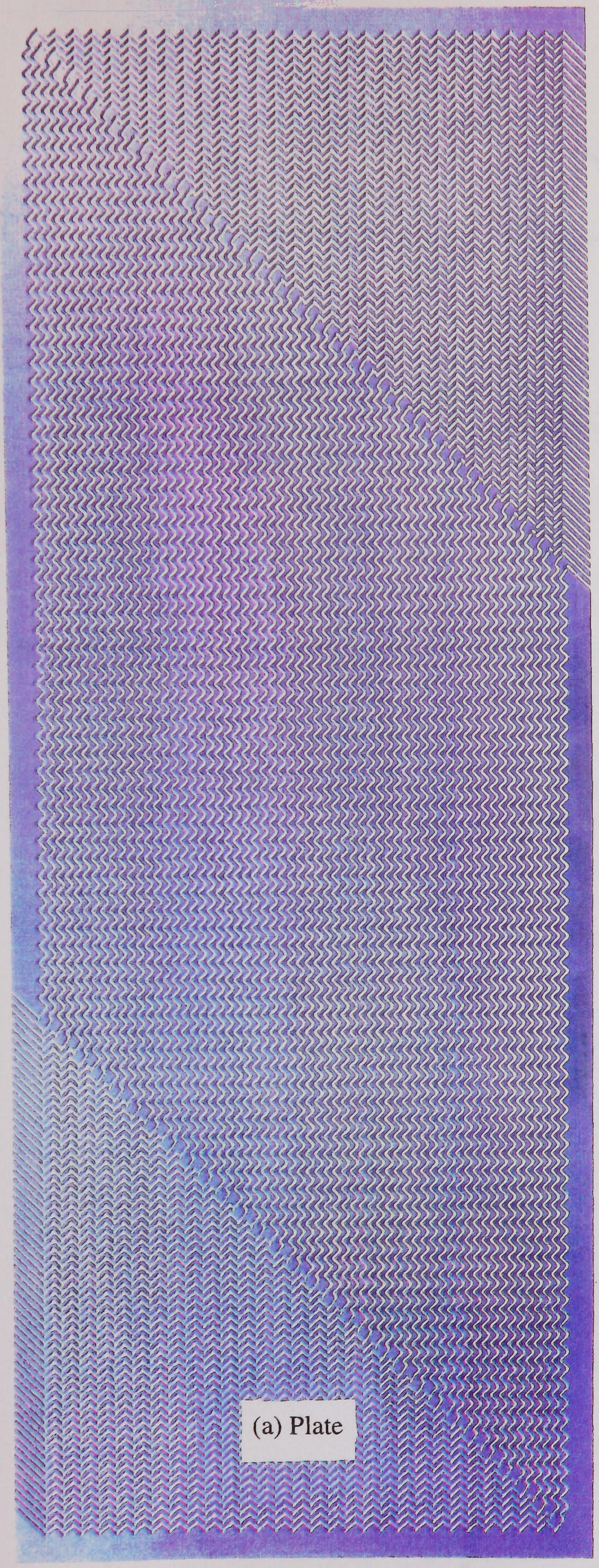

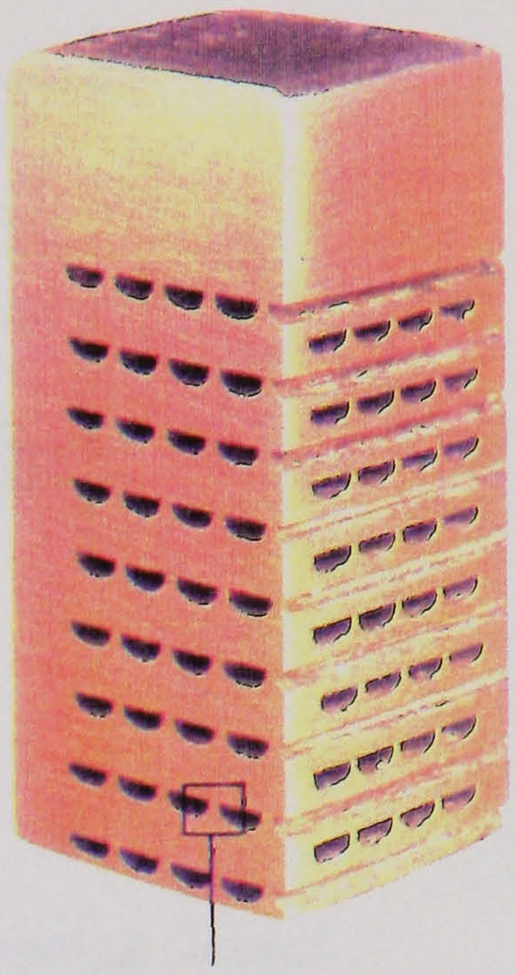

(b) Bonded Core

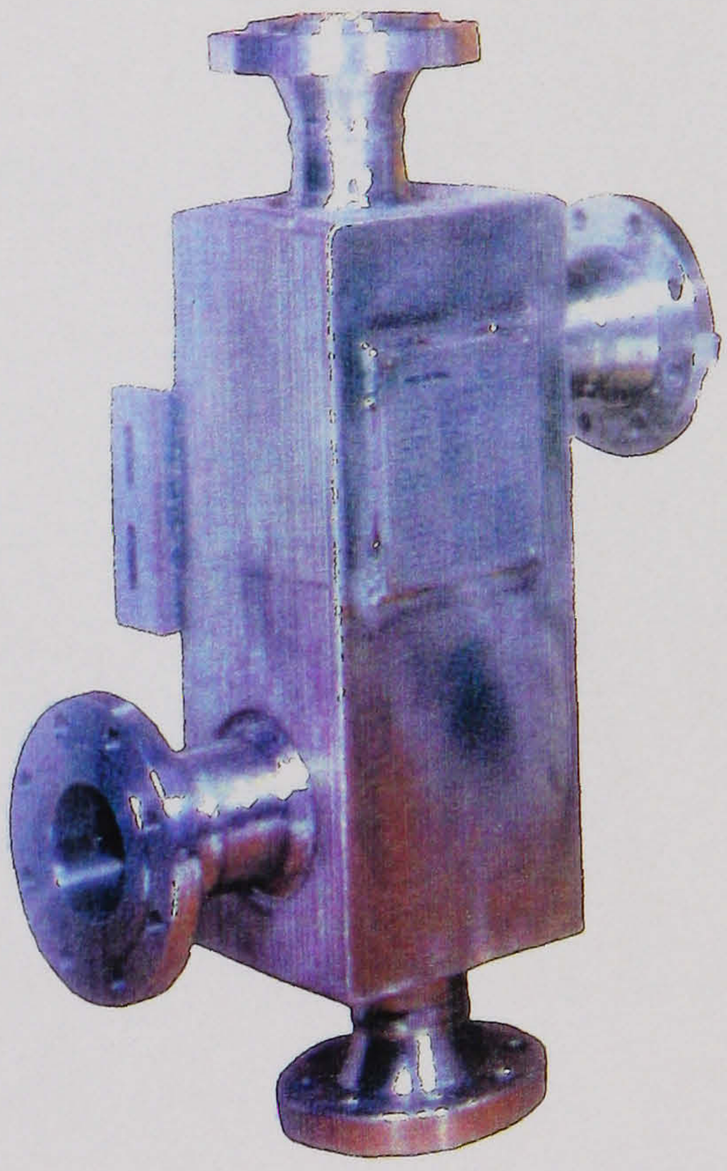

(c) Assembled PCHE

Figure 1.4 Printed Circuit Heat Exchanger Showing Typical Plate and Bonded Core

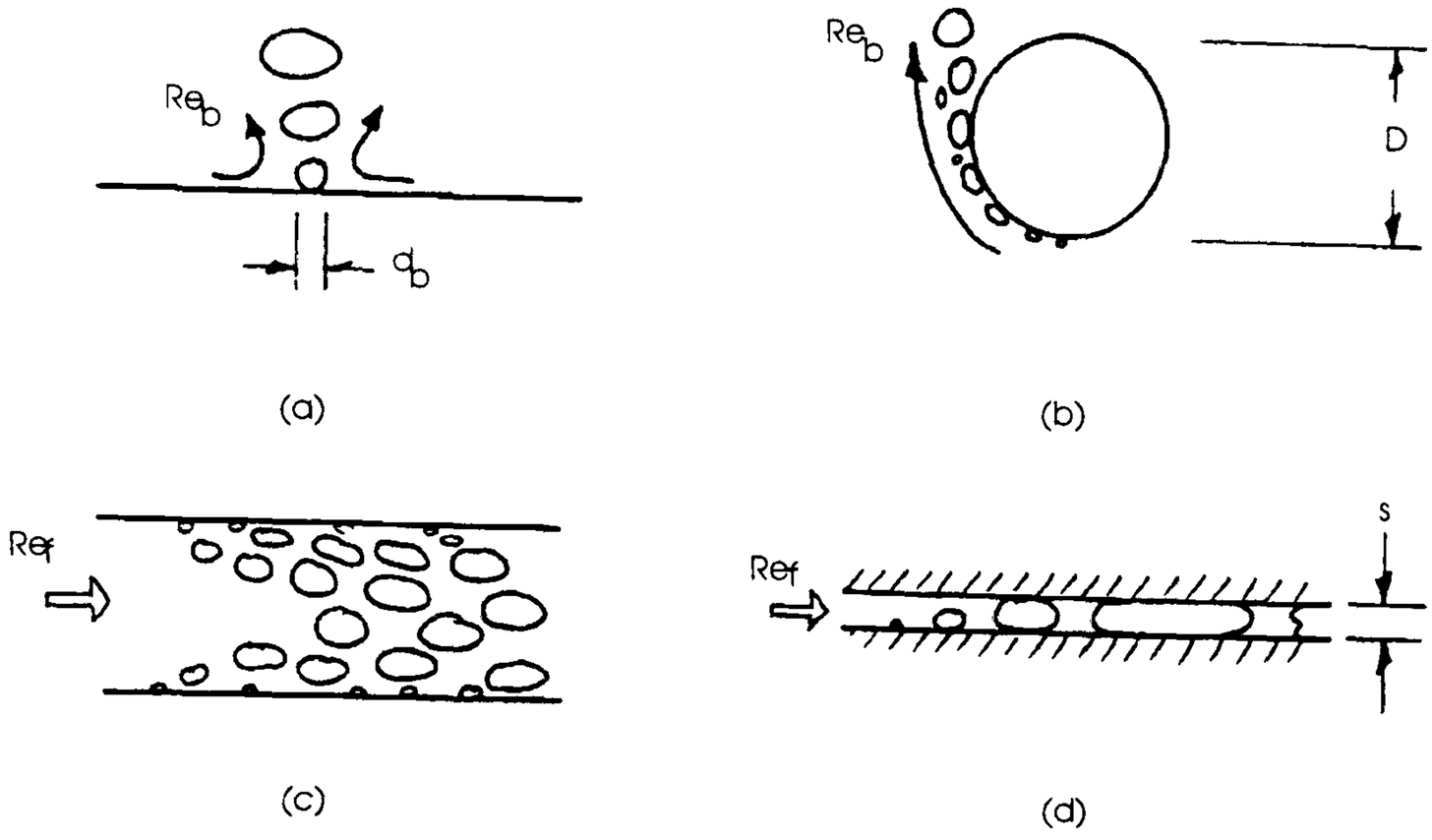

Figure 1.5 Geometrical Arrangements of Surfaces on which Boiling Occurs

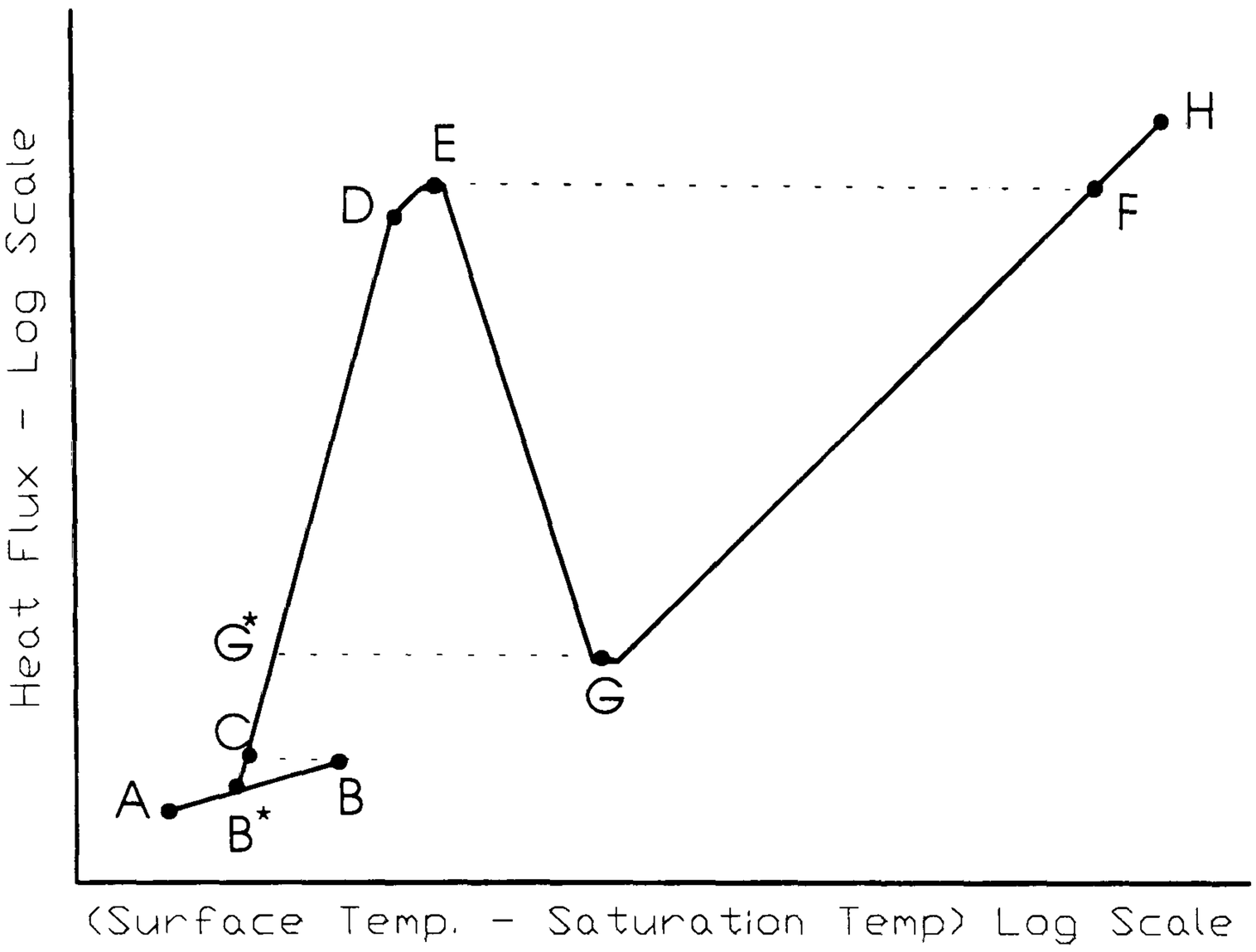

Figure 1.6 Typical Pool Boiling Curve

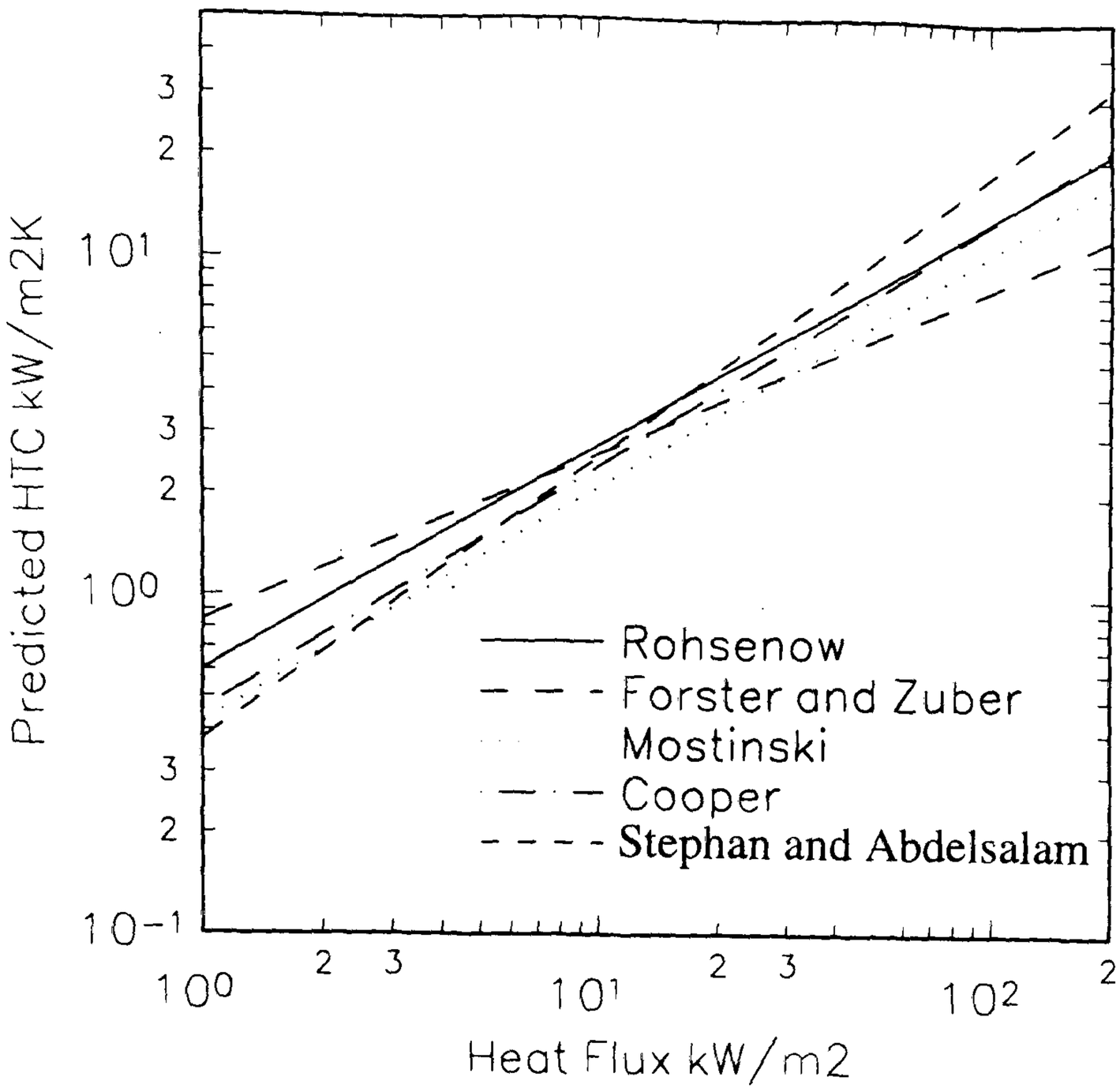

(a) Water

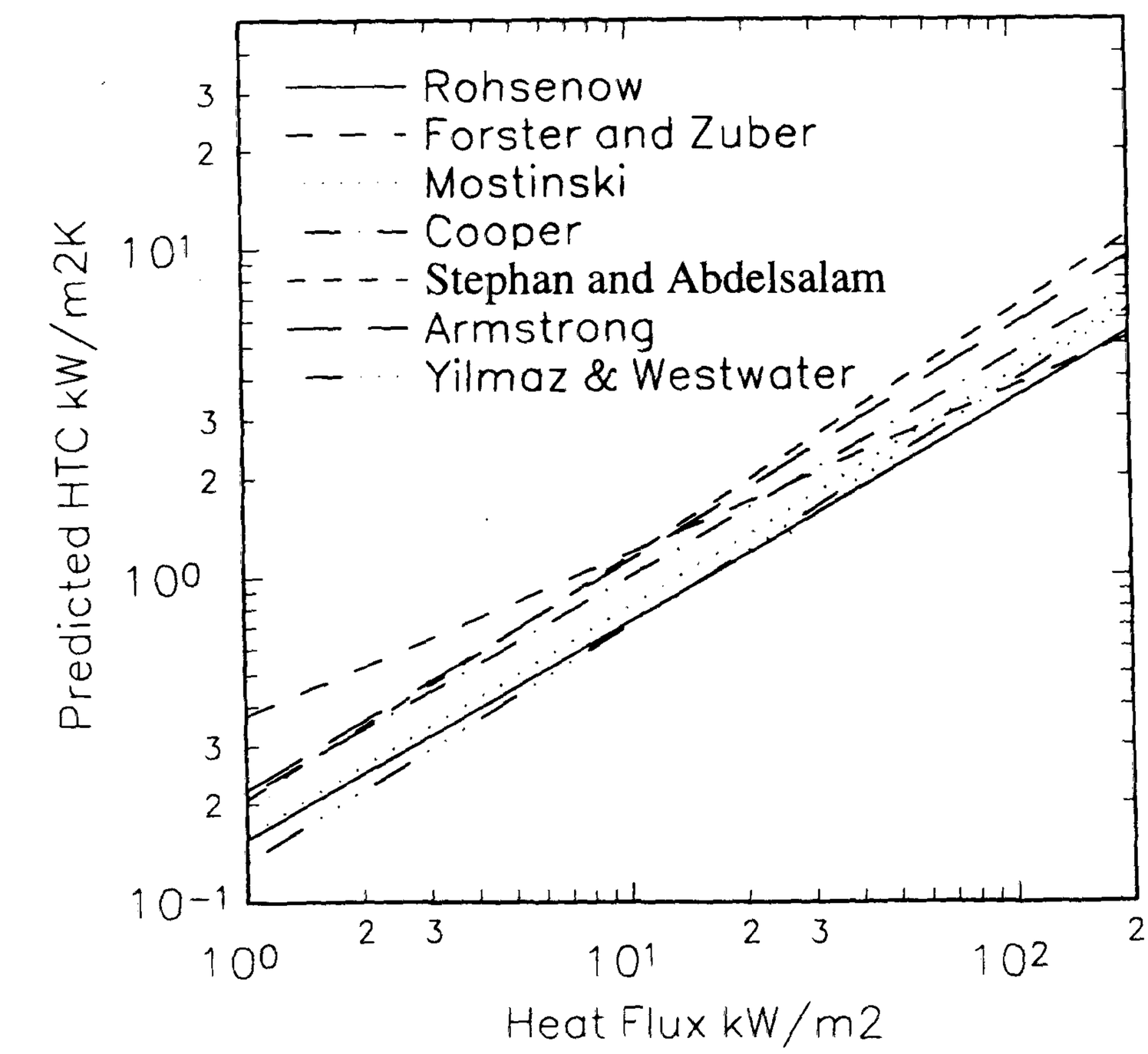

(b) R113

Figure 1.7 Application of Pool Boiling Correlations at Atmospheric Pressure

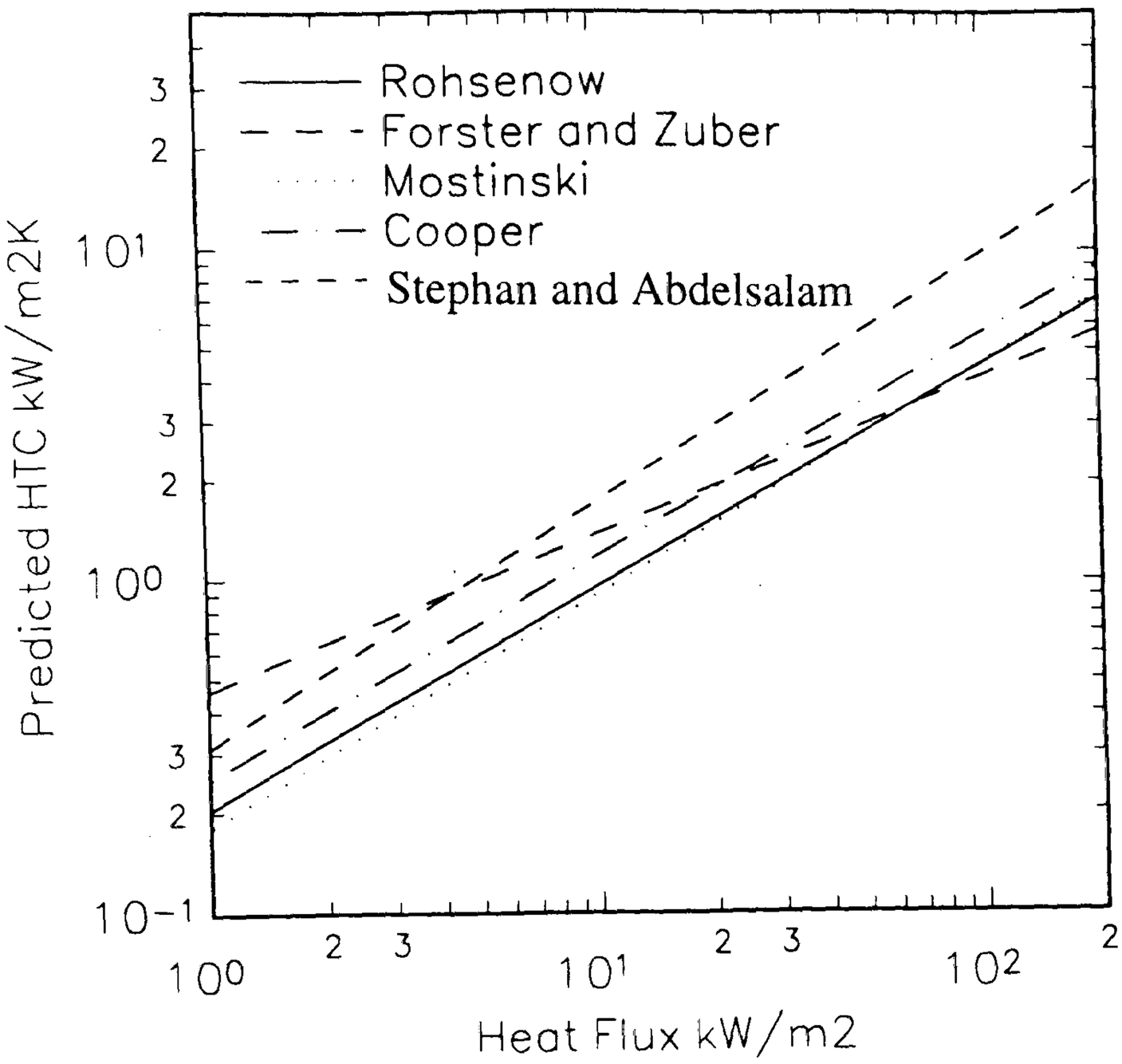

(c) **R141b**

Figure 1.7 Application of Pool Boiling Correlations at Atmospheric Pressure (Cont)

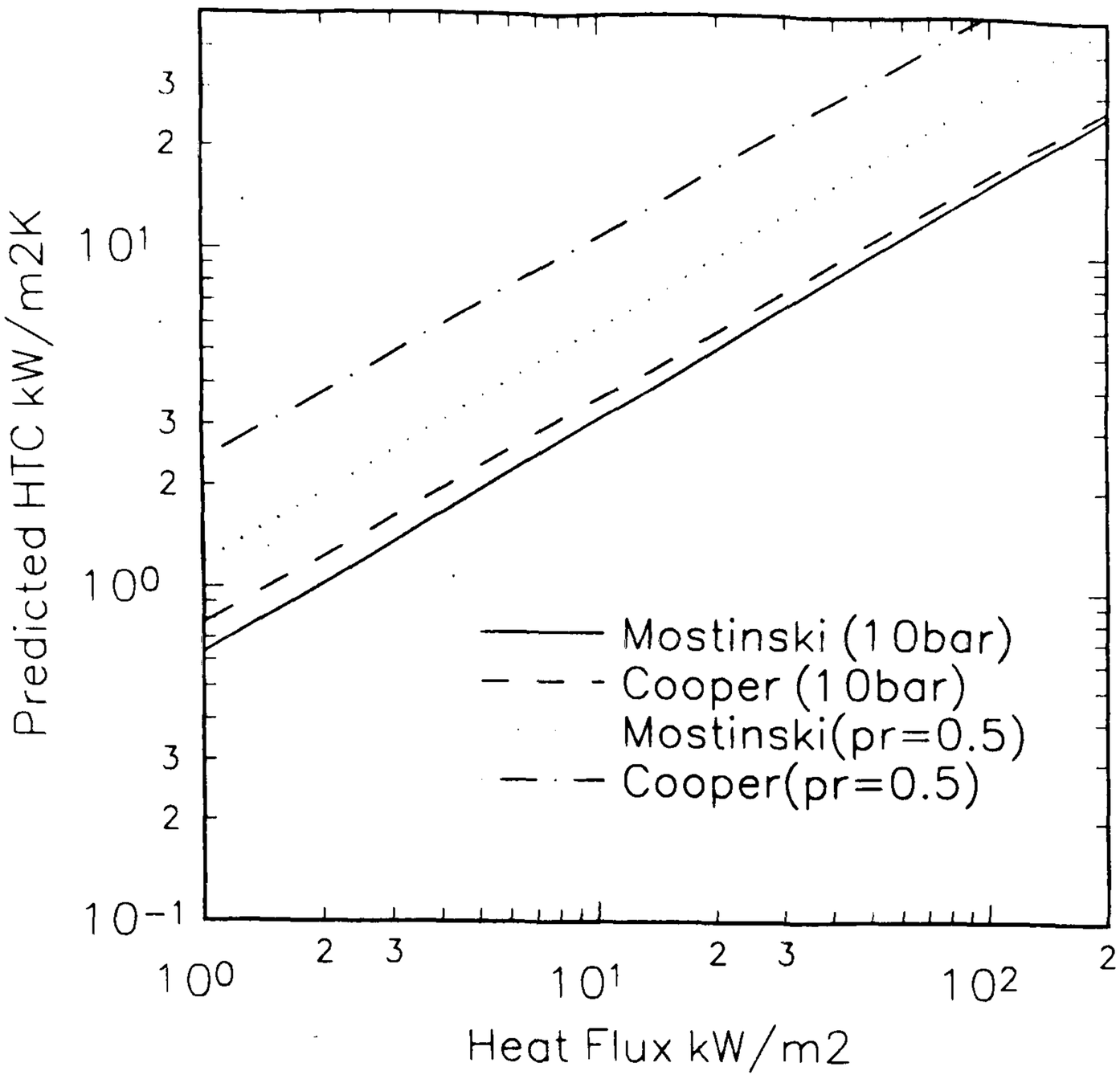

(a) Water

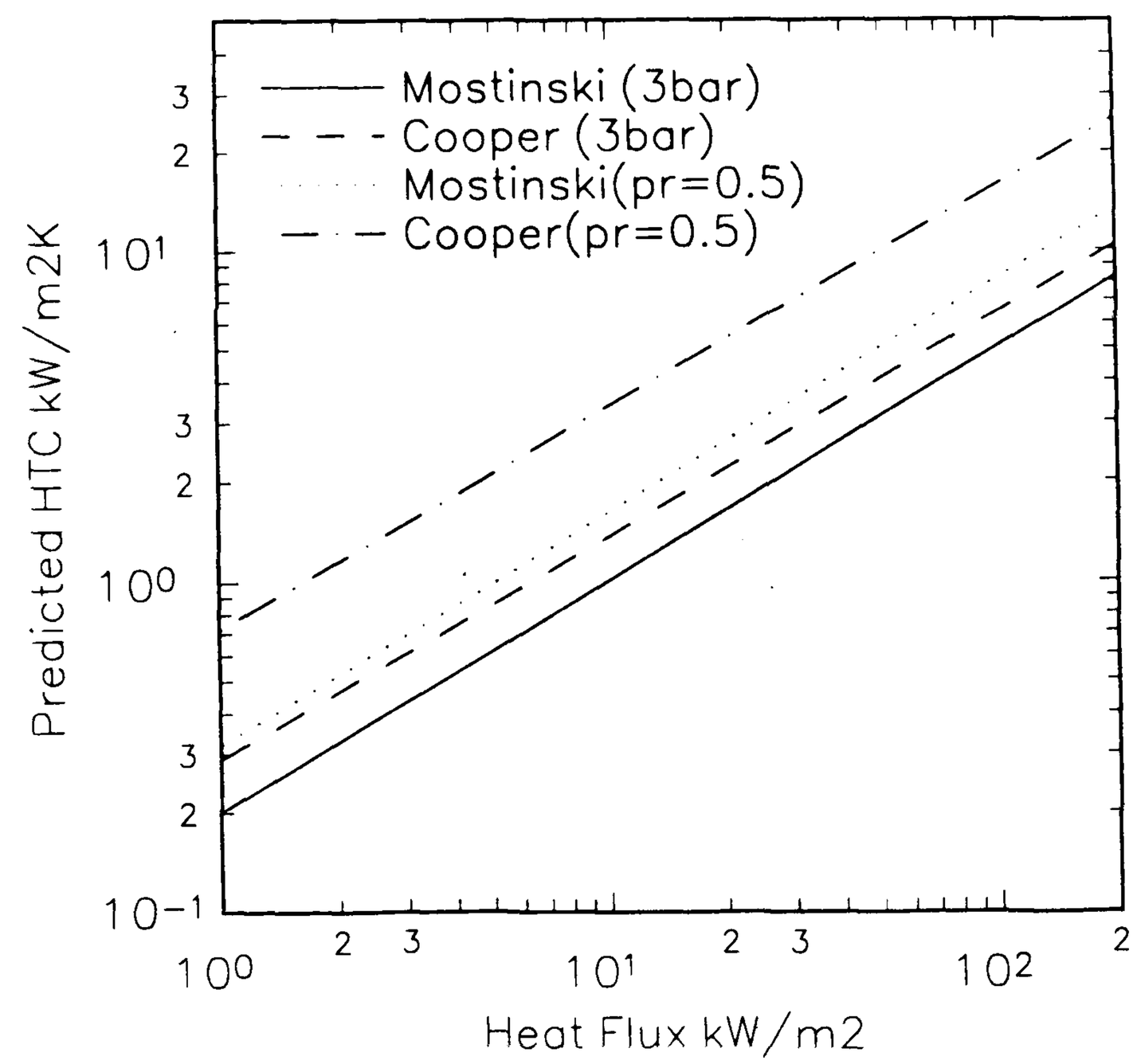

(b) R113

Figure 1.8 Application of Pool Boiling Correlations at Elevated Pressure

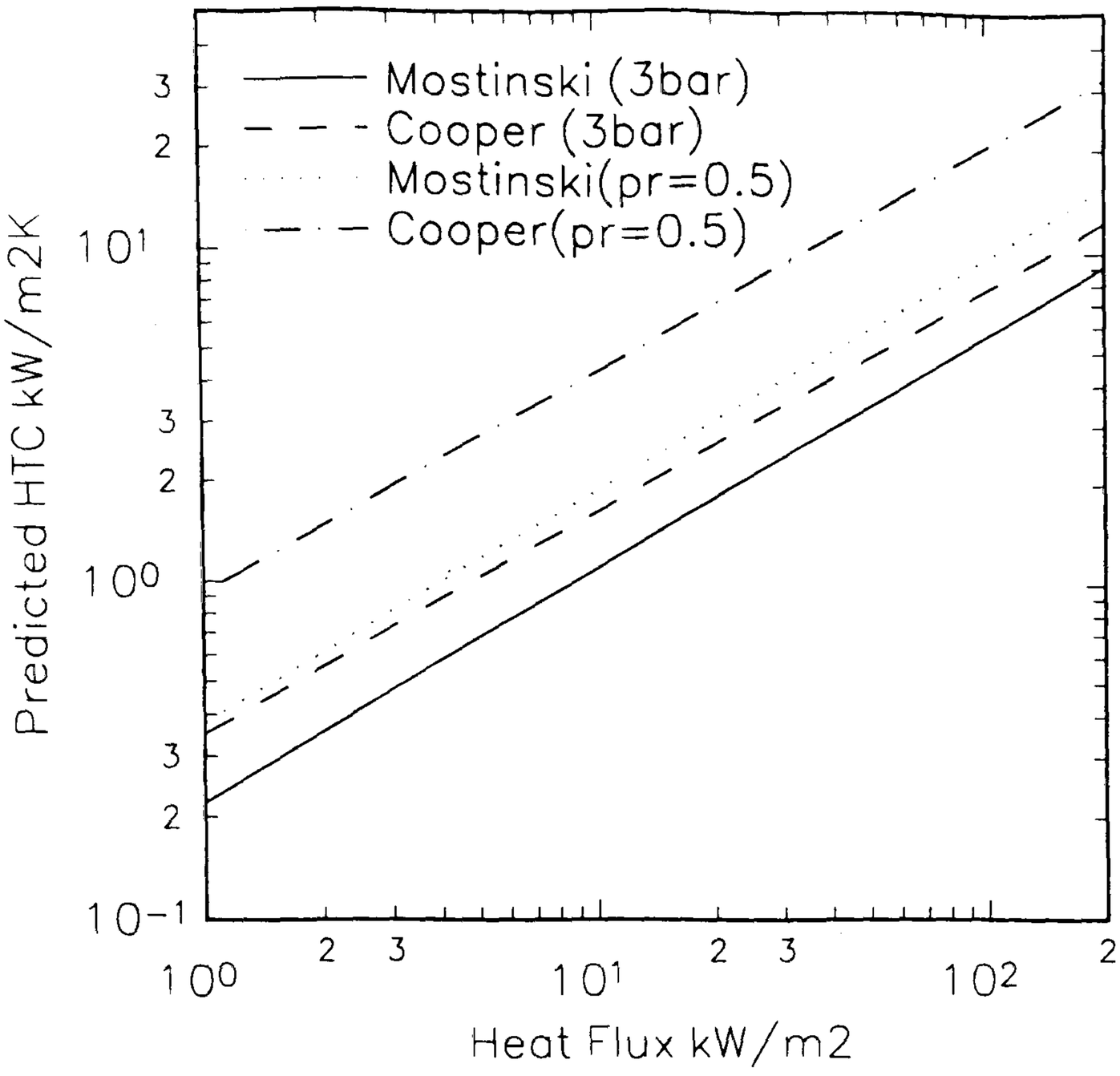

(c) R141b

Figure 1.8 Application of Pool Boiling Correlations at Elevated Pressure : (Cont)

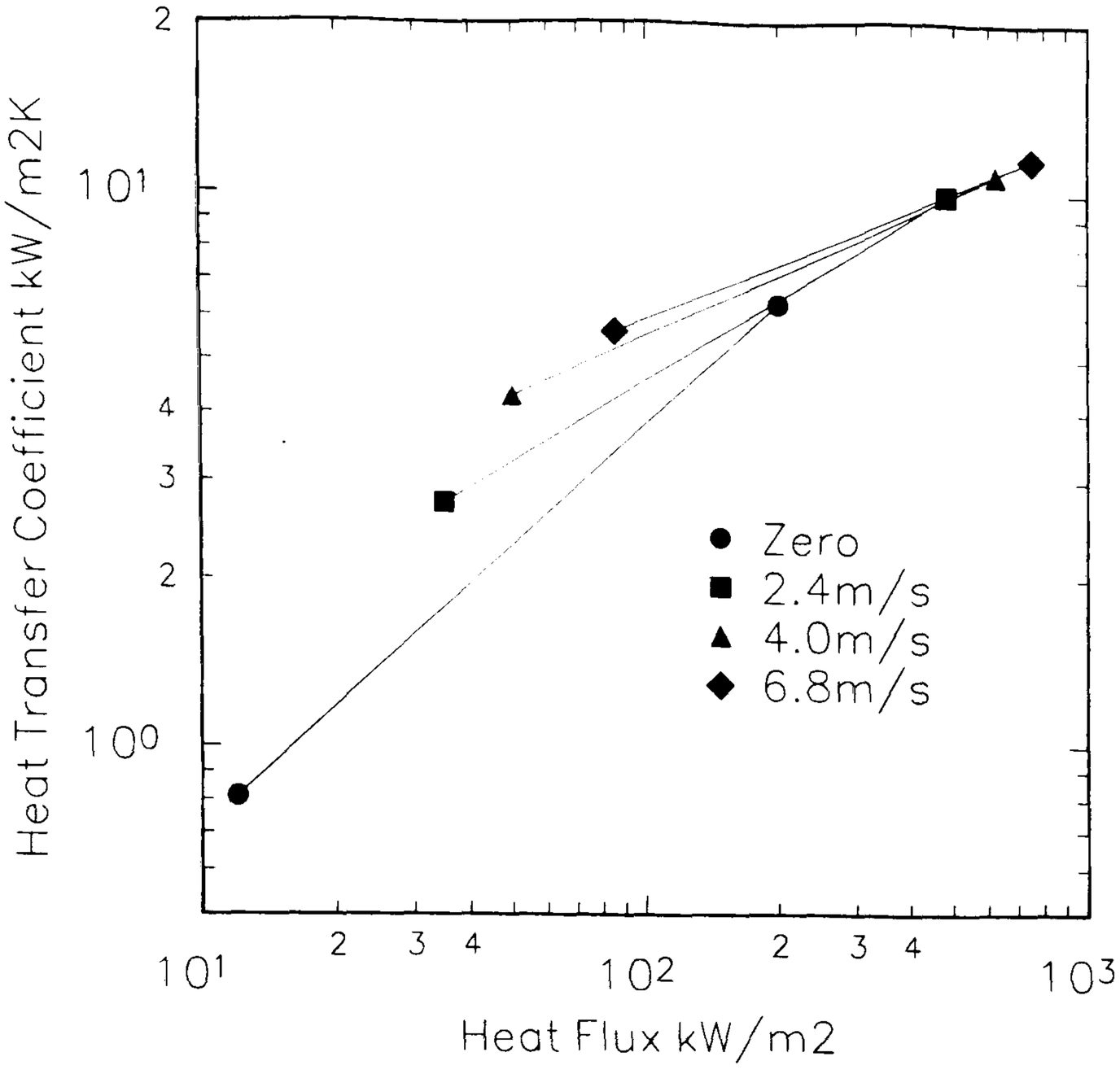

(a) Heat Transfer Coefficient against Heat Flux

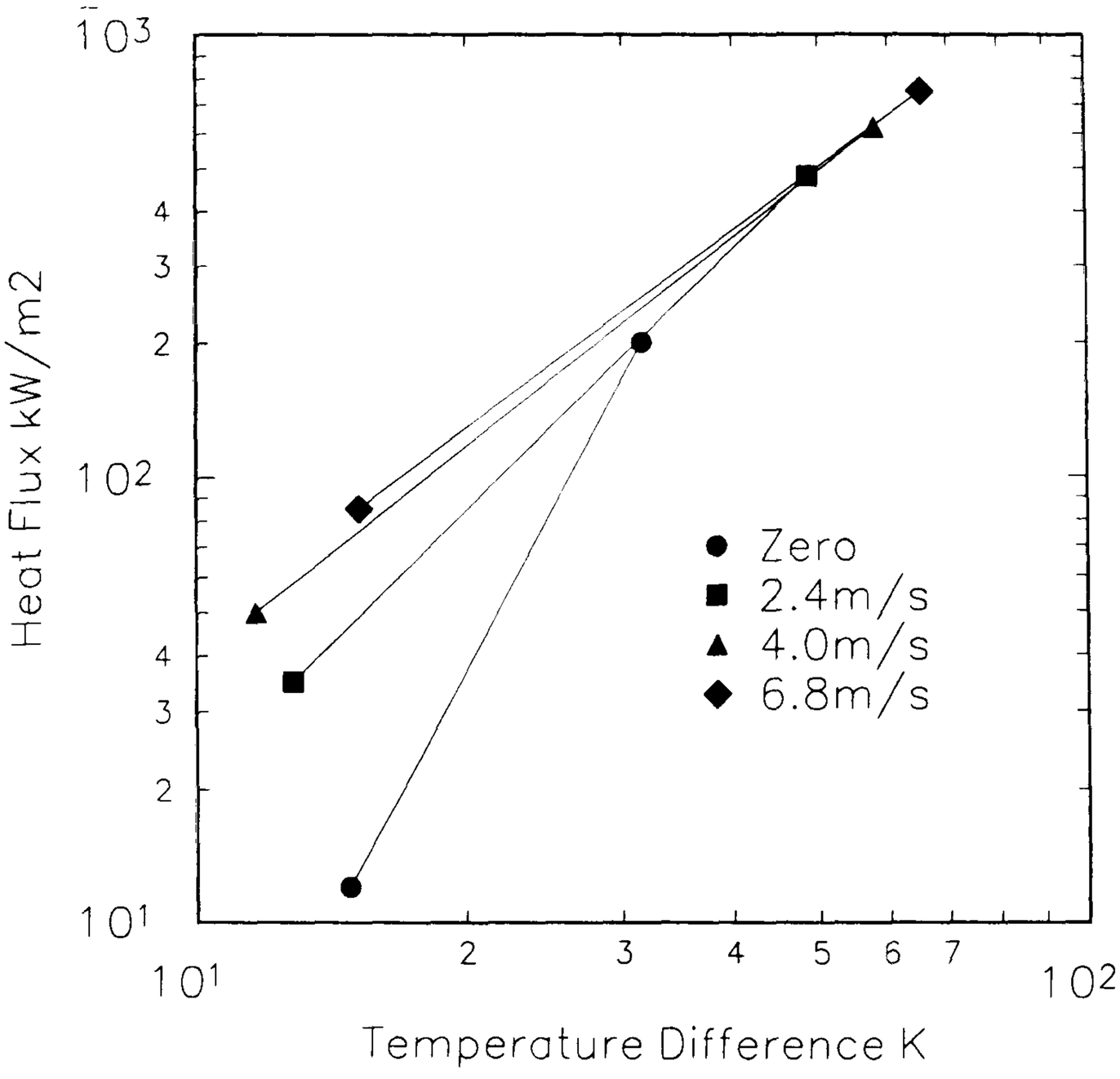

(b) Heat Flux against Temperature Difference

Figure 1.9 Correlation of Yilmaz and Westwater (1980) Showing Extent of Data

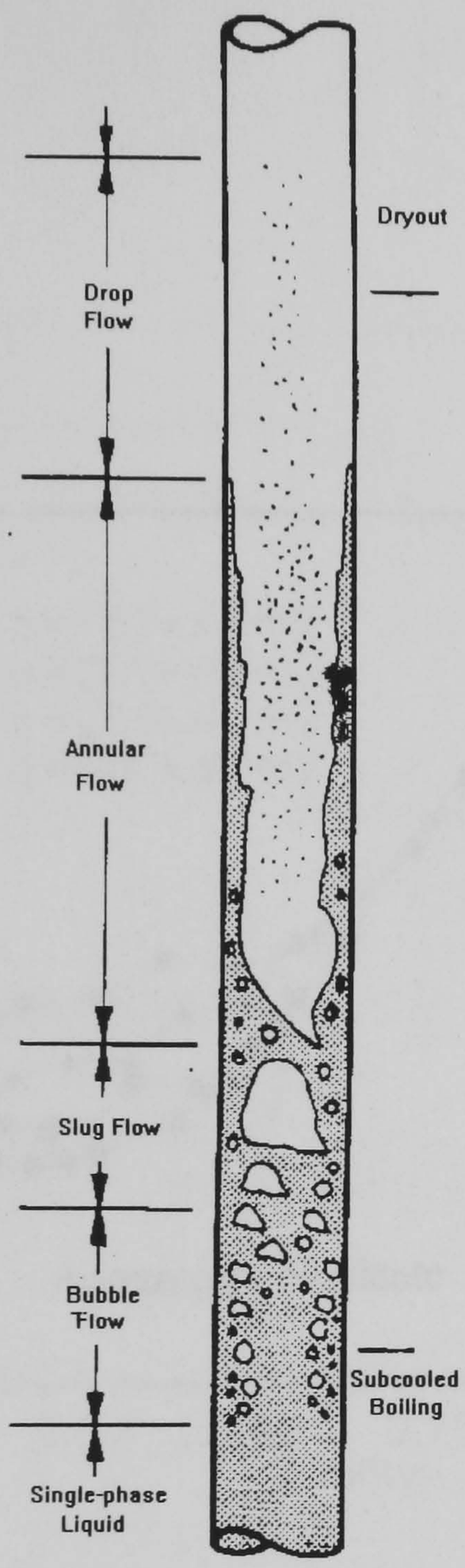

Figure 1.10 Flow Regimes in a Vertical Tube (Collier 1982)

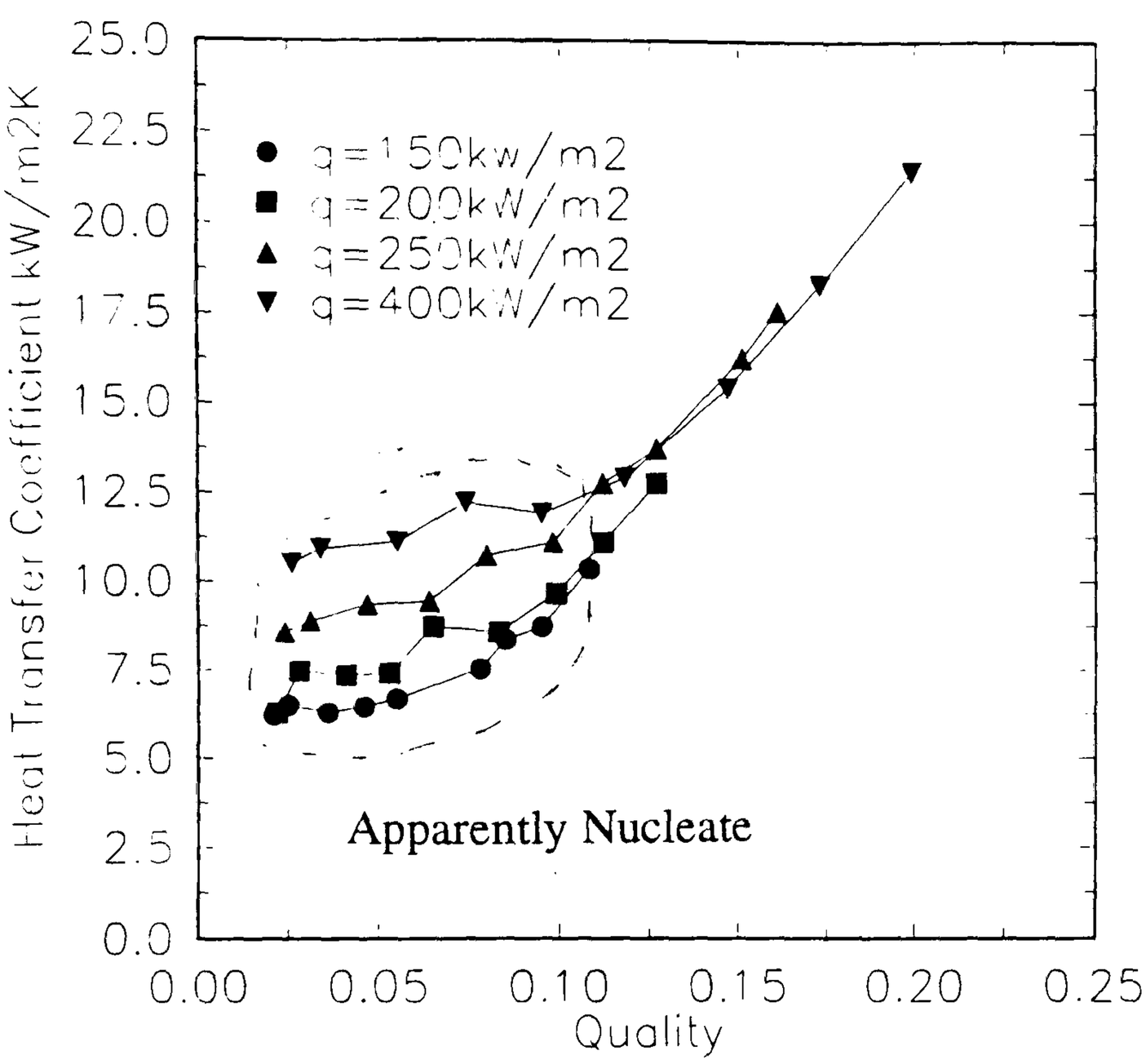

Figure 1.11 Data of Cooper (1989) Showing Apparently Nucleate and Convective Regions

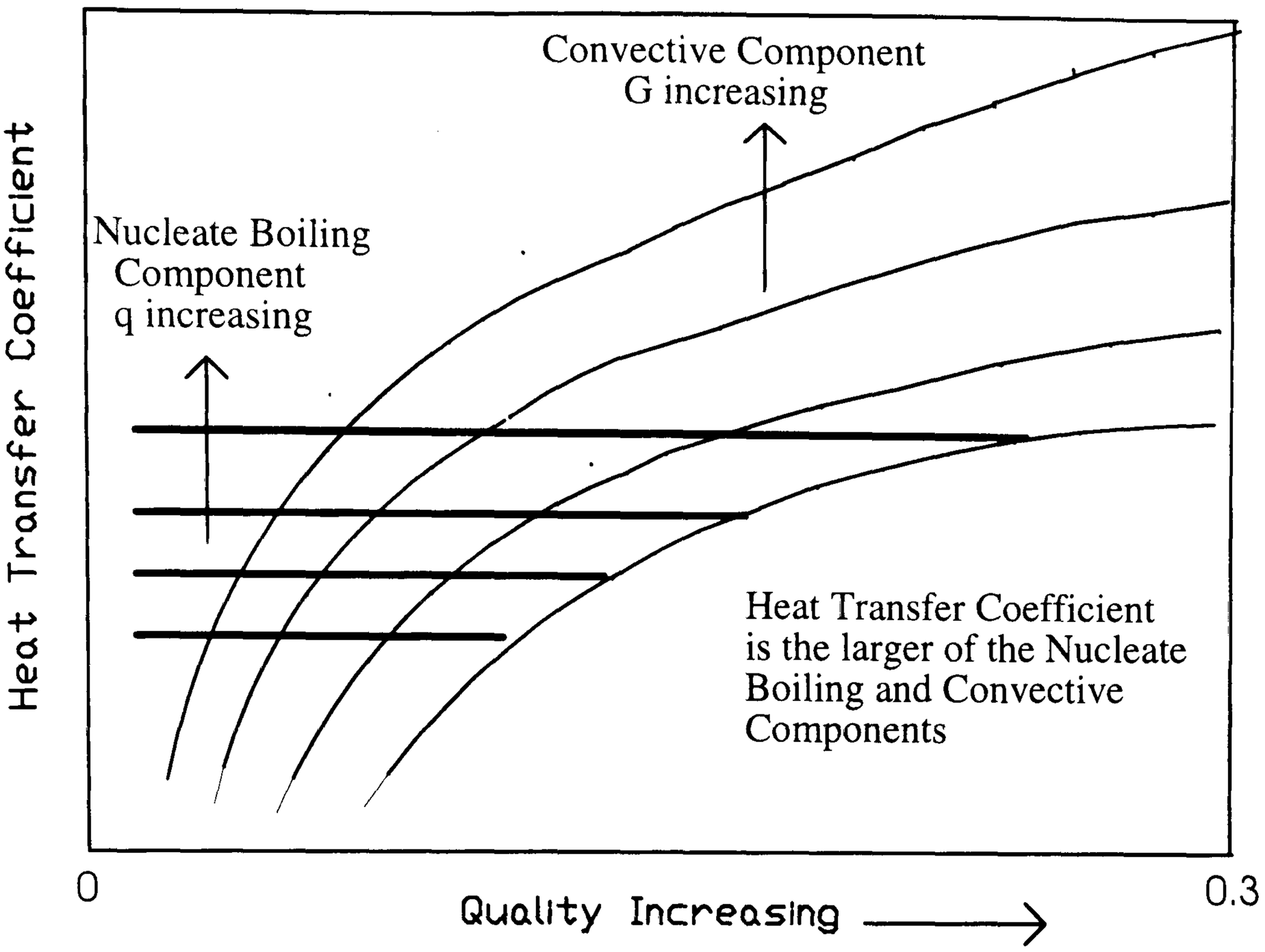

Figure 1.12 (a) Schematic Representation of a Flow Boiling Map

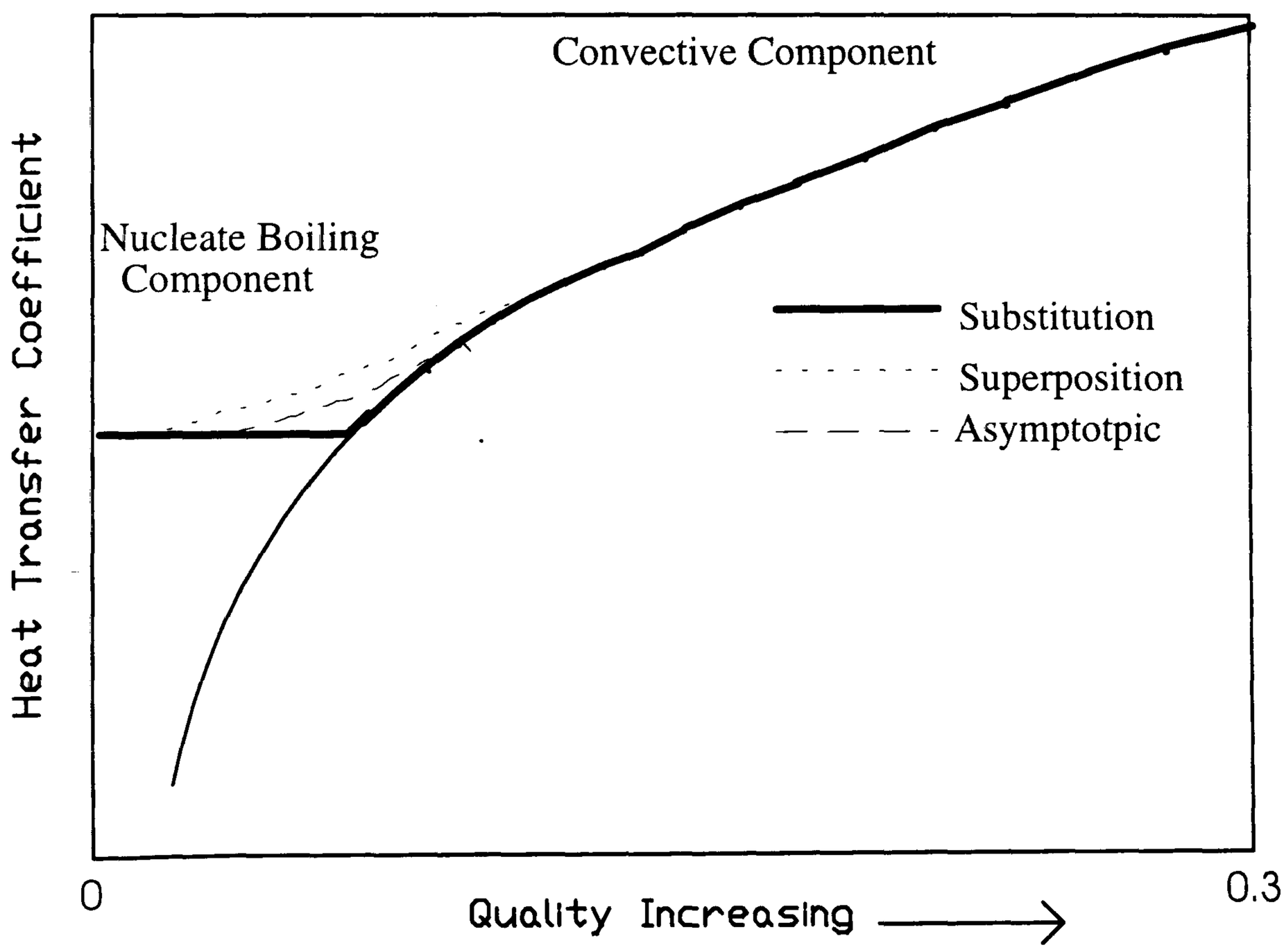

Figure 12(b) Schematic Representation of the Combination of Nucleate and Convective Boiling Components

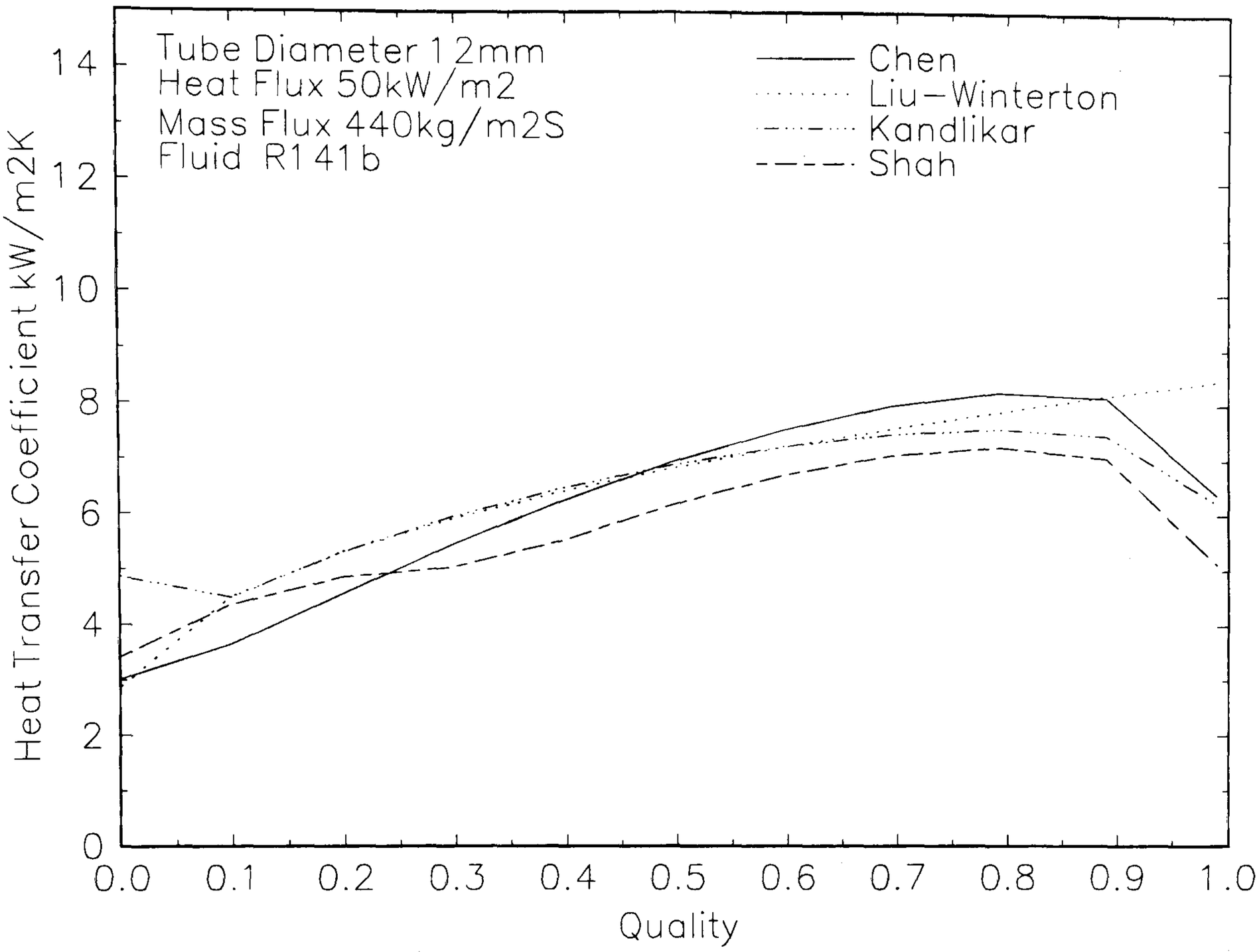

(a)

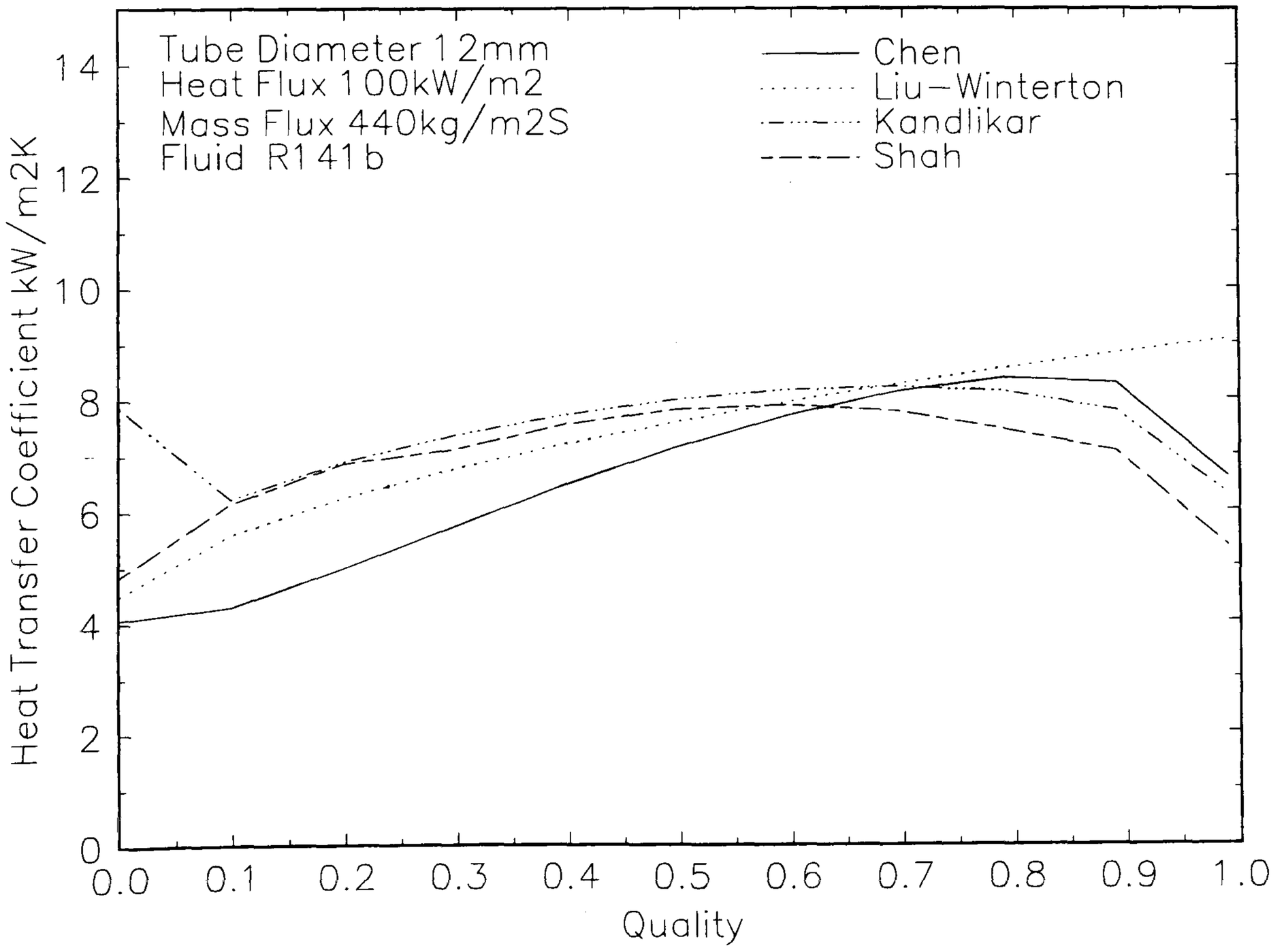

(b)

Figure 1.13 Application of Flow Boiling Correlations to Evaporation in 12mm Tube

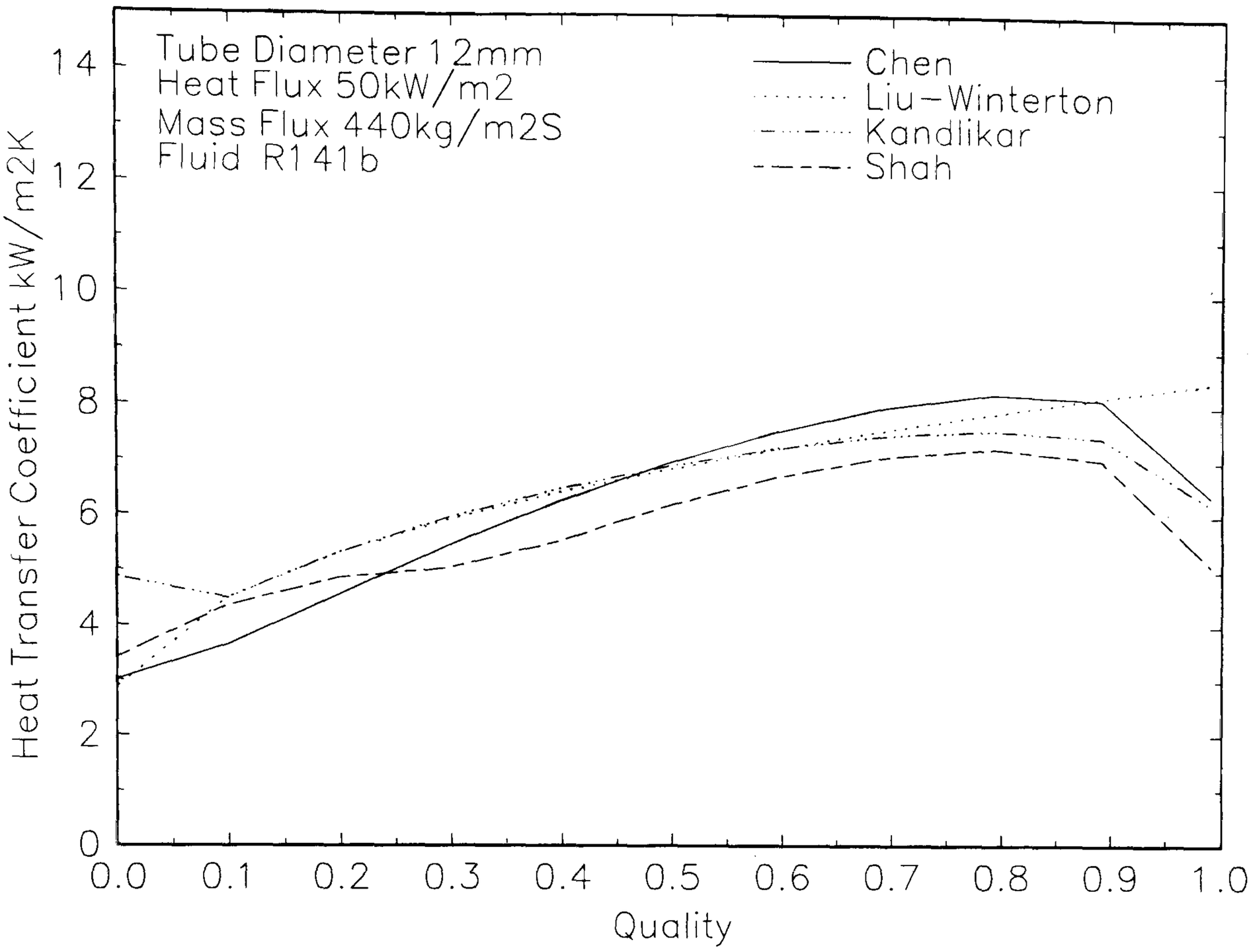

(a)

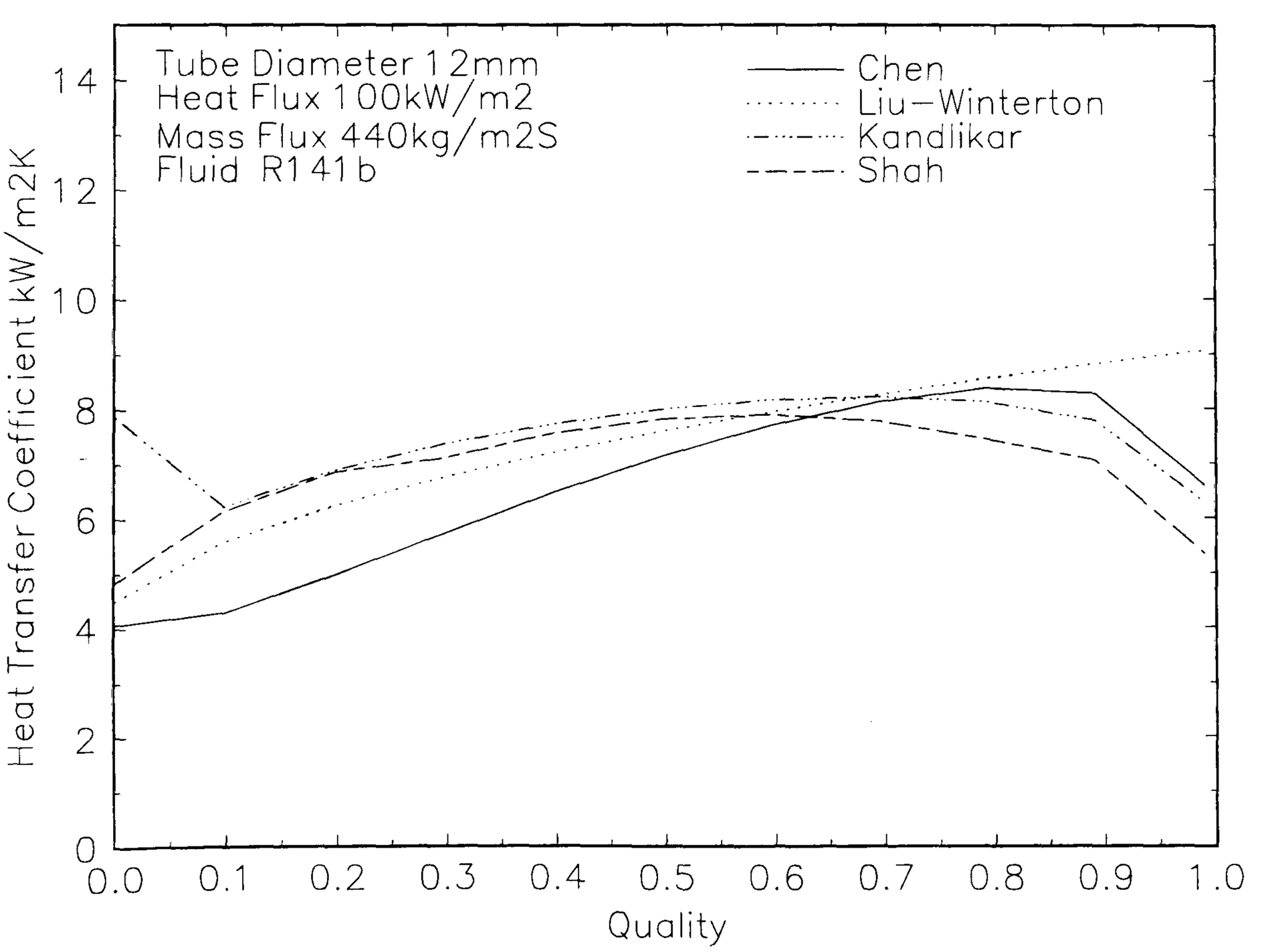

(b)

Figure 1.13 Application of Flow Boiling Correlations to Evaporation in 12mm Tube

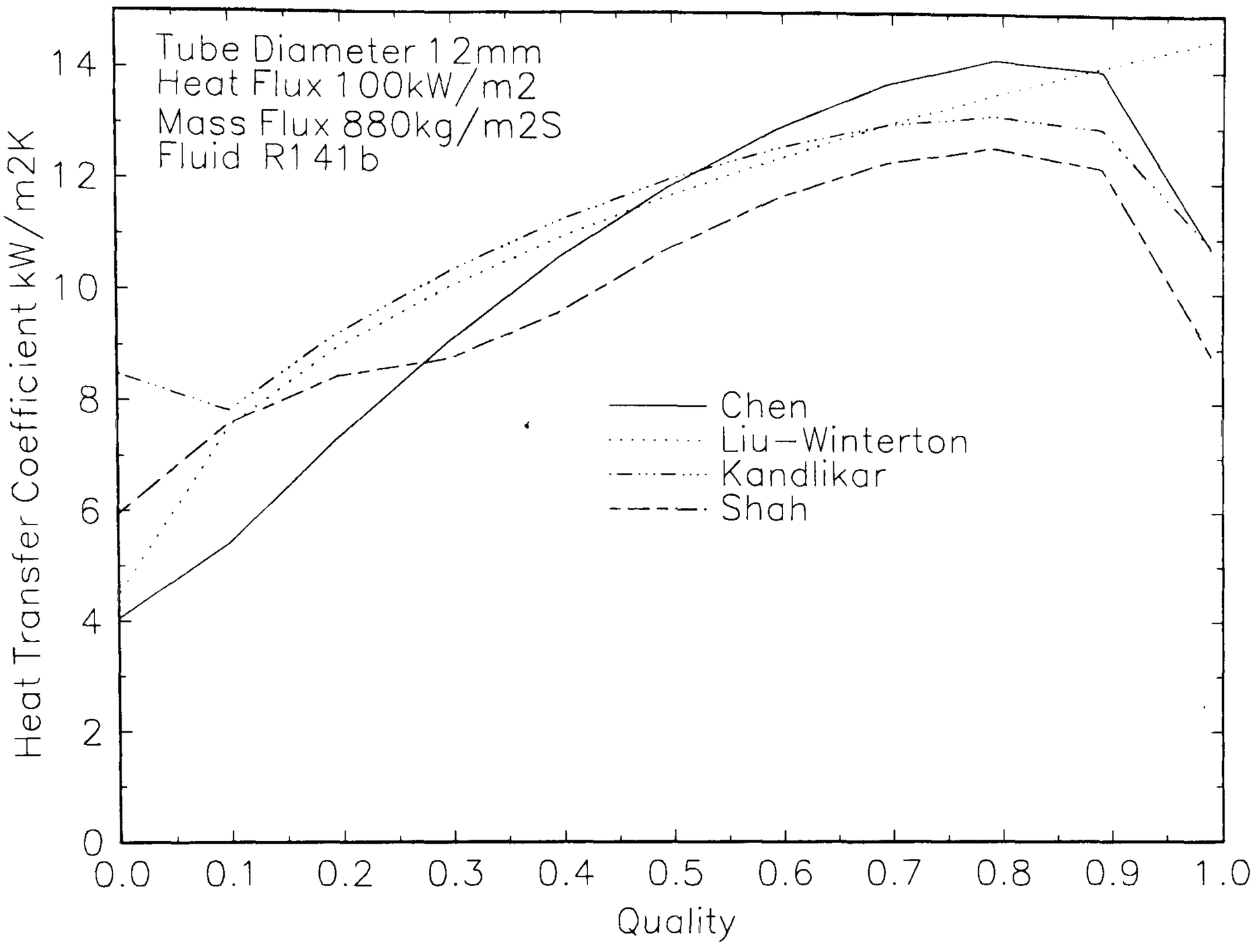

(c)

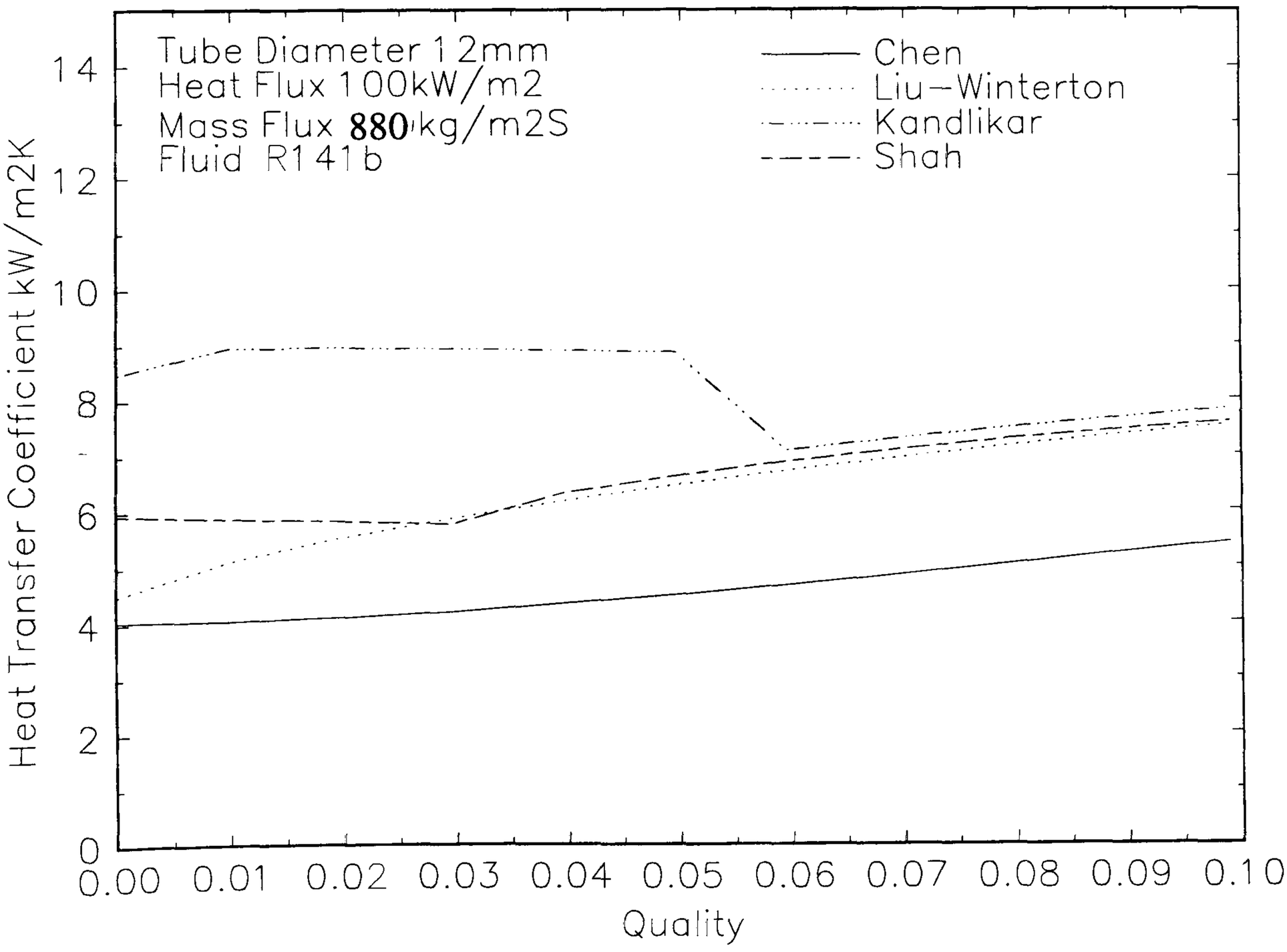

(d)

Figure 1.13 Application of Flow Boiling Correlations to Evaporation in 12mm Tube (cont)

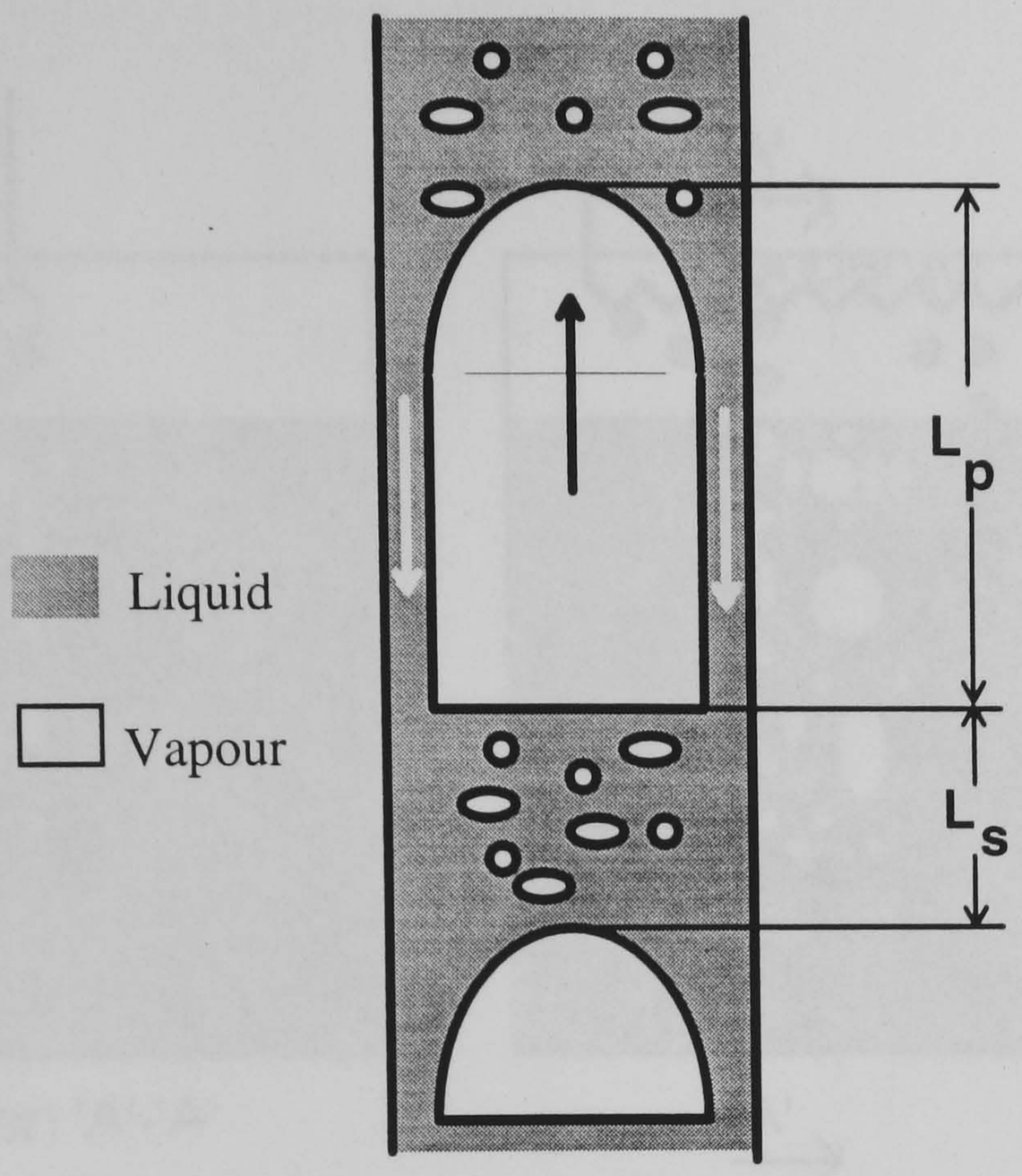

Figure1.14 Schematic Representation of Slug Flow
(Adapted from Wadekar 1991)

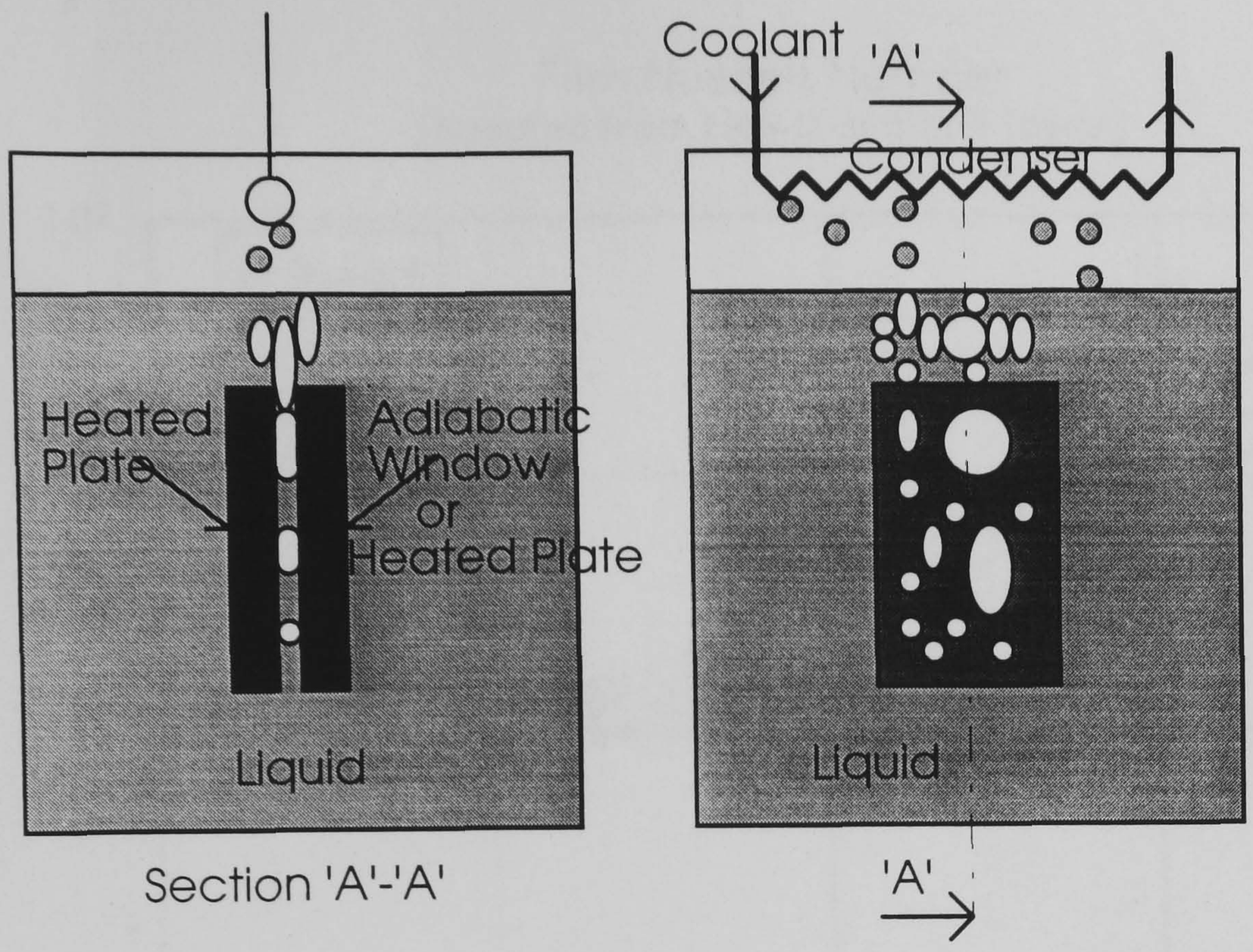

Fig. 2.1 Schematic Representation of Confined Pool Boiling

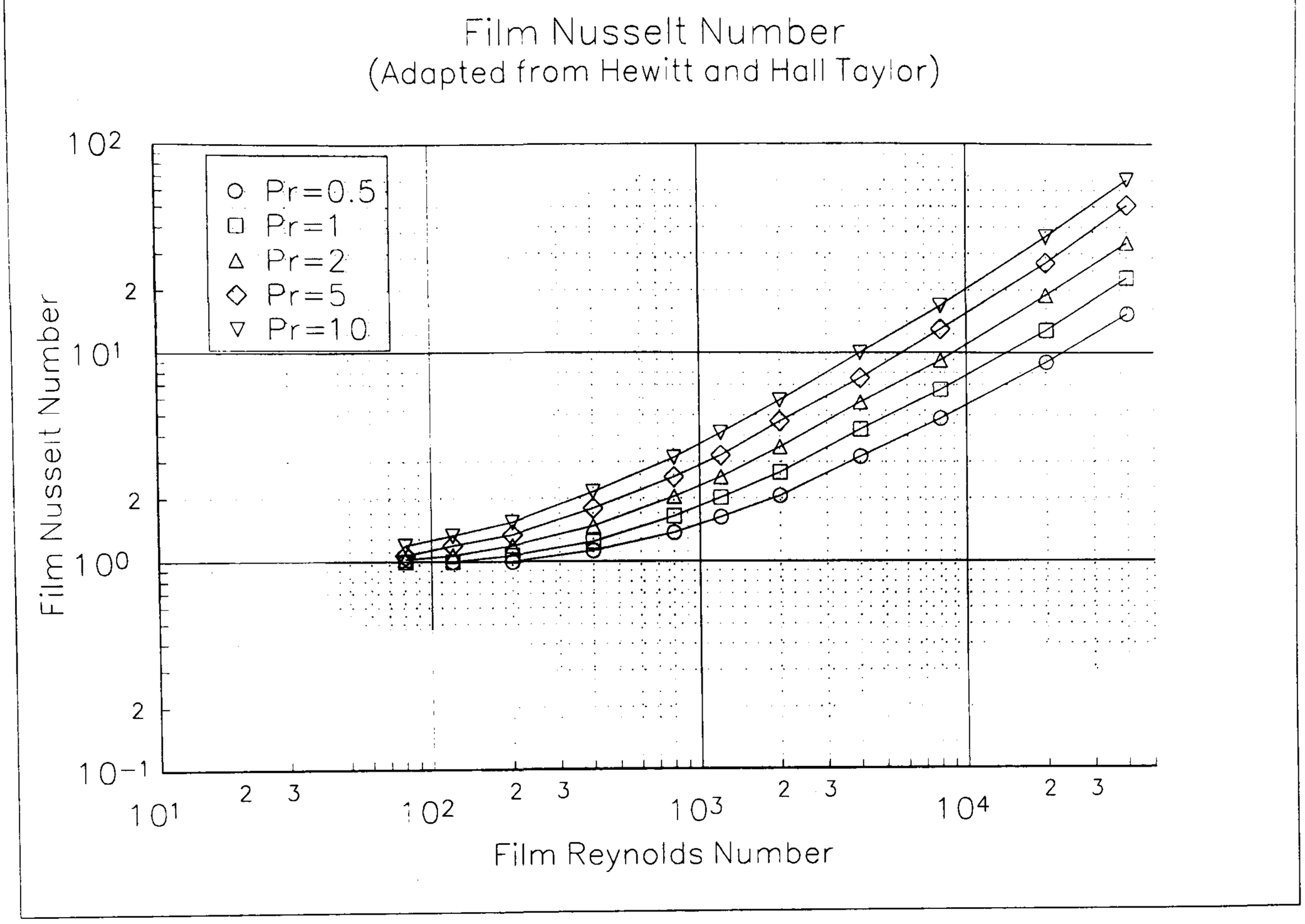

Fig.2.2 Relationship Between Film Nusselt and Reynolds Numbers
(Adapted from Hewitt and Hall Taylor 1970)

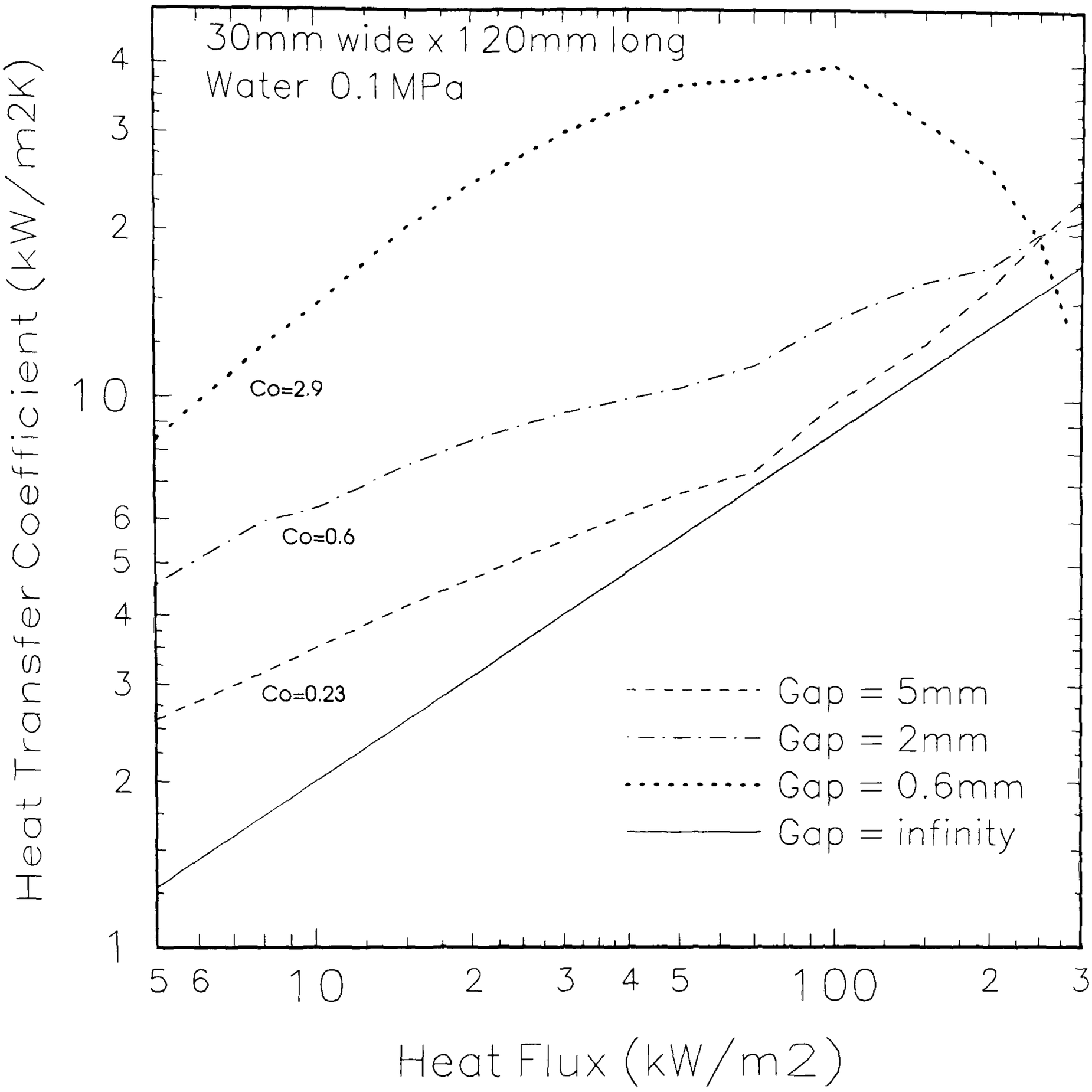

Figure 2.3 Variation of Heat Transfer Coefficient with Heat Flux in a Narrow Space
(Adapted from Fujita and Uchida 1990)

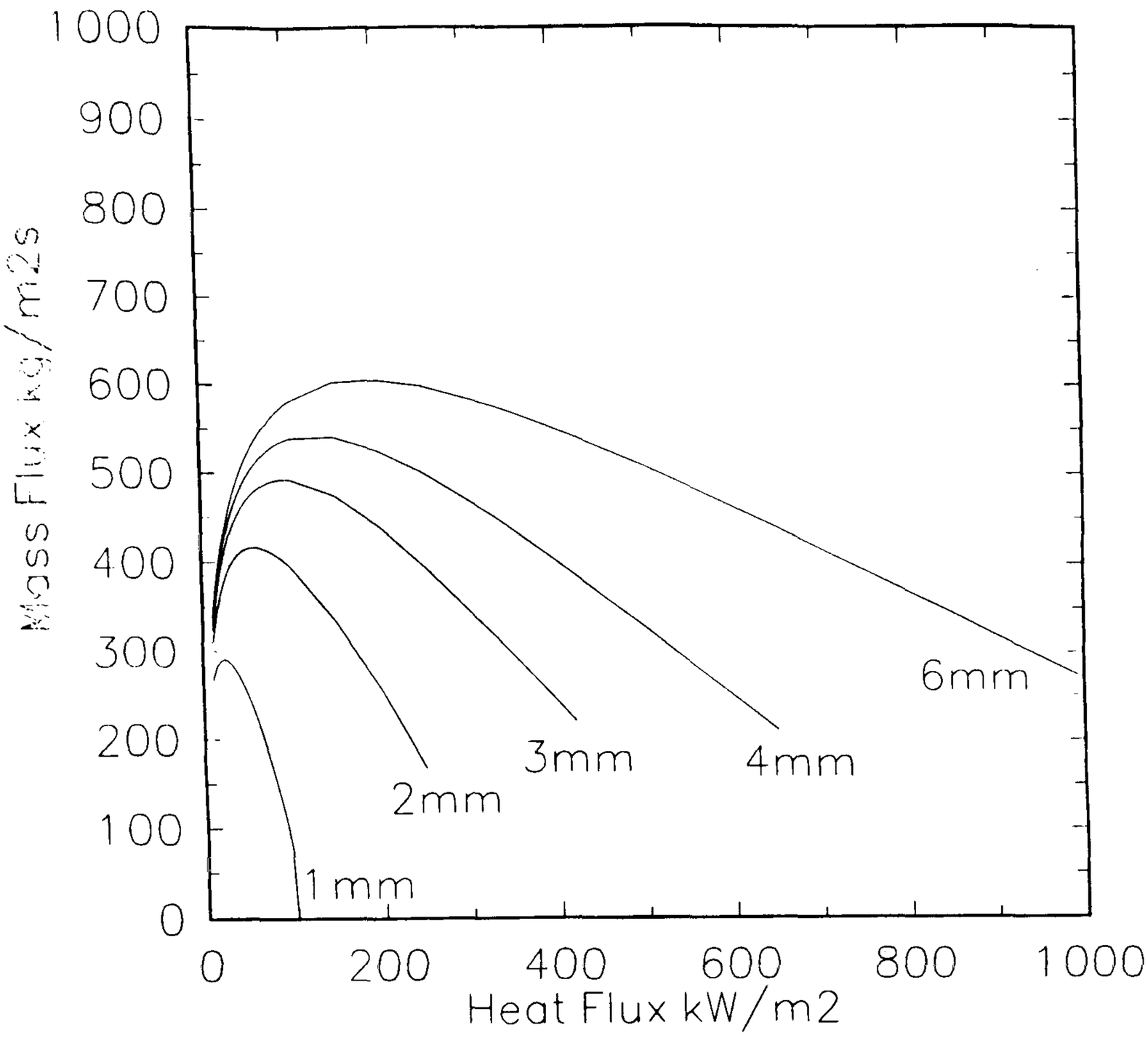

Figure 2.4 Mass Flux Predicted using Method of Bar-Cohen and Schweitzer (1985)
(Water, 1 Atm, Geometry of Bar-Cohen and Schweitzer)

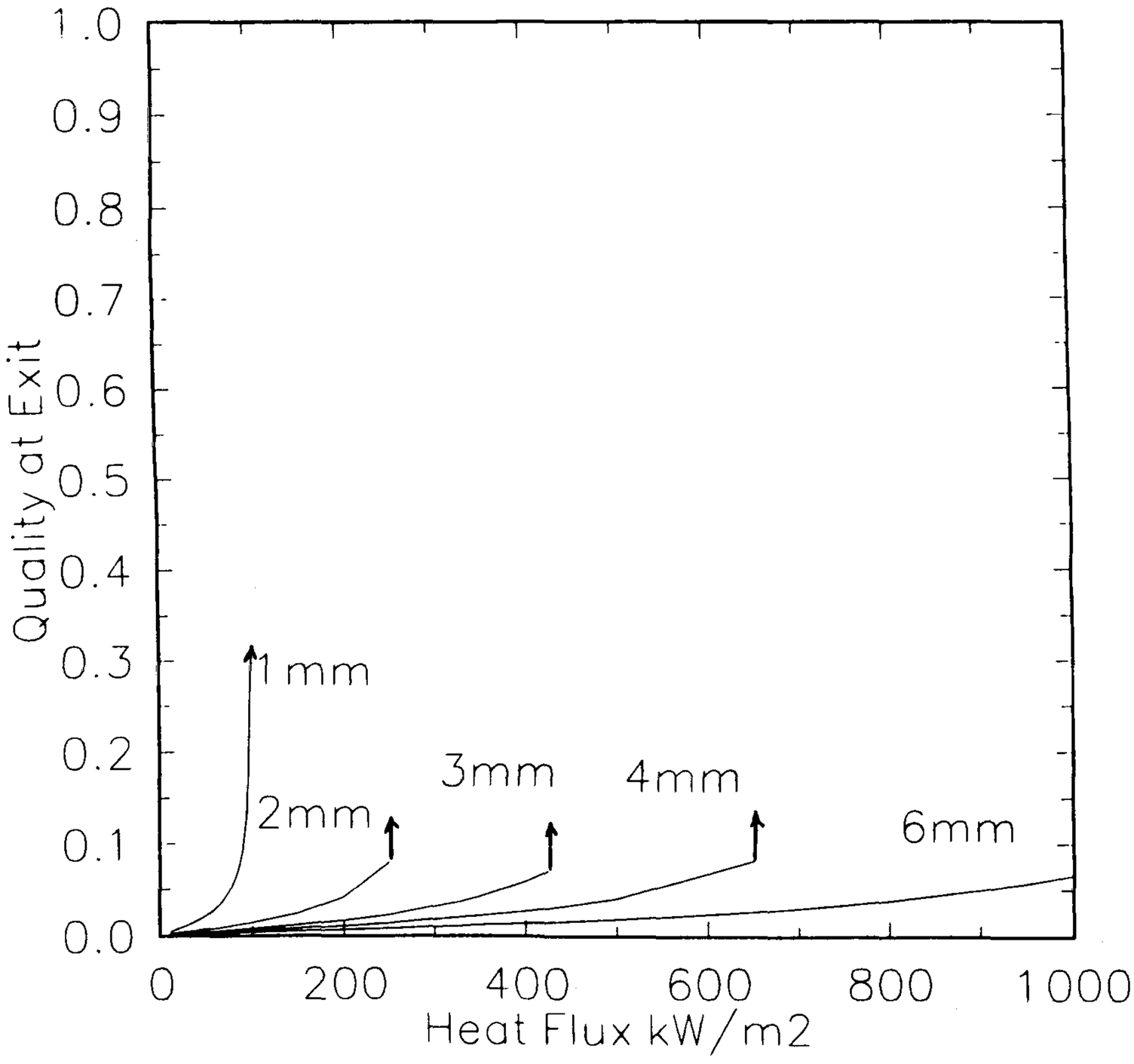

Figure 2.5 Quality Predicted using Method of Bar-Cohen and Schweitzer (1985)
(Water, 1 Atm, Geometry of Bar-Cohen and Schweitzer)

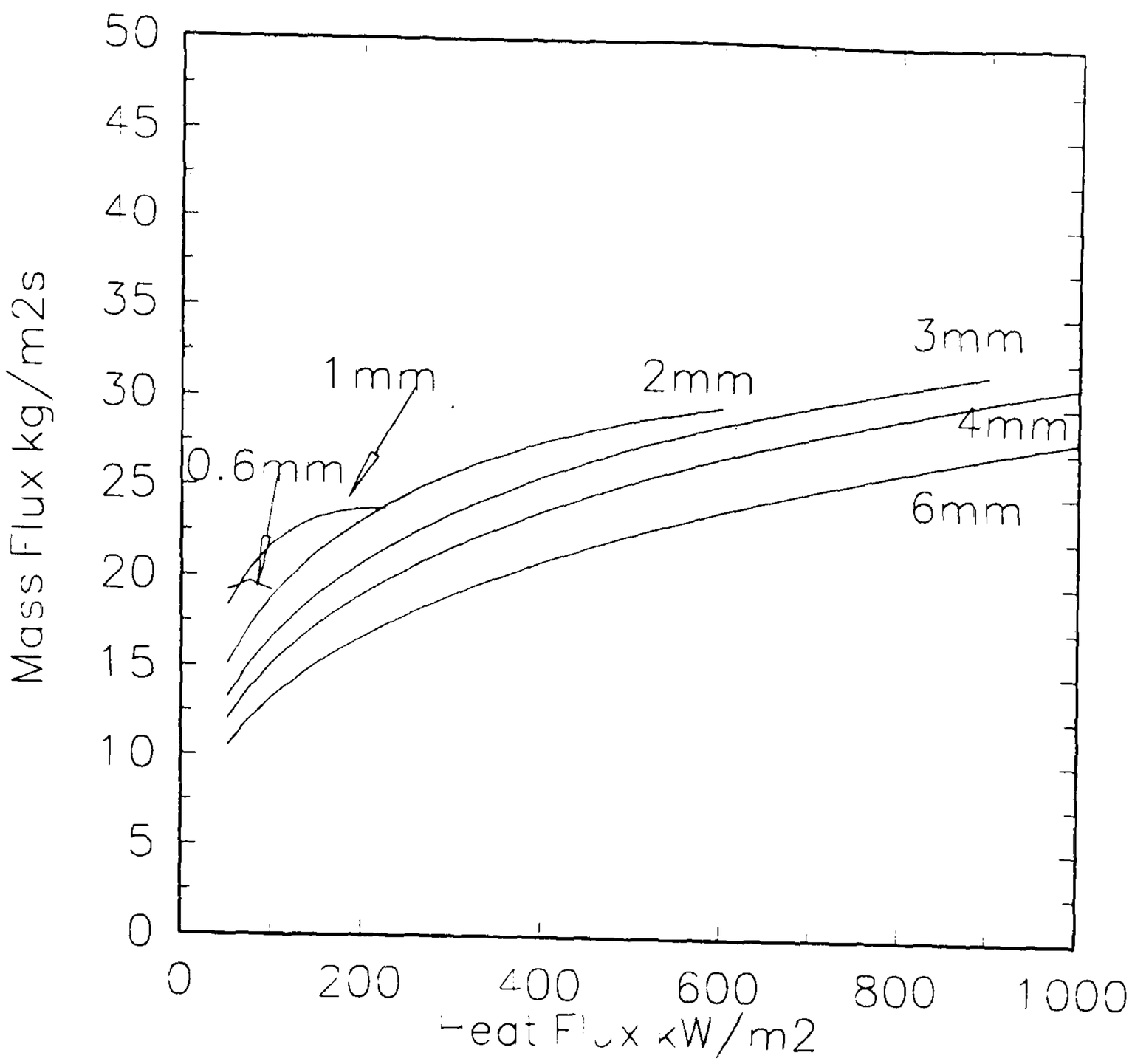

Figure 2.6 Mass Flux Predicted using Method of Fujita and Uchida (1990)
(Water, 1 Atm, Geometry of Bar-Cohen and Schweitzer)

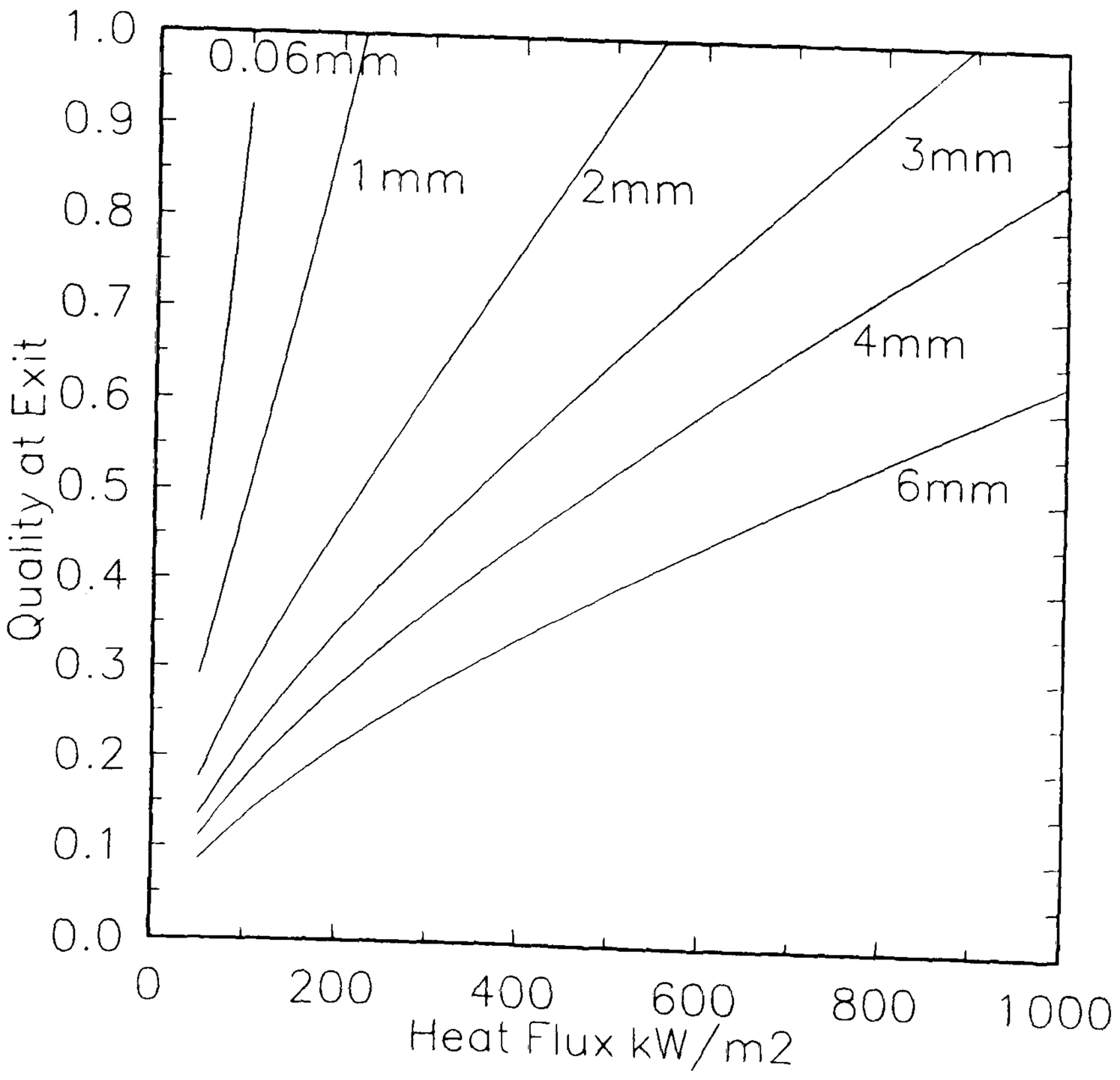

Figure 2.7 Quality Predicted using Method of Fujita and Uchida (1990)
(Water, 1 Atm, Geometry of Bar-Cohen and Schweitzer)

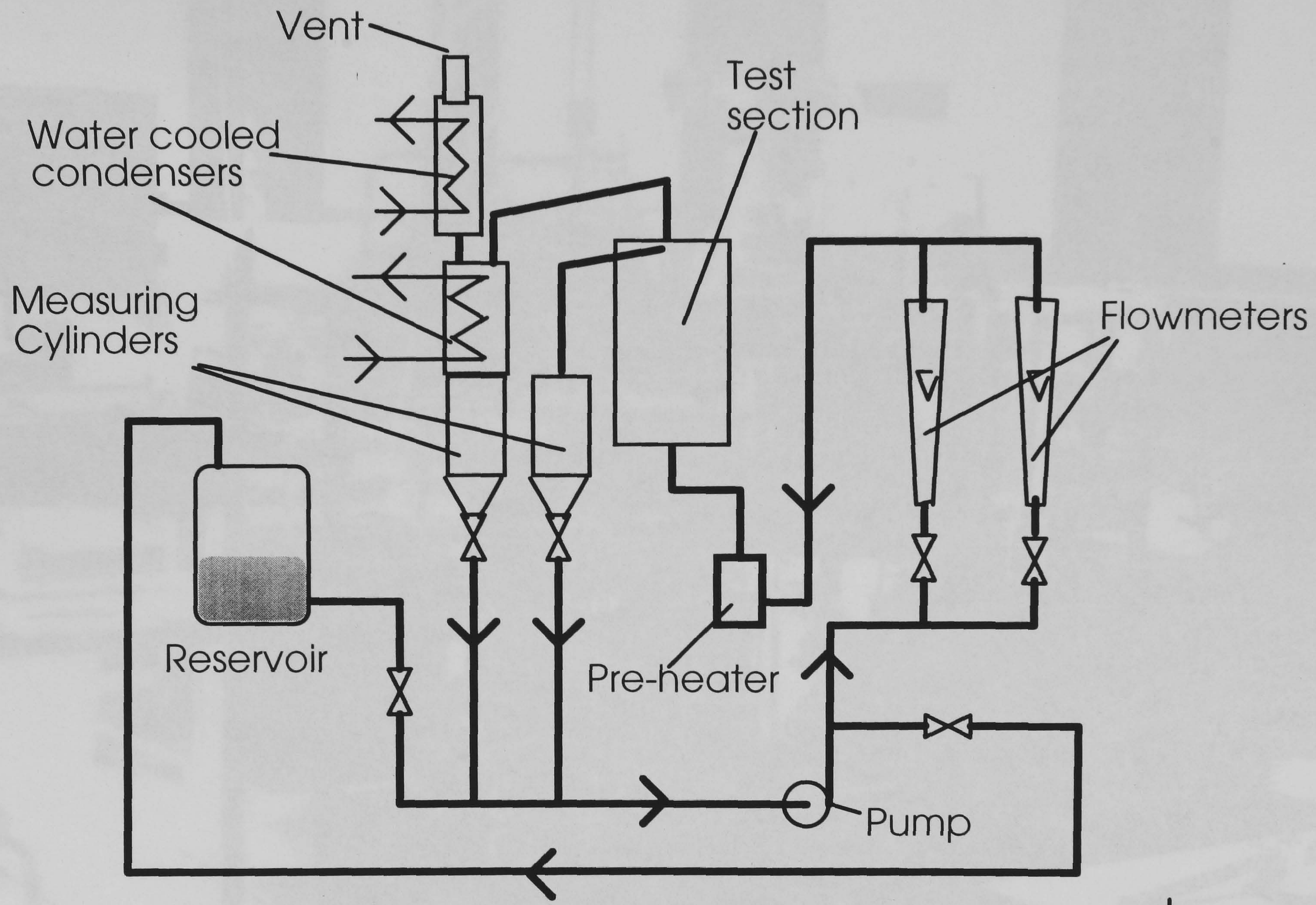

Fig 3.1 Schematic Diagram of Mark I Test rig

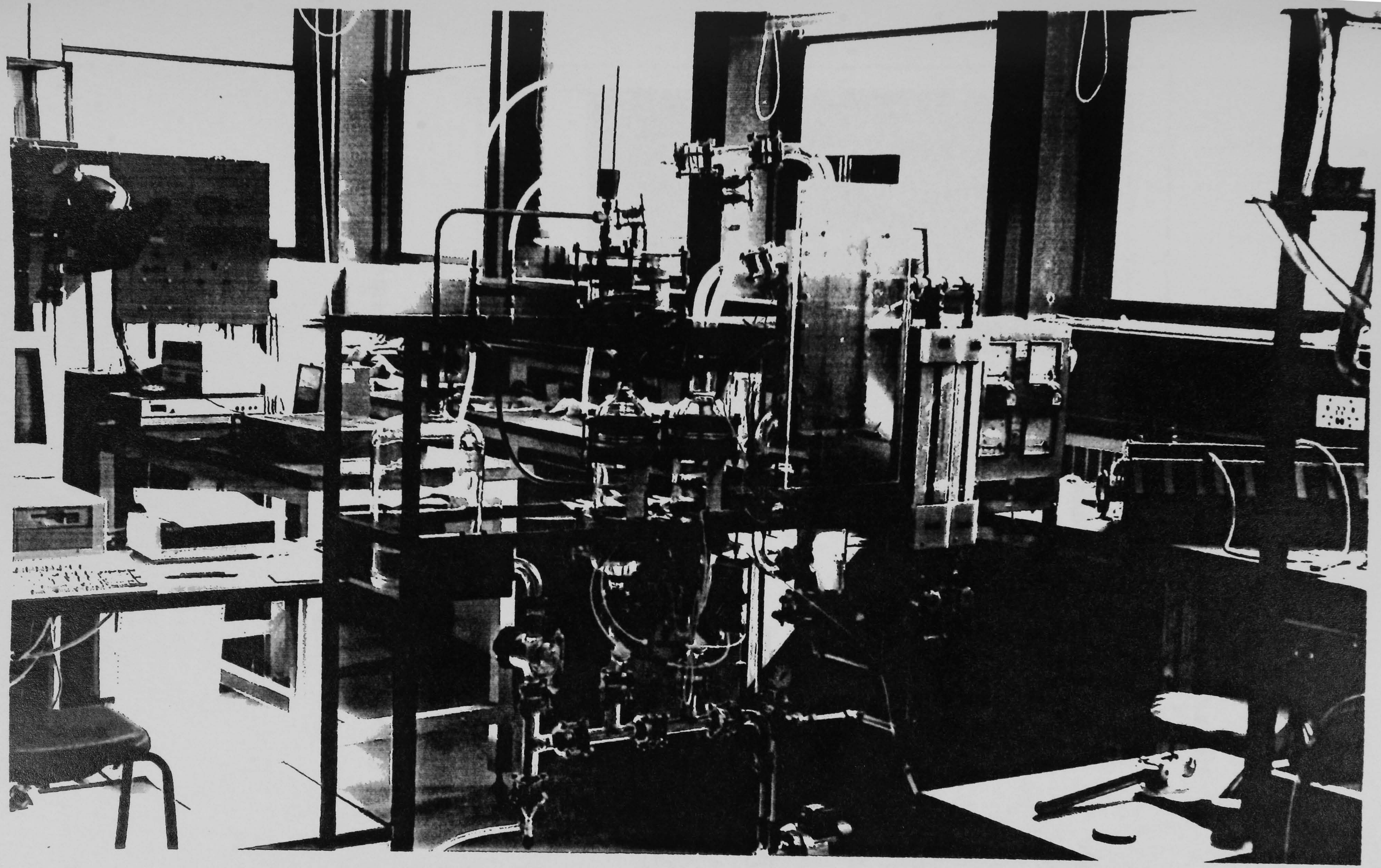

Figure 3.2 Photograph of Test Rig Mark I

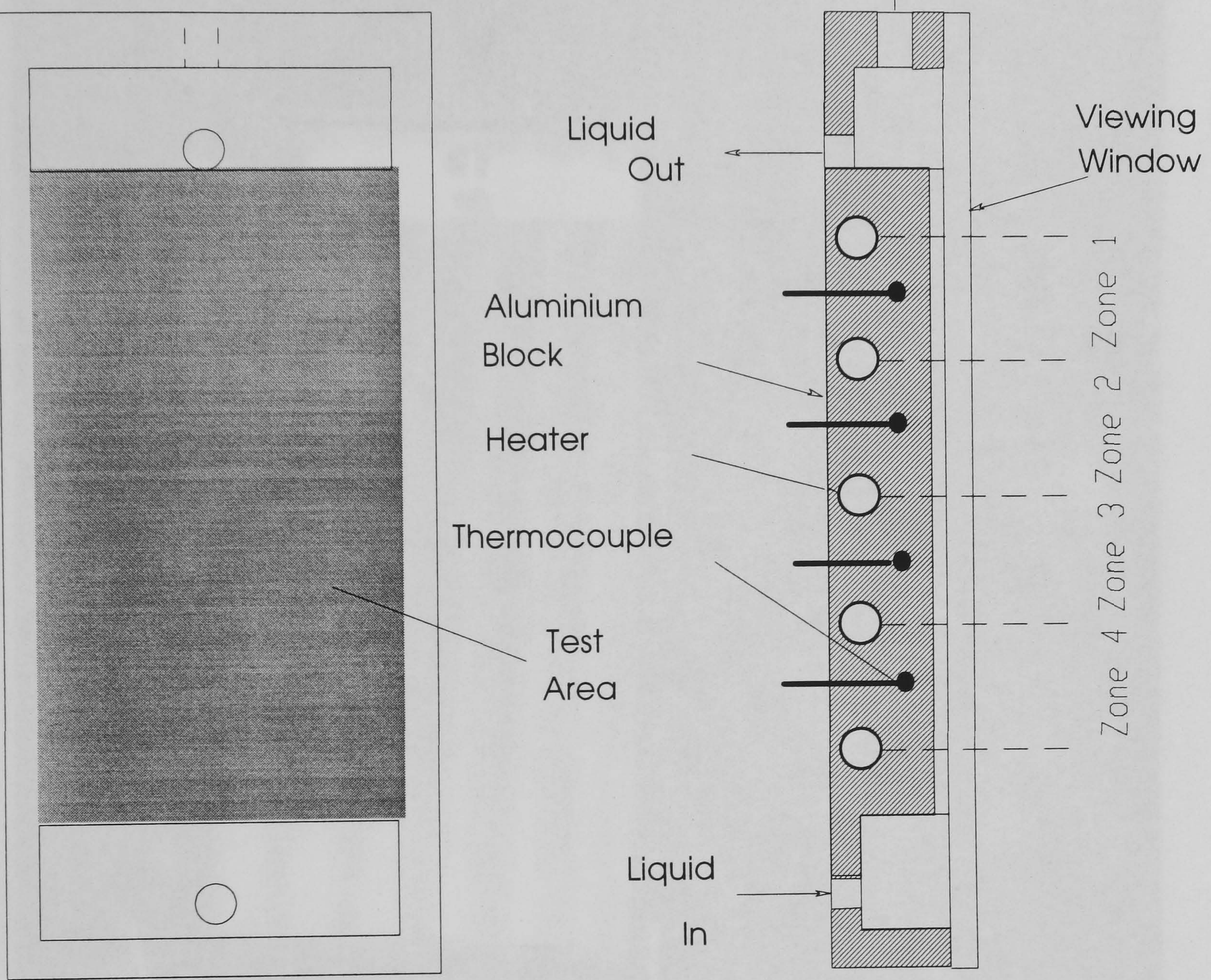

Figure 3.3 Schematic Diagram of Test Section - Test Rig Mark 1

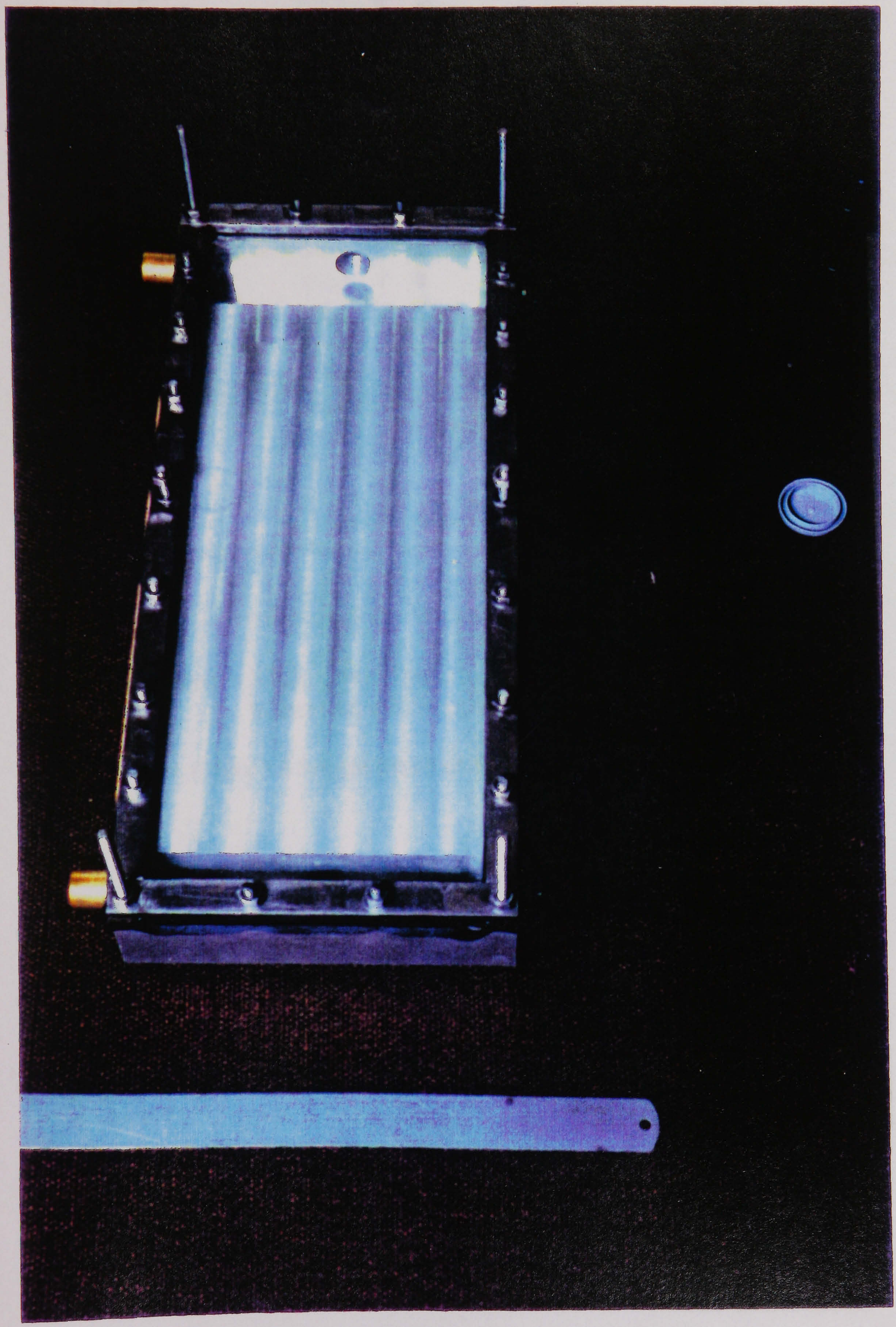

Figure 3.4 Photograph of Test Section - Test Rig Mark I

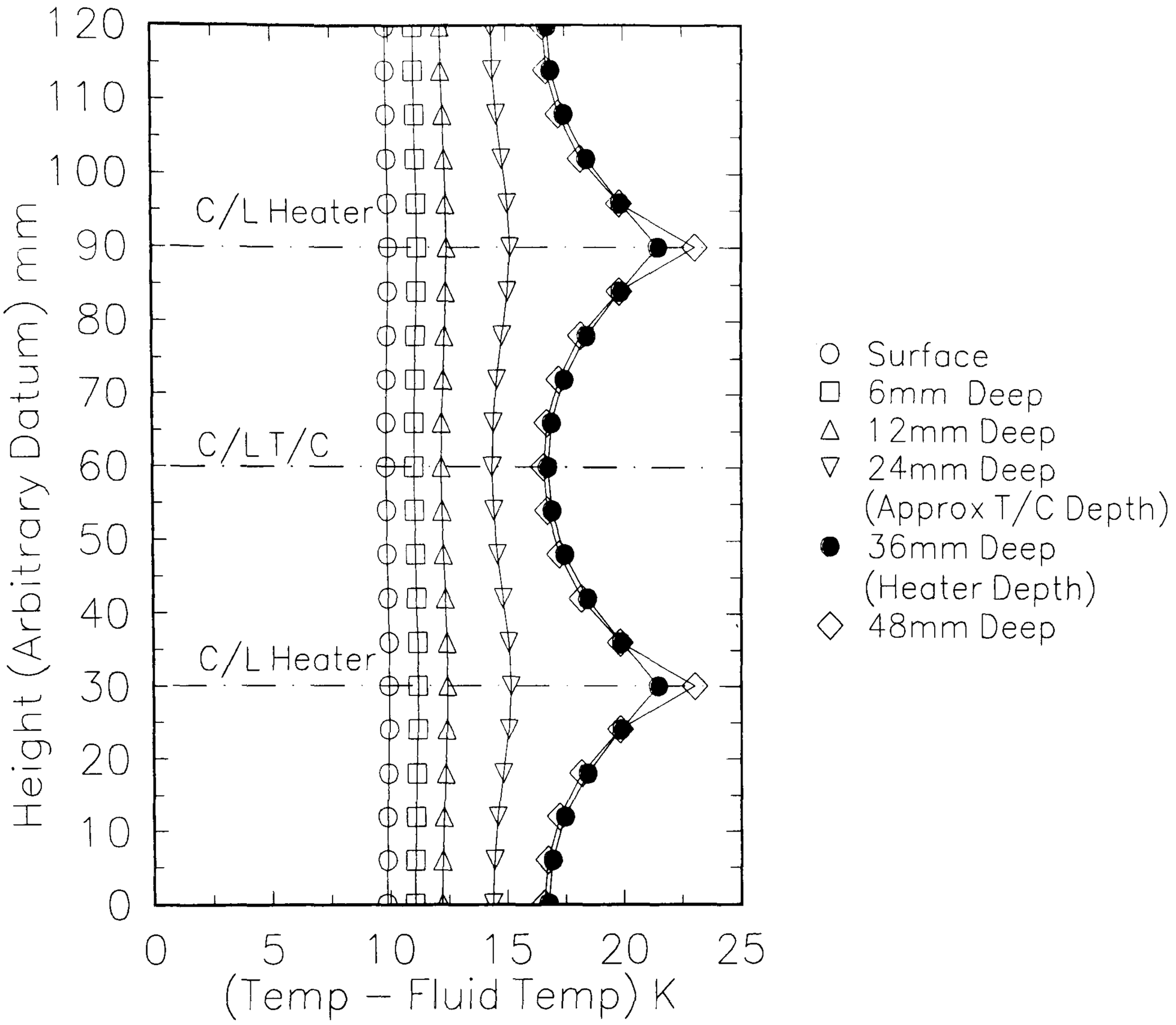

Aluminium Block, 48mm Thick, Heater 36mm from Front Surface
Heater Output 2.666 kW/m, α=4500W/m^2

Figure 3.5 Sample Result of Finite Difference Analysis

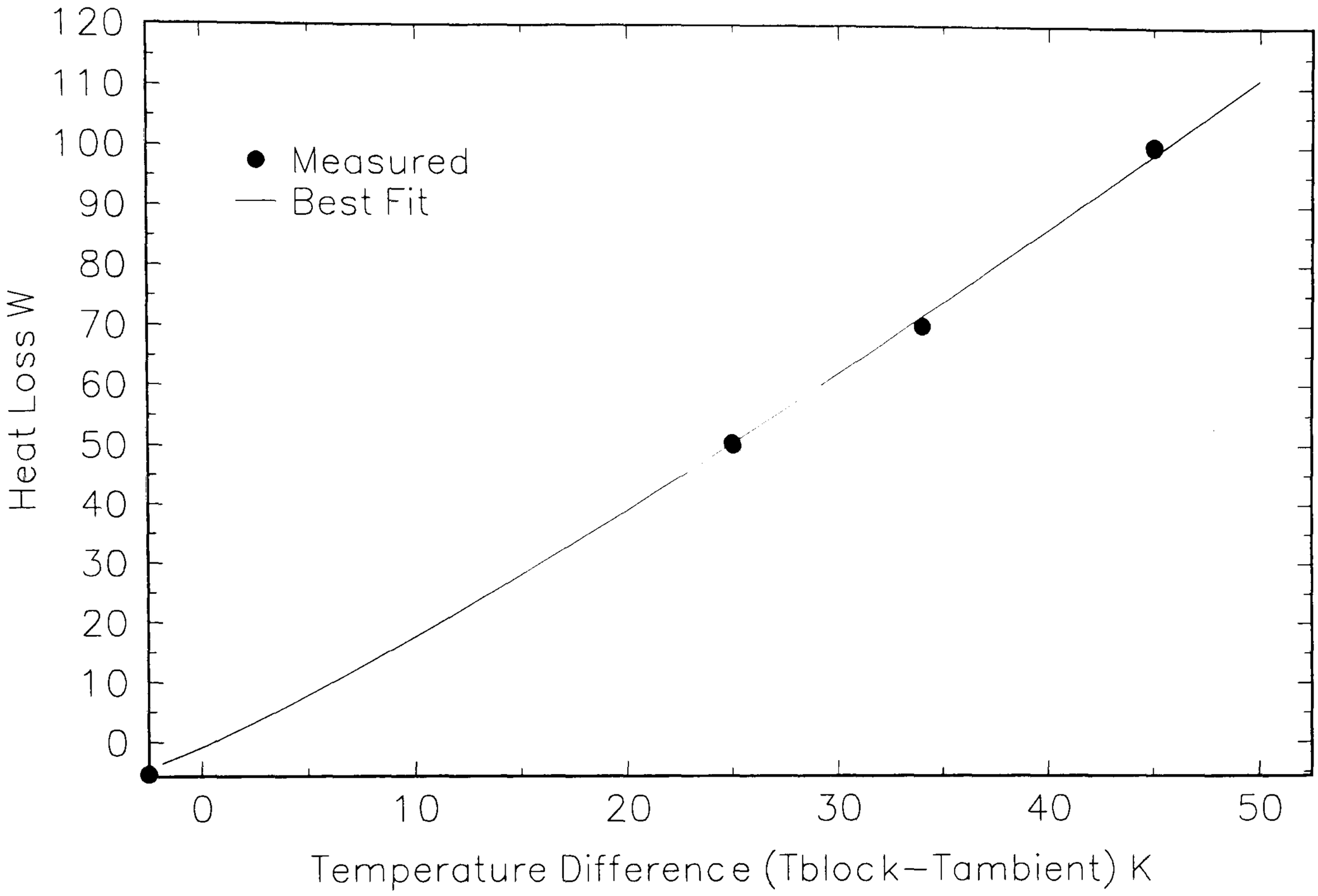

Figure 3.6 Relationship Between Test Section Temperature and Heat Loss

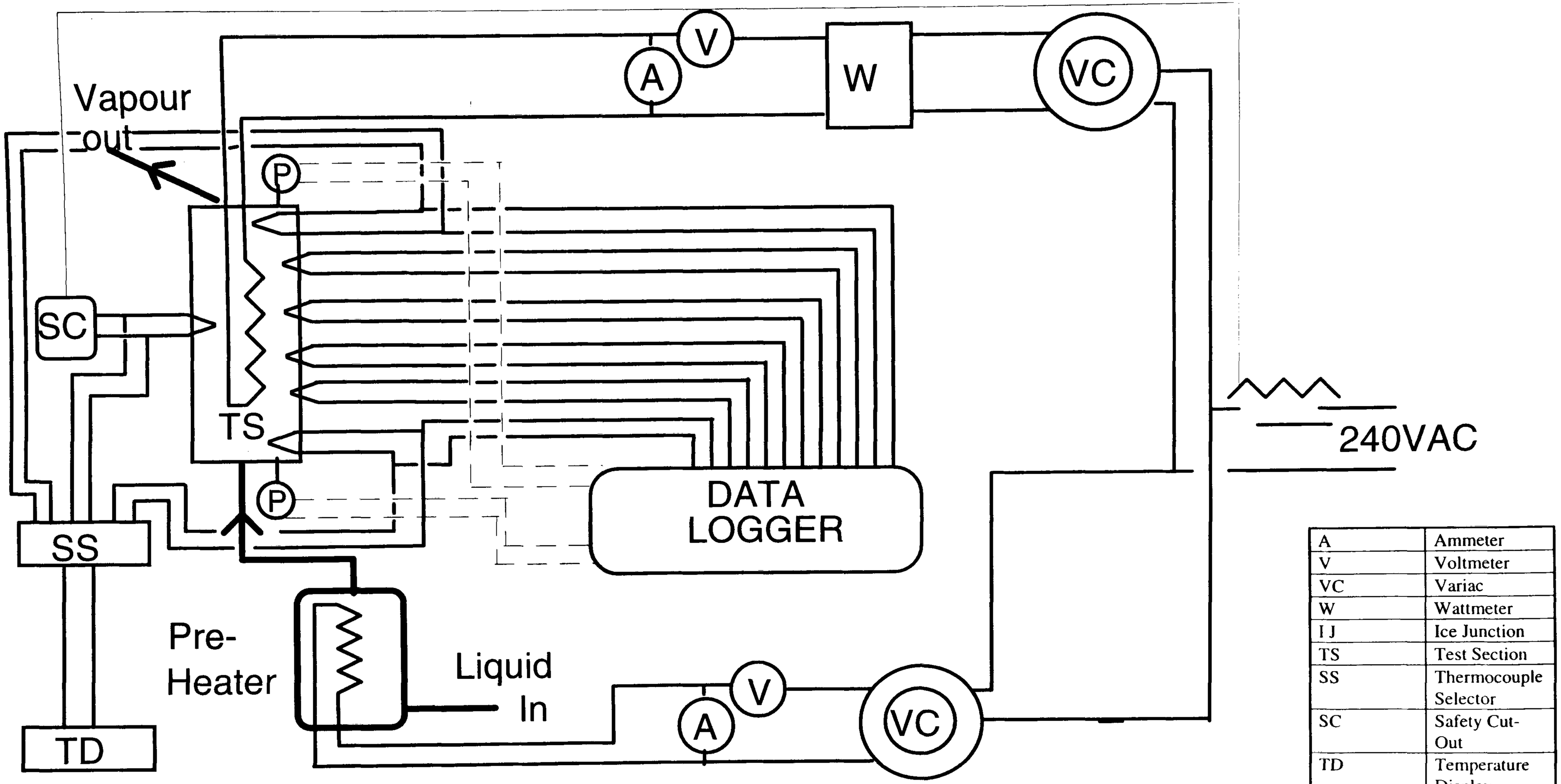

A	Ammeter
V	Voltmeter
VC	Variac
W	Wattmeter
I J	Ice Junction
TS	Test Section
SS	Thermocouple Selector
SC	Safety Cut-Out
TD	Temperature Display
⟸	Thermocouple
P	Pressure gauge and transducer

Figure 3.7 Simplified Schematic Diagram of Instrumentation - Mark I Rig

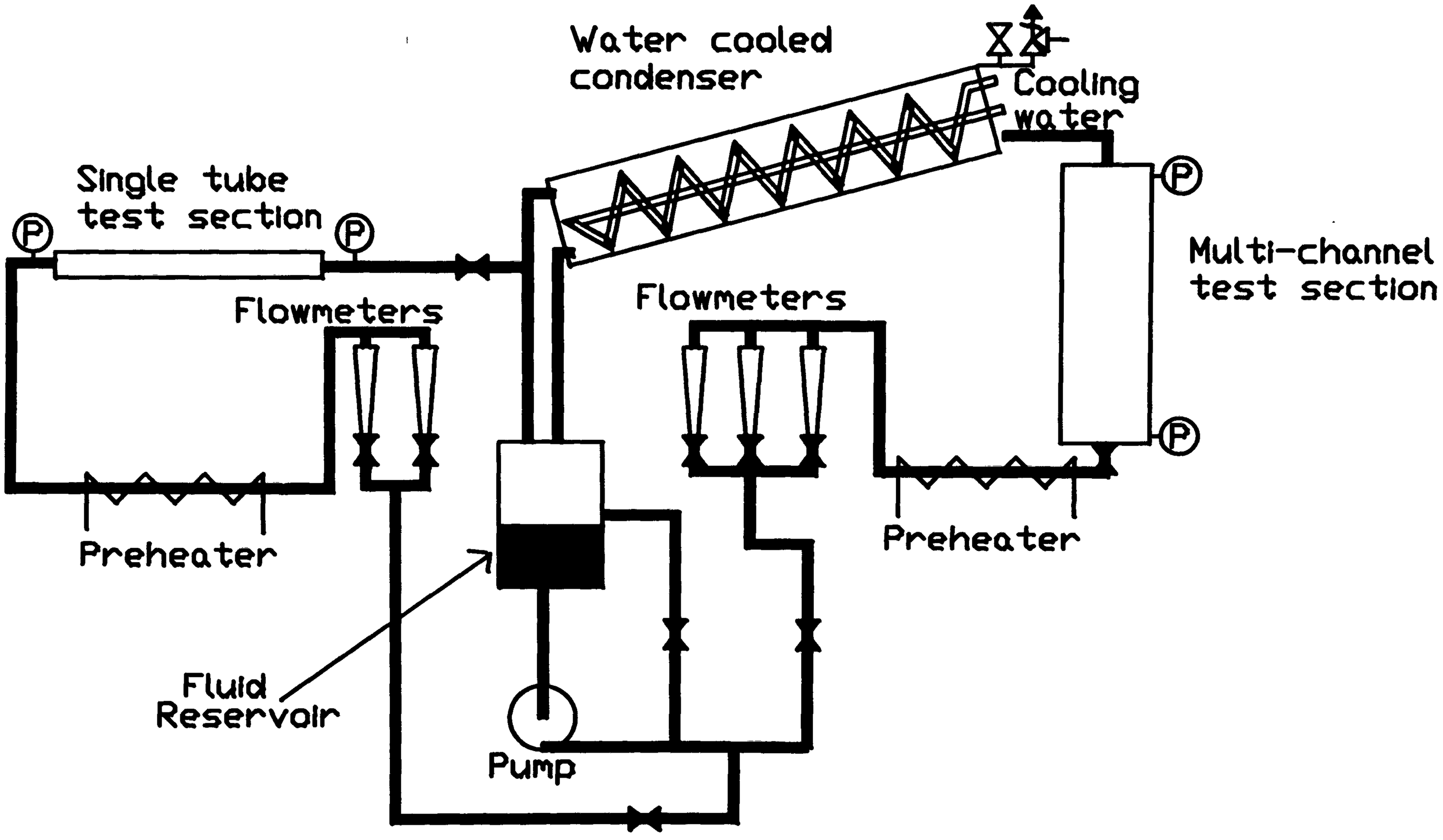

Fig 3.8 Schematic Diagram of Mark II Test rig

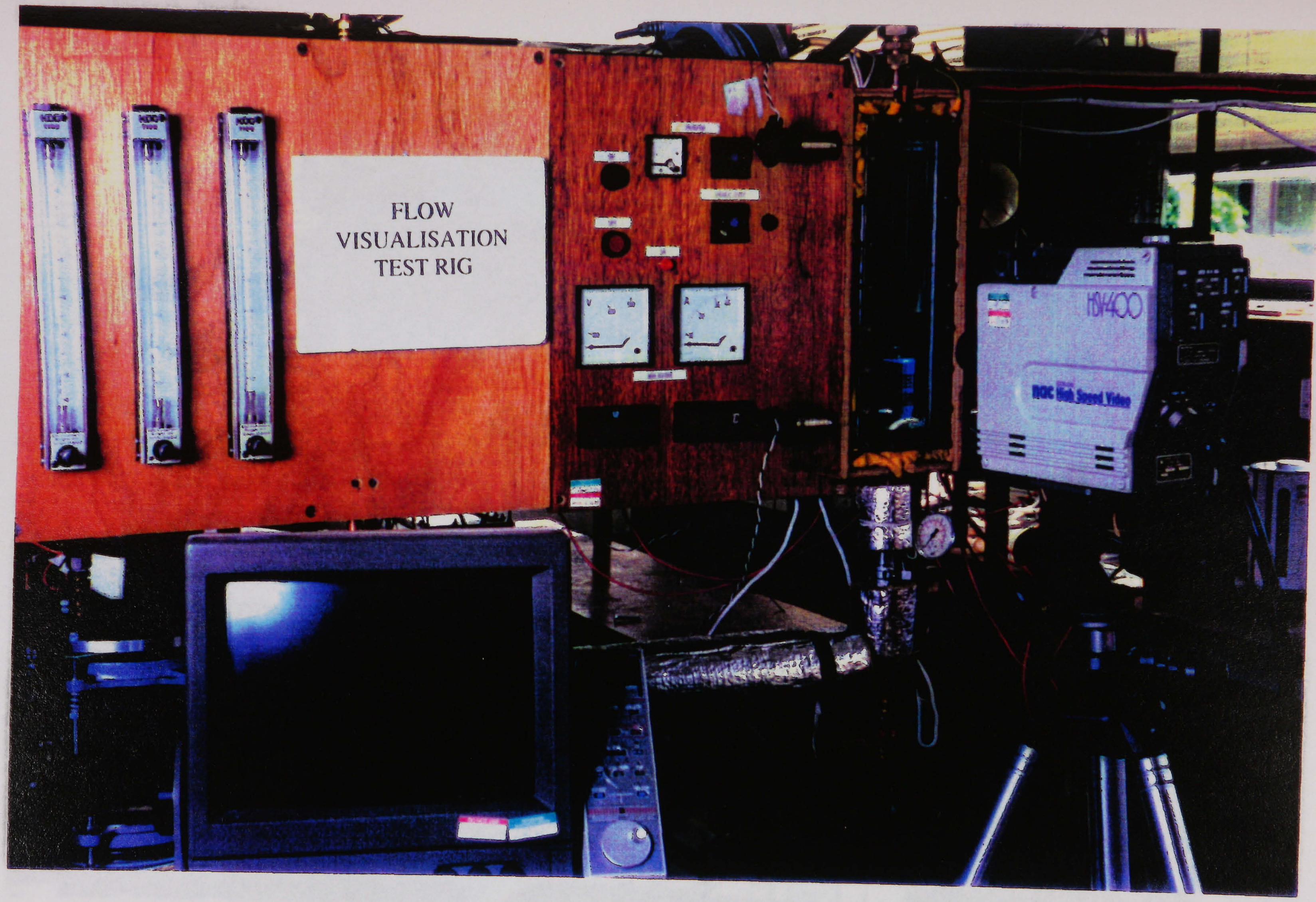

Figure 3.9 Photograph of Test Rig Mark II
showing Flow Visualisation Test Section

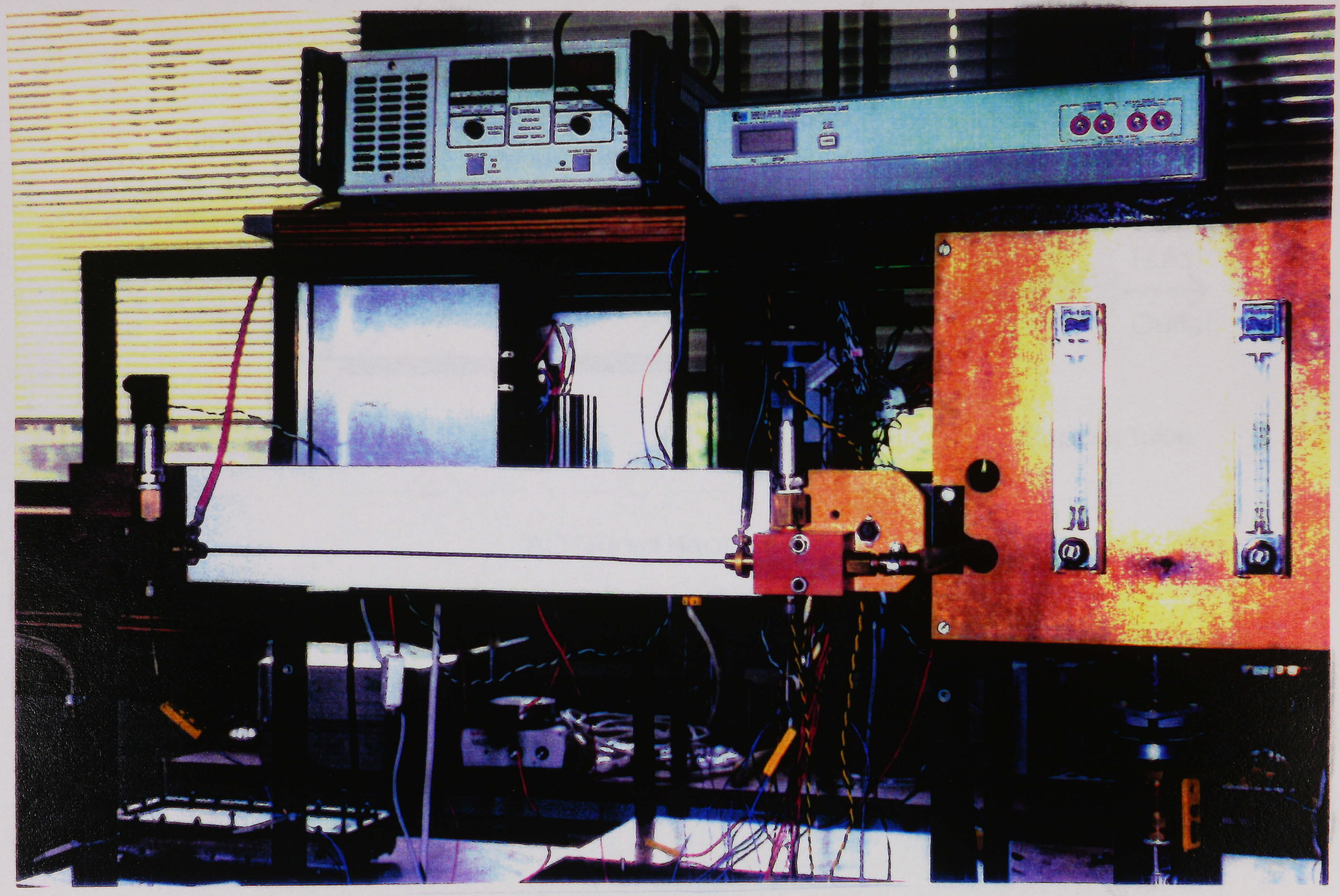

Figure 3.10 Photograph of Test Rig Mark II
showing Single Tube Test Section

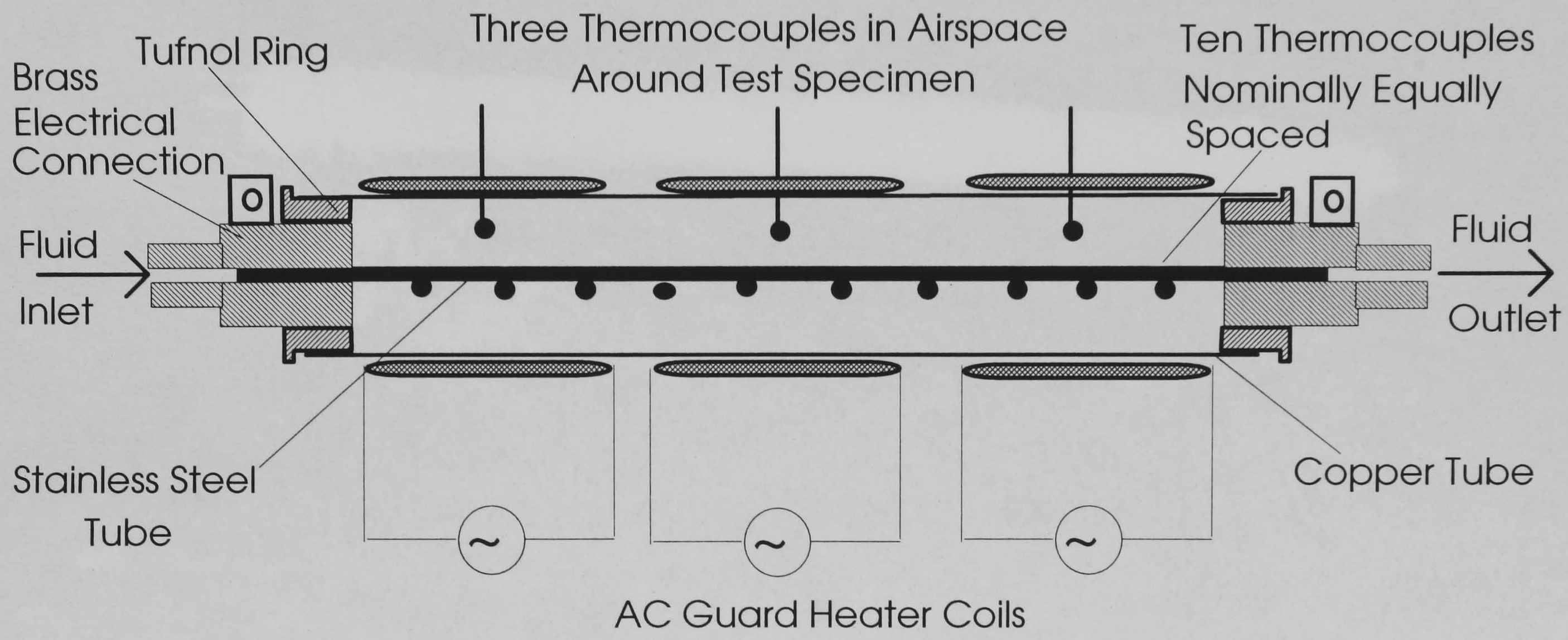

Figure 3.11 Schematic Diagram of Single Tube Test Section

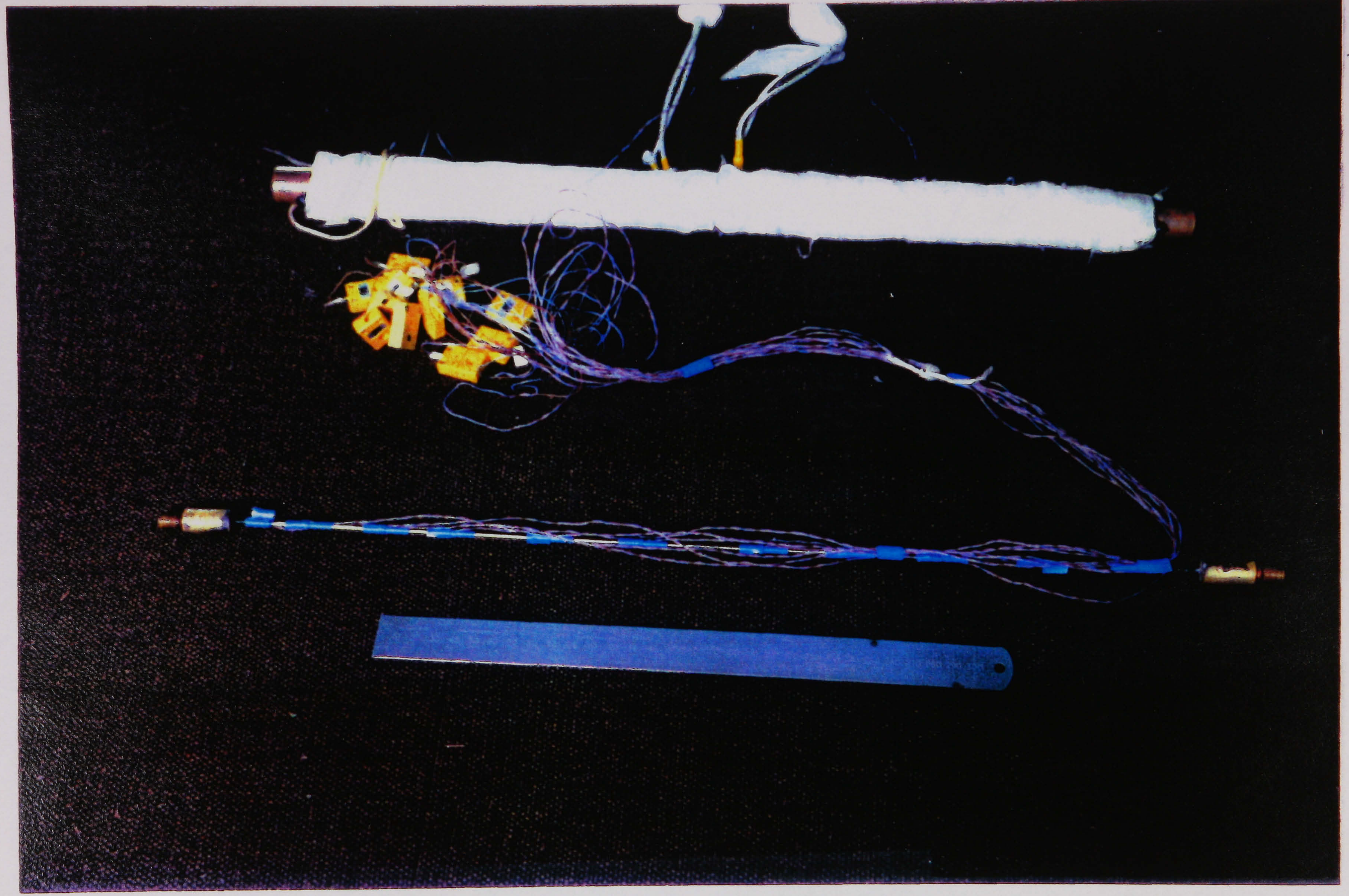

Figure 3.12 Single Tube Test Section with Thermocouples Attached
Guard Heaters Removed

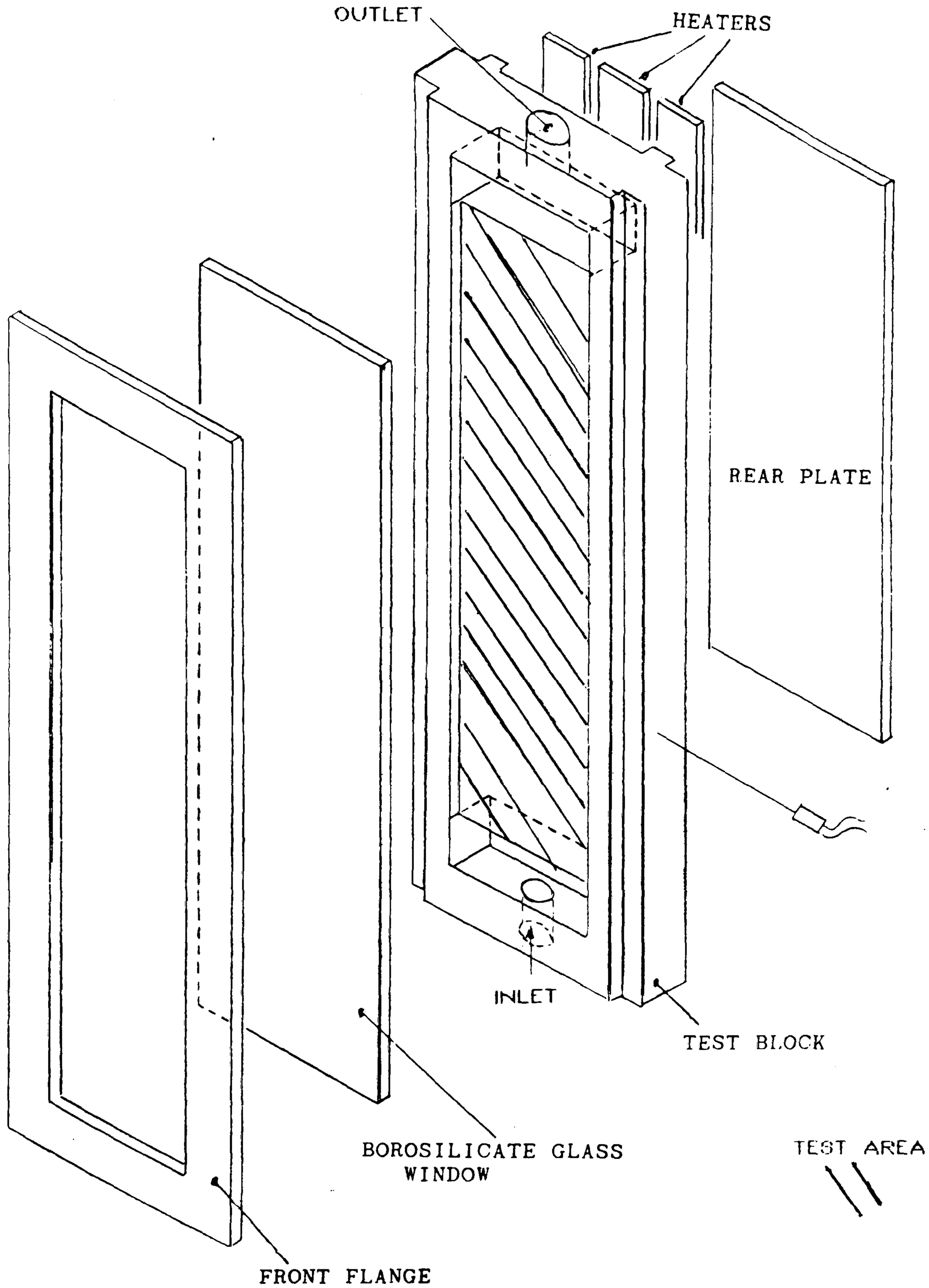

Figure 3.13 Exploded View of Flow Visualisation Test Section-Mark II Rig
(Fasteners and Casing Omitted)

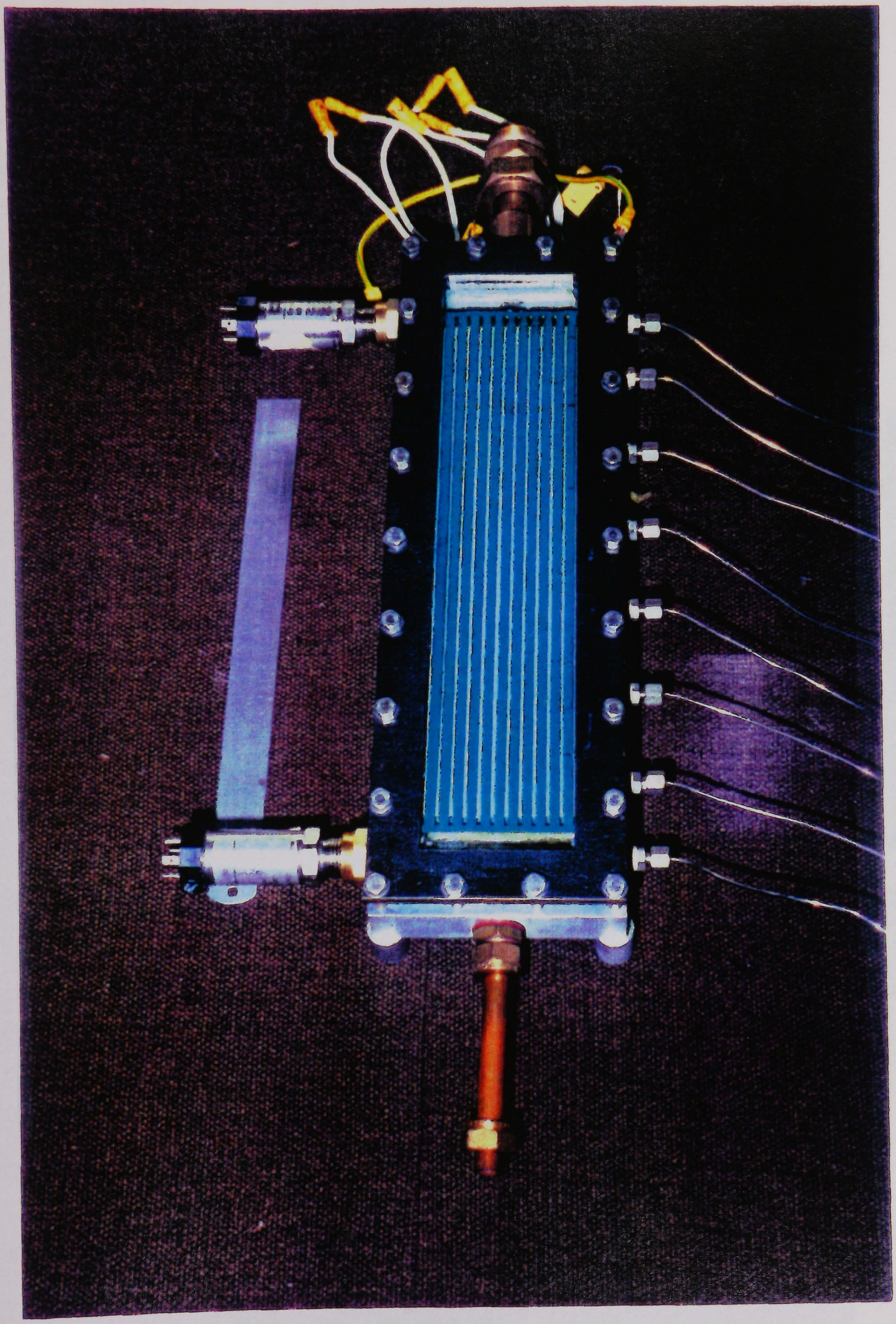

Figure 3.14 Photograph of Flow Visualisation Test Section

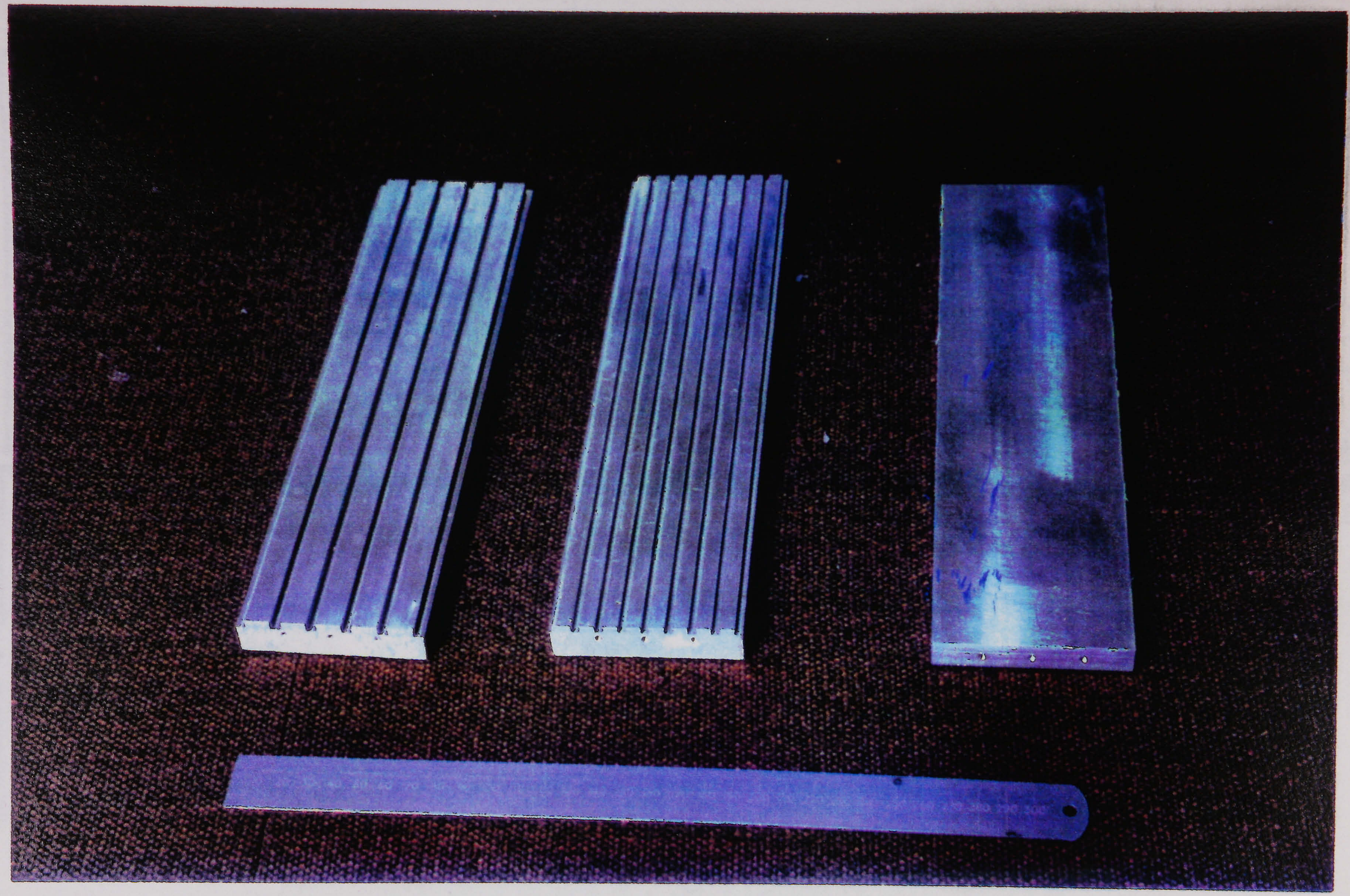

Figure 3.15 Photograph of Test Blocks Showing Flat-plate and Multi-Channel Geometries

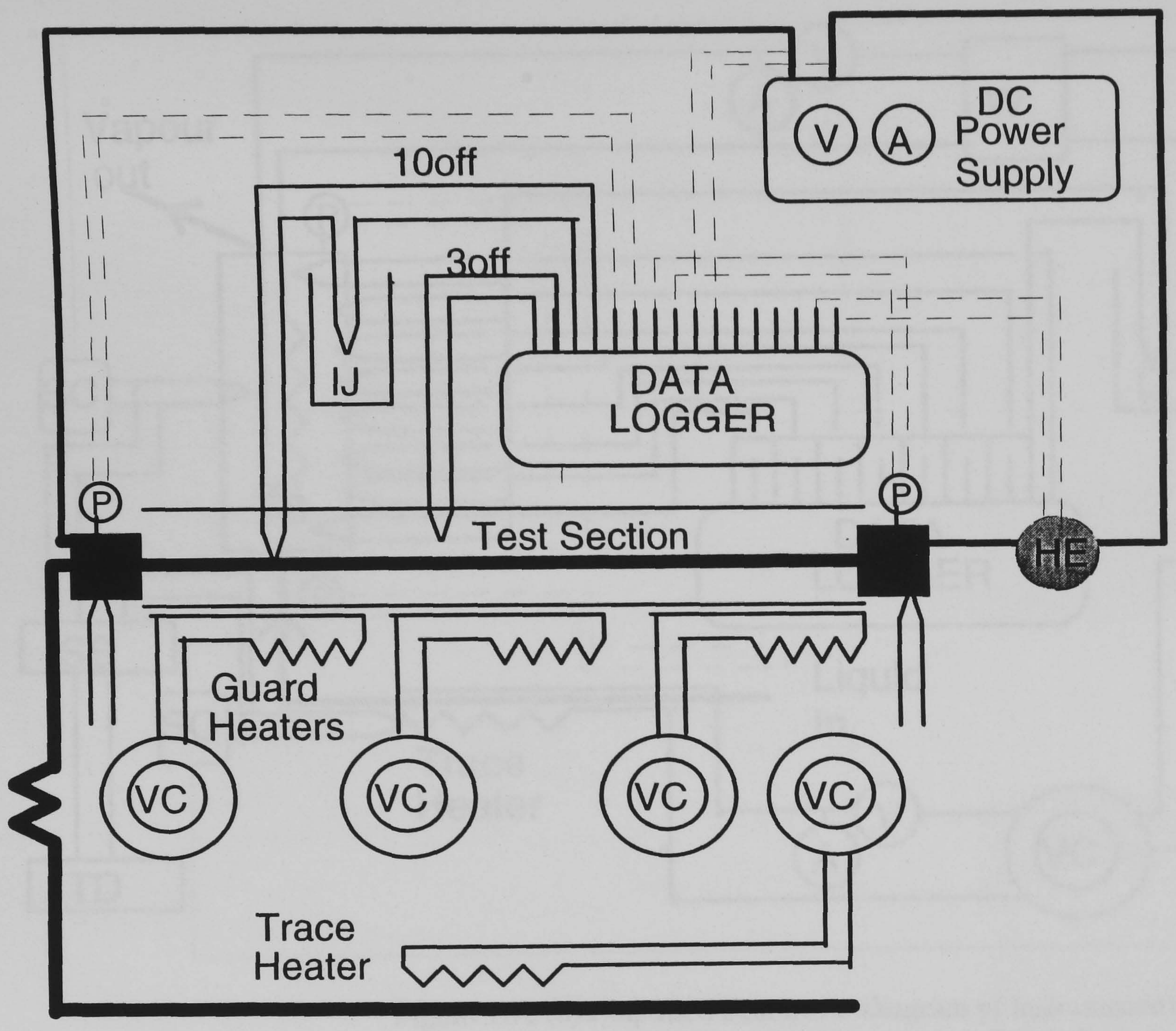

VC	Variac
I J	Ice Junction
HE	Hall Effect Transducer
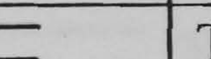	Thermocouple
P	Pressure gauge and transducer

Key to Figure 3.16(a)

Figure 3.16 (a)Simplified Schematic Diagram of Instrumentation -Mark II Rig
Single Tube Test Section

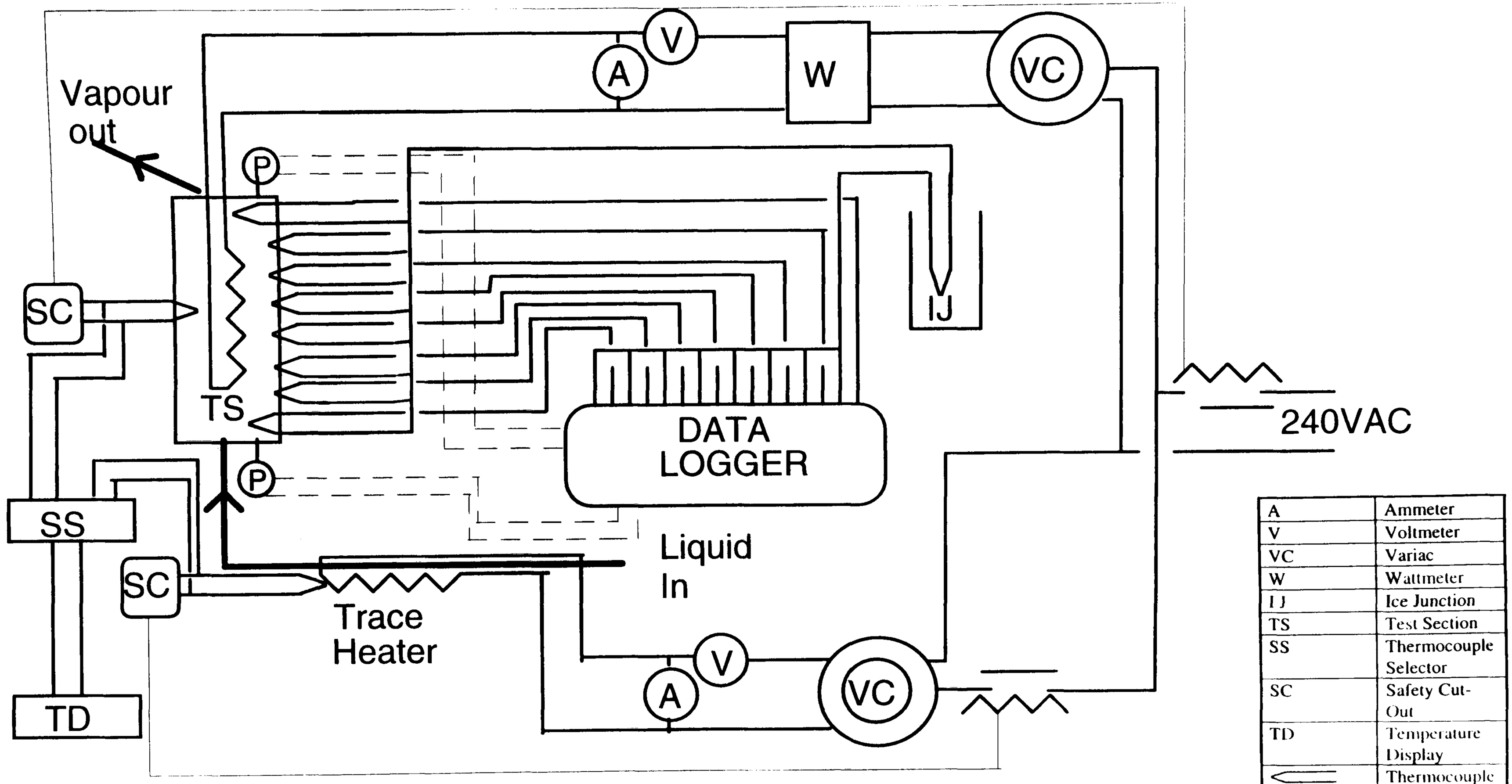

A	Ammeter
V	Voltmeter
VC	Variac
W	Wattmeter
I J	Ice Junction
TS	Test Section
SS	Thermocouple Selector
SC	Safety Cut-Out
TD	Temperature Display
	Thermocouple
P	Pressure gauge and transducer

Figure 3.16 (b)Simplified Schematic Diagram of Instrumentation -Mark II Rig
Flow Visualisation Test Section

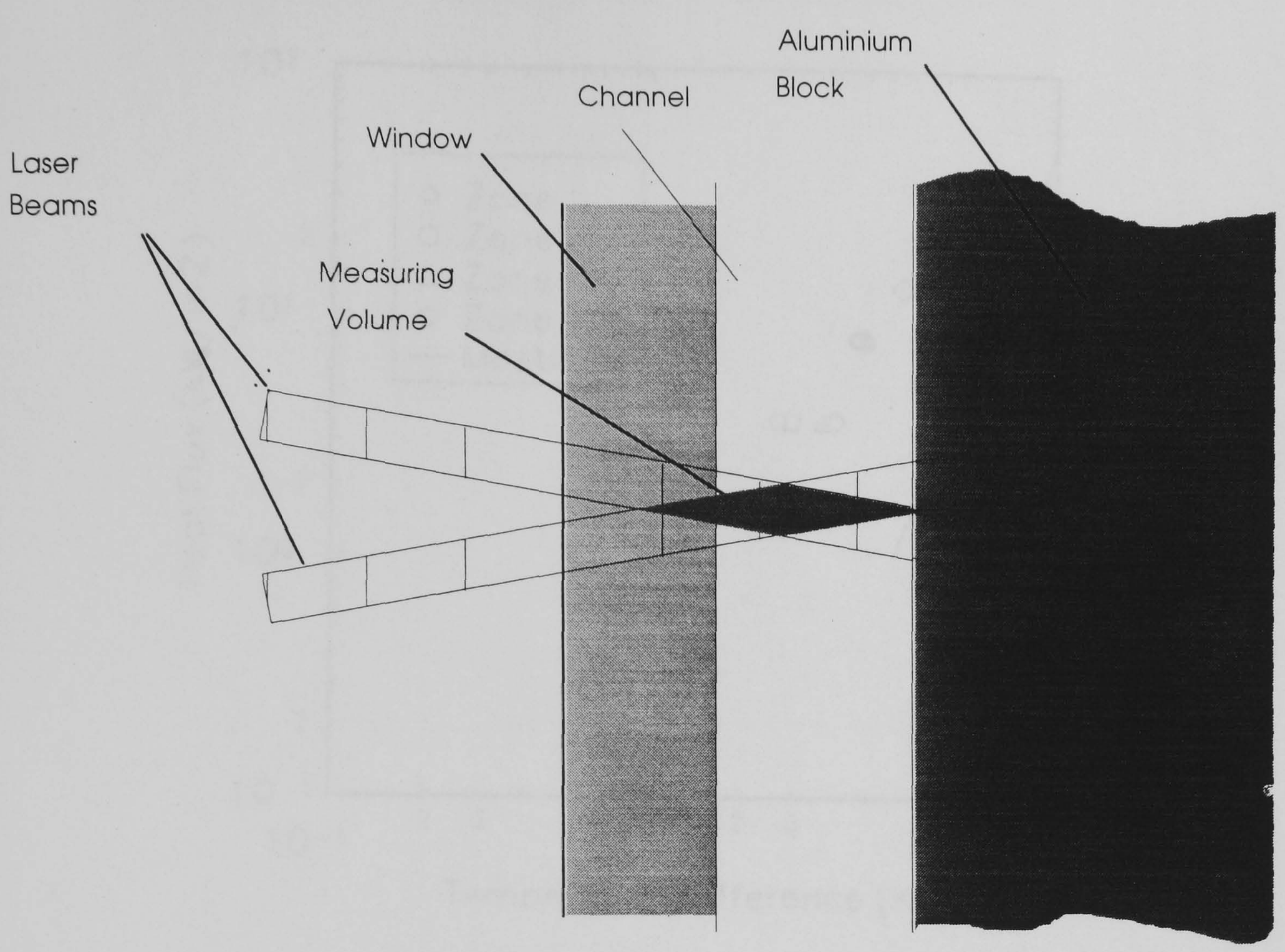

Fig 3.17 Schematic Diagram of LDA Measuring Volume Applied to Small Channel

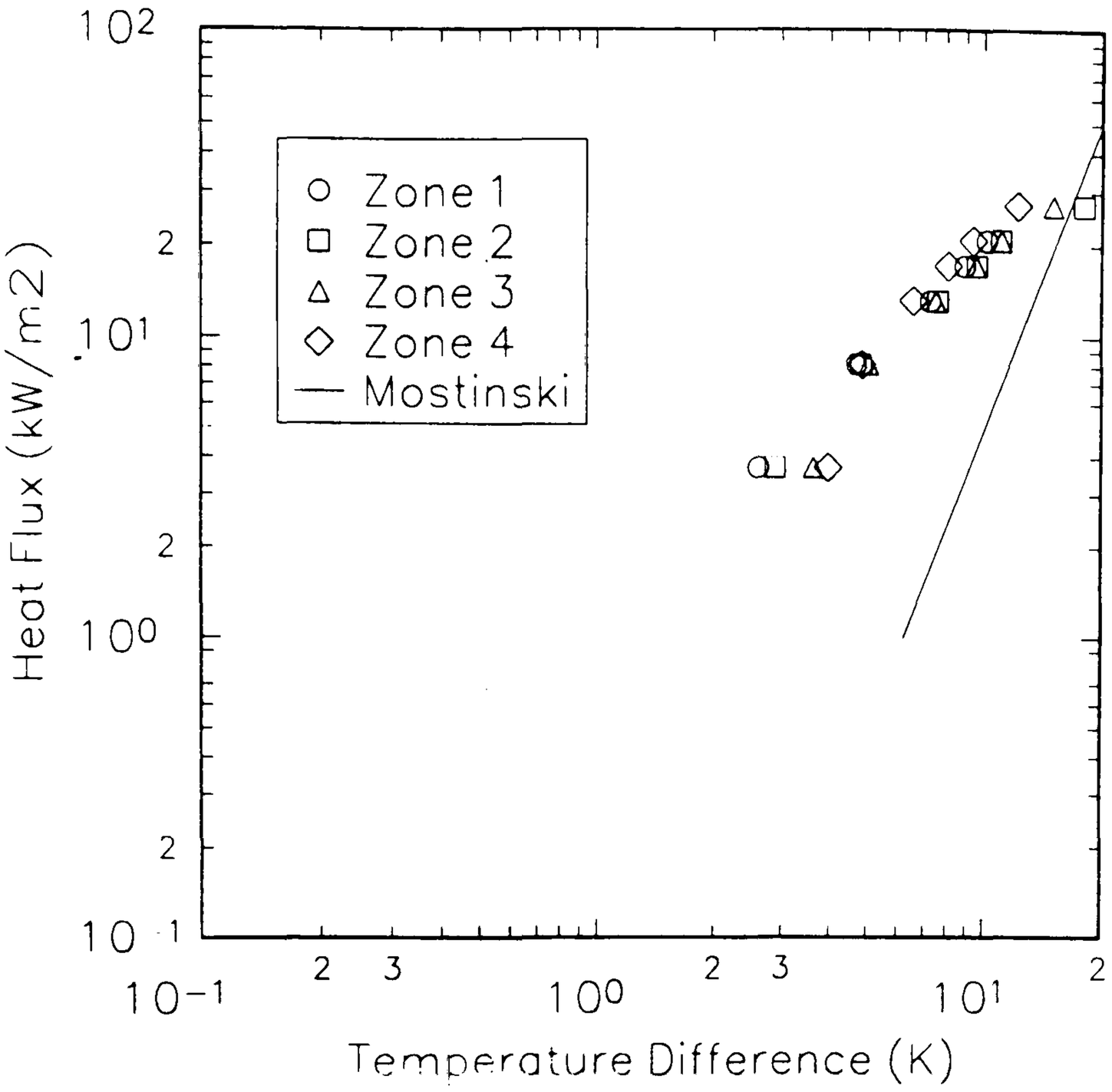

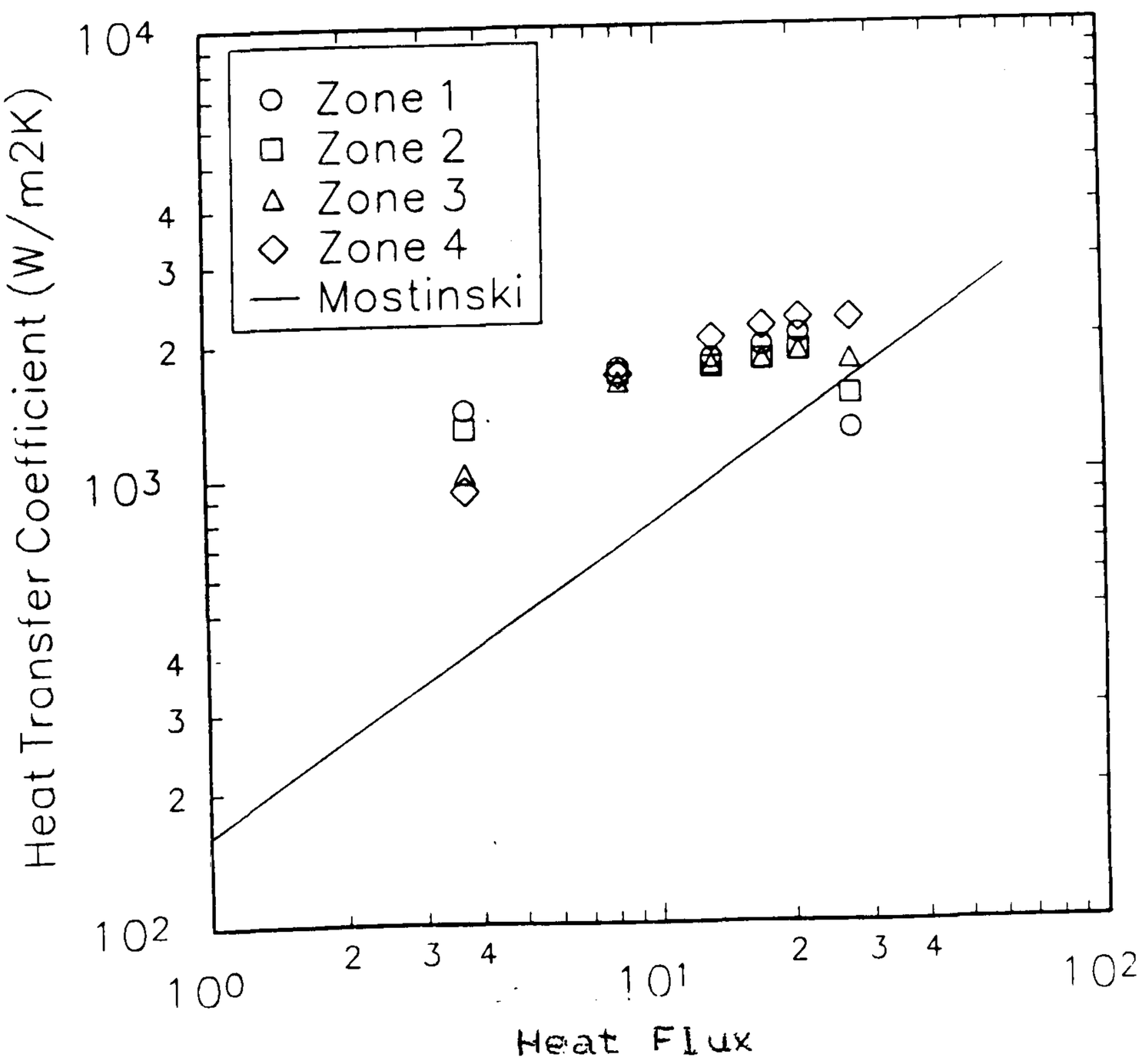

Figure 3.18 Heat Transfer Results
Flat Plate, 1 mm gap, 1 bar, G=67kg/m^{2}s, R113

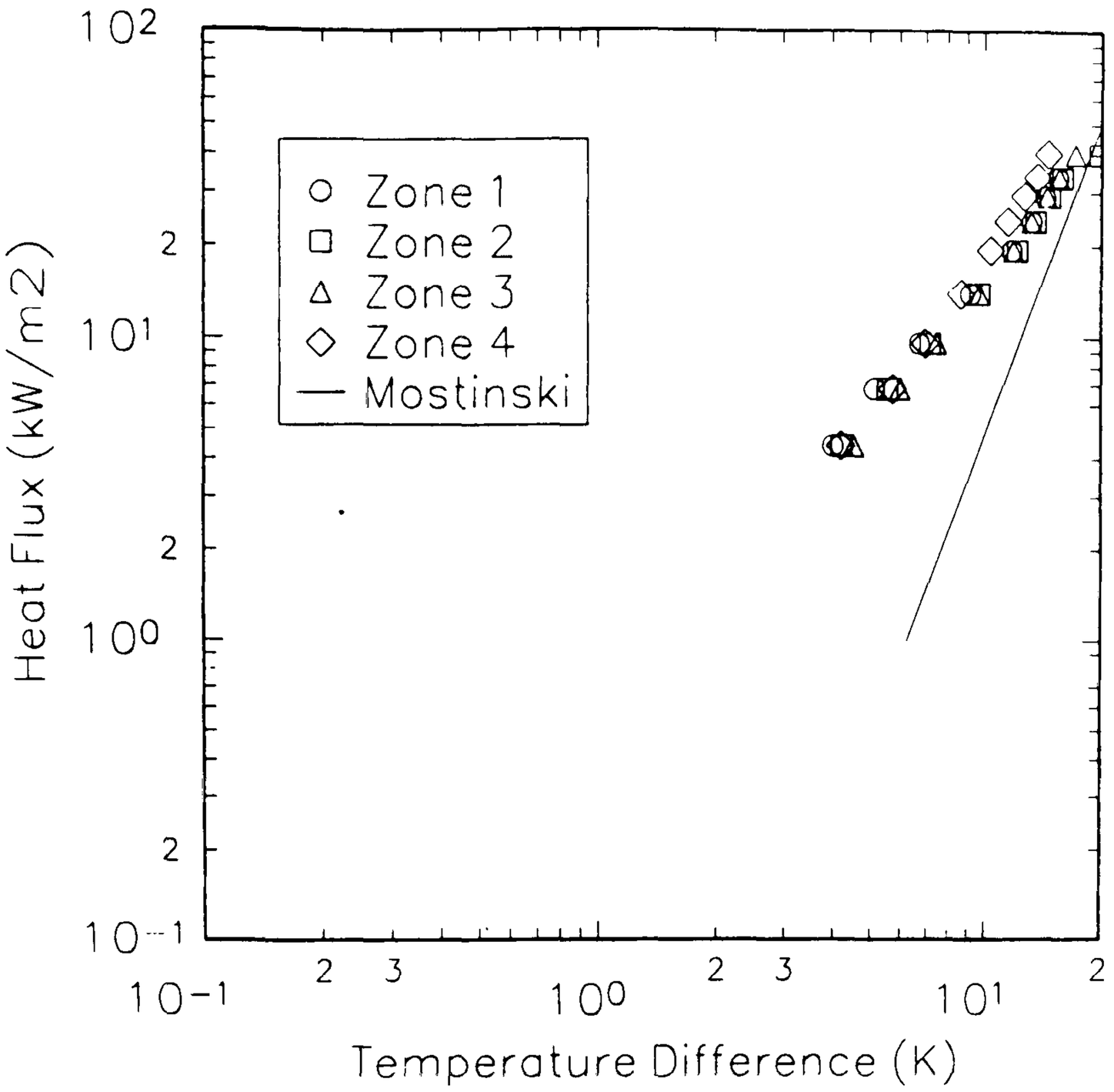

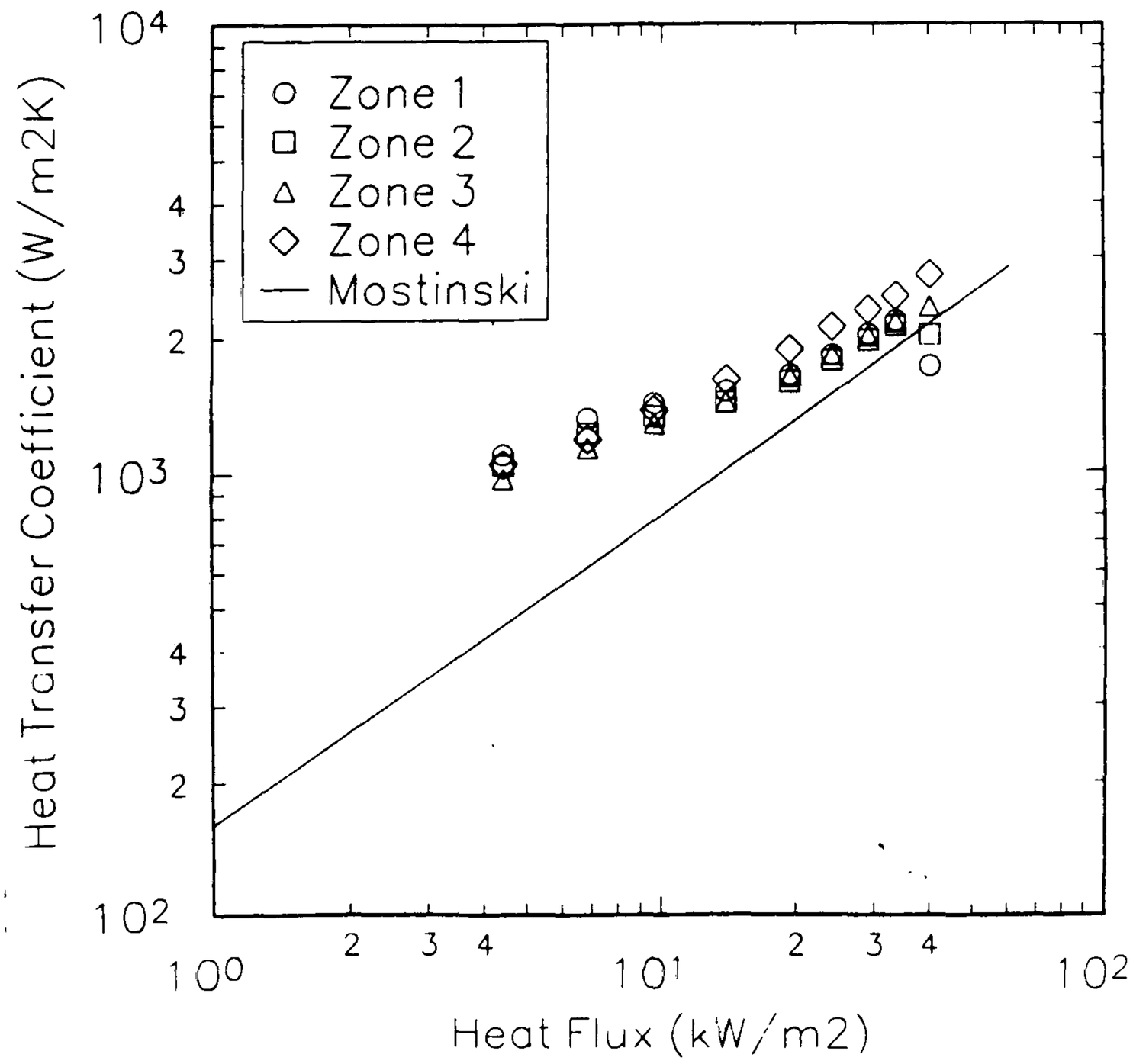

Figure 3.19 **Heat Transfer Results**
Flat Plate, 2 mm gap, 1 bar, G=67kg/m^{2}s, R113

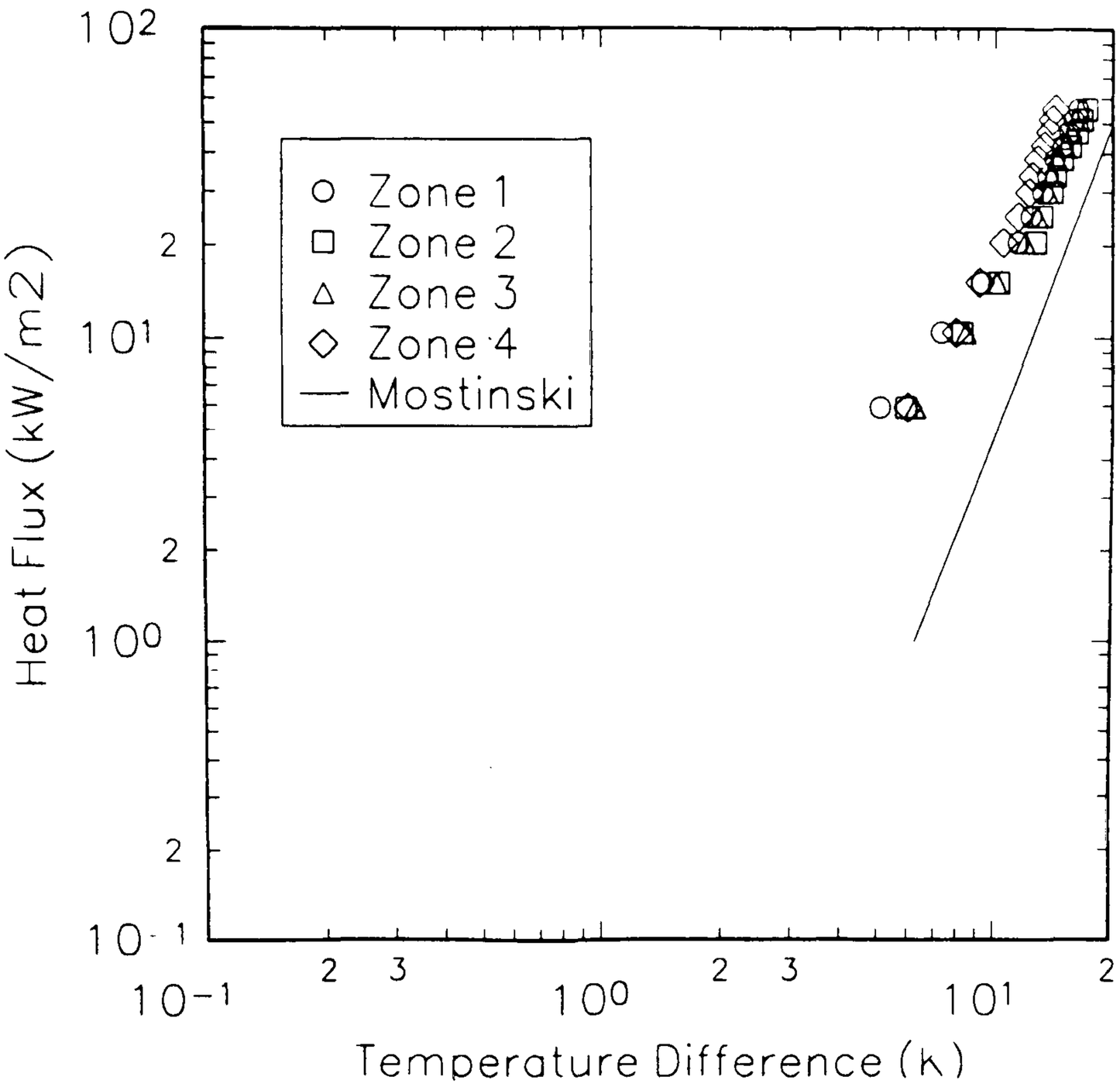

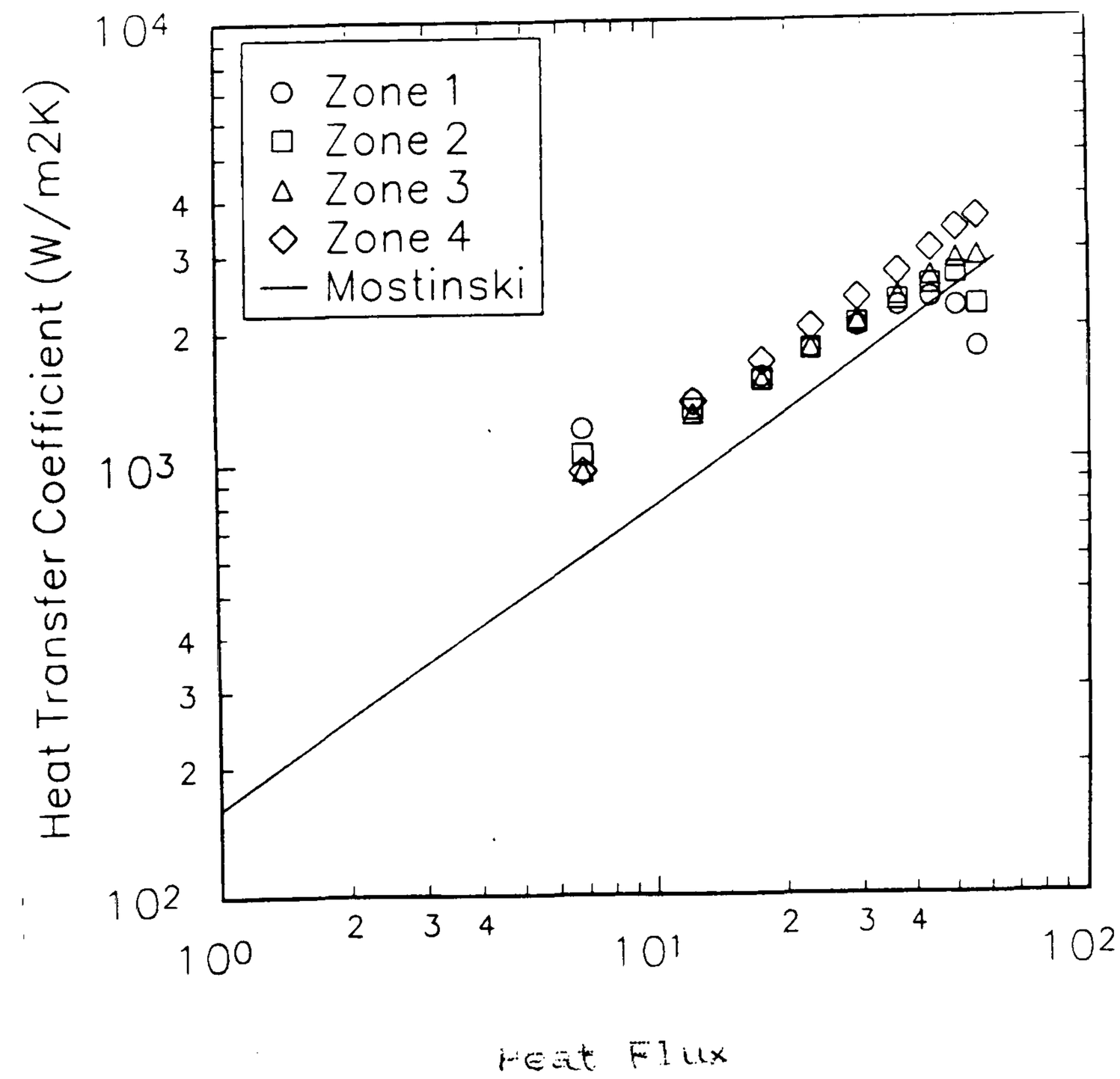

Figure 3.20 Heat Transfer Results
Flat Plate, 3 mm gap, 1 bar, G=67kg/m^{2}s, R113

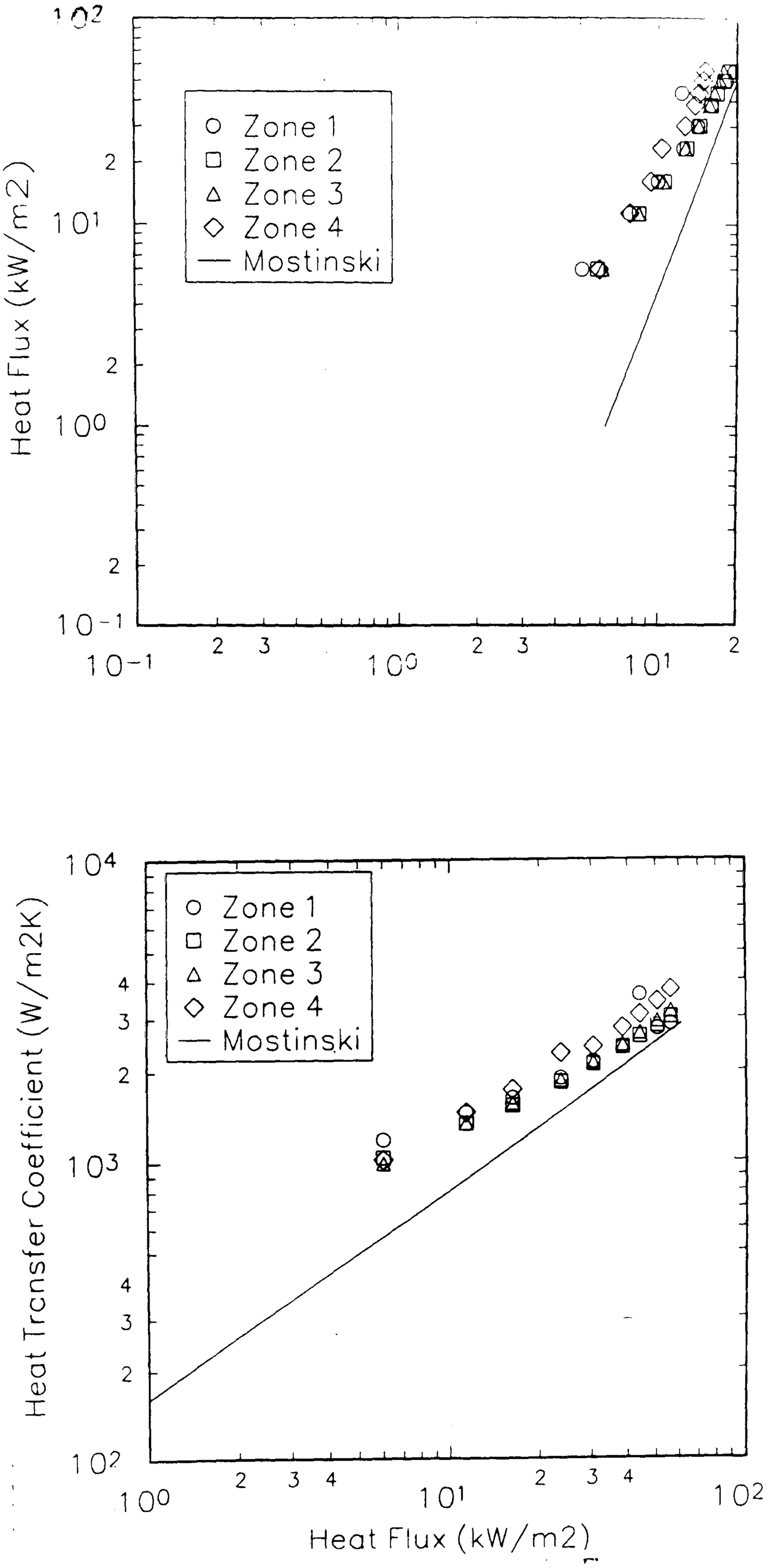

Figure 3.21 **Heat Transfer Results**
Flat Plate, 4 mm gap, 1 bar, G=50.3kg/m^{2}s, R113

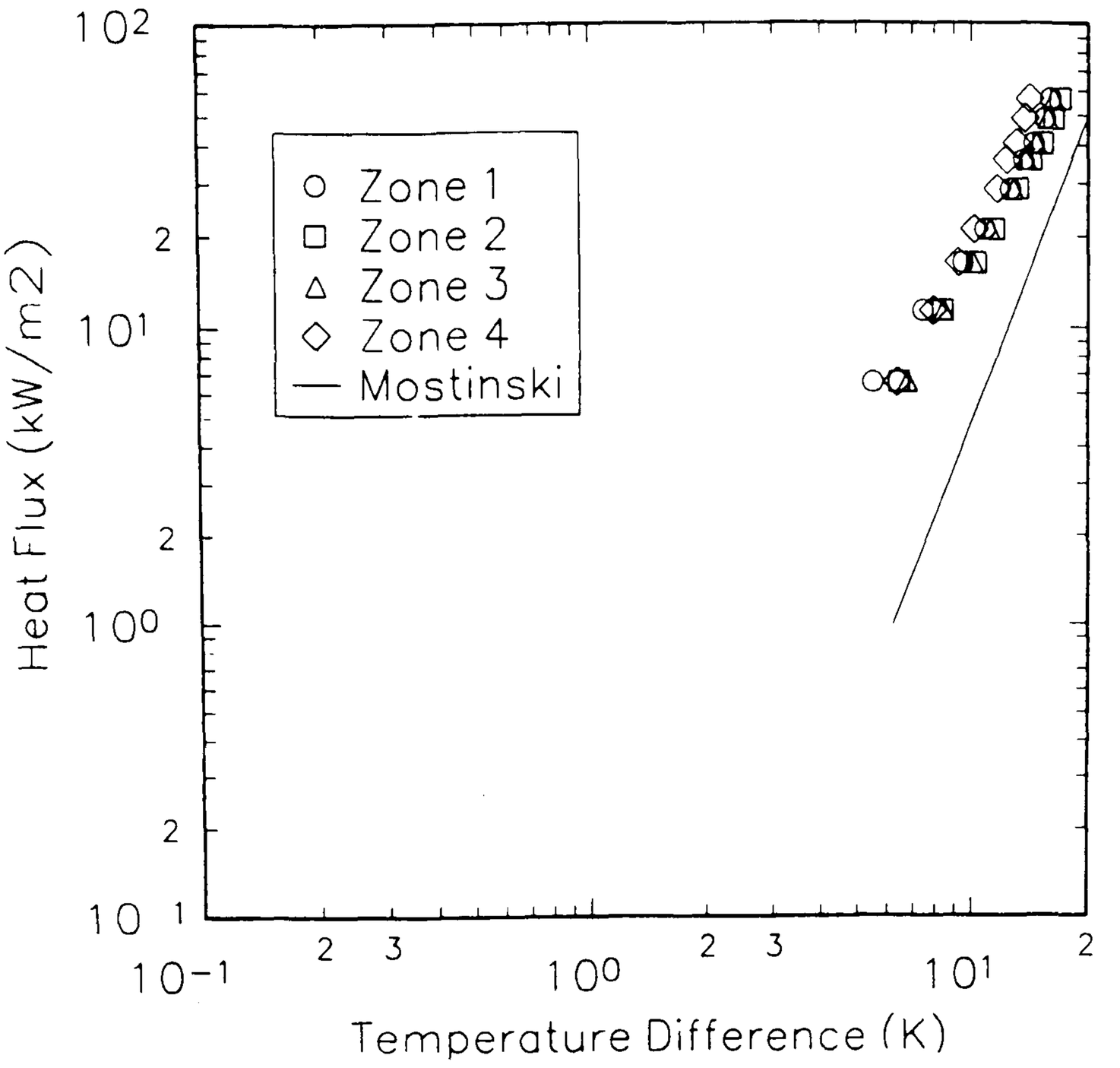

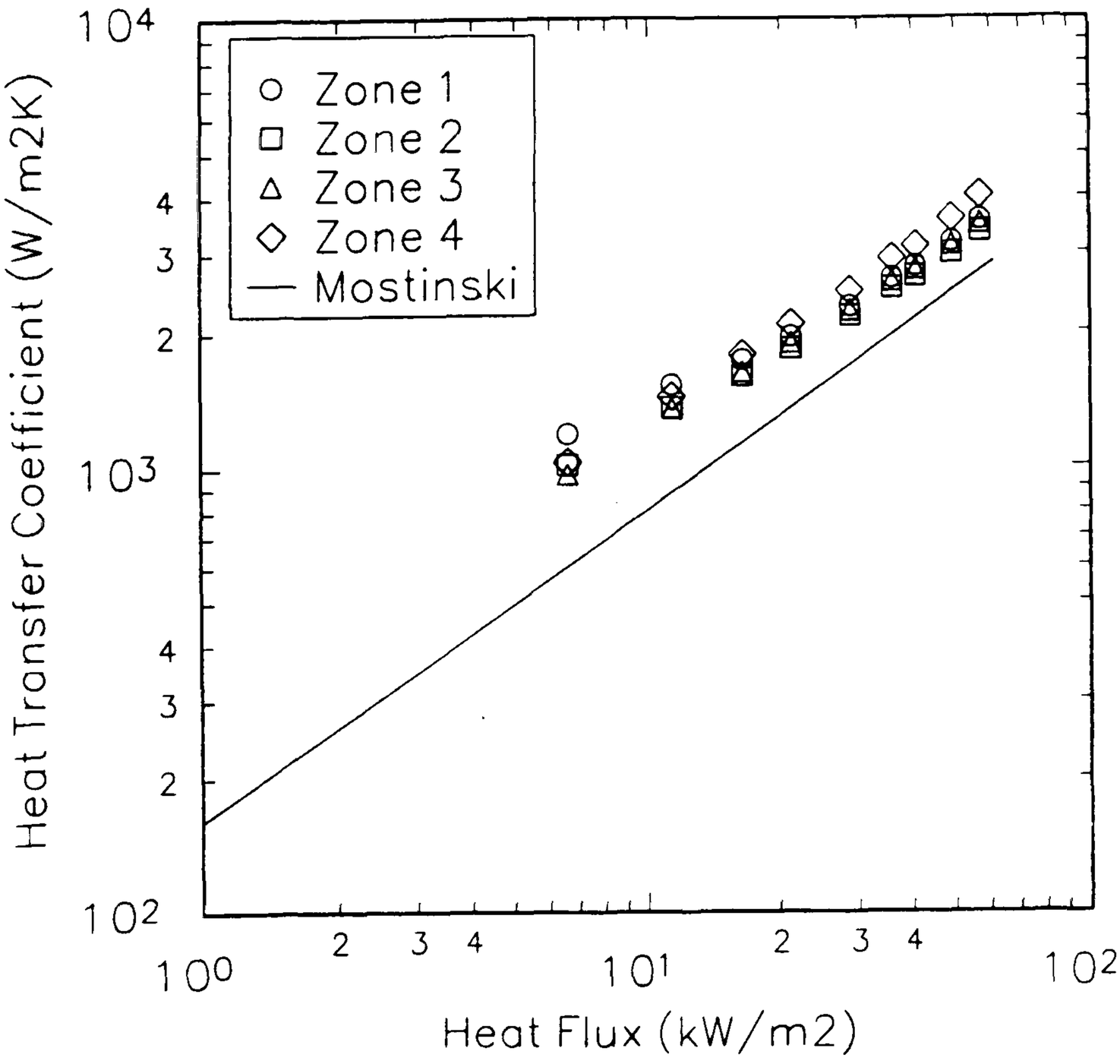

Figure 3.22 **Heat Transfer Results**
Flat Plate, 6 mm gap, 1 bar, G=56kg/m^{2}s, R113

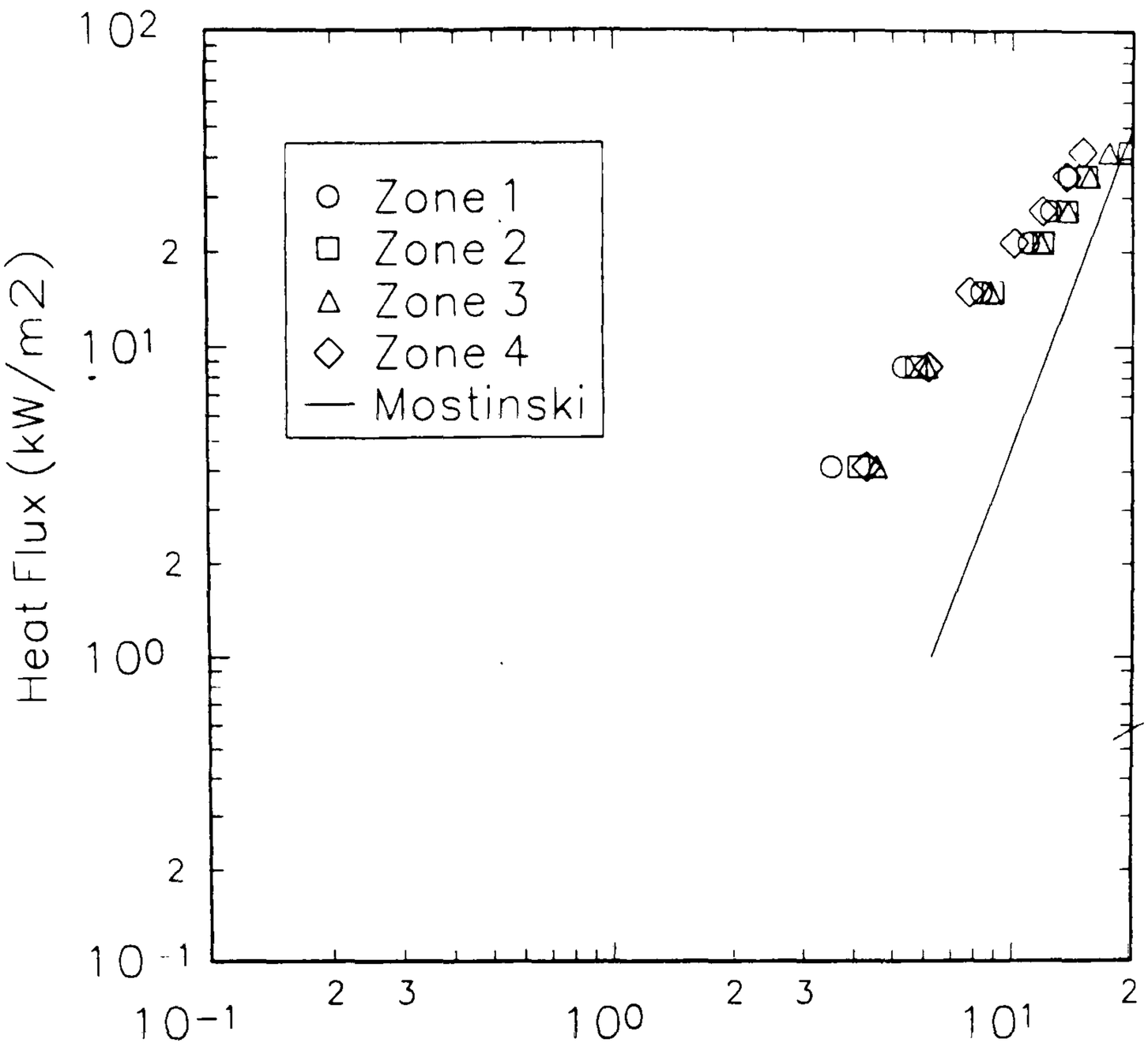

Figure 3.23 Heat Transfer Results
Flat Plate, 1 mm gap, 1 bar, G=134kg/m^{2}s, R113

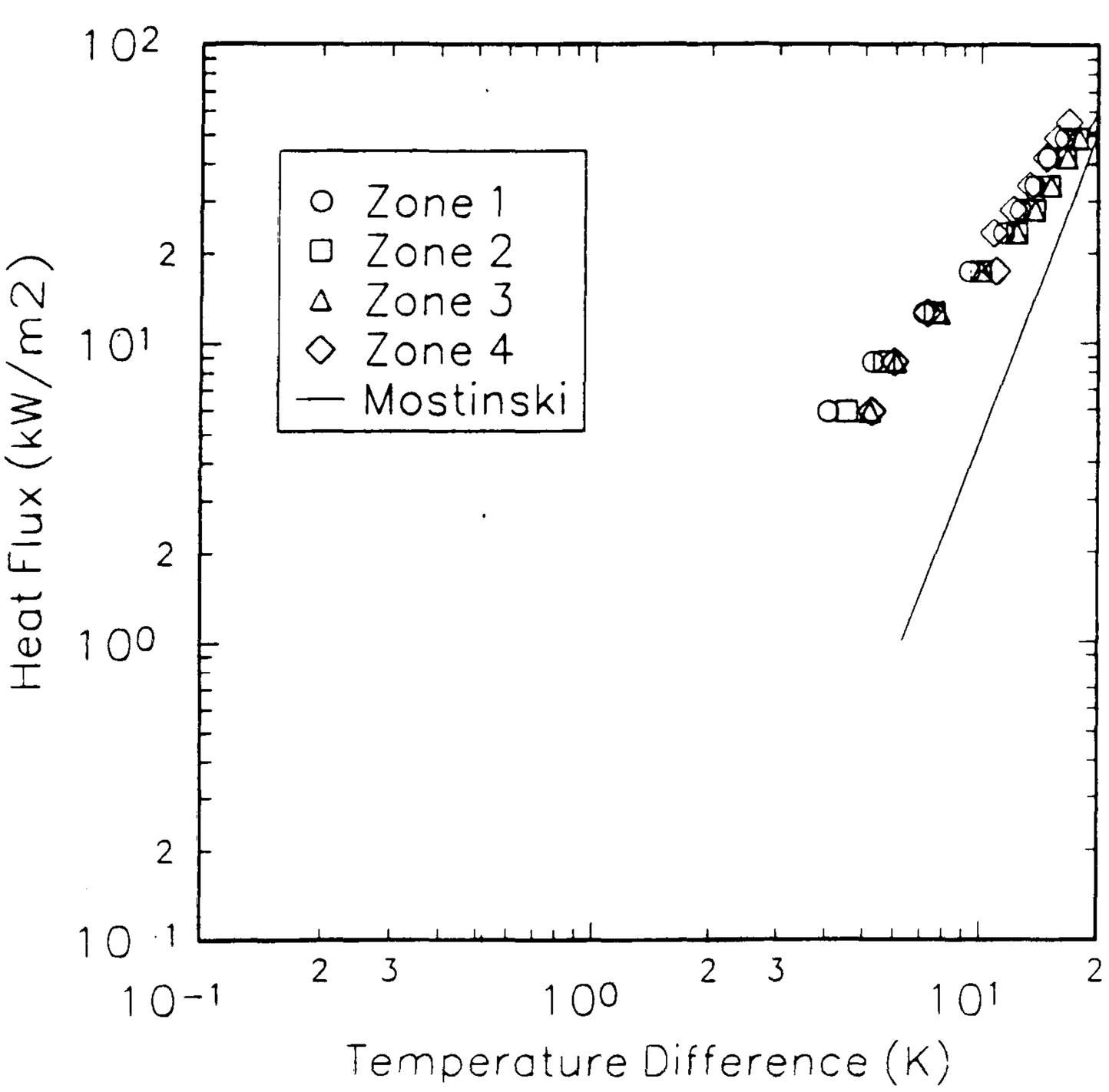

Figure 3.24 Heat Transfer Results
Flat Plate, 1 mm gap, 1 bar, G=201kg/m^{2}s, R113

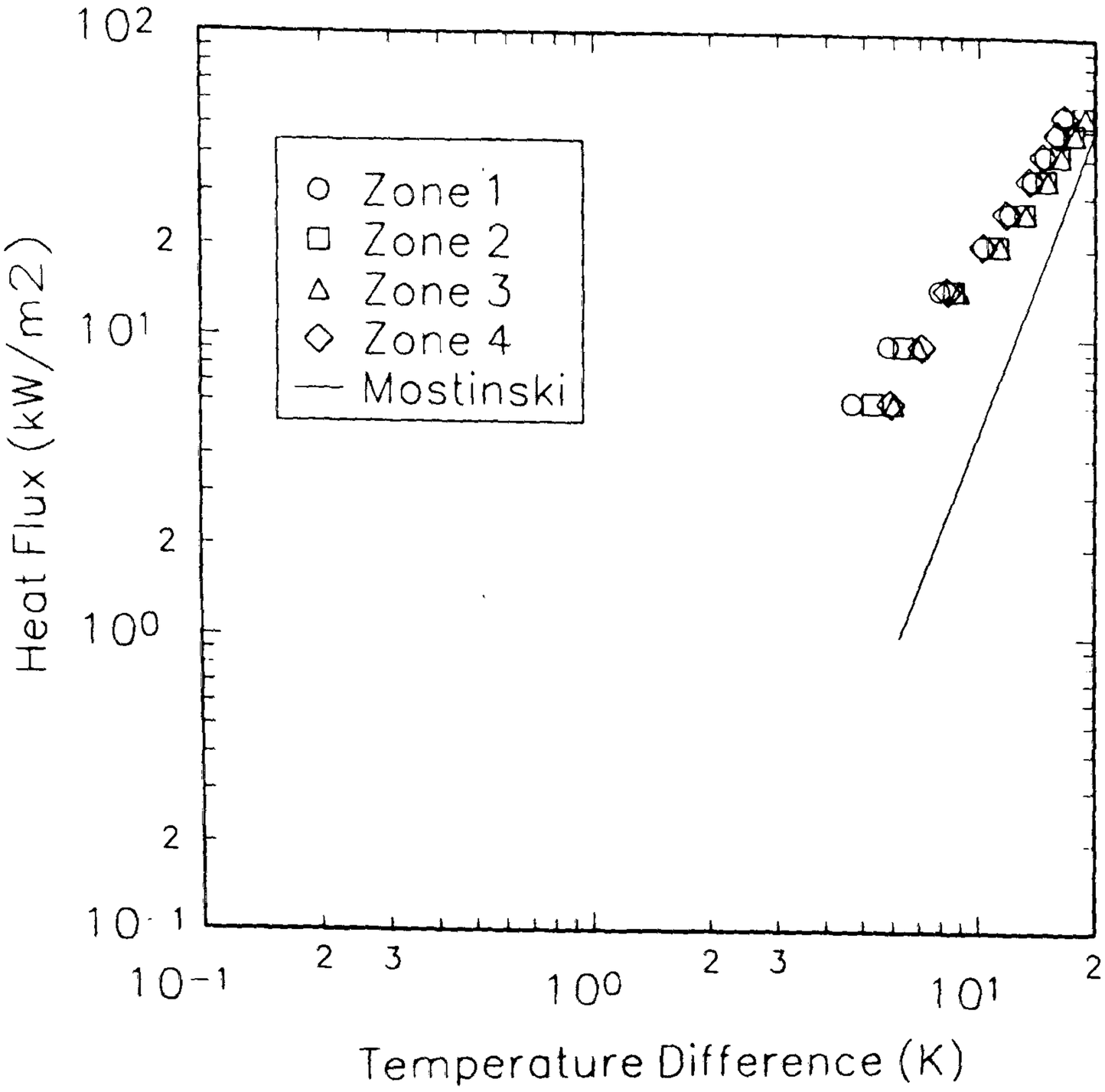

Figure 3.25 **Heat Transfer Results**
Flat Plate, 1 mm gap, 1 bar, G=268kg/m^{2}s, R113

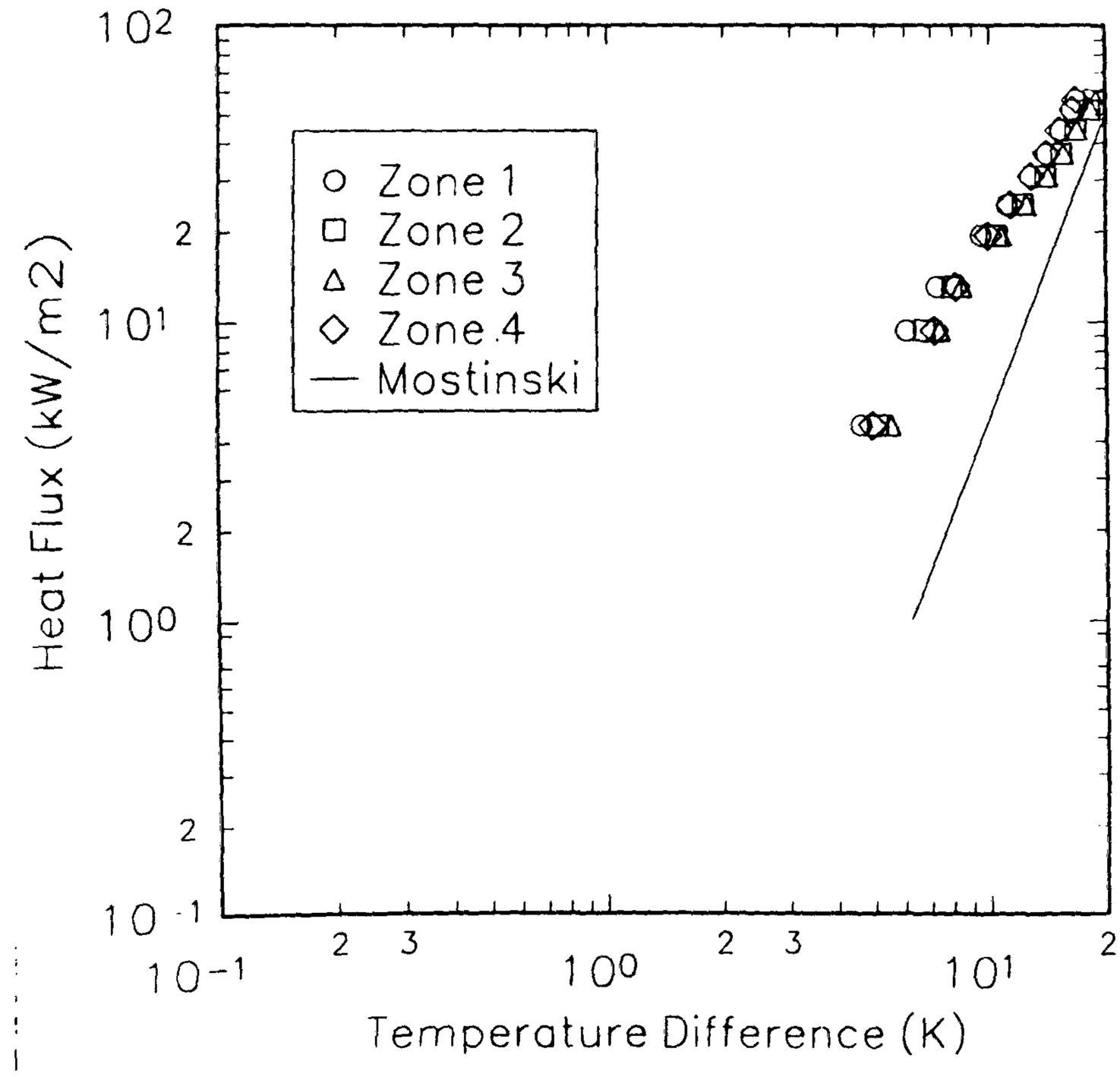

Figure 3.26 **Heat Transfer Results**
Flat Plate, 1 mm gap, 1 bar, G=335kg/m^{2}s, R113

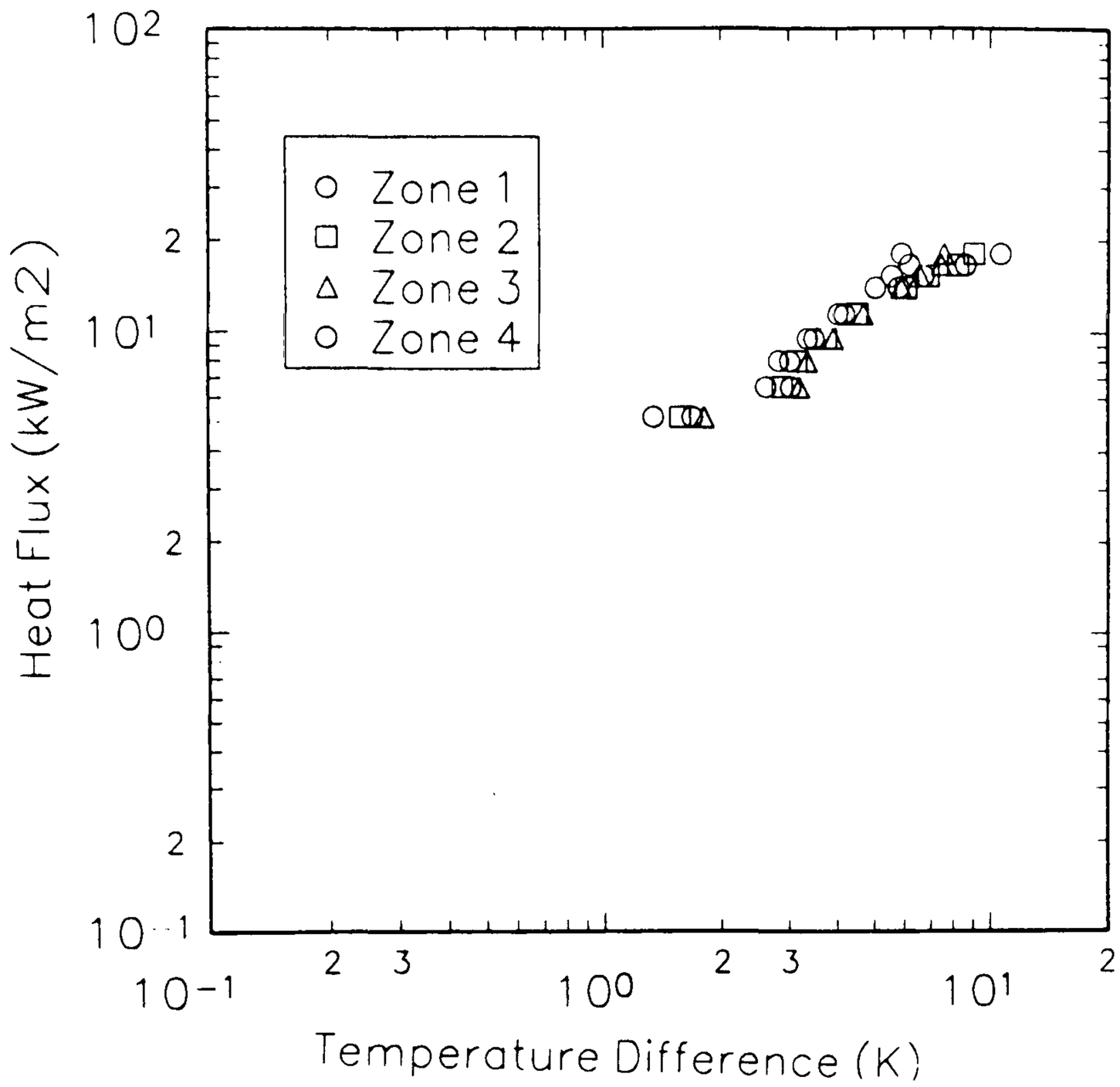

Figure 3.27 Heat Transfer Results
Geometry 1, 1 bar, G=124kg/m^{2}s, R113

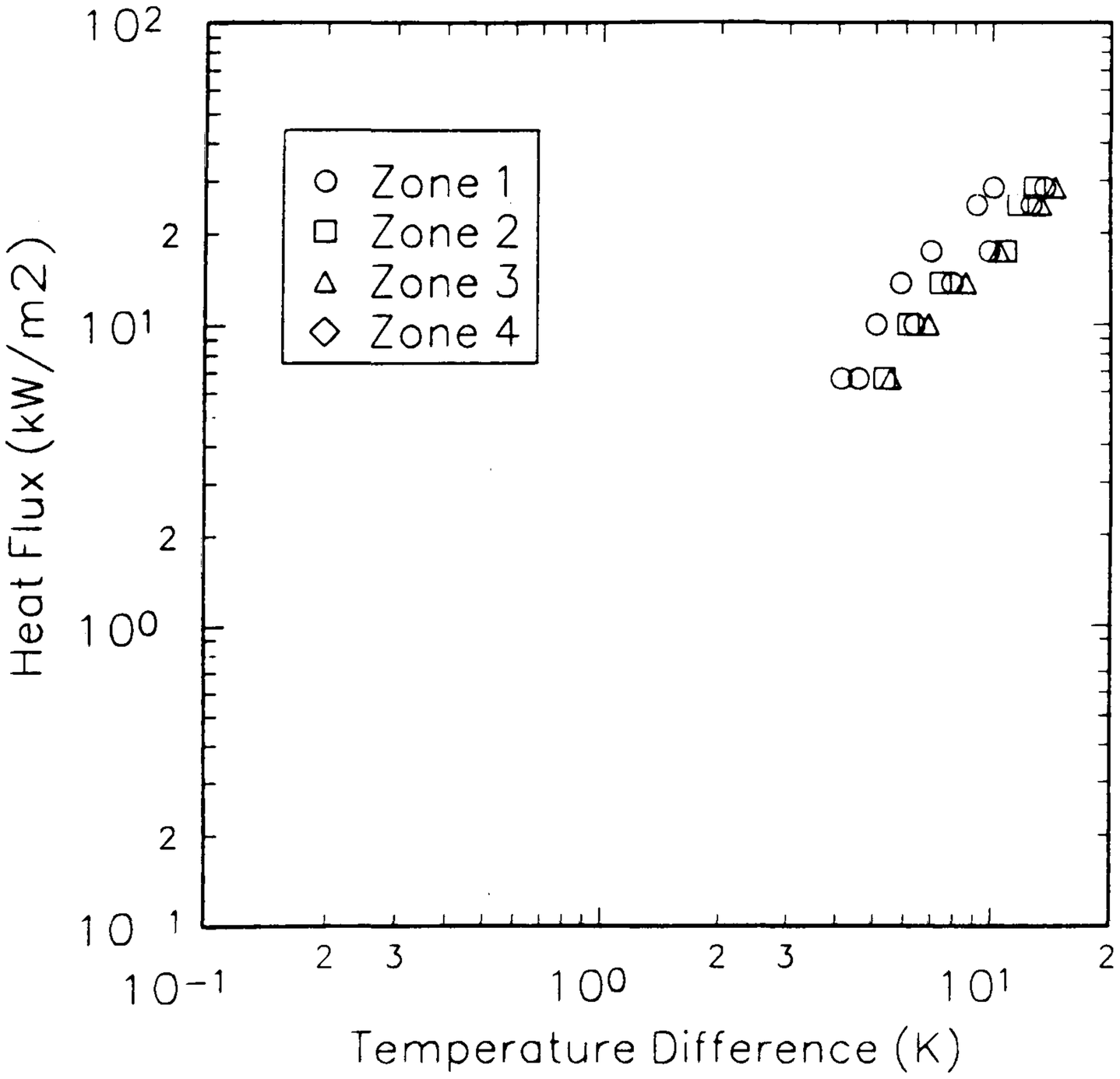

Figure 3.28 Heat Transfer Results
Geometry 1, 1 bar, G=620kg/m^{2}s, R113

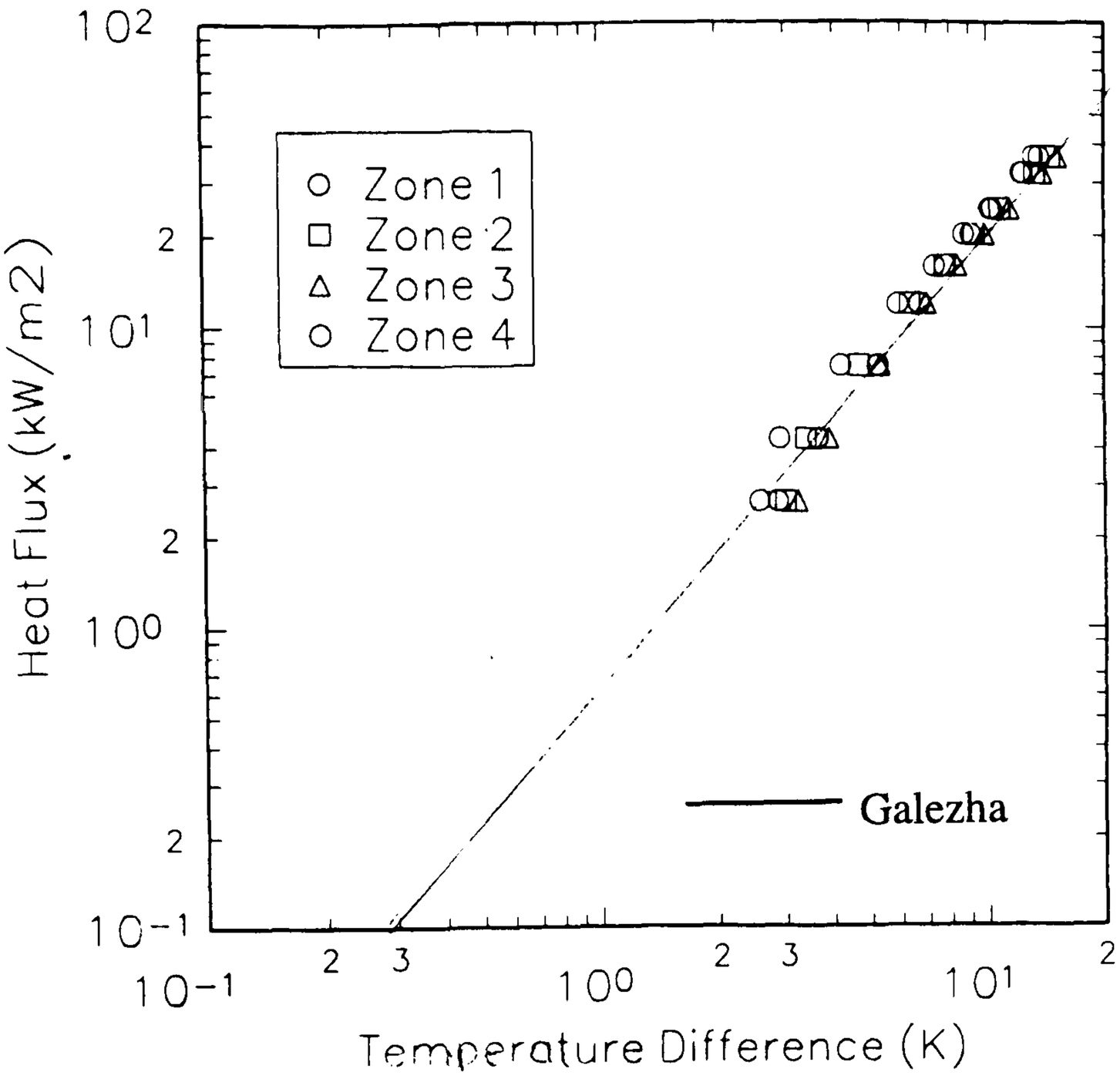

Figure 3.29 Heat Transfer Results
Geometry 2, 1 bar, G=312kg/m^{2}s, R113

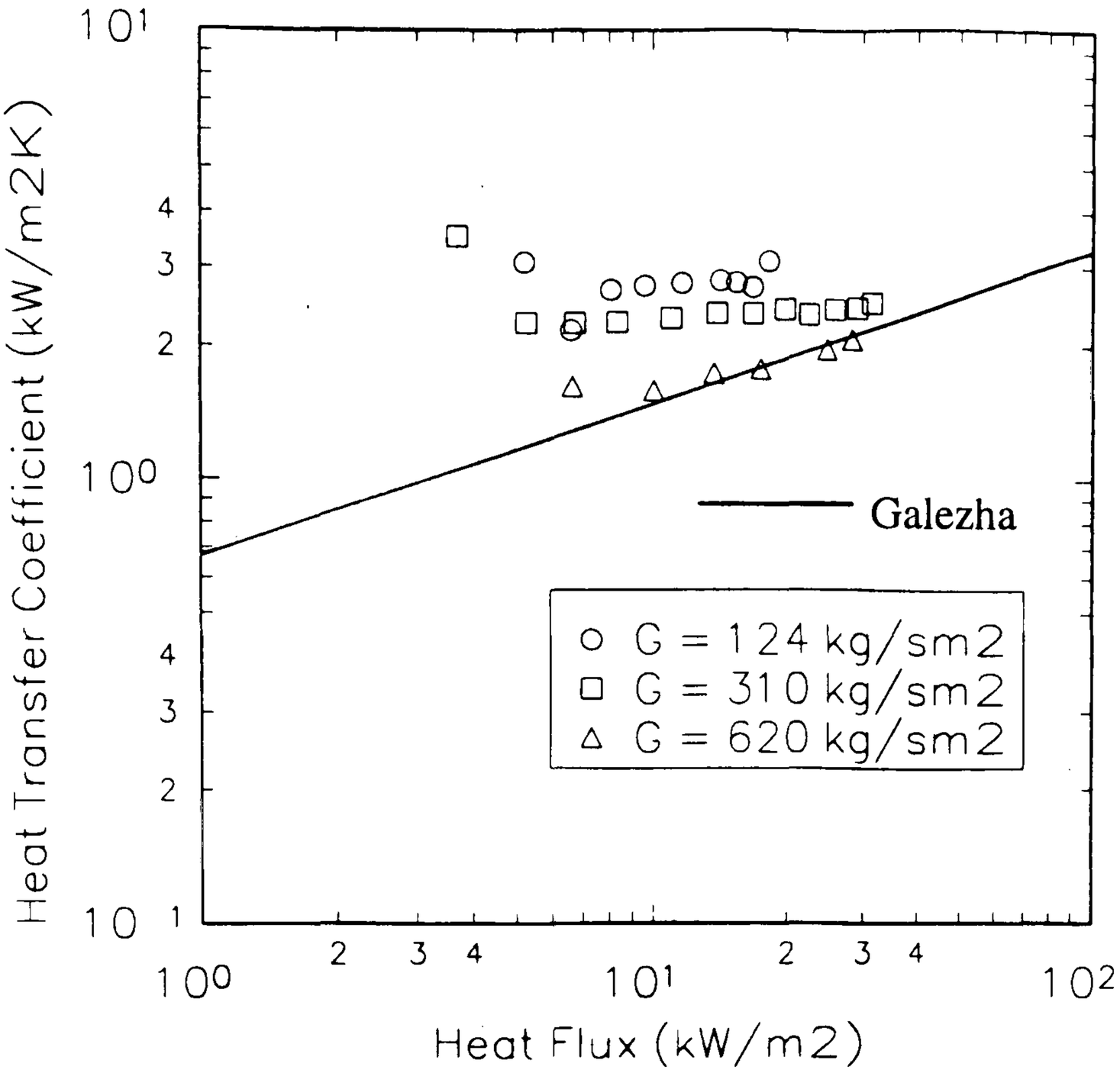

Figure 3.30 Heat Transfer Results
Geometry 1, 1 bar, Zone 4 (ref Fig.3.3), R113

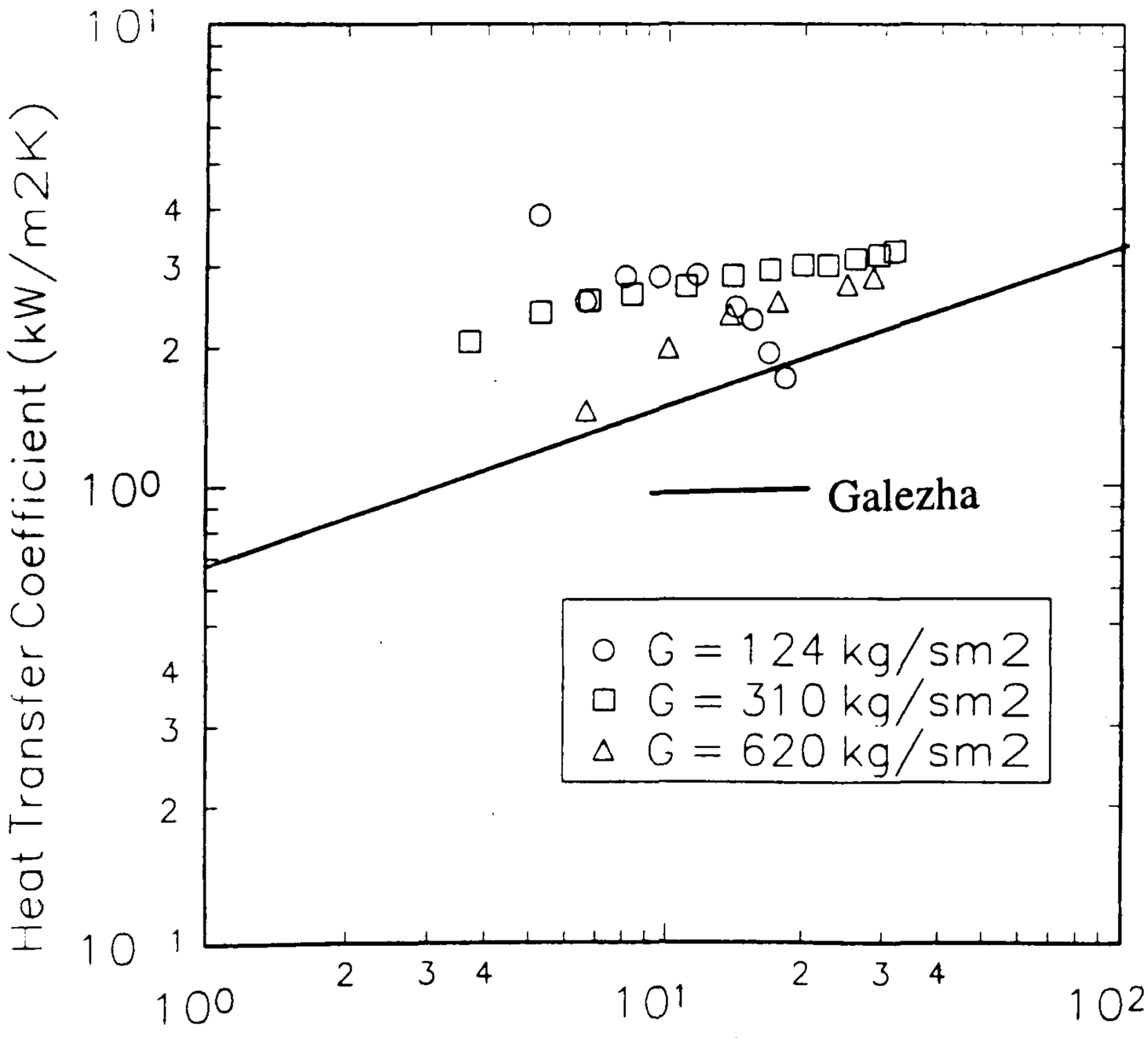

Figure 3.31 Heat Transfer Results
Geometry 1, 1 bar, Zone 1 (ref Fig.3.3), R113

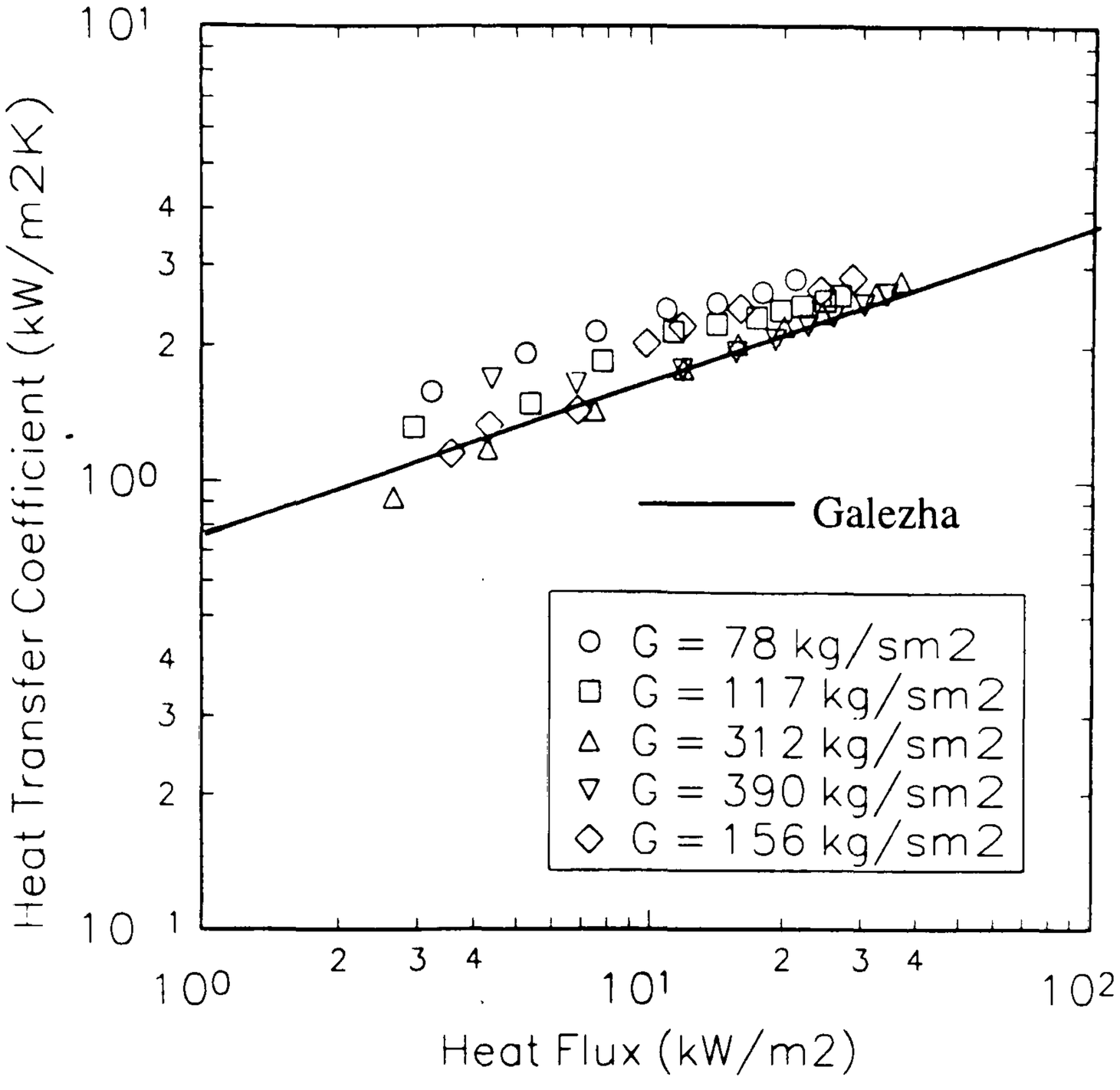

Figure 3.32 **Heat Transfer Results**
Geometry 2, 1 bar, Zone 4 (ref Fig.3.3), R113

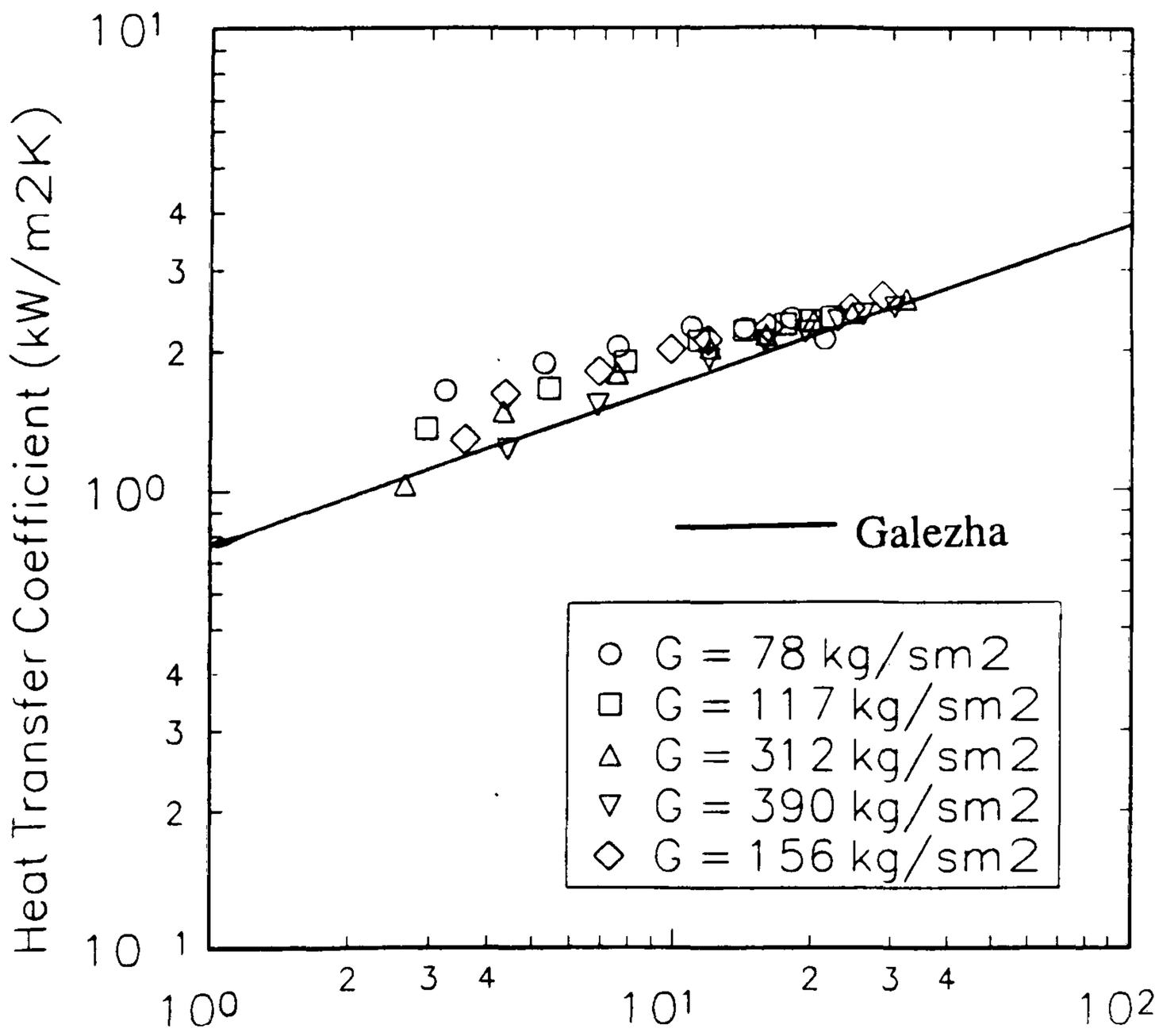

Figure 3.33 **Heat Transfer Results**
Geometry 2, 1 bar, Zone 1(ref Fig 3.3), R113

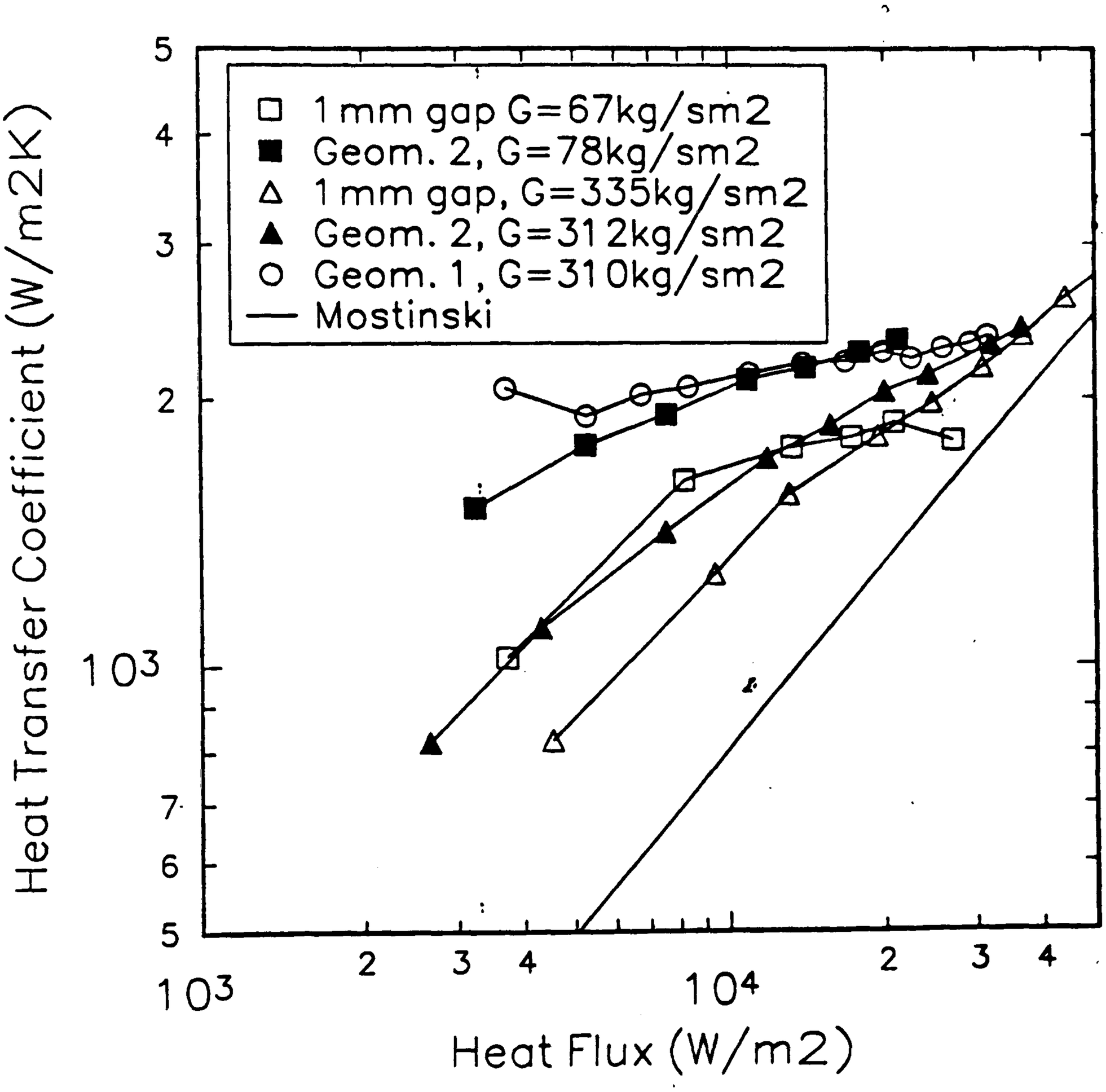

Figure 3.34 Heat Transfer Results
Sample from all Geometries - Mark I Rig

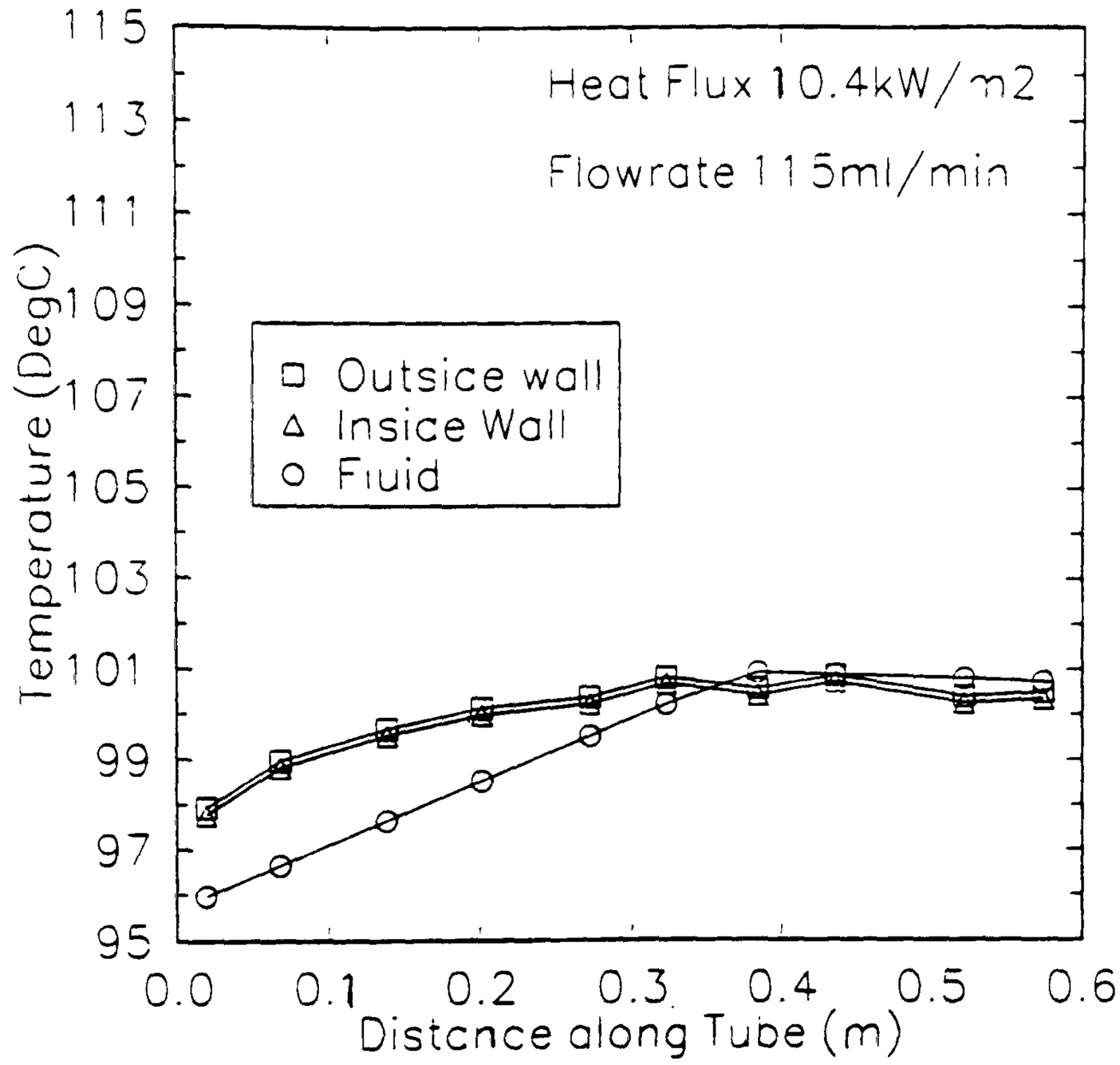

Figure 3.35 Sample Result showing Temperature Profiles along Test Section (Low Heat Flux, 2.87 mm ϕ, Water)

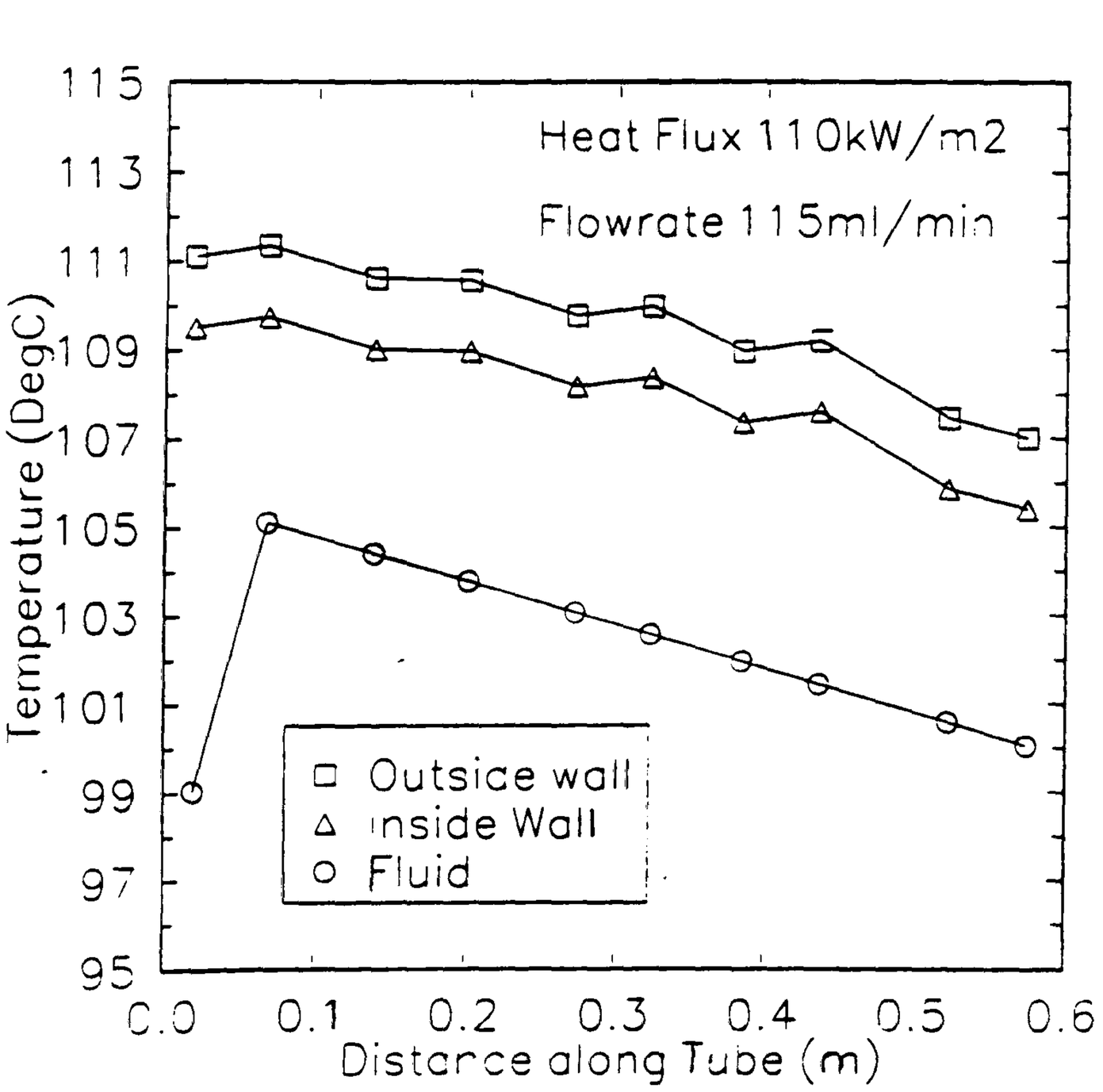

Figure 3.36 Sample Result showing Temperature Profiles along Test Section (High Heat Flux, 2.87 mm ϕ, Water)

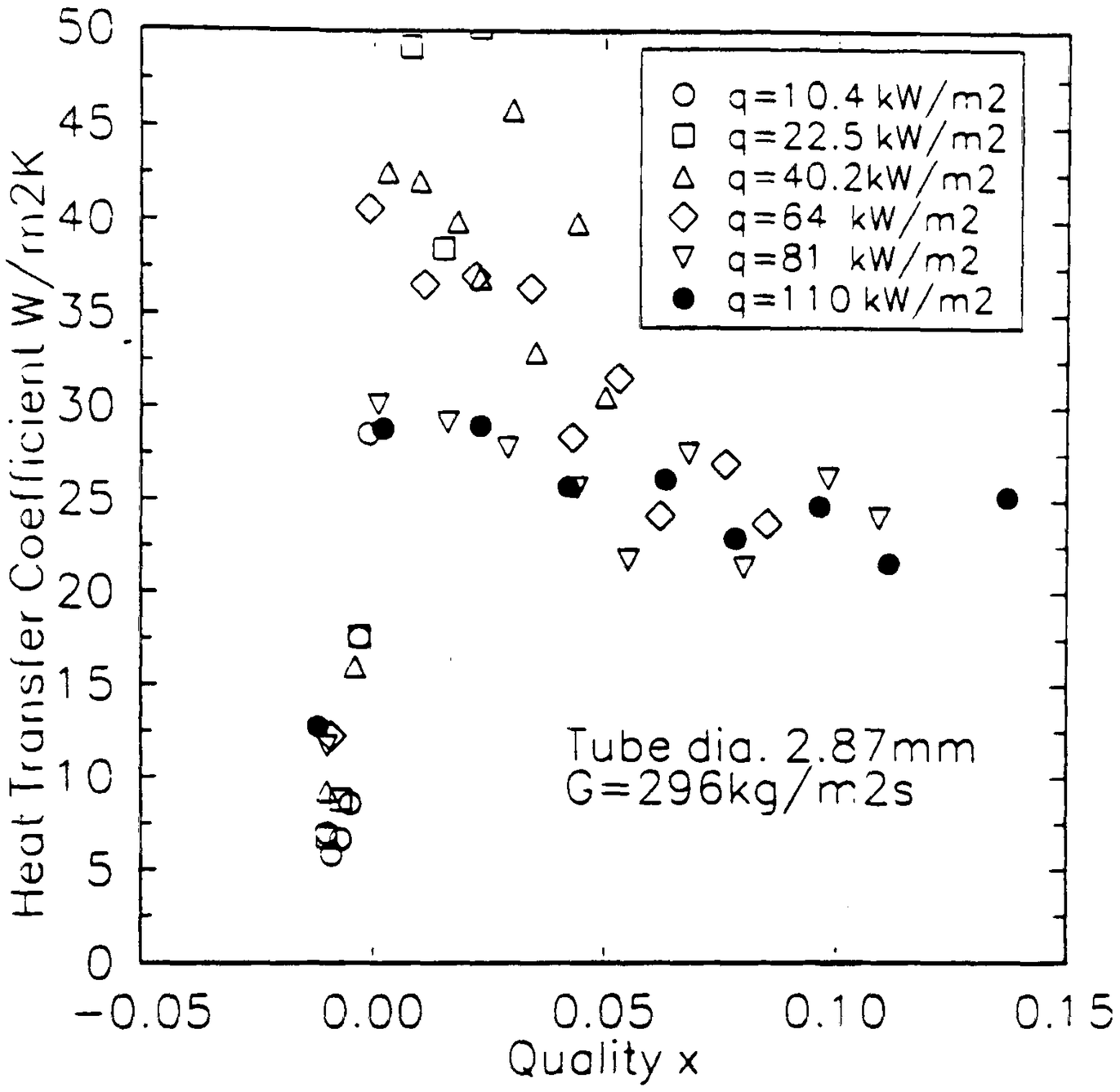

Figure 3.37 Variation of Measured Heat Transfer Coefficient (2.87 mm ϕ - Water)

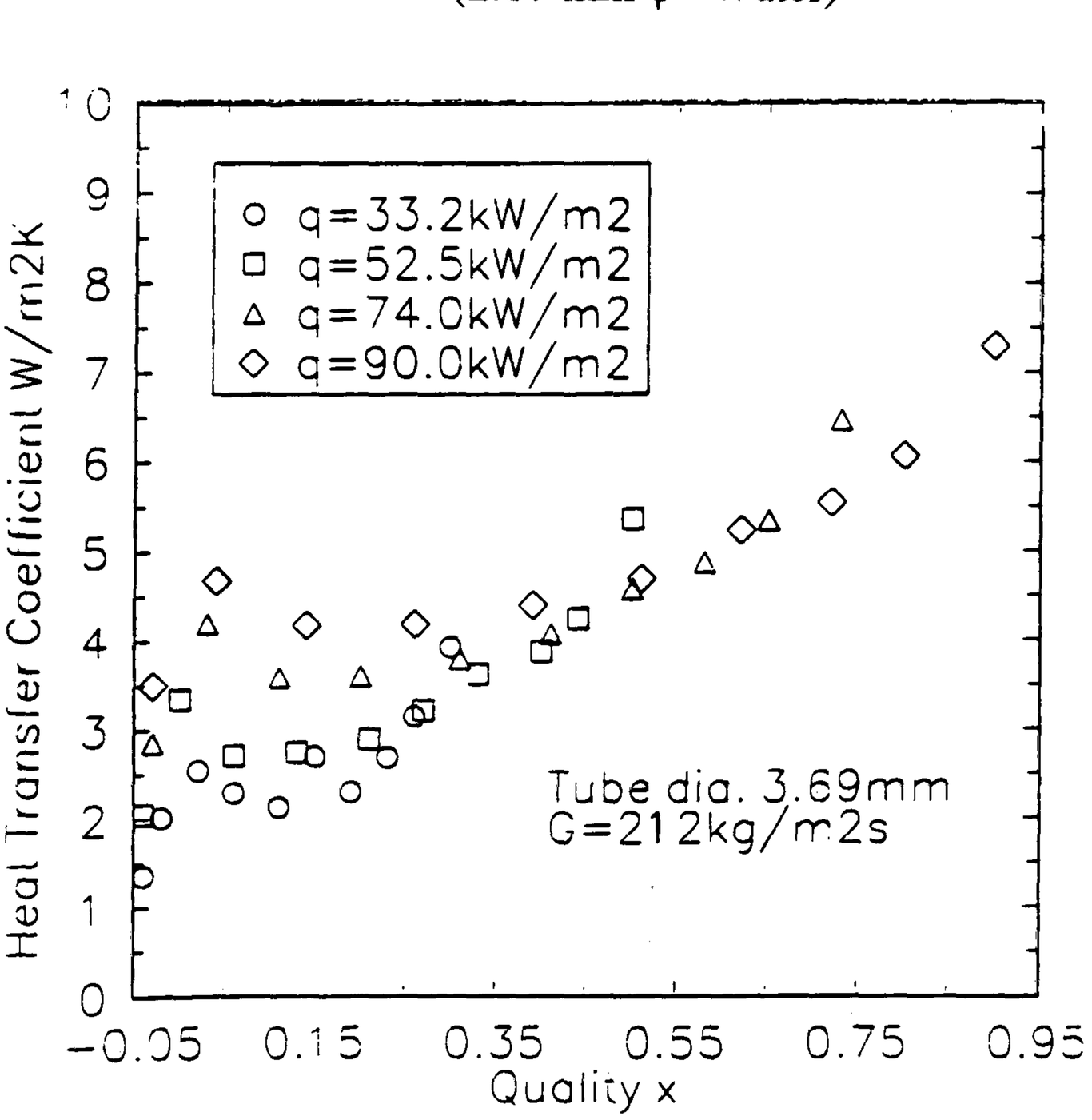

Figure 3.38 Variation of Heat Transfer Coefficient with Quality (3.69 mm ϕ - R141b)

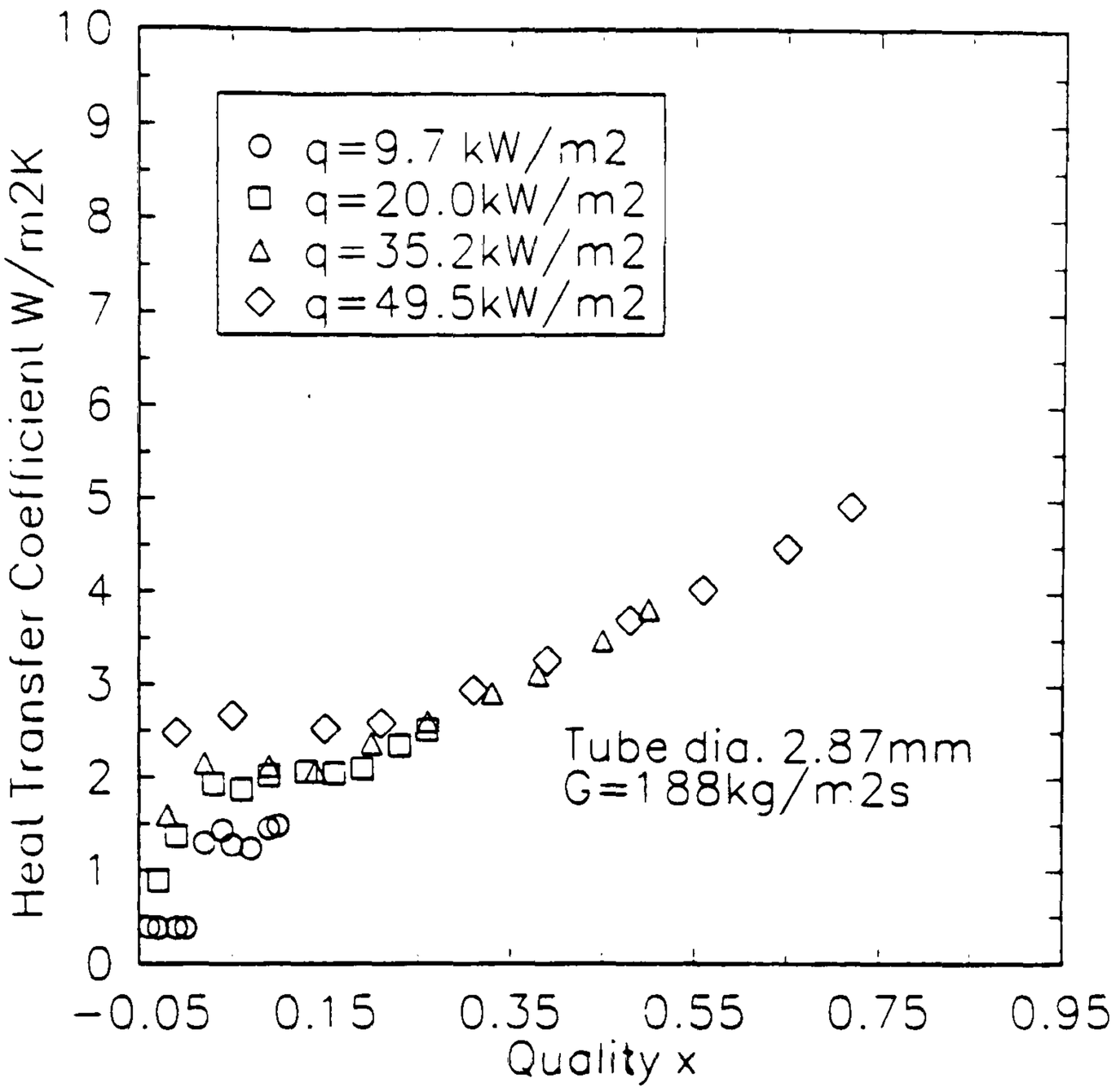

Figure 3.39 Variation of Heat Transfer Coefficient with Quality (2.87 mm ϕ - R141b)

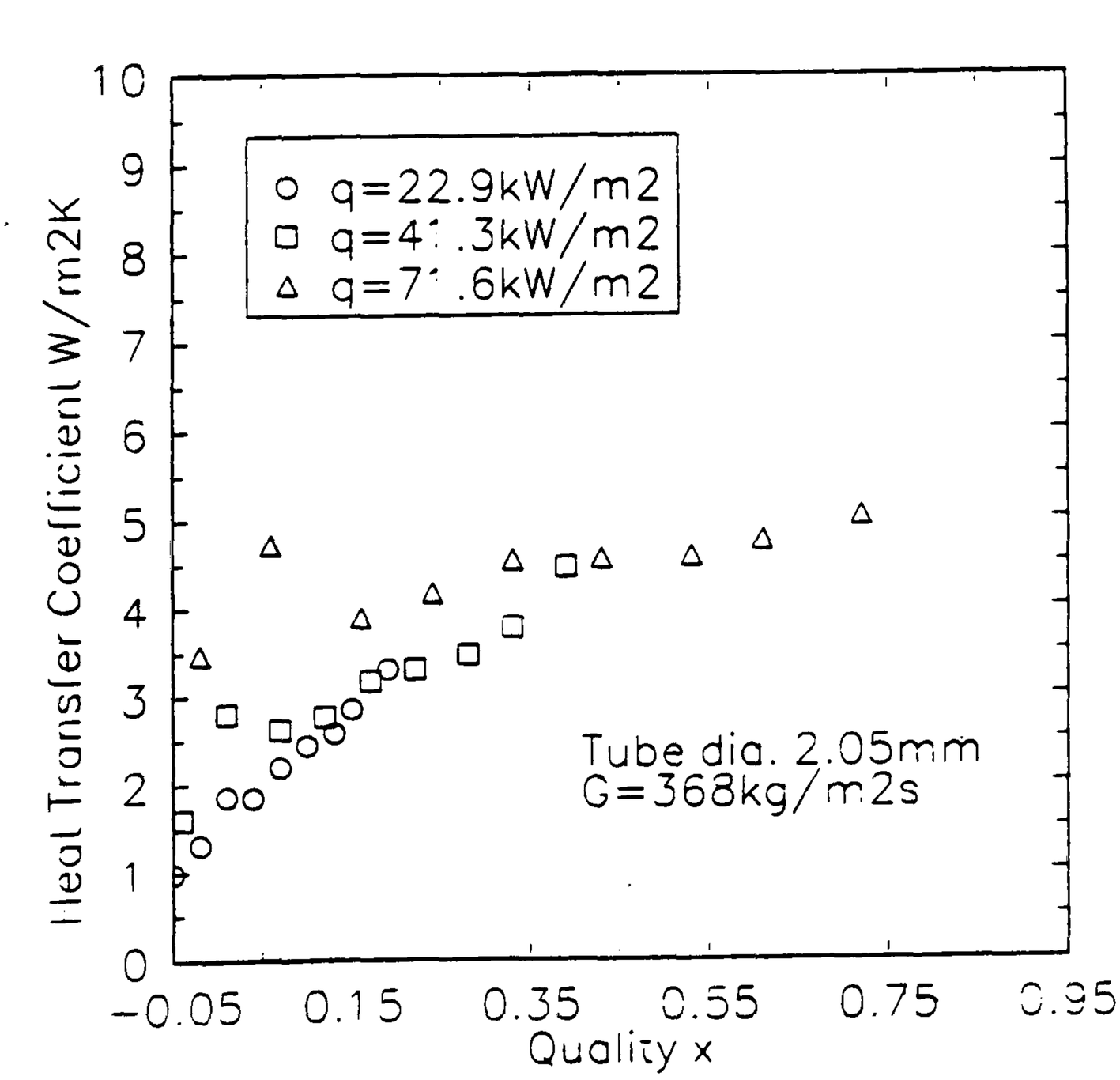

Figure 3.40 Variation of Heat Transfer Coefficient with Quality (2.05mmϕ - R141b)

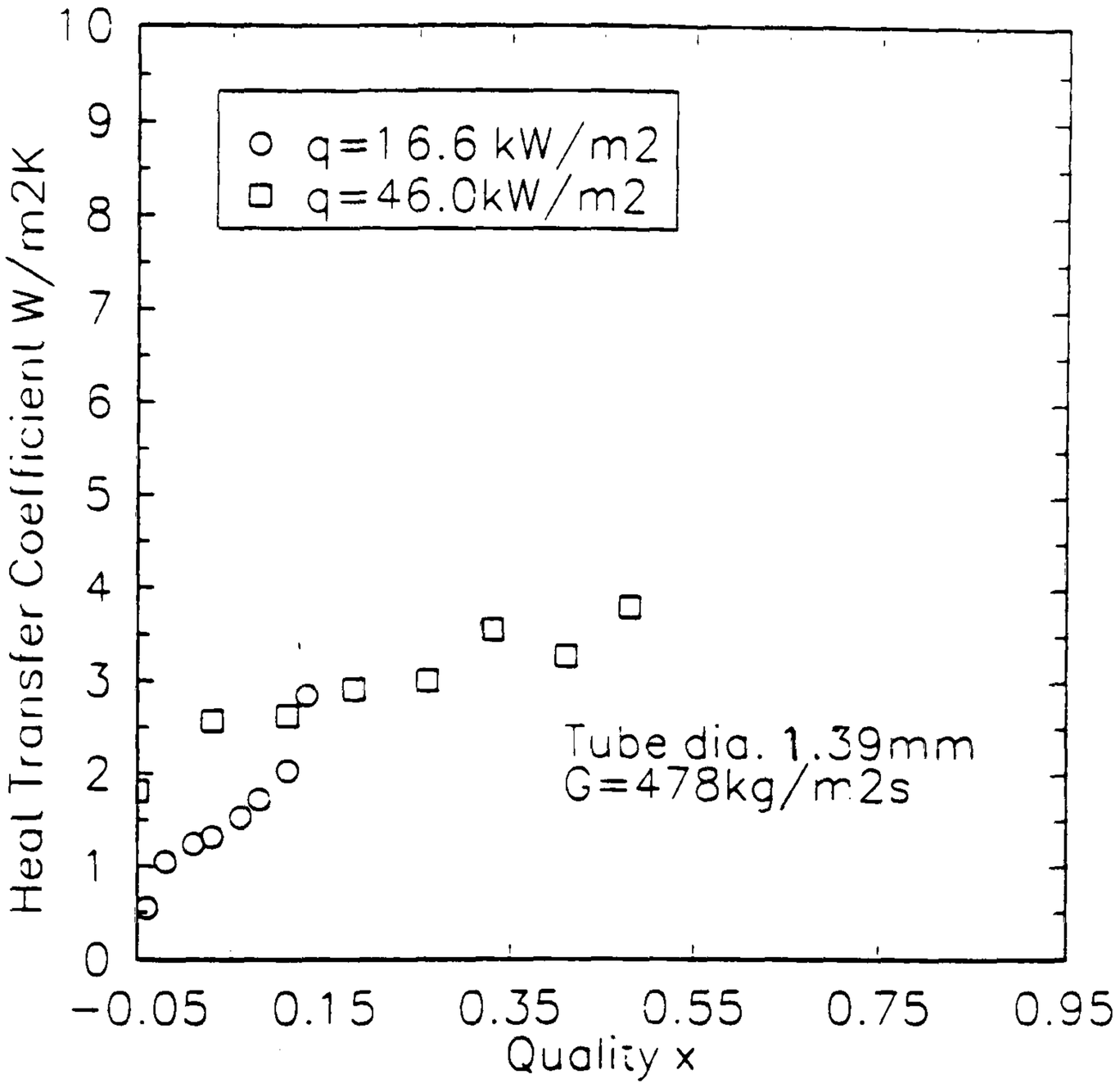

(a) Moderate mass flux

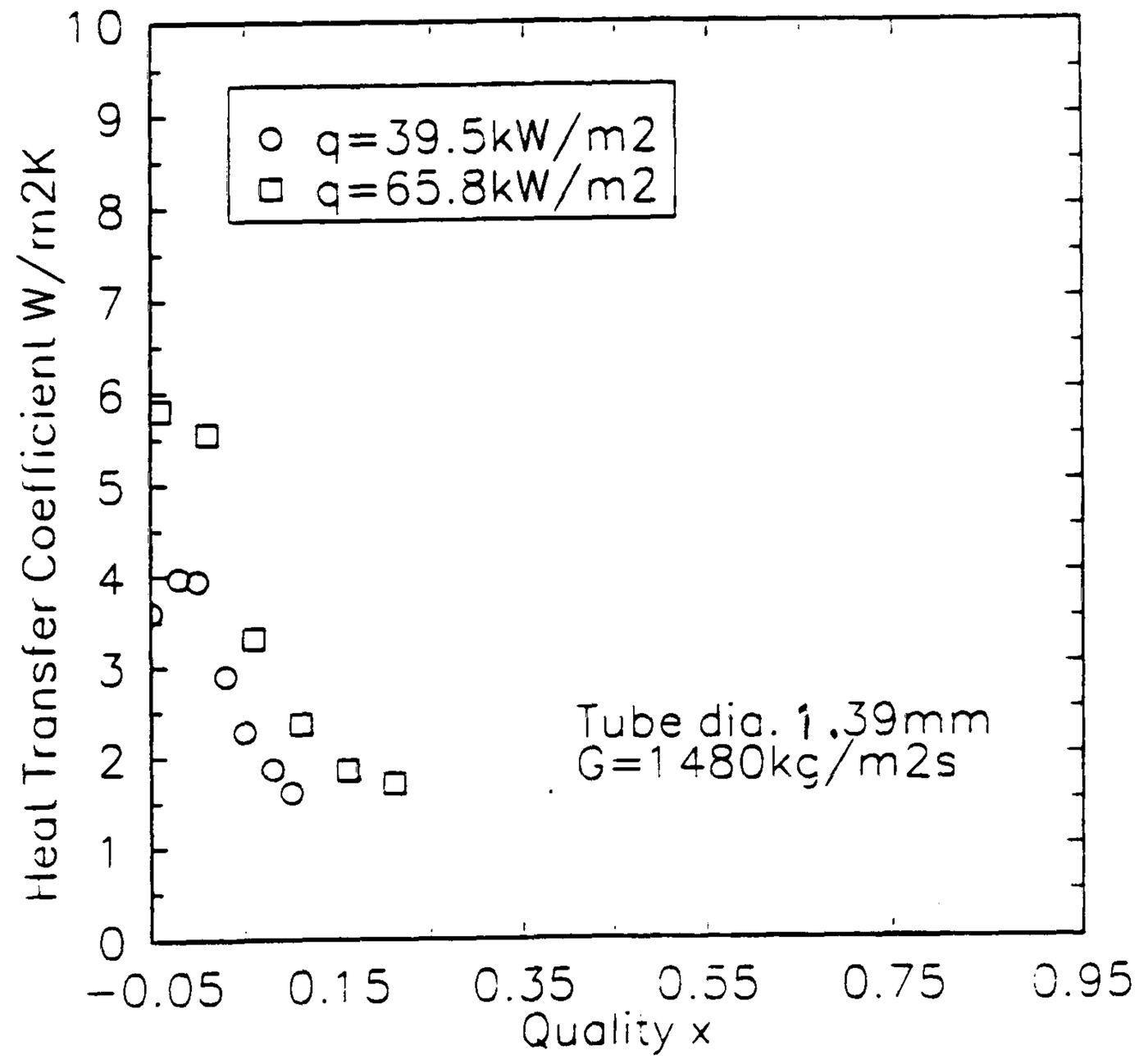

(b) High mass flux

Figure 3.41 Variation of Heat Transfer Coefficient with Quality (1.39 mm ϕ - R141b)

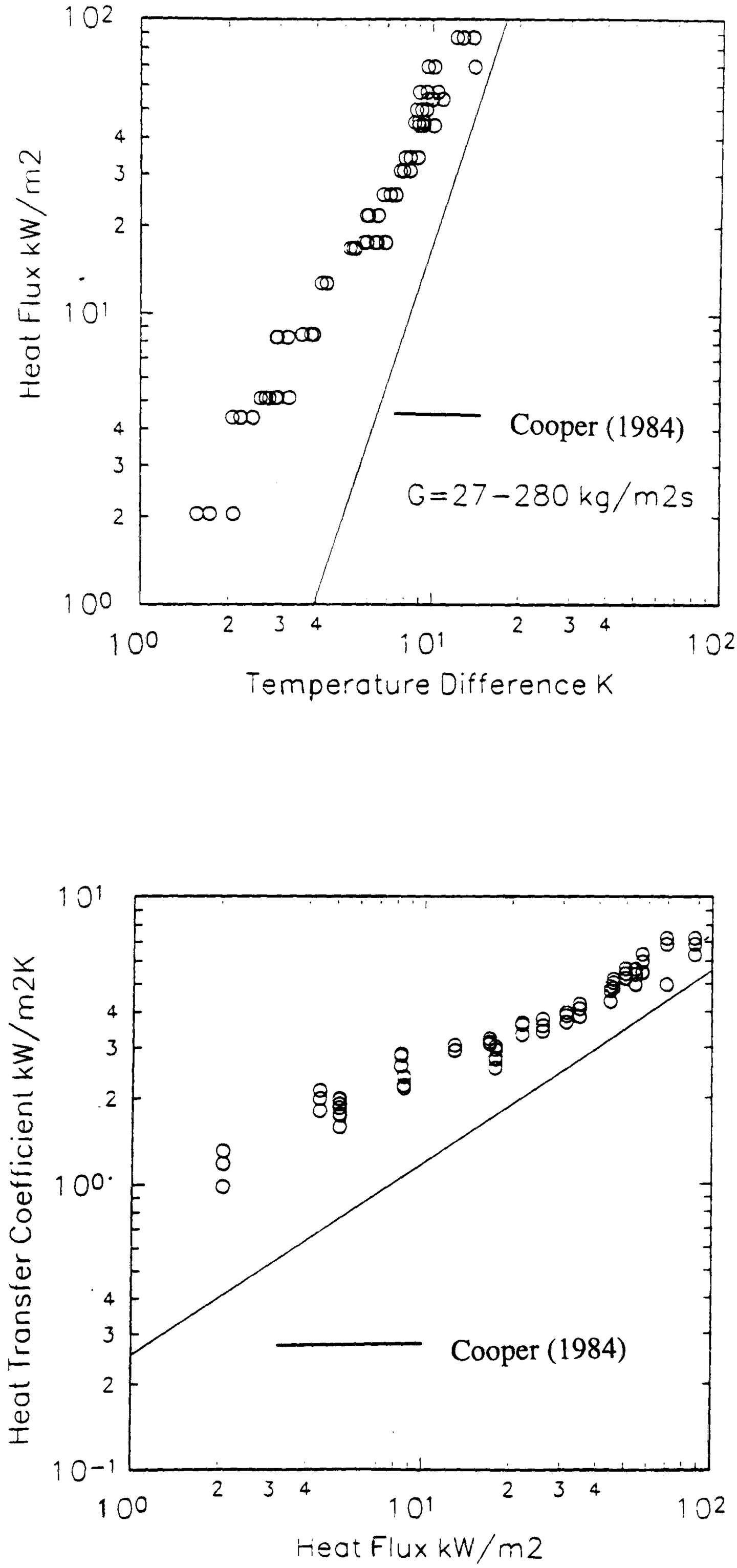

Figure 3.42 Heat Transfer Results
Flat Plate, 1.125 mm gap, 1 bar No Splitter, R141b

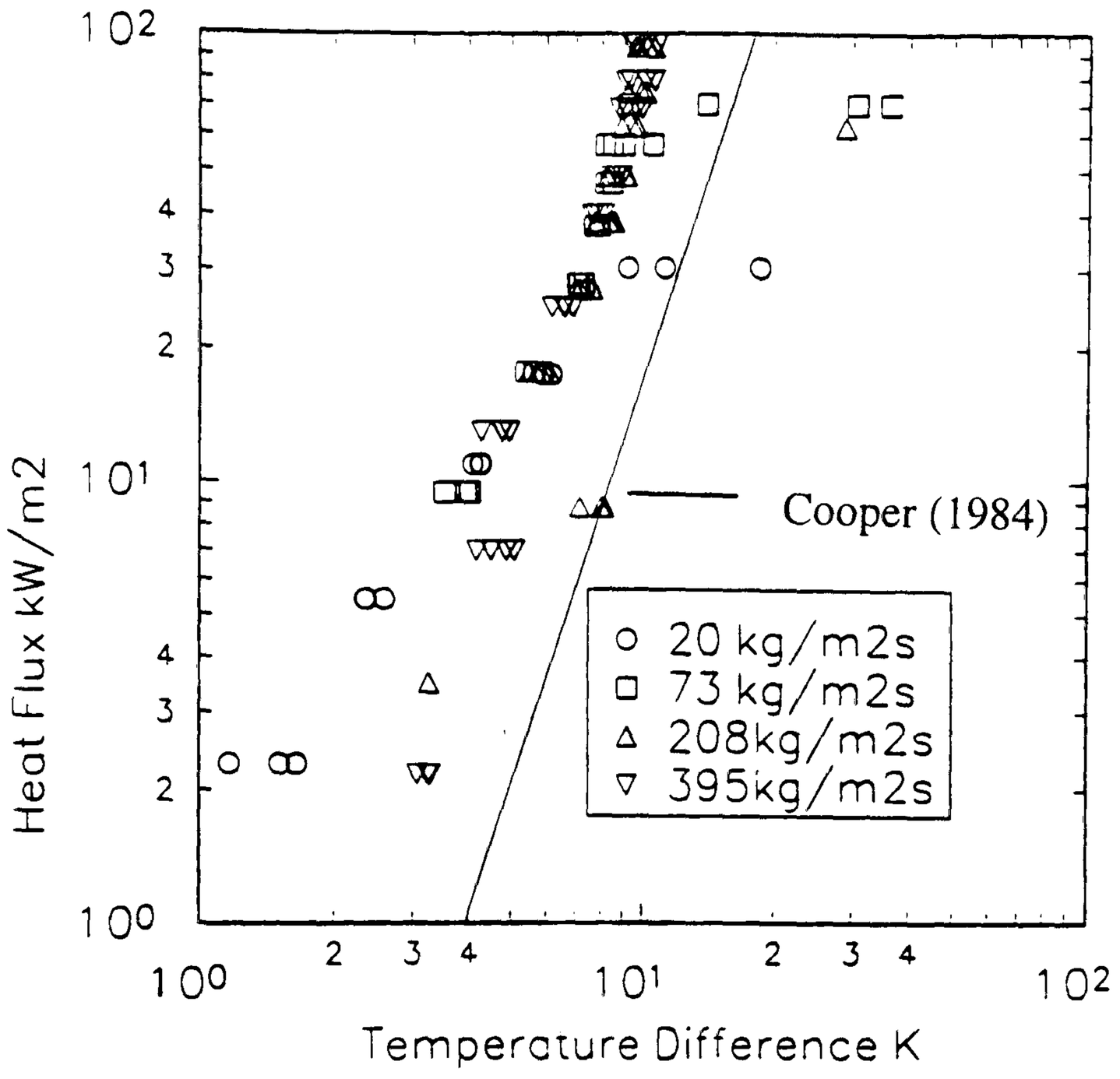

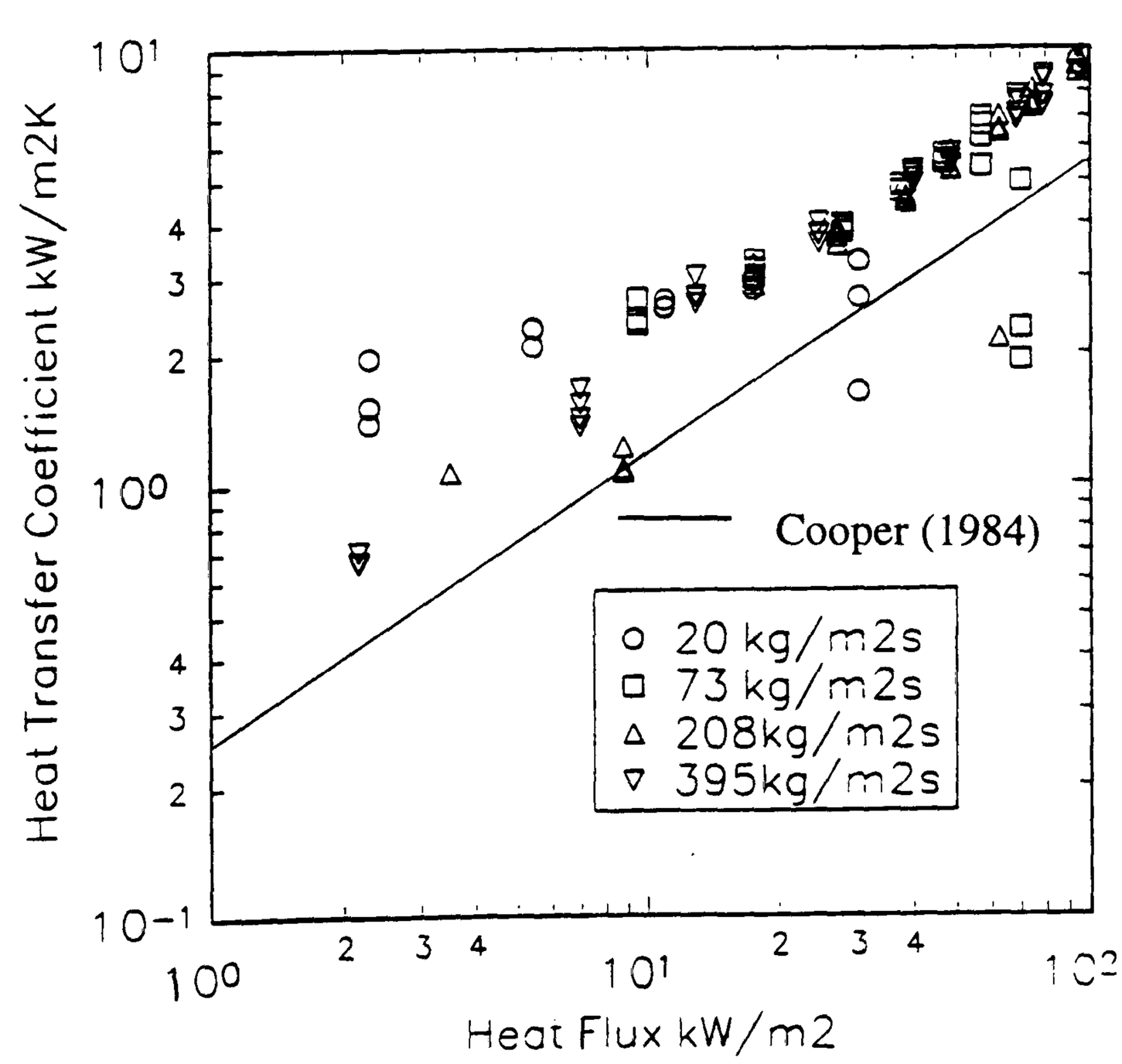

Figure 3.43 **Heat Transfer Results**
Flat Plate, 1.125 mm gap, 1 bar 1 Splitter, R141b

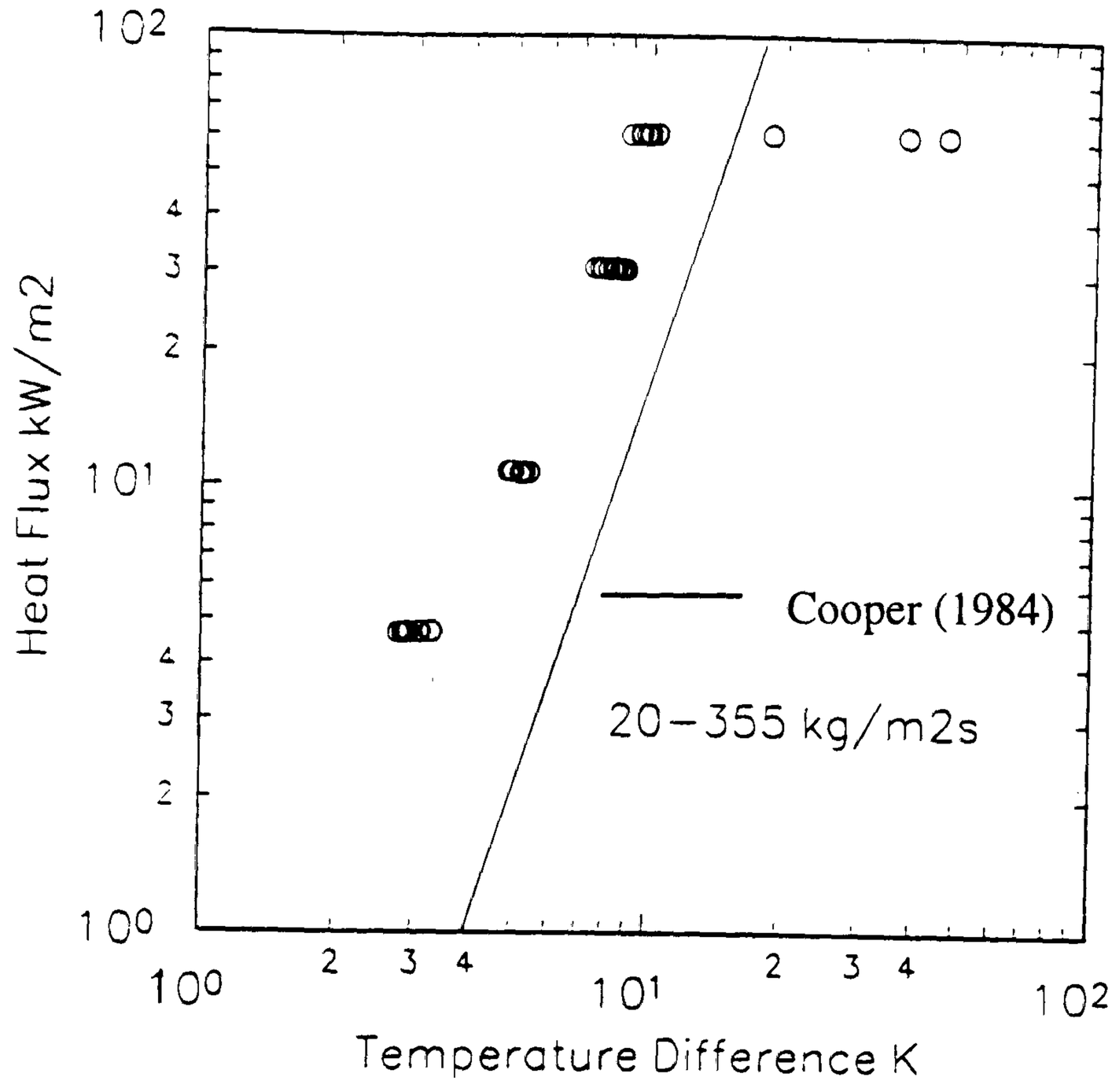

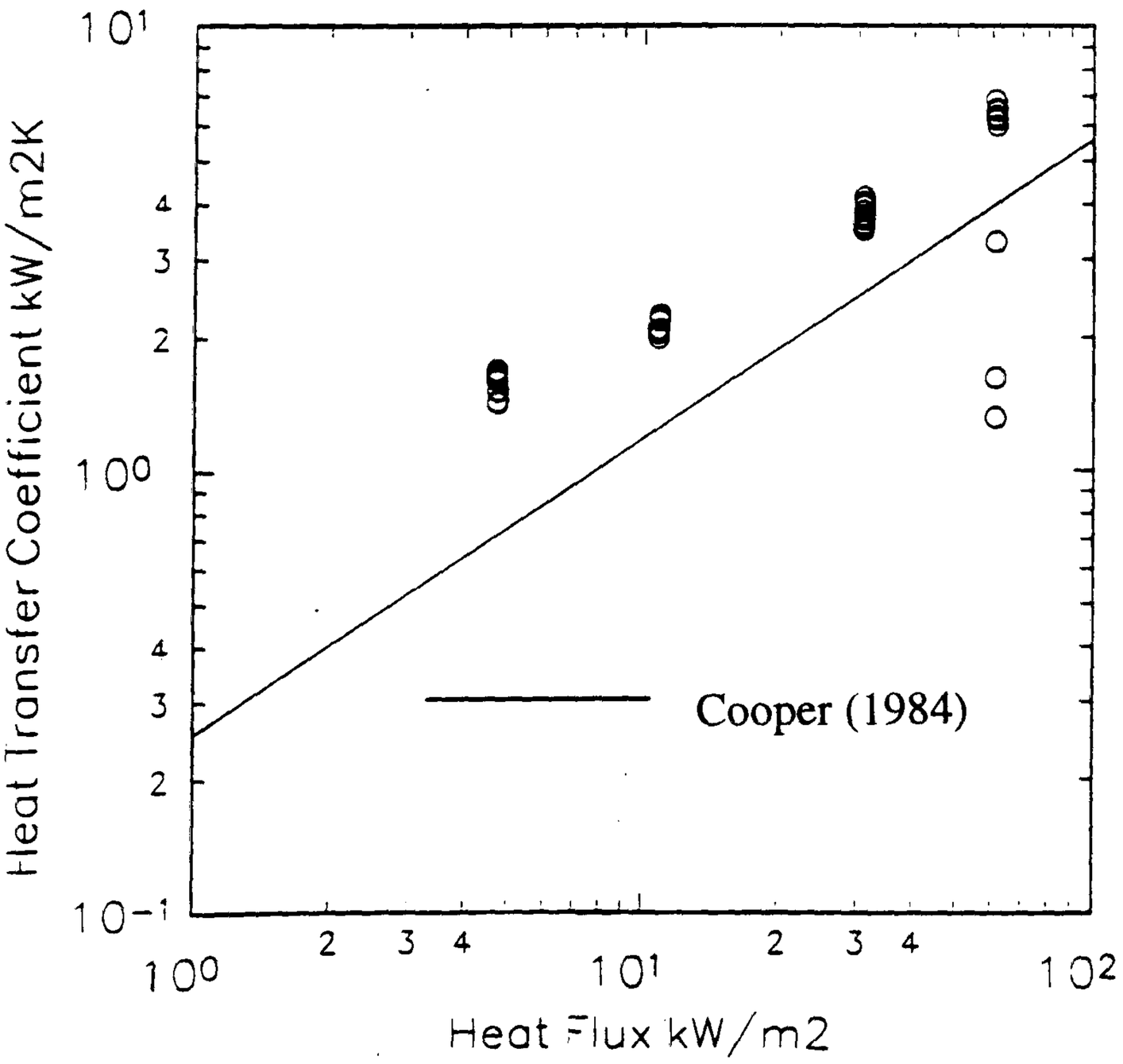

Figure 3.44 **Heat Transfer Results**
Flat Plate, 1.5 mm gap, 1 bar No Splitter, R141b

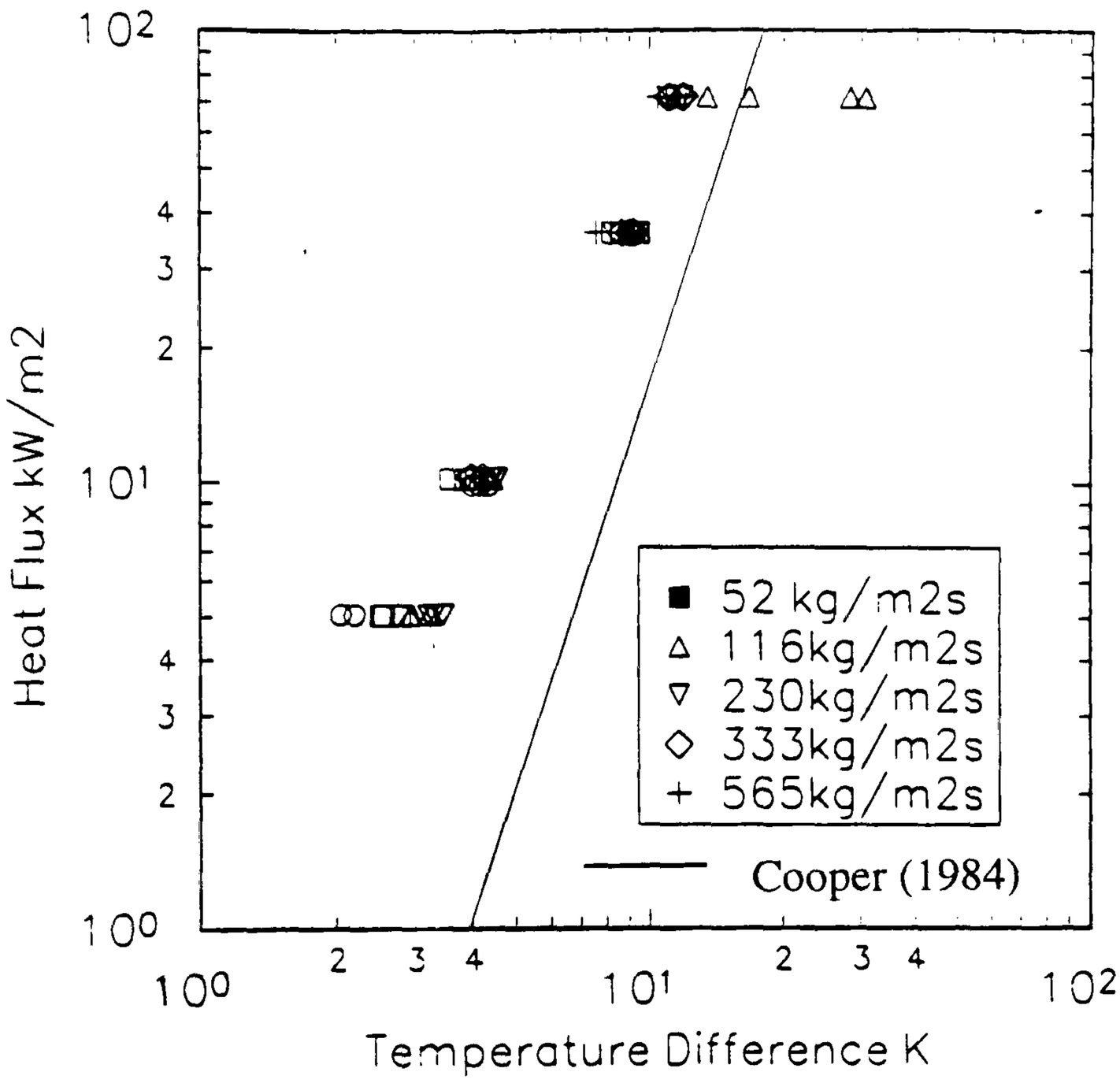

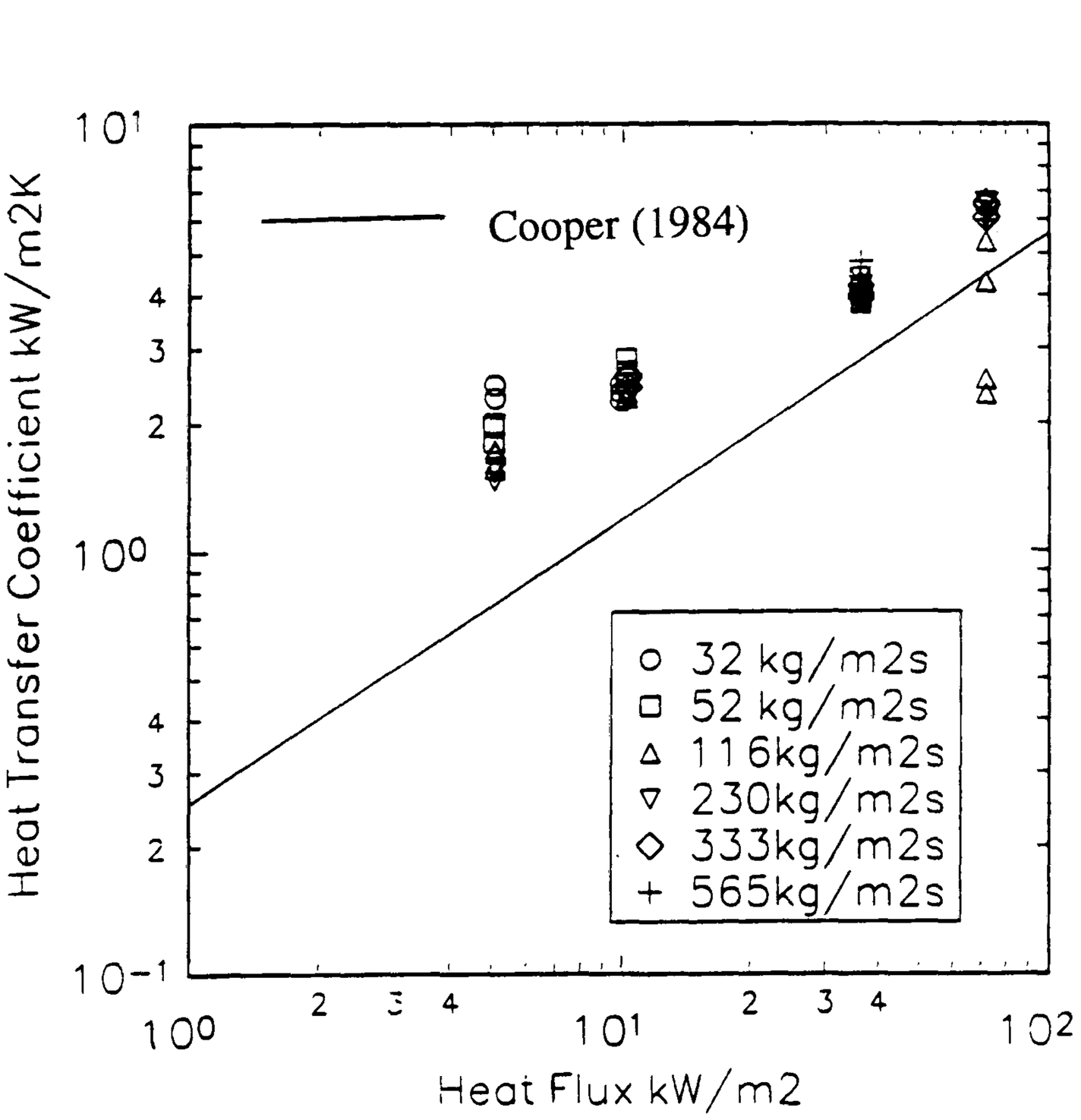

Figure 3.45 **Heat Transfer Results**
Flat Plate, 1.5 mm gap, 1 bar 2 Splitters, R141b

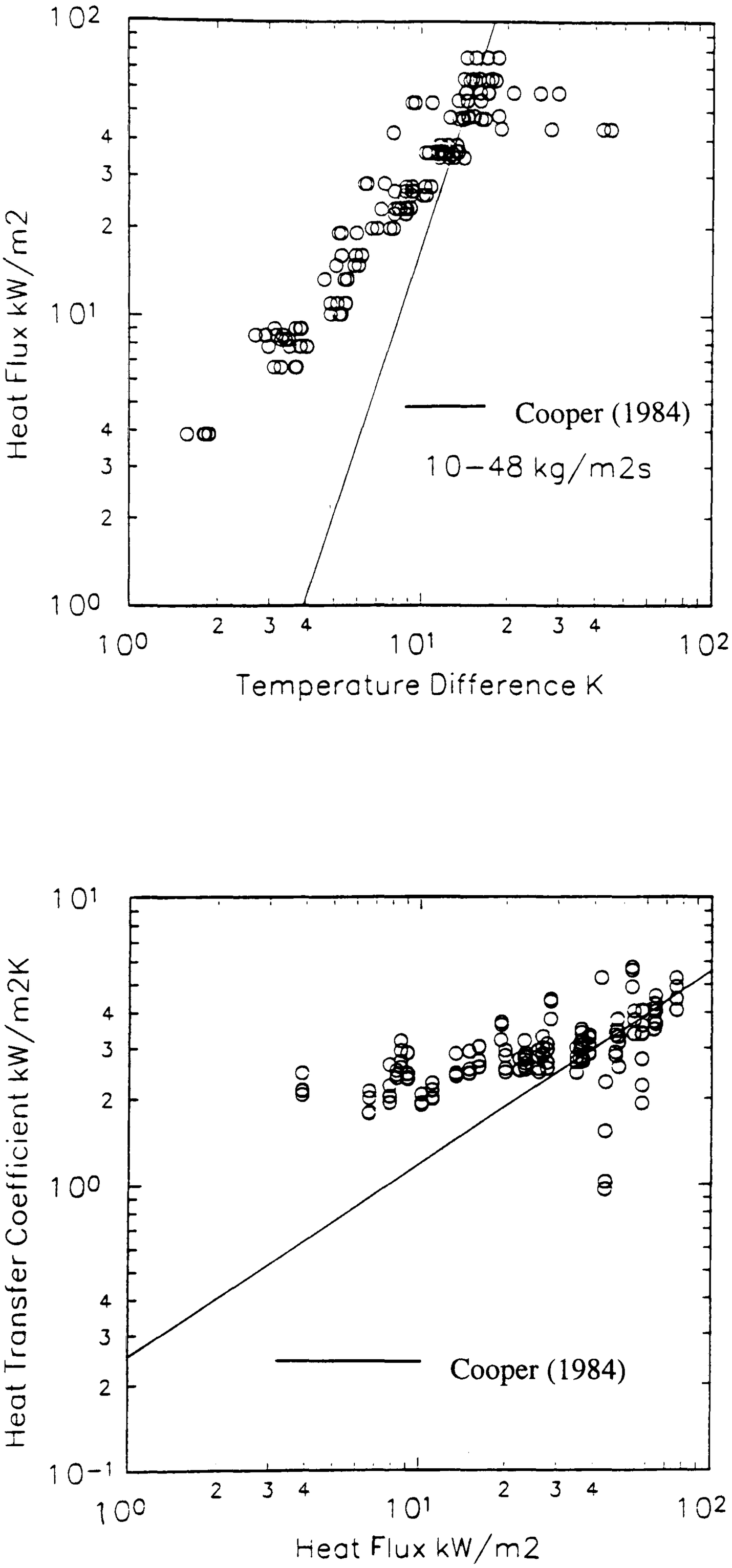

Figure 3.46 Heat Transfer Results
Flat Plate, 4.5 mm gap, 1 bar No Splitter, R141b

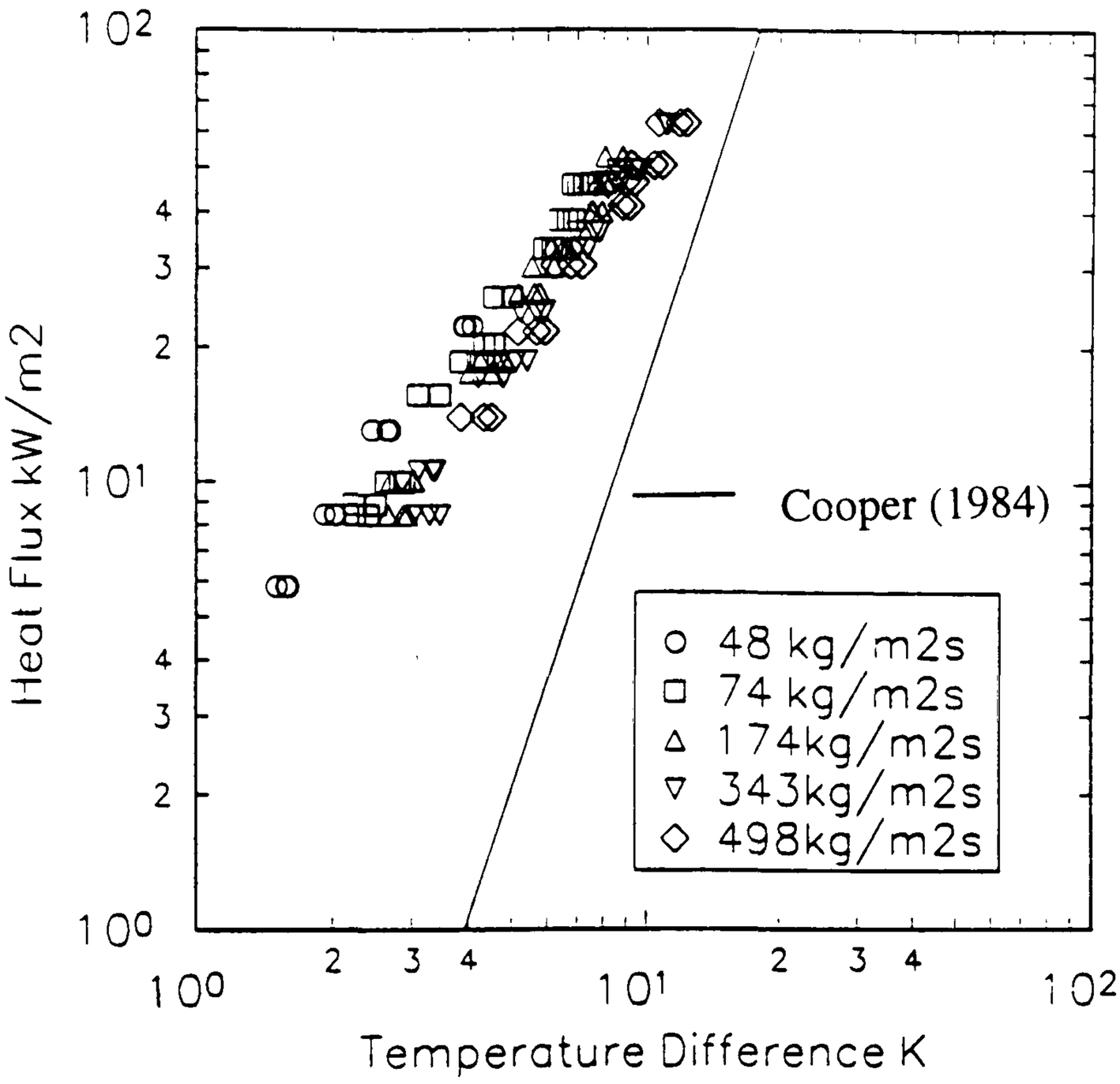

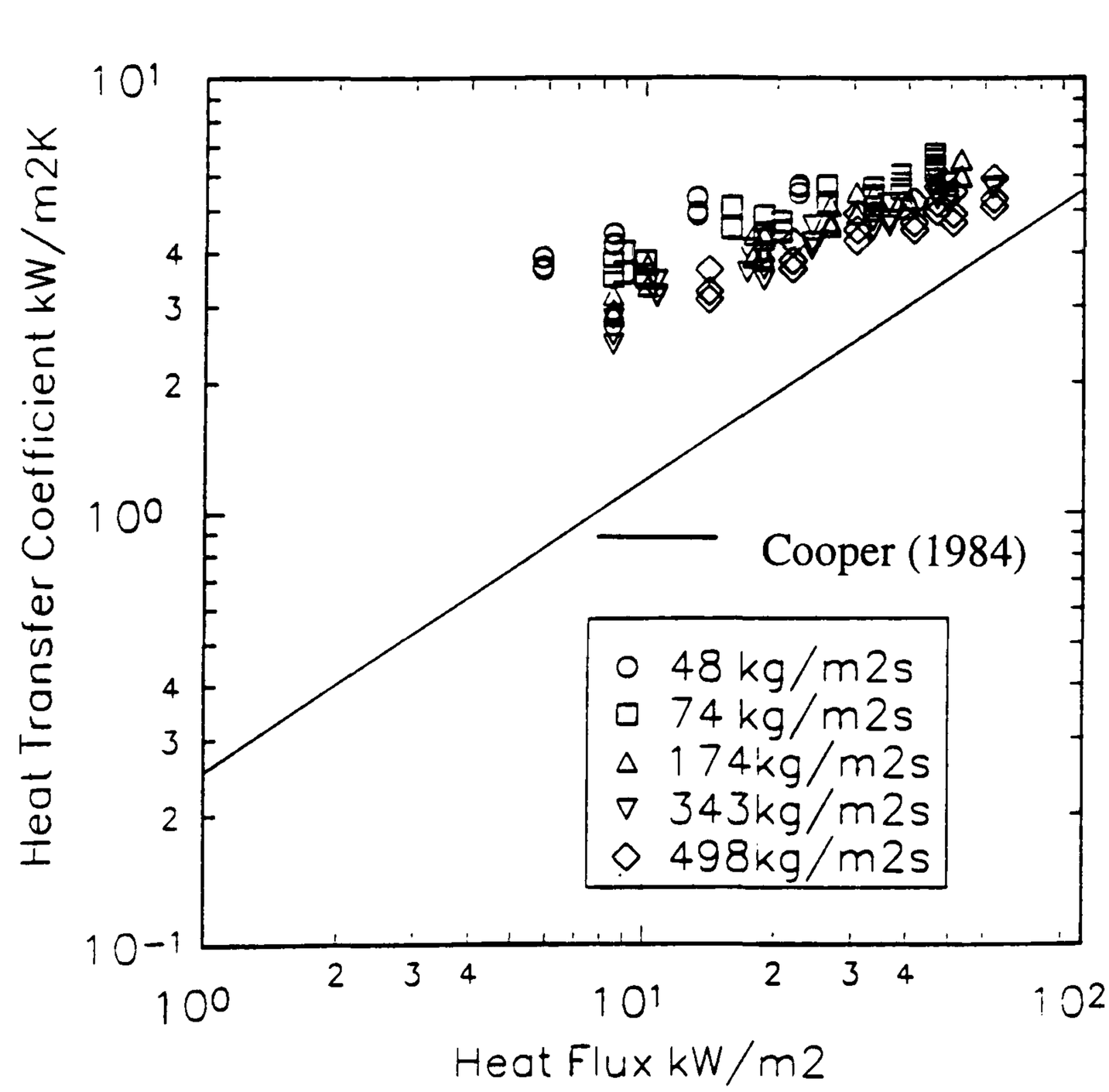

Figure 3.47 **Heat Transfer Results**
Multi-Channel, 2 mm □, 1 bar R141b

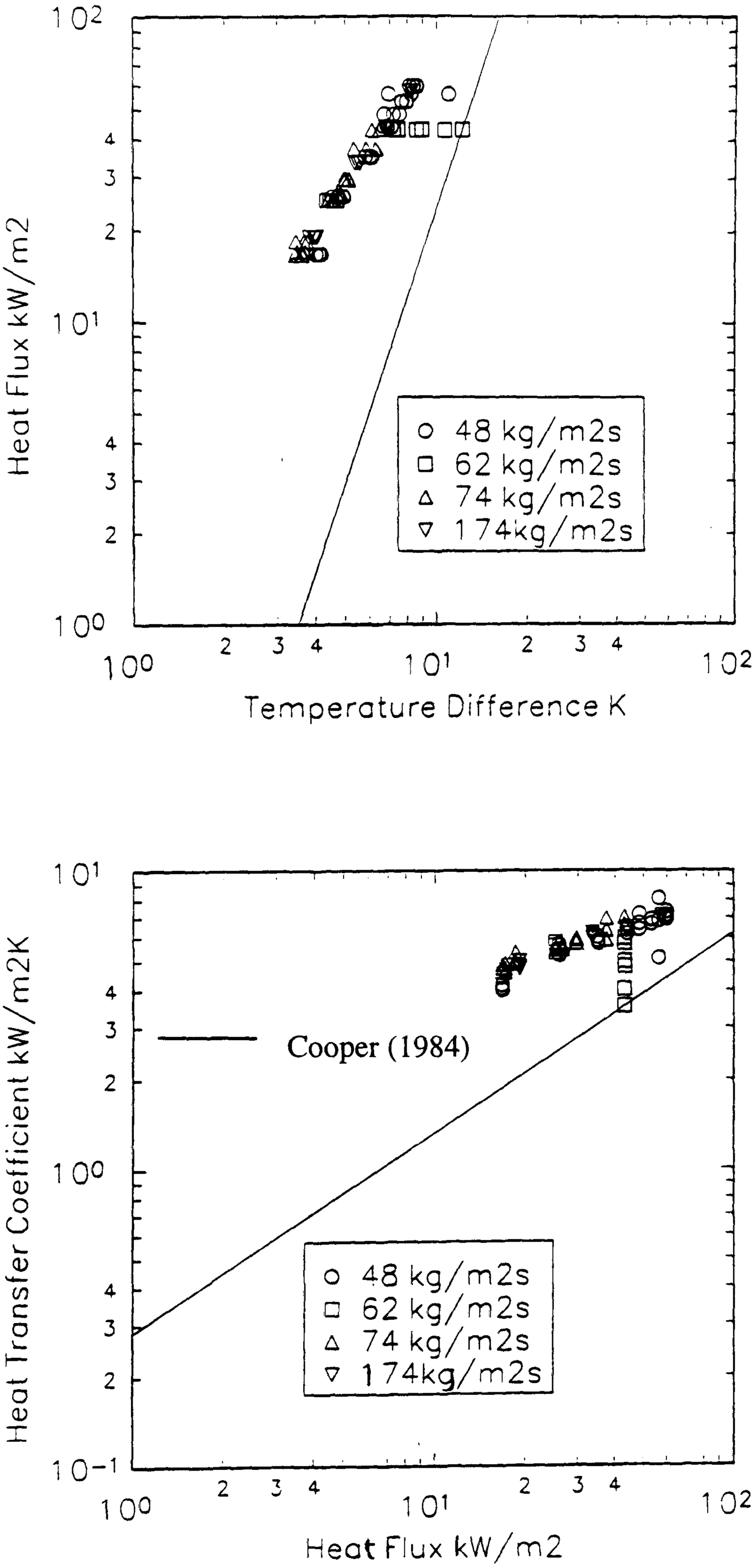

Figure 3.48 **Heat Transfer Results**
Multi-Channel, 2 mm □, 1.5 bar R141b

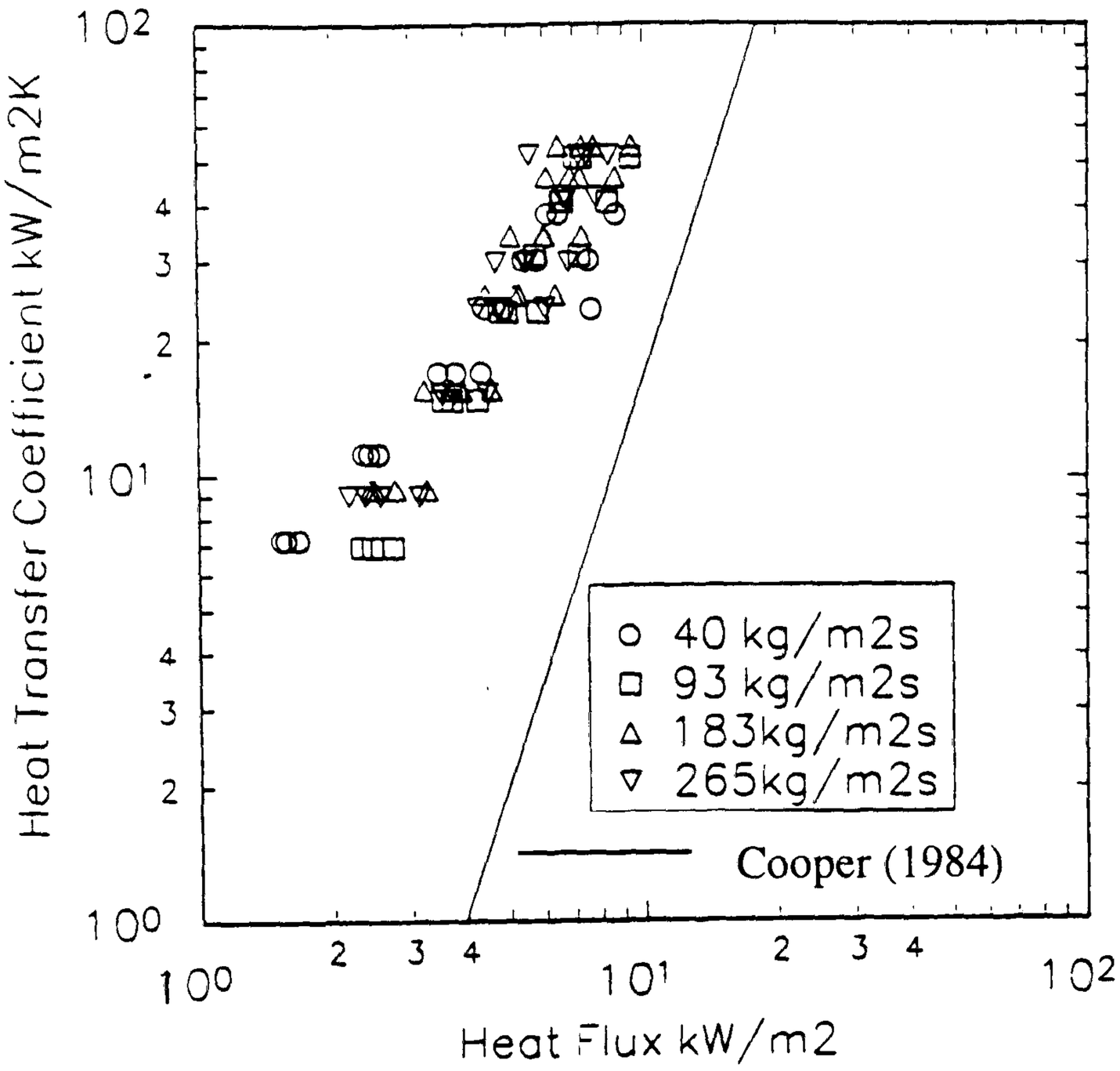

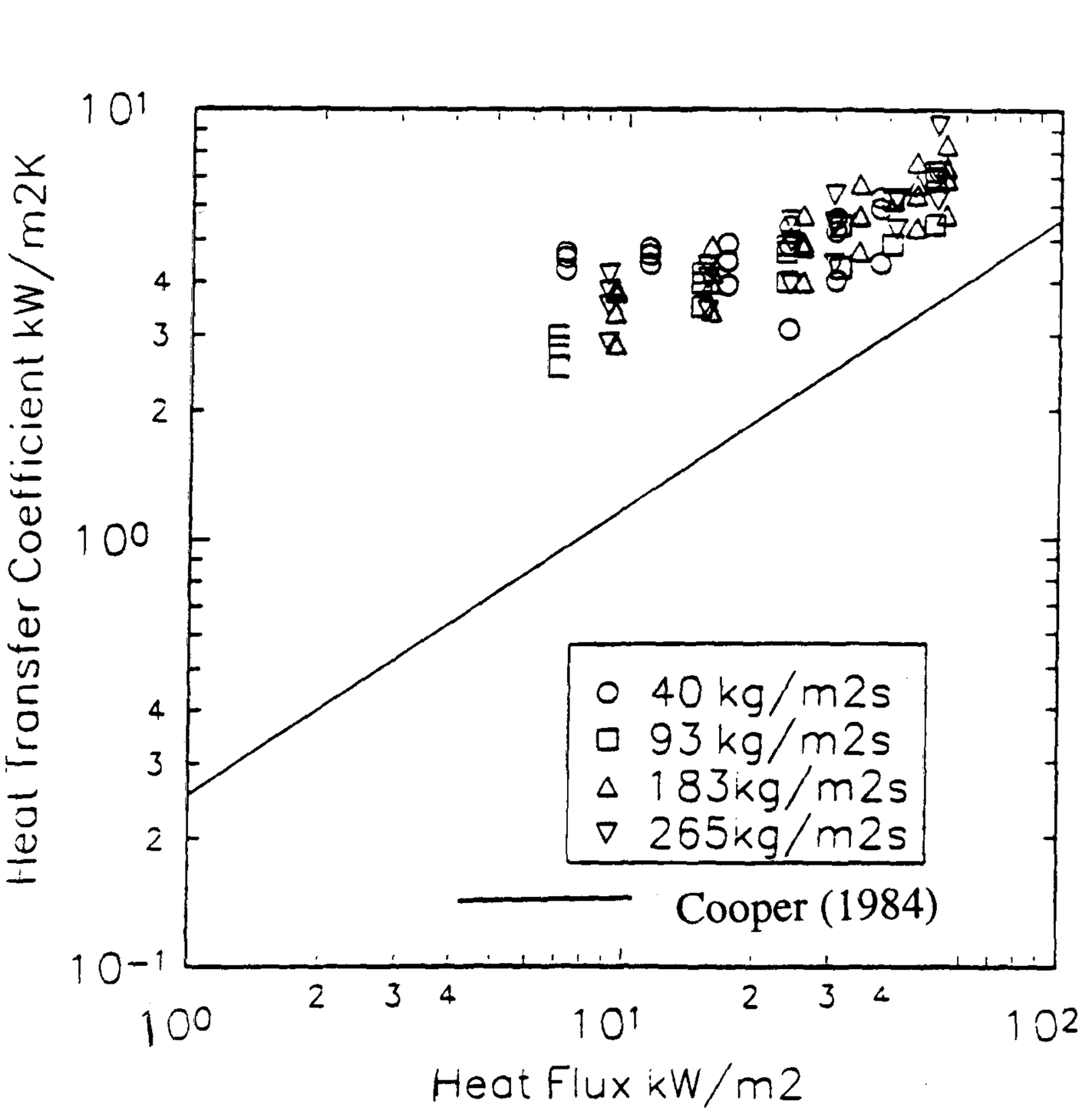

Figure 3.49 **Heat Transfer Results**
Multi-Channel, 3 mm □, 1 bar R141b

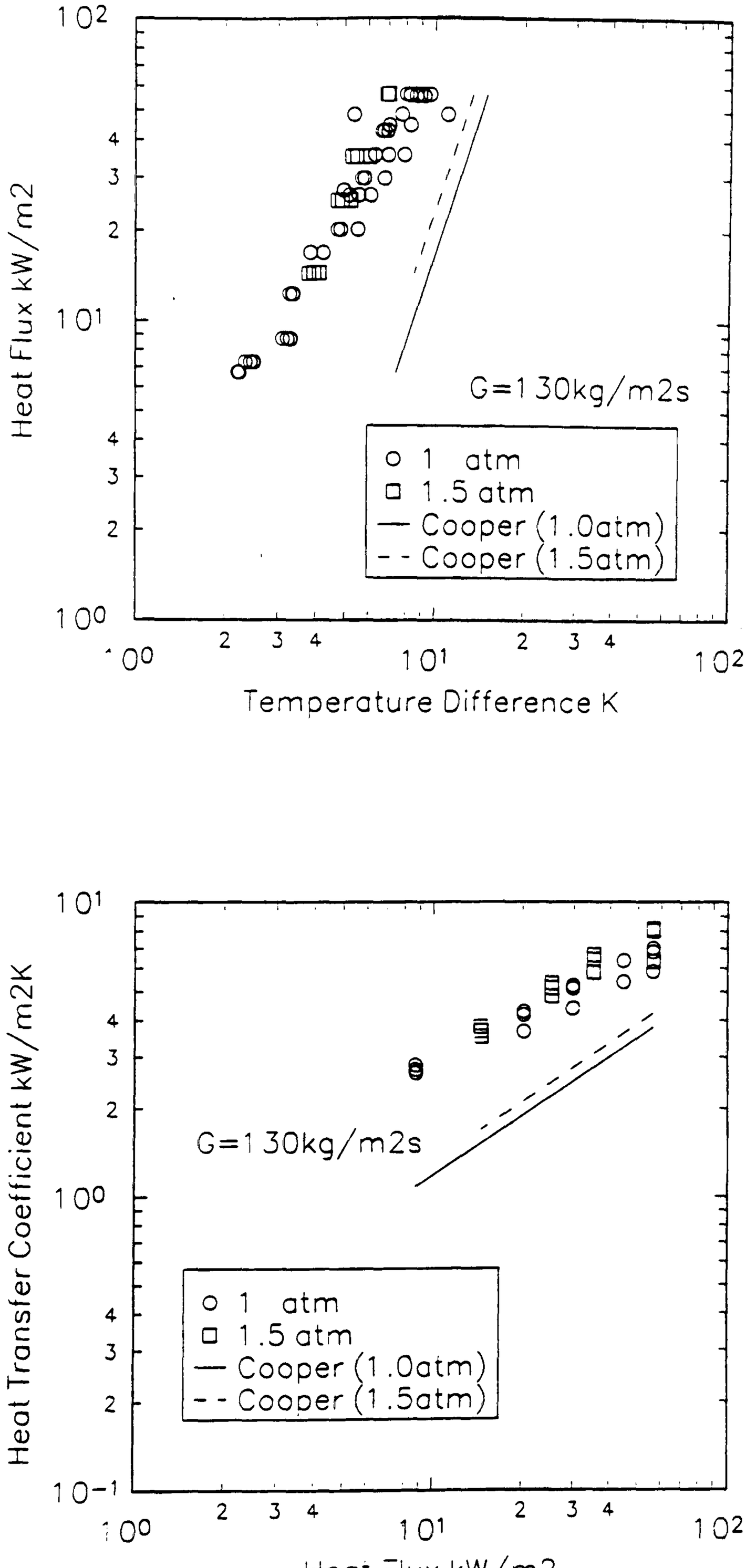

Figure 3.50 Heat Transfer Results
Multi-Channel, 3 mm □, 1 and 1.5 bar R141b

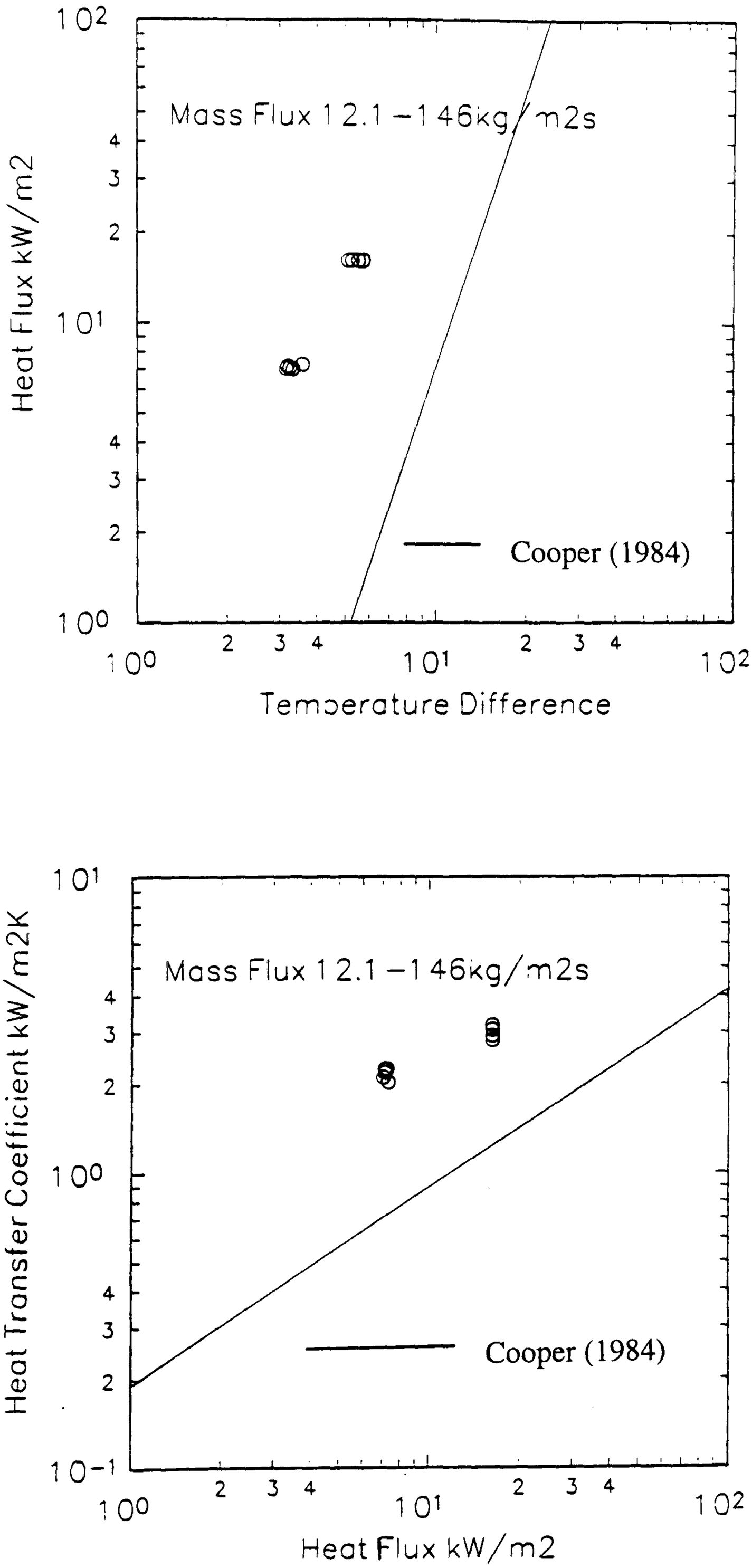

Figure 3.51 Heat Transfer Results
Flat Plate, 1.5 mm gap, 1 bar No Splitter, PP1

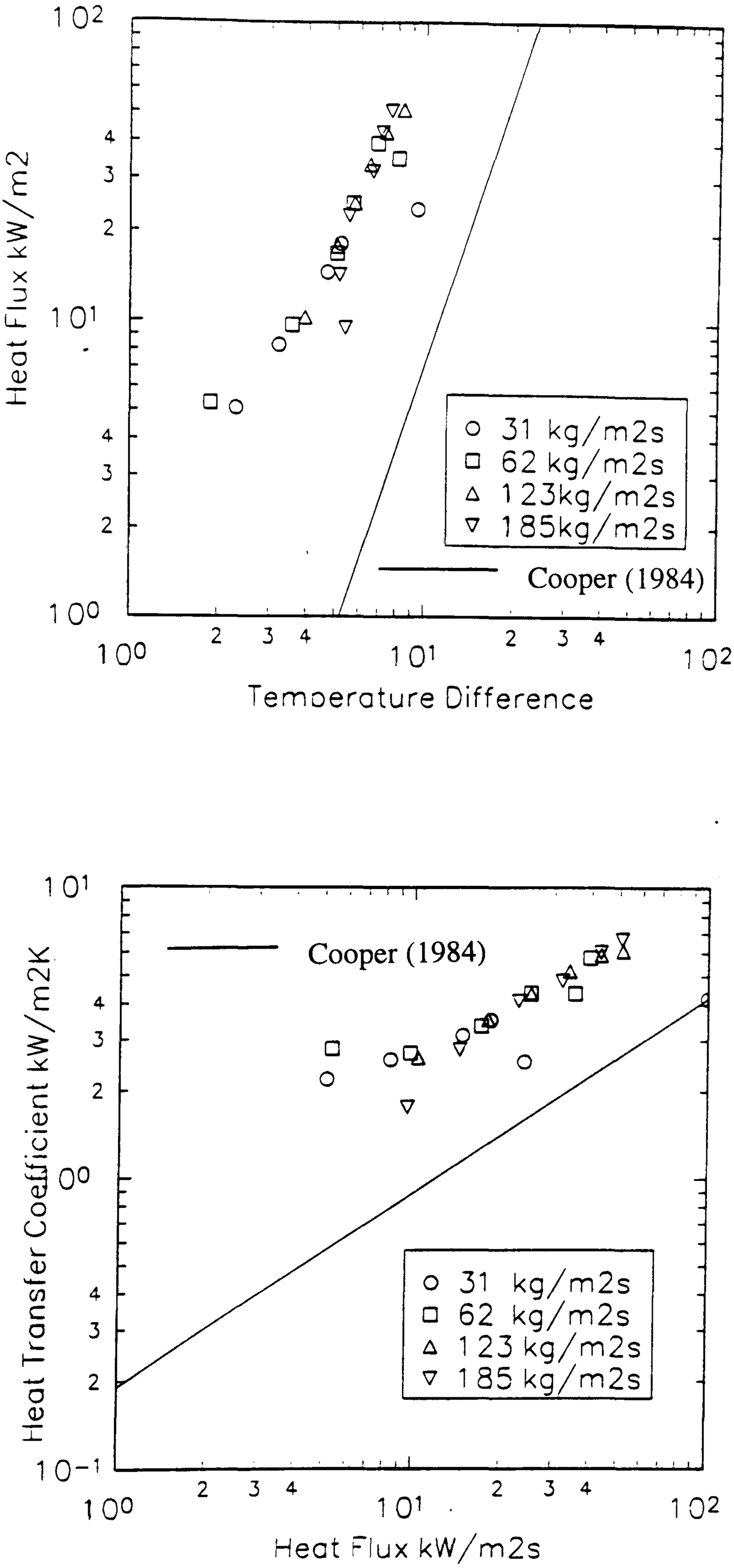

Figure 3.52 Heat Transfer Results
Multi-Channel, 3 mm □, 1 bar PP1

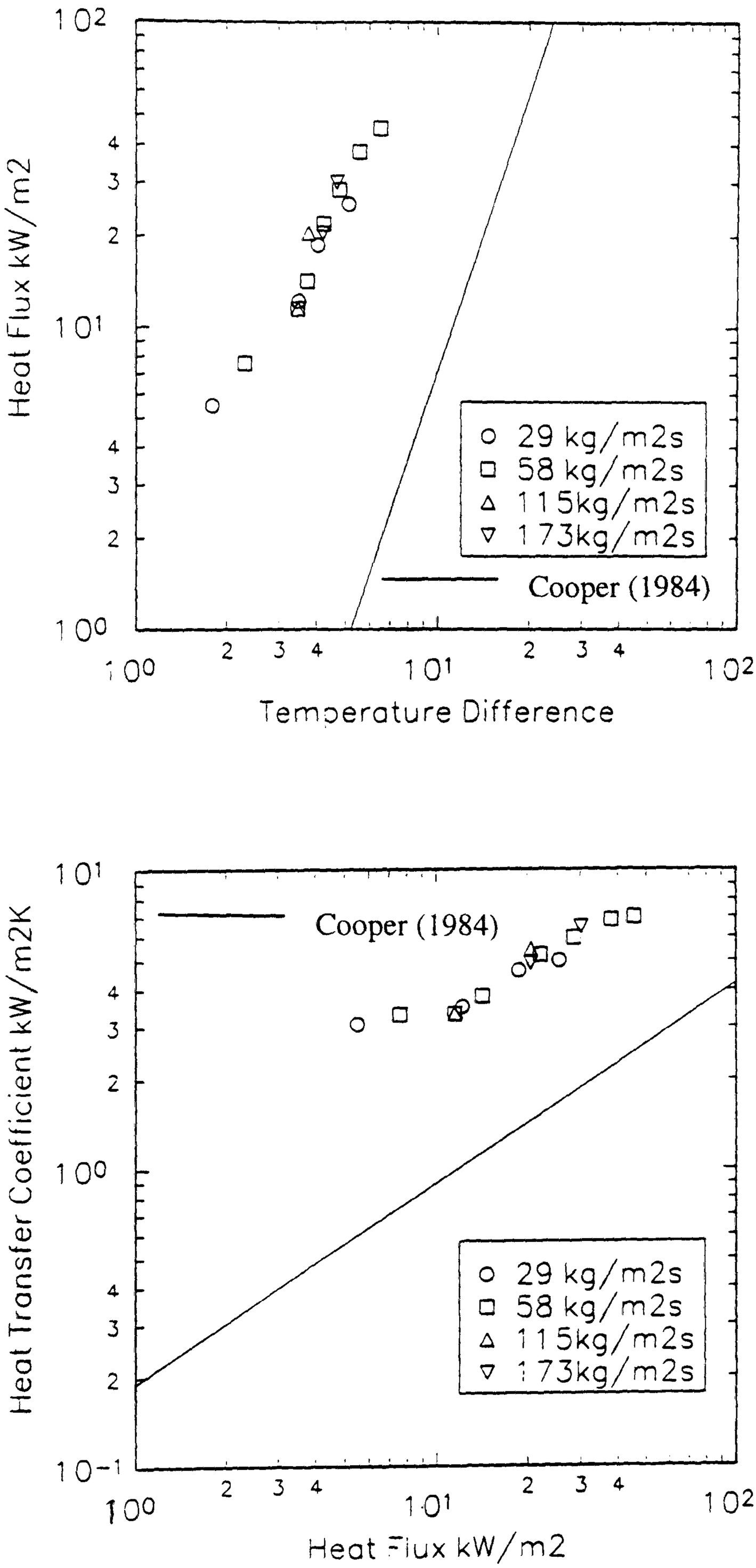

Figure 3.53 Heat Transfer Results
Multi-Channel, 4 mm □, 1 bar PP1

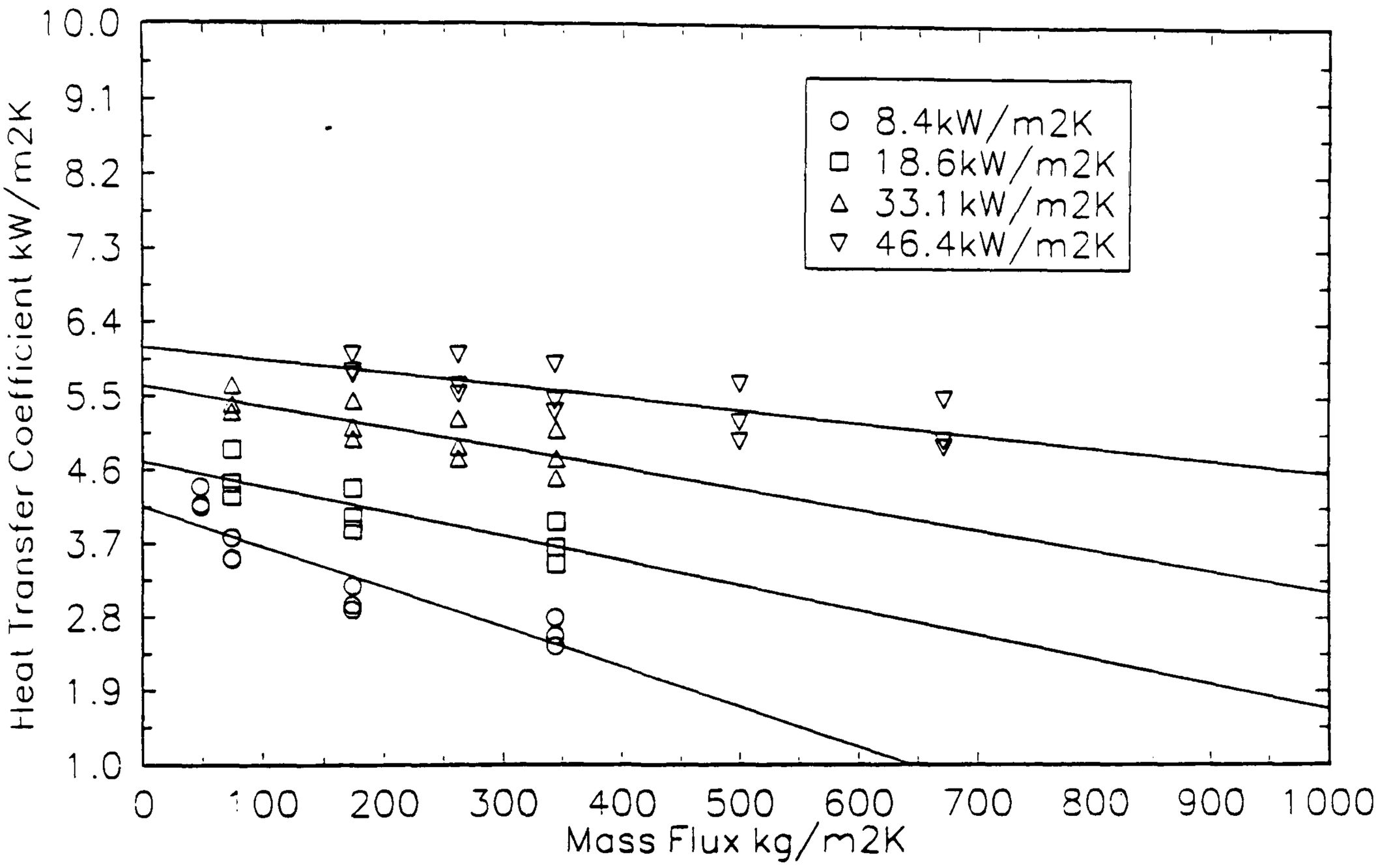

Figure 3.54 Influence of Mass Flux on Heat Transfer Coefficient
(Multi-channel,2mm □, R141b)

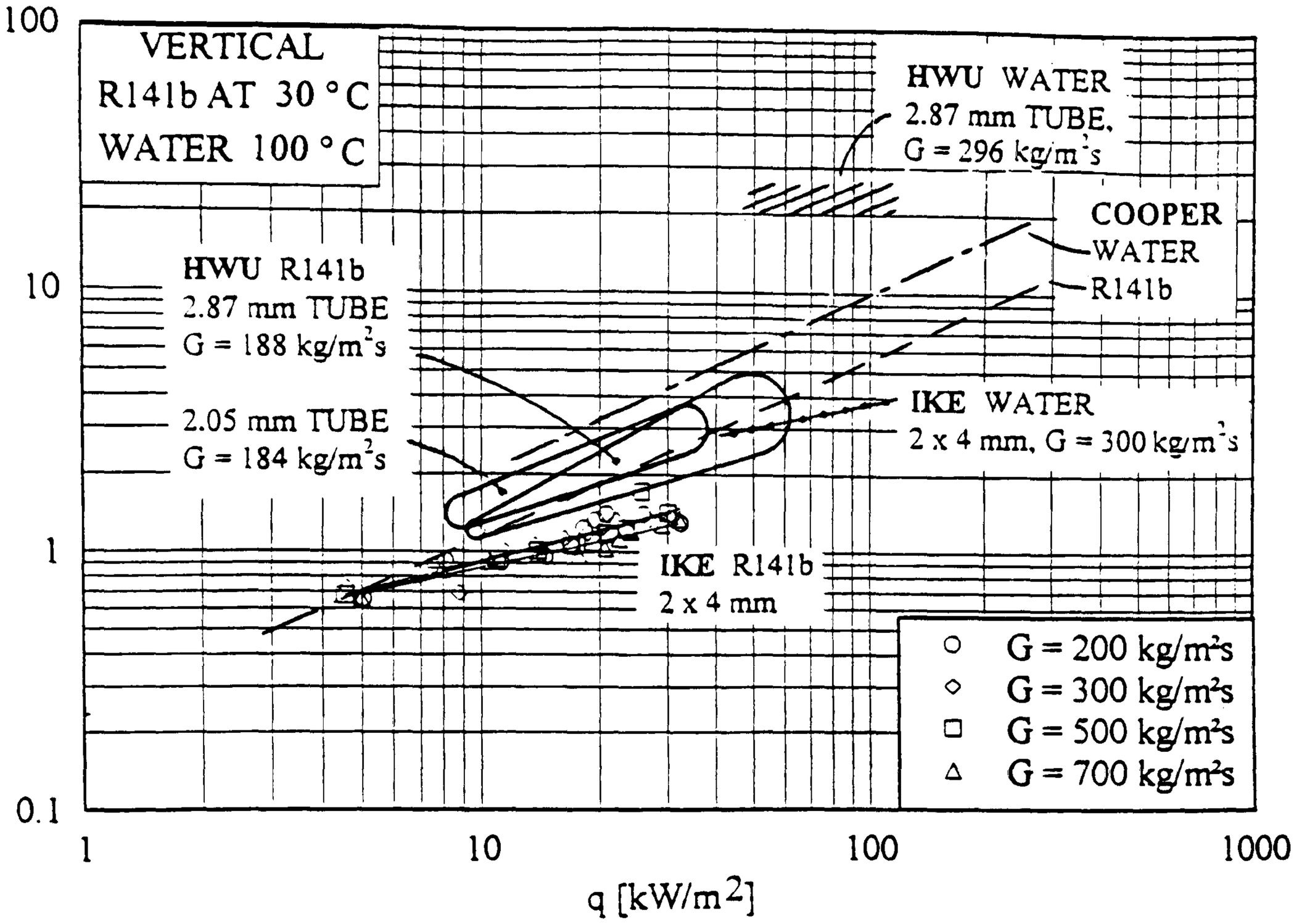

Figure 3.55 Comparison of Results with Work of IKE
(Single Channel)

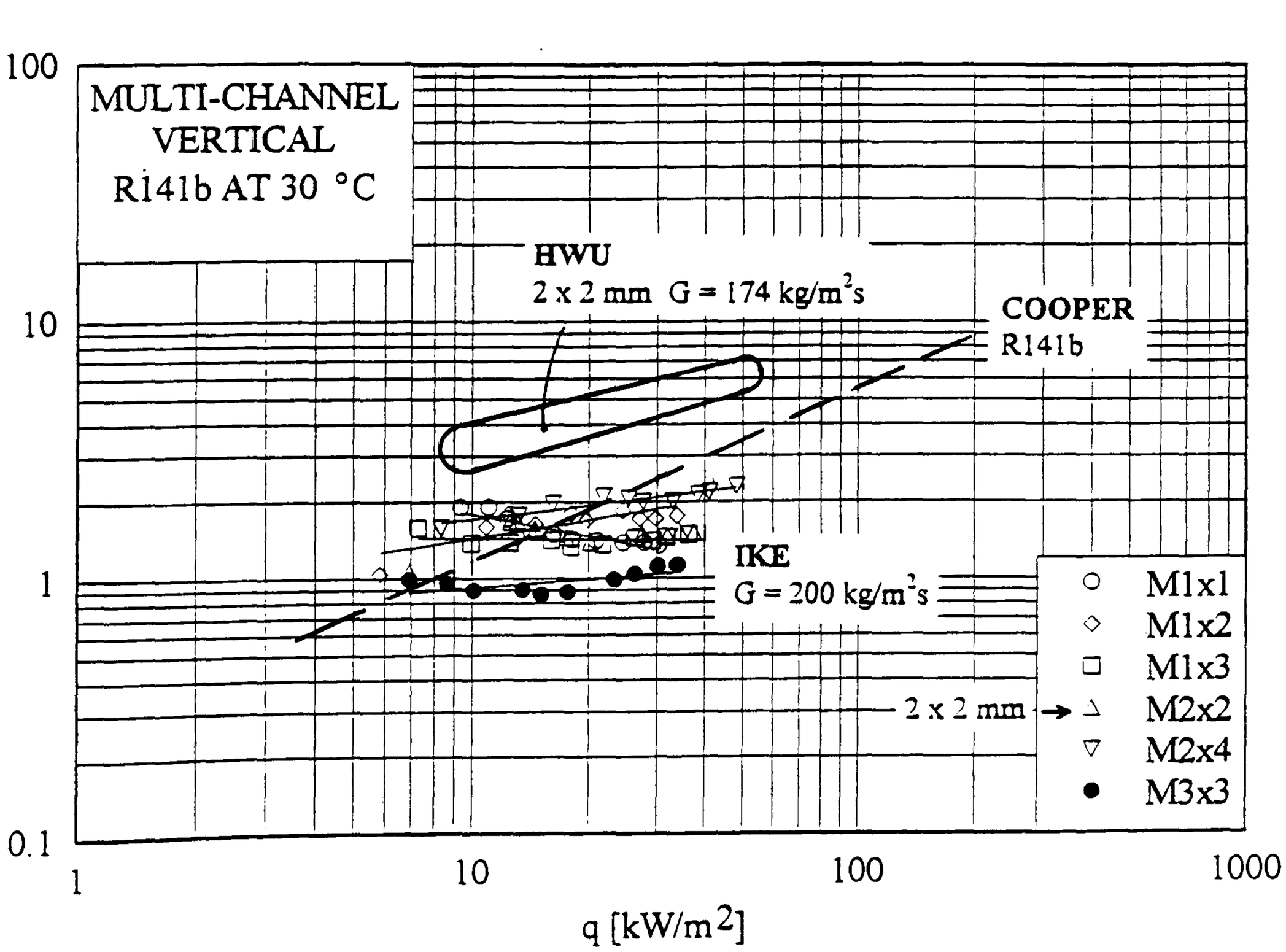

Figure 3.56 Comparison of Results with Work of IKE
(Multi-Channel)

(From Cornwell et al., 1995)

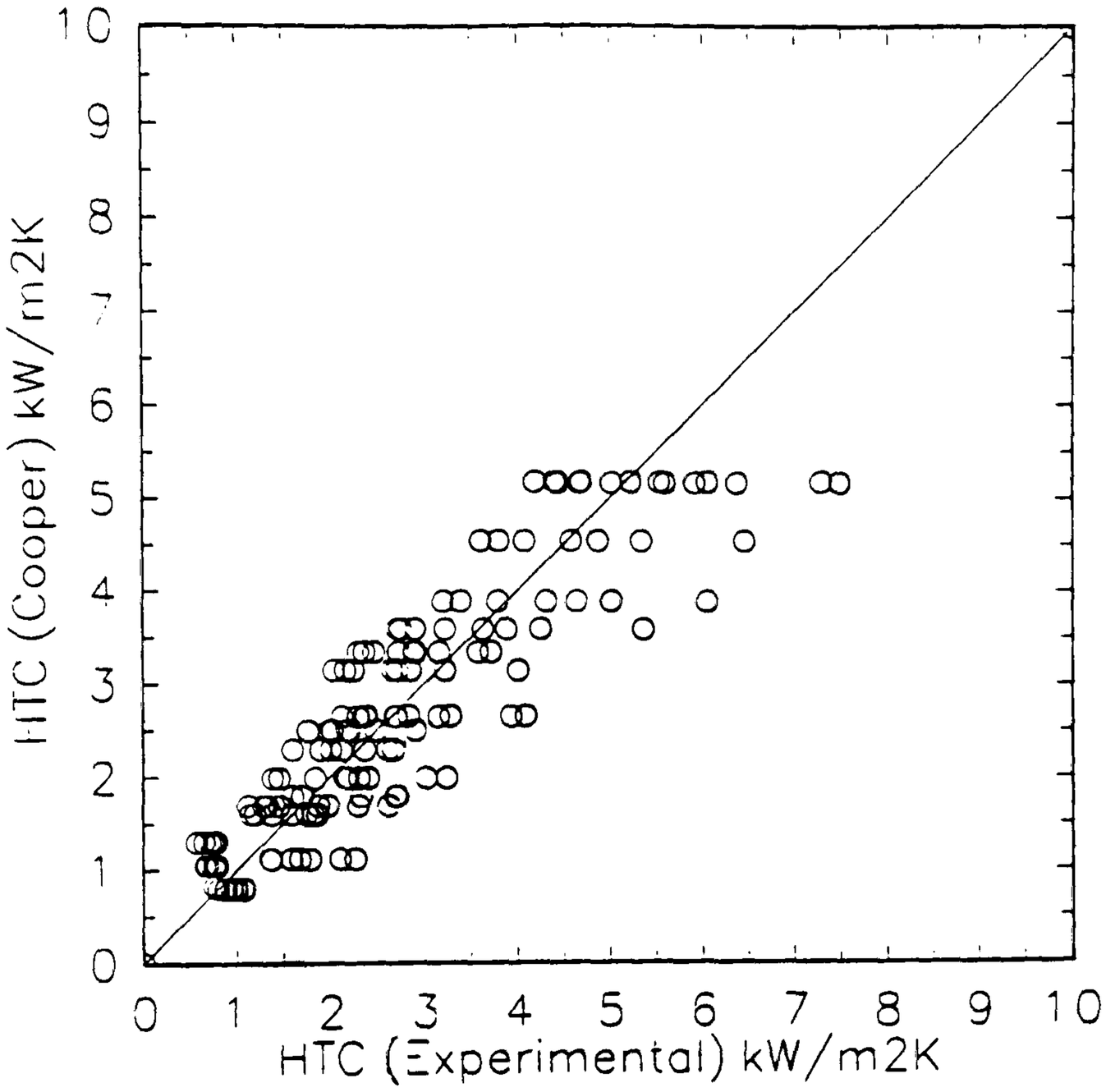

Figure 3.57 Comparison of Results with Correlation of Cooper (1984) - 3.69 mm Tube

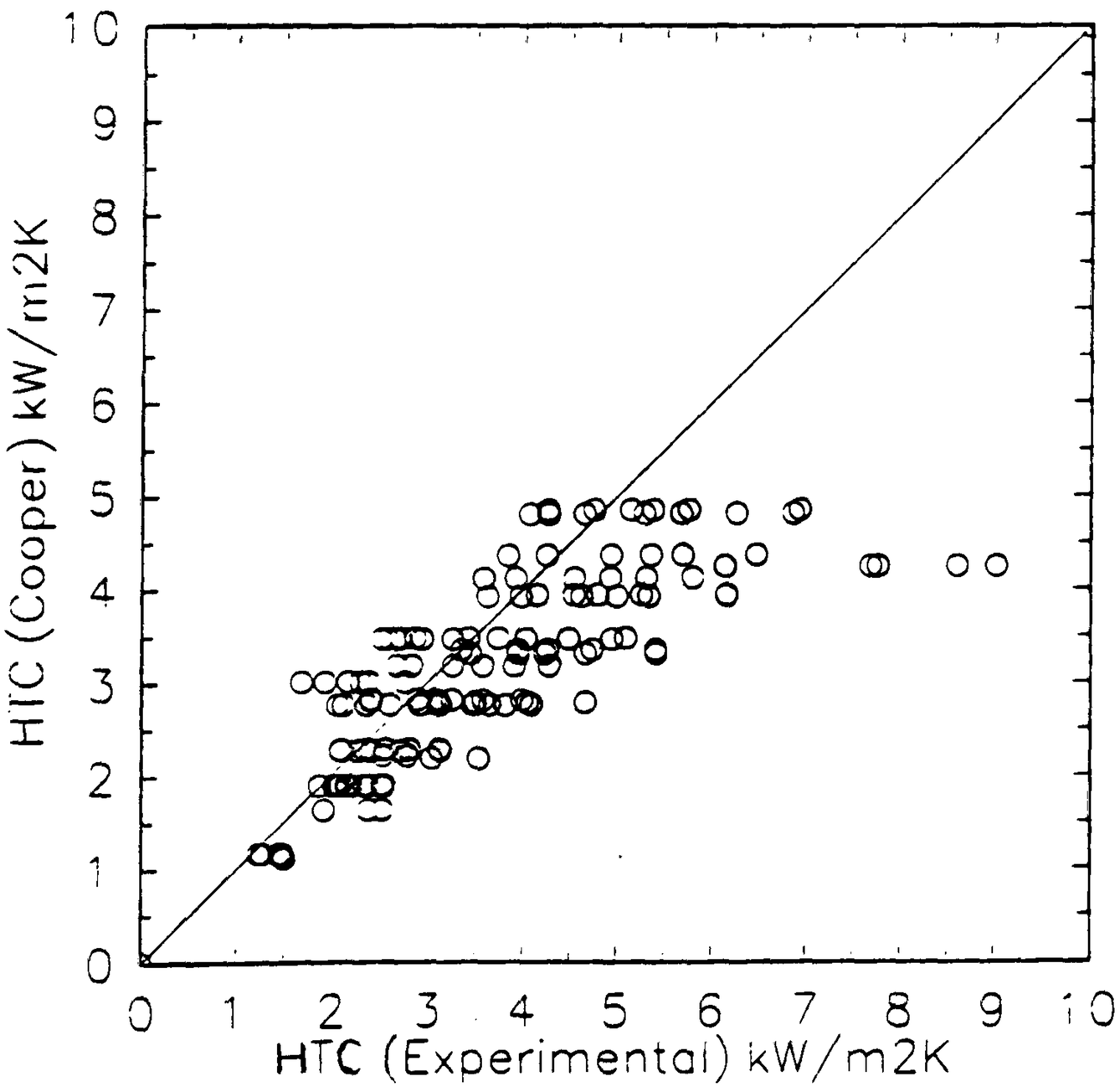

Figure 3.58 Comparison of Results with Correlation of Cooper (1984) - 2.87 mm Tube

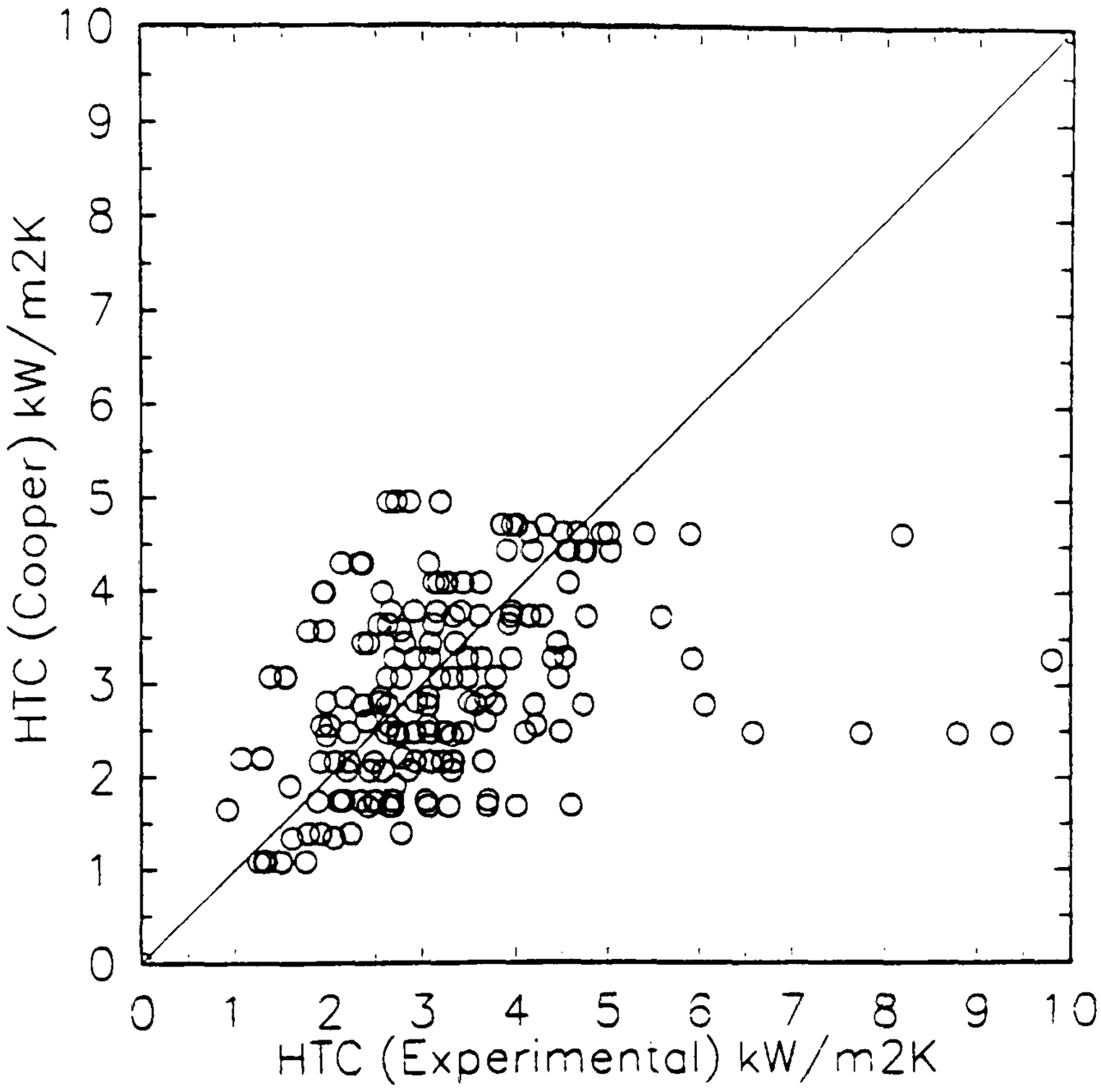

Figure 3.59 Comparison of Results with Correlation of Cooper (1984) - 2.05 mm Tube

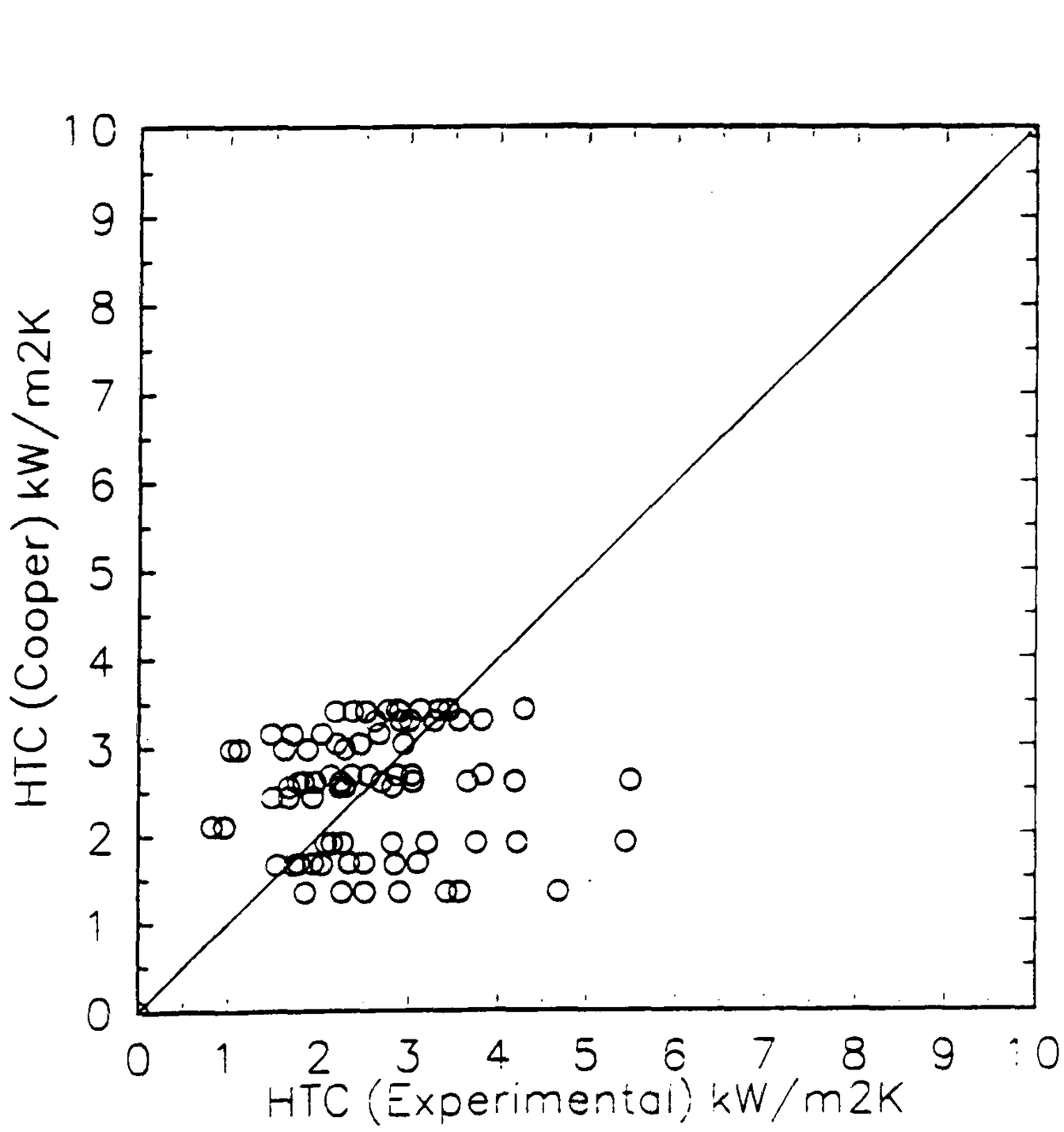

Figure 3.60 Comparison of Results with Correlation of Cooper (1984) - 1.39 mm Tube

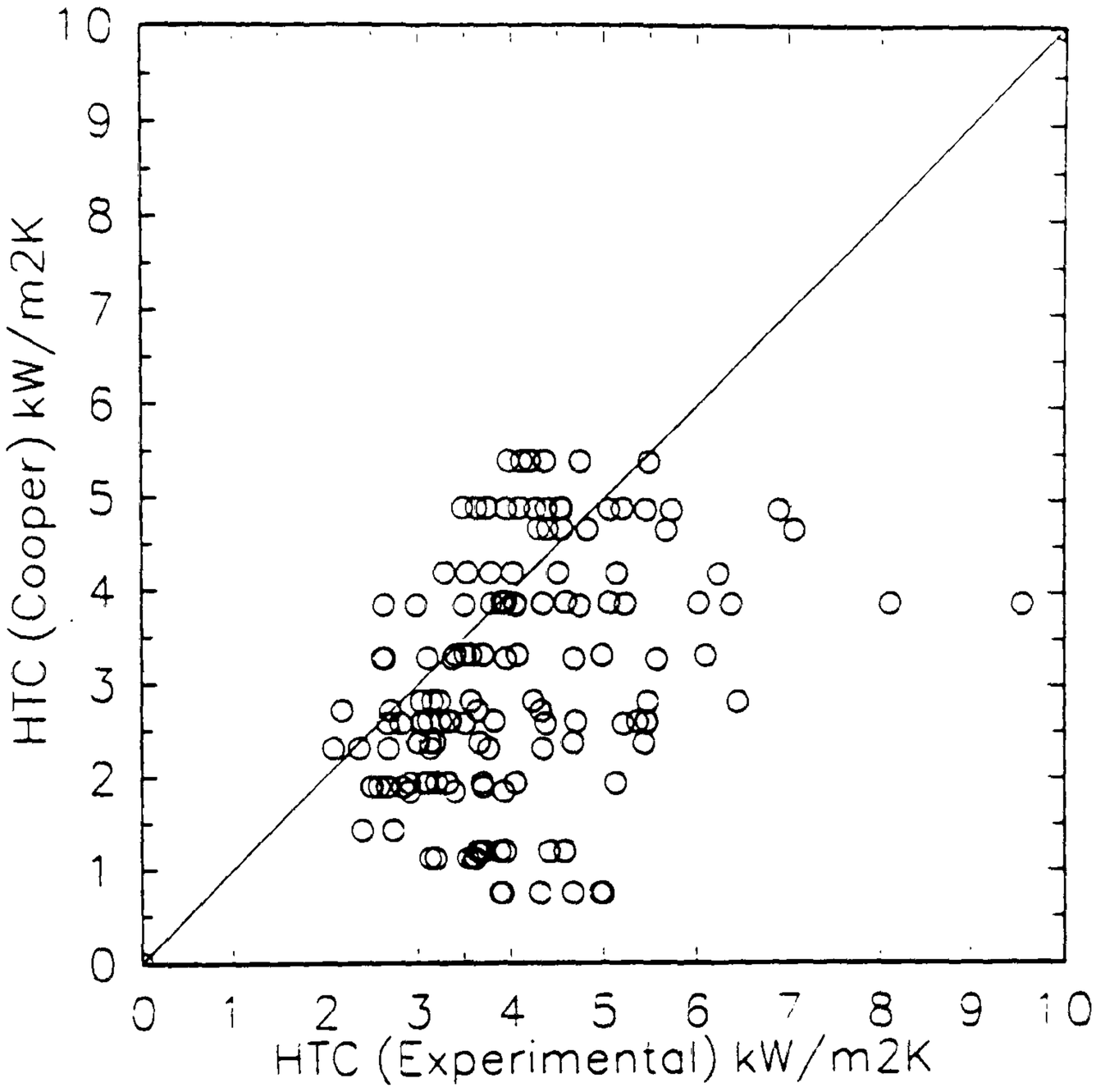

Figure 3.61 Comparison of Results with Correlation of Cooper (1984) - 2.10 mm Square Tube

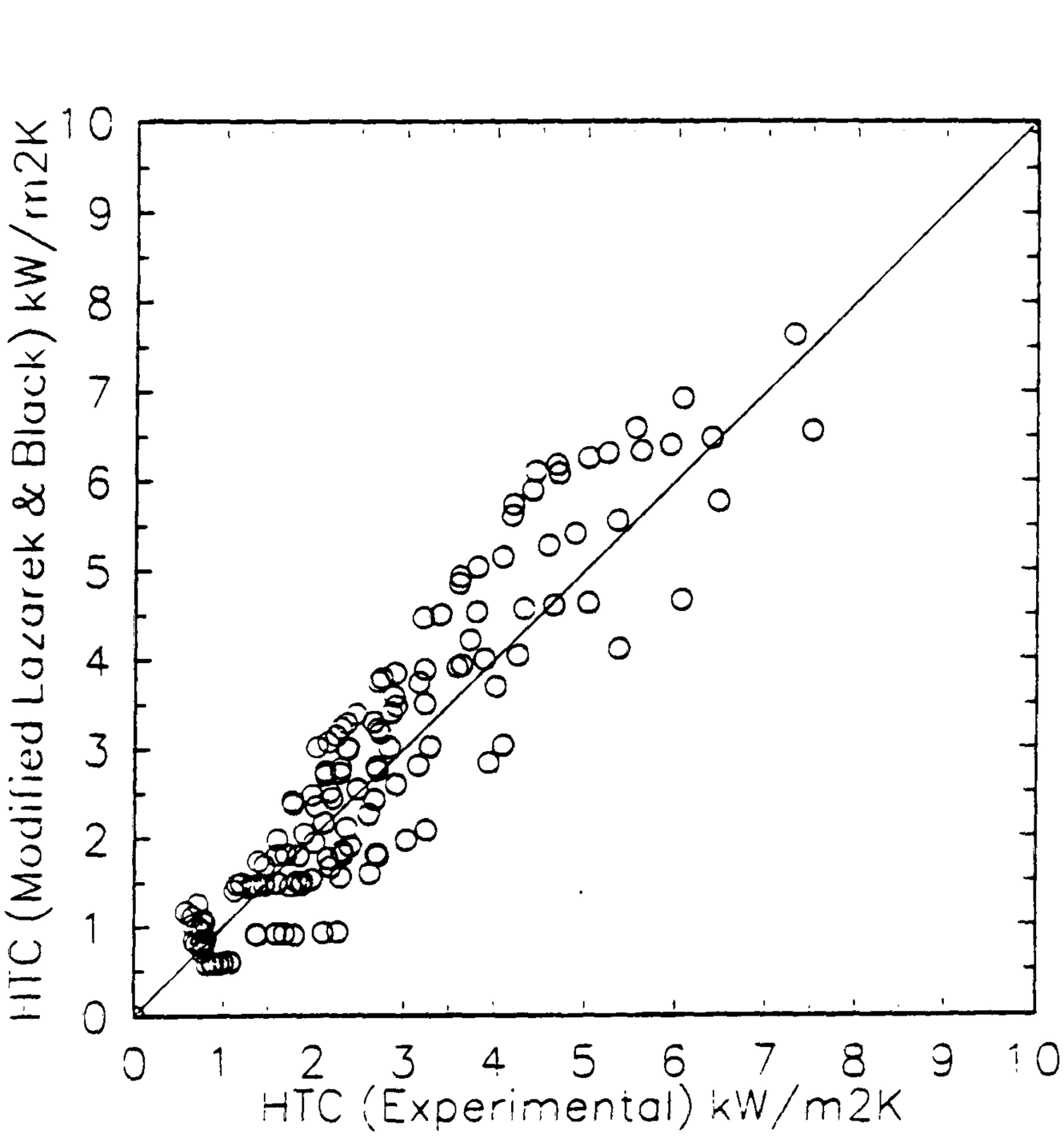

Figure 3.62 Comparison of Results with Modified Correlation of Lazarek and Black (1982) - 3.69 mm Tube

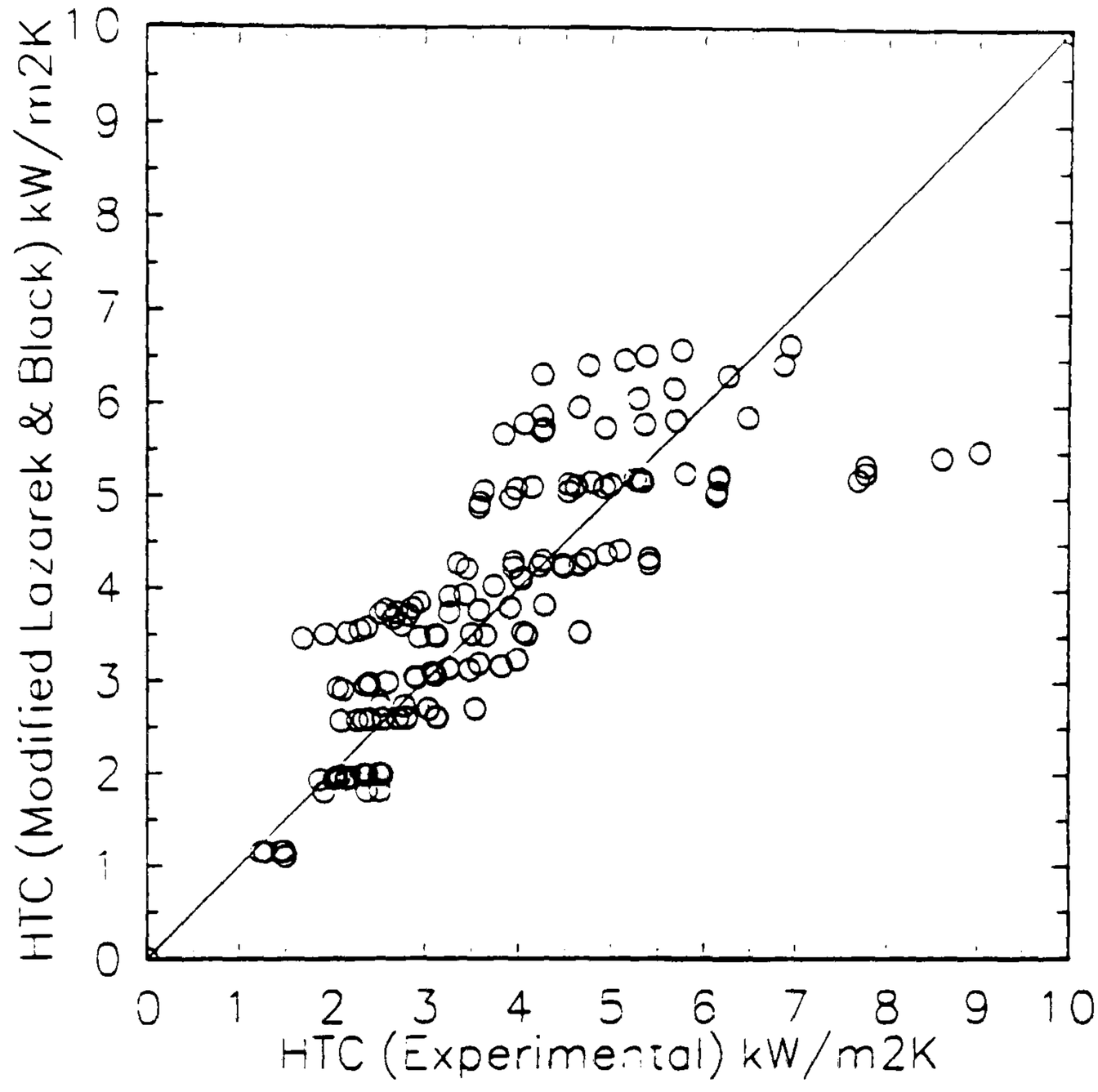

Figure 3.63 Comparison of Results with Modified Correlation of Lazarek and Black (1982) - 2.87 mm Tube

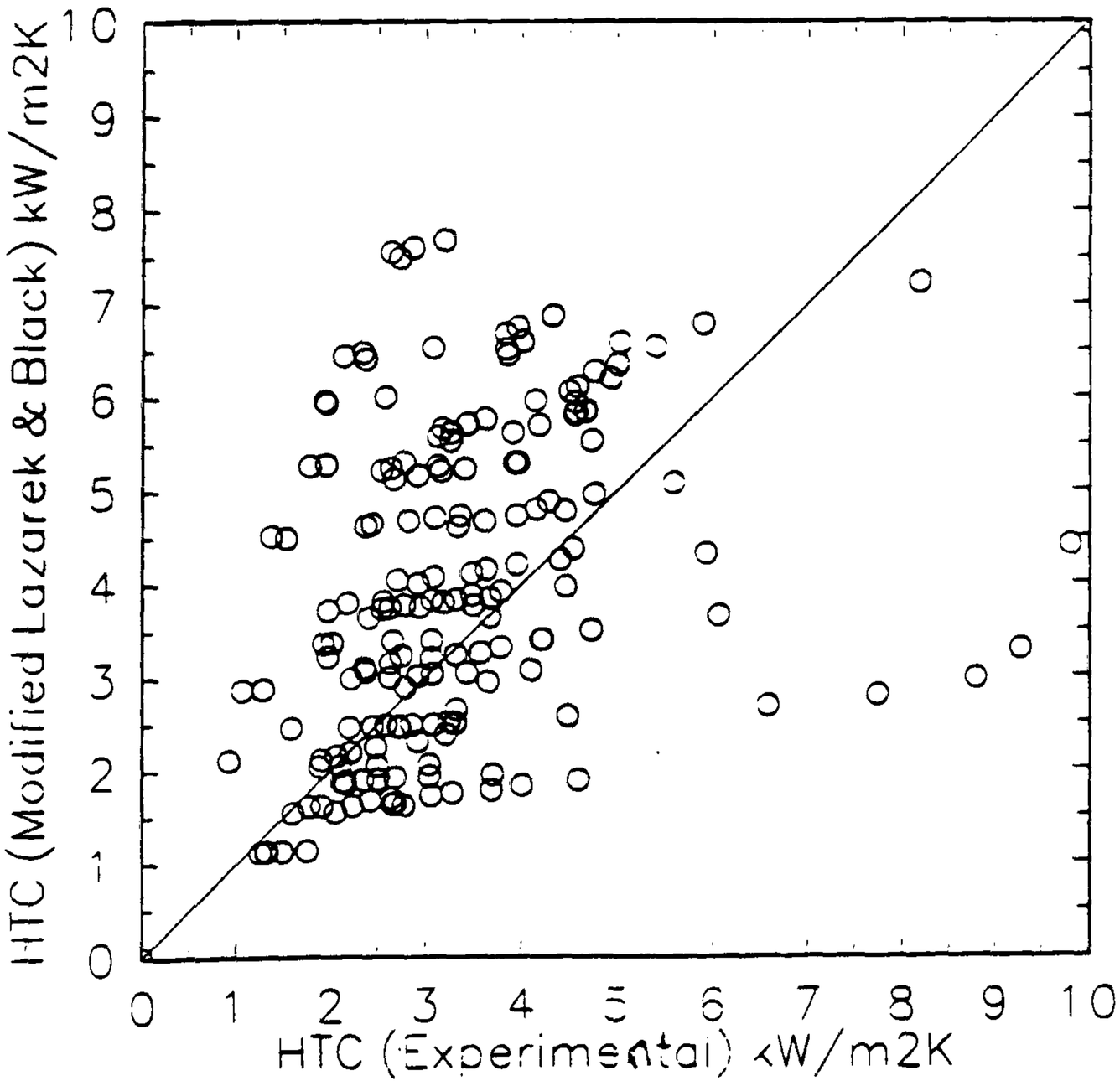

Figure 3.64 Comparison of Results with Modified Correlation of Lazarek and Black (1982) - 2.05 mm Tube

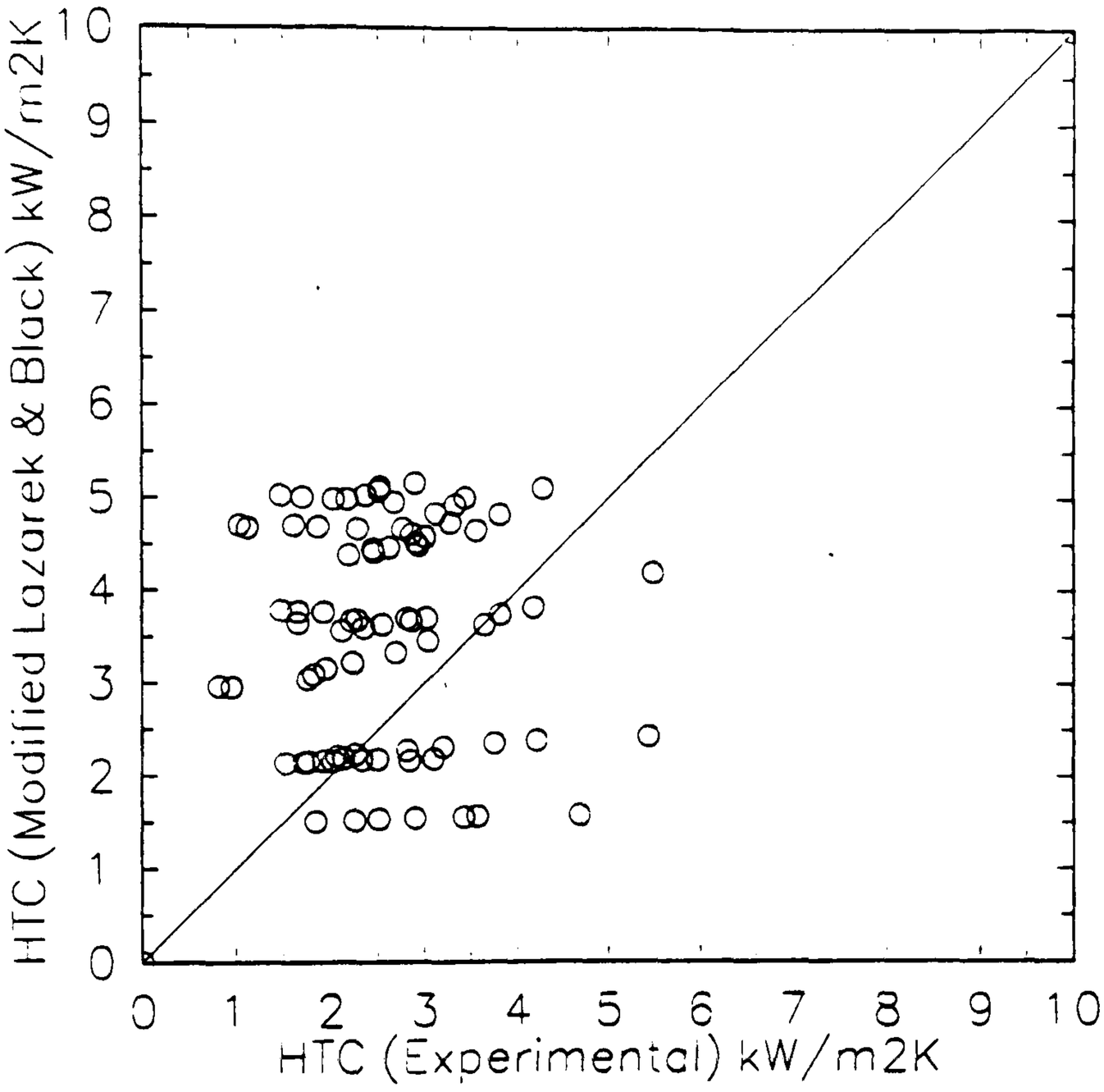

Figure 3.65 Comparison of Results with Modified Correlation of Lazarek and Black (1982) - 1.39 mm Tube

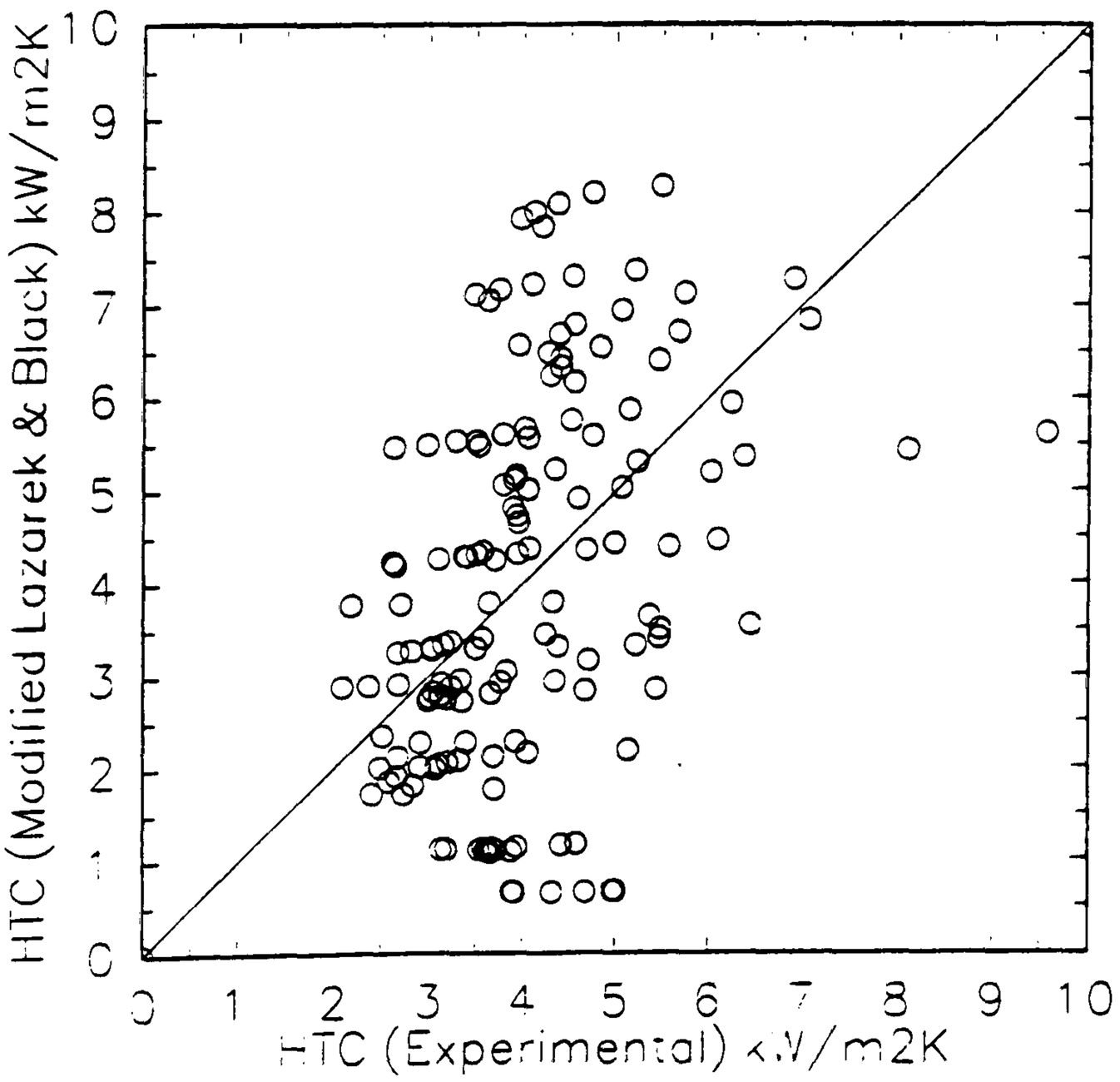

Figure 3.66 Comparison of Results with Modified Correlation of Lazarek and Black (1982) - 2.10 mm Square Tube

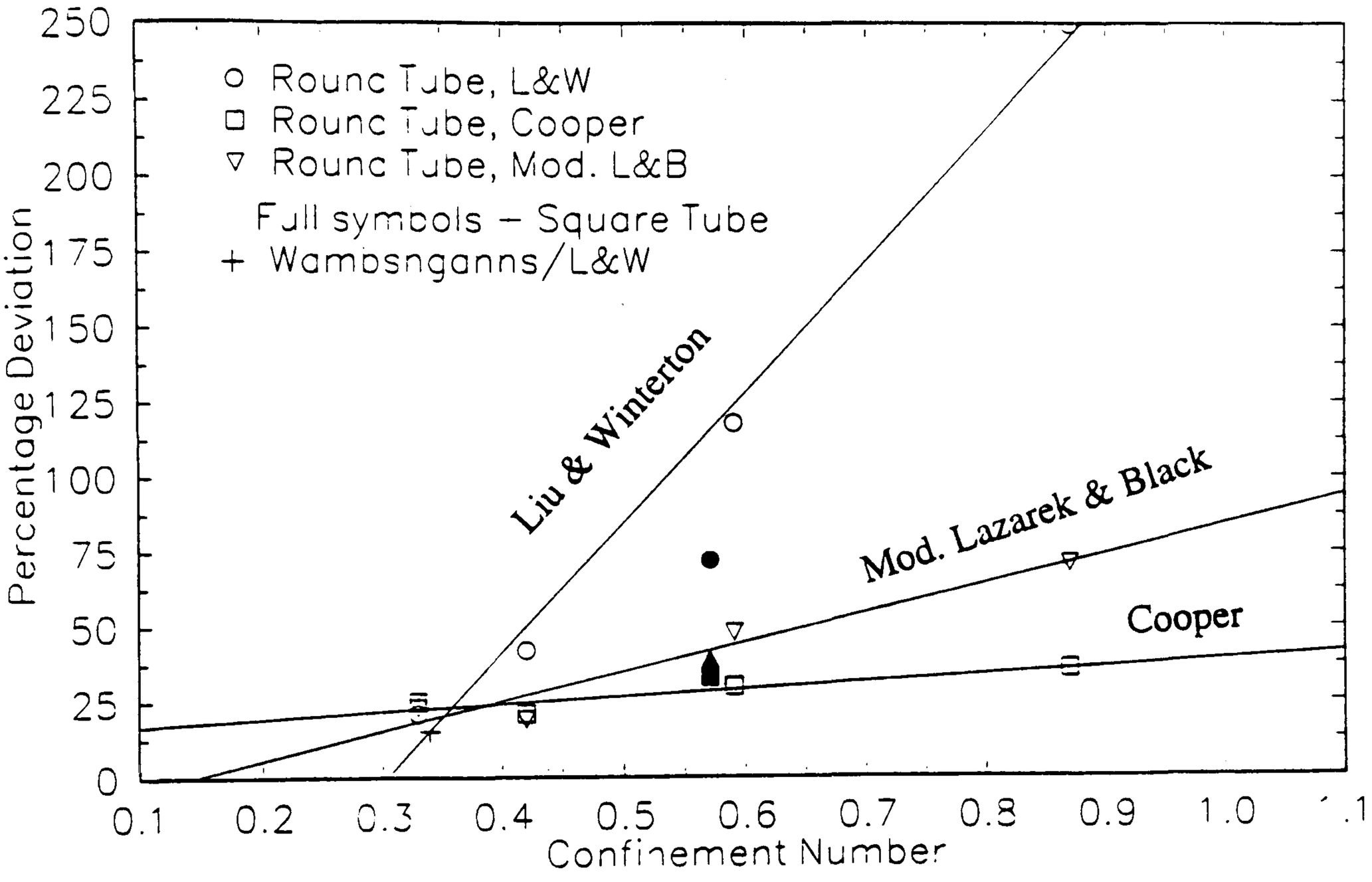

Figure 3.67 Deviation of Measured Results from Correlations with Increasing Confinement

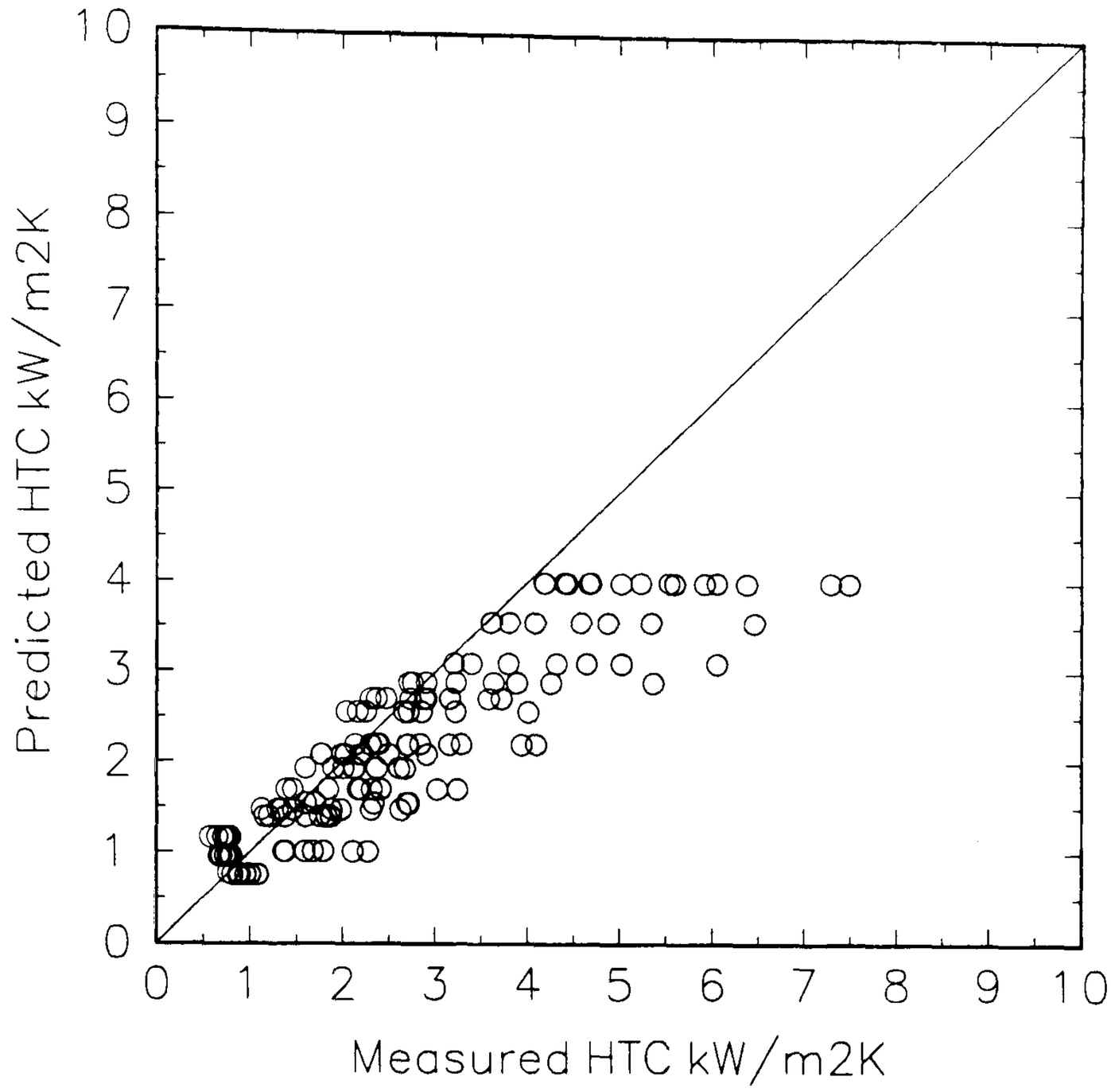

Figure 3.68 Comparison of Results with Correlation of Tran Wambsganss and France (1995) - 3.69 mm Tube

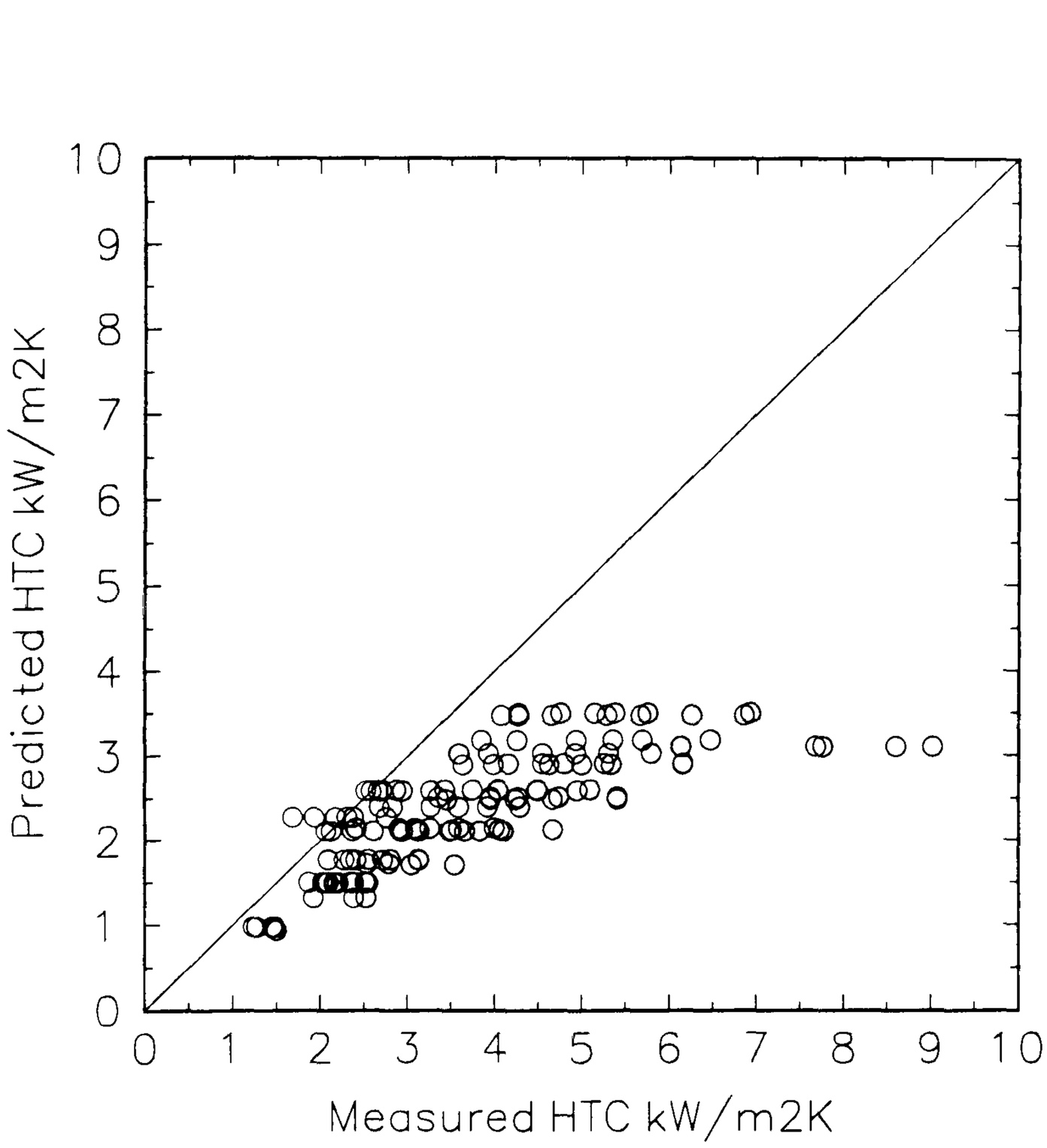

Figure 3.69 Comparison of Results with Correlation of Tran Wambsganss and France (1995) - 2.87 mm Tube

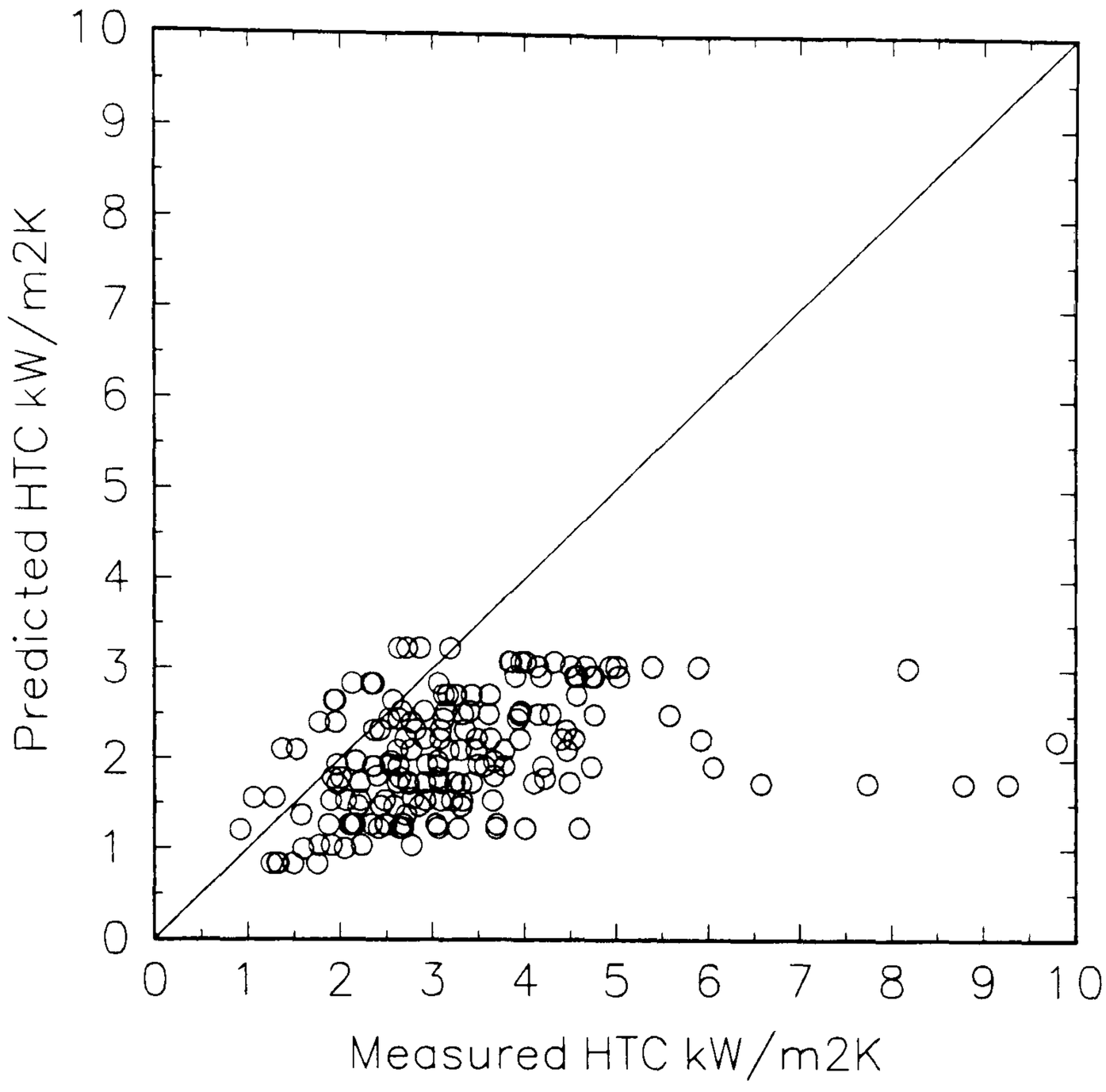

Figure 3.70 Comparison of Results with Correlation of Tran Wambsganss and France (1995) - 2.05 mm Tube

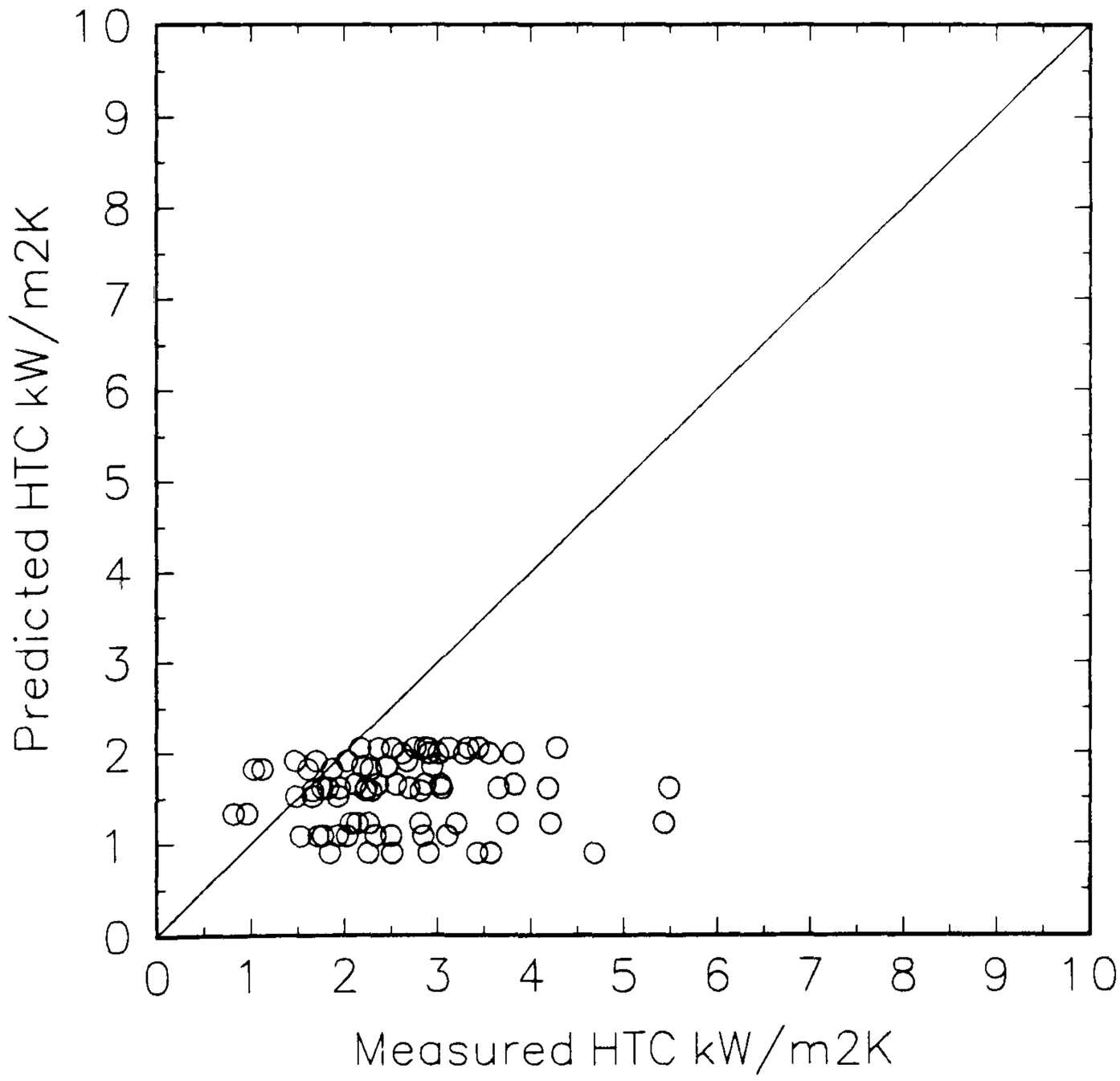

Figure 3.71 Comparison of Results with Correlation of Tran Wambsganss and France (1995) - 1.39 mm Tube

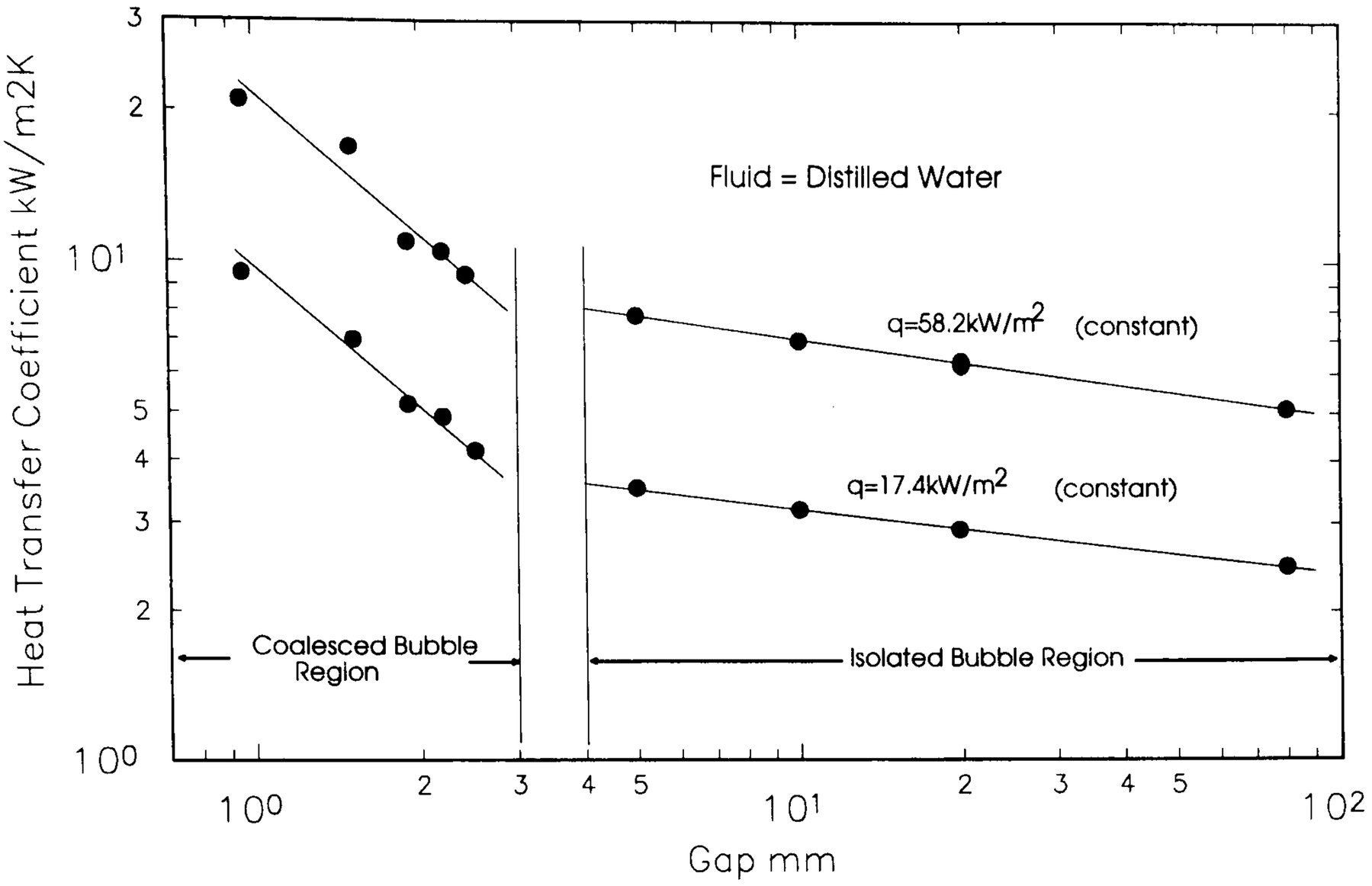

Figure 4.1 Variation of Heat Transfer Coefficient with Gap Size
(From Nishikawa and Fujita, 1990)

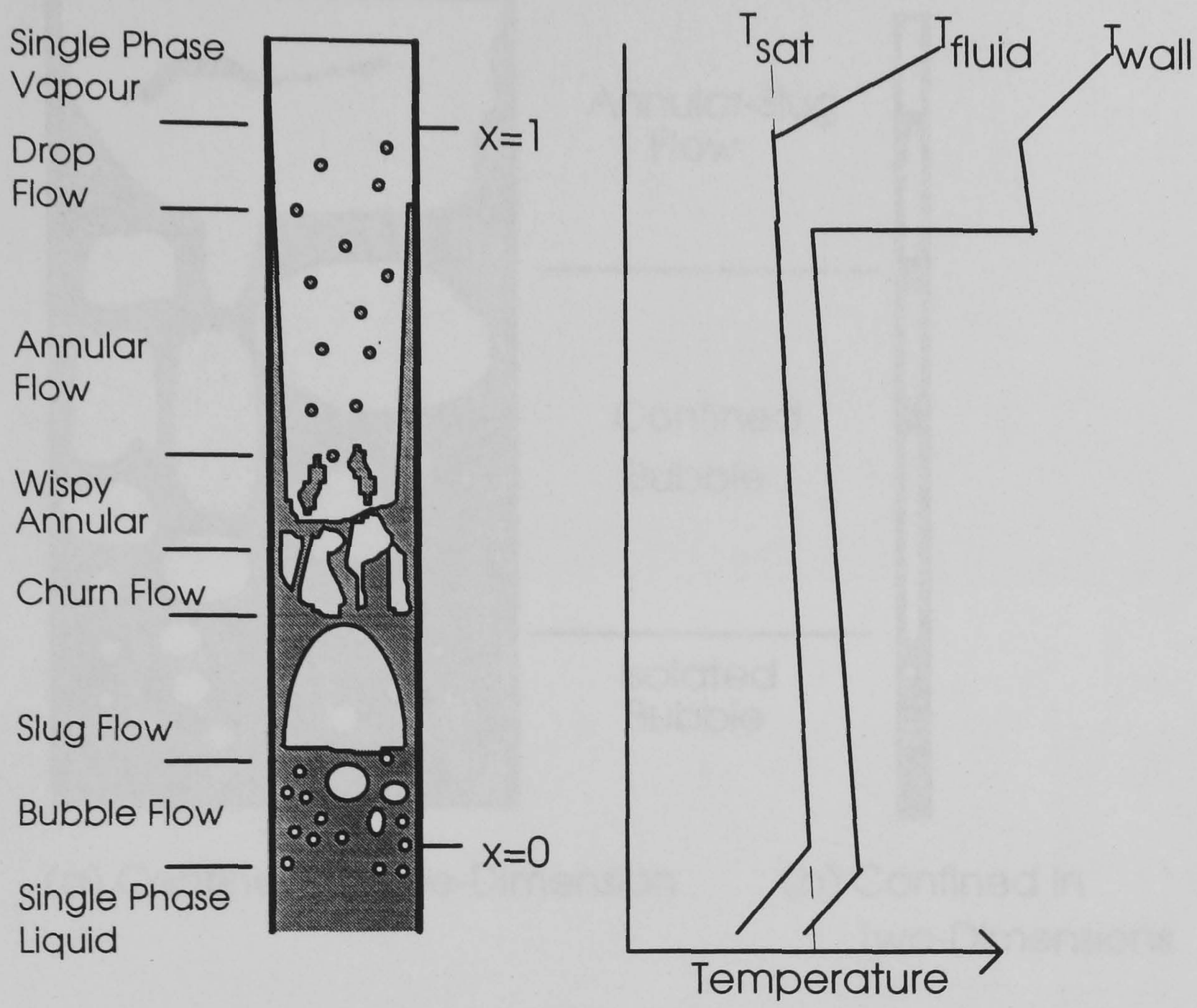

Figure 4.2 Flow Regimes in Vertical Tube and Representative Longtitudinal Temperature Variation

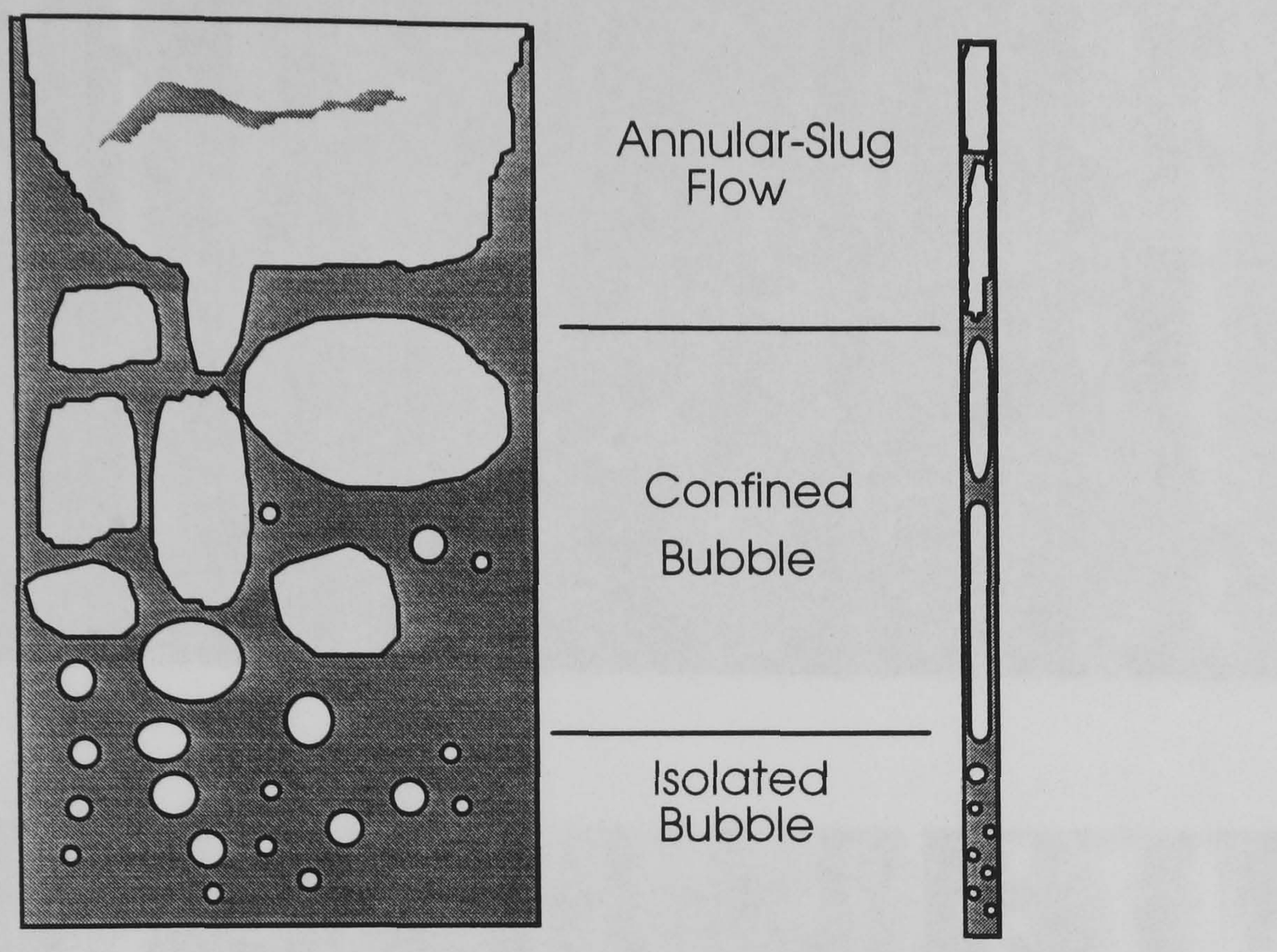

Figure 4.3 Schematic Representation of Flow Regimes in Confined Spaces

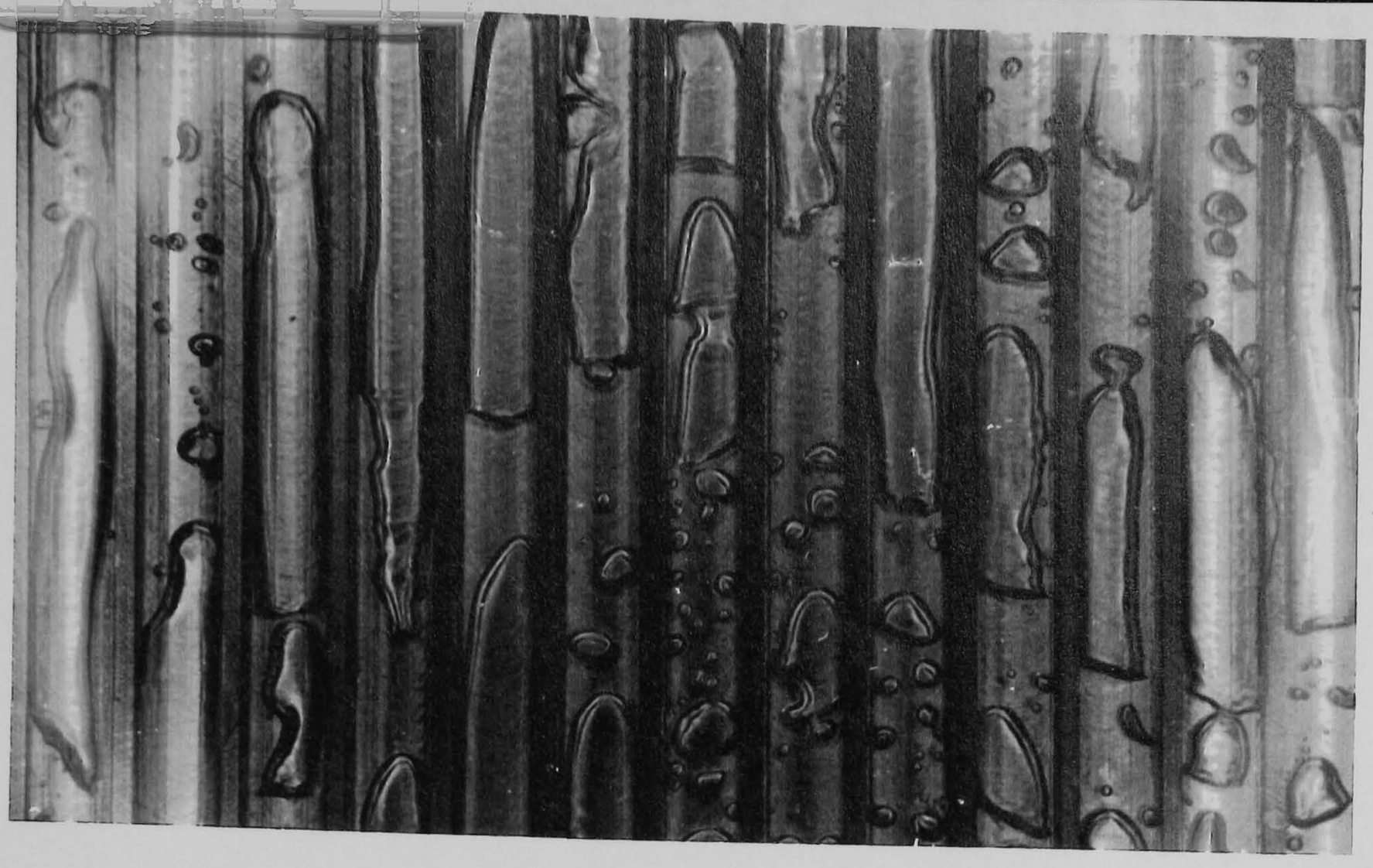

(iii)
q = 6.85kW/m²
x = 0.08

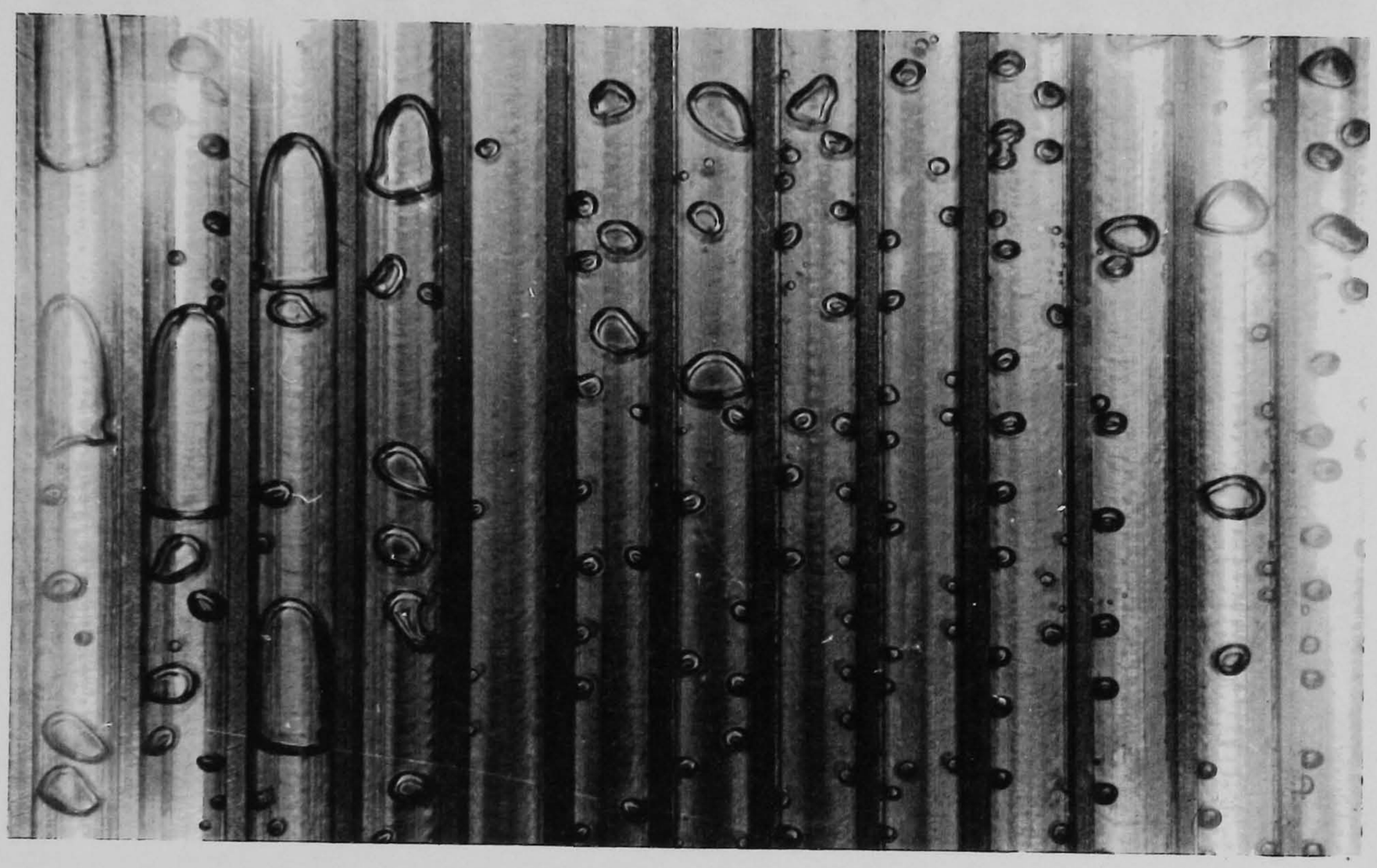

(ii)
q = 4.33kW/m
x = 0.05

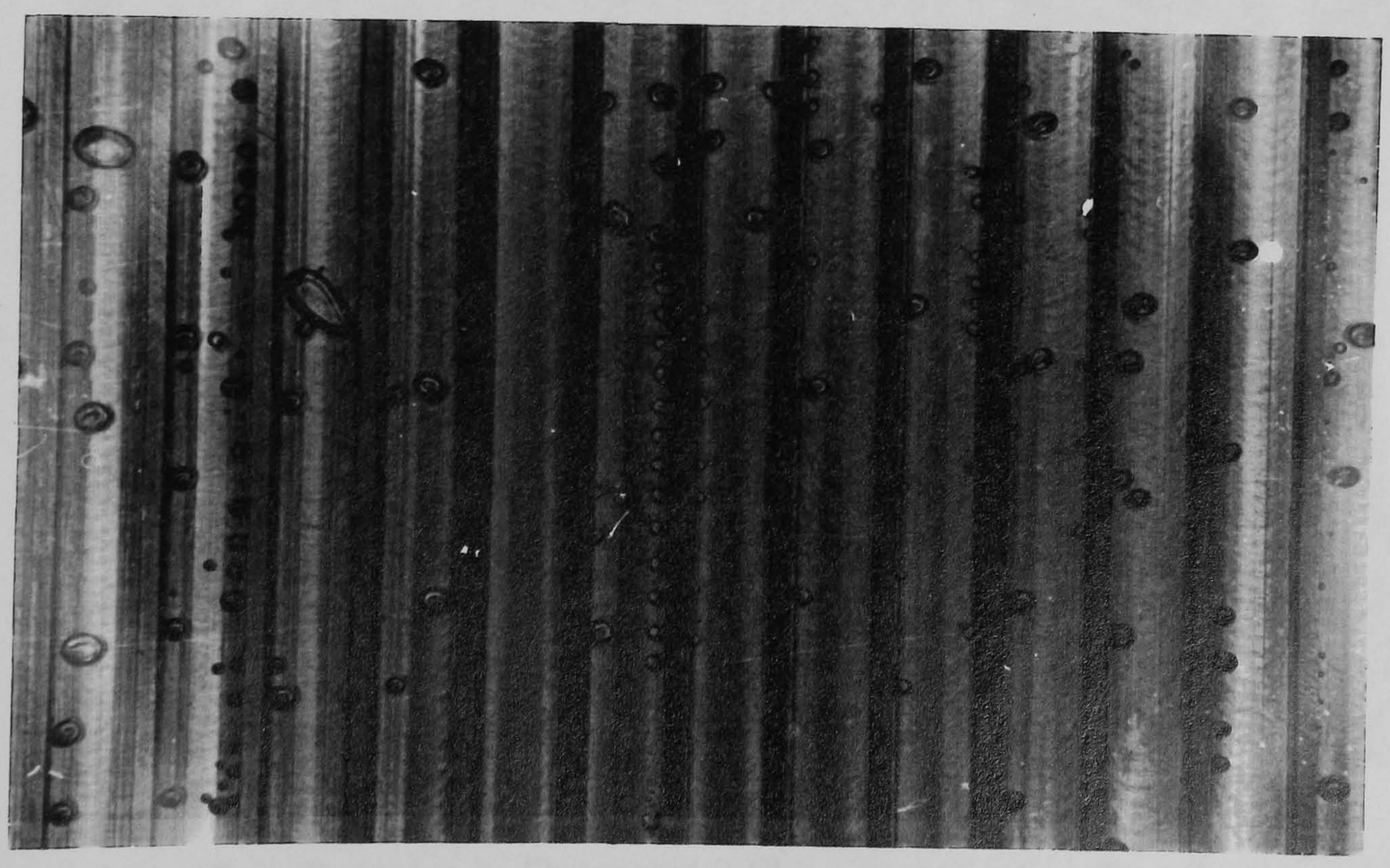

(i)
q = 2.55kW/m²
x = 0.03

Figure 4.4(a) Flow Regimes in Geometry 2 Flow Visualisation Test Section Mark I.
(G=156kg/m²s, Zone 3, R113)

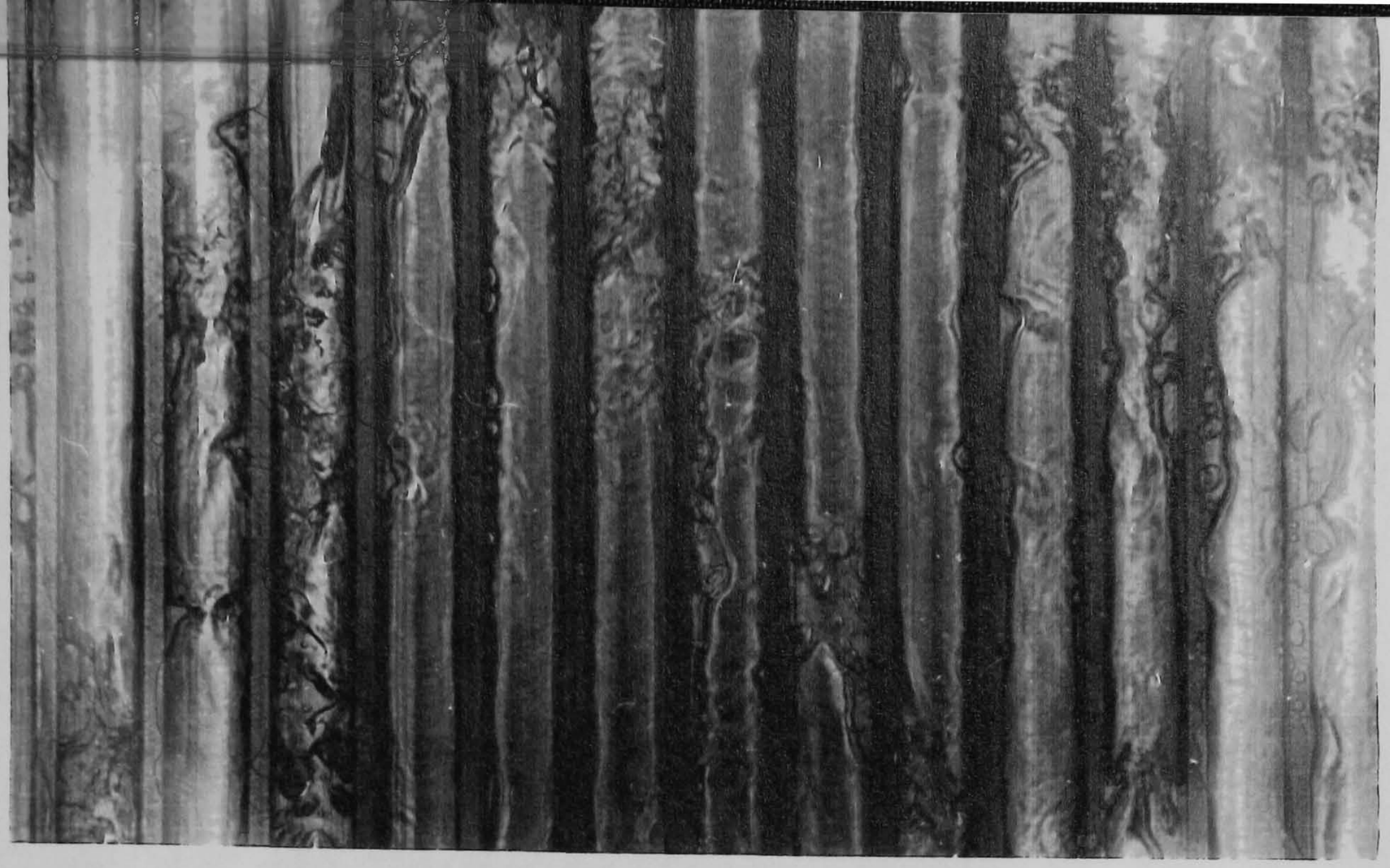

(vi)
q = 16.0kW/m²
x = 0.20

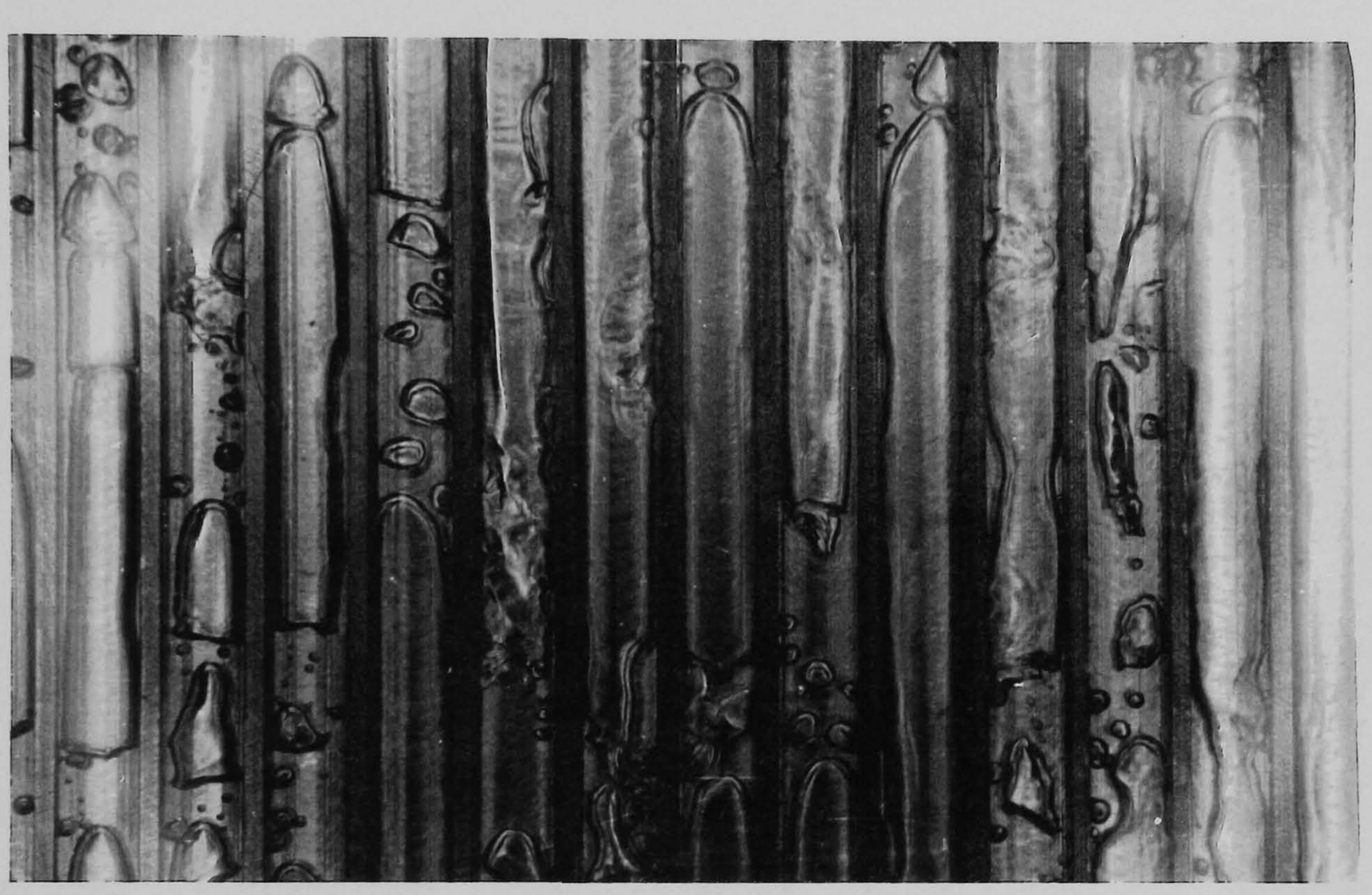

(v)
q = 11.8kW/m²
x = 0.14

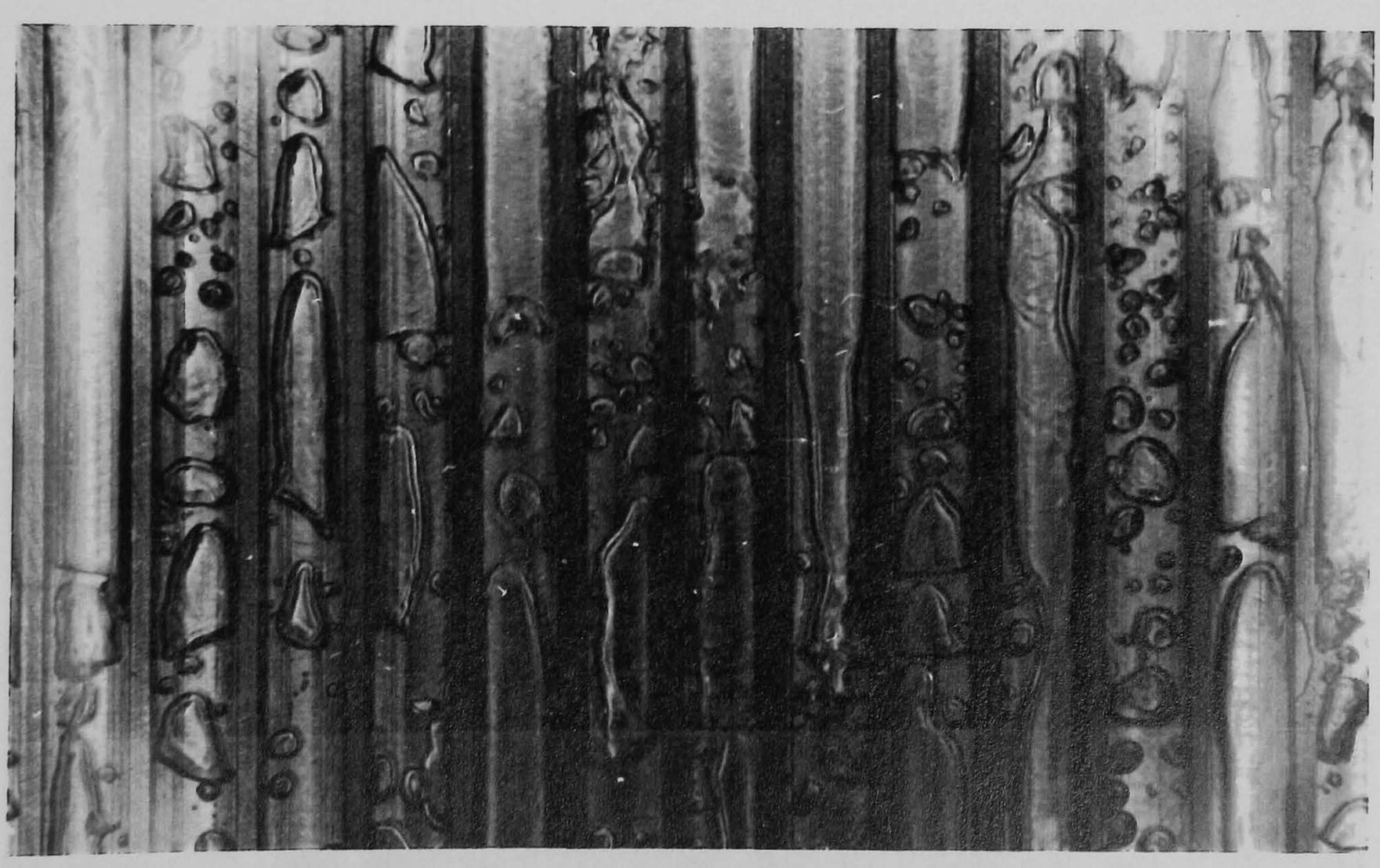

(iv)
q = 9.79kW/m²
x = 0.12

Figure 4.4(a) Flow Regimes in Geometry 2 Flow Visualisation Test Section Mark I.
(G=156kg/m²s, Zone 3, R113)
(Cont)

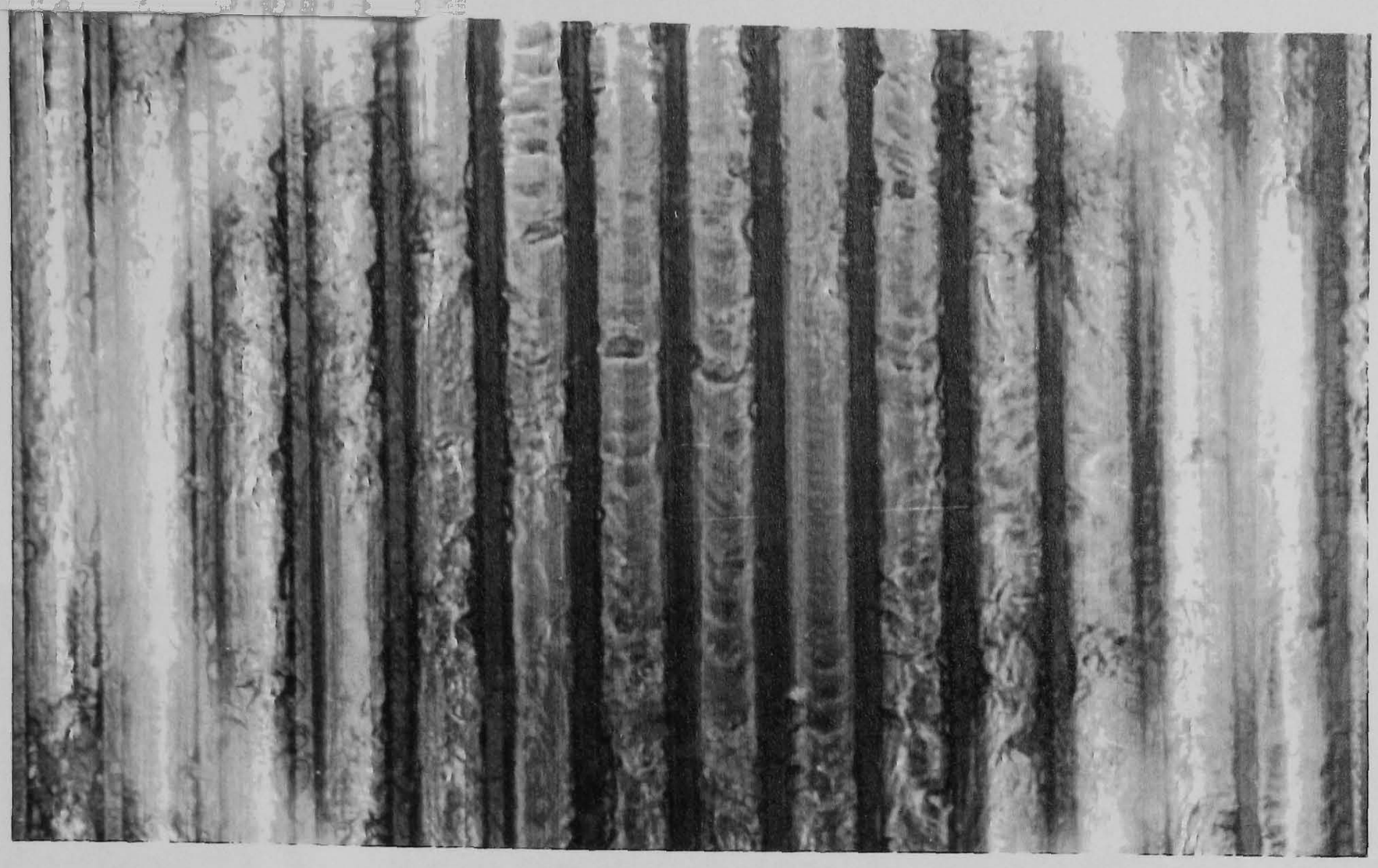

(ix)
q = 32.9kW/m²
x = 0.40

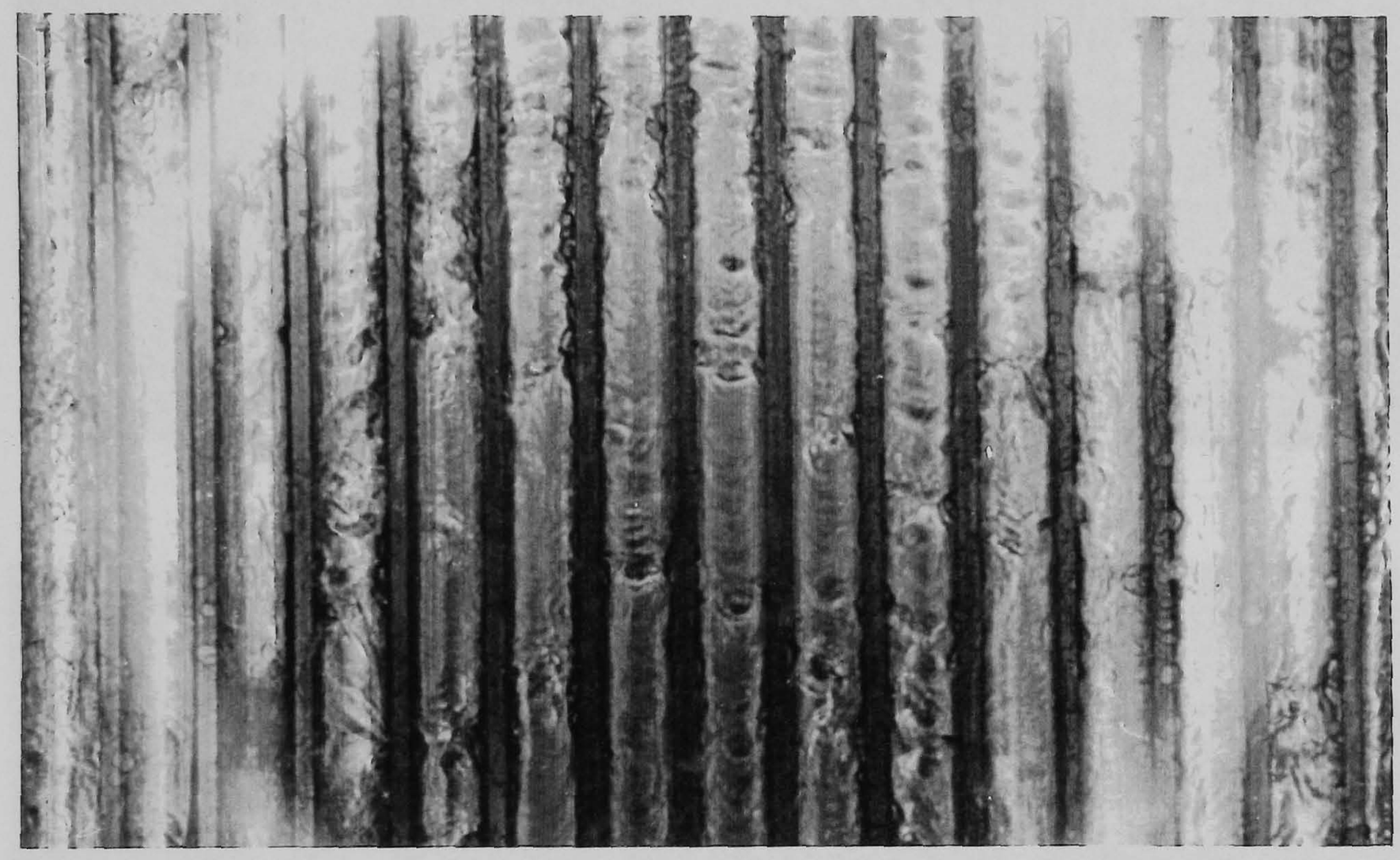

(viii)
q = 28.5kW/m²
x = 0.35

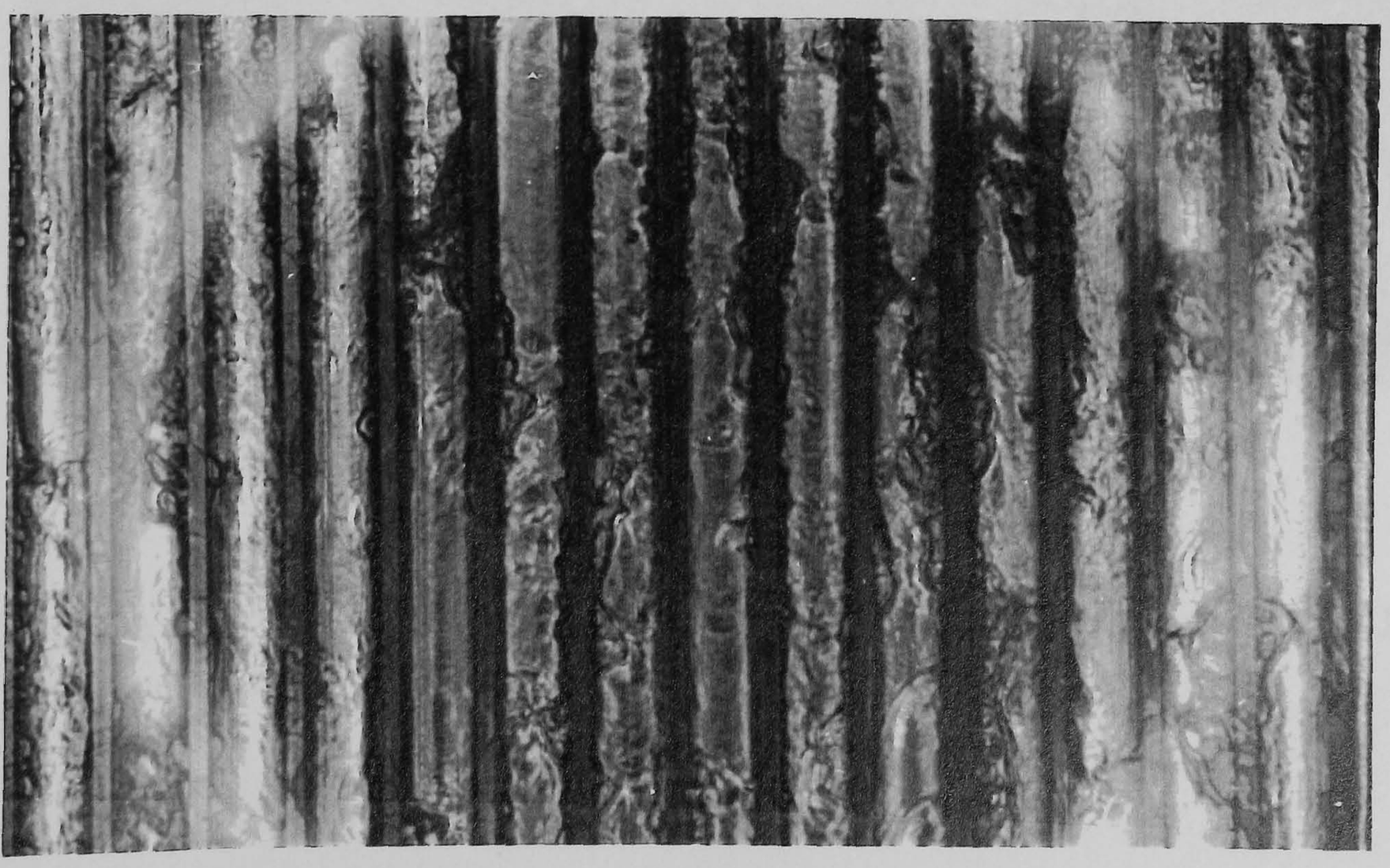

(vii)
q = 24.2kW/m²
x = 0.30

Figure 4.4(a) Flow Regimes in Geometry 2 Flow Visualisation Test Section Mark I.
(G=156kg/m^{2}s, Zone 3, R113)
(Cont)

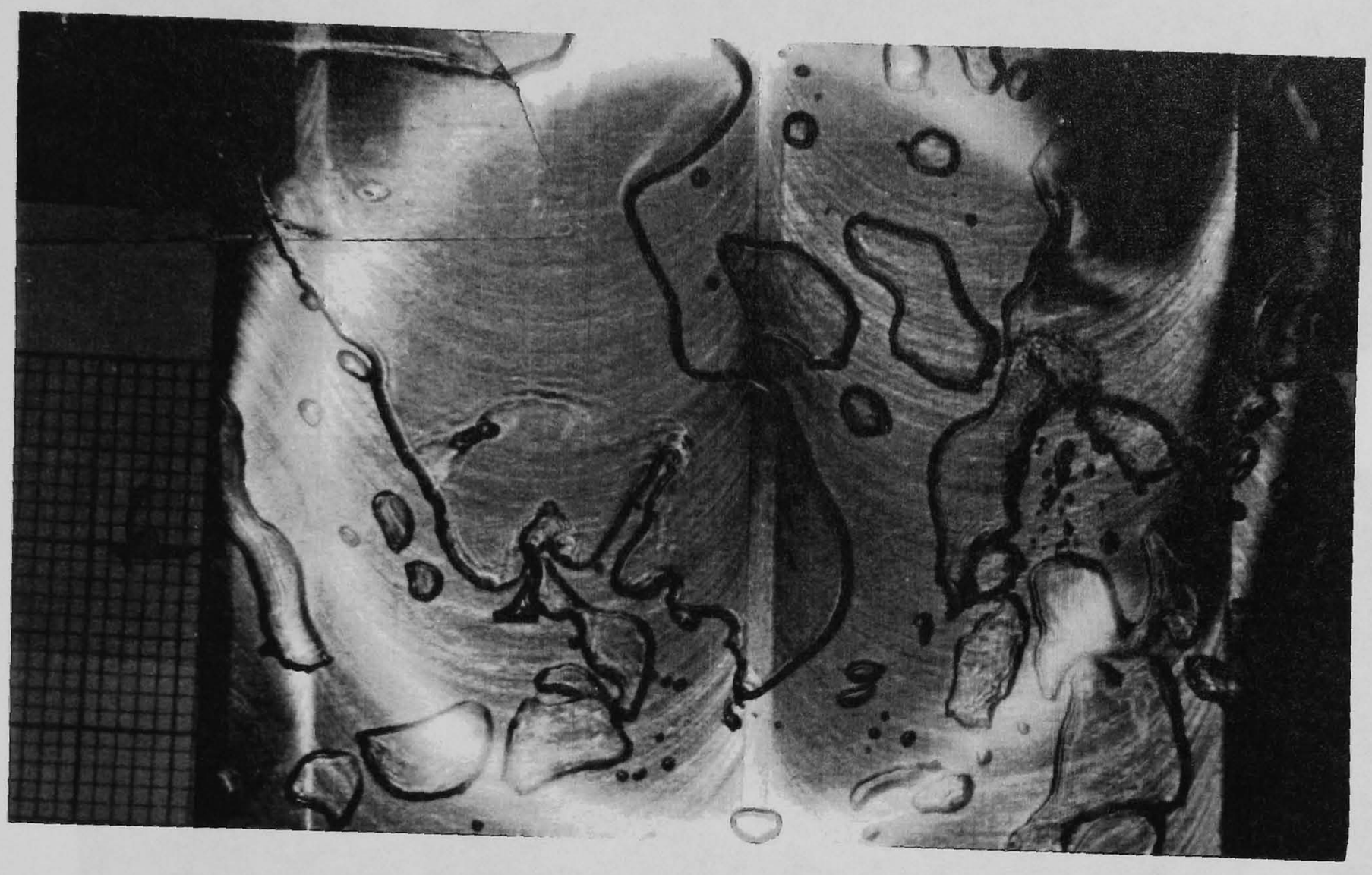

(ii)
x =0.05

(i)
x =0.04

Figure 4.4(b) Flow Regimes in Front of Flat Plate 1mm Gap- Test Section Mark I.
(G=134kg/m^{2}s, Heat Flux= 3.2kW/m^2, R113)

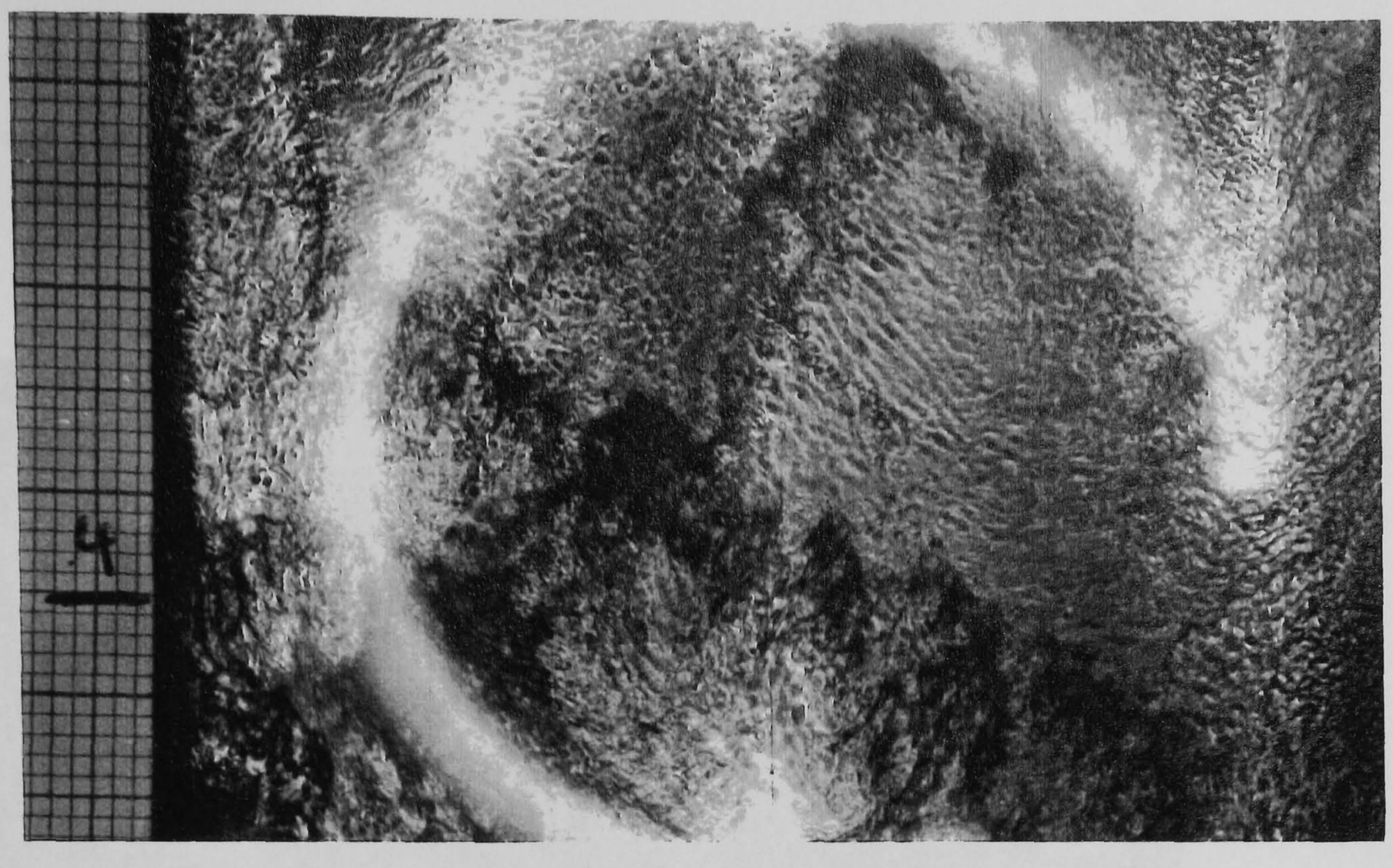

(iii)
x =0.17

(ii)
x =0.11

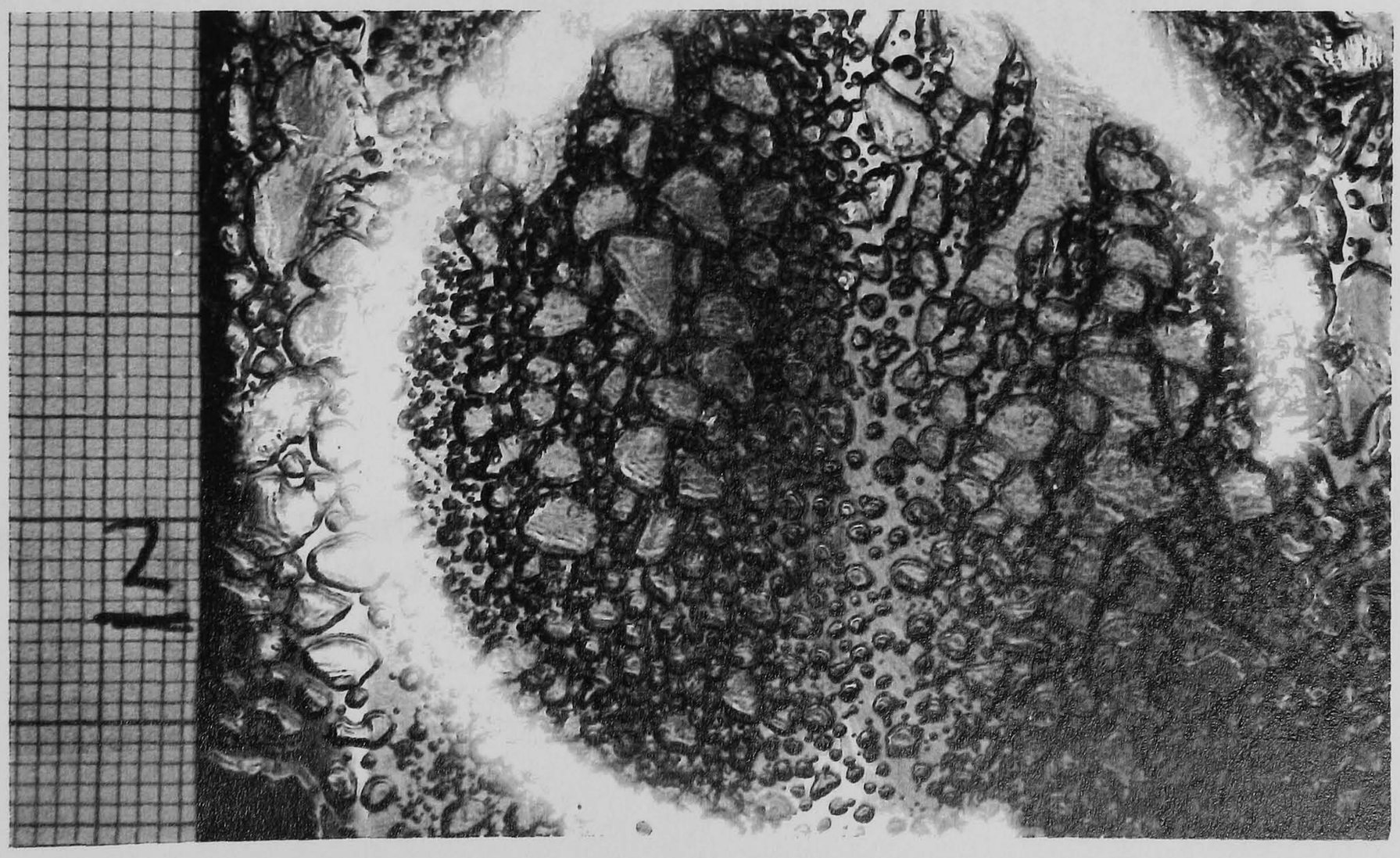

(i)
x =0.06

Figure 4.4(c) Flow Regimes in Front of Flat Plate 1mmGap- Test Section Mark I.
(G=335kg/m^{2}s, Heat Flux= 44kW/m^2, R113)

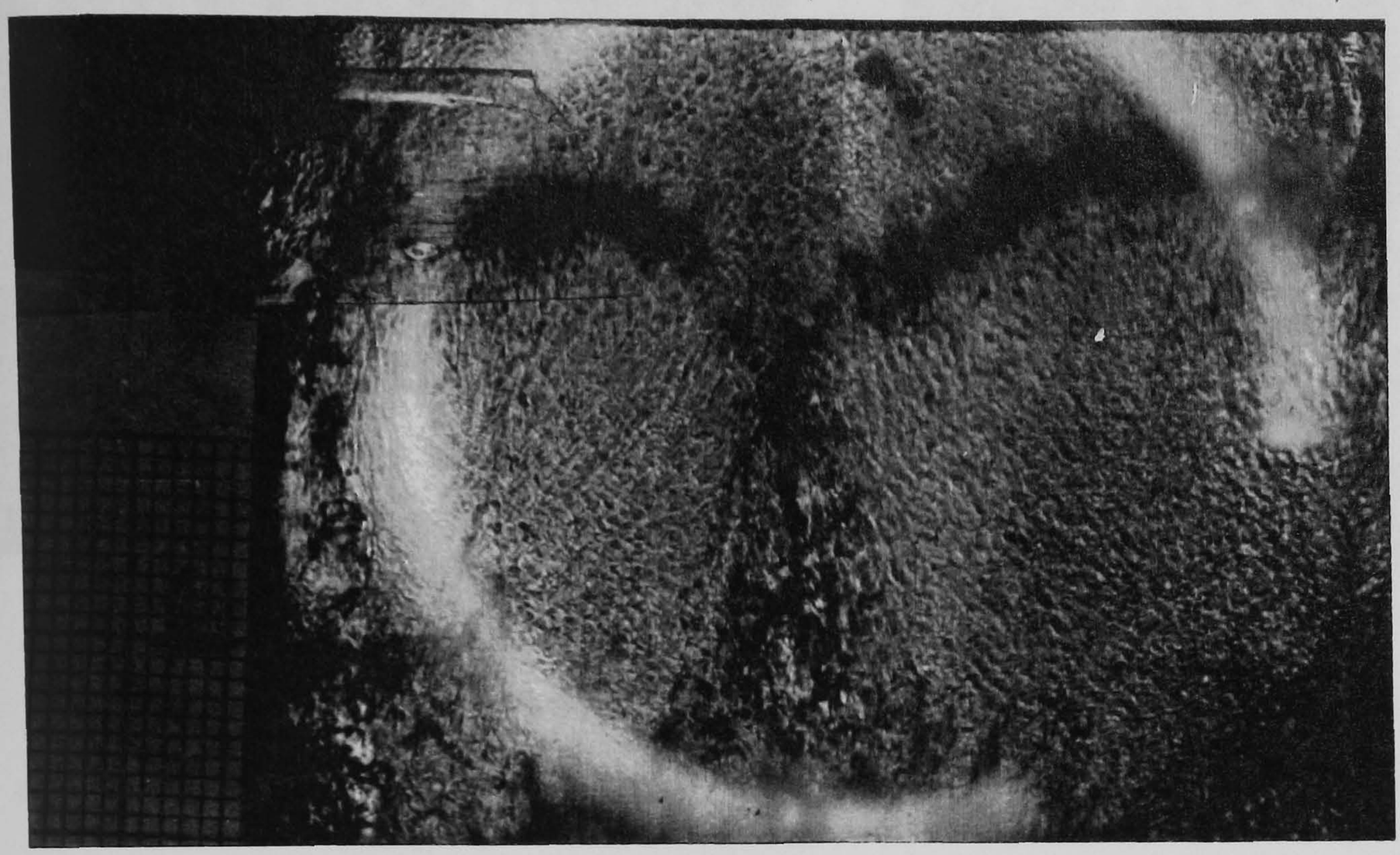

(v)
x =0.26

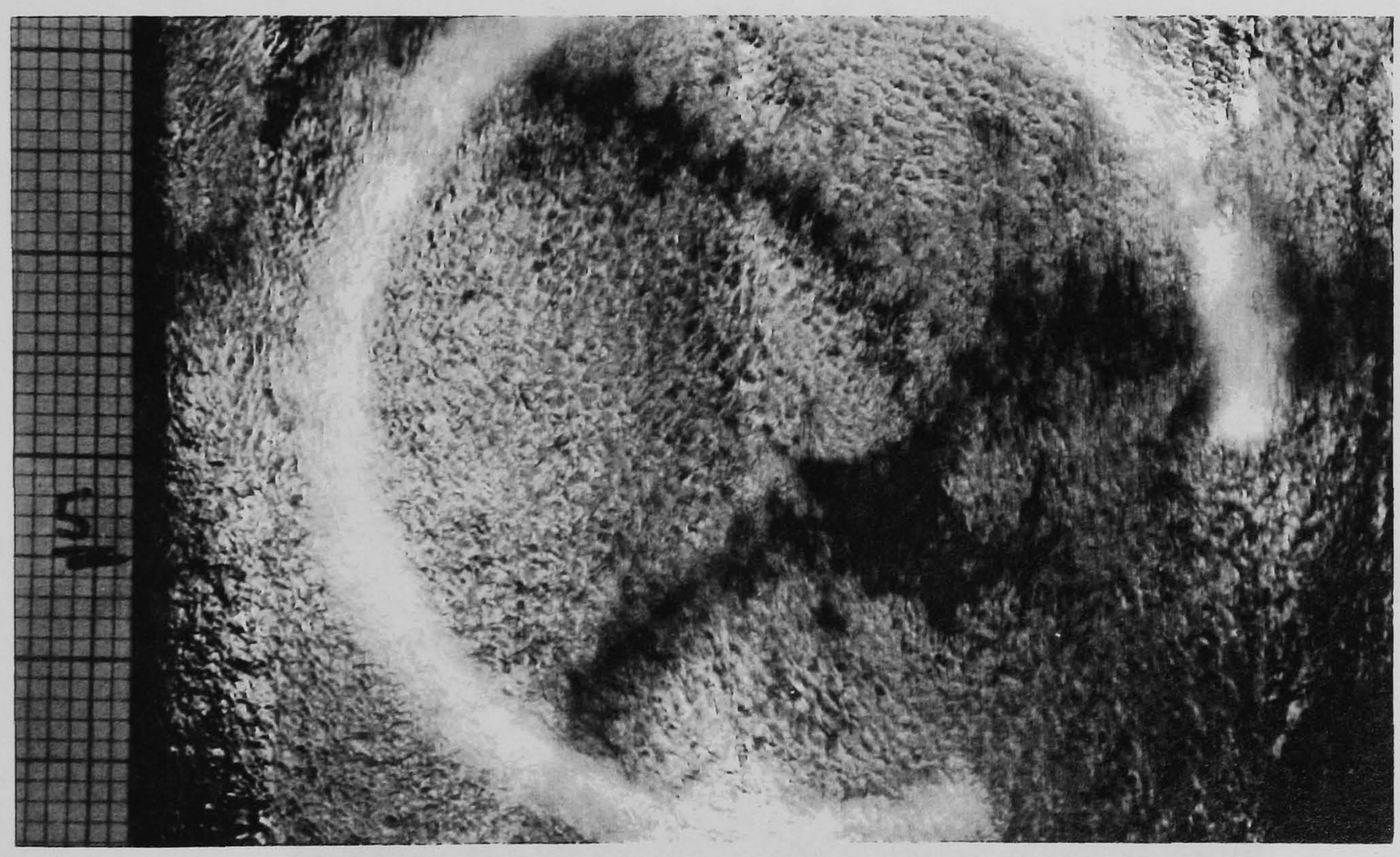

(iv)
x =0.22

Figure 4.4(c) Flow Regimes in Front of Flat Plate 1mmGap- Test Section Mark I.
(G=335kg/m^{2}s, Heat Flux= 44kW/m^2, R113)
(Cont)

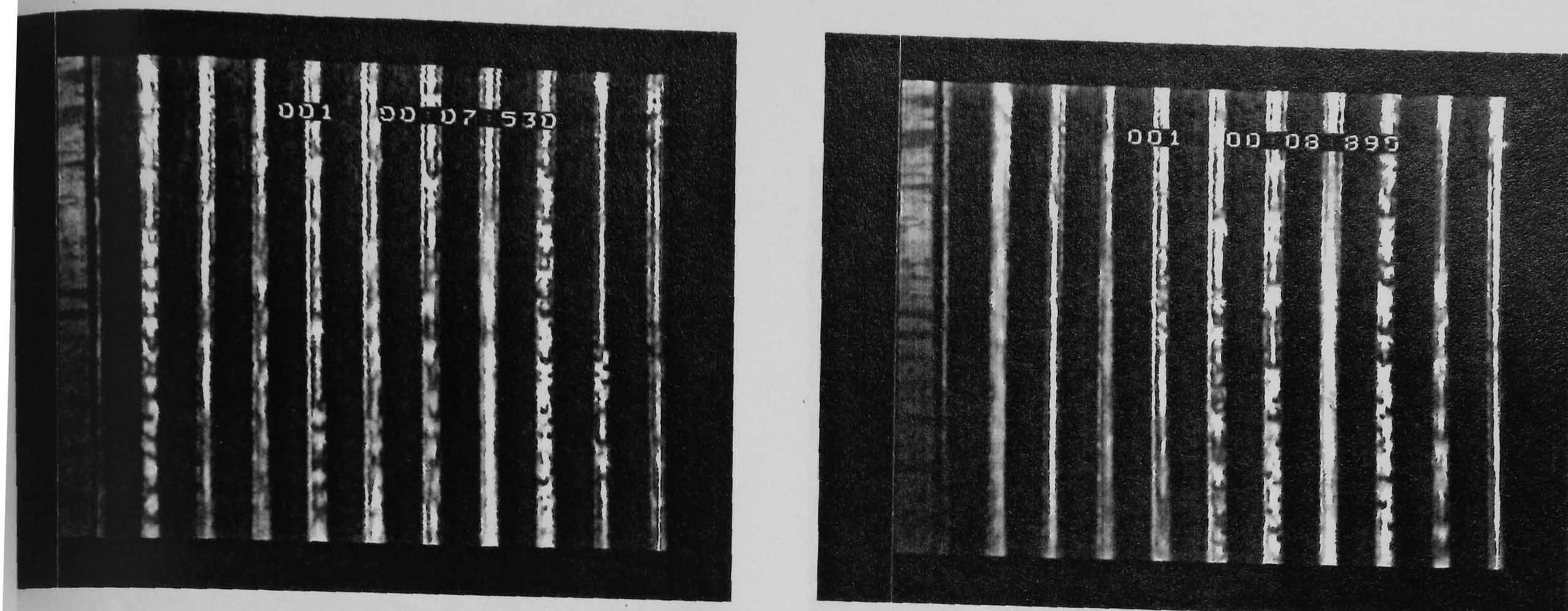

$G=61.5kg/m^2s$, $q=9.2kW/m^2$, x=0.04

Figure 4.4(d) IB, CB and ASF Regimes in Parallel Multi Channels
Test Rig Mark II, 2mm □, R141b

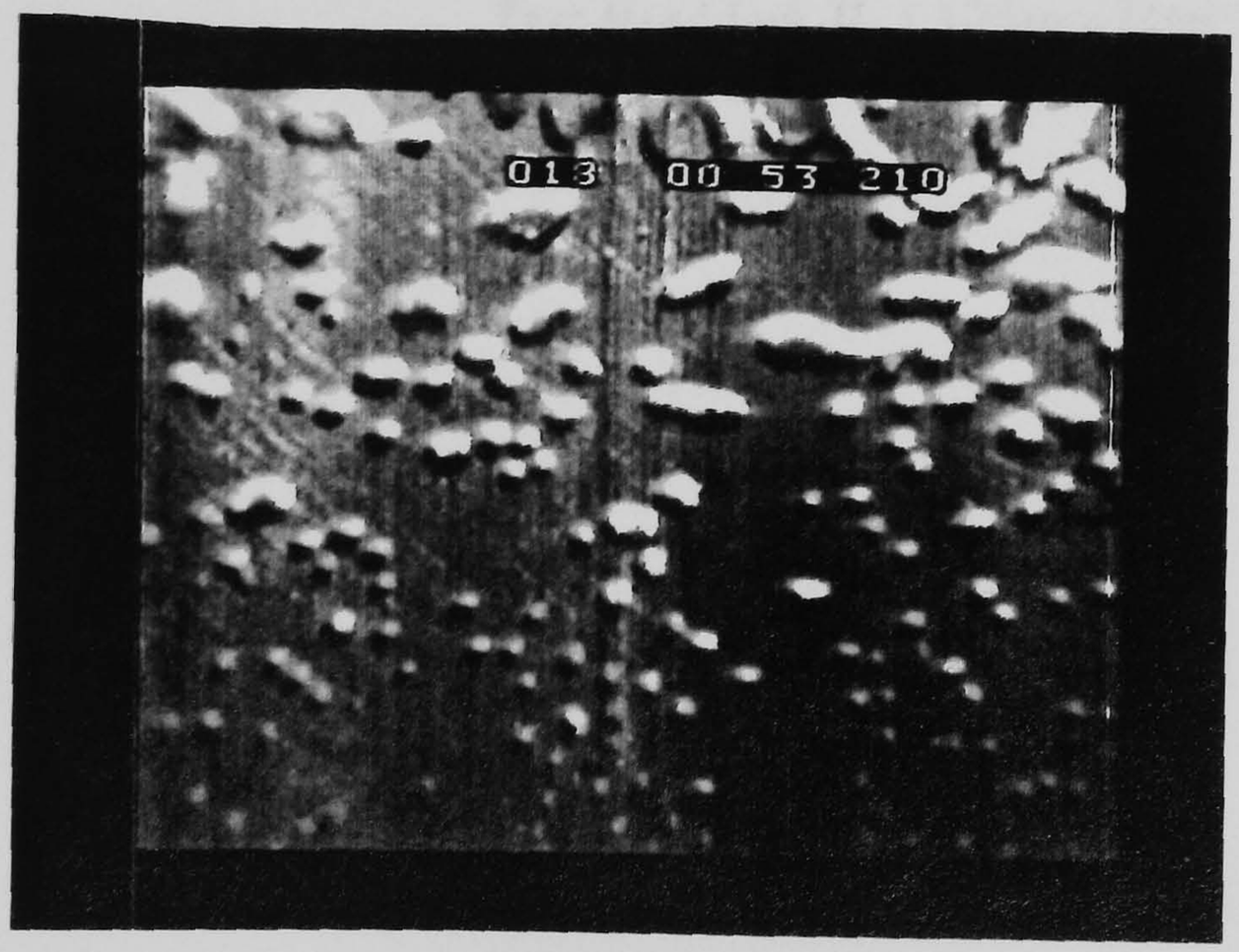

Figure 4.4(e) Isolated Bubbles Developing into Confined Bubbles
Test Rig Mark II, 1.125mm Gap, R141b
(View 60mm wide)

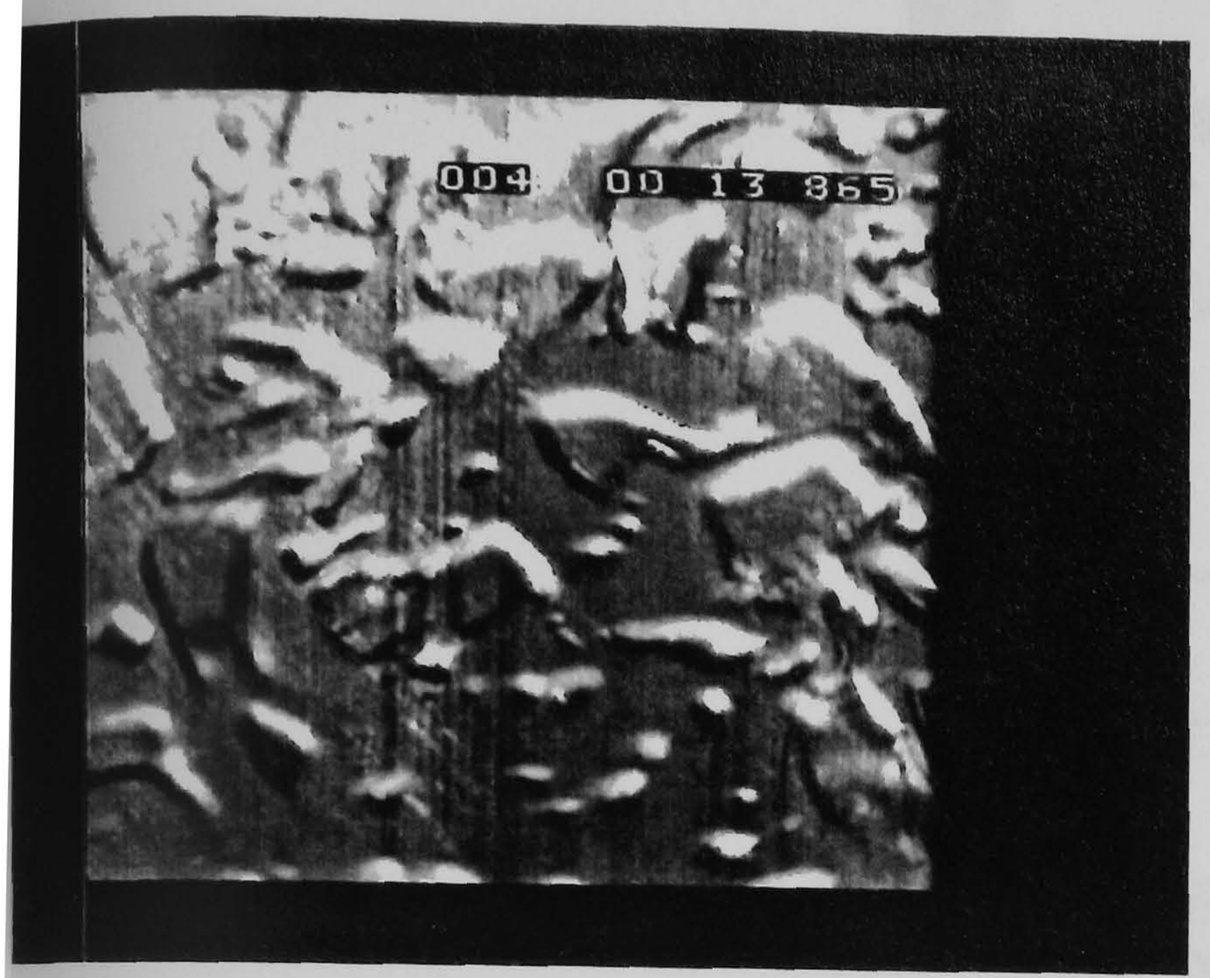

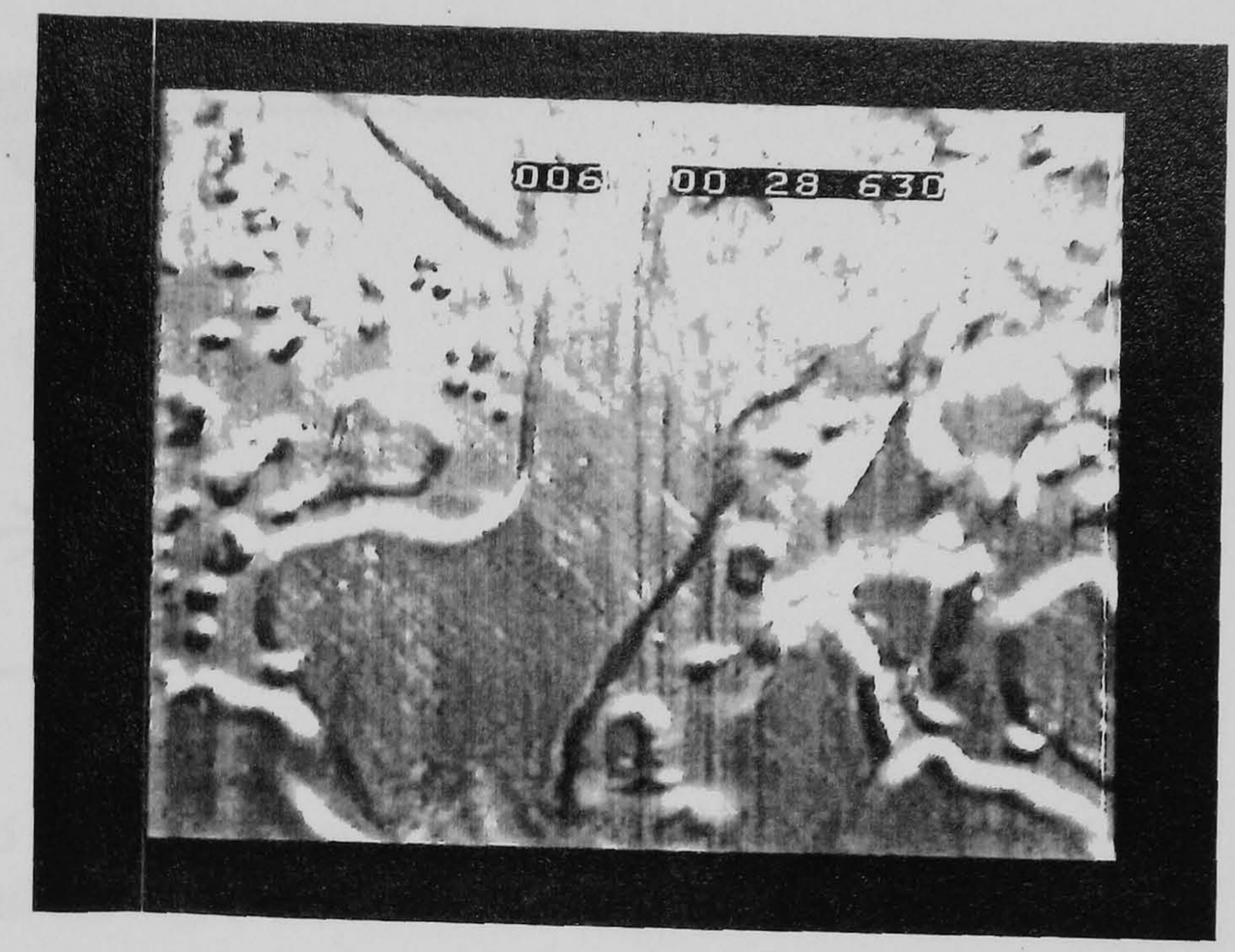

G=16.8kg/m^{2}s, q=4.69kW/m^2,x=0.04

Figure 4.4(f) Confined Bubble Regime
Test Rig Mark II, 1.125mm Gap, R141b
(View 60mm wide)

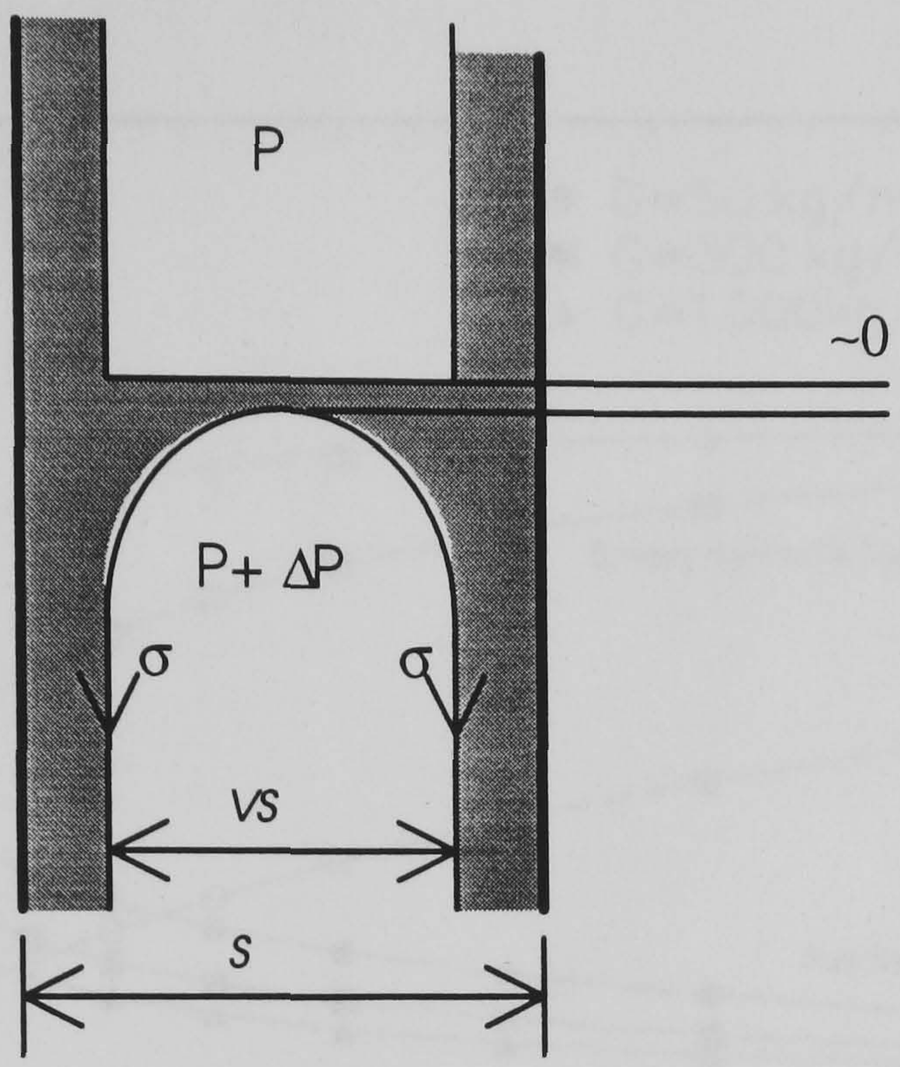

Figure 4. 5 Idealised Liquid Bridge as Used in the Analysis of Lowry and Kawaji (1988)

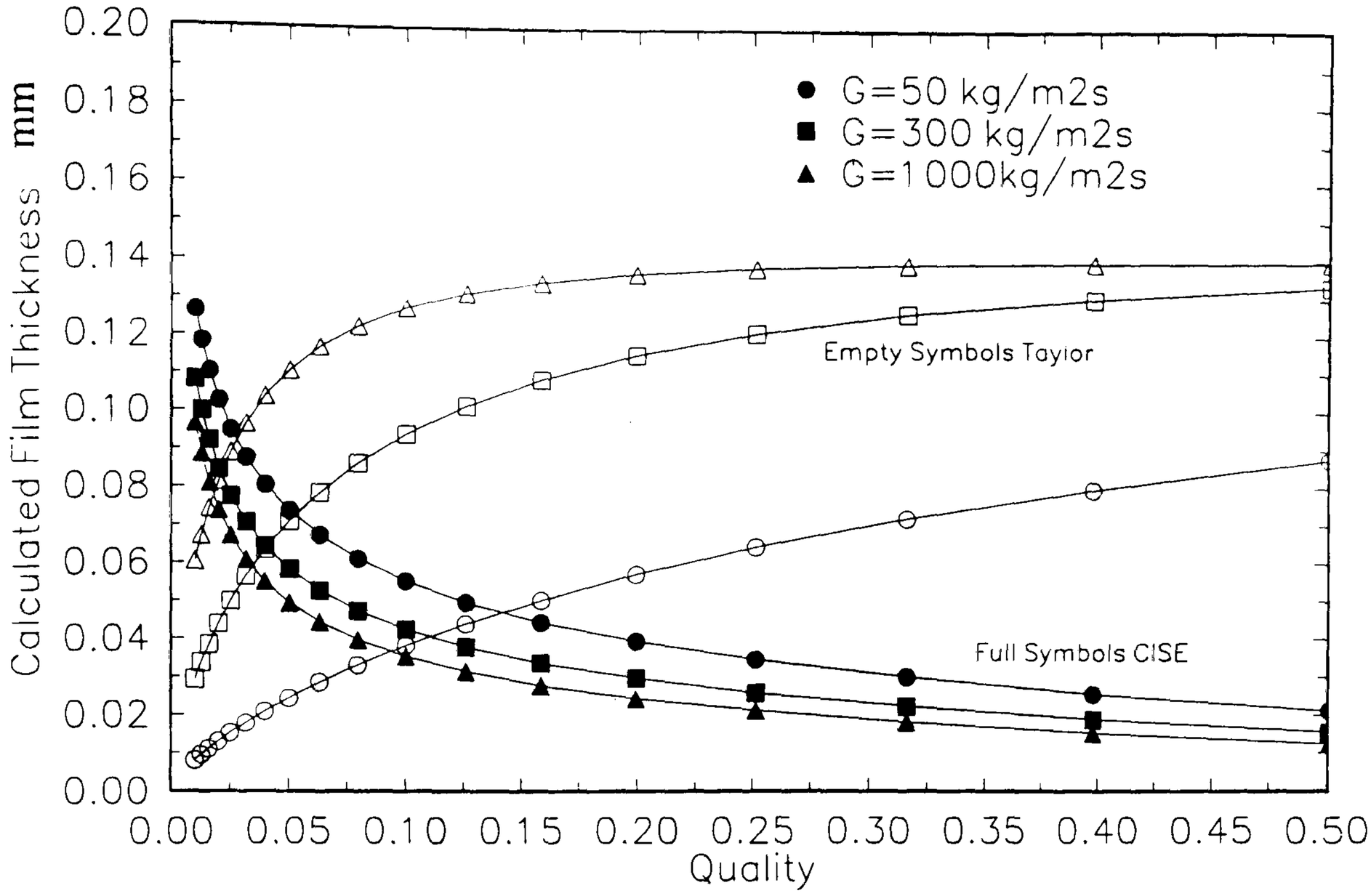

(a)Tube Diameter 1.0mm

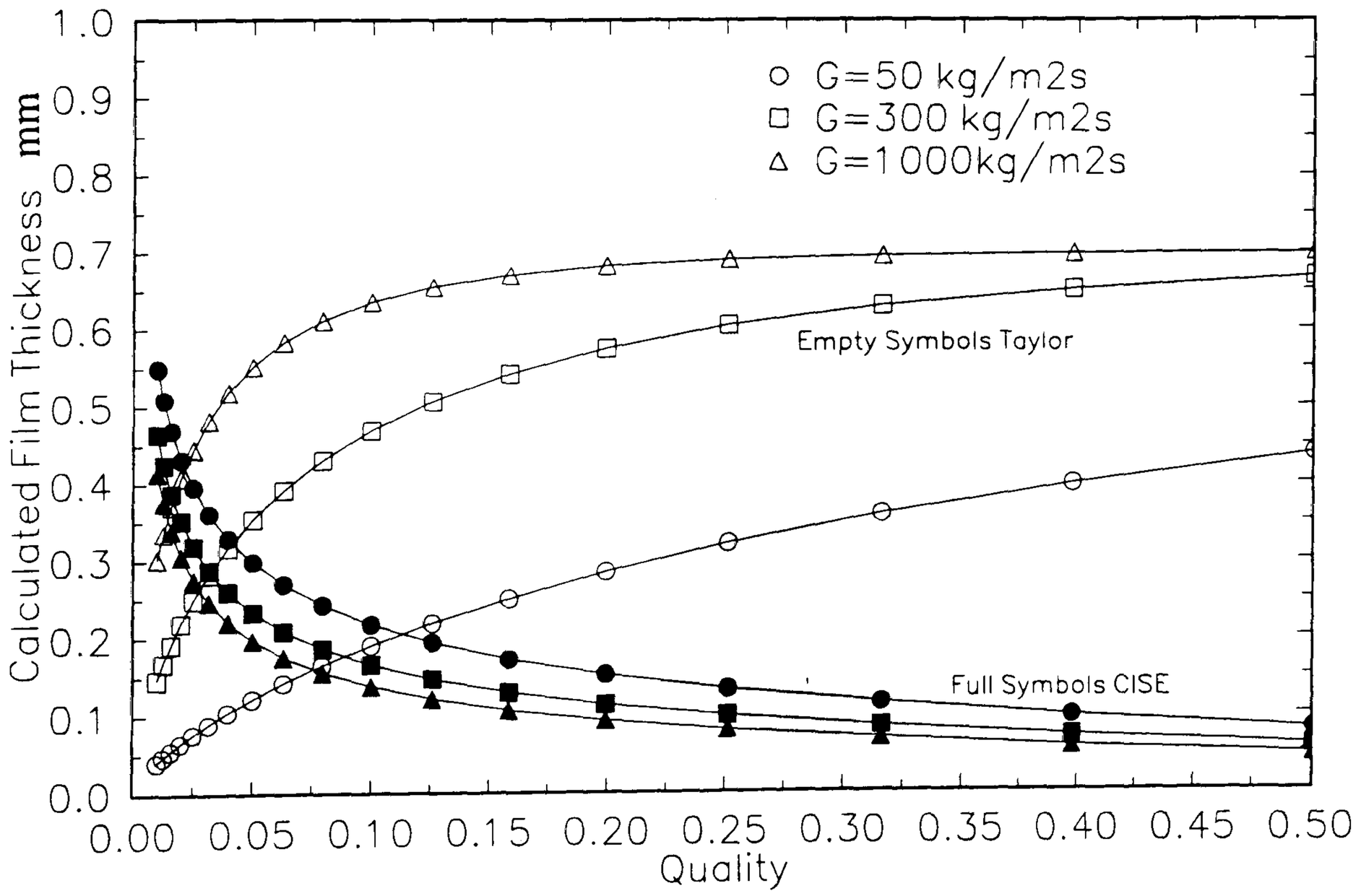

(b)Tube Diameter 5mm

Figure 4.6. Predicted Film Thicknesses Used in Prediction of Onset of Annular-Slug Flow

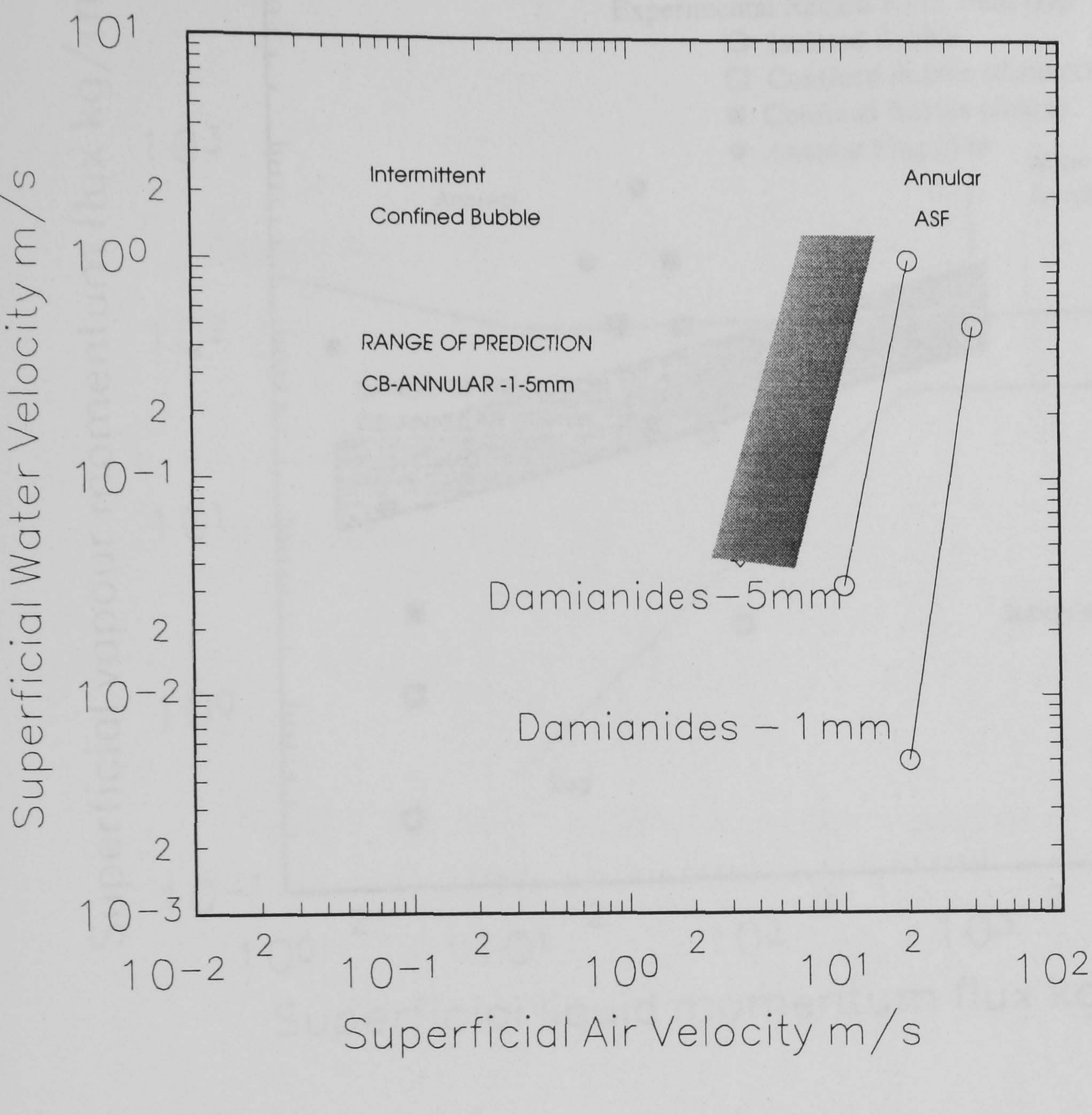

Figure 4.7 Comparison of Model with Data of Damianades and Westwater (1988)

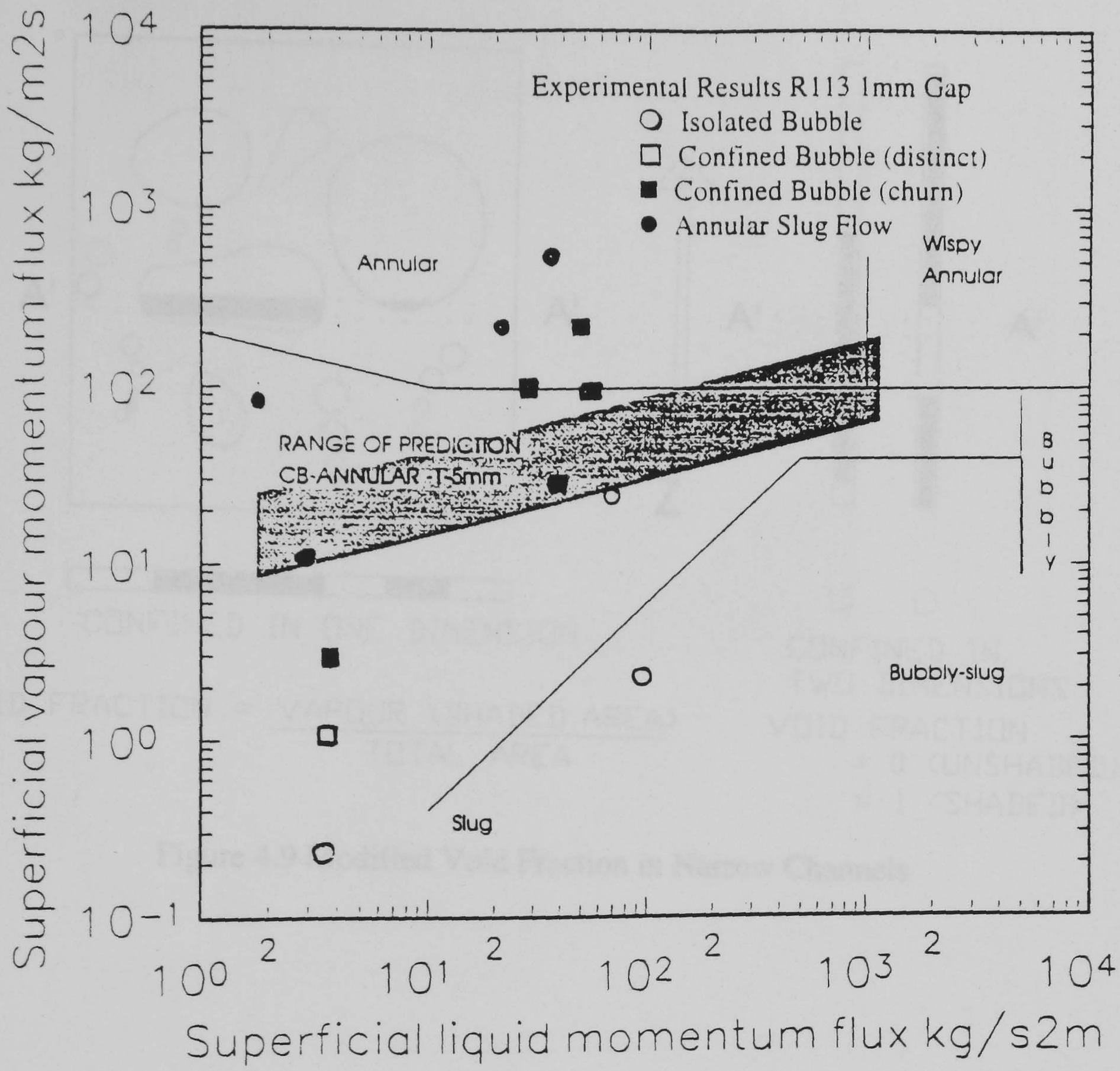

Figure 4.8 Comparison of model predictions with Map of Hewitt and Roberts(1969)

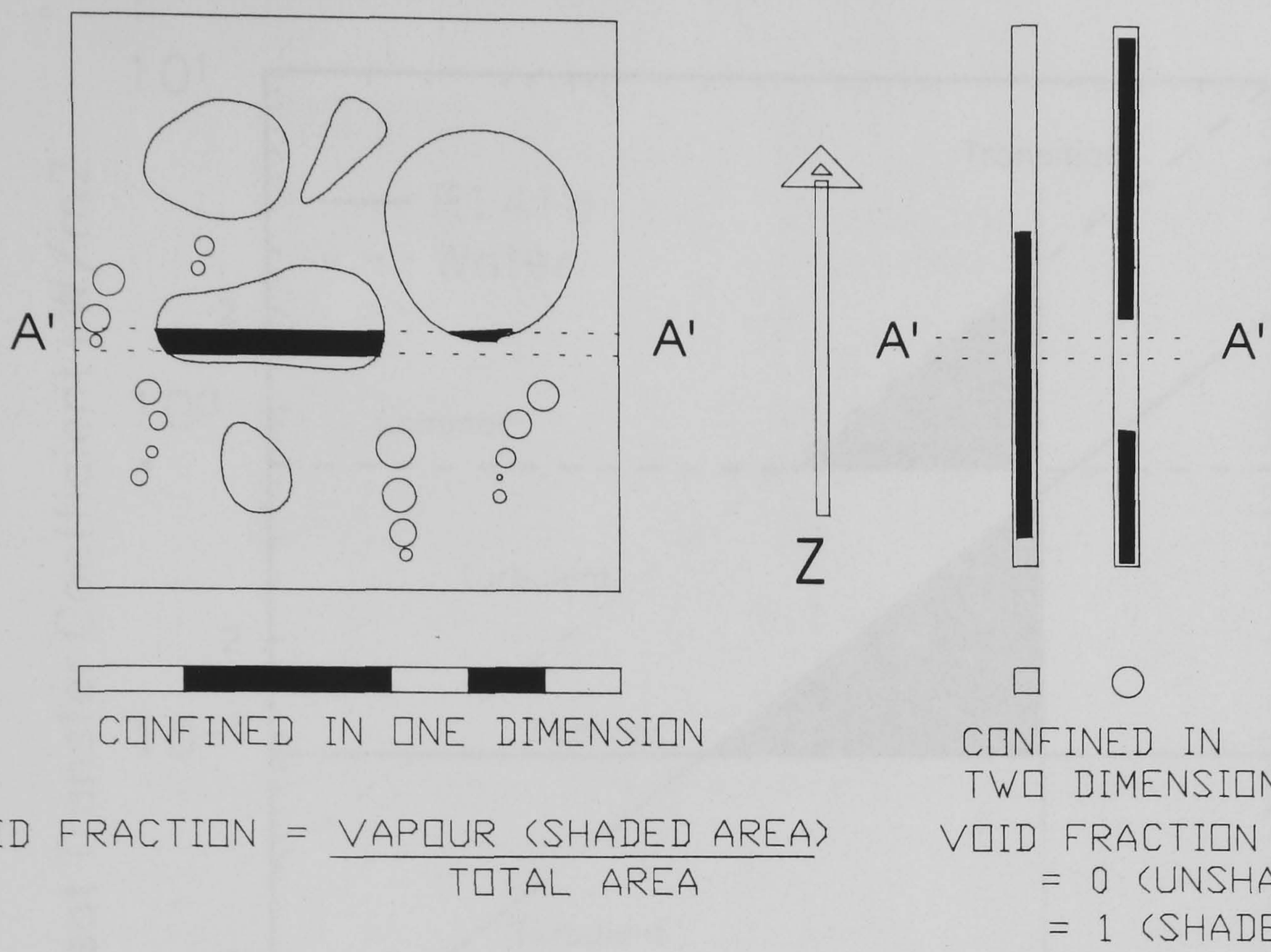

Figure 4.9 Modified Void Fraction in Narrow Channels

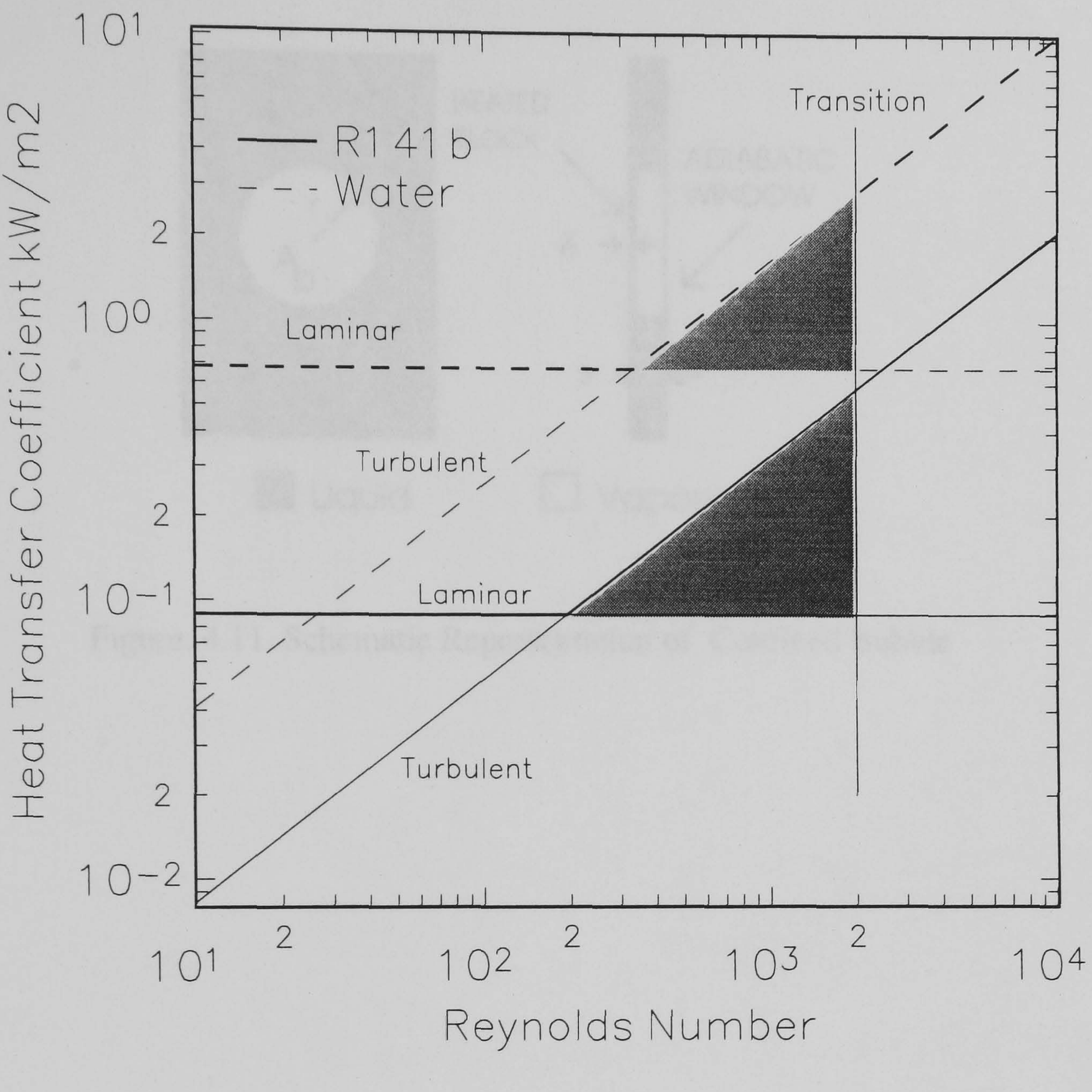

Figure 4.10 Enhancement Due to Transition from Laminar to Turbulent Flow

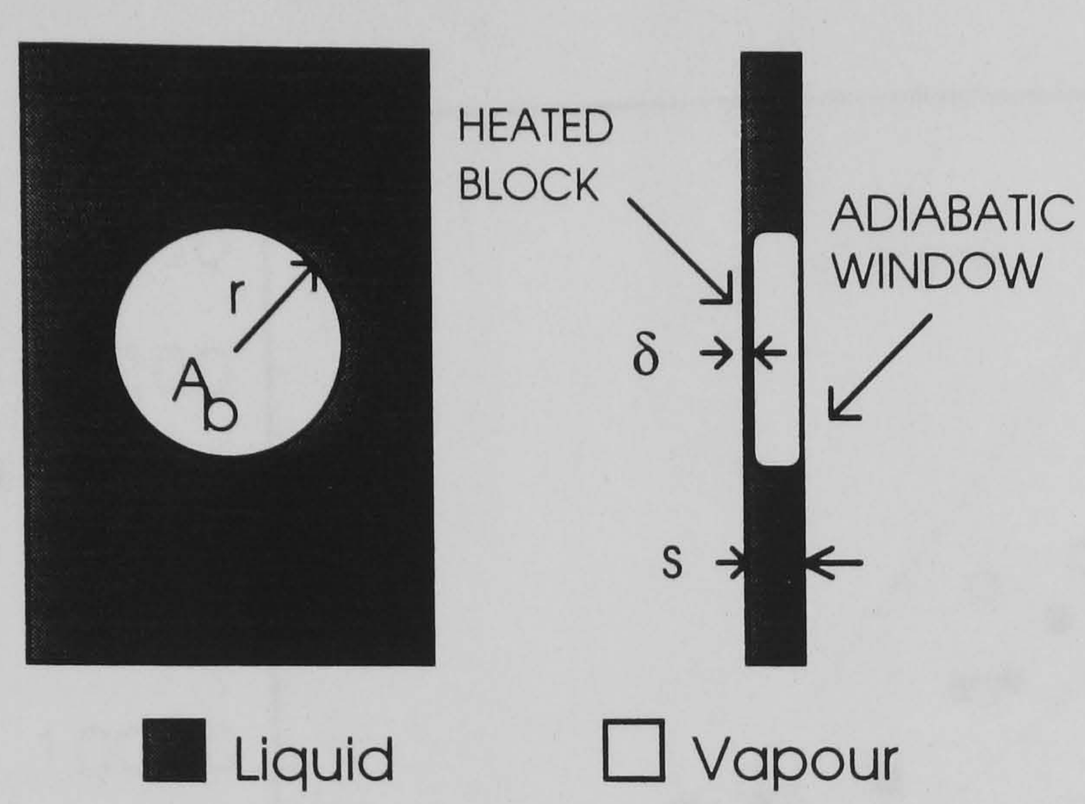

Figure. 4.11 Schematic Representation of Confined Bubble

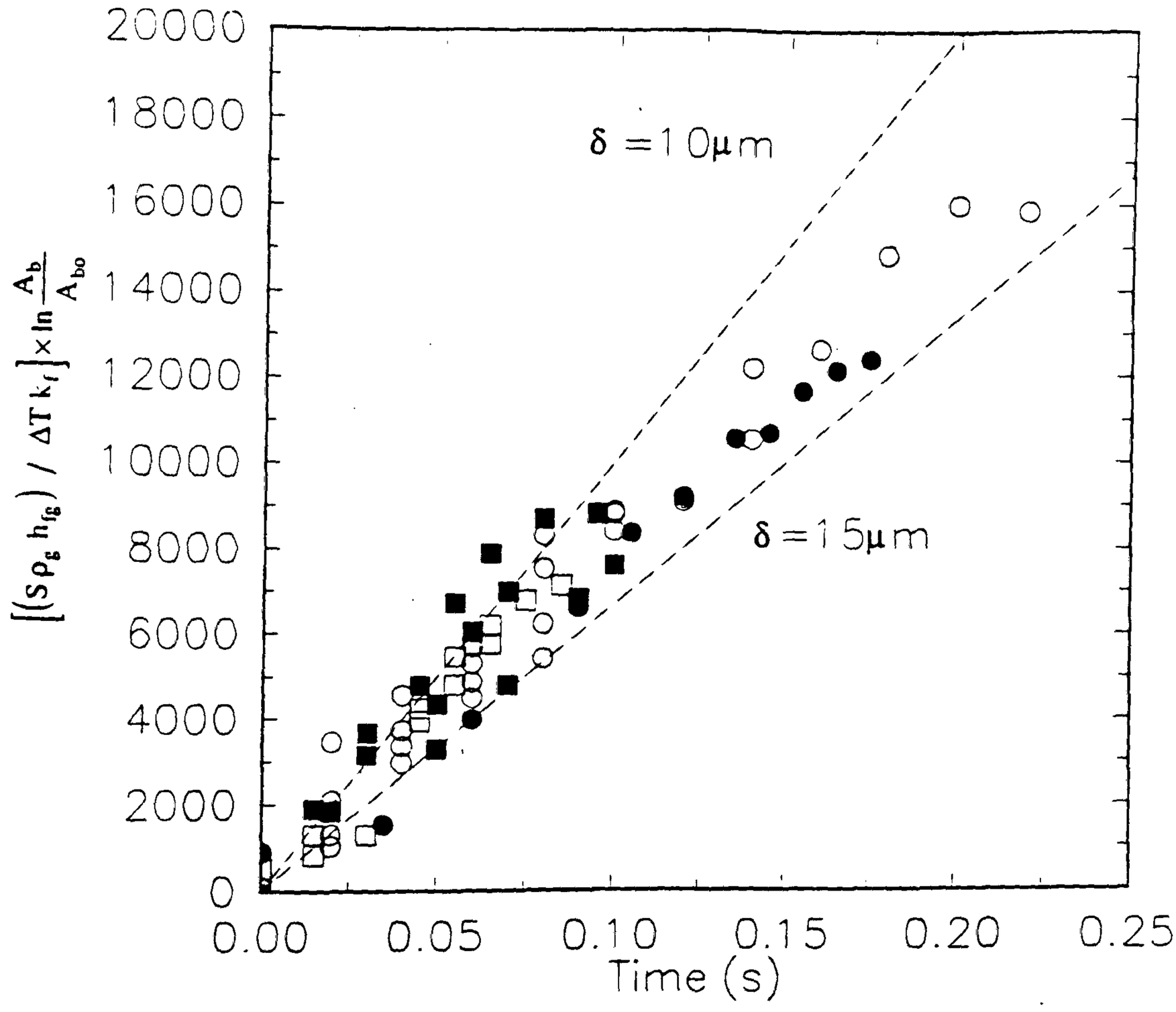

Figure 4.12(a) Estimate of Microlayer Thickness under Confined Bubble R113

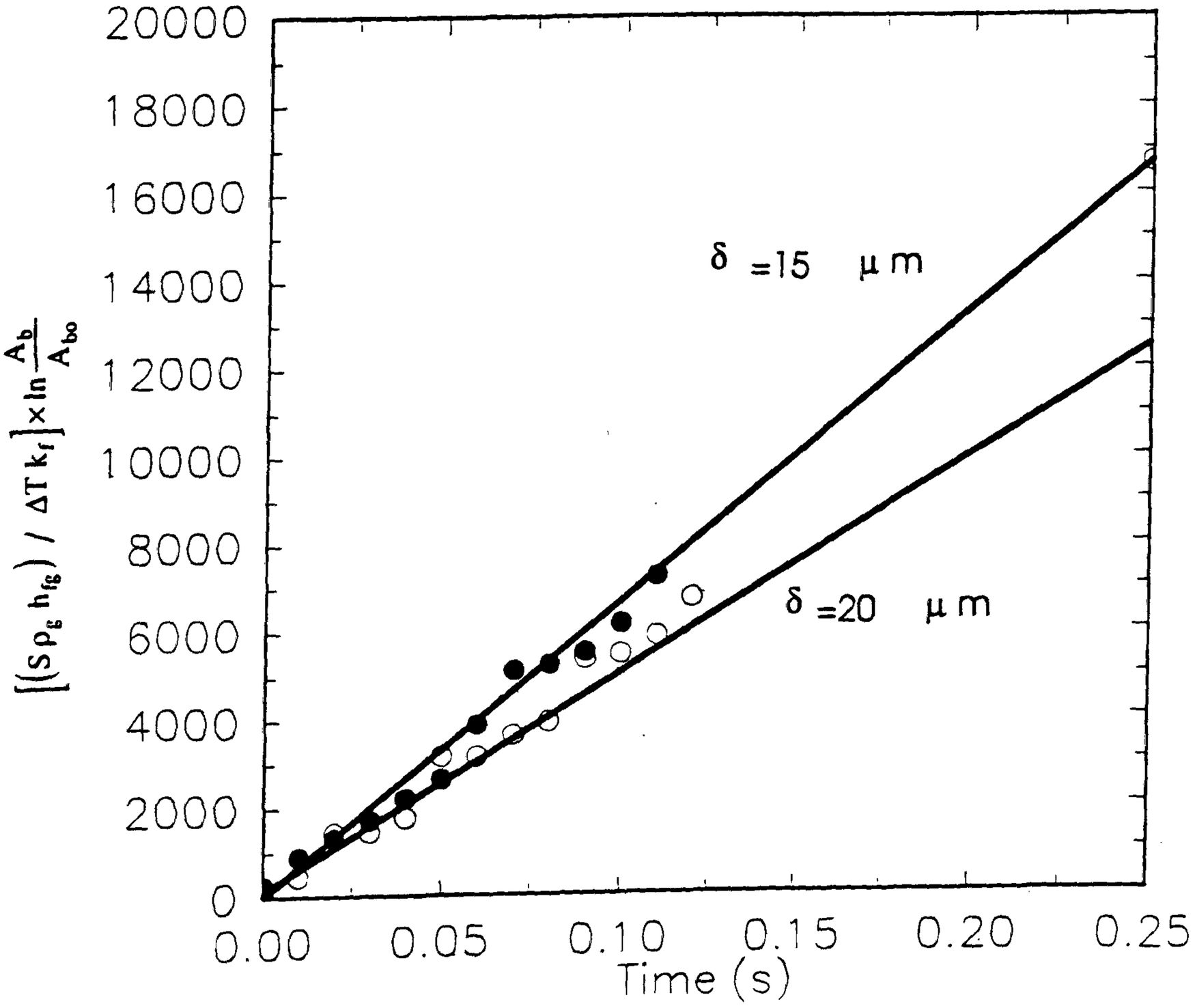

Figure 4.12(b) Estimate of Microlayer Thickness under Confined Bubble R141b

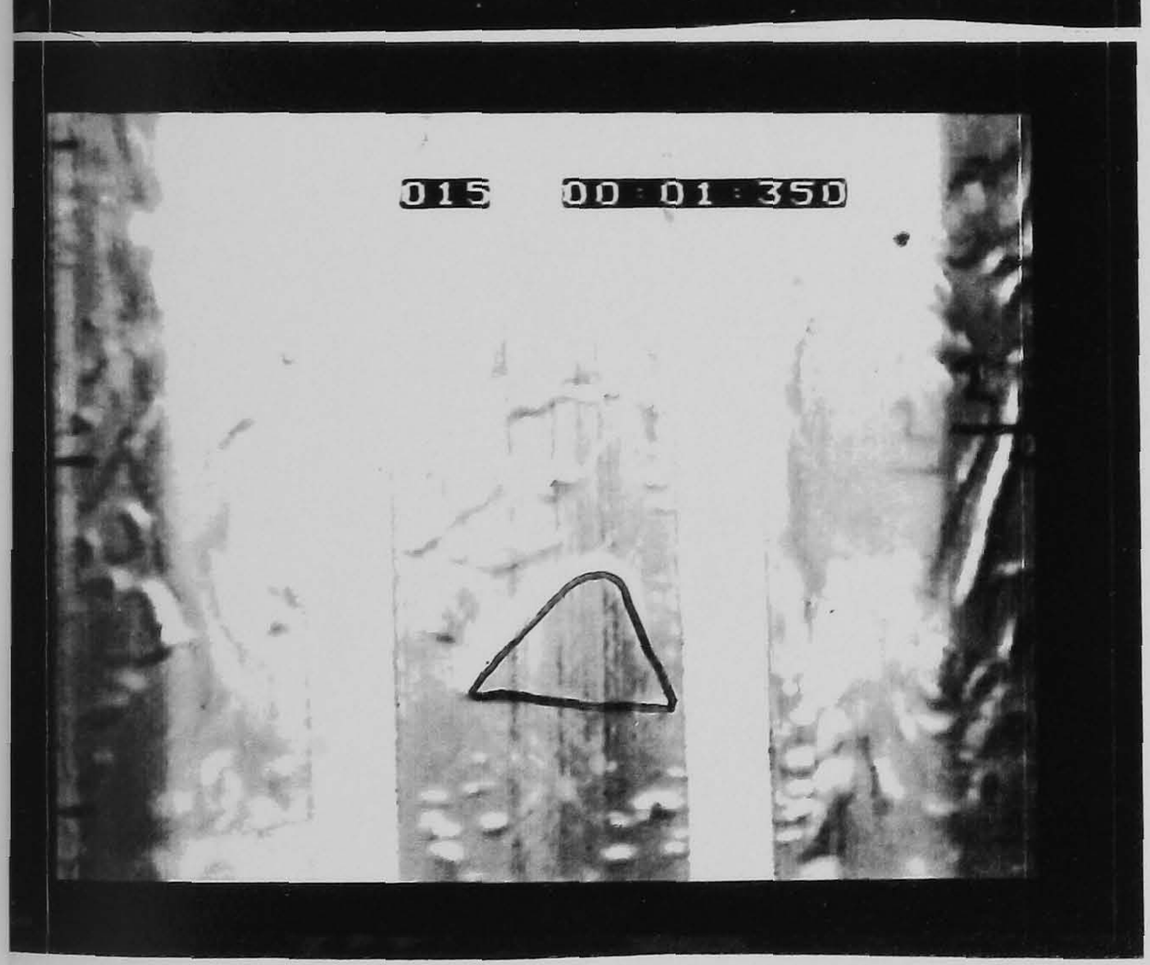

Figure 4.13 Video Sequence Showing Growth of Bubble R141b-2

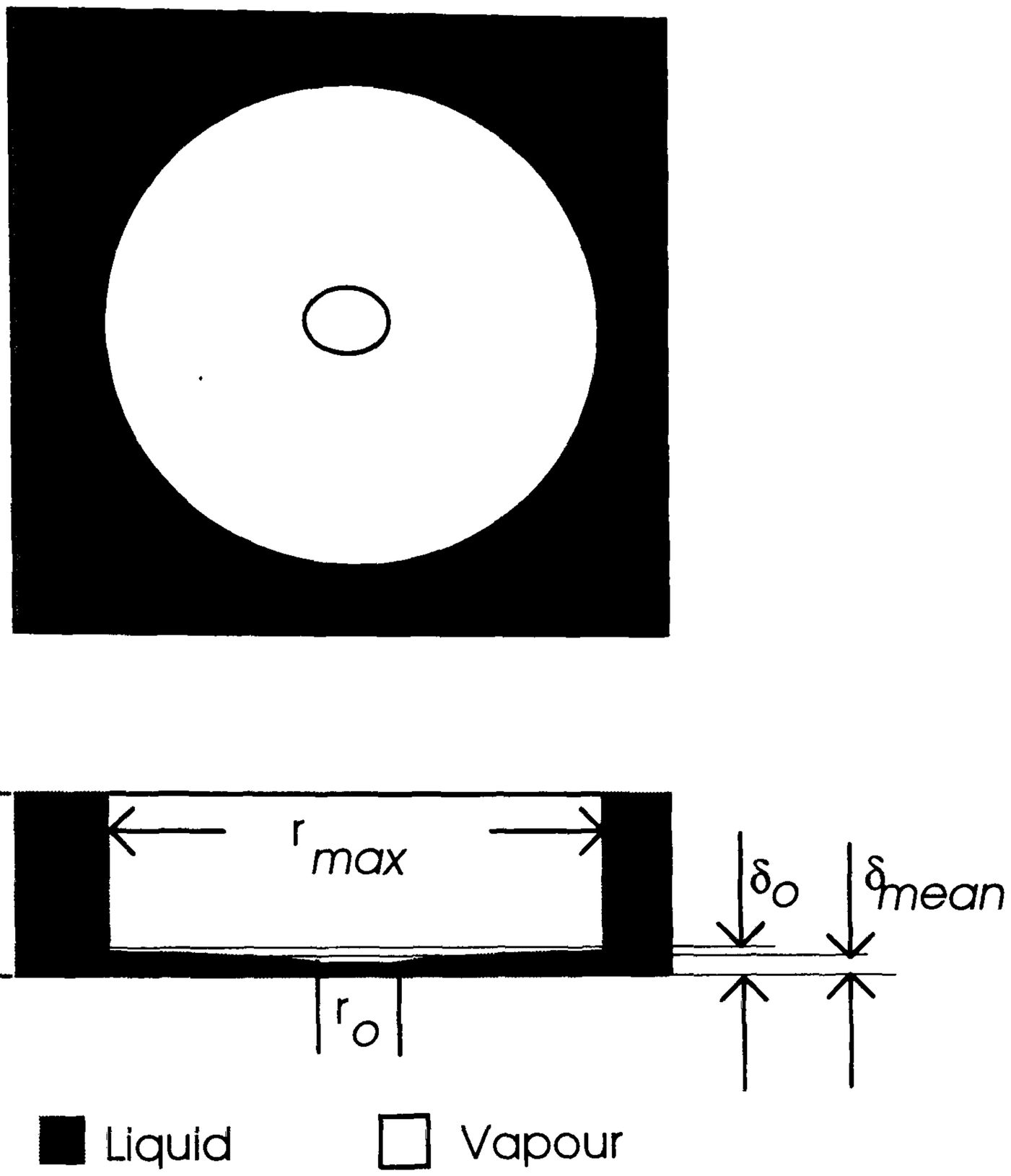

Figure 4.14 Schematic Diagram Showing Film Profile (Not to Scale)

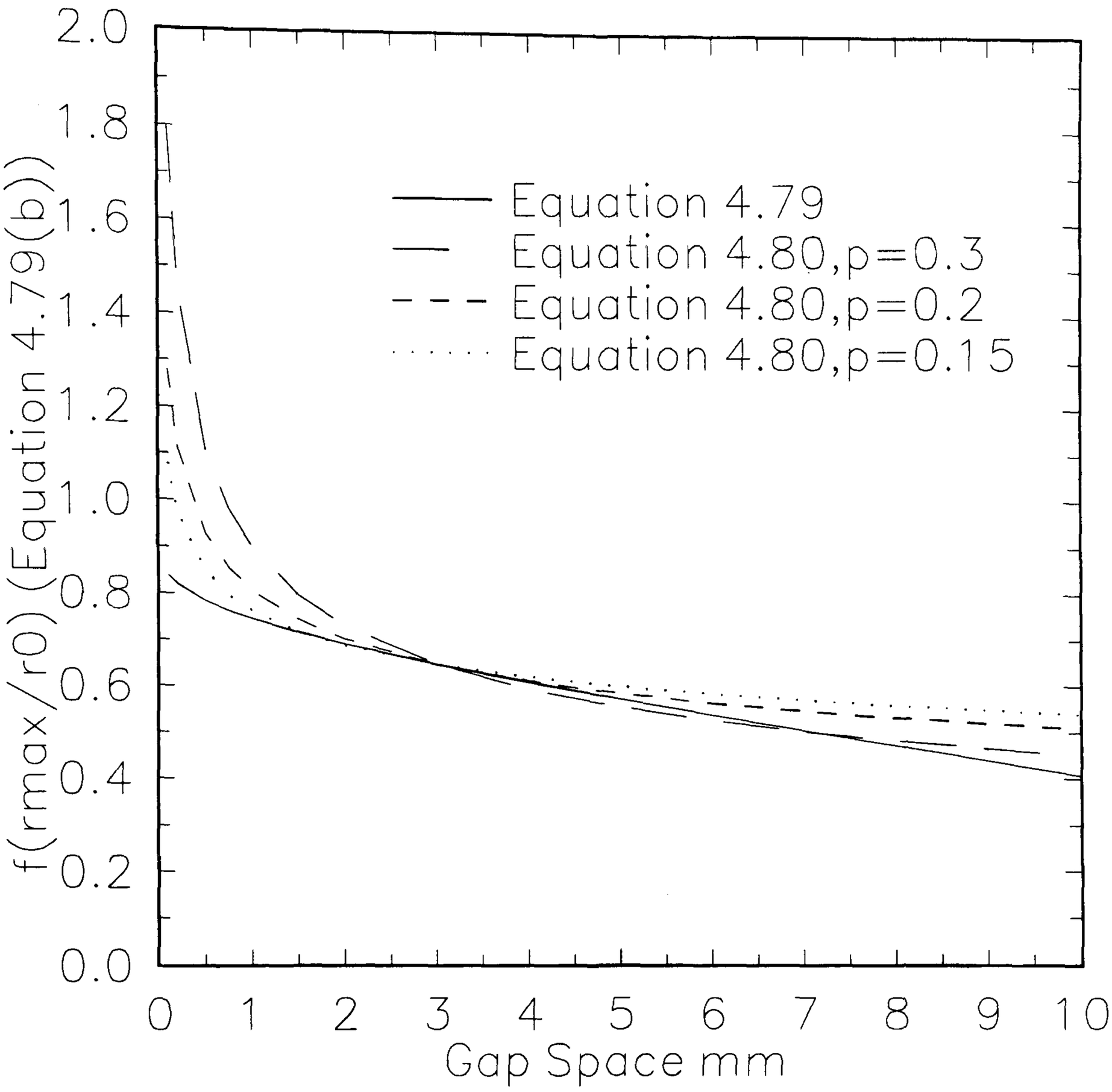

Figure 4.15 Predicted Influence of Gap Spacing

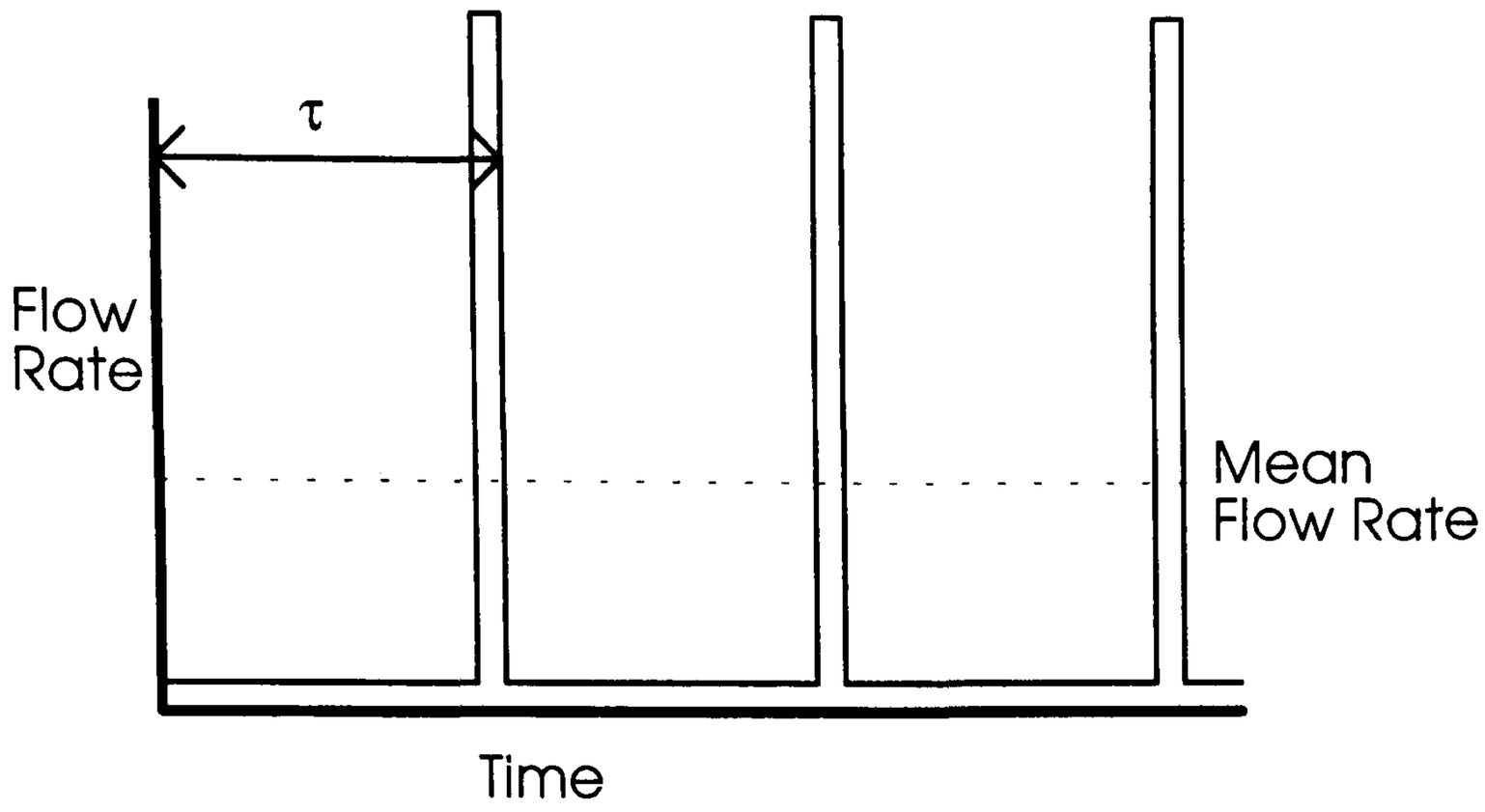

Figure 4.16. Schematic Representation of Pulsed Flow

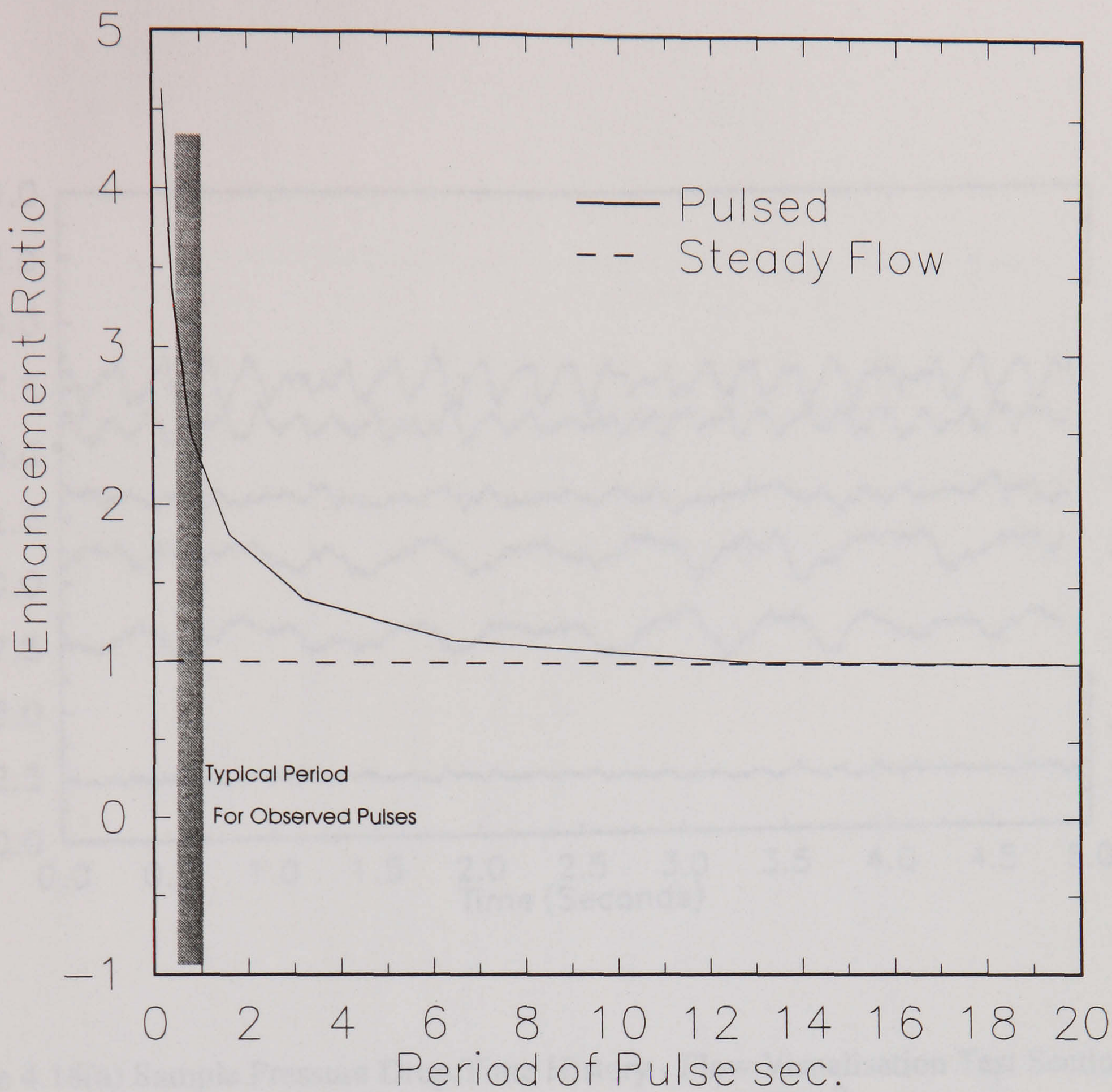

Figure 4. 17 Enhancement due to Pulsing Flow in Tube
(Water, Tube diameter 2.87mm,
Nusselt No. 3.65)

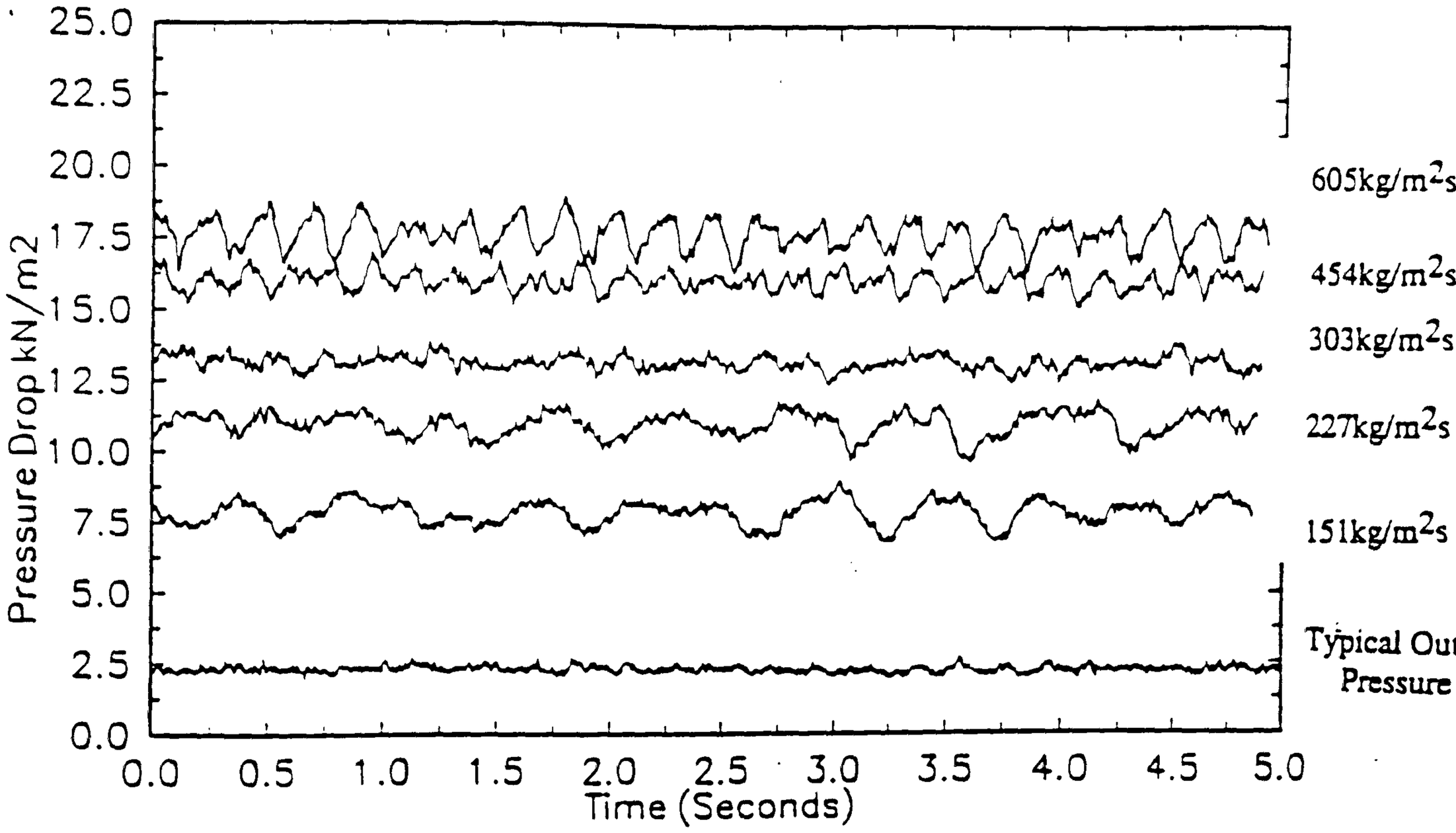

Figure 4.18(a) Sample Pressure Drop Time History - Flow Visualisation Test Section
(R141b, Channels 2mm square, q=46kW/m^2)

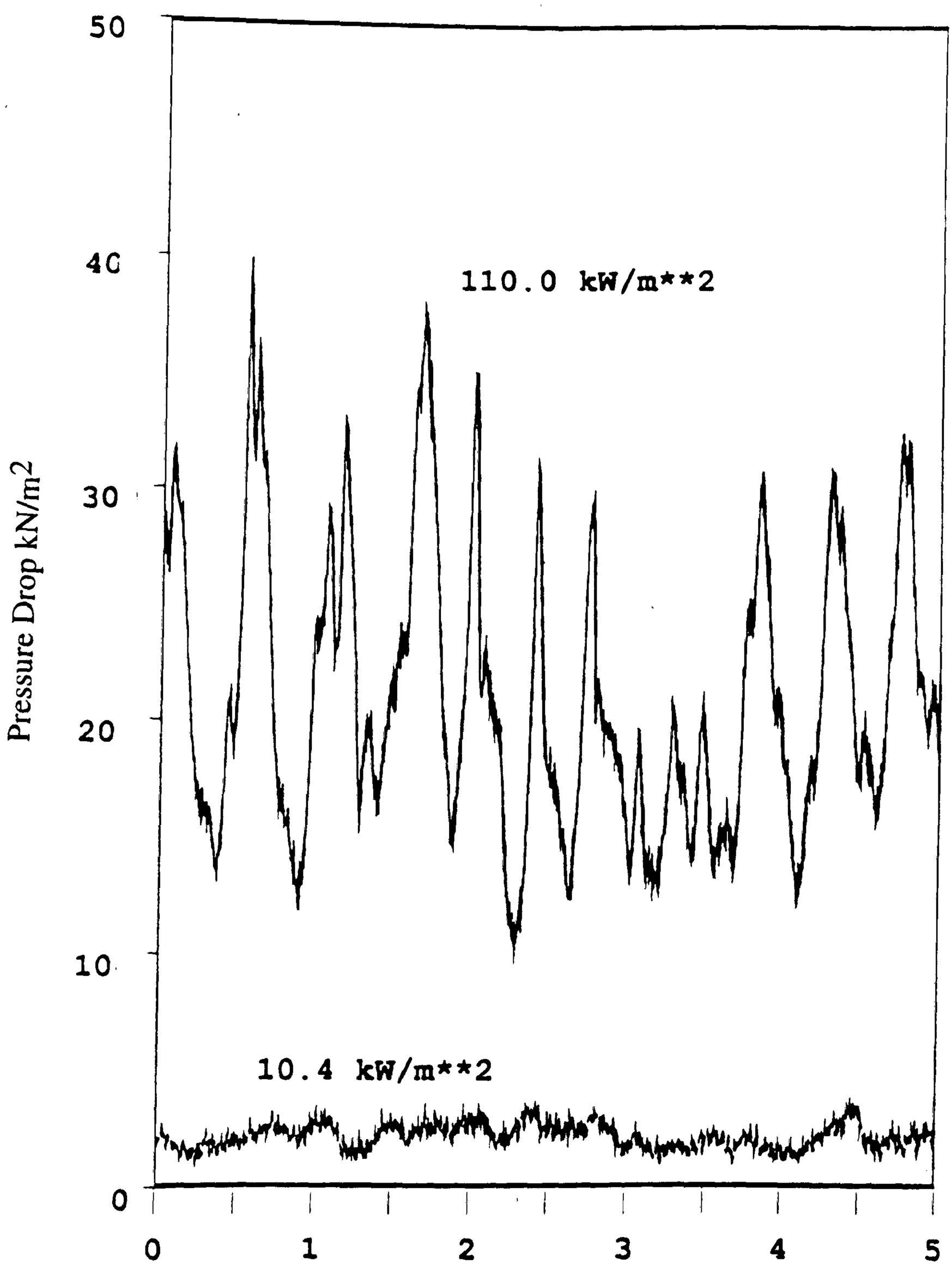

Figure 4.18(b) Sample Pressure Drop Time History - Single Tube Test Section
(Water, Tube Diameter 2.87mm, G=300kg/m^{2}K)

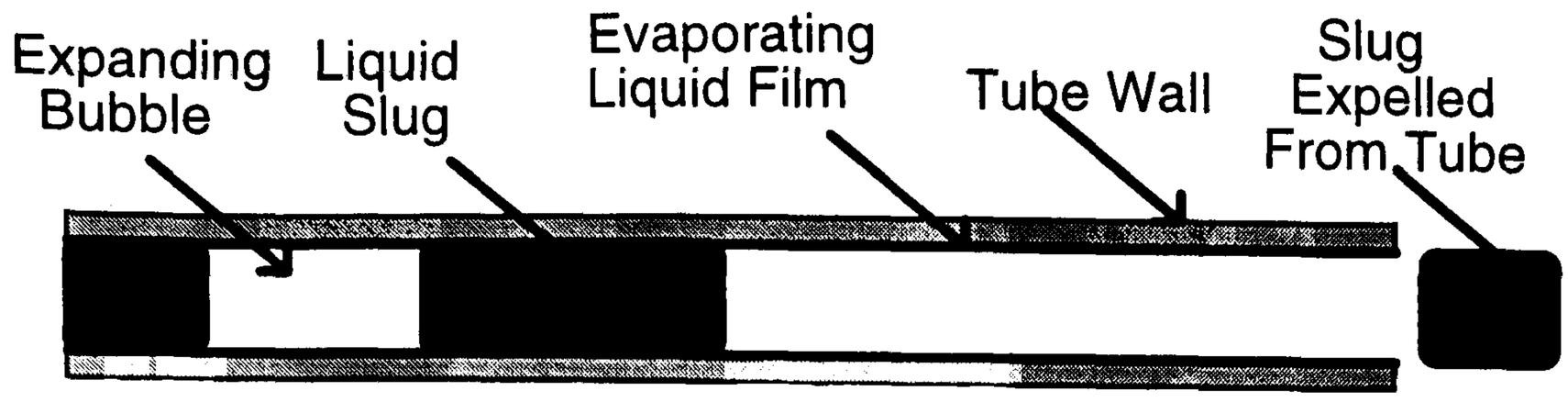

Figure 4.19 Model of Processes in Boiling in Confined Bubble or Annular Slug Flow

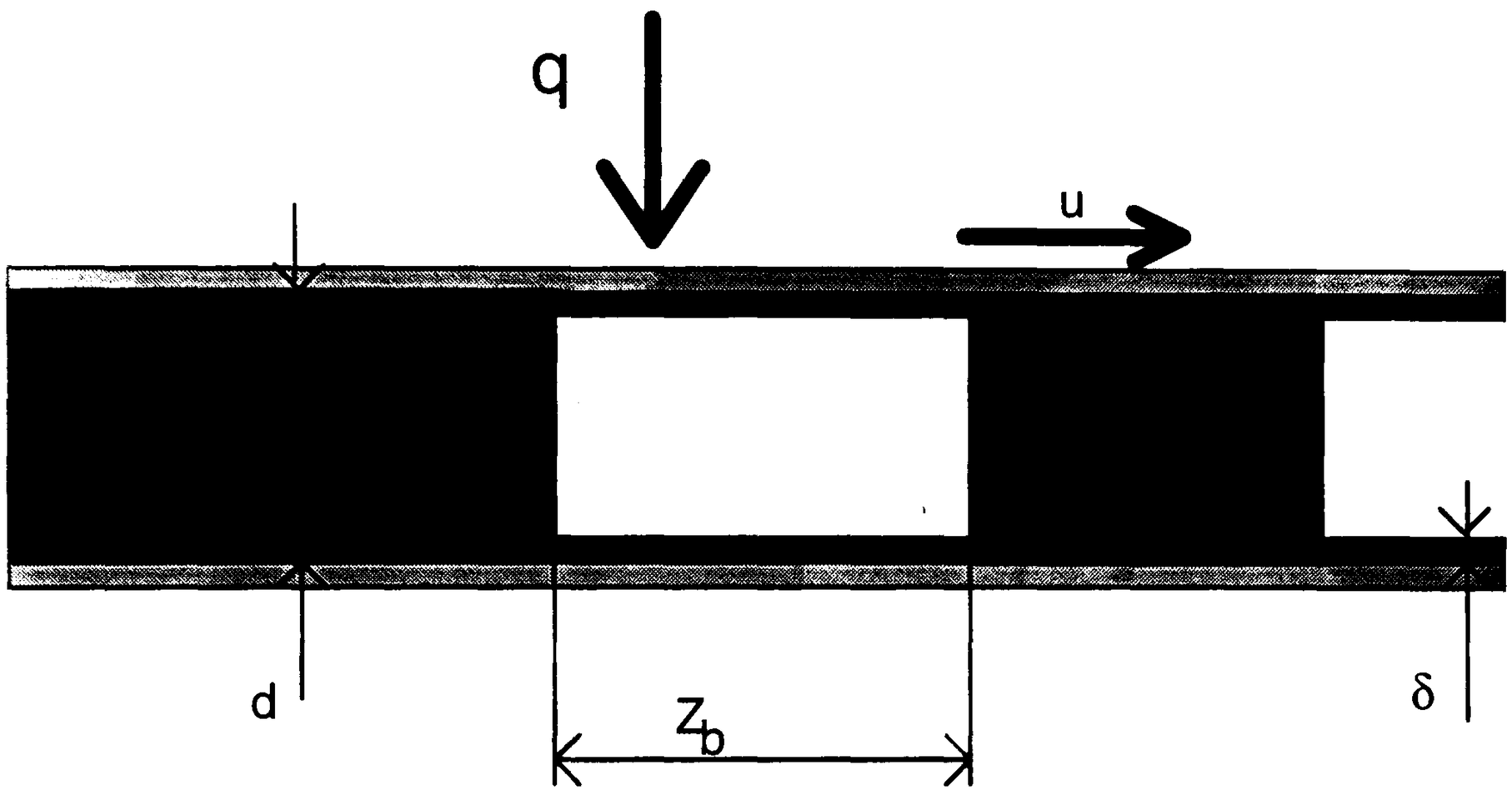

Figure 4.20. Nomenclature Used in Analysis of Pressure Fluctuations

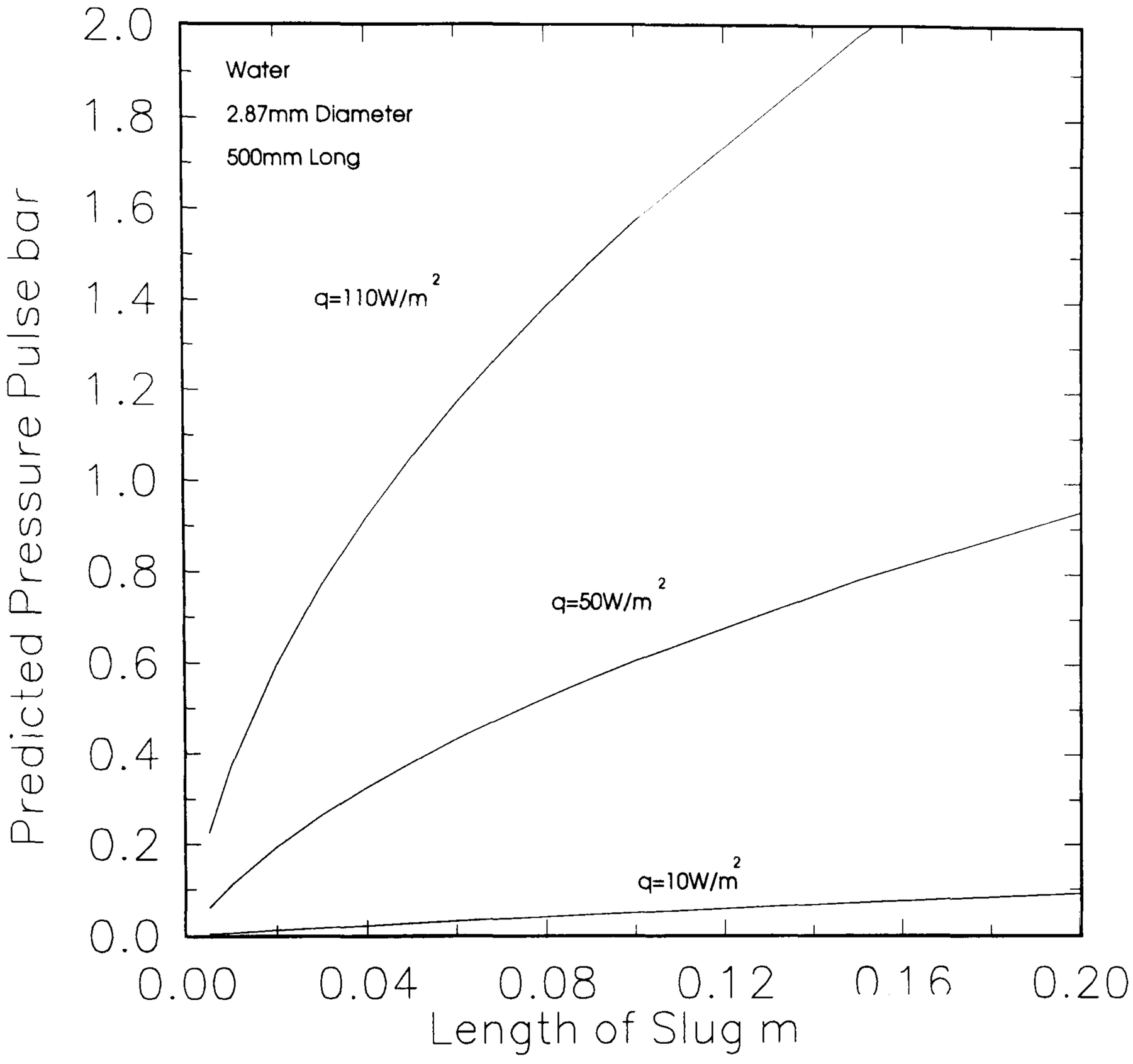

Figure 4.21(a) Magnitude of Pressure Pulse Caused by Acceleration of Slug

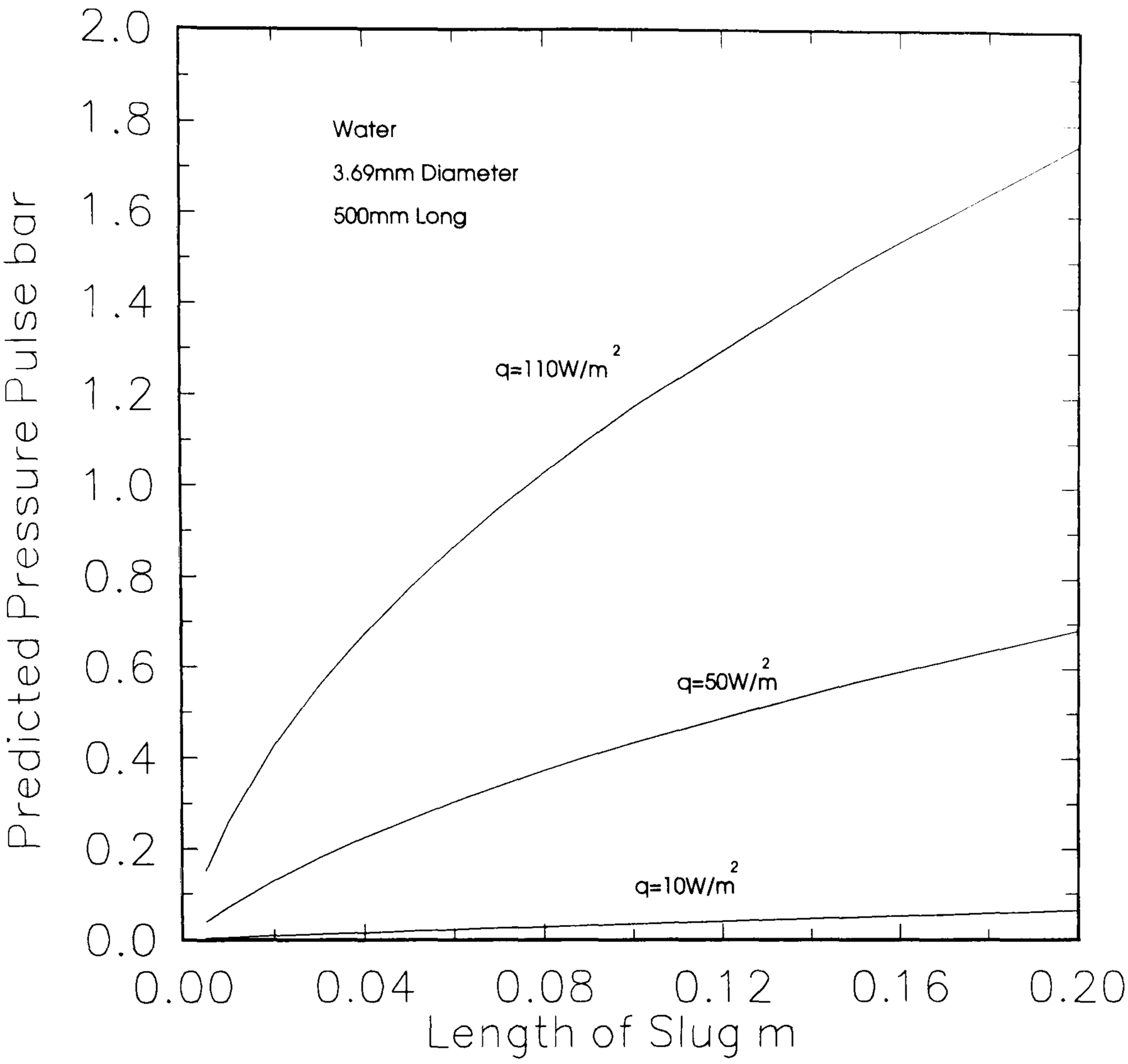

Figure 4.21(b) Magnitude of Pressure Pulse Caused by Acceleration of Slug

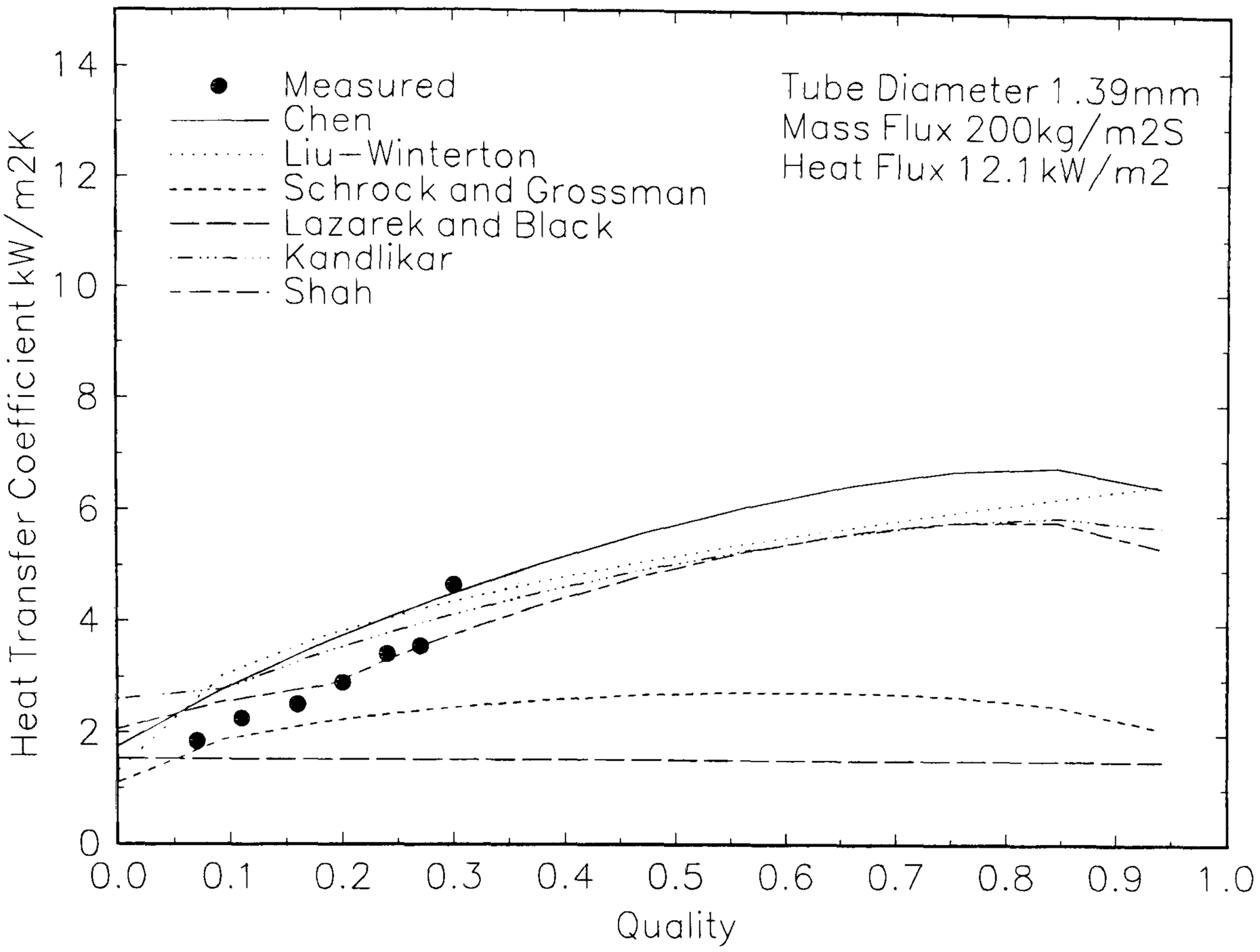

(a)

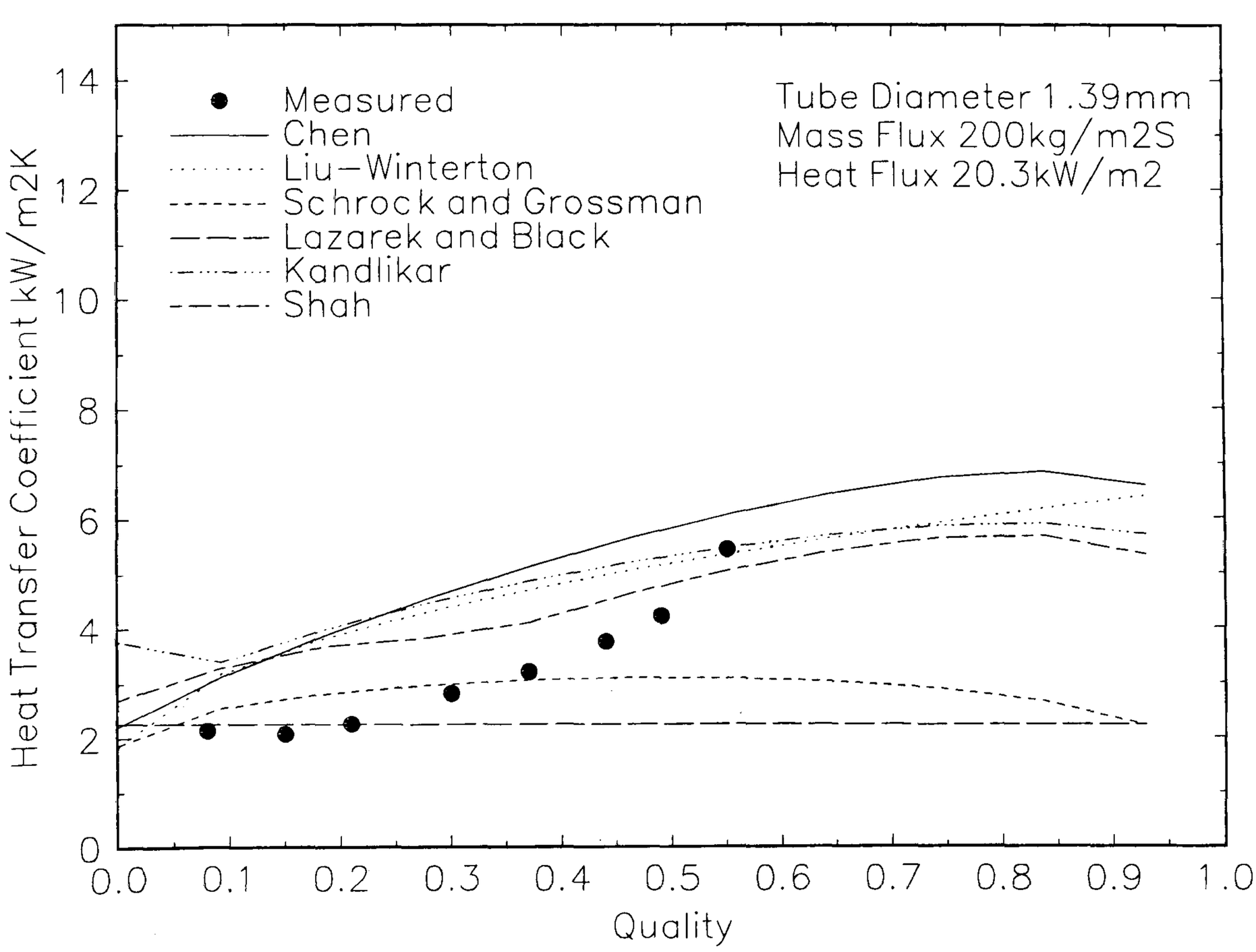

(b)

Figure 5.1 Comparison of Measured Data with Predictions of Published Correlations for 1.39mm Diameter Tube

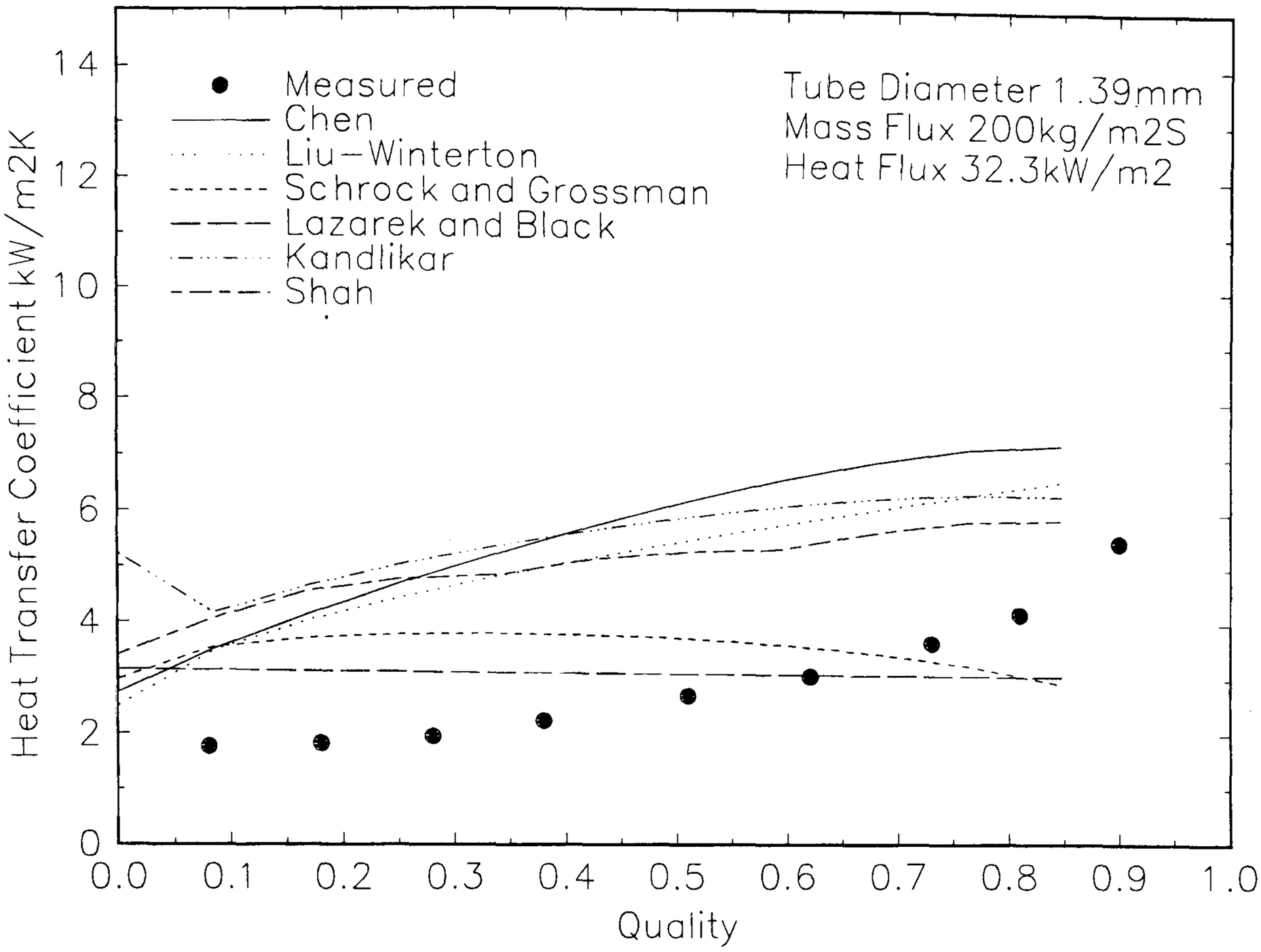

(c)

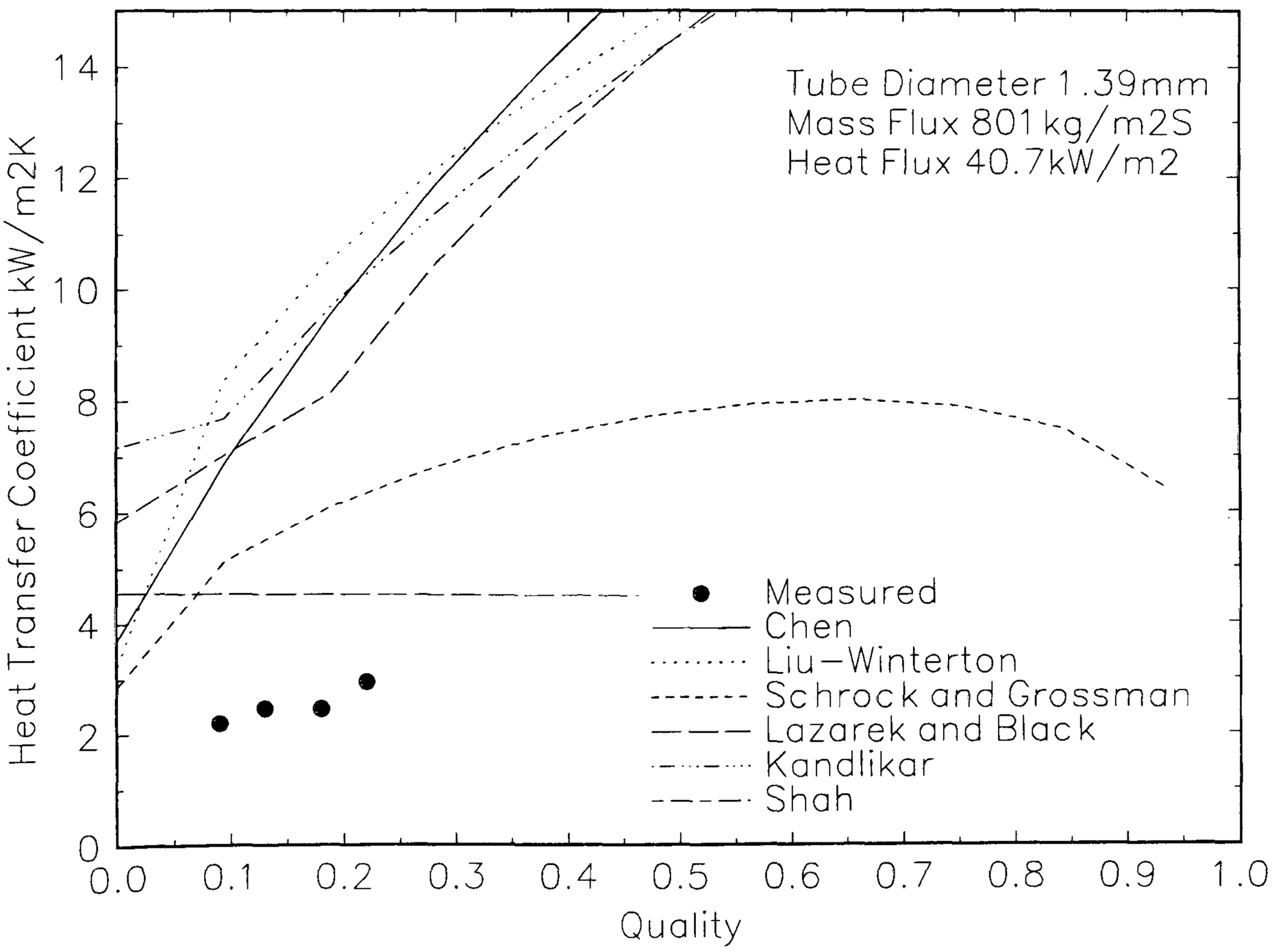

(e)

Figure 5.1 Comparison of Measured Data with Predictions of Published Correlations for 1.39mm Diameter Tube (R141b) (Cont)

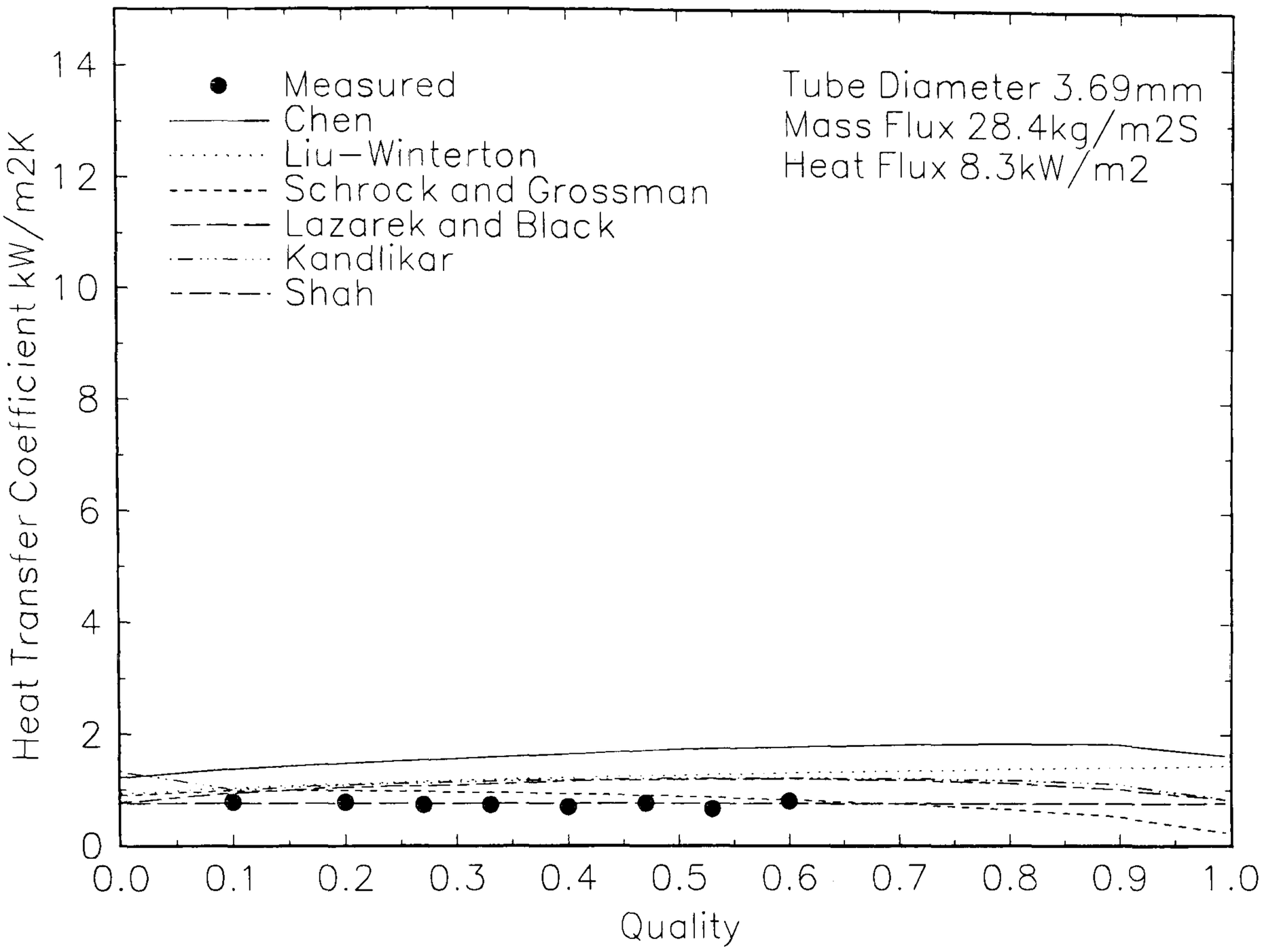

(a)

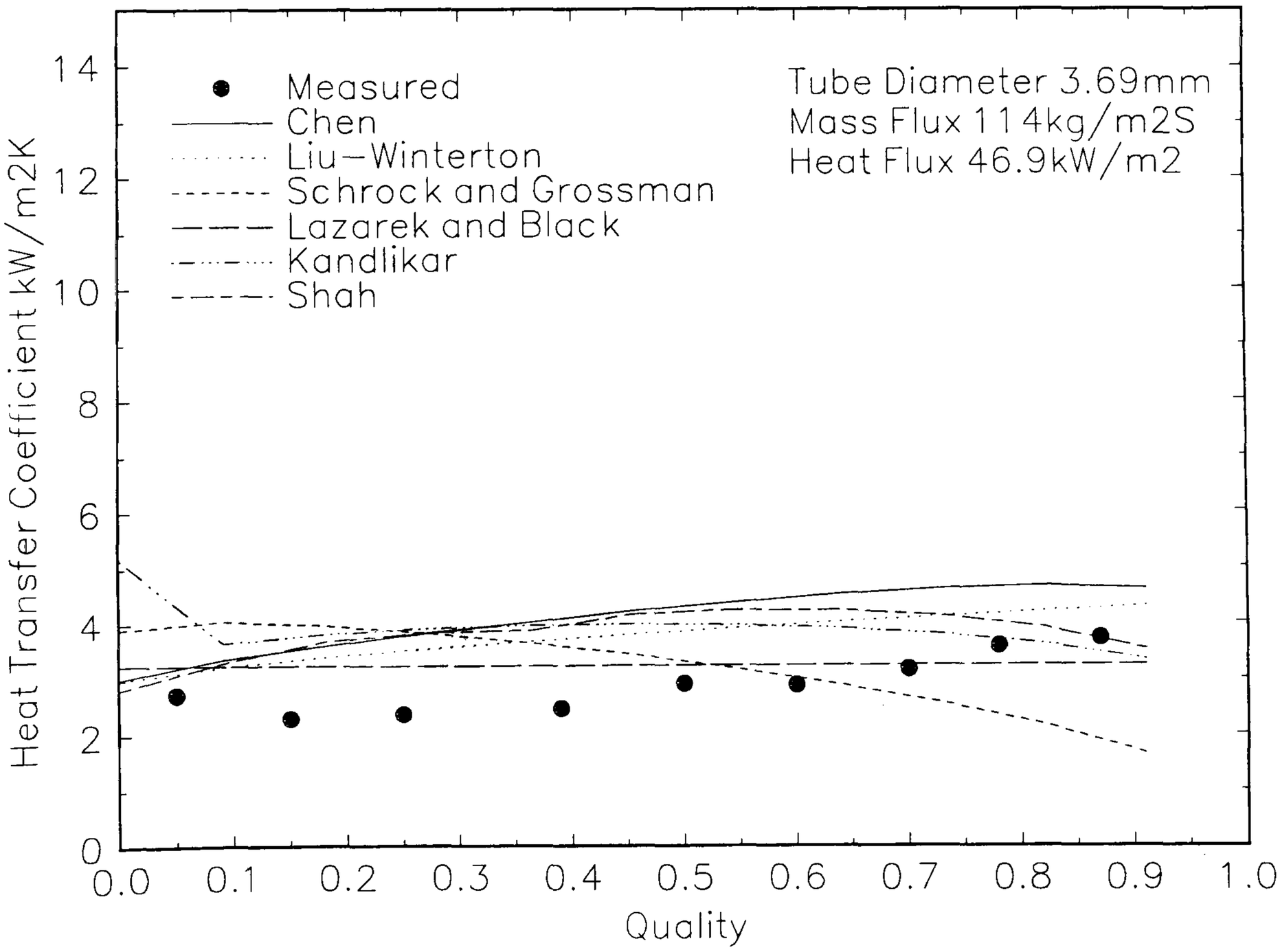

(b)

Figure 5.2 Comparison of Measured Data with Predictions of Published Correlations for 3.69mm Diameter Tube (R141b)

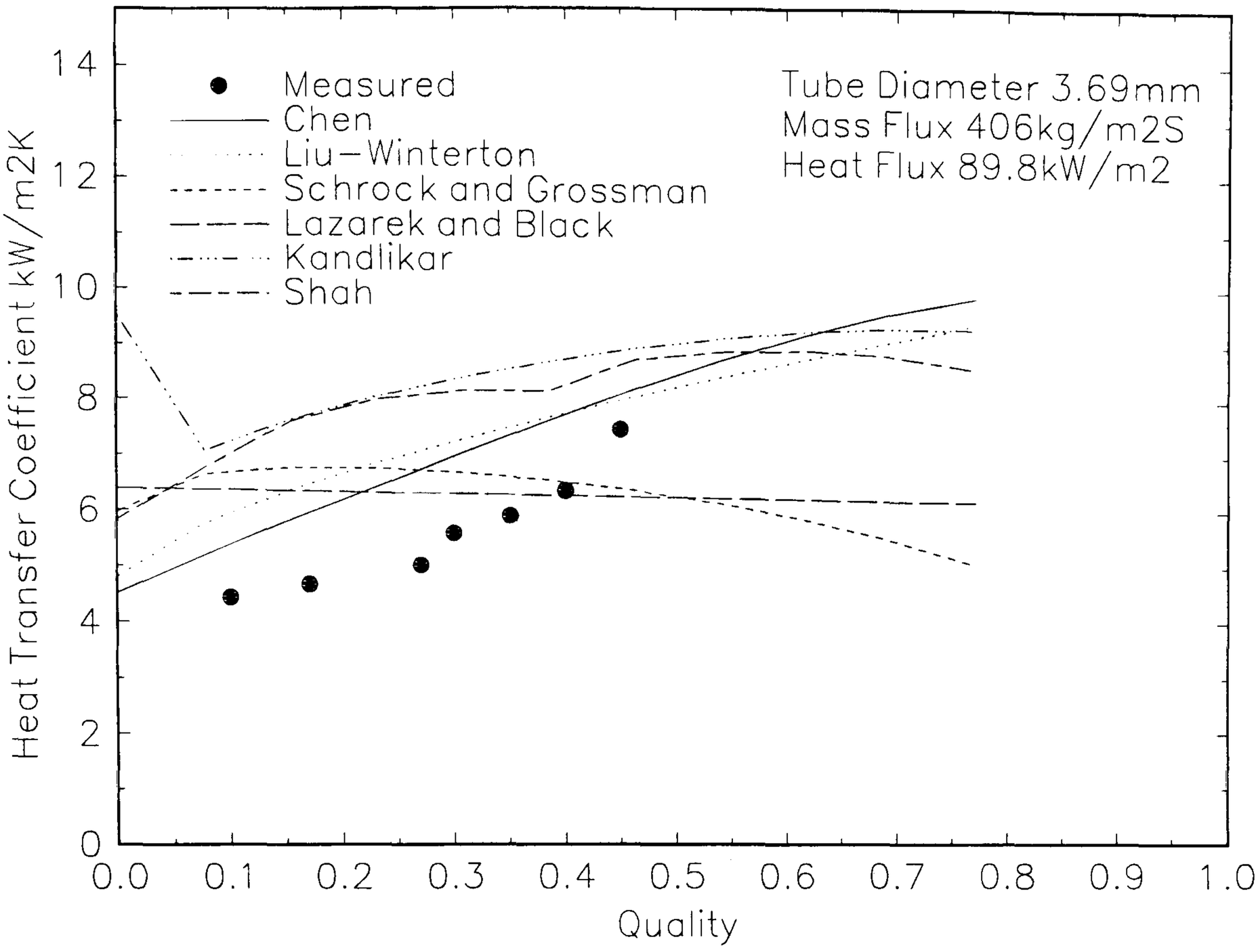

(c)

Figure 5.2 Comparison of Measured Data with Predictions of Published Correlations for 3.69mm Diameter Tube (R141b)(Cont)

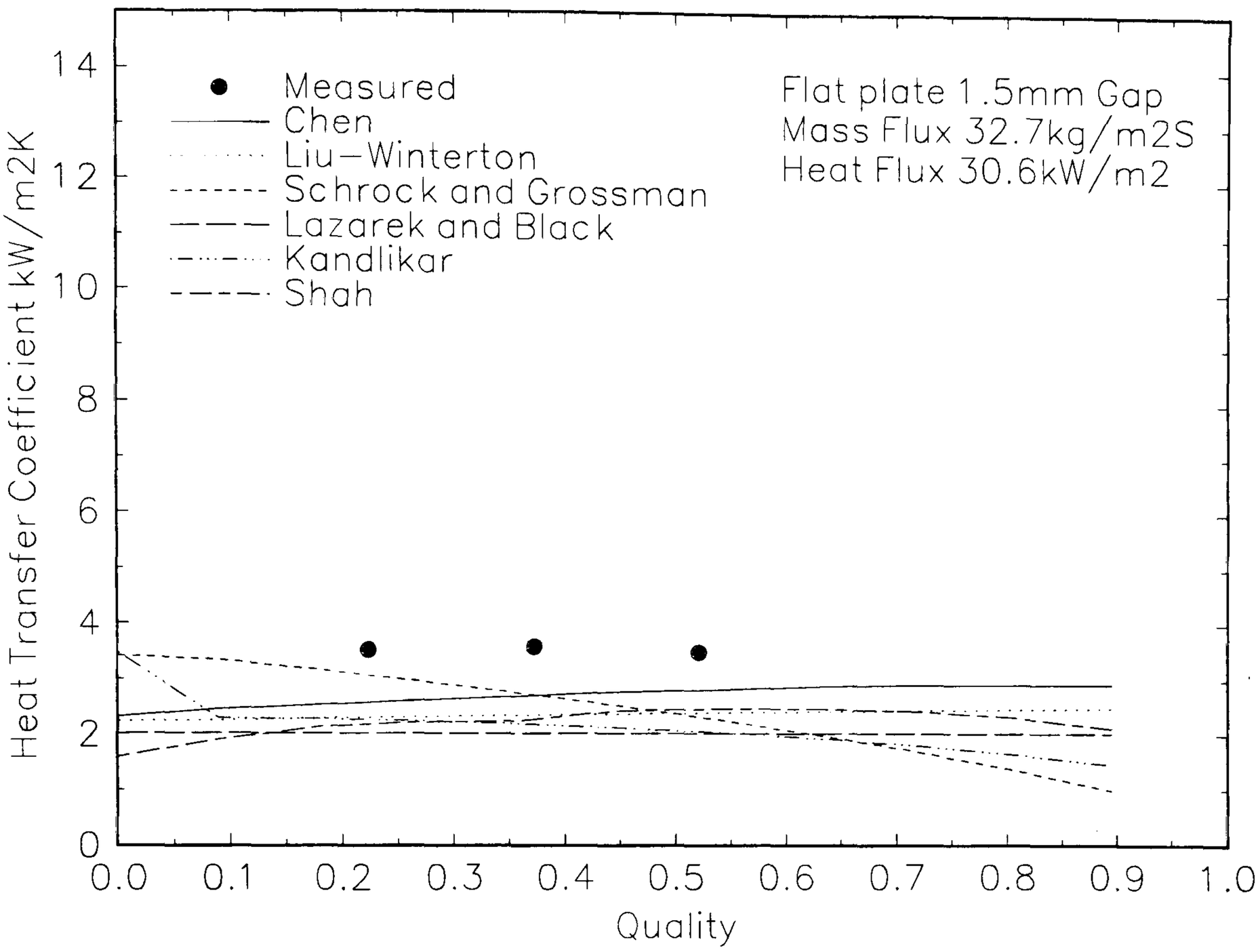

(a)

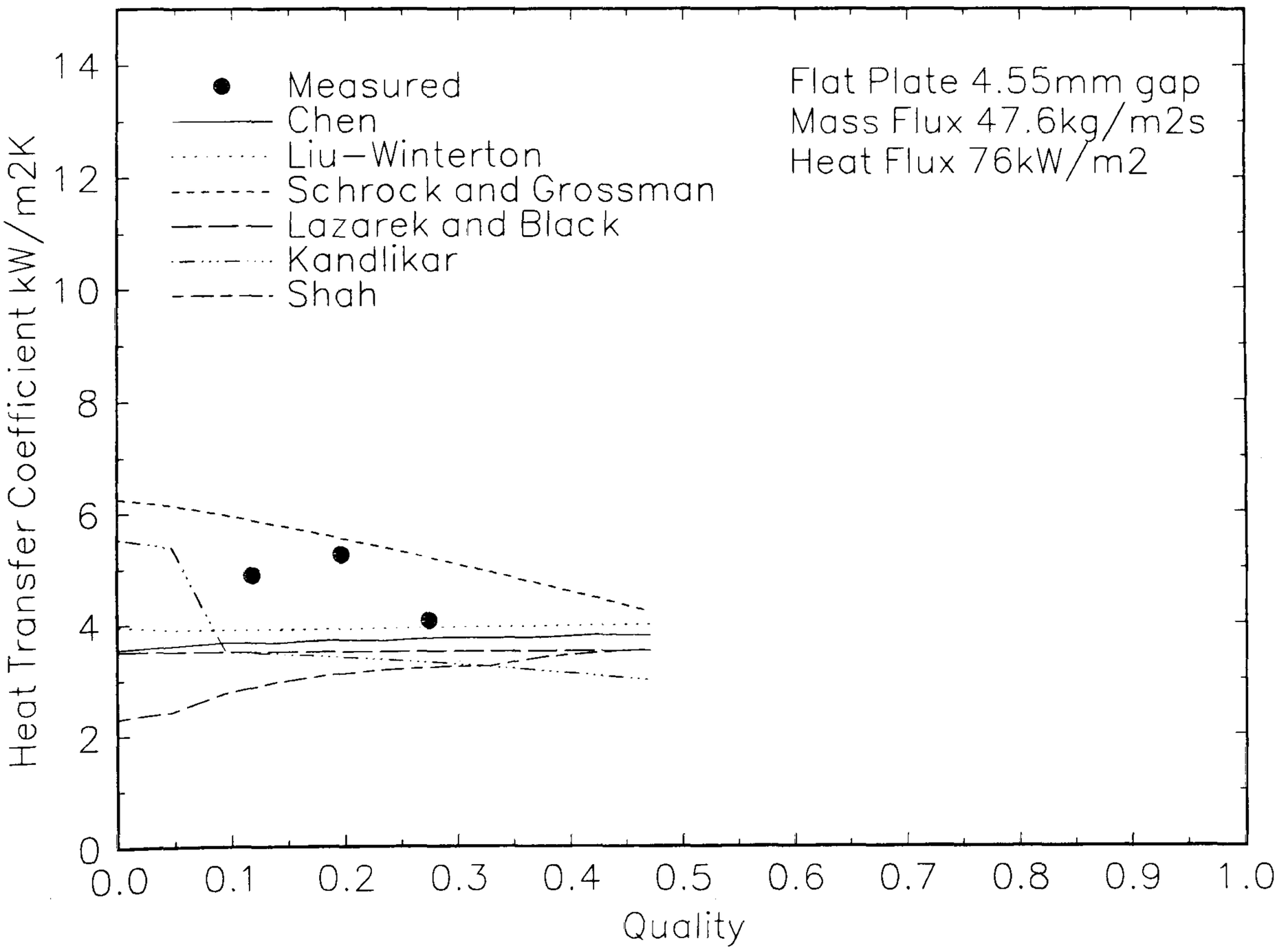

(b)

Figure 5.3 Comparison of Measured Data with Predictions of Published Correlations for Flat Plate Geometries (R141b)

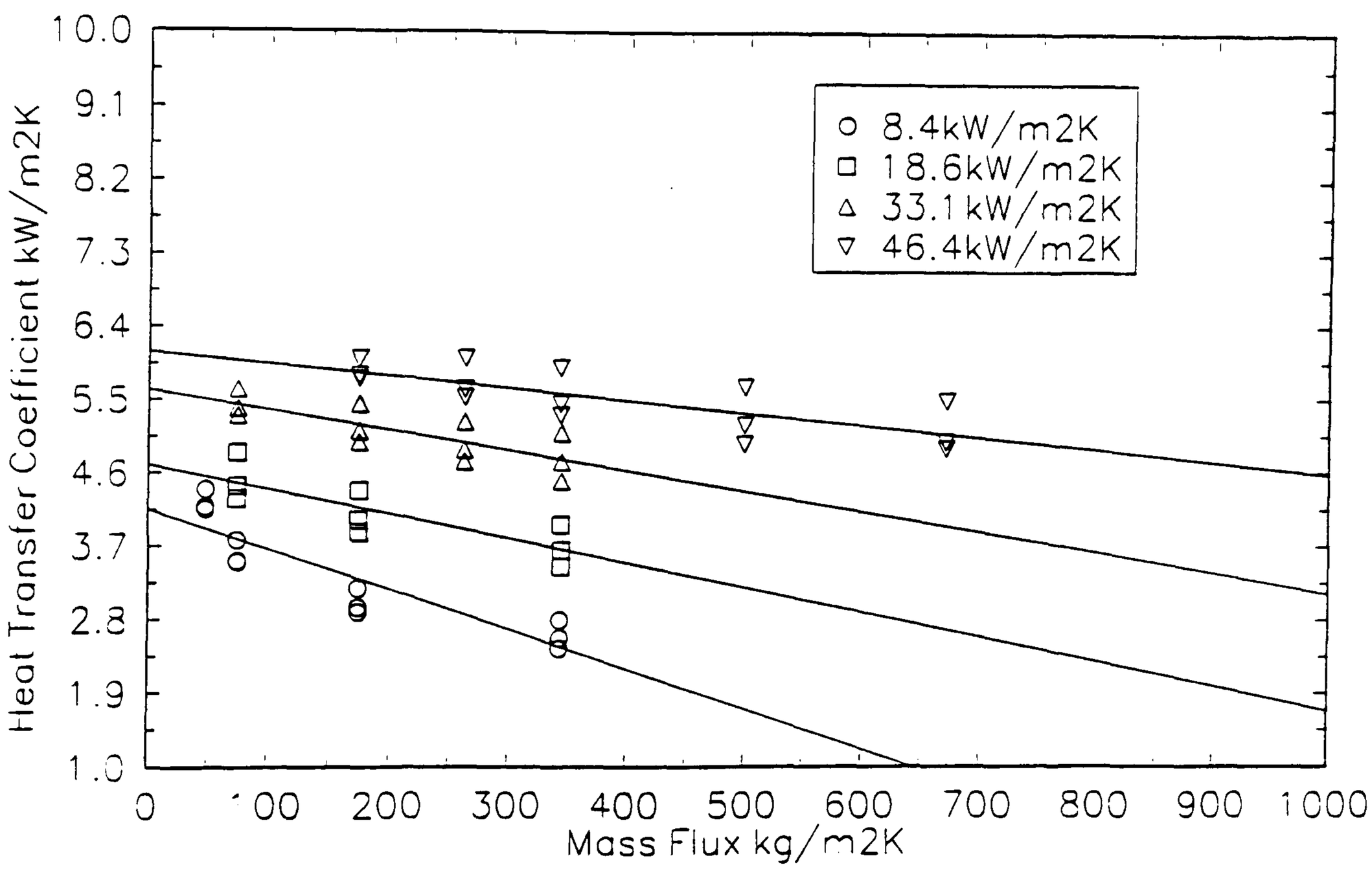

Figure 5.4. Influence of Mass Flux on Heat Transfer Coefficient
(2mm multi-channel, R141b)

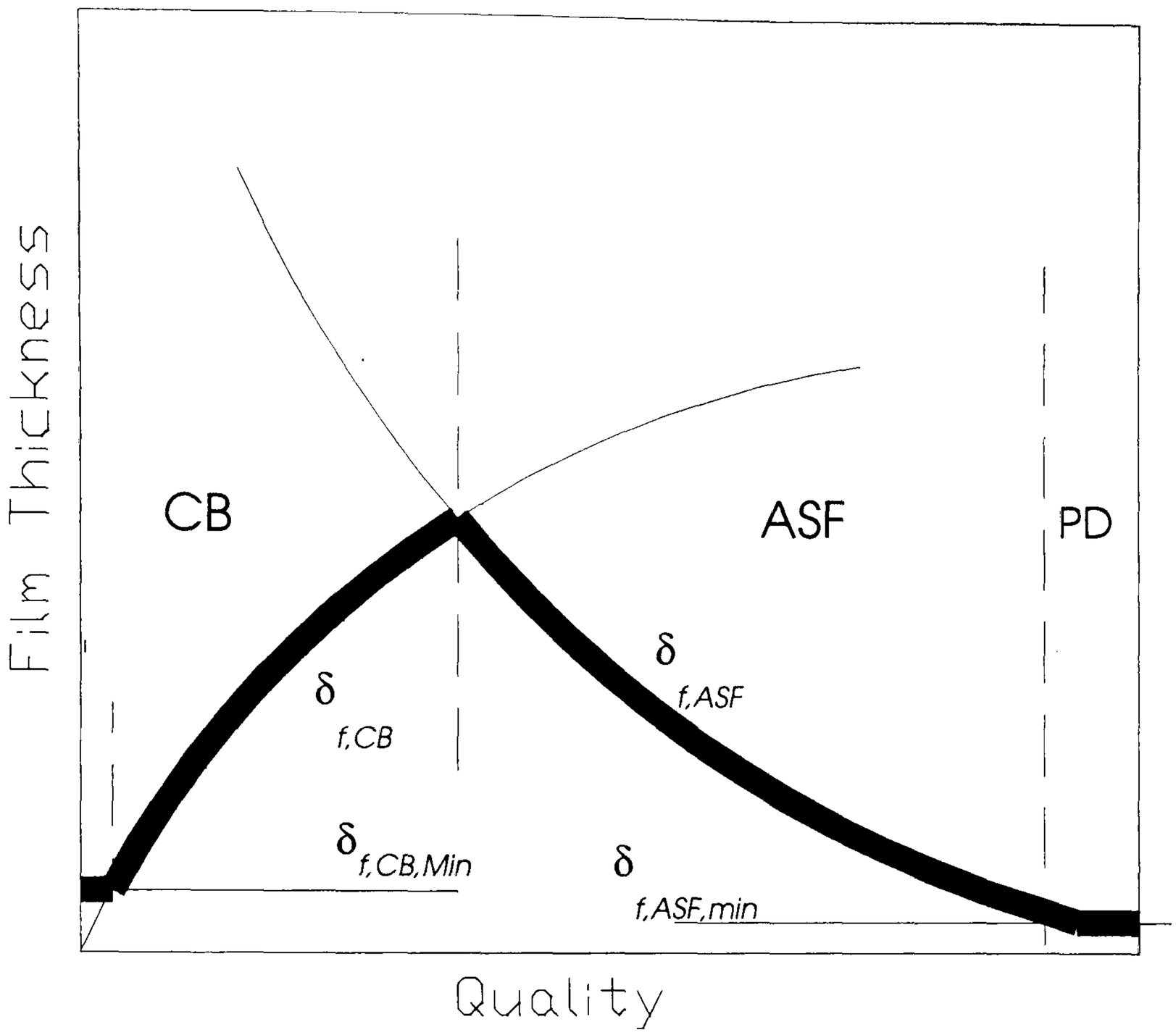

Figure 5.5 Schematic Representation of Variation of Film Thickness

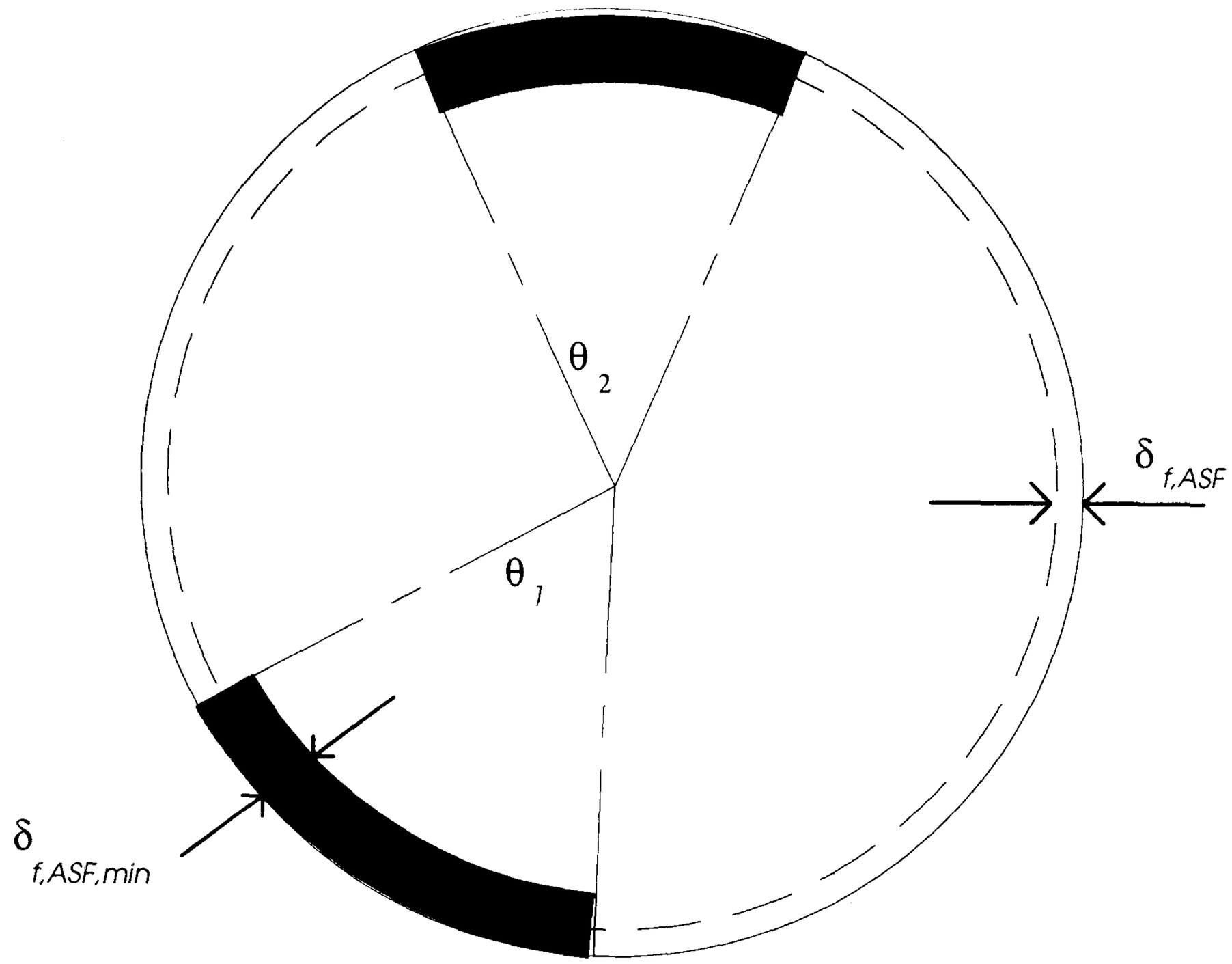

The volume in the film  = the volume if the film were uniformly distributed at the predicted thickness $\delta_{f,ASF}$.

$$r\sum\theta\delta_{f,ASF,min} = 2\pi r\delta_{f,ASF}$$

$$P_W = \frac{\text{Wetted area}}{\text{Total Area}} = \frac{\delta_{f,ASF}}{\delta_{f,ASF,min}}$$

Figure 5. 6 Film Thickness and Wetted Area in Partial Dryout Regime

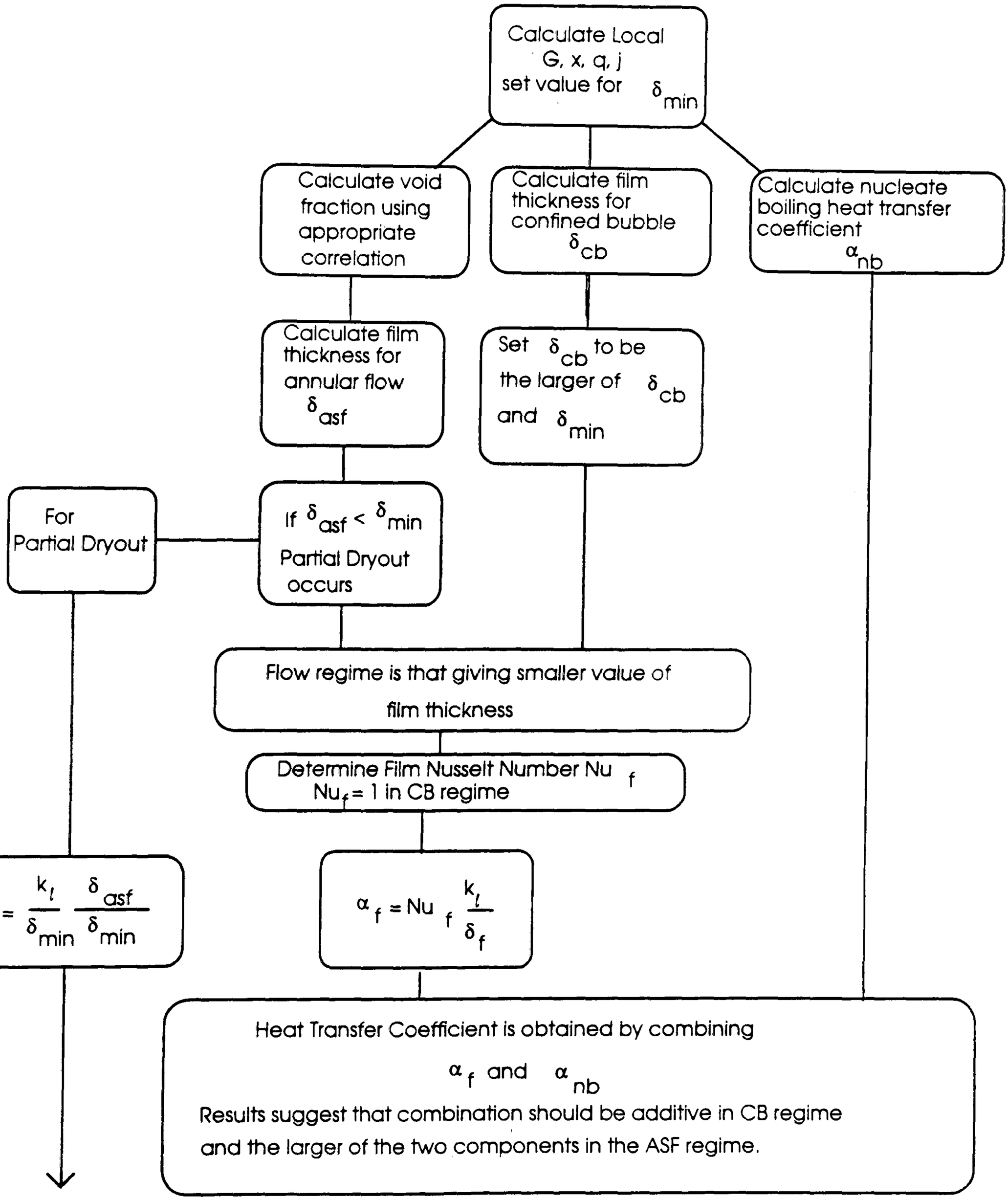

Figure 5.7 Flow Diagram for Model for Predicting Heat Transfer Coefficients in Narrow Channels

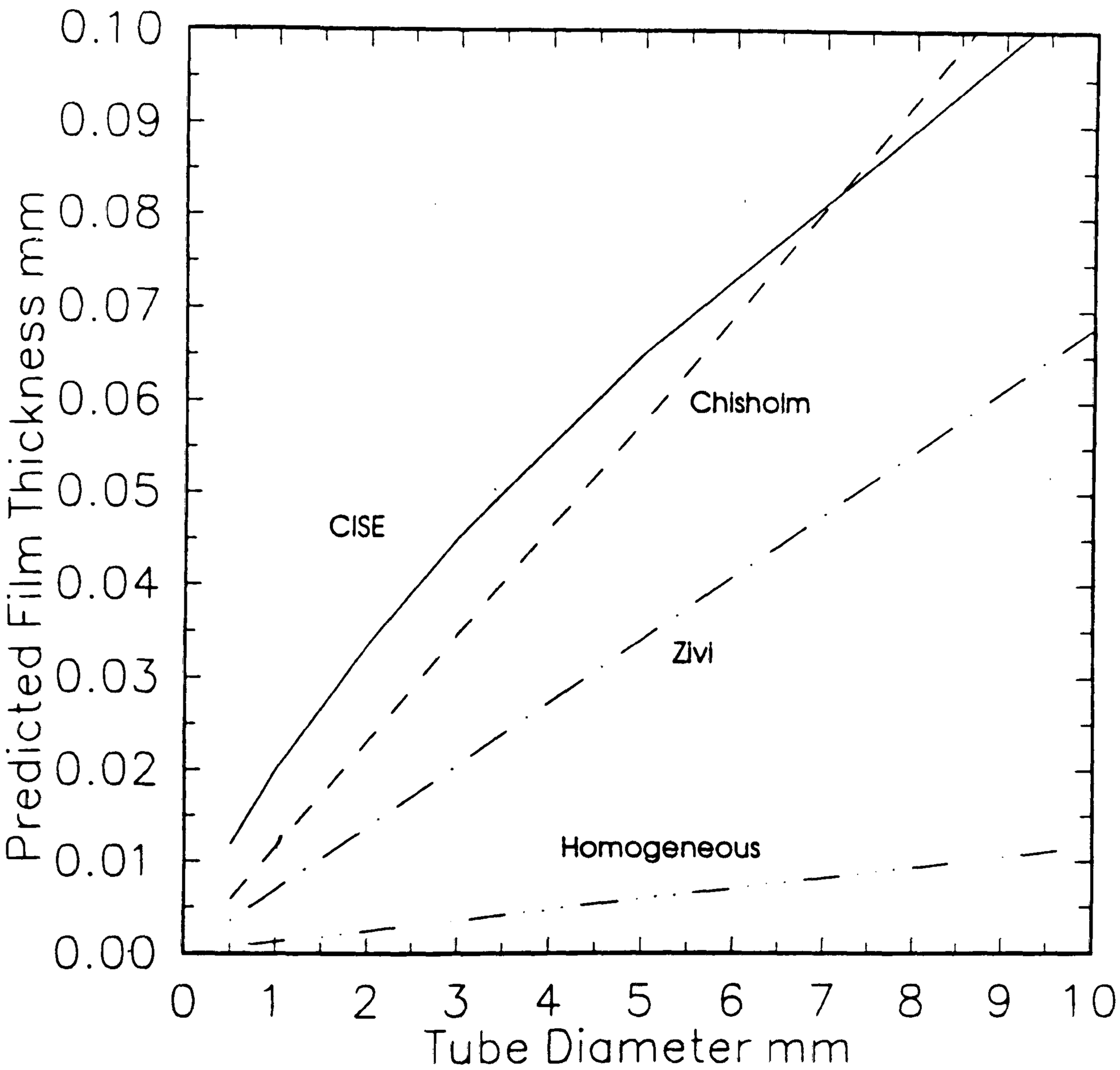

Figure 5.8 Variation in Predicted Film Thickness
R141b, x=0.5, G=300kg/m^{2}s

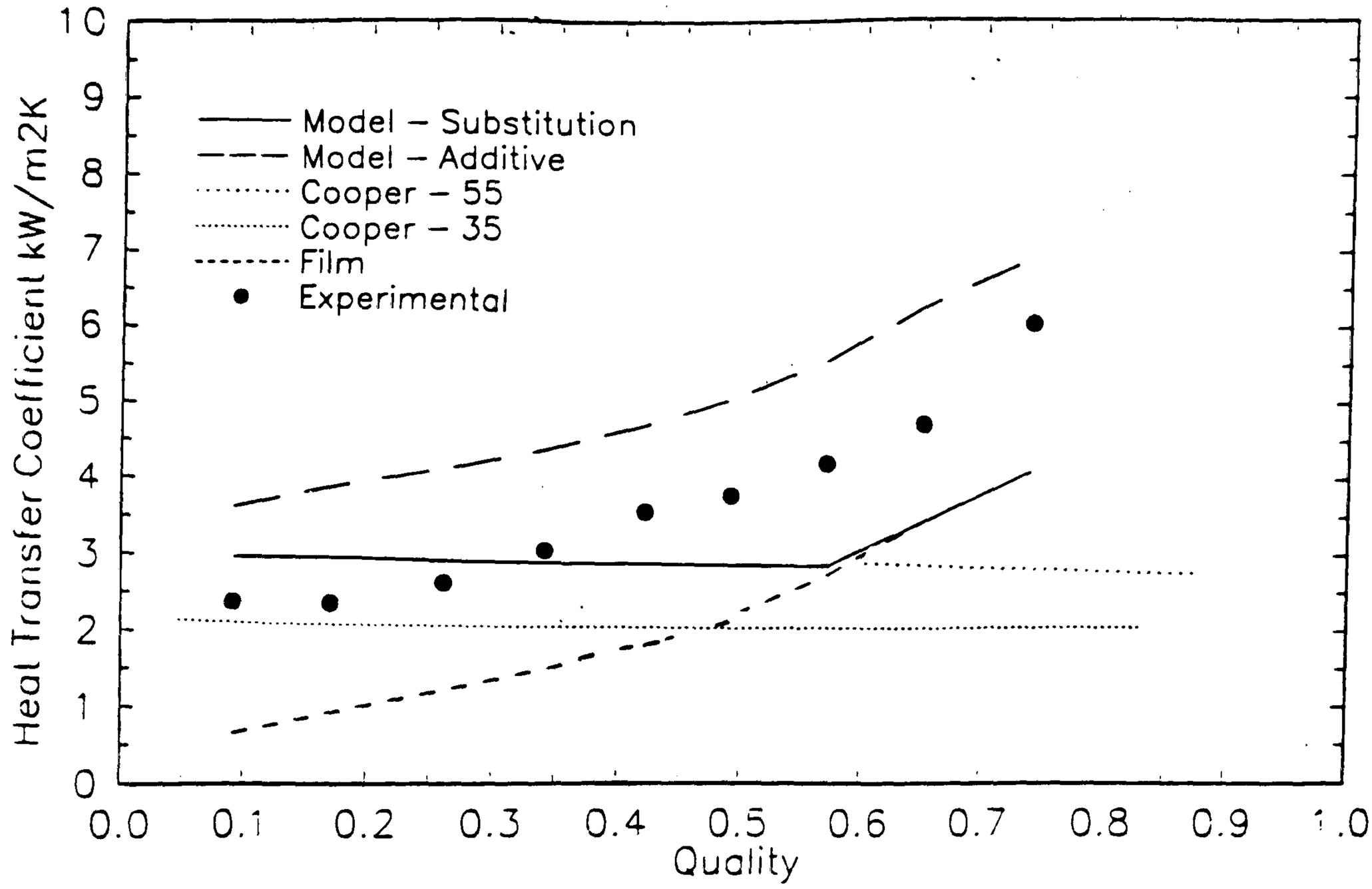

(a) Confined Bubble - Taylor, Film Thickness - CISE, Film Nusselt Number =1

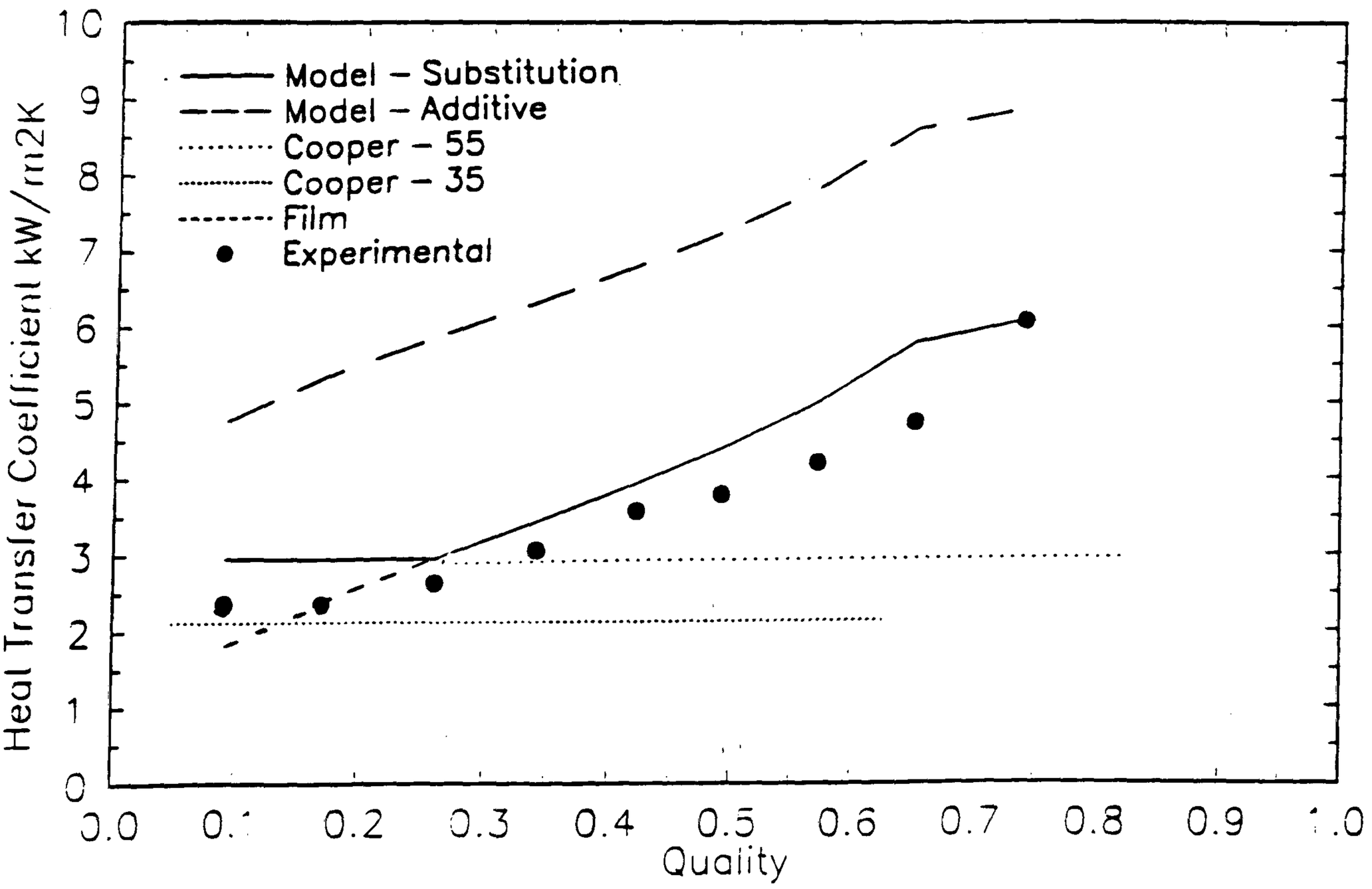

(b) Confined Bubble - Taylor, Film Thickness - CISE. Film Nusselt No.- Hewitt

Figure 5.9 Comparison of Various Implementations of the Proposed Model with Sample Results
(R141b, 2.05mm Tube, G=184kg/m^{2}s, q=35.6kW/m^2)

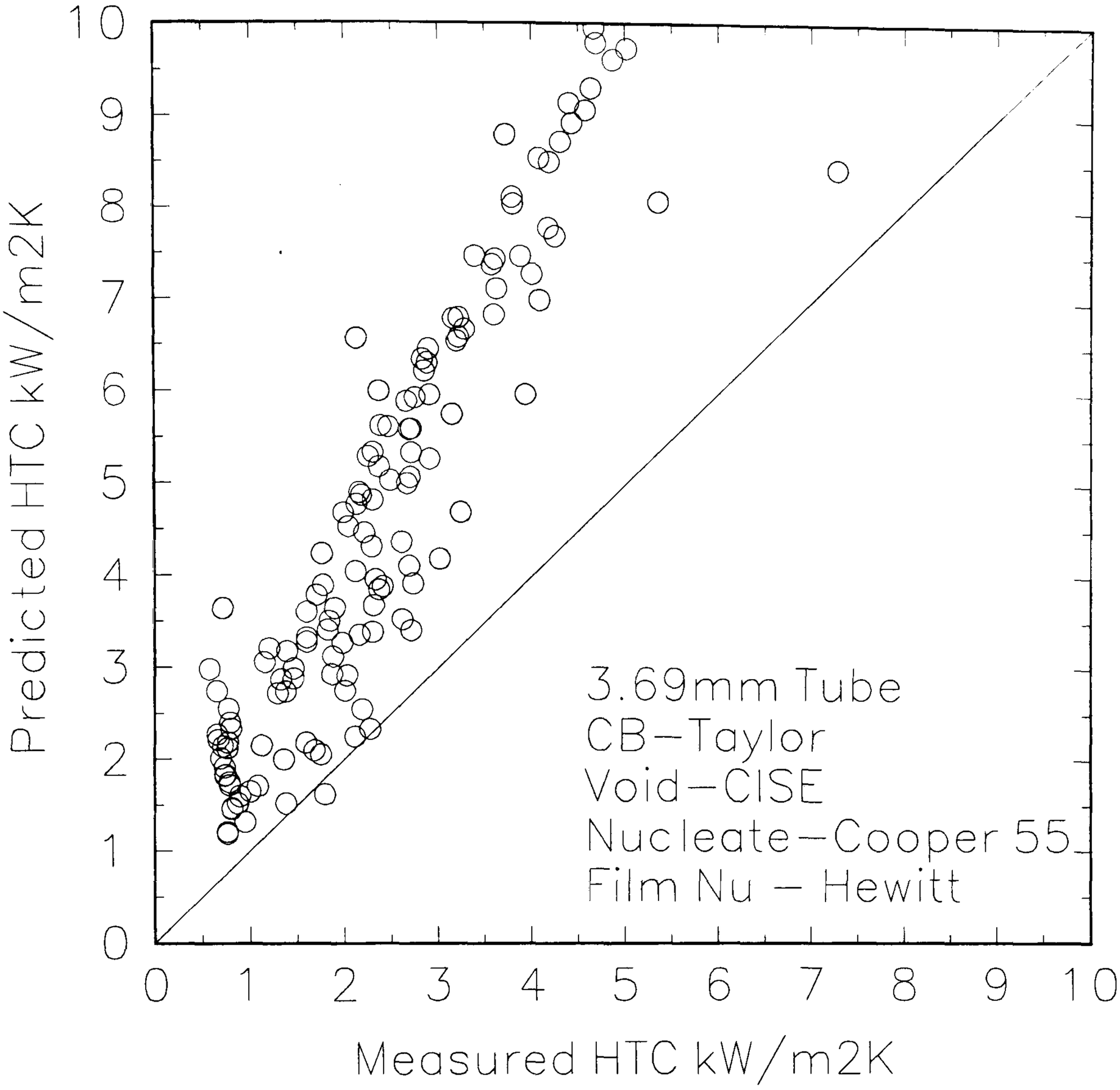

Figure 5.10 (a) Comparison of Measured and Predicted Heat Transfer Coefficients
R141b, 3.69mm, Film and Nucleate Boiling Coefficients Added

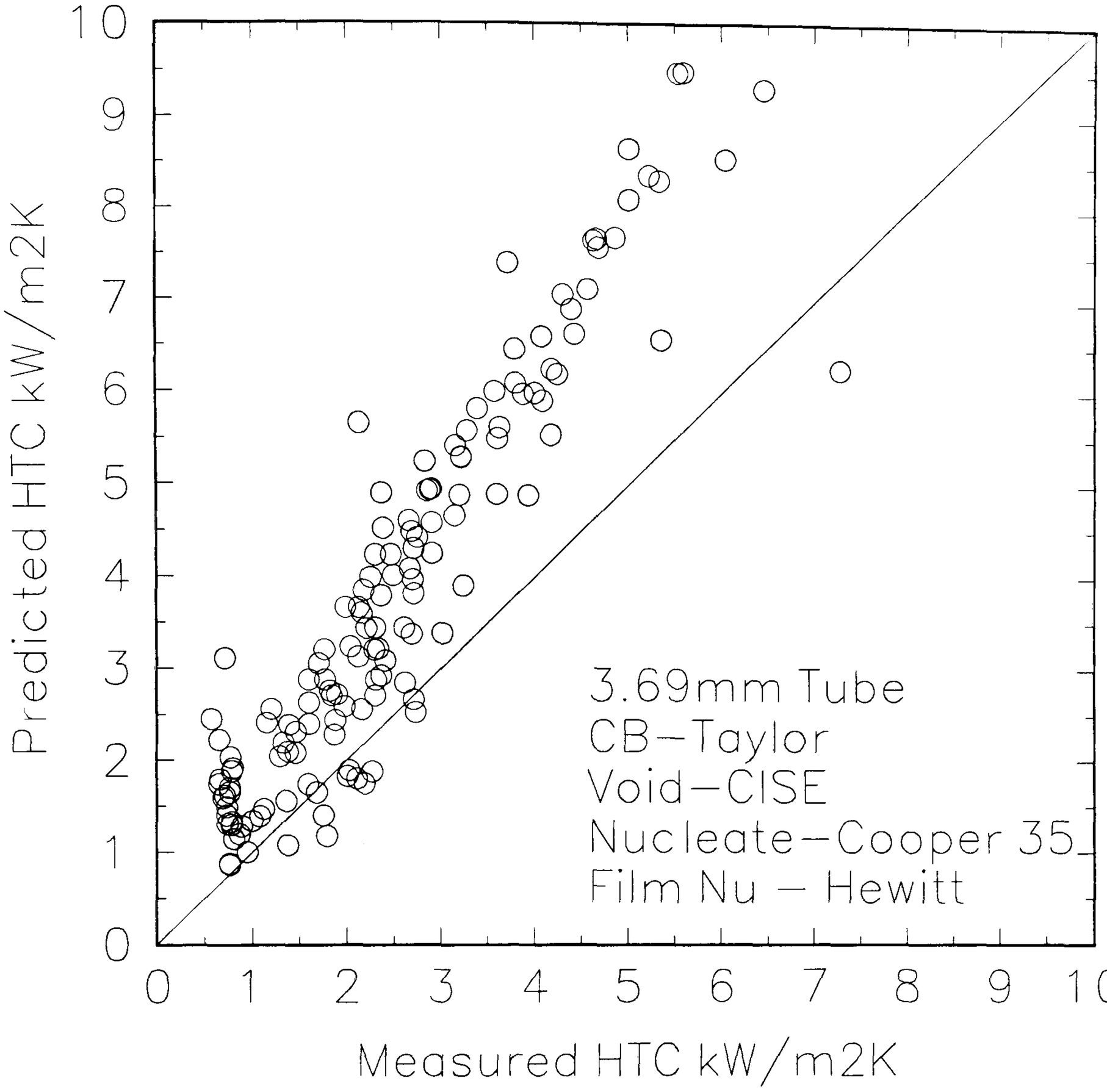

Figure 5.10 (b) Comparison of Measured and Predicted Heat Transfer Coefficients
R141b, 3.69mm, Film and Nucleate Boiling Coefficients Added

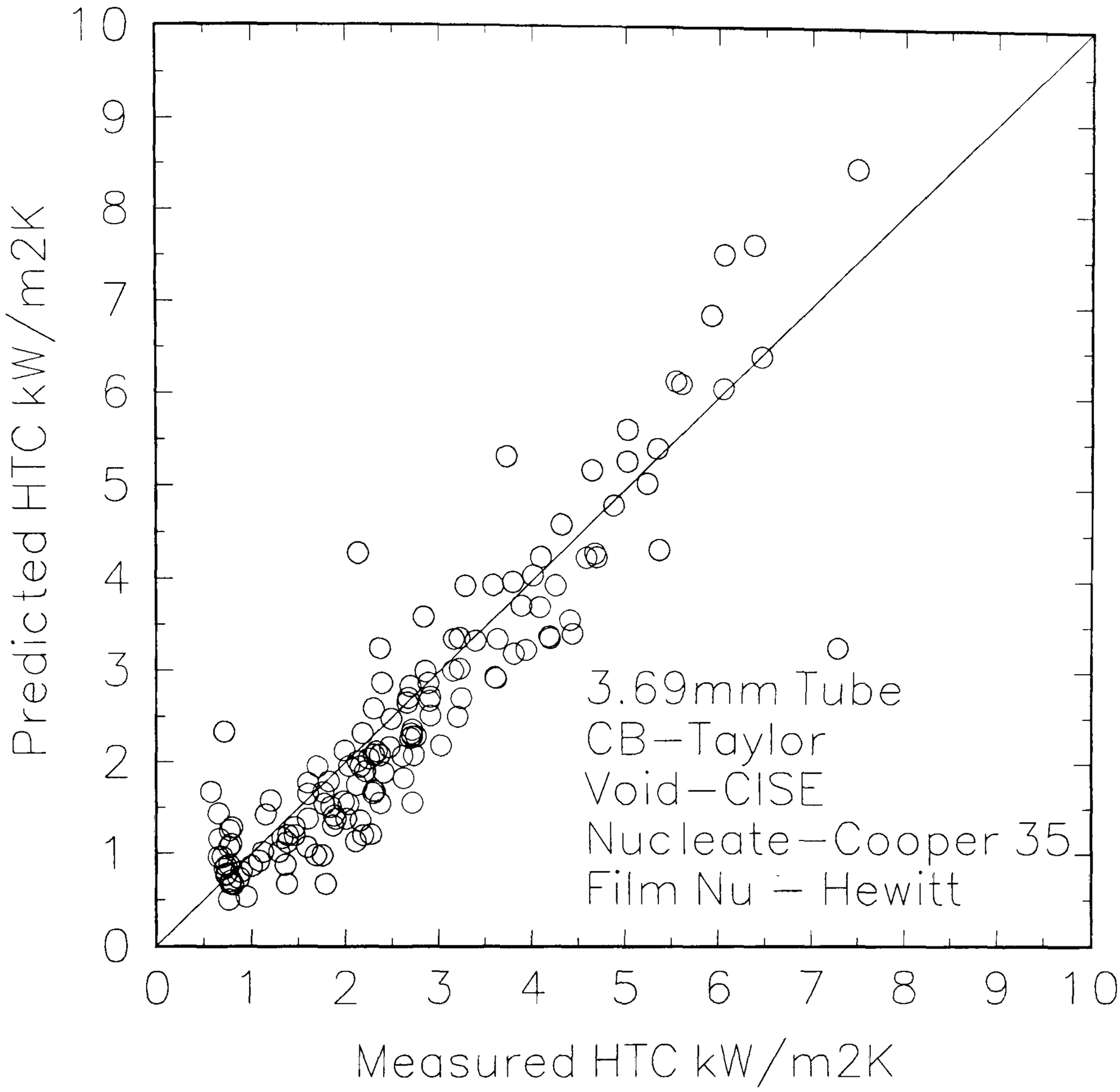

Figure 5.10 (c) Comparison of Measured and Predicted Heat Transfer Coefficients
R141b, 3.69mm,
HeatTransfer Coefficient = Larger of Film and Nucleate Boiling Coefficients

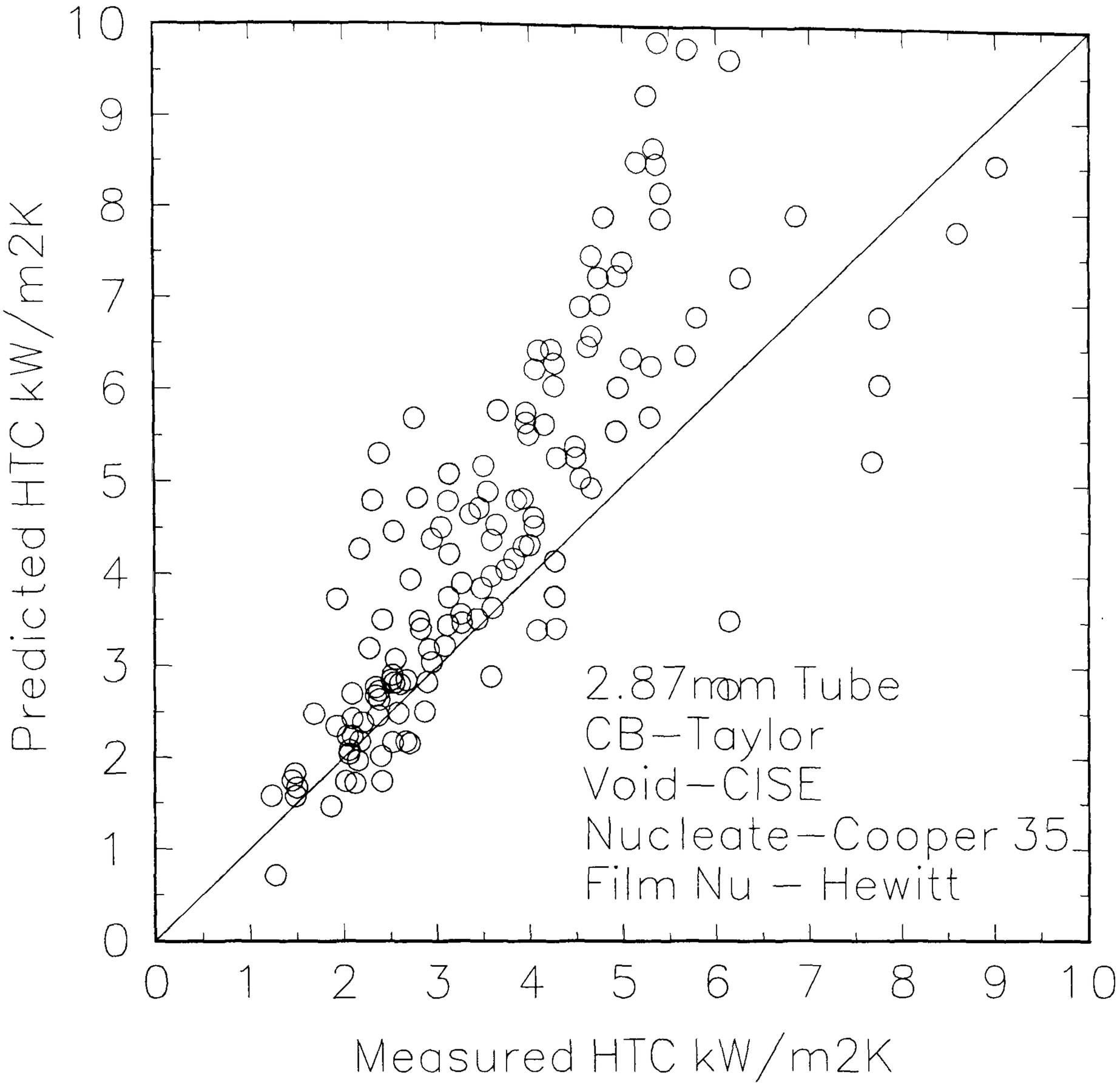

Figure 5.11 Comparison of Measured and Predicted Heat Transfer Coefficients
R141b, 2.87mm,
HeatTransfer Coefficient = Larger of Film and Nucleate Boiling Coefficients

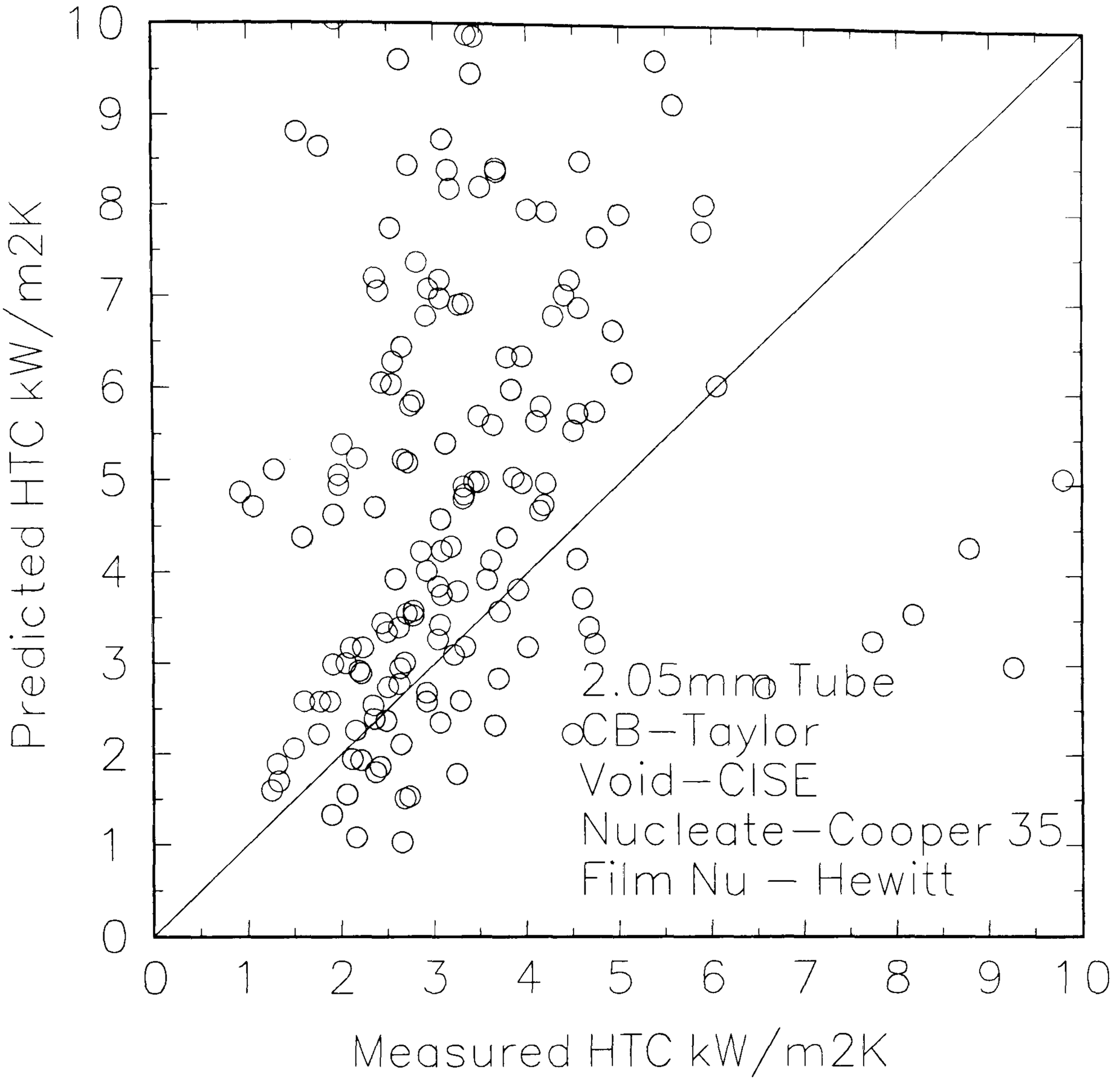

Figure 5.12 Comparison of Measured and Predicted Heat Transfer Coefficients
R141b, 2.05mm,
HeatTransfer Coefficient = Larger of Film and Nucleate Boiling Coefficients

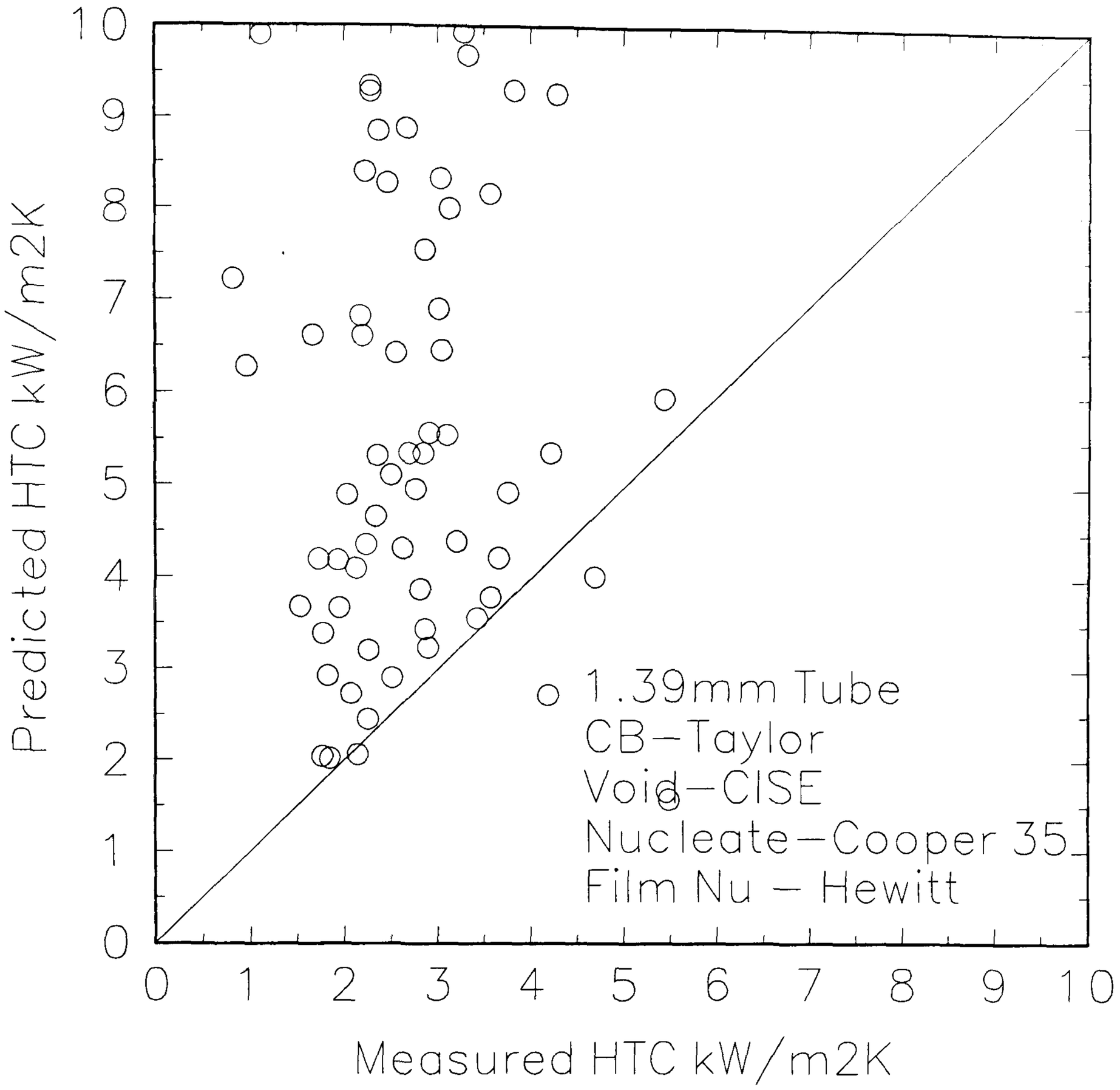

Figure 5.13 Comparison of Measured and Predicted Heat Transfer Coefficients
R141b, 1.39mm,
HeatTransfer Coefficient = Larger of Film and Nucleate Boiling Coefficients

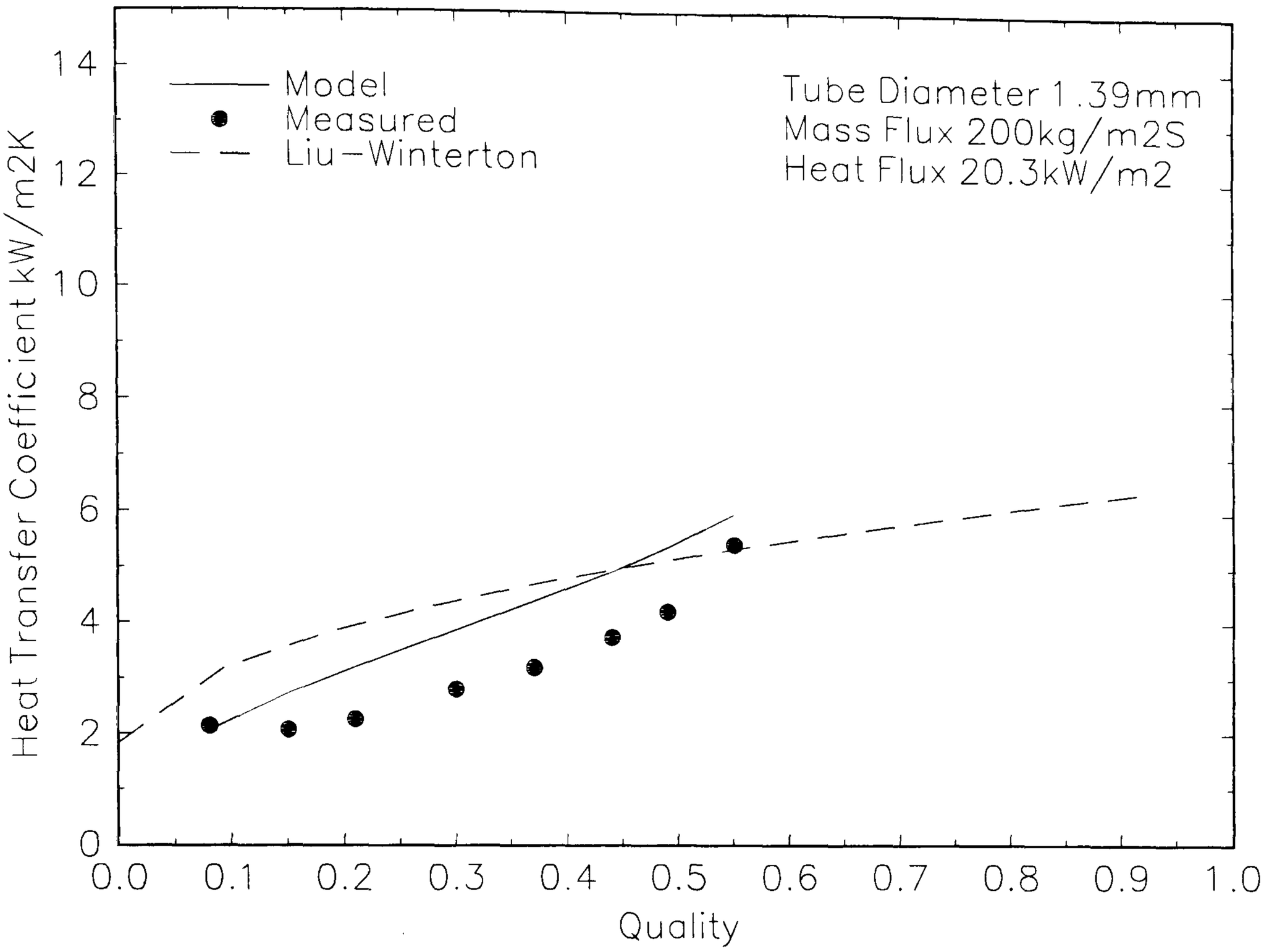

(a)

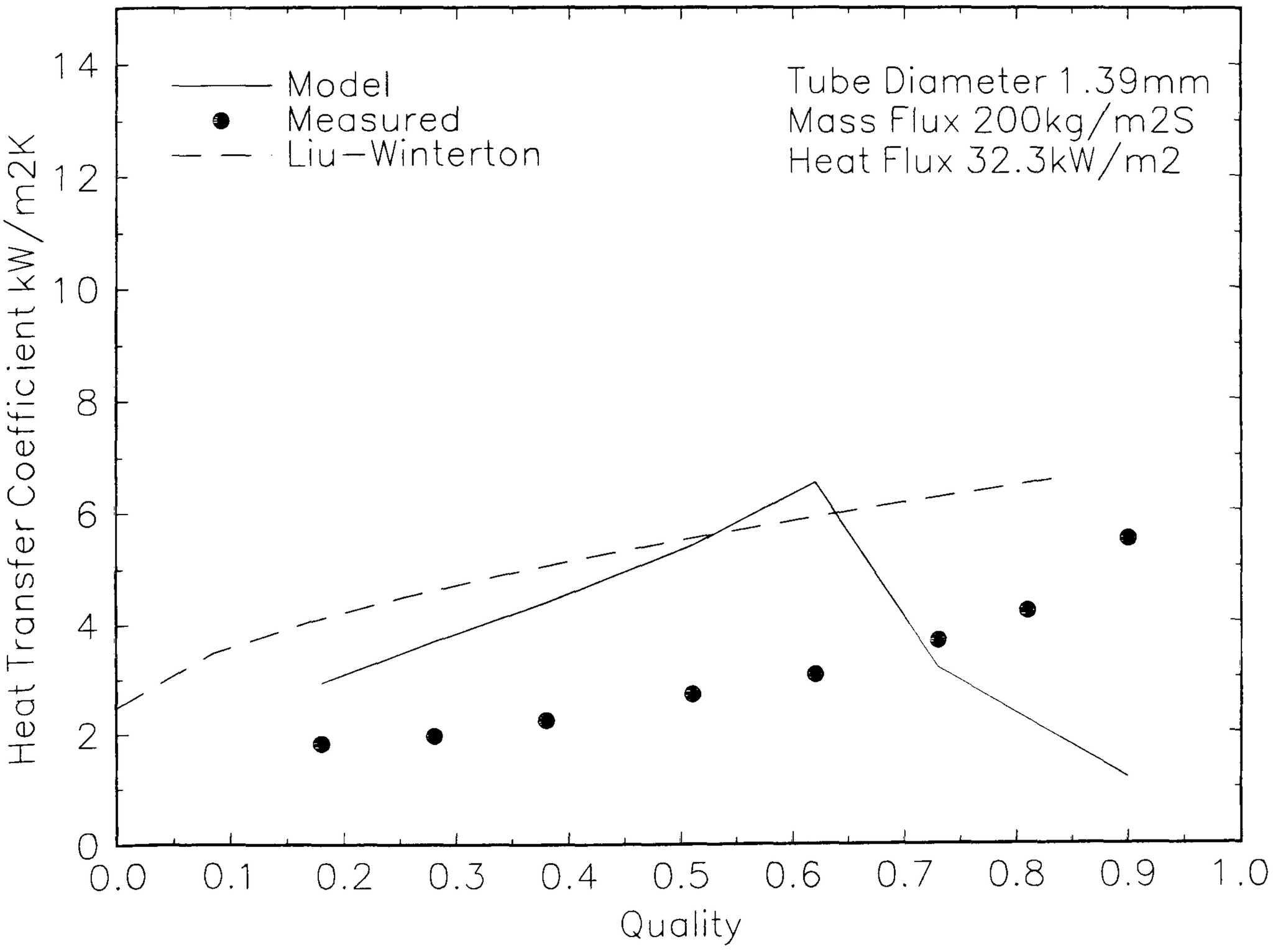

Figure 5.14 Comparison of Various Implementations of the Proposed Model with Sample Results
(R141b, HeatTransfer Coefficient = Larger of Film and Nucleate Boiling Coefficients)

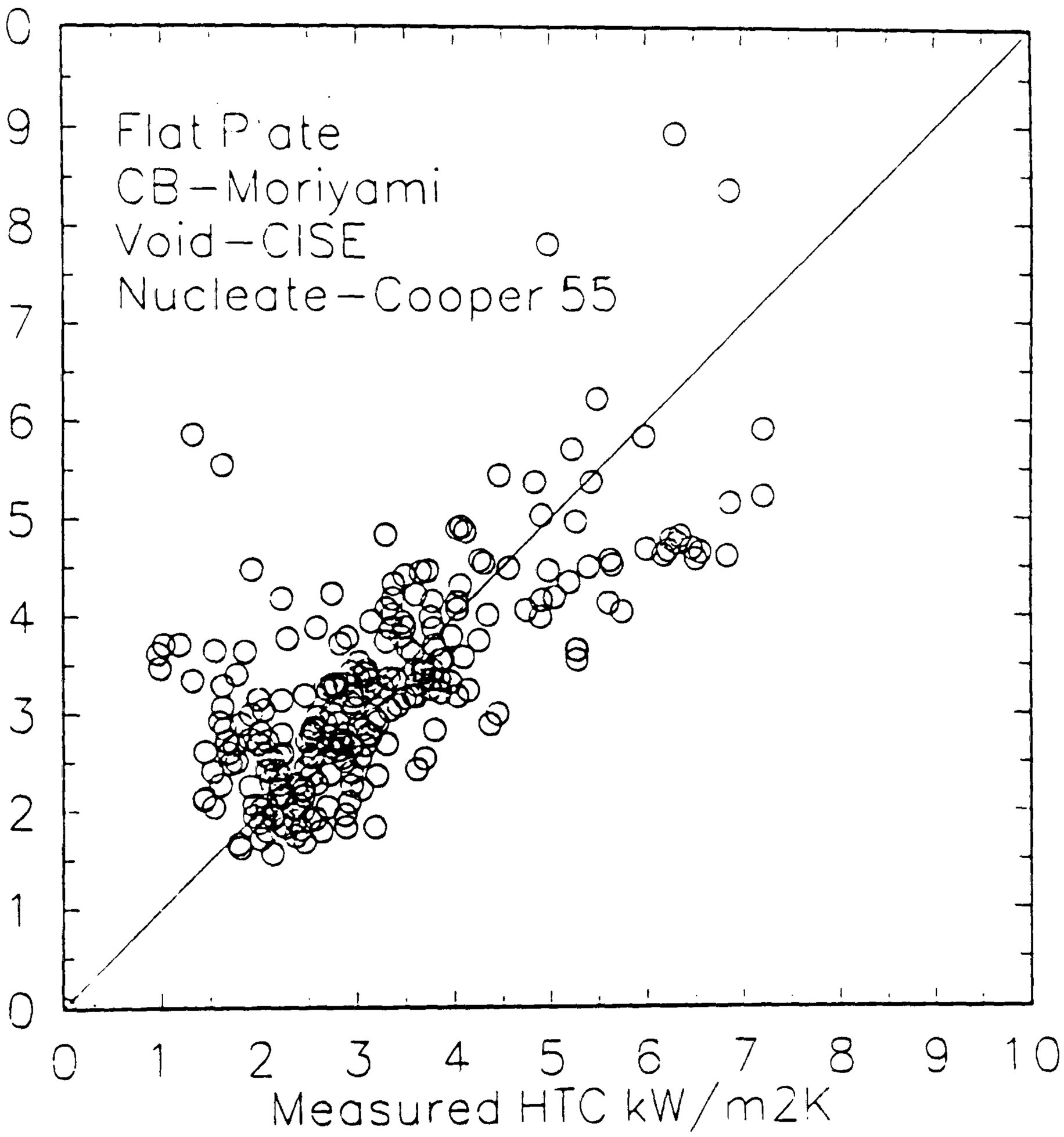

Figure 5.15 Comparison of Measured and Predicted Heat Transfer Coefficients
R141b, Flat Plate Geometry, Gap 1.125-4.5mm,
HeatTransfer Coefficient = Sum of Film and Nucleate Boiling Coefficients

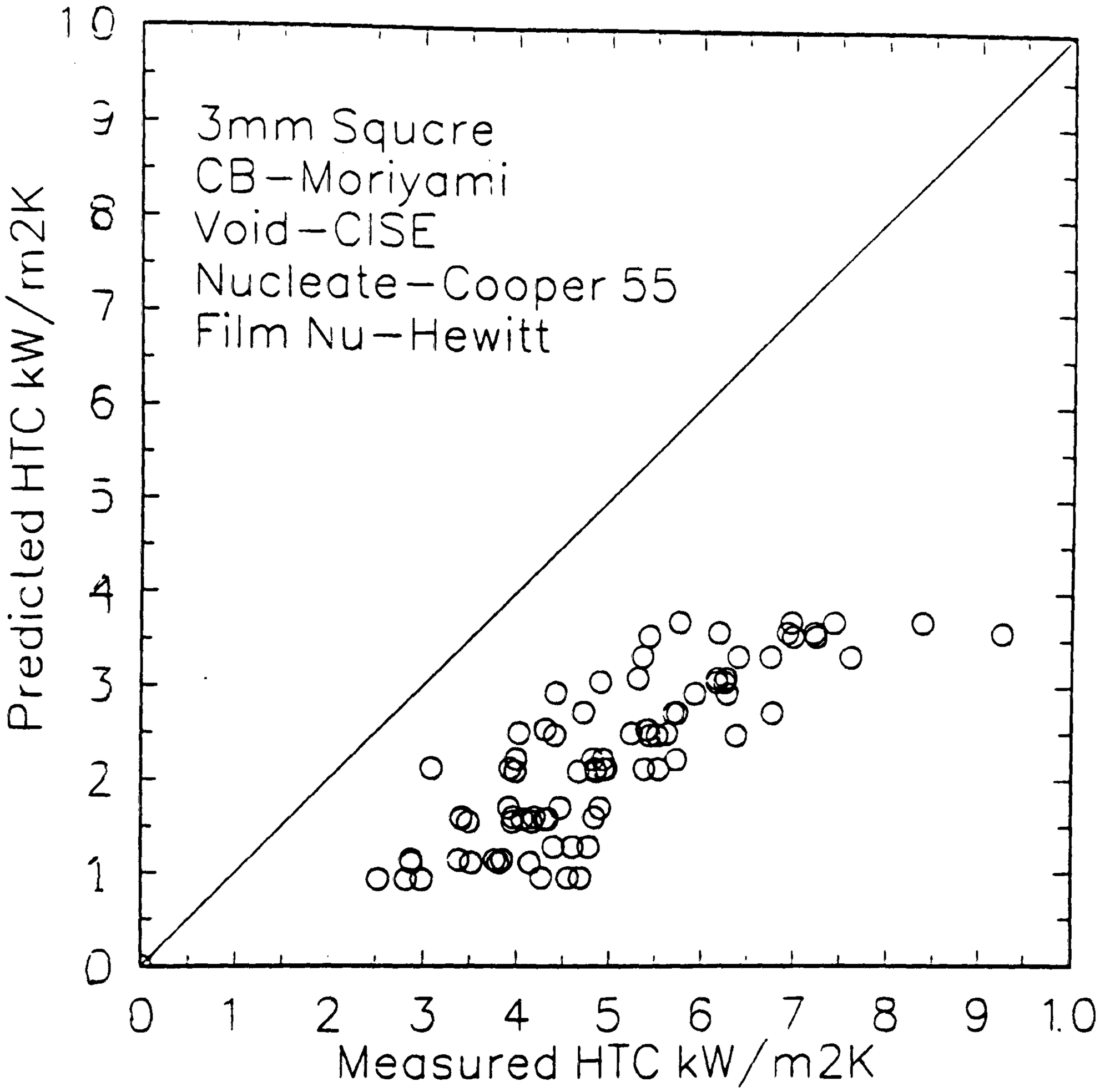

Figure 5.16 Comparison of Measured and Predicted Heat Transfer Coefficients
R141b, Multi-Channel Geometry,3mm □ Channels
HeatTransfer Coefficient = Larger of Film and Nucleate Boiling Coefficients

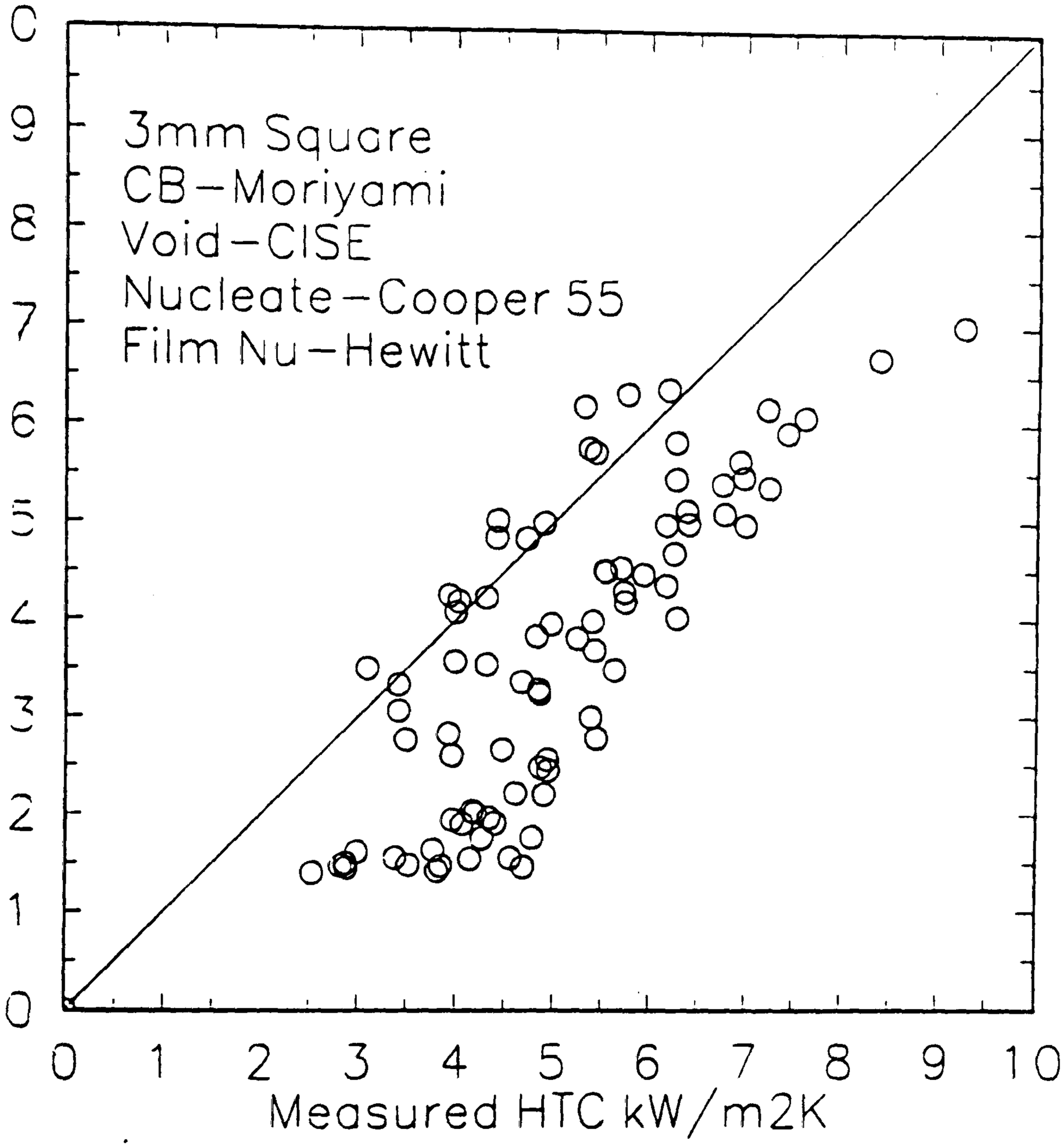

Figure 5.17 Comparison of Measured and Predicted Heat Transfer Coefficients
R141b, Multi-Channel Geometry,3mm □ Channels
HeatTransfer Coefficient = Sum of Film and Nucleate Boiling Coefficients

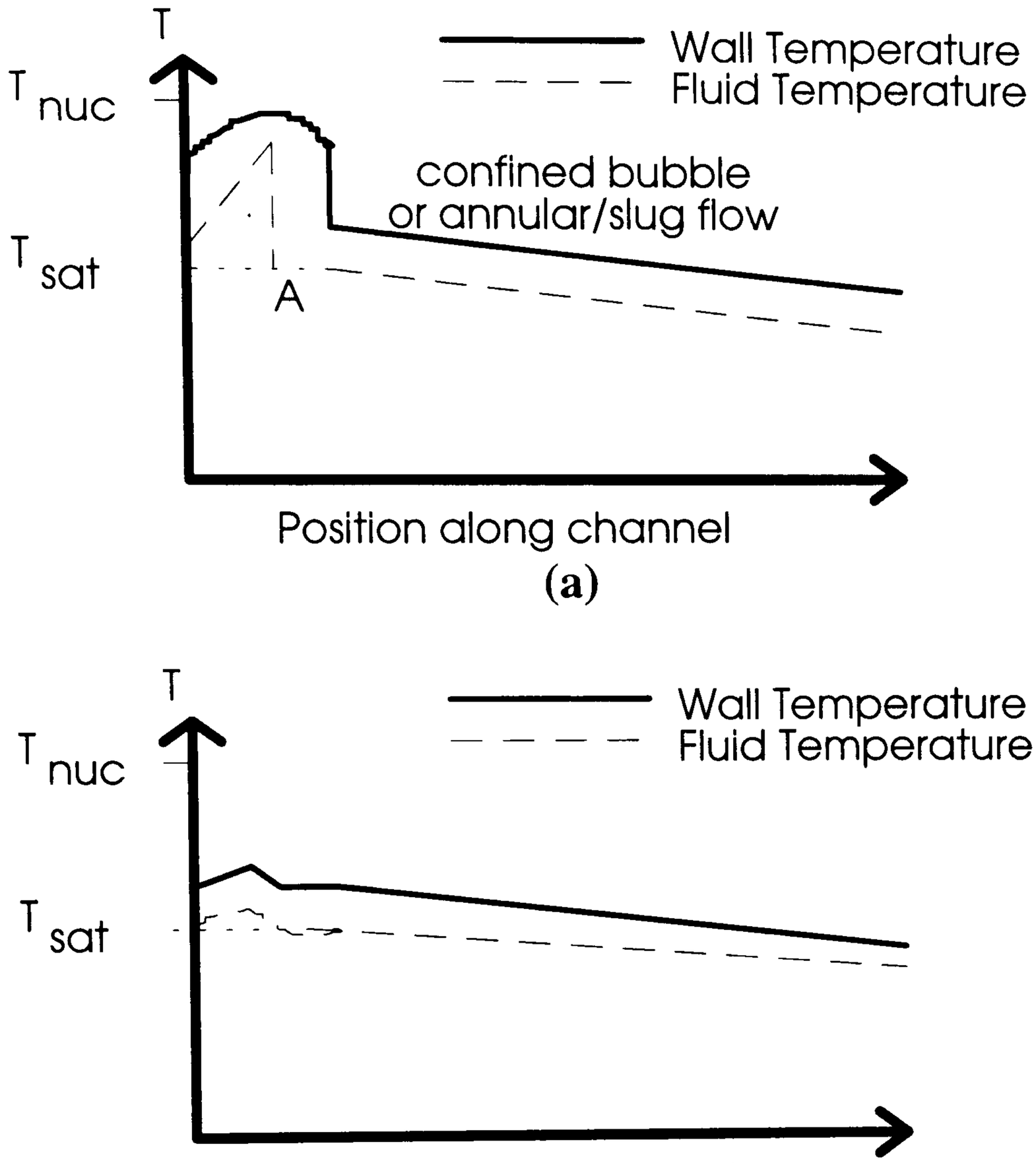

Figure A3.1 Temperature profiles along electrically heated narrow channel

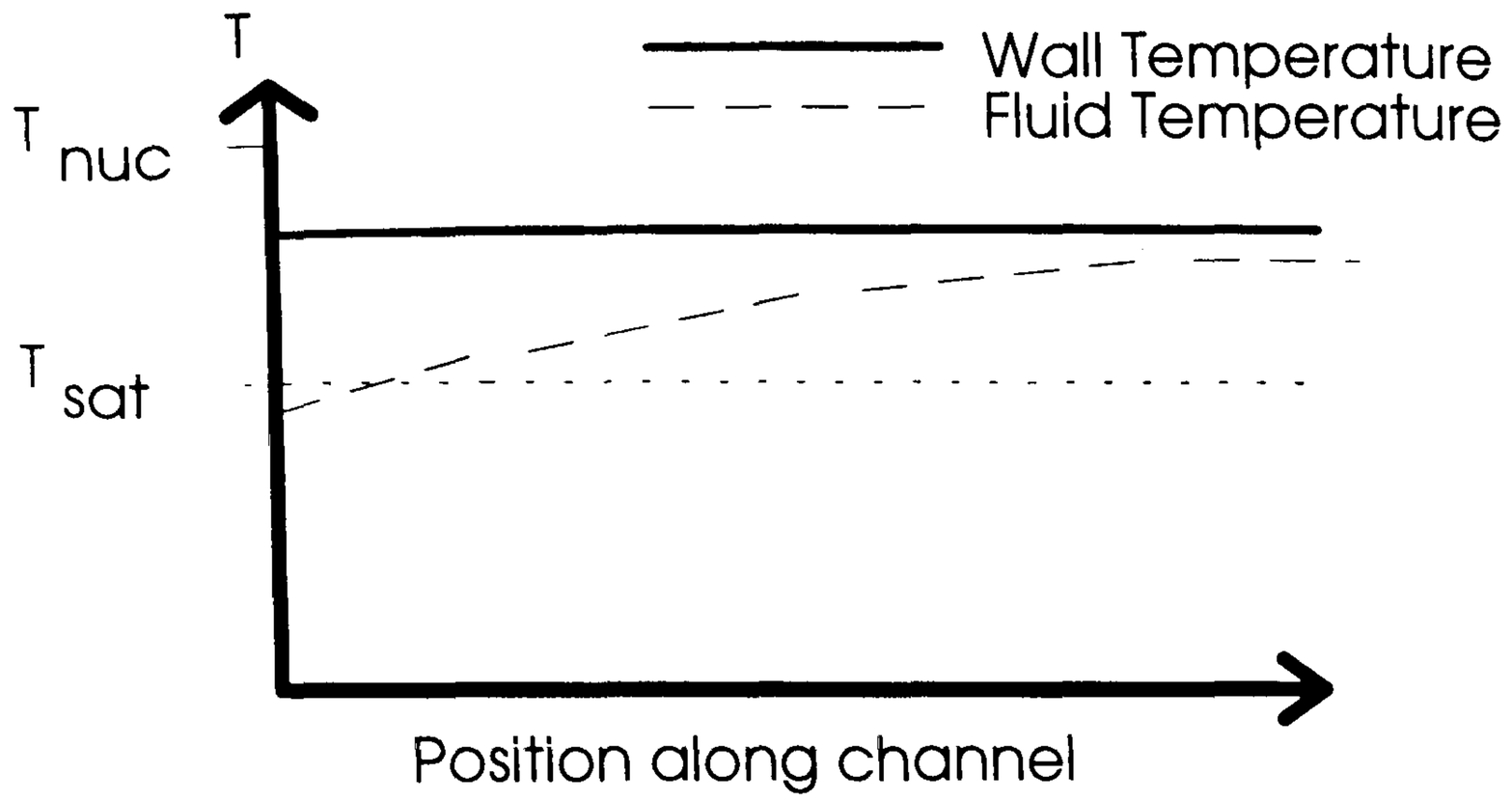

Figure A3.2. Temperature profile along narrow channel maintained at a constant temperature
(close to the fluid saturation temperature)